The metabolism of starch in the model legume *Lotus japonicus*

Cécile Vriet

Thesis submitted to the University of East Anglia for the degree of Doctor of Philosophy

September 2010

Abstract

The metabolism of transitory starch is of central importance to many aspects of plant growth and development. Studies carried out on *A. thaliana* have greatly enhanced our knowledge of the pathways involved, highlighting their complexity. However, information about these pathways in other species is lacking. In particular, almost nothing is known about the metabolism of transitory and storage starch in legumes, a family that includes some of the most agriculturally important forage and grain crops.

In this study, the model *Lotus japonicus* was used to explore the metabolism of starch in legumes and investigate its importance for several agriculturally important traits. Characterisation of mutants from a forward genetic screen was linked with TILLING reverse genetics to assemble a comprehensive suite of starch mutants. These mutants were used to elucidate the main components of starch synthesis and degradation in *L. japonicus*. Although these components were for the most part conserved with those in *A. thaliana* and other species, the control of flux through the pathways and their importance in sustaining normal plant growth were shown to be different. Whereas a severe deficiency in starch synthesis had much less effect in *L. japonicus* than in A. *thaliana*, the loss of the capacity for starch degradation had a much more profound consequence for plant growth. Further investigation of these differences may lead to a better understanding of the regulatory mechanisms linking the metabolism of starch with plant growth. This suite of *L. japonicus* mutants was also used in combination with a collection of annual and perennial species of the genus *Lotus* to investigate the importance of carbon partitioning for the perenniality trait. Results of this analysis suggested that root starch reserves play an important role in determining the vegetative re-growth vigour in perennial *Lotus* species.

A mes grands-parents, Jean et Odette Rigault;
A mes parents et mes frères, Robert, Maryline, Guillaume et Rémi Vriet;
En mémoire de ma grand-mère, Odette Vriet.

Contents

List of Figures

List of tables

Acknowledgements

The writing of this PhD thesis and the work presented in it would not have been done without the support, encouragement, and help of many people.

First of all, I would like to thank my PhD supervisors, Dr. Trevor Wang and Professor Alison Smith for giving me the great opportunity to work on this research project at the John Innes Centre (Norwich, UK) and for their supervision. I am extremely grateful to Professor Alison Smith for her valuable guidance, critical comments and suggestions of experiments, and for her great help for the writing of my research paper. The writing of this PhD thesis turned out to be very challenging; I am deeply grateful to her and my current supervisors at CropDesign NV (Gent, Belgium), Dr. Christophe Reuzeau and Dr. Wim Van Camp, for their patience, support and encouragement during its writing. I would like to thank Professor Alison Smith and Dr. Trevor Wang for reading and giving me comments on my thesis chapters. I also would like to thanks my advisor, Dr. Philip Wigge for interesting discussions and his advice during my PhD committee meetings.

Part of the work presented in this thesis has been published in the journal Plant Physiology (Vriet et al., 2010; Appendix 2). Many thanks go to my co-authors, and in particular to Dr Andreas Brachmann for his great help and contribution for the mapping of the forward screen mutations, to Tracey Welham, Jodie Pike, and Dr. Jillian Perry for their initial work on the isolation of starch metabolism mutants from forward genetic screen and TILLING, and to Shusei Sato for providing me with genome sequence information. I am also grateful to Tracey Welham and Marilyn Pike for doing the few last experiments needed for the re-submission of my manuscript.

I also would like to thank all the people at the John Innes Centre that helped on the realisation of this research project one way or another. Special thanks go to the horticultural staff for taking care of my plants, to Andrew Davis, for doing some of the imaging of my plants, and to Sue Bunnewell for making the microscopy sections. Many thanks also go to the European Commission for the funding (Marie Curie fellowship; EU EST Programme 019727).

Special thanks go to people of Dr. Trevor Wang and Professor Alison Smith's lab, and in particular to Dr. Lionel Hill, Dr. Jillian Perry, Dr. Fran Robson, Dr. Irmi Horst, Tracey Welham, and Baldeep Kular for their kindness, friendship, and for the many interesting discussions about science and beyond.

I own many thanks to my friends at JIC, especially Akiko Sugio, Alexandre Robert-Seilaniantz, Debora Gasperini, René Dreos, Victoria Nicholls, Clare Simpson, and Rita Lei

with whom I have had wonderful discussions at lunch times. My greatest thanks go to Akiko, Alex, Debora, and René for their wonderful kindness, great friendship and advice, and for their patience and perseverance in trying to improve my cooking skills. I am also forever grateful to them for dragging me out of the lab from time to time to go on wonderful trips in the nice Norfolk countryside, and for great dinners in restaurant or at their homes. It is where my best memories of my time in Norwich lie, thanks ever so much for all this! A very special thank go to Akiko and Alex for their touching and fantastic support and encouragements during difficult times. Thanks a lot as well to my friends from France, and in particular to Céline Leroy for keeping in touch.

At last but not least, I would like to thank my family, and in particular my parents, my two brothers, and my grand parents for their love, support, understanding, and for always being there when I needed some help or encouragements.

A very big thank you again to all the people mentioned above!

Cécile Vriet

Gent, Belgium
21 September 2010

CHAPTER 1

General Introduction

If I have seen further it is by standing on the shoulders of giants

Isaac Newton

CHAPTER 1: General Introduction

1.1. Carbohydrate metabolism in plants

Plants are photoautotrophic organisms that, together with bacteria, possess the ability to use the energy from sunlight to reduce carbon dioxide and other simple nutrients into all the primary and secondary metabolites required for growth and development. Plants can be divided into two functional parts with regard to this photosynthetic activity: sources and sinks (Sonnewald and Willmitzer, 1992). Sources are defined as the parts of the plant in which there is net fixation and reduction of carbon dioxide into assimilates, whereas sinks are the organs characterised by a net import of these molecules. Photosynthesis is principally active in mature mesophyll cells of the leaves (the sources), and the assimilates, primarily sucrose, are transported to developing organs such as roots, tubers, flowers, fruits or seeds (the sinks) where they are stored or immediately metabolised. This relationship between source and sink tissues/organs changes throughout the plant life cycle as the sink strength or the number of sink organs competing for the common pool of carbohydrates varies according to the developmental stage. In addition, this partitioning of carbon can also be influenced by environmental conditions either abiotic (e.g. atmospheric carbon dioxide concentration, temperature) or biotic (e.g. pathogen attack) (Wardlaw, 1990; Farrar and Williams, 1991; Herbers et al., 2000).

The sugars produced and exported through the plant are not only vital as substrates to sustain the metabolism of cells, they are also important signalling molecules. Indeed, sugar status is known to modulate carbon metabolism in response to changing environmental conditions, depending on the availability of other nutrients (Stitt and Krapp, 1999; Coruzzi and Bush, 2001; Coruzzi and Zhou, 2001). This ensures optimal synthesis and use of carbon and energy resources. Generally, a high level of sugars promotes growth and carbohydrate storage whereas a low sugar level enhances photosynthesis and reserve mobilization. In addition, soluble sugars have been postulated to act as regulatory molecules in many different developmental processes including the control of seed and embryo development, the formation of adult structures (e.g. leaves, tubers, roots, nodules), the induction of flowering, and leaf senescence (Bernier et al., 1993; Borisjuk et al., 2004; Gibson, 2005; Rolland et al., 2006; Wingler et al., 2006).

As well as partitioning assimilates between source and sink tissues and organs, almost all plants studied to date also perform another form of partitioning: the partitioning of the photoassimilates between sugars and starch.

1.2. Nature and importance of starch

1.2.1. Transitory and storage starch

There are two types of starch: transitory and storage starch. In source leaves during the day, a proportion of the products of photosynthesis are exported from the chloroplast to the cytosol where they are converted to sucrose. Concurrently, the remaining part of the photoassimilates is partitioned into starch within the chloroplast. This starch (referred as 'transitory starch' hereafter) is remobilized during the subsequent night and thereby provides a steady supply of carbon for export to sink tissues and to sustain growth and energy metabolism of the plant through the dark period (Zeeman and ap Rees, 1999). This conversion of starch to sucrose at night in plant leaves is one of the most important daily fluxes of carbon on earth, involving tens of millions of tons of carbon every night (Niittylä et al., 2004).

In contrast, storage starch is a medium- to long-term (from several days to several months) form of carbon store found in specialized plastids of non-photosynthetic tissues and organs such as seeds, roots and tubers. This starch is synthesised from imported photoassimilates (mainly sucrose), normally during a particular developmental phase (e.g. seed development), to be degraded during a subsequent phase (e.g. seed germination).

1.2.2. Starch granule composition and structure

Starch consists of two distinct homopolymers of glucose: amylopectin and amylose. Amylopectin is a highly branched polymer that contains α-1,4-linked glucose chains (glucans) connected by α-1,6 branch points whereas amylose, which is almost free of α-1,6 branch points, is essentially linear. These two polysaccharides are assembled together inside plastids to form the starch granule – a three dimensional semi-crystalline particle (Figure 1). This crystalline nature is associated with the highly organised architecture of the amylopectin component, and thus will vary according to the ratio of amylose and amylopectin. The structure of amylopectin is brought about by the non-random distribution of branch points, with regions of high-branch frequency alternating with regions devoid of branches, so as to enable neighbouring linear chains to align in parallel arrays of double helices. This conserved architecture allows the dense packaging of glucose units (Myers et al., 2000; Smith, 2001). Amylopectin accounts for 70% to more than 90% of the starch depending of the plant species and organs, the developmental stage of that organ and, to

some extent, the growth conditions of the plant (Martin and Smith, 1995; Zeeman et al., 2002).

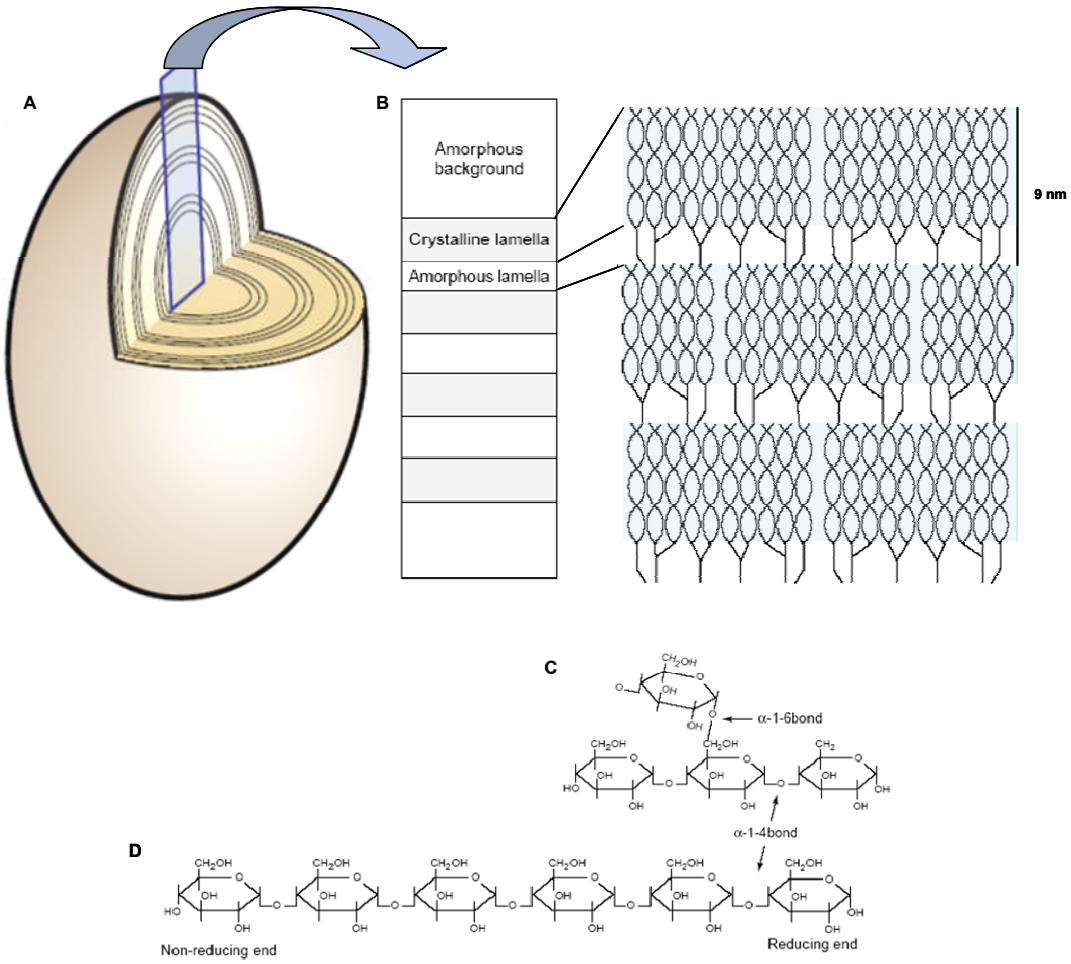

Figure 1. Starch granule structure and composition.
Modified from Jobling et al. (2004) and Teltow et al. (2006). **A**. Schematic representation of the starch granule structure composed of amorphous and semi-crystalline zones. Together, these two zones form a growth ring of several hundred nm across. The semi-crystalline zone consists of alternating crystalline and amorphous lamellae. The size of the starch granule varies from 1 to 100 μm in length, depending on the plant species and tissue. **B**. Enlargement of a growth ring showing the arrangement of the alternating crystalline and amorphous lamellae. The crystalline lamellae contains amylopectin molecules formed by chains of glucose units organized into clusters. Adjacent chains within a cluster form double helices that pack together in ordered arrays. The amorphous lamellae, high in α-1,6 branch points, contains amylopectin in a less ordered state together with amylose. **C** and **D**. Representation of the glycosyl bonds in amylopectin (C) and amylose (D). Amylose is essentially linear while amylopectin is highly branched with α-1,6 linkages.

Differences between transitory and storage starches are found in the structure of amylopectin (branch length distribution) and in the morphology and appearance of the starch granules (Tomlinson et al., 1997; Zeeman et al., 2002). Starch granules found in leaves are generally disc-shaped, and are usually smaller (1-10 μm) than those in storage organs (1-100 μm), probably because their synthesis usually occurs over a shorter period of time. The appreciable variation in the number, size, and morphology of the starch granules in the storage tissues of different species suggest that these characteristics are at least partially genetically determined. Lastly, the starch granule also contains small amounts of proteins, lipids and minerals (mainly phosphate), the amount of which is dependent on the botanical source (Martin and Smith, 1995).

1.2.3. Industrial and agronomic importance of starch

Starch is not only the most important carbohydrate reserve in plants, it is also a major component of the human diet (about half of the calories consumed by humans comes from starch). It is also an important raw material for many industrial processes in the food, textile, paper, and adhesives industries (Jobling, 2004), including the production of biodegradable plastics (Mooney, 2009). Importantly as well, starch is used as a source of energy, for the production of bioethanol (so-called first generation biofuel; Smith, 2008), or even hydrogen (Zhang et al., 2007).

In its native form, starch has a limited number of industrial uses, essentially as a thickener or binder. Upon heating in water, however, starch swells and increases in viscosity, to form a gel upon cooling. The composition and structure of the starch granules affects the properties and functionalities of starches. Amylose and amylopectin in particular differ dramatically in their physical characteristics (amyopectin forms pastes when heated in water, whereas amylose form gels). The ratio amylose:amylopectin therefore has an important impact on the applications of starch. Many treatments and chemical modifications, including cross-linking, cationisation, and partial hydrolysis, are often carried out after extraction to modify the functionality of starch, and increase its versatility. Some other modifications such as change in the amylose, amylopectin, and phosphate content, however, are often expensive and difficult to achieve *in vitro*. Since the desirable physical properties of starch vary considerably between plant species and organs, crop species used as a source of starch have long been selected for particular applications. For instance, tuber and root starch both have larger granules and lower protein and lipid contents than starches from cereal endosperms. Consequently, these starches form clear, bland pastes upon processing, and are excellent for food applications. Potato tuber starch, on top of that has a high content of phosphate, which coupled to the large size of its granules, gives it a very high swelling power (Jobling, 2004).

Yet, the vast majority of starch currently used by the industry is cereal starch because of its convenience for transport and storage.

Over the past two decades, the great progress made in understanding the metabolism of starch, and the isolation of many of the genes involved in the pathway, together with advances in the genetic modifications of crops, has made possible the production of novel starches with improved functionality *in planta*. For instance, mutation of the *Waxy* gene that encodes a Granule Bound Starch Synthase (GBSS; see section 1.3.1) leads to the production of amylose-free starch. Thus, in addition to *waxy* mutants of maize, barley, sorghum, and potato that have been known for years, *waxy* potato plants have recently been developed by genetic engineering (Amflora, BASF Plant Science) and are now commercially available. These amylose-free starches present many advantages for the food industry and paper manufacturer, in particular, as they yield clear and stables pastes, and have improved freeze-thaw stability compared to normal starches (Zheng et al., 1998; Jobling et al., 2002). High-amylose starches are also of great interest because of their high gelling strength, which makes them especially useful for sweets. High-amylose starches can also be processed into 'resistant starches' that have nutritional benefits (Bird et al., 2000). In plants, this high-amylose phenotype is caused by the inhibition of the activity of an enzyme involved in the synthesis of starch (Starch Branching Enzyme; see section 1.3.1). Other variations between species and organs that affect starch properties in ways valuable to industry include the branching of amylopectin, the phosphate content of the starch, and granule size and shape (Jobling et al., 2004).

Beside its use in industrial processes, starch plays a primary role in storage organs and tissues, many of which are of agronomic importance. High starch content is a desired trait for all the starch-rich seeds of cereal crops used as a major dietary source of energy for humans (for example, maize, rice, wheat, sorghum, and barley). Similarly, tuber and tuberous root starches are also very important agronomically (e.g. potato tubers and cassava roots), and an increased starch content in these tissues has already been successfully achieved by genetic modification (e.g. Ihemere et al., 2006).

1.2.4. Importance of starch in plant growth and development

As mentioned above, the role of transitory starch in many species is to provide the plant with a supply of carbon during the night, when photosynthesis cannot take place. Starch can also act as an overflow sink for newly assimilated carbon when the rate of assimilation exceeds the demand for sucrose (Caspar et al., 1985; Schulze et al., 1991; Ludewig et al., 1998). By acting as a buffering agent of the carbon balance of the plant, this transitory starch plays a central role in growth and development. Hence, *A. thaliana* mutants deficient in the

synthesis of starch (reduced-starch and starch-free mutants), or mutants with a reduced capacity to degrade it (starch-excess mutants) generally display a reduced rate of growth under many environmental conditions, especially when grown under short days (Caspar et al., 1985; Lin et al., 1988a and b; Caspar et al., 1991; Schulze et al., 1991). In wild-type (WT) plants, an artificial extension of the night beyond the normal end of day results in the depletion of starch in leaves, and in an abrupt reduction of the plant growth rate (Gibon et al., 2004). This impaired rate of growth in both the mutants severely altered in leaf starch metabolism, and in the WT plants submitted to extended dark periods, is accompanied by large transcriptional changes indicative of carbon starvation (Smith and Stitt, 2007; Usadel et al., 2008). Taken together, this strongly suggests that, at least in some species such as *A. thaliana*, the transitory storage of carbon as starch is essential for maintaining the metabolism and growth of the plant during the night.

In addition to this central role in plant growth, starch metabolism is involved in many development and environmentally-induced processes, including responses to pathogen attack and nutrient availability, acclimation to abiotic stresses (e.g. cold and drought stresses), senescence, and flowering (MacDonald et al., 1970; Chatterton and Silvius, 1981; Paul and Stitt, 1993; Martindale and Leegood, 1997; Corbesier et al., 1998; Schulze et al., 1991; Handford and Carr, 2007). Its importance in flowering initiation is revealed in several of the *A. thaliana* mutants that cannot accumulate starch to a normal level, or accumulate it in excess. In addition to the impaired rate of growth, such mutants usually display a delay in flowering independent of their slower rate of growth (Caspar et al., 1985; Eimert et al., 1995; Yu et al., 2000). Yu et al. (2000) hypothesized that this late floral initiation in the starch-deficient mutants could be directly caused by their lack of starch, which is normally degraded to provide the plant with soluble sugars that serve as a signal for the initiation of flowering. In agreement with this hypothesis, the late-flowering-phenotype of one of these mutants (*pgi1-1*; see section 1.3.1) could be reversed upon addition of soluble sugars (sucrose, fructose, or glucose) to the growth medium (Yu et al., 2000), therefore suggesting an important role played by carbohydrate metabolism in flowering time. As an alternative hypothesis, Eimert et al. (1995) suggested that starch accumulation and flowering may share a common pathway. The delayed flowering and increased starch accumulation phenotype of rice transgenic plants overexpressing the ethylene receptor ETR2 suggest that hormonal signals may also be involved (Wuriyanghan et al., 2009). Hence, the molecular mechanism responsible for this interaction between starch metabolism and flowering induction is likely to be complex.

Despite the importance of starch metabolism, our comprehension of how starch is degraded and the mechanisms underlying the regulation of its metabolism is still incomplete. Our understanding of the pathways of starch synthesis and degradation in leaves, however,

has dramatically improved over the past few years, especially from studies carried out in *A. thaliana*. In the next sections, I shall review our current knowledge of the metabolism of transitory starch in source leaves, and of storage starch in seeds, fruits, roots and tubers.

1.3. The metabolism of transitory starch in source leaves

1.3.1. The pathway of starch synthesis

1.3.1.1. The synthesis of ADP-glucose

In the light, photosynthetic CO_2 fixation in leaves drives, through the Calvin cycle, the synthesis of glyceraldehyde-3-phosphate (G3P). This molecule is used as precursor both for the synthesis of sucrose (that is further stored in the cytosol or exported to the rest of the plant), and for the synthesis of starch (Figure 2 and Figure A1). This synthesis of starch occurs entirely inside the chloroplast. In a first step, and still as part of the Calvin cycle, one molecule of G3P and one of dihydroxyacetone phosphate (DHAP) combine to produce fructose-1,6-bisphosphate, which is subsequently converted to fructose-6-phosphate (Fru6P). This reaction is catalysed by the enzymes aldolase and fructose-1,6-bisphosphatase.

The chloroplastic isoform of phosphoglucoisomerase (PGI, EC 5.3.1.9) is the first enzyme involved in the synthesis of starch beyond the Calvin cycle. This dimeric enzyme catalyzes the reversible isomerisation of Fru6P into glucose-6-phosphate (Glc6P) (Smith and Doolittle, 1992). In *A. thaliana*, mutants lacking this enzyme show a reduced level of starch in leaves, but still accumulate starch in heterotrophic tissues (e.g. seeds and root cap cells). Such mutants also display a delayed flowering time when grown in short day conditions (Yu et al., 2000).

The next step in the pathway of starch synthesis involves the plastidic phosphoglucomutase (PGM, EC 2.7.5.1), which catalyzes the conversion of Glc6P to glucose-1-phosphate (Glc1P). Importance of this enzyme for photosynthetic starch synthesis in chloroplasts is illustrated by the *A. thaliana pgm* mutant isolated from forward screens (Caspar et al., 1985). This mutant, which has a completely starch-free phenotype, has a reduced rate of photosynthesis, an impaired growth rate and a delayed flowering time when grown in short day conditions. This mutant is characterised by very high level of soluble sugars (sucrose, glucose and fructose) during the day (10-fold increase over the wild-type) but has very low sugar levels during the second part of the night. Futhermore, it also shows higher invertase and sucrose synthase activities, but lower AGPase activity (Caspar et al., 1985; Gibon et al., 2004; Blasing et al., 2005).

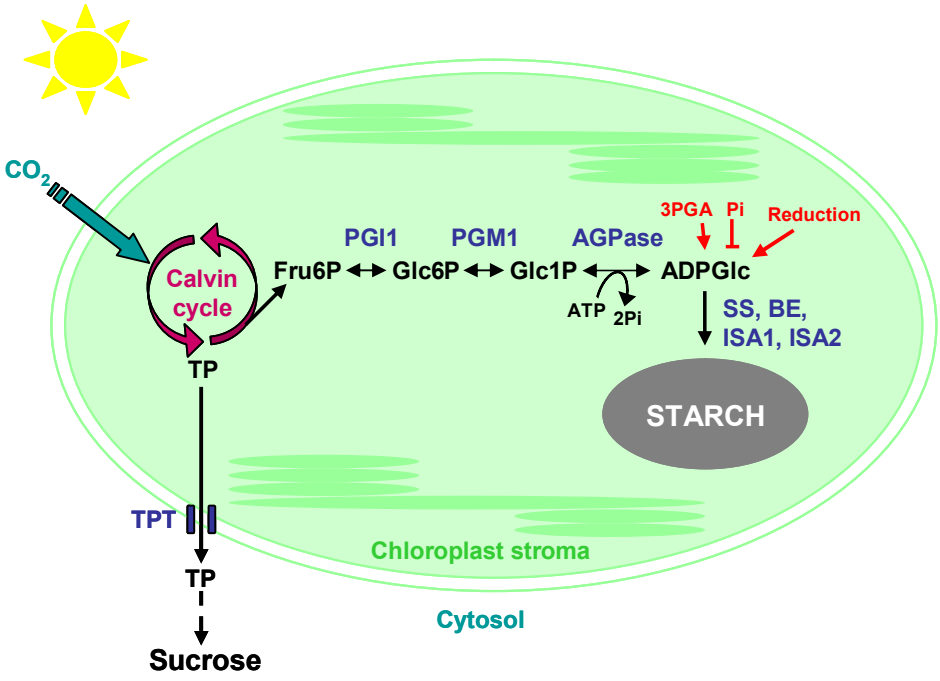

Figure 2. Proposed pathway of transitory starch synthesis in *A. thaliana*.
A fraction of the carbon assimilated via the Calvin cycle is exported to the cytosol for the synthesis of sucrose. The remaining fraction (about half of the newly assimilated carbon in *A. thaliana*) is used for starch synthesis within the chloroplast. This flux of carbon into starch is primarily controlled via the allosteric regulation (activation by 3PGA and inhibition by Pi) and redox-activation of the AGPase enzyme (in red). The core set of starch metabolic enzymes and transporters involved are in blue. Abbreviations: PGI1, phosphoglucoisomerase, plastidal isoform; PGM1, phosphoglucomutase, plastidial isoform; AGPase, ADPglucose pyrophosphorylase; SS, starch synthases (SS1, SS2, SS3, SS4, GBSS); BE, starch branching enzymes (SBE1, SBE2, SBE3); ISA1 and ISA2, isoamylases (debranching enzymes, DBE); TP, triose-phosphate; TPT, triose-phosphate transporter; 3PGA, 3-phosphoglycerate; Pi, inorganic phosphate.

Adenosine 5' diphosphate glucose (ADPGlc) pyrophosphorylase (AGPase, EC 2.7.7.27) is a key enzyme in the pathway of starch biosynthesis. This enzyme catalyses the synthesis of ADPGlc and PPi from Glc1P and ATP. This constitutes the first committed step of starch synthesis (Neuhaus et al., 1990; Kleczkowski et al., 1991; Green and Hannah, 1998). AGPase in higher plants is a heterotetramer ($\alpha 2\beta 2$) composed of two large (LS) and two small (SS) subunits (Anderson et al., 1990). The small subunit is responsible for the catalytic activity while the large subunit plays a regulatory function. This large subunit is sensitive to two allosteric effectors: 3-phosphoglycerate (3-PGA), acting as an activator and Pi, acting as an inhibitor (Sanwal et al., 1968; Ball and Preiss, 1994; Kleczkowski et al., 2000). Most plants possess one or two SS genes and several LS genes that are differentially expressed between different tissues and organs (Smithwhite and Preiss, 1992; Singh et al., 2002; Crevillen et al., 2005; Ohdan et al., 2005; Rosti et al., 2006; Lee et al., 2007). In addition to this tissue-specific pattern of expression, the different LS isoforms have been shown to

confer distinct kinetic and regulatory properties to the heterotetrameric enzyme (Crevillen et al., 2003). Such evidence suggests that heterotetramers are formed to respond to substrates and allosteric effectors in a way that is best suited to the particular metabolic demand of a given plant organ or tissue. In *A. thaliana*, four LS genes (*AtAPL1, AtAPL2, AtAPL3* and *AtAPL4*) and two SS genes (*AtAPS1, AtAPS2*) have been identified, of which one (*AtAPS2*) was found to be non-functional (Crevillen et al., 2003). The APS1/APL1 heterotetramer, the main AGPase isoform expressed in leaves, was found to have the highest affinity for substrates and sensitivity to allosteric effectors in comparison to AGPase containing the three other isoforms. These isoforms were mainly expressed in sink tissues (Crevillen et al., 2003 and 2005). Mutants lacking either APS1 (*adg1* mutant) or APL1 (*adg2* mutant) display a strong starchless phenotype in leaves (Lin et al., 1988a; Lin et al., 1988b).

1.3.1.2. Elongation and branching of the glucan chain

Starch synthases (SS, EC 2.4.1.21) are the enzymes responsible for the transfer of the glucosyl moiety of the soluble precursor ADPGlc to the non-reducing end of an α-1,4 glucan chain during starch synthesis. Plants possess multiple isoforms of SS that can be classified into two groups according to their conserved sequence and function. The first group of SS genes encodes isoforms primarily involved in the synthesis of amylose while the second group contains genes exclusively involved in amylopectin biosynthesis. Genes belonging to the first group encodes isoforms named granule-bound starch synthases (GBSS). In many species, *GBSSI* genes appear to be expressed mostly in storage organs whereas *GBSSII* genes are responsible for the synthesis of amylose in non-storage tissues such as leaves (Fujita and Taira, 1998; Nakamura et al., 1998; Vrinten and Nakamura, 2000; Edwards et al, 2002). The second group of SS genes, which is involved solely in the synthesis of amylopectin, encodes the isoforms SSI, SSII, SSIII and SSIV. Analyses of mutants lacking each of these isoforms suggest that they possess specific roles, each of them acting on the elongation of an amylopectin chain of a defined length. The synthesis of the shortest chain of glucan (10 glucosyl units or less) is achieved through the activity of SSI, while SSII preferentially elongates medium-length chains (12-24 glucosyl units), and SSIII, the longest chains (Commuri and Keeling, 2001; Zeeman et al., 2007a). Consistent with this model, the SSII and SSIII isoforms were shown to make distinct and synergetic contributions to the synthesis of amylopectin in potato plants (Edwards et al., 1999; Lloyd et al., 1999) although some overlapping functions between the two were recently found in *A. thaliana* (Zhang et al., 2008). In this species, SSIII was also shown to influence the rate of transitory starch synthesis (Zhang et al., 2005). In contrast to the three other SS single null mutants, plants lacking SSIV display a severely reduced growth rate with no modification in amylopectin structure or composition but a dramatic decrease in the number of starch granules and

increase in their size (Roldan et al., 2007). From these observations, the authors suggested that the SSIV isoform is involved in the priming of starch granule formation. This theory has further been supported by the finding that mutants lacking both SSIII and SSIV fail to initiate any starch granules and remain starchless (Szydlowski et al., 2009). Another SS gene, named SSV (At5g65685), has been identified in the genome of *A. thaliana* and other plant species. However, the function of the enzyme encoded by this gene is still unknown (Deschamps et al., 2008b).

In addition to the activity of the SS isoforms, the formation of amylopectin in the chloroplast requires the creation of branch points clustered at regular intervals on the glucan chains. These α-1,6 branch points are the result of the activity of the starch branching enzymes (BEs, also named SBEs; EC 2.4.1.18). The reaction involved is a glucanotransferase reaction which consists of the cleavage of internal α-1,4-linkages, and the transfer of glucan segments of six or more glucose residues to the same or a neighbouring chain of the amylopectin molecule (Borovsky et al., 1975). Higher plants contain multiple isoforms of BE that fall into two classes: class I (also named class B) and class II (also known as class A) based on their amino acid sequence (Burton et al., 1995). These two major classes of BE differ in the length of the glucan chain transferred and their substrate specificities: BEI proteins have a high affinity for amylose and preferentially transfer longer glucan chains than BEII. In contrast, their BEII counterparts preferentially branch amylopectin (Guan and Preiss, 1993; Takeda et al.., 1993). Three BE genes (BE1, BE2, BE3) have been identified in *A. thaliana.* Sequence comparisons indicate that BE2 and BE3 belong to the SBEII class, while BE1 is not related to the standard plant SBE class I or II (Dumez et al., 2006). This gene which has orthologs in rice and poplar has relatively recently been classified within a third class named SBEIII (Han et al., 2007). The down-regulation of BEI activity seems to have no or only minimal effect on the amount of starch synthesised and its composition in most plant species studied (Blauth et al., 2002; Satoh et al., 2003; Dumez et al., 2006). In contrast, a lack of BEII activity has been shown to reduce the branching frequency of amylopectin and its synthesis, resulting in an increased amylose to amylopectin ratio, both in photosynthetic and non-photosynthetic tissues (Bhattacharyya et al., 1990; Stinard et al., 1993; Jobling et al., 1999; Nishi et al., 2001; Dumez et al., 2006).

Debranching enzymes (DBEs, EC 3.2.1.41) have traditionally been associated with the pathway of starch degradation. However, evidence indicates that these enzymes also play a role in starch synthesis. DBEs fall into two groups in plants: isoamylase-type and pullulanase-type (also named limit-dextrinase; LDA). These enzymes hydrolyse α-1,6 linkages and β-limit dextrin. Three isoamylase-type proteins (ISA1, ISA2 and ISA3), and one pullulanase (LDA) exist in *A. thaliana*. The loss of either ISA1 or ISA2 activity results in the accumulation of water-soluble phytoglycogen instead of starch (Zeeman et al., 1998b;

Delatte et al., 2006a). Based on this observation, a model has been prosposed to explain the role of DBEs in starch synthesis. This model suggests that these enzymes play a 'clearing' role by removing the soluble glucans not attached to the starch granule so as to prevent the accumulation of phytoglycogen (Zeeman et al., 1998b). A second model has also emerged that rather proposes a 'glucan-trimming' activity for the DBEs. In this model, DBEs remove the branch points of amylopectin that could otherwise disturb the crystallisation of the starch granule (Ball et al., 1996; Myers et al., 2000).

1.3.2. The pathway of starch degradation

As discussed above (section 1.2.4), transitory starch is the main source of carbon to maintain growth and metabolism during the night in many plant species. The pathway of starch degradation (Figure 3 and Figure A1) that is relatively more complex than the pathway of starch synthesis can be divided into three main steps. The first one corresponds to the initial attack of the starch granule and involves a cycle of phosphorylation and dephosphorylation events at its surface. Subsequently, starch is hydrolysed into maltose, the major product of starch degradation, and to a lesser extent into glucose. Lastly, these products are then exported from the chloroplast to the cystosol where they are further metabolised.

1.3.2.1. Phosphorylation and initial hydrolytic attack on the intact starch granule

Several *A. thaliana* mutants with a starch-excess (sex) phenotype, in whose the starch content of leaves at the end of the night is higher than that of the wild-type plants, have been isolated from forward screens. One of them, designated *sex1*, has a drastic starch-excess phenotype in leaves associated with a strong reduction of phosphate content and increased amylose content (Caspar et al., 1991). This mutant also has elevated starch contents in flowers, seeds and root tips. Map-based cloning of the mutated gene in *sex1* (Yu et al., 2001) revealed that it encodes a glucan-water dikinase (EC 2.7.9.4), an enzyme located at the surface of the starch granule that transfers a β-phosphate group of ATP to a proportion of the glucose residues of amylopectin. This GWD1 enzyme (originally called R1 protein) had already been identified as a starch-bound protein essential for starch degradation in potato leaves and tuber (Lorberth et al., 1998). As in *A. thaliana*, mutant potato plants lacking GWD1 had a loss of phosphate groups covalently linked to the amylopectin fraction of starch and a starch-excess phenotype in leaves. In *A. thaliana* starch granules, approximately 1 in 2000 glucose residues carries a phosphate group (Yu et al., 2001). These phosphate groups were shown to be specifically transferred to the C6 position of glucose residues by the GWD1 enzyme (Ritte et al., 2006). The starch-excess phenotype of the *gwd1* (*sex1*)

mutants suggests that this phosphorylation of amylopectin by GWD1 is necessary for the initial attack on the starch granule. Consistent with this essential role for normal starch degradation, GWD1 was found to bind the surface of the starch granules at night only (Ritte et al., 2000). In addition, the phosphorylation of glucans on the surface of the starch granules was also higher at night than during the day (Ritte et al., 2004).

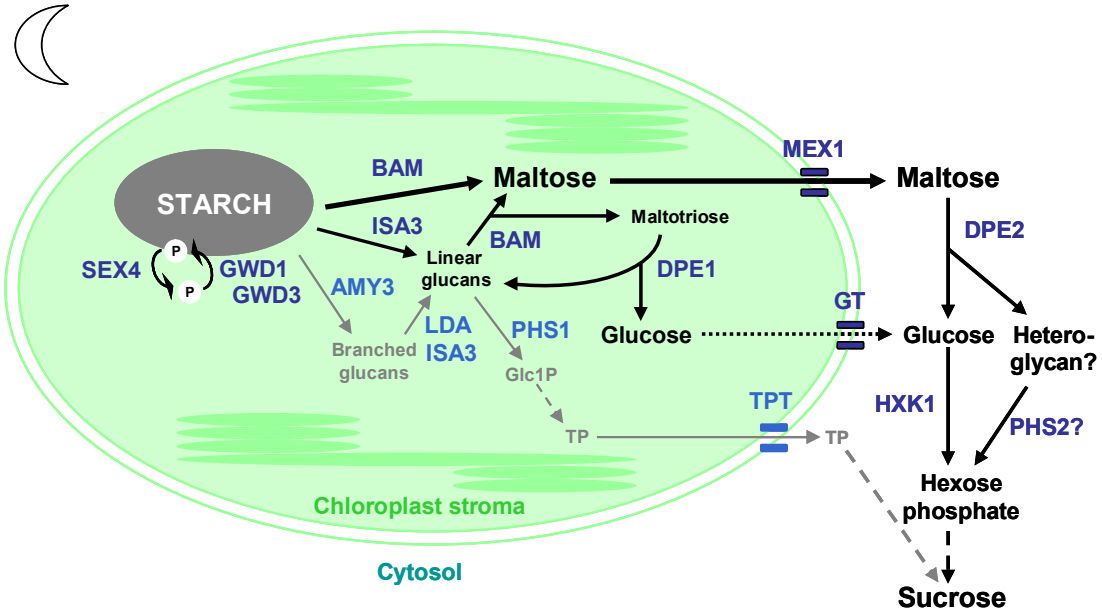

Figure 3 Proposed pathway of transitory starch degradation in A. thaliana.
During the night, starch is degraded to release maltose and glucose. First, phosphorylation by GWD1 and GWD3, and dephosphorylation by SEX4 occurs at the surface of the starch granule. This may allow the action of BAM and ISA3. This results in the release of maltose and linear glucans that can be further metabolised into maltose and glucose by BAM and DPE1. Loss of any of these enzymes reduces starch degradation and causes a starch excess phenotype. Alternatively, linear glucans can be degraded by PHS1 into Glc1P. The starch granule can also be attacked by AMY3 activity to release branched glucans that can be degraded by LDA and ISA3. Loss of PHS1, AMY3 or LDA, however, does not cause a starch excess phenotype suggesting that these reactions do not constitute the main pathway of starch degradation in *A. thaliana* (shown in grey and light blue). Next, maltose and glucose are exported from the chloroplast to the cytosol (via the transporters MEX1 and GT, respectively) to be further metabolised into hexose phosphates and sucrose by enzymes including DPE2, and possibly also PHS2. The sugar molecules would then be used to support the growth and energy metabolism of the plant during the dark period. Steps involving several enzymatic reactions for which the importance is not known are represented with broken arrows. The importance of the glucose transporter in starch degradation has yet to be established (dashed arrow). Abreviations: GWD1, glucan water dikinase 1; GWD3, glucan water dikinase 3, also named phosphoglucan, water dikinase (PWD); BAMs, beta-amylases (BAM3 and BAM4); ISA3, isoamylase (debranching enzyme); DPE1, disproportionating enzyme; AMY3, alpha-amylase 3; LDA, limit dextrinase (also called pullulanase: debranching enzyme); MEX1, maltose transporter; GT, glucose transporter; TPT, triose-phosphate transporter; DPE2, maltose transglucosidase; PHS1, glucan phosphorylase, plastidial isoform. PHS2, glucan phosphorylase, cytosolic isoform; HXK1, hexokinase 1.

A second starch phosphorylating enzyme that was identified in a starch-bound protein fraction (Kotting et al., 2005) was named phosphoglucan, water dikinase (PWD; also known as GWD3 and referred as such thereafter). In contrast to GWD1 that phosphorylates the glucose residues in C6 position, the GWD3 enzyme exclusively phosphorylates them in their C3 position. Importantly, this phosophorylation by GWD3 requires that the glucan substrate has been previously phosphorylated in C6 position. In other words, GWD3 acts downstream of GWD1 and is dependent on its prior action (Zeeman et al., 2007a and b). Loss of GWD3 activity also results in increased leaf starch content relative to the wild-type. This phenotype, however, is much less pronounced than in the *gwd1* mutant plants, at least in *A. thaliana* (Baunsgaard et al., 2005; Kotting et al., 2005). It is worth noting that another *GWD* gene has been identified in the genome of *A. thaliana* and other species (Glaring et al., 2007). However, the enzyme encoded by this gene (named *GWD2*) is not required for normal starch degradation, although capable of phosphorylating α-glucans *in vitro* (Glaring et al., 2007).

Recently, loss of a dual-specificity protein phosphatase (DSP4; also named PTPKIS1) was found to be responsible for the phenotype of another starch excess mutant: the *sex4* mutant of *A. thaliana* (Niittylä et al.., 2006; Sokolov et al., 2006). Like the *gwd1* and *gwd3* mutants, the starch-excess phenotype of *sex4* arises from impaired starch degradation at night. In addition, *sex4* mutants accumulate phosphorylated intermediates of starch degradation (Kotting et al., 2009). The authors also showed that the SEX4 protein is able to dephosphorylate the starch granule surface as well as soluble glucan chains. It is interesting to note that the ortholog of this enzyme in humans is a protein called Laforin that is implicated in the control of glycogen metabolism. Laforin deficiency results in the accumulation of aberrant glycogen particles (polyglucosans or lafora bodies) that leads to neuronal dysfunction and early death (Worby et al., 2006; Gentry et al., 2006 and 2007). Another putative chloroplastic phosphatase named LSF1 (for LIKE SEX4, previously PTPKIS2) may also be involved in this dephosphorylation of starch (Comparot-Moss et al., 2010).

1.3.2.2. Metabolism of branched and linear glucans, and production of maltose

As mentioned above, the class of enzymes involved in the degradation of leaf starch has been widely discussed. α-amylases (AMY; EC 3.2.1.1) and other endoamylases hydrolytically cleave α-1,4 linkages resulting in the production of a mixture of linear and branched malto-oligosaccharides (MOS). These enzymes were previously thought to be responsible for the initial attack of the starch granule in leaves as it is the case in the endosperm of germinating cereal seeds (cf section 1.4.2). However, evidence suggests that, in leaves, AMY activity does not have an important role in starch degradation, at least under normal growth conditions. The *A. thaliana* genome encodes three AMY proteins (AMY1, 2,

and 3) of which, only one, AMY3, is localised in the chloroplast (Zeeman et al., 1998a; Yu et al., 2005). Knock-out mutants of this plastidial α-amylase in *A. thaliana* showed normal rates of starch degradation (Smith et al., 2003). Starch metabolism was also normal in the triple mutant *amy1/amy2/amy3* (Yu et al., 2005).

Recent data from studies performed in *A. thaliana* and potato indicate that the starch granules are degraded by exo-amylolysis and debranching activities rather than by endo-amylolysis activity. This exo-amylolysis is carried out by a group of amylase named β-amylases (BAM; EC 3.2.1.2) which catalyze the removal of maltose units from the non-reducing end of α-glucan chains, while the debranching action is carried out by debranching enzymes (DBE). Loss of specific isoforms of BAM (BAM3 in *A. thaliana*; PCT-BMY in potato) and the DBE ISA3 in leaves from *A. thaliana* and potato results in reduced rates of starch degradation (Scheidig et al., 2002; Hussain et al., 2003; Wattebled et al., 2005; Delatte et al., 2006b; Fulton et al., 2008). *In vitro*, BAM3 and ISA3 recombinant proteins have a high level of activity on soluble glucans, but each shows very little capacity to degrade the starch granule (Scheidig et al., 2002; Hussain et al., 2003). However, the release of glucan increases when both enzymes are used in combination (Edner et al., 2007), suggesting that these two enzymes act synergistically. Indeed, as an exo-amylase, BAM can act only on the outer chains of the branched glucans to produce a surface of short chains on which it cannot act further. ISA3 activity is necessary to remove the branch points and uncover longer chains that BAM can then continue to hydrolyse. In agreement with this model, Delatte et al. (2006b) showed that short glucan chains accumulated on the granule surface of *A. thaliana isa3* mutants, probably because they were no longer efficiently removed by the debranching activity of ISA3. Further, *in vitro* hydrolysis of the starch granule surface by BAM3 and ISA3 was found to be enhanced upon the simultaneous phosphorylation and dephosphorylation of the glucan residues at the surface of the starch granule by GWD and SEX4 activities (Edner et al., 2007; Kotting et al., 2009). This observation has led to a model for starch degradation in leaves involving the synergistic action of GWD1, GWD3, SEX4, and the starch degrading enzymes BAM3 and ISA3 (Edner et al., 2007; Zeeman et al., 2007a and b; Kotting et al., 2009). In this model, the phosphorylation by GWD1 and GWD3 has been proposed to result in the uncoiling of the amylopectin double helices, thereby allowing the BAM and ISA enzymes to access the glucan chains. This hypothesis was supported by the fact GWD3-catalysed C3 phosphorylation disturbs the structure of the amylopectin molecule (Hansen et al., 2009). The removal of the phosphate groups by the action of SEX4 is also required since β-amylases cannot efficiently hydrolyse phosphorylated glucans (Edner et al., 2007).

The model described above places BAM3 and ISA3 as key players in the enzymatic hydrolysis of the starch granule in leaves of *A. thaliana* at night. Yet, it is possible that other

enzymes may also play a role in starch degradation and/or compensate at least partly for their functions when they are missing. Recent evidence shows that this is the case. Loss of the DBE limit dextrinase LDA (aka pullulanase, PU1) has no effect on the rate of starch degradation as observed in the *isa3* mutant (Wattebled et al., 2005; Delatte et al., 2006b). The *isa3/lda* double mutant however showed a greater reduction of starch content than the *isa3* mutant. This suggests that in the absence of ISA3, LDA is necessary for the degradation of starch (Delatte et al., 2006b). Furthermore, AMY activity was increased and soluble branched glucan accumulated during the night in the double mutant. Thus, it is likely that in the absence of ISA3, the degradation of starch occurs through the endo-amylolytic attack of AMY3 that provides soluble substrates for LDA (Delatte et al., 2006b). Although these two last enzymes are not essential for starch degradation under normal growth-room conditions, they could be important under specific conditions, for instance under exposure of the plant to stresses. Similarly, additional isoforms of BAM (out of the nine β-amylases enzymes encoded in the genome of *A. thaliana*, four are predicted to be chloroplastic) have recently been shown to participate in the degradation of starch under normal or stress conditions. Thus, BAM1 was found to play an overlapping role with BAM3 (Fulton et al., 2008). Suprisingly, *bam4* mutants also showed elevated levels of starch despite the BAM4 protein lacking β-amylase activity (Fulton et al., 2008). The authors suggested that BAM4 facilitates or regulates the degradation of starch upstream and independently of BAM1 and BAM3.

The result of the combined action of the enzymes mentioned above is the release of maltose and maltotriose from the starch granule. The maltotriose then released – too short to act as a substrate for BAM (Chapman et al., 1972) can further be degraded by this enzyme after action of another plastidial enzyme called disproportionating enzyme, or D-enzyme (also referred as DPE1; EC 2.4.1.25). This enzyme transfers two of the glycosyl units from maltotriose to another glucan chain (making them available for hydrolysis by the β-amylase) and releases a glucose molecule. This role is supported by the fact that knock-out mutants of DPE1 in *A. thaliana* show a reduced rate of starch degradation at night accompanied by accumulation of maltotriose and grow slower than the WT plants (Critchley et al., 2001).

Alpha-1,4 glycosyl bonds can be cleaved by starch phosphorylase (SP; EC 2.4.1.1) to produce Glc1P. Only one plastidial isoform of α-glucan starch phosphorylase has been predicted from the genome sequence of *A. thaliana*. This isoform referred as PHS1 could be responsible for the hydrolysis of linear glucan chains to glucosyl monomers but its role in starch degradation is still unclear. Under normal growth conditions, *A. thaliana* and potato plants lacking PHS1 do not display any impairment in starch degradation, suggesting that one or more isoforms of β-amylases rather than the plastidial starch phosphorylase plays an important role in this process (Sonnewald et al., 1995; Zeeman et al., 2004a). However, PHS1 could play a role under specific conditions. *phs1* mutant plants develop small lesions

on their leaves that are bordered by cells accumulating large amounts of starch, and are sensitive to any sudden drought and salt stress (Zeeman et al., 2004a and b). One possible explanation is that the loss of this enzyme activity could compromise the ability of the plant palisade and mesophyll cells to tolerate any transient water stress, leading to cell death. Under these stress conditions in WT plants, phosphorolysis could supply substrates for the plastidial oxidative pentose phosphate pathway that would generate reducing power required for the scavenging of reactive oxygen intermediates (Zeeman et al., 2004a and b).

1.3.2.3. Fate of maltose in the cytosol

According to the model presented above, the main products of starch degradation in the chloroplast in leaves are maltose, and to a lesser extent, glucose (Weise et al., 2004; Lu and Sharkey, 2006). To be further used for the metabolism of the cell and growth of the plant during the night, these products must be exported to the cytosol. Information about this export comes from studies performed on isolated chloroplasts from different species (Stitt and ap Rees, 1980; Stitt and Heldt, 1981; Kruger and ap Rees, 1983), and from the characterisation of chloroplast envelope glucose and maltose transporters: glucose can be exported through a glucose transporter (Schafer et al., 1977; Weber et al., 2000; Servaites et al., 2002) while the export of maltose is carried out by the maltose transporter MEX1. Evidence that this protein constitutes the major route by which maltose is exported in higher plants come from the analysis of the *A. thaliana* mutant lacking this protein (Niittylä et al., 2004). This mutant accumulates high levels of maltose inside the chloroplast during the night, and starch degradation is decreased (Niittylä et al., 2004; Lu et al., 2006). Once exported from the chloroplast, evidence suggests that the fate of maltose involves a transglucosidase termed DPE2. This enzyme transfers one of the glucose molecules of maltose to an, yet unknown, acceptor, releasing the other as free glucose. Mutants lacking DPE2 accumulate a very high level of maltose (Chia et al., 2004; Lu and Sharkey, 2004) like those lacking MEX1. It is likely that the free glucose molecule thus released from maltose by DPE2 is converted to hexose-phosphate by a hexokinase enzyme. The metabolism of the second glucosyl moiety from maltose remains to be discovered. It is possible to speculate that it is transferred to a cytosolic carbohydrate molecule (heteroglycan) which would be subsequently acted on to release free glucose or hexose-phosphate molecules (Fettke et al., 2009). A cytosolic isoform of the glucan phosphorylase (PHS2) has been proposed to be involved in this reaction (Smith et al., 2005).

1.4. The metabolism of storage starch in sink tissues and organs

1.4.1. Why distinguish the metabolism of storage and transitory starch?

Historically, the metabolism of storage starch, rather than transitory starch, was the subject of most, if not all, studies because of its ready availability as well as its economic and agronomic importance. Hence, the plants used for these studies were mostly important storage starch crops such as maize, rice, pea and potato. Only in the last decade has the metabolism of starch in leaves received increasing attention with the development of the model plant *A. thaliana* and the discovery of its primary importance to plant growth.

Transient starch is made within living cells, synthesised and mobilized on a daily basis in leaves. In contrast, storage starch constitutes a long term reserve of carbon synthesised in organs and tissues that can be structurally and metabolically very different from the leaves. As a result, the control and even the nature of the pathway is expected to be different between the two types of starch, and from one tissue or organ to another. Evidence shows that this is indeed the case (Zeeman et al., 2007). To start with, the first steps of the synthesis of transitory and storage starch are fundamentally different. As presented above, the starch synthesised in leaves is made from the photoassimilates coming from the Calvin cycle. In contrast, the synthesis of starch in non-photosynthetic organs and tissues requires the import of sucrose as first step. Catabolism of this sugar produces the substrates Glc-6-P and ATP. These are imported into the plastids from the cytosol via specific translocators of the plastid envelope (Neuhaus and Wagner, 2000). This differs from the synthesis of starch in leaves where the Glc-6-P and ATP are made photosynthetically within the plastid. Likewise, the degradation of starch also occurs differently depending on the organs and tissues, and the function it fullfills. Differences regarding the nature of the enzymatic pathway and its regulation are the subject of the following paragraphs, and of section 1.5.2.

1.4.2. Starch synthesis and degradation in cereal and legume seeds

The core pathway of starch synthesis in seeds (Figure 4) has been well characterised for all major cereal crops (maize, wheat, rice, and barley) and for pea. Detailed studies of the enzymes involved have revealed a similar scheme of starch formation to that in leaves. In pea, for instance, mutants affected in starch synthesis carry mutation at five loci that encode several of the enzymes involved in starch synthesis (branching enzyme, AGPase, plastidial isoform of PGM, and two starch synthases: *r, rb, rug3, rug5, and lam* mutants, respectively; Wang et al., 1998). Mutations at these loci lead to change in starch content and in polymer (amylose and amylopectin) composition, and alter the structure of the starch granule. Except for *lam*, all these mutations also alter the shape of the seed, from round to wrinkled

(Bogracheva et al., 1999). Some significant differences, however, exist between the pathway of transitory and storage starch synthesis, some of which are presented below.

First, starch synthesis in seeds requires the involvement of a sucrose synthase enzyme (also known as Susy) that converts sucrose and UDP into UDP-Glc and fructose. It is this UDP-Glc that, after conversion to into Glc6P, will be used for the synthesis of starch. A deficiency in Susy in developing maize endosperm (*shrunken1* mutant; Chourey et al., 1998) or pea embryo (*rug4* mutant; Craig et al., 1999) results in a reduced starch content.

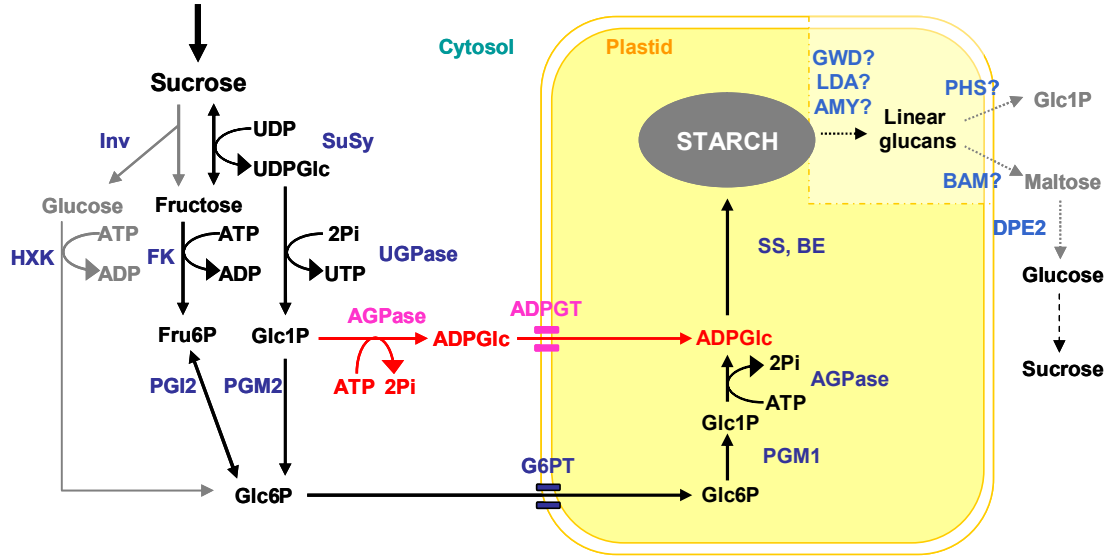

Figure 4. Proposed pathway of storage starch synthesis and degradation.
Susy plays a key role in this pathway by converting the sucrose coming from the source tissue of the plant into hexose phosphates. These Glc6P molecules would then be used for the synthesis of starch in the plastid. One exception to this is the existence in cereal endosperms of an alternative pathway. In this tissue, a cytosolic isoform of the AGPase enzyme produces ADPGlc that is transported from the cytosol to the amyloplast to be used for starch synthesis (reactions and proteins involved are shown in red and purple). In contrast to starch synthesis, the pathway of starch degradation in heterotrophic tissues and organs is still largely unknown. In germinating legume cotyledons, the amylopast membrane disintegrates so that starch degradation is catalysed by cytosolic enzymes. Evidence suggests that glucan phosphorylase plays an important role in this degradation. In germinating cereal endosperm, both the amyloplast envelope and the plasma membrane disintegrate. Degradation of starch in this non-living tissue is thought be hydrolytic (i.e. involvement of amylases) rather than phosphorolytic (i.e. via glucan phosphorylase). To date, almost nothing at all is known about the way starch is degraded in other storage organs such as potato tubers. Abbreviations for enzymes and transporters are: Susy, sucrose synthase; UGPase, UDP-glucose pyrophosphorylase; Inv, Invertase; HXK, hexokinase; PGM, phosphoglucomutase; FK, fructokinase; PGI, phosphoglucoisomerase; AGPase, ADP-glucose pyrophosphorylase; SS, starch synthase; BE, starch-branching enzyme; ADPGT, ADP-glucose/ADP transporter; G6PT, glucose-6-phosphate/phosphate transporter.

Another distinctive feature of the synthesis of storage starch in grasses (Poaceae or Gramineae, also known as cereals) is the involvement of a cystosolic isoform of the APGase enzyme in addition to the plastidial one. This is the case for instance in maize, barley, and wheat endosperms in which this cytosolic isoform accounts for 85 to 95% of the total AGPase activity depending of the species (Denyer et al., 1996b; Thorbjørnsen et al., 1996b). Evidence that this cytosolic isoform is essential for starch synthesis in the endosperm come from the study of two maize mutants: *shrunken2* (*sh2*) and *brittle2* (*bt2*) that carry mutations in the genes encoding the small and large subunit of AGPase, respectively. These mutants display a strong reduction of the level of starch accumulation in the endosperm that correlates well with the reduction seen in their AGPase activity (Giroux and Hannah, 1994). Further evidence for the importance of a cytosolic AGPase comes from the reduced starch and increased ADP-Glc contents found in the *brittle1* (*bt1*) mutant. BT1 encodes an amyloplast envelope protein thought to be an ADP-Glc transporter (Shannon et al., 1998; Kirchberger et al., 2007). Thus, grass endosperm cells possess two separate ways of providing ADP-Glc for starch synthesis: via the plastidial, or via the cytosolic AGPase. The emergence, conservation, and dominance of this endosperm-specific pathway (also referred to as the 'alternate pathway') through the grass family, and during the domestication of cereals, suggest that it has a selective advantage in this plant family (Comparot-Moss and Denyer; 2009). It has been hypothesised that the synthesis of ADP-Glc in the cytosol may enable the production of starch in a more energy-efficient manner than when it is synthesized in the plastid, by drawing upon the relatively abundant pool of ATP present in the cytosol, rather than the more limited plastidial pool of ATP (Comparot-Moss and Denyer, 2009).

Starch degradation in cereal seeds (Figure 4) has also been relatively well studied due to its social and economic importance; the sugars produced during germination can be fermented to alcohol. In this unusual tissue ─ the starch-containing cells die upon seed maturation ─ the complete degradation upon germination of starch requires the co-operative action of several hydrolytic enzymes (AMY, BAM, DBE, and α-glucosidase enzyme) that are also found in other non-photosynthetic storage organs, and in photosynthetic tissues (Fincher et al., 1989; Sun and Hanson, 1990; Sissons et al., 1994; Sissons and MacGregor, 1994). In contrast to leaves, however, it appears that in cereal endosperm, there is no cycle of phosphorylation and dephosphorylation involving the GWDs and SEX4 enzymes, nor any direct attack by BAM activity occuring. Rather, the attack on the starch granule seems to be exclusively catalysed by AMY (Fincher et al., 1989). Another important difference between these tissues is the final product of the degradation of starch: in cereal endosperm, the main product is glucose, whereas in living cells, the main products of starch degradation are sucrose and hexose phosphate. This difference affects the nature and control of the pathway:

starch degradation must be coordinated with metabolic demand in the same cell in a leaf but not in an endosperm

In contrast, starch degradation in legume seeds is not well studied. Nevertheless, evidence suggests that the degradation of this starch follows again a different scheme that may involve the action of starch phosphorylase following the endo-amylolytic attack of the starch granule (Juliano and Varner, 1969; Tarrago et al., 1976).

1.4.3. Starch synthesis and degradation in potato tubers and in roots

The mechanisms underlying the transport and unloading of photoassimilates and their subsequent use for starch synthesis in heterotrophic organs such as potato tubers (Figure 4) have been broadly studied, and are in general well characterised. As in seeds, Susy activity plays an important role for the synthesis of starch (positive correlation) in these organs as demonstrated by the study of susy-antisense potato tubers (Zrenner et al., 1995). Invertases perform the hydrolysis of sucrose into glucose and fructose in an irreversible manner. Interestingly, studies of these Susy-deficient plants revealed that the hydrolysis of sucrose by invertases cannot compensate for the loss of Susy (Zrenner et al., 1995).

In contrast to the conversion of sucrose to starch, the degradation of starch in these heterotrophic tissues, and its regulation is still largely unknown (Smith et al., 2005). Likewise, the metabolism (both synthesis and degradation) of starch in roots and other vegetative tissues has only been very poorly studied so far, and very little is know about the nature of the pathway and enzymes of starch synthesis and degradation active in these tissues.

As described above, the pathways of starch synthesis and degradation vary significantly between tissues and organs of plants. In addition to this, the metabolism of starch has also been found to vary considerably with plant species, and with environmental conditions thanks to a very tight, and yet highly flexible, regulation. This constitutes the subject of the next section.

1.5. Regulation of the metabolism of transitory and storage starch

As sessile organisms, plants are exposed to numerous stimuli in an environment which is in constant change (e.g. fluctuations in the availability of light, water and nutrients, or in pathogen attack). Facing this challenge, plant metabolism is highly flexible. This plasticity is of vital importance as it allows the plant to achieve environment-induced changes in

phenotypes and thus ensure its survival in the prevailing conditions. The accumulation and degradation of transitory starch is no exception to this as described below.

1.5.1. The regulation of starch synthesis and degradation in leaves

1.5.1.1. Regulation of the rate of starch synthesis and degradation

The synthesis of starch during the day in *A. thaliana* and many other plant species is clearly not a simple overflow for photoassimilates in surplus to the immediate demand for metabolism and growth. Rather, evidence shows that in these species enough starch is synthesized during the day to match the anticipated amount of carbohydrates that will be required during the following night. Hence, a change in daylength leads to a modification in the partitioning between sugars and starch with the rate of starch synthesis being inversely related to the length of the light period. In other words, *A. thaliana* plants growing under short day (SD) conditions would have a faster rate of starch accumulation than those growing under long day (LD) conditions. Moreover, the longer the night period, the greater is the proportion of carbon being partitioned into starch during the day. Thus, *A. thaliana* plants in a 6 h photoperiod accumulate 80% as much as starch as in a 12 h photoperiod (Gibon et al., 2004).

Similarly, the rate of starch degradation is also tightly controlled in *A. thaliana* and adjusted to the length of the photoperiod so that the rate of starch degradation at night in SD (i.e. long nights) is slower than in LD conditions. This ensures that a constant supply of sugars is available through the whole night (Smith and Stitt, 2007). Two different kinds of control of this degradation of starch could occur, firstly at the onset of the dark period, and secondly through the night. Starch degradation usually starts after a short delay following the transition from light to dark. Therefore, the depletion of sugars, rather than the absence of light, has been suggested to be the most important factor triggering the degradation of starch (Zeeman and ap Rees, 1999). Sugar signalling pathways could play a role in this process (Rolland et al., 2002; Moore et al., 2003). Following this short delay, starch degradation occurs at a remarkably constant rate throughout the night so that the starch reserves are almost completely depleted at the end of this period (Smith e al, 2005; Zeeman et al., 2007a). Notably, this linear degradation of starch was also observed in mutants that accumulated a reduced amount of starch due to reduction in AGPase activity (Lin et al., 1988). Further evidence that this regulation is not only tight but also very flexible comes from studies of plants submitted to abnormal changes in the length of the light and dark period. It was found that when plants entrained to a long day photoperiod were submitted to an early night halfway through the photoperiod, their rate of starch degradation slowed down. Conversely, plants entrained to short days exhibited an increased rate of starch degradation when the photoperiod was doubled in length (Lu et al., 2005). Similar

experiments were performed by Gibon et al., 2004 who showed that the adjustment of the degradation rate to the length of the photoperiod could be achieved within three days.

These remarkable adjustments show that, in *A. thaliana*, the synthesis and degradation of starch are closely coupled to the diurnal energy demand of the plant, itself dependent on the environmental conditions such as the length of day and night. The importance of this control for the plant carbon economy is reflected by the results of experiments in which plants were subjected to a further period of darkness at the end of a normal 12 h night. Under this condition, and within few hours, massive modification of the leaf transcriptome (up-regulation of the expression of genes involved in amino-acid, lipid, cell wall degradation, and many other classes, such as protein turnover and RNA metabolism) suggests that the plant is entering a carbon starvation mode (Thimm et al., 2004; Gibon et al., 2004). However, the mechanisms by which plants sense the amount of starch present at the end of the day, and are able to anticipate the length of the following night and fine-tune the rate of starch turnover accordingly so as to achieve optimal growth, remain largely unknown. Recent research (Graf et al., 2010) has shown that the circadian clock plays a central role in controlling this conversion of starch to sugars in leaves at night, and that failure to set the right rate of starch degradation leads to reduction in plant growth.

It must be mentioned, however, that the timing and pattern of starch degradation is likely to be different in plants growing under natural conditions than in controlled environments. For instance, in some species, the degradation of leaf starch can also occur at the start and end of the day when light levels are relatively low. Furthermore, starch degradation can also be induced during the photoperiod under conditions promoting high rates of photorespiration (Smith et al., 2005). This suggests that, under natural environments, the mechanisms controlling starch turnover are likely to respond to a wide range of complex inputs.

There is evidence that the accumulation and degradation of starch is controlled at the transcriptional and post-translational level, involving factors such as the level of light and metabolites. The possible or established influence of these different controls is presented below, first concerning the synthesis of starch, and then its degradation.

1.5.1.2. Regulation of the enzymes of starch synthesis: the example of AGPase

Flux control analyses have allowed the identification of the enzymes of starch synthesis that exercise the greatest degree of control in this pathway. Under low light conditions, most of the flux control resides in the reaction catalysed by AGPase. Under high light, the flux control is shared between several enzymes. 50% of the control is still exerted by AGPase while the remaining 50% is shared between PGI, PGM, and SBE (Neuhaus and Stitt, 1990). AGPase therefore exerts a considerable control over starch synthesis in leaves. Consequently, this enzyme has been extensively studied and a complex and high level of

regulation of its activity has been discovered. A summary of our current understanding of this regulation is presented below.

AGPase has been found to be regulated both at the transcriptional and post-translational level. At this second level, the modulation of the enzyme activity is of two types: allosteric and redox regulation. First, AGPase is allosterically regulated by two effectors with antagonistic actions: 3-phosphoglycerate (3-PGA), which leads to the activation of AGPase, and inorganic phosphate (Pi), that inhibits AGPase when its concentration increases (Ghosh and Preiss, 1966). Changes in 3-PGA and Pi contents are themselves controlled by the level of sucrose synthesis in the cytosol: during periods of active photosynthesis, the production of energy in the form of NADPH and ATP is high, resulting in an increase of chloroplastic 3-PGA and triose phosphate from CO_2 reduction, and a decline of chloroplastic Pi from the synthesis of ATP. At the same time, the transfer of 3-PGA and triose phosphates to the cytosol in exchange of Pi from the cytosol is enhanced. Reduced Pi and increased 3-PGA and triose phosphate in the cytosol activate the cytosolic fructose 1,6-bisphosphatase (FBPase) and sucrose phosphate synthase (SPS) enzymes, leading to increased sucrose synthesis. When the rate of photosynthesis is high relative to the demand for sucrose, the 3-PGA to Pi ratio in the chloroplast is also high and the AGPase enzyme is activated, resulting in increased ADP-Glc synthesis. Hence, the newly assimilated carbon will be preferentially directed toward starch synthesis under sucrose sufficiency conditions. Conversely, when the demand for sucrose is high, the ratio of 3-PGA to Pi in the chloroplast will be low. Thus, the AGPase enzyme activity will be inhibited, and the flux of carbon through the pathway of starch synthesis will be restricted so as to allow a greater synthesis of sugars (Trethewey and Smith, 2010).

Studies carried out in *A. thaliana*, potato and pea have revealed that AGPase is also redox regulated, and that this regulation is modulated by change in sugar level via two different sugar signalling pathways - either by sucrose, via a pathway dependent on the SNF1-related kinase SnRK1, or by glucose, via the involvement of hexokinase (HK) (Geigenberger et al., 2005). Another sugar, trehalose-6-phosphate (T6P) was also found to promote the post-translational redox activation of AGPase (Kolbe et al., 2005). Furthermore, the authors showed that this activation by T6P was modulated by cytosolic sucrose levels, and depended on the expression of SnRK1. In all cases, the activation of AGPase by redox modification (reduction of a disulfide bridge) is thought to be mediated by a thioredoxin enzyme. AGPase can also be redox-regulated via a light-dependant signal involving the action of a ferredoxin and thioredoxin reductase (Buchanan and Balmer, 2005).

Lastly, the highly responsive activation of the AGPase genes by sugar and light signals constitutes another level of regulation. Genes encoding the different isoforms of the large subunits and the small subunit of the enzyme were found to be strongly and differentially

regulated by sugar and light/dark exposures in leaves of *A. thaliana* and other plant species (Sokolov et al., 1998; Wingler et al., 2000; Hendriks et al., 2003). However, it is important to note that protein and enzyme activity level did not follow these rapid changes in gene expression (Sokolov et al., 1998)

The regulation of AGPase described above is the best characterised example of a regulatory mechanism implicated in the synthesis of starch. However, many other enzymes involved in carbon partitioning have also be found, or are likely to be subjected to similar regulation. Redox reactions, in particular, have been proposed to play an important role in the metabolism of plants by modifying the activity of numerous enzymes involved in carbon partitioning in response to light and sugars (Geigenberger et al., 2005). Similarly, SnRK1 and HK have been shown to play a role in the regulatory network that controls the expression and post-translational activation of several sugar- and starch-related enzymes (Smeekens et al., 2000).

1.5.1.3. Regulation of the enzymes of starch degradation

As for starch synthesis, several regulatory mechanisms act on the enzymes of the starch degradation pathway. Transcriptional and post-transcriptional controls as well as feedback inhibition or activation by metabolites may play a role in the control of flux through this pathway (Smith et al., 2005; Zeeman, et al., 2007).

Transcripts of several of the genes encoding starch- and maltose-metabolizing enzymes were found to be co-expressed and levels showed a strong diurnal rhythm (Smith et al., 2004). Expression of the genes *GWD1, GWD3, ISA3, AMY3, DPE1* and *PHS1* was shown to be under the control of the circadian clock (Harmer at al., 2000; Schaffer et al., 2001). Importantly, however, the amount of the corresponding proteins was found to be maintained relatively constant throughout the diurnal cycle (Yu et al., 2001, Smith et al., 2004; Lu et al., 2005). This lack of correspondence between transcript and enzyme levels highlights the complexity of starch metabolism and suggests that post-transcriptional and post-translational regulation is certainly more important in controlling the amounts of enzymes and their activities *in vivo* on a diurnal basis (Smith et al., 2004).

Post-translational control of the enzyme activities involved in starch degradation occurs at several levels. First, the level of metabolites of starch degradation could influence the rate of the degradation through feed-back regulation (Smith et al., 2005; Zeeman, et al., 2007). It was proposed that such mechanism may be responsible for the phenotype of the *A. thaliana dpe1*, *dpe2* and *mex1* mutants. Although the DPE1, DPE2 and MEX1 proteins are only involved downstream of the attack of the starch granule, their loss-of-function results in a reduced rate of starch degradation. Because these mutants accumulate abnormally high levels of maltose or maltotriose (Critchley et al., 2001; Chia et al., 2004; Lu and Sharkey,

2004; Nittylä et al., 2004) it is possible to speculate that these malto-oligosaccharides (MOS) may inhibit the enzymes directly involved in the hydrolysis of starch. Maltose for instance was shown to inhibit BAM activity at high concentration (Lizotte et al., 1990). Alternatively, these MOS could also compete with granular starch for the binding and activities of enzymes involved in starch degradation.

The redox activation of enzymes constitutes another mechanism implicated in the regulation of starch degradation. In contrast to starch synthesis, however, only a light-independent pathway could be responsible for the redox activation of the enzymes of starch degradation. In spinach, BAM was thus found to interact with a thioredoxin (Balmer et al., 2003), and it was hypothesized that this type of redox modulation could also apply for GWD1 and SEX4 (Mikkelsen et al., 2005; Sokolov et al., 2006).

Lastly, it is interesting to note that in *A. thaliana isa* mutants that accumulate soluble phytoglycogen instead of starch, the tight regulatory mechanism of the degradation does not take place, and the phytoglycogen reserves are depleted before the end of the night (Zeeman et al., 1998b; Delatte et al., 2005). This suggests that the controlled degradation of starch at night is dependent on the presence of granular starch and/or that the cycle of phosphorylation and dephosphorylation events taking place at the surface of the starch granule plays a major role in this control.

1.5.2. The regulation of storage starch metabolism

Surprisingly very little is known so far about the mechanisms involved in the regulation of the synthesis and turnover of storage starch in non-photosynthetic tissues compared to those of transitory starch metabolism. Some examples of the regulatory mechanisms involved, mainly from studies performed in potato tubers on the conversion of sucrose to starch, are presented here.

First, as for the synthesis of transitory starch in leaves, AGPase exerts an important level of control over the synthesis of storage starch in potato tubers and cereal seeds (Sweetlove et al., 1998 ; Giroux et al., 1996; Smidansky et al., 2002, 2003, and 2007). In addition, analyses performed in potato tuber suggested that in this storage organ, a large proportion of the control of starch synthesis resides outside the committed, linear pathway. Thus, antisense suppression of the amyloplastidial ATP translocator (sometimes referred to as the adenylate transporter) resulted in a strong reduction in starch synthesis in potato tubers. The control coefficient of this transporter that supplies the AGPase substrate ATP to the plastid was estimated to be 0.78 (Tjaden et al., 1998). SnRK1 has also been shown to exert an important external control over starch accumulation in potato tubers (Tiessen et al., 2003; McKibbin et al., 2006).

Since protein phosphorylation and dephosphorylation play a ubiquitous role in regulating cellular processes, protein kinases and phosphatases are also likely to be involved in the regulation of starch accumulation and degradation. Finally, evidence suggests that some of the enzymes of the starch metabolic pathway may work within complexes and that there are probably more interactions between enzymes than those already identified (Tetlow et al., 2004a and b).

1.6. Conservation and evolution of starch metabolism across the plant kingdom

Most living organisms accumulate either glycogen or starch as a carbon reserve. Both are made of glucose units. However, while glycogen is a polymer constituted of branched glucose chain lengths of uniform size distribution, the distribution of chain lengths in the amylopectin polymer of starch is polymodal. Of the two energy storage polymers, glycogen is the most widespread: it is found in archaea, bacteria and in most eukaryotes. In contrast, starch is restricted to plants and algae that are believed to be descendants of an endosymbiotic event involving a glycogen-synthesizing eukaryotic host cell, and a starch synthesising prokaryotic endosymbiont. This event introduced the plastid organelle into the eukaryotic cells and rendered them able to perform oxygenic photosynthesis. Most likely, the prokaryotic symbiont was an ancestor of the present-day group V cyanobacteria (Deschamps et al., 2008a). Indeed, whereas other bacteria synthesize glycogen, this group of cyanobacteria synthesize large, insoluble, polysaccharide granules resembling starch granules (Schneegurt et al., 1997; Nakamura et al., 2005). In contrast to glycogen, these starch-like granules are osmotically inert, and therefore could have presented the advantage of allowing the accumulation in the cell of the biopolymer in large amounts (Comparot-Moss and Denyer, 2009).

Three eukaryotic lineages are known to descend from the common eukaryotic ancestor that underwent the endosymbiosis event mentioned above: the Chloroplastida (land plants and green algae), the Rhodophyceae (red algae), and the Glaucophyta (freshwater algae having peptidoglycan-containing plastids known as cyanelles). Importantly, in plants and green algae, starch accumulates within the plastid, whereas organisms of the Glaucophyta and Rhodophyceae lineages accumulate starch in their cytosol. This cytosolic starch (also known as floridean starch) involves the use of UDP-Glc as substrate and is thought to be comprised purely of amylopectin (Yu et al., 2002). It has been shown that, despite the difference in the nature and location of the synthesis of starch between the Chloroplastida and red algae lineages, their starch synthesis pathways share a common origin and represent a chimera of the host and endosymbiont storage glucan synthesis (Patron and Keeling, 2005).

Genome analyses of many model and crop plants have revealed that the metabolism of starch is for large part conserved from the early photosynthetic organisms mentioned above to the higher plants we know today. However, many significant and interesting differences can be found from one plant species to another, some of which have already been mentioned in the previous sections. One notable difference, for instance, is the presence in the endosperms of grasses (e.g. maize, rice, wheat, barley, sorghum) of a cytosolic isoform of the AGPase enzyme in addition to the plastidial one (see section 1.4.2). This relative recent evolution of the cytosolic ADP-Glc synthesis is estimated to coincide with the evolution of monocots to grasses approximately 70 Mya (Comparot-Moss and Denyer; 2009). This contrasts with the conservation of the plastidial ADP-Glc synthesis which location in the symbiont/plastid most likely remained constant through the evolution of Chloroplastidida (Deschamps et al., 2008a).

The extent to which transitory starch accumulates in leaves and its importance in supplying carbon to the plant during the night differs dramatically between species. In some species starch constitutes a major form of storage whereas in others it can be viewed much more as an 'overflow' product of photosynthesis. In *A. thaliana*, where starch constitutes a source of carbon indispensable for the plant to avoid carbon starvation and growth arrest during the night, about half of the products of photosynthesis are partitioned into starch within the chloroplast (Zeeman et al., 1999). In this species, as well as in soybean, cotton, and tobacco, starch synthesis is 'constitutive', in that photoassimilates will be partitioned into starch even if there is still a demand for sucrose. However, alternative strategies exist in plants in relation to the importance and extent to which starch accumulates and is degraded. In pea and spinach, for instance, evidence suggests that the photoassimilates are channelled into starch only when the demand for sucrose synthesis is exceeded by the rate of photosynthesis. In this 'overflow' model, starch accumulates when the sucrose supply exceeds the capacity of the leaf cells to use and store it, and the demand from sink tissues (Zeeman and Rees, 1999). This difference in strategy of carbon partitioning is notably reflected in the phenotype of mutants altered in the synthesis of starch. Hence, for some species such as *A. thaliana* and tobacco, this starch is important for normal growth (Caspar et al., 1985; Lin et al., 1988a; Schulze et al., 1991; Huber and Hanson, 1992). In contrast, starchless mutants of pea, for instance, grow normally (Harrison et al., 2000), possibly because, in addition to starch, these plants also store sucrose in their leaves. Lastly, in many grasses, photoassimilates are used to produce sucrose and fructan both for export and to be stored in vacuoles, prior to being used as a supply of carbon during the night (Smith et al., 2005; Smith and Stitt, 2007).

In some species there may be significant variations in the metabolism of starch depending on developmental conditions. In tobacco, for instance, the diurnal pattern of starch turnover changes dramatically through leaf development. Thus, a strong diurnal turnover of starch

was observed in younger leaves whereas in older leaves much less of the starch was diurnally remobilized, and its level progressively increased. Subsequently, during senescence, all of the starch was degraded and the resulting products exported from the leaves before their abscission (Matheson et al., 1962 and 1963).

In addition to this, the predominant pathway of starch degradation (i.e. phosphorolytic versus hydrolytic) in the chloroplasts of source leaves may be species-dependent. In *A. thaliana*, starch degradation occurs mainly via hydrolysis. This assumption is supported by the 18:1 ratio of amylolytic to phosphorolytic activity, the fact that the phosphorylase activity in chloroplasts was estimated to be too low to sustain the rate of starch degradation (Lin et al., 1998c), and by more recent evidence from the study of knockout mutants showing that BAM activity is required for normal starch degradation, while PHS1 is not (see section 1.3.2 and reference therein). Moreover, the nature of the main products of transitory starch degradation, namely maltose and glucose (Servaites and Geiger, 2002; Weise et al., 2004) also favour this model. However, the situation may not be the same in other species. In pea, for instance, early studies suggested that starch degradation is mainly phosphorolytic. Indeed, pea chloroplasts do not contain significant activities of α-amylase or β-amylase, but do contain sufficient starch phosphorylase activity to mediate the observed rate of starch degradation (Stitt et al., 1978).

Remarkably little is known to date about the metabolism of starch in legume species other than pea, and its function in biological processes such as the accumulation of reserves in seeds, the fixation of atmospheric nitrogen via symbiosis with rhizobial bacteria, or perenniality and vegetative re-growth. These agronomically important traits are the subjects of the following paragraphs together with an introduction on the importance of legumes in agriculture and the species developed as model legumes.

1.7. Legumes and model legumes

1.7.1. The importance of legumes in agriculture

The legume family (Fabaceae or Leguminosae) is the third-largest family of flowering plants (Angiosperms), comprising approximately 700 genera and around 18 000 species (Doyle and Luckow, 2003). Legumes grow in a wide range of habitats and show extraordinary diversity (Doyle and Luckow, 2003). They possess many characteristics of agronomic importance, making them the second most agriculturally important group after the grass family. Firstly, legume seeds represent an important source of protein and oil both for human food and livestock feed. Major protein-rich legume crop seeds for human

consumption are common bean (*Phaseolus vulgaris*), chickpea (*Cicer arietimum*) and pea (*Pisum sativum*), while those grown for their high oil content are mainly soybean (*Glycine max*) and peanut (*Arachis hypogea*). Furthermore, legumes are also grown as forage crops for animal feed (Singh et al., 2007). This includes species like alfalfa (*Medicago sativa*), clover (*Trifolium pratense*), and bird's-foot trefoil (*Lotus corniculatus*). Hence, legumes comprise some of the most agriculturally important crops and account for about a third of the world's primary crop production (Graham and Vance, 2003). Moreover, legumes are also increasingly recognised as a source of valuable secondary compounds, some of which have health promoting effect (e.g. isoflavones; Dixon and Sumner, 2003). Lastly, because of their capacity for phosphorus and symbiotic nitrogen fixation (see section 1.8), legumes provide an opportunity to develop more sustainable agricultural systems by providing a free and renewable source of phosphate and nitrogen, thus reducing the need of fertilizers. Given their conservative strategy of growth, perennial legume crops are of current and potential agronomic importance for forage, grain production and the production of biofuels.

1.7.2. *Lotus japonicus* as model system

Although *A. thaliana* represents a powerful plant model because of its characteristics and the numerous tools and facilities developed for its analysis, it does not represent a suitable system for studying all physiological and developmental processes exhibited within the plant kingdom. This includes legume-specific processes such as the fixation of nitrogen via symbiosis with *rhizobia*.

Studies on legume genomics first focused on the species of agronomic importance (e.g. pea, bean and soybean). However, many of their characteristics (e.g. large genome size, tetraploidy, transformation and regeneration difficulties) limited the use of these species as experimental systems and pointed out the need for the development of a model legume plant. In fact, not one, but two legume species: *Lotus japonicus* and *Medicago truncatula* have been chosen and developed as model systems. Both species exhibit desired characteristics for genetic and genomic analyses, including a relatively small genome (450-500Mbp; only three to four times that of *A. thaliana*), a diploid and autogamous nature, as well as a relatively short generation time and a susceptibility to *Agrobacterium tumefaciens* (Kuchuk et al., 1990; Handberg and Stougaard, 1992). The impetus for the development of these two models was justified solely for the study of the rhizobium-legume symbiosis. Symbiotic nitrogen fixation by *rhizobia* in legumes take place in specialised organs called root nodules. Nodules of *L. japonicus* and *M. truncatula* represent the two classes of nodule ontogeny, determinate and indeterminate development, respectively (Brewin, 1991). In addition, the sequencing of these two legume genomes provides a unique opportunity for synteny comparisons (Cannon

et al., 2006; Sato and Tabata, 2006; Gepts et al., 2005; Young et al., 2005). These two model legumes have benefited, over the past few years, from the development of a wide range of genetic and genomics resources, a summary of which is presented below with a particular focus given on *L. japonicus*.

L. japonicus is a temperate perennial species native to Japan, Korea and China that belongs to the genus *Lotus.* This genus is large and extremely diverse (Figure 5), comprising about 200 species distributed worldwide (Arambarri, 2000a and b) and found in a broad range of habitats. Most of these species are grow in temperate regions although there are also subtropical and tropical species. These species have been divided into two classes according to their origin of diversity: the old world species that occurs in the Mediterranean region, including part of Europe, Africa and western Asia, and the new world species, native from western North America (Arambarri et al., 2000a and b). These species are highly polymorphic and vary for numerous genotypic traits (e.g. ploidy, number of chromosomes) and phenotypic characters such as growth habit (annuality versus perenniality), reproduction type (self-fertility), and flowering time. Among the genus *Lotus*, three species: *L. corniculatus* (broadleaf bird's-foot trefoil), *L. glaber* (also called *L. tenuis*, narrowleaf trefoil) and *L. uliginosus* (greater bird's-foot trefoil) are commonly used in agriculture for pasture and forage.

L. japonicus is a self-fertile, diploid species with a relatively small genome (472 Mb) consisting of six pairs of chromosomes (Jiang et al., 1997; Sato et al., 2008). Genomics in this species was initiated in 1999 with a collection of Expressed Sequence Tags (ESTs) and followed in 2000 by the start of the sequencing of its genome (ecotype Miyakojima, MG-20) using a whole-genome shotgun sequencing approach in combination with BAC end sequencing (Sato et al., 2008). To date, genome sequences of about 67% of the genome (315 Mb) likely to cover 93.1% of the gene space have been determined (Sato et al., 2008). Moreover, as of May 2009, a total of 192,409 *L. japonicus* ESTs derived from a variety of organs have been generated and clustered into 20,996 unique sequences (from DCFI Gene Index of *L. japonicus*; http://compbio.dfci.harvard.edu/tgi/plant.html). These ESTs have been used in several transcriptome analyses (Asamizu et al., 2004). Information generated by the *Lotus* genome and cDNA sequencing projects are available on public databases and at the following website: http://www.kazusa.jp/lotus/index.html. In addition to the accumulation of ESTs and genome sequences, research on *L. japonicus* also benefits from the development of a wide range of resources, including transcriptomic, metabolomic, and functional genomic tools (see section 4.1.3 for a detailed description of the functional genomic resources available, and the following publications for a review of all the 'omics' tools developed for legume research: Udvardi et al., 2005; Sato et al., 2006; Varshney et al., 2009). As for genetic analyses, three high-density genetic linkage maps have been

established, two are inter-specific linkage maps based on a *L. japonicus* x *L filicaulis* cross and a *L. japonicus* x *L burtii* cross, while the third is based on an intra-specific cross between the two most divergent accessions of *Lotus japonicus*: Gifu (B-129) and Miyakojima (MG-20) (Hayashi et al., 2001; Kawaguchi et al., 2001; Sandal et al., 2002).

Lastly, since *L. japonicus* has adapted to a variety of environmental conditions, it is thought to possess a broad range of genetic variation. This natural variation could be used to investigate potential traits of agronomic importance (e.g. plant height, seed yield, cold tolerance) by Quantitative Trait Locus (QTL) mapping. Thus far, 108 wild accessions of *L. japonicus* have been collected across the whole of the Japanese archipelago. A list of ecotypes with phenotypic data as well as information on location and climate are available from 'Legume base' (http://www.shigen.nig.ac.jp/lotusjaponicus/index_e.html). Available also for natural variation and QTL analysis are recombinant inbred lines (RILs) between Gifu and MG-20. These lines have already proved useful in several studies (Sandal et al., 2006; Gondo et al., 2007).

Figure 5. Illustration of the diversity of inflorescences in species of the genus Lotus.
Top row, right to left: *L. alpinus*, *L. berthelotii*, *L. nevadensis*. Middle row: *L. scoparius*, *L. oblongifolius*, *L. creticus*. Bottom row: *L formosissimus*, *L. corniculus*, *L. maritimus*, *L. uliginosus*.

1.8. Symbiotic nitrogen fixation

Nitrogen and phosphate availabilities constitute two major limitations to plant growth. In order to facilitate the uptake of these nutrients, many species have elaborated symbiotic interactions with microbial partners. Most legume species possess the capacity to form such interactions with two microbial partners: nitrogen-fixing rhizobial bacteria and phosphorus-fixing mycorrhizal fungi. It has been estimated than over 80% of all the land plants are able to form mycorrhizal symbiosis (Morgan et al., 2005), a symbiosis thought to be ancient (Oldroyd and Downie, 2004). In contrast, symbiotic nitrogen fixation with the gram-negative soil bacterium rhizobium has evolved more recently (Oldroyd and Downie, 2004) and is found in nearly all species (90%) belonging to the legume family. These two symbioses allow legumes to grow in soil low in phosphate and nitrogen without the need to add fertilizers, thus making them ideal crops for sustainable agriculture. In contrast, in well-fertilised soil in which nitrogen is readily available, these symbioses may reduce plant growth rather than promote it due to the high symbiont demand for carbon (Morgan et al., 2005). The nitrogen-fixing bacteria provide the plant with nitrogen in the form of ammonium, whereas the mychorrhizal fungus aids in the uptake of phosphate. In exchange, the host plant assures a supply of carbohydrate to the symbiont. Such processes involve complex interactions between the two symbiotic partners. The process of symbiotic nitrogen fixation in legumes is presented below.

The fixation of atmospheric nitrogen (N_2) consists in its reduction into ammonium (NH_4^+) by the nitrogenase enzyme complex which is found in *rhizobia*. The reaction catalyzed by the nitrogenase is as follow: N2 + 8 H+ + 8 e− + 16 ATP → 2 NH3 + H2 + 16 ADP + 16 Pi To fix the nitrogen, legumes plants have adapted to live in a symbiotic relationship, and a special root organ, the nodule, has evolved to allow nitrogenase function since this enzyme requires an environment very low in oxygen and very high in ATP. The generation of ATP, however, requires a high flux of oxygen. Nodules house the nitrogen-fixing *rhizobia* and surround them with an oxygen diffusion barrier as well as providing a high amount of oxygen which is bound to a protein called leghemoglobin. The establishment of this nitrogen-fixing symbiosis is a complex mechanism that requires a) the intracellular infection of the host plant cells by the bacterium, b) the development (organogenesis) of the nodules, and c) the fixation of nitrogen *per se*. As mentioned above (in section 1.7.2) two type of nodule organogenesis exist depending of the legume species: determinate (e.g. in *Lotus*, soybean, common bean) and indeterminate (e.g. in *Medicago*, pea, and clover).

First, signals between the *rhizobia* and the plant are needed in order to initiate the development of the nodules: flavonoid and isoflavonoid signalling molecules are released by the plant that attract the *rhizobia* on the plant root hair surface and induce the secretion of bacterial molecules (lipochitin oligosaccharides) known as Nod factors. The structure of

these Nod factors determines the host specificity (Morgan et al., 2005). Their recognition by the plant receptors allow the infection to occur. This step is known to involve a rapid influx and oscillation of Ca^{2+} in the cytosol of the root hair cells. This so-called Ca^{2+} spiking then leads to the cessation of tip growth, the curling of the root hair, and the formation of tubular structures: the infection threads, which allow penetration of the bacteria into the root tissue. At the same time, inner (in indeterminate nodules) or outer (in determinate) cortical cells are activated, de-differentiate, and divide. Their successive divisions lead to the formation of a nodule primordium. The infection threads grow towards the primordium, and when they reach it, *rhizobia* are released into the cytoplasm of their cells. These intracellular *rhizobia* differentiate into bacteroids. Simultaneously, a number of primordium cells generate a meristem. In determinate nodules, cell expansion of a transient meristematic region determines the nodule growth. In contrast, in indeterminate nodules, this meristem is persistent, allowing continued nodule growth. The resulting mature symbiotic organ is composed of different zones, along a differentiation gradient, and of a mix of uninfected and infected cells. The uninfected cells contain a large number of amyloplasts while the infected cells are densely packed with nitrogen-fixing bacteroids and contain small vacuoles (Imaizumi-Anraku et al., 1997; Hossain et al., 2006).

Nitrogen fixation is dependant of carbon supply to the bacteroids. Sucrose is transported from the shoot of the plant host to the infected cells of the nodules where it is further metabolised to furnish the bacteroids with decarboxylic acids (presumed to be malate) for their respiration, to fuel the reduction of nitrogen to ammonia by the nitrogenase enzymes, and provide carbon skeletons for the subsequent assimilation of ammonia into amino acids by the plant (Gordon et al., 1995; Galvez et al., 2005). Thus the net carbon flux from the plant's phloem tissue to the bacteroids results in a net nitrogen flux in the opposite direction, from the bacteroids to the xylem tissue of the plant (Schulze et al., 2004).

Because this nitrogen fixation process is so energetically expensive and consumes carbon, nodule formation only occurs when it is beneficial for the growth of the plant, under nitrogen-limiting conditions. Furthermore, not all plant cells are invaded by bacteria. This suggests that the plant is able to restrict the invasion by *rhizobia*. This process by which the plant avoids excessive nodulation and is able to inhibit the emergence of further nodules is called autoregulation of nodulation (Magori and Kawaguchi, 2009).

1.9. Legume seed development and filling

The success of germination and early plant growth is in large part determined by the physiological and biochemical characteristics of the mature seed. Of central importance for

this success are the reserves that are stored in the seed to be used as source of energy during the heterotrophic growth phase of germination and early seedling growth. In addition to their central position in the life cycle of higher plants, seeds such as those of grain legumes and cereals crops are major food sources. In cereal grains, the major storage tissue is the endosperm while in legumes seeds, the principal organs of reserves storage are the embryonic cotyledons.

The major components of legume seeds are proteins (referred to as storage proteins), carbohydrates (mainly starch), and lipids (often triacylglycerols). Their levels vary between species. The protein content in mature seeds of *Lotus* and soybean is about 40% of the dry weight (Gallardo et al., 2008; Dam et al, 2009) while the protein content in *Medicago* ranges between 30 and 40% depending of the genotypes (Djemel et al., 2005). Seeds of pea exhibit a lower protein content (about 20 to 25%). In this species, the major constituent is starch (accounting for up to 50% of the dry weight). The starch content in mature seeds of *Lotus*, soybean and *Medicago* is very low (less than 1%). This is because starch in seeds of these species is either not synthesised in large amounts, or is completely degraded during seed maturation, probably to provide carbon skeletons for the synthesis of other compounds (Gallardo et al., 2008). Lipids in *Lotus* constitute 7% of the mature seed dry weight while the lipid content in pea is between approximately 1.5 and 3%. In contrast, the lipid content in soybean can be higher than 20% (Dam et al., 2009).

Seed development and maturation in legumes consists of three different phases: histodifferentiation (or cell division phase; also referred as pre-storage phase), seed filling (or enlargement phase; also named storage phase), and desiccation. The histodifferentiation phase is characterised by cell division. Cell divisions are first confined to the endosperm and seed coat, and then concern the embryo. During the seed-filling phase, the growth of the embryo occurs by cell enlargement. This phase is associated with the synthesis and accumulation of reserves (Munier-Jolain and Salon, 2003).

During the pre-storage phase, nutrients coming from the phloem are downloaded into the seed-coat. A transient accumulation of protein and starch occurs in this tissue which controls the supply of nutrient to the embryo, thus regulating the cell division phase (Panitz et al., 1995). During this phase, high activities of seed-coat associated acid invertases play an important role by creating a high hexose environment that promotes the embryo cell division (Weber et al., 2005). Indeed, flow of sucrose from the phloem has been specifically implicated, and the acid invertase activity and hexose concentration in the apoplast have been shown to be positively correlated with the final cell number of the embryo (Munier-Jolain and Salon, 2003).

With the cessation of cell division, the embryo enters a transition phase during which it develops from a meristem-like structure into a highly differentiated storage organ.

Simultaneously, it also becomes green and photosynthetically active. As an adaptation to the low oxygen environment of the maturing embryos, respiration decreases and the energy state increases (Borisjuk et al., 2003 and 2004). This transition is accompanied by a switch from a hexose-based metabolism controlled by invertases, to a sucrose-based metabolism controlled by sucrose synthase activity (Weber et al., 1995; Sturm et al., 1999). This differentiation process is induced by the changing oxygen/energy conditions and by a high rate of sucrose transport into the embryo that also promotes storage activities (Rosche et al., 2002). Indeed, in seeds, as in other plant organs and tissues, sucrose has a dual function, both as a nutrient sugar and as a signalling molecule. In legume seeds, sucrose acts on transcriptional and post-translational levels to affect carbon fluxes and trigger storage-associated processes (Smeekens et al., 2000; Koch et al., 2004). Other factors including the hormone abscisic acid (ABA) and SnRK1 kinases have been shown to be involved in this regulatory network controlling seed differentiation (Weber et al., 2005).

During the storage phase, nutrients continue to be transported to the embryo where they are metabolised into storage compounds. Sucrose synthase activity is thus associated with starch synthesis in the embryo (Déjardin et al., 1997). Besides, sucrose regulates the activity of several enzymes involved in reserve accumulation. Notably, sucrose induces the up-regulation of the enzyme phosphoenolpyruvate carboxylase (PEPC; EC 4.1.1.31) whose activity correlates with seed protein content (Sugimoto et al., 1989; Rolletschek et al., 2004; Weber et al., 2005).

Proteins involved in cell division are abundant during the early stages of seed development. Their levels then decrease during seed filling, prior the accumulation of the major storage proteins (Gallardo et al., 2003). In legumes, the storage proteins consist for large part of globulins. There are two main groups of globulins that have been classified depending of their sedimentation coefficient: legumins and vicilins. Accumulation of these storage proteins is highly regulated by the supply of nutrients (Golombek et al., 2001). In addition, the energy state could also control the partitioning of assimilates into the different storage products. Energy demand is lowest for starch, intermediate for proteins, and highest for lipids. In *Vicia* embryos, for instance, protein accumulation is initiated in regions rich in ATP while starch is first detected in region with lower ATP content. This results in the pattern of starch accumulation being inversely oriented to that of the storage protein legumin during the transition phase (Borisjuk et al., 2003).

Seed development depends on interactions between the plant and the seed, and on interactions between the genotype and the environment of the plant. As presented above, the first phase (histodifferenciation) seems to be maternally controlled (Weber et al., 2005). Cell division rate varies according to the supply of carbon and nitrogen (Munier-Jolain and Salon, 2003). Evidence suggests that hormones and environmental factors may also play a role in

the control of this mitotic activity in the seed (Ozga et al., 2002). However, this first phase also seems to depend of the embryo genotype (Domoney et al., 2006). Switch from the maternal tissues to the filial tissues (embryo) control during the transition phase is marked by the initiation of a nutrient uptake system based on the formation of transfer cells, an increased sucrose uptake, and the generation of embryonic sink strength (Weber et al., 2005). Carbon supplied during the second phase (seed filling) seems to derive mainly from recent photosynthate rather than from remobilized carbon, while the supply of nitrogen to the seed depends both upon N_2 fixation and the retrieval of nitrogen from the soil (Domoney et al., 2006).

Attempts have been made to improve the nutritional quality of legume seeds because of their importance in our diet and that of other animals. For instance, an increase of seed protein content while maintaining seed yield is a target of pea breeding (Gallardo et al., 2008). Such a goal may be achieved by increasing nitrogen remobilization or uptake by the plant, or by modifying the embryonic control of nutrient uptake and metabolism. This strategy has already been employed with success, for example, in *Vicia* (Rolletschek et al., 2004). Seed-specific expression of a bacterial PEPC in this legume species induced a shift of metabolic fluxes from sugars and starch into organic acids and free amino acids that resulted in an increased protein content with no consequence on seed yield (the decreased number of seed per pod found in the transgenic plants was compensated by an increase in seed dry weight; Rolletschek et al., 2004). Furthermore, legume seeds also contain a certain number of undesirable and antinutritional components that are the target of research and breeding programs aiming at impoving their nutritional quality (Wang et al., 2003).

1.10. Perenniality and vegetative re-growth

1.10.1. Annuality *versus* Perenniality

Annual plants undergo their entire life cycle from seed to seed within a single growing season. That is to say, all the different part of the plant (roots, stems and leaves) die annually, and only the seed bridges the gap between one generation and the next. In contrast, plants that are able to persist for several growing seasons are called perennials. These plants go back to vegetative growth following seed production, and are able to grow back each year following overwintering, for instance, through the persistence of vegetative organs such as roots, rhizomes, stolons, or tubers. A third class of plants, which require two years to complete their life cycle, are called biennials. The flowering of these plants is delayed by a requirement for winter vernalisation. Both annual and biennial plants are monocarpic.

Monocarpic plants die following flowering and seed setting. They are often, but not necessarily short lived; there are also some monocarpic perennials. Most perennials, however, are polycarpic: flowering and seed production occurs many times during their life time, and over many years, interspersed by period of vegetative growth (Munné-Bosch, 2007). In addition, some plants can behave as an annual or a perennial depending of local climatic and geographic growth conditions. Lastly, perennial plants can be classified into three classes, depending on their growth habit: woody (trees and shrubs), creeping (strategy based on asexual, clonal reproduction), and herbaceous, which vegetative growth is thought to result from the activity of apical meristems sustained by nutrients accumulated in storage organs (Munné-Bosch, 2007). Discussion on the perenniality trait in the following section and elsewhere in the text concerns this third class of herbaceous, polycarpic perennial plant species versus their annual counterparts.

1.10.2. Majors determinants of perenniality

How perennials are able to undergo successive cycles of vegetative growth and flowering that are synchronized to the changing seasons has not been extensively studied and is not yet fully understood. In the past, meristem determinacy and programmed cell death have been suggested to be the two major determinants of perenniality (Thomas et al., 2000). The authors also suggested that this important difference between annual and perennial growth was likely to result from relatively minor changes in the relationship between genes involved in apical meristem determinacy on the one hand, and programmed senescence and cell death processes on the other, hence the proposed quantitative nature of this trait. In 2002, Battey and Tooke hypothesized that the transition to flowering and the molecular mechanism controlling it could be another determinant factor of perenniality. Their study highlighted several important points. First, that meristem determinacy is an important feature of flowering in many annual species. Conversely, in perennials, the ability to preserve active axillary meristems (ie meristem indeterminancy) past the reproduction period is crucial to the initatiation of another period of outgrowth (also termed post-sexual cycle re-growth; Lammer et al., 2004). Hence, failure to impose determinacy in annual species could be the basis for perennial growth. In addition, flowering and senescence processes are linked in annuals, the senescence being triggered by seed setting. Conversely, two keys features of perennial growth are the conservation of the vegetative meristem during and past the flowering phase, and the separation of flowering from senescence. Perennials also share two other features: a tendency for a delay between flower initiation and emergence, and the regulation of the duration of flowering (Battey and Tooke, 2002). Lastly, perennials also distinguish themselves from monocarpic annual plants by their ability to suspend growth

during a dormant period and then resume it, often seasonally, in reponse to change in environmental conditions (e.g. cold and daylength; Rohde and Bhalerao, 2007). Despite these important differences between annual and perennial species, Battey and Tooke (2002) suggested that the basis of flowering control could be similar between them, and that the life-form was likely to result from quantitative relationships between genes involved in vegetative growth, flowering and senescence. Such a hypothesis is supported by the fact that a switch between an annual and biennial strategy can be accounted for the expression level of a single gene involved in the control of flowering time (Michaels and Amasino, 2000). Further, the fact that either of the two strategies can be found among closely related plant species or varieties (e.g. in wheat; Cox et al., 2006) tends to support this idea that a change between these life forms might not require major genetic innovation.

This crucial importance of meristem determinacy and floral transition in determining the annual or perennial growth status of the plant has since been confirmed by three recent and very interesting studies in tomato and *A. thaliana* (Shalit et al., 2009; Melzer et al., 2008; Wang et al., 2009). Results of these studies showed that change in the expression of only a few genes involved in the control of flowering time was able to affect determinacy of all meristems, and confer phenotypes common to the polycarpic perennial lifestyle to a monocarpic annual species that included limitation of the duration of flowering, increased longevity, and even induction of secondary growth reminiscent of that found in woody perennial species.

Evidence suggests that the partitioning of the plant resources may also be an important determinant of the perenniality trait. In general, annual species and fast-growing species tend to maximize resource acquisition, whereas perennials and slow-growing species rather maximize the conservation of resources (Aerts and Chapin, 2000). This theory is supported by studies on leaves comparing annual with perennial species. Indeed, annuals are characterized by leaf traits that allow the acquisition of a high level of carbon while perennial species possess leaf characteristics linked to persistence and defence (Garnier and Laurent, 1994). Comparison of annual and perennial species also suggests that they differ in their senescence process, both in term of their intrinsic rate of leaf senescence, with perennials being less sensitive to senescence signals that closely-related annuals species (Thomas and Howarth, 2000), and at the whole-plant level (Munné-Bosch, 2008). Further, it may be hypothesised that the ability of the plants to store nutrient resources in perennial organs and remobilize them may also play an important role for their perennial lifestyle, especially in determining their capacity for vigorous re-growth.

Resources in annual plants are thought to be for the most part directed to reproduction, whereas in perennials, the resources are believed to be also directed to persistent, storage organs. Thus, the annual strategy can be explained as a way of increasing the number of

progeny surviving, since higher number of viable progeny is expected to be produced by a redistribution of the nutrients from the plant to the seed during senescence. This strategy may represent a long term advantage by allowing a higher rate of genetic diversity. Conversely, the perennial strategy may represent a more effective strategy, particularly in certain unfavourable and highly competitive environments where the plants have to compete with other organisms for space, light and a limited amount of nutrients. In such conditions, the fact that perennials re-grow from structures and resources that have survived through the winter may represents a benefit over their annual relatives as this strategy potentially allows them to become larger, stronger and thus more competitive from one year to the next.

1.11. Research objectives

The aim of this work was to increase our understanding of the metabolism of transitory and stored starch in legumes, and investigate its role in perenniality and re-growth, symbiotic nitrogen fixation, and seed development, three traits of agronomic importance in legumes. *L. japonicus* represents an excellent model to study this since it is a perennial and temperate legume species as well as a close relative of several species used as forage crops, and is able to nodulate. Furthermore, *L. japonicus* also benefits from the recent development of many genomic resources.

First, I have performed a series of bioinformatic analyses aiming at characterising the metabolism of starch in *L. japonicus*. These included detailed gene sequence, phylogenetic and gene expression analyses of the set of genes involved in starch synthesis and degradation in this species. In addition, I also carried out some biochemical assays designed to establish the diurnal pattern of starch accumulation and degradation in source leaves of MG-20 and Gifu, two ecotypes widely used for research in *L. japonicus*. I extended this analysis to other organs and tissues, and throughout development. Results of these analyses can be found in Chapter 3. In this chapter, the similarities and differences found between the pathway of starch metabolism in *A. thaliana* and in other plants species are also discussed.

Prior the start of this PhD research project, a collection of putative mutants altered in starch synthesis and degradation had been established using forward and reverse genetic screens on an EMS-mutagenised population of *L. japonicus*. In Chapter 4, I will present the isolation of these mutants, the identification of the mutations in the forward screened mutants, and the generation of additional mutants via TILLING. In the next Chapter (Chapter 5), I will describe the results of genetic, biochemical, and physiological analyses I performed on them. In particular, I will focus on the new information gained from the molecular and phenotyping

analysis of the mutants. This functional characterisation provided insights into the nature of the pathway and the importance of starch for several aspects of plant growth and development and symbiotic nitrogen fixation in *L. japonicus*. Results from structure-function relationship analysis of key enzymes of the starch metabolism pathway are also presented in this chapter.

I used both this collection of starch metabolism mutants together with a suite of natural genetic variants of the genus *Lotus* to test the hypothesis that the partitioning of carbon as starch in roots is important for vegetative re-growth in perennial species. Evidence gained from this analysis supports an important role played by root starch in determining the capacity of perennial *Lotus* plants to re-grow following cutting-back. Results of this analysis are presented in Chapter 6.

Finally, I will discuss the comprehensive and unique collection of *L. japonicus* starch metabolism mutants established in this study and how my work has contributed to a deeper understanding of the pathways of starch metabolism and its regulation, and the importance of carbon partitioning for growth and development in perennial, nitrogen-fixing legume species.

CHAPTER 2

Materials and Methods

Anyone who has never made a mistake has never tried anything new

Albert Einstein

CHAPTER 2: Materials and Methods

2.1. Plant material, rhizobial strain, and growth conditions

2.1.1. Plant ecotypes, species, and rhizobial strain

L. japonicus (Regel) K. Larsen accessions (aka ecotypes) Gifu (B-129) and Miyakojima (MG-20) were used as wild types (WT) for experimental analyses. All forward and reverse genetic mutants used in this study were generated in Gifu. Seeds of this accession were treated with ethylmethane-sulphonate (EMS) which resulted in a population of plants with random point mutations (Perry et al., 2003 and 2009). This population was used both for TILLING (Targeted Induced Local Lesions In Genomes; McCallum et al., 2000) and forward genetic screens. The rhizobium *Mesorhizobium loti Tono* strain was used to inoculate *L. japonicus* plants for acetylene reduction assays (see section 2.14).

Several species of the genus *Lotus*, were also used in this study. Seeds of the wild accessions and the RI lines were ordered from the NBRP (National BioResource Project; http://www.shigen.nig.ac.jp/bean/lotusjaponicus/top/top.jsp). Annual and perennial species of *Lotus* were kindly donated by the Germplasm Resource Information Network (GRIN; http://www.ars-grin.gov/) of the USDA/ARS (United States Department of Agriculture/Agriculture Research Service). A list of the plant species and ecotypes used in this study can be found in Table 1. For some experiments, plants of *Arabidopsis thaliana* ecotype Columbia (Col) were used as comparators. Some analyses were also performed on a set of annual and perennial species of *A. thaliana* obtained from TAIR (http://www.*A. thaliana*.org/; Table 1)

2.1.2. Crossing and plant generation used for analyses

Homozygous mutants in Gifu background, which had been selected from the EMS mutagenesis screen, were out-crossed, and then subsequently back-crossed at least once to the ecotype MG-20. These crosses needed to be carried out to reduce the number of background mutations generated by EMS, and eliminate their possible effects on the phenotype and establish a mapping population for the identification of the forward screen mutations. In a few cases where the results of rough mapping (see section 2.9.2) revealed that the mutations lay in a region of genome translocation between the two parents Gifu and MG-20 (Kawaguchi et al., 2005), *Lotus burtii* rather than MG-20 was used as crossing partner.

Table 1A

Scientific name and synonyms	USDA ID	Life form
Lotus angustissimus	PI 368894	annual
Lotus arabicus	PI 214109	annual
Lotus arenarius	PI 319020	annual
Lotus burtii	n/a	perennial
Lotus collinus	PI 641351	annual
Lotus conimbricensis	PI 308033	annual
Lotus corniculatus var. corniculatus (aka L. filicaulis)	PI 464684	perennial
Lotus denticulatus	PI 236862	annual
Lotus edulis	PI 244281	annual
Lotus gebelia	PI 464824	perennial
Lotus glinoides	PI 246736	annual
Lotus halophilus (aka L. pusillus)	PI 300237	annual
Lotus japonicus, ecotype B-129 (aka Gifu)	n/a	perennial
Lotus japonicus, ecotype MG-20 (aka Miyakogusa)	n/a	perennial
Lotus mearnsii	PI 226275	perennial
Lotus ornithopodioides	PI 442514	annual
Lotus palustris (aka L. lamprocarpus)	PI 311427	perennial
Lotus parviflorus (aka L. hispidus)	PI 415815	annual
Lotus peregrinus (aka L. carmeli)	PI 368905	annual
Lotus subbiflorus (aka L. hispidus)	PI 631785	annual
Lotus tenuis (aka L. glaber)	PI 302922	perennial
Lotus uliginosus (aka L. pedunculatus)	W6 20479	perennial
Lotus unifoliolatus (aka L. purshianus; L. americanus)	PI 338644	perennial
Lotus weilleri	PI 196332	annual

Table 1B

Species name	USDA ID	Life form
Medicago arabica	PI 495200	Perennial
Medicago cancellata	PI 440491	Annual
Medicago carstiensis	PI 641414	Annual
Medicago cretacea	PI 641510	Perennial
Medicago heyniana	PI 537136	Perennial
Medicago hybrida	PI 538998	Annual
Medicago marina	PI 516711	Annual
Medicago muricoleptis	PI 495401	Perennial
Medicago noeana	PI 495407	Perennial
Medicago papillosa	PI 464704	Annual
Medicago pironae	PI 253450	Annual
Medicago polymorpha var. polymorpha	PI 206695	Perennial
Medicago praecox	PI 495434	Perennial
Medicago prostrata	PI 577446	Annual
Medicago sativa subsp. falcata	PI 631682	Annual
Medicago sativa subsp. glomerata	PI 641405	Annual
Medicago sativa subsp. sativa	PI 536533	Annual
Medicago sauvagei	PI 499155	Perennial
Medicago saxatilis	W6 5898	Annual
Medicago secundiflora	PI 537238	Perennial
Medicago soleirolii	PI 537242	Perennial
Medicago suffruticosa	PI 304529	Annual
Medicago tenoreana	PI 499161	Perennial
Medicago truncatula	PI 384648	Perennial

Table 1C

Species name	NASC stock code	Life form
Arabidopsis arenosa (Care-1)	N3901	Perennial
Arabidopsis lyrata subsp. lyrata	N22696	Perennial
Arabidopsis lyrata subsp. petraea	N3219	Perennial
Arabidopsis suecica (Sue1)	N22505	Perennial
Arabidopsis halleri	N9852	Perennial
Arabidopsis thaliana, ecotype Columbia (Col0)	n/a	Annual
Arabidopsis thaliana, ecotype Landsberg erecta (Ler)	n/a	Annual
Arabidopsis korshinskyi (Olimarabidopsis cabulica)	N4653	Annual
Capsella rubella	N22697	Annual
Olimarabidopsis pumila	N3700	Annual

Table 1. List of *Lotus, Arabidopsis*, and *Medicago* species and ecotypes mentioned in this study. Continued on next page.

Table 1. List of *Lotus, Arabidopsis*, and *Medicago* species and ecotypes mentioned in this study. Continued.
Lotus and *Arabidopsis* species and ecotypes listed here were analysed in this study; *Medicago* species were selected for further analysis on the importance of carbon allocation for perenniality and re-growth. Seeds of all the species of the *Lotus* and *Medicago* genus (Table 1A and 1B, respectively) were ordered from the USDA GRIN germplasm (http://www.ars-grin.gov/) at the exception of *L. burtii* and *L. japonicus*, ecotype Gifu and MG-20 that were obtained from the John Innes Centre's germplasm collections. The life form information corresponds to the one given by the USDA database. Seeds of all the *Arabidopsis* species (Table 1C) were ordered from the TAIR database (http://www.*A. thaliana*.org/) at the exception of seeds of *Arabidopsis thaliana*, ecotypes Col0 and Ler that were from Alison Smith's laboratory (John Innes Centre). Information on the life form of these species was obtained from Al-Shehbaz and O'Kane (2002) and Clauss and Koch (2006).

Crossings were performed as described in Jiang and Gresshoff (1997), using the homozygous mutant as male parent (i.e. pollen donor; in Gifu background for first out-cross), and MG-20 WT as female parent unless otherwise indicated. When forward genetic mutants were crossed for the first time with MG-20 (referred to as out-cross, designed as B1), it was possible to confirm that the F1 plant resulted from a true cross by marker analysis. In case of the TILLING reverse genetic mutants, the hybrid nature of the F1, and therefore its heterozygosity for the mutation, could be confirmed by genotyping (see section 2.6.7). In both cases, seeds from crossed plants (B1F1) were collected, sown, and the corresponding F2 segregating population screened for the mutant phenotype. There were two possibilities: either the mutation responsible for the mutant phenotype was known (as for the mutants from TILLING, and the forward genetic mutants for which the mutation had been identified), or it was yet not known (uncharacterised mutants isolated from forward screens). In the first case (mutation known), the F2 population could be genotyped for the mutation as well as phenotyped, and homozygous and heterozygous plants for the mutant and WT alleles were isolated, self-fertilised, and their seeds (F3 generation) harvested. Both the homozygous mutants and their WT segregants (or their progeny) were used for most analyses, to allow more accurate mutant *versus* WT comparison. The number of background mutations will be similar between the two, as will be the genome background. Mutants were generally back-crossed several times (see Chapter 4). The same procedure was carried out for the subsequent crosses (referred to as back-crosses, designated B2, B3, etc). In contrast, when the back-crossings were performed on forward screen mutant lines for which the mutation of interest was unknown, the hybrid nature of the F1 could only be assessed by analyzing the phenotype of their progeny (i.e. segregation for mutant phenotype in the F2). In this case, only homozygous mutants - based on the phenotype – were kept and allowed to self-fertilize. The subsequent offspring (generally F3 or F4) were used for analysis with the two WT parents, MG-20 and Gifu as controls. The number of back-crosses and generation of the plants used in each experiment are stated in the text. Lastly, crosses between mutants of several of the mutant lines were also performed for complementation analyses, (aka allelism

tests) to determine whether mutations responsible for the phenotypes of independent mutant lines were carried by the same locus (no complementation will occurs and the F1 plants will show the mutant phenotype) or by different loci (the WT phenotype will be restored in the F1 plants).

2.1.3. Plant and bacteria growth conditions

Plants were grown with 12 h light, 12 h dark, or with 16 h light, 8 h dark either in a greenhouse or in a controlled environment chamber or room (CER) as stated in the text. In greenhouses, plants were grown with supplementary, artificial lighting (high pressure sodium lamps) with a minimum light level at 200 µmol quanta photosynthetically active radiation (PAR) $m^{-2}s^{-1}$ (supplemental lighting put for a period of 16 h, from 12 to 4 pm; from September until April) or without supplemental lighting (referred to as natural light conditions; from April until September). In the controlled environment chamber or room, the humidity was 75% and the day/night temperature 22 °C/18 °C. Light intensity was ca. 200 µmol quanta PAR $m^{-2}s^{-1}$ in the controlled environment room (CER), and ca. 100 µmol quanta PAR m^{-2} s^{-1} in growth chamber (SANYO MLR-350 and -351; SANYO E&E Europe B.V., Loughborough, UK).

For most experiments, and unless otherwise indicated in the text, plants were grown in F2 compost (Levington, Scotts Professional, Ipswich, UK). In a few cases, plants were grown in a mixture of perlite:vermiculite (1:1) to allow easier harvesting of the root samples. When this was the case, plants were fed twice a week with Hornum solution containing 5 mM NH4NO3, 3 mM KNO3 (Handberg and Stougaard, 1992). For most experiments, seeds were scarified with sand paper before sowing on compost. Once sown, seeds were covered with a clear plastic propagator top that was removed after full emergence of the cotyledons. For some experiments (for plant culture *in vitro*, germination capacity assay, or when resources of seeds of a particular genotype were limited), seeds were scarified, sterilized with 10% (v/v) bleach (containing 1% available chlorine), and incubated in sterile water overnight (ON) at 4 °C. These seeds were then germinated on water agar (15 $g.L^{-1}$ Difco bacto-agar) for three to seven days before transfer to compost or growth media.

Plants for acetylene reduction assay were transferred from compost to perlite:vermiculite (1:1 v/v) after seven to eight weeks of growth, and fed twice a week with nitrogen-free nutrient solution (Broughton and Dilworth, 1971). Roots of the plants were truncated at the time of transfer to stimulate lateral root formation and aid the production of nodules upon inoculation with *Mesorhizobium loti* strain *Tono*. These bacteria were grown on TY medium (5 $g.L^{-1}$ tryptone, 3 $g.L^{-1}$ yeast extract, 10 mM $CaCl_2$).

2.1.4. *In vitro* culture of pods

For *in vitro* culture of pods, peduncles carrying mature flowers were harvested, and the end of the peduncle immediately immersed in distilled water (dH_2O). Subsequent procedures were carried out under aseptic conditions. The entire peduncles were surface sterilized with 10% (v/v) bleach (containing 1% available chlorine), and then rinsed repeatedly in sterile water. The peduncles were re-cut at the end and inserted through a hole in the lid of a 50 mL tube filled with autoclaved Murashige and Skoog (MS) medium (micro and macro elements including vitamins, pH 5.8; Duchefa Bioechemie B.V., Haarlem, The Netherlands) with or without 3% (w/v) sucrose, then transferred to a growth chamber with 16 h light, 8 h dark for about four weeks.

2.2. Cutting-back experiments and biomass measurements

Cutting-back experiments were performed in order to mimic grazing and determine the capacity for vegetative re-growth of natural and induced variants of *Lotus* for root starch content. Unless otherwise indicated, these experiments were carried out on plants grown from seeds in F2 compost (Levington, Scotts Professional, Ipswich, UK).and the cutting back were performed on mature plants that were flowering and setting seeds. More details about the developmental stage of the plants and the environmental growth conditions under which they were grown for the cutting back experiments are given in the text and figure legends of chapter 6. The shoot and root fresh weight and ratio were measured by cutting off the shoot at 1 to 2 cm from the base of the stem. For plants that were allowed to re-grow, shoots and leaves present at the base of the stem were removed. Fresh weight measurements were performed immediately after harvest. The root system was weighed after being washed with water to remove soil, and then blotted on absorbent paper to remove excess water. Fresh weight measurements of the 'new shoot' and root after re-growth (generally six weeks post cutting) were performed the same way. For dry weight measurement, plant material was placed into a glass beaker and dried in an oven (Qualivac, LTE Scientific Ltd., Oldham, UK) for two to four days at 80 °C until the weight was constant.

2.3. Pollen viability and germination assays

2.3.1. Cytological observation of pollen grains

Pollen viability was assessed using two different dyes: 1% (w/v) acetocarmine (1 g acetocarmine in 100 mL 45% acetic acid), and fluorescein diacetate (FDA; 2 $\mu g.mL^{-1}$ FDA prepared by diluting 2 $mg.mL^{-1}$ stock solution (in acetone) in 0.4 M mannitol solution as described by Zhang et al. (2001) with a few minor modifications. In addition, pollen was also stained with iodine (Lugol's solution) to check the accumulation of starch (see section 2.4). Anthers were collected from flowers at anthesis and the pollen grains were released on a glass slide by gently squashing the anthers with fine forceps. Pollen grains were covered with the staining solution and a coverslip applied for observation under a microscope. Iodine and acetocarmine stained pollen grains were observed and photographed with a Zeiss Axioskop light microscope (Carl Zeiss Ltd., Welwyn Garden City, UK). Fluorescein stained pollen grains were examined and imaged with a Leica DM 6000 microscope using a fluorescent filter for green dyes (L5; exitation at 460-500 nm, and emission at 512-543 nm) and a DFC420 digital camera (Leica Microsystems Ltd., Milton Keynes, UK).

2.3.2. *In vitro* pollen germination assay

In vitro germination of pollen grains was performed as described by Nashilevitz et al. (2009) with some modifications. Flowers from at least three plants of each genotype were harvested at anthesis. Three anthers per flower were removed and placed into a microfuge tube containing 0.5 mL of germinating solution (10% sucrose, 2 mM boric acid, 2 mM calcium nitrate, 2 mM magnesium sulfate, and 1 mM potassium nitrate). After shaking to release the pollen grains, tubes were incubated at 25 °C for 24 h in the dark. Germination capacity was assessed at several time points by examining the germinating pollen grains under a light microscope (Zeiss Axioskop). Germinating pollen was also stained with acetocarmine, FDA, and iodine.

2.4. Iodine staining of plant tissues

Iodine staining was used to estimate the amount of starch present in different plant tissues and genotypes. With the exception of embryos and seeds, iodine staining of all plant tissues was performed as follows: pigments were removed by heating in 80% (v/v) ethanol for 30 min at 70 °C before letting the tissue decolorise in contact of natural or artificial light for several hours. When needed, several washes with 80% (v/v) ethanol were performed until the plant tissue became completely white. Tissues were then covered with iodine (Lugol's solution) generally for 10-20 min. Stained tissues were washed once with water to remove excess iodine prior to imaging. Stained tissues were observed with either a Leica MZ8

binocular or on a Zeiss Axioskop light microscope. Iodine staining of developing embryos and mature seeds differed from this protocol in that the pigments were removed by incubation in chloroform:ethanol:water (v:v:v; 5:5:1) prior to treatment with 80% ethanol.

Unless otherwise stated in the text, leaf samples of the mutant plants were harvested at the end of the light period for mutants defective in starch synthesis, and at the end of an extended dark period of up to 44 h for the mutants defective in starch degradation.

2.5. Microscopy of leaf starch granules

Sample embedding and sectioning for light microscopy (LM) and transmission electron microscopy (TEM) were carried out by Sue Bunnewell (JIC, Norwich, UK). For each genotype, one leaflet of a fully developed leaf from the top of plant was cut into pieces of about 0.5 cm^2, pooled with those of two other biological replicates, and placed in a fixation solution of 2.5% (v/v) glutaraldehyde in 0.05 M sodium cacodylate, pH 7.3. After vacuum infiltration, the fixative was washed out by three successive 10 min washes in 0.05 M sodium cacodylate before fixing in 1% (w/v) OsO_4 for 1 h at room temperature (RT). Samples were then washed three times for 10 min in dH_2O, and then submitted to dehydration series of ethanol solutions. Once dehydrated, the samples were gradually infiltrated with LR White resin (London Resin Company, Reading, Berkshire) by successive changes of resin:ethanol mixes over approximately 24 h at RT. Lastly, samples were transferred into gelatine capsules filled with resin, and allowed to polymerise for 16 h at 60 °C. Sections were prepared with a glass knife using a Reichert Ultramicrotome (Leica Microsystems).

For LM, 0.5 μm semi-thin sections were applied to glass slides, and stained with 0.5% (w/v) toluidine blue in 0.5% (w/v) borax solution. Sections were subsequently stained with a drop of Lugol's solution then covered with a cover slip for observation and imaging using either the Zeiss Axioskop light microscope or the Nikon Eclipse E800 fluorescent microscope (Nikon Precision Europe GmbH, Livingston, Scotland). Micrographs with this second microscope were captured with a Pixera Pro ES600 digital camera (Pixera Co., San Jose, USA). Ultrathin sections of between 95 to 100 nm for TEM were prepared from the same embedded material used to obtain the LM sections. These TEM sections were prepared and imaged by Sue Bunnewell (JIC, Norwich, UK).

2.6. General molecular methods

2.6.1. Isolation of DNA

Genomic DNA was extracted with phenol:chloroform as follows: a few young leaves were harvested on ice or dry ice in collection tubes (96-well plate, 1000 µL-well; Qiagen Ltd., Surrey, UK) containing a tungsten carbide bead (Qiagen). After addition of 400 µL of 200 mM Tris-HCl (pH 7.5), 250 mM NaCl, 25 mM EDTA, 0.5% w/v SDS pre-heated to 65 °C, they were homogenized in a mixer mill (Retsch MM300; Retsch GmbH, Haan, Germany) for 2 min at 30 oscillations s^{-1}. The rack was turned 180° and the grinding repeated. After a 60 min incubation at 65 °C, samples were centrifuged at 5000 g for 10 min and 300 µL of supernatants were treated with 200 µL of phenol:chloroform:isoamyalcohol (v:v:v; 25:24:1), pH 8.0. DNA was precipitated at -20 °C for at least 60 min with 220 µL isopropanol and 20 µL 3 M sodium acetate (NaAc), pH 5.2, before centrifugation at 5000 g for 45 min. The DNA pellet was washed with 200 µL 70% (v/v), air dried, and re-suspended in 10 to 50 µL of TE (10 mM Tris-HCl, pH 8.0; 0.1 mM EDTA, pH 8.0) or nuclease-free water at 4 °C for at least one hour. Samples of 1 µL were diluted 1:6 with 6X DNA loading dye (10 mM TrisHCl, pH 7.6; 60 mM EDTA, 60% glycerol; 0.03% (w/v) bromophenol blue, 0.03% (w/v) xylene cyanol) were subjected to electrophoresis on 1% agarose gels to check integrity and estimate concentration. In most cases, samples were also treated with RNAse. Five- to ten-fold dilutions were used for further experiments.

In some instances, DNA extraction for Polymerase Chain Reaction (PCR) was carried out using FTA cards. This was performed according to the manufacturer's instructions (Whatman Ltd., Kent, UK).

2.6.2. Isolation of RNA

Plant material was harvested and ground in liquid nitrogen using a pestle and mortar. Total RNA was extracted with CONCERT™ reagent (Invitrogen Ltd., Paisley, UK), and purified using the RNeasy kit Minikit™ with one-column DNAse I treatment (Qiagen) as described by the manufacturer. RNA was eluted with nuclease free water and the RNA content determined using a Picodrop™ spectrophotometer (Picodrop Ltd., Saffron Walden, UK). Absorbance was measured at 260 nm (nucleic acid) and 280 nm (protein) to access the purity of the samples with the calculated ratio A_{260}/A_{280}. A ratio between 1.8 and 2.1 indicates a high purity RNA. One µL of the RNA samples diluted 1:2 with 2X RNA loading dye (95% formamide (v/v); 0.5 mM EDTA; 0.05% (v/v) SDS; 0.025% (w/v) bromophenol blue; 0.025% (w/v) xylene cyanol) were also subjected to electrophoresis on 1% agarose gels to check RNA integrity.

2.6.3. Primer design

Gene-specific primers for PCR for genotyping, candidate gene sequencing, and RT-PCR analysis were designed using the Primer3 software (http://frodo.wi.mit.edu/cgi-bin/primer3/primer3_www.cgi; Rozen and Skaletsky, 2000) and the CODDLE program (Codons Optimized to Discover Deleterious Lesions; http://www.proweb.org/coddle/) to identify intronic and exonic region of genes. Primers were generally 20 bp in length, and with an annealing temperature close to 60 °C. Whenever possible, primers for RT-PCR were designed as intron-spanning so as to avoid non-specific gene - instead of/in addition to cDNA - amplification. Primers were ordered from Sigma-Genosys. A list of the primers used can be found in Table 2.

2.6.4. Polymerase Chain Reaction (PCR)

DNA amplifications by PCR were performed either using classical Taq polymerase (Amersham Biotech, Freiburg, Germany), or using the TaKaRA ExTaq™ polymerase kit (TAKARA Biotechnology Inc., Shiga, Japan). When the classical Taq polymerase was used, PCR was performed with a 10 µL reaction mix containing the template (genomic DNA, 1 ng-1 µg), 1X PCR Buffer, 0.2 mM dNTPs, and 0.5 U of the Taq polymerase. The PCR program used was as follows: an initial denaturation at 95 °C for 3 min: followed by 28-35 cycles of 94 °C, 1 min, annealing temperature, 1 min; 72 °C, 1 min/kb; and a final extension step at 72 °C for 10 min. Amplification with the TaKaRA ExTaq™ polymerase was performed according to the manufacturer's instructions. In both cases, the cycling conditions (number of cycles and extension time) were optimised for each primer pair, and using an annealing temperature about 5 °C below the melting temperature of the primers given by the supplier, Sigma-Genosys. PCR was performed using a MJ Research PTC-200 Peltier Thermal Cycler (MJ Research, Inc., Waltham, USA).

2.6.5. cDNA synthesis and semi-quantitative RT-PCR

Reverse transcription was performed with 5 µg of RNA using SuperScript II reverse transcriptase (Invitrogen) and oligo(dT)15 primers (Promega Ltd., Southamtpon, UK) according to the manufacturers' instructions. All samples were measured in technical triplicates on three biological triplicates consisting of leaf material harvested from three single plants and extracted individually. The housekeeping genes Ubiquitin 10 (UBQ10) and Elongation factor α (EFα) were used as reference genes (internal standards).

Table 2A

Gene	Primer name	Primer sequence 5'-3'	Position
PGI1	LjPGI1_1F	TGGTCAAAACCTGAAAACAAAACAC	-79
	LjPGI1_1R	TTCCAATTTCCATCCCAGTATTTCC	1118
	LjPGI1_2F	GGAATGAGTTTTGCTAAATGTTCTT	1311
	LjPGI1_2R	TCATCATTGCATAGTCATACAGAAA	2472
	LjPGI1_3F	GCTAAATTTTGACTCGCTCCCAATC	3484
	LjPGI1_3R	ATAGAGTCCATTAGGCTGGTTCAGA	3982
	LjPGI1_4F	ATTGTTGCTCAGGAGCCCTAGTTTC	4822
	LjPGI1_4R	AACTCATGCTTTCATGAGGATCCAG	5841
	LjPGI1_5F	CGAAGTCCATGATTATGCCACTAAA	6431
	LjPGI1_5R	CCAAAACAACTTATTGCAACCTGCT	6983
PGM1	LjPGM1_1F	GTGGCACCTGTGTTTCCTTT	-178
	LjPGM1_1R	TGCAATACAAAAGCCAGCAG	1407
	LjPGM1_2F	TGTTCAATTCATTGCCTCCA	1238
	LjPGM1_2R	CCTGGTGAGGAAGACCCTCT	2843
	LjPGM1_3F	CCCAGTTCATGGAAAATGAGA	2850
	LjPGM1_3R	TTGAATTCTTTCCTCTGTGGTG	4485
	LjPGM1_4F	AAACGGGCTCCTAGTGTTGA	5818
	LjPGM1_1634R	CATCTGCAAACTGGAGGACA	7315
	LjPGM1_1374F	TGACCACATTCGTGAGAAAGA	6463
	LjPGM1_4R	CGGGAACAGGTTGATTCACT	8257
APL1	LjAPL1_1F	CACACAGTGCTTCATGTGGA	-98
	LjAPL1_1R	CTGCCATAGAAACCCCAGAG	1401
	LjAPL1_2F	GGTGGTACCAGCTGTTTGGT	1188
	LjAPL1_2R	TTGCTTTCAGGTCTGCTCCT	2837
	LjAPL1_3F	GGAAAATTCGCACCTCAAAG	2635
	LjAPL1_3R	TGGACATCCAACCACATGAA	4356
	LjAPL1_4F	AAGCACCAAAGCCTTATTGG	4203
	LjAPL1_4R	GCGGCATTGGAATATCAAGA	5794
GWD1/SEX1	LjGWD1_6F	GGAGGGCAGATCTGGAATTT	-1349
	LjGWD1_6R	GAACAAACAGAATCCAATCAAAA	325
	LjGWD1_7F	GAGTGTCAGCAAAGGCAAGA	105
	LjGWD1_7R	CTCCCTCATCTTTTCCTGGT	1802
	LjGWD1_8F	AGGTCTCCTGAATTGACTGGA	1477
	LjGWD1_8R	TCAAATAAGCAAAAAGTGCAAAA	3466
	LjGWD1_9F	GAAAAAGCTGGGAAGCCTAA	3305
	LjGWD1_9R	TGGCTAGCTGGTTAGTGTGC	4993
	LjGWD1_10F	GAGAGGCATGGCAACAATCT	4801
	LjGWD1_10R	TCCAACCTTCAGTGTCCTCA	6233
	LjGWD1_11F	TCAGAAAGGTCCTGCAATCA	5699
	LjGWD1_11R	TGACAACAACCACCAACACC	6401
	LjGWD1_1F	TCTCTCCAGGCACTGATTGA	6033
	LjGWD1_1R	CGTAAGCTAAGGATCGCAAA	7523
	LjGWD1_2F	CAGTTTTCATGCCCTGGACT	8767
	LjGWD1_2R	TGGCATATCTGGTGTCAGGA	10401
	LjGWD1_3F	ACTTGACGTGCTTGCACCAT	11234
	LjGWD1_3R	TGAAAACTTCCCTGGATCAAA	12963
	LjGWD1_4F	TGTGTTCTCAAGCCCAGTTT	13551
	LjGWD1_4R	CTTCTCTTGTTCGCCAGGAT	15239
	LjGWD1_5F	TGCCCCCATTTTAATGTTGT	15569
	LjGWD1_5R	TCAAACACACAGATTCACCAAA	17133

Table 2. Primers used for gene sequencing, TILLING, genotyping, and RT-PCR analysis. Continued on next page.

Table 2A continued

Gene	Primer name	Primer sequence 5'-3'	Position
GWD3/PWD	LjGWD3_1F	CCGAATCAATCAATCGACAA	-128
	LjGWD3_1R	GATATCCGCGCATCAAAATC	1463
	LjGWD3_2F	CGCTTAAGCAAAGCCATGTA	1617
	LjGWD3_2R	CAACTCCTAAGTCATGTTCCACA	3077
	LjGWD3_3F	AATTCCACGCTCCAAATGTC	5733
	LjGWD3_3R	CCATGTTGAACTTGATTGATGG	7467
	LjGWD3_4F	TGCTCCATCTTGCAATAGTCT	8956
	LjGWD3_4R	ATGGACCAAGTGCCTCTGAA	14339
	LjGWD3_5F	TCAACAGACCCCTACACATGA	15920
	LjGWD3_6F	GTCGCCTTTGTAACGTGTGA	14899
	LjGWD3_6R	ATTCCGGACCTTGAACCTCT	16339
	LjGWD3_7F	GCTGTTCATTTGAAGGATGC	16061
	LjGWD3_7R	AGAGGTTCAAGGTCCGGAAT	16320
	LjGWD3_8F	CGTGCTTCCTCTATACCTCAGAA	17645

Table 2B

Gene	Primer name	Primer sequence 5'-3'	Position
PGM1	LjPGM1_TILL_2F(T2F)	GGTGCTCTGGATCGTGTTGCTGAA	6257
	LjPGM1_TILL_2R(T2R)	TCCAGAAAAACGGTGGGGAAACAA	7558
APL2	LjAPL2_TILL_1F	AAAGCAGACCCAAAAAGTGTGGCTTCC	358
	LjAPL2_TILL_1R	TGTCAACATGCTGCAAATTTTGGCAAT	1643
	LjAPL2_TILL_2F	TGAAGGCATGCCACTTGATTTTCTTGA	1320
	LjAPL2_TILL_2R	ATGCTGTGATGCAGGATAAGTGTGTGC	2817
APS1	LjAPS1_TILL_2F	GCATAGGCGGAACCAGGAAAAACC	698
	LjAPS1_TILL_2R	TCCAATGGAAGTTGCACCAGGAAT	1981
	LjAPS1_TILL_1F	TGCCCAGCAGAGTCCTGAGAATCC	1253
	LjAPS1_TILL_1R	GACGGAGGCAAATATCGTGGTTGG	2582
GWD1/SEX1	LjGWD1_TILL_1F	CAAAGTAGATCGTTCTTTCACCTTGACCA	9502
	LjGWD1_TILL_1R	ATGCTCATTTTCCTGGGAAGCAAACAC	10685
	LjGWD1_TILL 2F	GGAGGAATATGAAGCAGCTCGACAAGA	3124
	LjGWD1_TILL 2R	AGCCACATGCTTTGCCACAAAATTACA	4702
GWD3/PWD	LjGWD3_TILL_1F	AGAGGTTCAAGGTCCGGAAT	16320
	LjGWD3_TILL_1R	GGCAGTAGGGGTCAAACAAC	17825

Table 2C

Gene	Primer name	Primer sequence 5'-3'	Position
GWD3/PWD	LjGWD3_RT-PCR_1F	AGCCAGAAGAATGTGGTGCT	7729
	LjGWD3_RT-PCR_1R	TGCCATCTTCATTTCCTTCC	7886
	LjGWD3_RT-PCR_2F	TTGCTATGCGTCAAAAGTGG	6189
	LjGWD3_RT-PCR_2R	CTCCCAGCAGCTGTTACCTC	14725
EF-1α	EF-1α_TC14056_1F	GGACAGACTCGTGAGCACGCAC	n/a
	EF-1α_TC14056_1R	CAGGCTTCAAGACACCAGTTTCAAC	n/a

Table 2. Primers used for gene sequencing, TILLING, genotyping, and RT-PCR analysis. Continued. The position given for each primer sequence corresponds to the nucleotide position of its 5' end from the start codon of the gene. For sequencing of the candidate genes affected by the forward genetic screen mutations, primers were designed to cover the whole coding sequence. **A**. Primers for gene sequencing and genotyping in relation to mutations discovered in the forward genetic screen. **B**. Primers for gene sequencing and genotyping in relation to mutations isolated by TILLING. **C.** RT-PCR primers for GWD3 transcript expression analysis

2.6.6. Agarose gel electrophoresis

DNA, RNA, PCR and RT-PCR products (1-2 µL, diluted 1:2 with 2X loading dye) were subjected to electrophoresis on 0.5 to 2% TBE (Tris Borate EDTA; 1X TBE: 89 mM Tris, 89 mM Boric acid, 2 mM EDTA) or TAE (Tris Acetate EDTA; 40 mM Tris, 20 mM Acetate, 1 mM EDTA) agarose gels containing ethidium bromide (0.5 $\mu g.mL^{-1}$) depending on the nucleic acid nature and fragment size. PCR products generated were visualised and imaged under ultraviolet (UV) light using a Molecular Imager system and the Quantity One Analysis software from Biorad (Biorad Laboratories, Inc., Hercules, USA). DNA fragment size and quantity were estimated by comparison with a 100 bp or 1 kb Ladder (New England Biolabs Inc., Ipswich, USA).

2.6.7. Genotyping via DNA sequencing and restriction analysis

Genotyping of individual plants was carried out using gene-specific primers as listed in Table 2. PCR products for sequencing were generated as described in section 2.6.4, using the TaKaRA ExTaq™ polymerase (TAKARA Biotechnology). Following PCR, 1 to 2 µL of PCR product were added to 10 µL of sequencing reaction mix provided by the ABI PRISM™BigDye™Terminator v3.1 Cycle Sequencing Ready Reaction Kit, and the sequencing reaction performed according to the manufacturer's instructions (Applied Biosystems, Foster City, USA). Automated DNA sequencing was performed on an ABI PRIM™ 377XL DNA sequencer (Perkins Elmer, Connecticut, USA) by the DNA sequencing Service at the JIC Genome Laboratory. DNA sequences were analysed either using the Chromas software (Technelysium Ltd., Helensvale, Australia), or using the Vector NTI® software (Invitrogen)

In some cases, mutation genotyping could be carried out by restriction analysis relatively quickly, robustly, and at a lower cost than by sequencing. When this was the case, genotyping was performed by PCR followed by treatment of the PCR products with restriction enzymes (Table 3). Enzymes used for this restriction analysis were ordered from either Roche (F. Hoffmann-La Roche Ltd., UK) or NEB (New England Biolabs). Reactions were carried out according to the manufacturers' instructions in a 25 µL volume containing 15 µL of restriction mix to which 10 µL of PCR product were added. One µL of sample was then loaded on agarose gel to determine the genotype of the plant tested.

Table 3. Mutant allele genotyping by sequencing and restriction analysis. Continued on next page.

Mutations from forward screen

			Mutation		PCR		Sequencing		Restriction analysis			
Gene	Line	Allele	Nt change	Effect	Primer set	Prod. size (bp)	Primer	Mutation position	Enzyme	Mutant prod. size (bp)	WT prod.size (bp)	Hetero. Prod. size (bp)
PGI1	SL 4715-2	pgi1-1	C917T	Q200*	1F/1R	1198	1R	201				
	SL 4308-12	pgi1-2	G3602A	W360*	3F/3R	499	3R	380				
	SL 5069-2	pgi1-3	G5047A	Splice junction	4F/4R	1020	4F	225	AluI	171, **317**, 240, 292	**91**, 171, **226**, 240, 292	**91**, 171, **226**, 240, 292, **317**
PGM1	SL 4725-4	pgm1-4	G1233A	Splice junction	1F/1R	1586	1R	174	PstI	**1586**	**175, 1411**	**175, 1411, 1586**
	SL 4867-11	pgm1-5	G377A	G95D	1F/1R	1586	1F	555	KpnI	**1586**	**559, 1027**	**559, 1027, 1586**
APL1	SL 5127-5	apl1-1	C4408T	S400L	4F/4R	1592	4F	205				
GWD1	SL 5215-2	gwd1-1	G4633A	E566K	9F/9R	1689	9R	360				
	SL 5358-3	gwd1-1	G4633A	E566K	9F/9R	1689	9R	360				
GWD3	SL 5104-12	gwd3-1	G7871A	Splice junction	6F/6R	1490	6F	404	ScrFI	**219**, 239, 303, 729*	**100, 119**, 239, 303, 729*	**100**, **119**, **219**, 239, 303, 729*

* 729 bp-long restriction prod. in MG-20 replaced by 327+402bp-long restriction prod. in Gifu

Mutations from TILLING

			Mutation		PCR		Sequencing		Restriction analysis			
Gene	Line	Allele	Nt change	Effect	Primer set	Prod. size (bp)	Primer	Mutation position	Enzyme	Mutant product size (bp)	WT product size (bp)	Hetero. product size (bp)
PGM1	SL 4490-1	pgm1-1	G6413A	D436N	T2F/T2R	1302	T2F	156	FokI	**1302**	**169, 1133**	**169, 1133, 1302**
	SL 755-1	pgm1-2	G6848A	W467*	T2F/T2R	1302	T2F	591				
	SL 1837-1	pgm1-3	G6932A	W495*	T2F/T2R	1302	T2R	626	BsrI	132, 257, 299, **614**	132, **246**, 257, 299, **368**	132, **246**, 257, 299, **368**, **614**
APL2	SL 933-1	apl2-1	G1104A	D236N	1F/1R	1286	1R	539				
	SL 443-1	apl2-2	G1471A	G275E	1F/1R	1286	1R	172				
	SL 501-1	apl2-3	C2369T	P383S	2F/2R	1498	2R	448				
	SL 4318-1	apl2-4	G2453A	Splice junction	2F/2R	1498	2R	364				
APS1	SL 529-1	aps1-1	G1059A	A111T	2F/2R	1284	2F	361	FauI	**1284**	**351, 933**	**351, 933, 1284**
	SL 4504-1	aps1-2	G1129A	S134N	2F/2R	1284	2F	431				
	SL 5072-1	aps1-3	G2379A	A359T	1F/1R	1330	1R	203				
	SL 4723-1	aps1-4	C1077T	L117F	2F/2R	1284	2F	379				
GWD1	SL1833-1	gwd1-2	G3303A	W303*	TILL_2F/2R	1579	2F	179				
	SL3001-1	gwd1-3	G3994A	W456*	TILL_2F/2R	1579	2R	708	BsrI			
	SL4958-1	gwd1-4	G3491A	R324K	TILL_2F/2R	1579	2F	367				
	SL0176-1	gwd1-5	C4236T	P497L	TILL_2F/2R	1579	2R	466	FokI			
	SL5535-1	gwd1-6	G9912A	A968T	TILL_1F/1R	1183	1F	410				
GWD3	SL692-1	gwd3-2	G16648A	G890E	TILL 1F/1R	1506	1F	328				
	SL639-1	gwd3-3	G16918A	G980E	TILL 1F/1R	1506	1F	598				
	SL4648-1	gwd3-4	C17437T	P1153L	TILL 1F/1R	1506	1R	388				

Table 3. Mutant allele genotyping by sequencing and restriction analysis. Continued.
Variants identified by TILLING with silent mutation (i.e. mutation not causing an amino acid change or mutation located within intron) or amino acid change with a PSSM difference given by PARSESNP < 0 have been ignored here. Only enzymes that were used for restriction analysis in this study are mentioned here, together with their restriction profile in the mutant variant, WT and heterozygote. The column 'site' corresponds to the restriction site of the enzyme, with the following number code: (1) if gained in variant, and (2) if lost from reference. Expected restriction profile was obtained by submitting the sequence of the gene retrieved from the Miyakogusa database (http://www.kazusa.jp/lotus/index.html; Sato et al., 2008) to the NEB Cutter v2.0 tool available at http://tools.neb.com/NEBcutter2/.

2.7. *In silico* analyses of genes and proteins

2.7.1. Gene and protein sequence analyses

Prediction of genes and their corresponding cDNA and amino acid sequences was performed using the Genscan (http://genes.mit.edu/GENSCAN.html; Burge et al., 1997; 1998), FGENESH (http://linux1.softberry.com/berry.html), and GenomeScan (http://genes.mit.edu/genomescan.html; Yeh et al., 2001) programs. Gene structures (i.e. exonic and intronic regions) were determined using the CODDLE program.

Multiple DNA and protein sequence alignments were performed using the Clustal W2 program available at http://www.ebi.ac.uk/Tools/clustalw2/index.html. Defaults settings were used unless otherwise indicated. Percent of identity between sequences at the genomic DNA, cDNA, and amino acid level was determined using this program. Multiple sequence alignments generated by Clustal W2 were used to draw phylogenetic trees using Dendroscope (http://www-ab.informatik.uni-tuebingen.de/software/dendroscope). Editing and analyses of the protein sequences alignments were performed using GeneDoc (http://www.nrbsc.org/gfx/genedoc/). Subcellular localisation predictions of the proteins were obtained using the TargetP (http://www.cbs.dtu.dk/services/TargetP/) and Predotar (http://urgi.versailles.inra.fr/predotar/predotar.html) programs.

The Blastp tool at NCBI (http://www.ncbi.nlm.nih.gov/), and Pfam and PROSITE databases (http://pfam.sanger.ac.uk/; http://www.expasy.ch/prosite/) were used to search for protein motifs and functional domains. The CAZy (Carbohydrate-Active enZYmes) database (http://www.cazy.org/) was searched for proteins containing a Carbohydrate Binding Motif (CBM). Secondary structures of proteins were predicted using the JPred program (http://www.compbio.dundee.ac.uk/www-jpred/). Three-dimensional structures of proteins were retrieved from the RCSB Protein Data Bank (PDB; http://www.rcsb.org/pdb/home/home.do) and visualised using the VMD and Swiss PDB viewer software (http://www.ks.uiuc.edu/Research/vmd/, and http://spdbv.vital-it.ch/,

respectively). The Swiss PDB viewer software was also used for *in silico* mutagenesis. Trials of three dimensional amino acid structure predictions by homology modelling were performed using PHYRE (http://www.sbg.bio.ic.ac.uk/phyre/), the Swiss Model server (http://swissmodel.expasy.org/), and Geno3D http://geno3d-pbil.ibcp.fr/cgi-bin/geno3d_automat.pl?page=/GENO3D/geno3d_home.html.

2.7.2. Identification of the starch metabolism gene homologs in *L. japonicus*

Genes encoding known enzymes of starch metabolism in *L. japonicus* were identified by searching the Miyakogusa genome database developed by the Kasuza DNA Research Institute (http://www.kazusa.jp/lotus/index.html; Sato et al., 2008) using the gene names as keywords and by peforming a Blastp with the protein sequences of their *A. thaliana* homologs against *L. japonicus* genome sequences. Hits that included clones and Selected Genome Assembly (LjSGA) sequences were selected for further analyses. These included use of the Clustal W2 program for protein sequence alignment of homologs and other members of the same gene family. From this, it was possible to assign with confidence the orthologs of known starch metabolism genes of other species in *L. japonicus* and discover duplication events in several instances. Alignments also allowed identification of problems associated with incorrect annotations, incorrect predictions, or incomplete sequences for the *L. japonicus* genes and proteins. Where the coding sequence retrieved was incorrectly predicted or partial, it was used to search the database for the contig containing the corresponding genomic sequence. A predicted full length coding sequence was then obtained using the programs FGENESH, Genscan, and GenomeScan programs (see above for web address and related publications).

When homologs of known genes encoding enzymes of starch metabolism could not be identified in the *L. japonicus* genome database using the approach mentioned above, Blastn or tBlastn searches were performed against the LjEST database (DCFI Gene Index of *L. japonicus* (http://compbio.dfci.harvard.edu/tgi/plant.html). Where possible, a partial or full length coding sequence was obtained by aligning several EST clones and the resulting sequence was used to search the Miyakogusa genome database or to screen Transformation-competent Artificial Chromosome (TAC) and Bacterial Artificial Chromosome (BAC) libraries.

2.8. Analysis of gene expression data from microarrays

Affymetrix gene chip data were retrieved from the 'Lotus Gene Expression Atlas' assembled by Andry Andriankaja and Michael Udvardi (personal communication; Samuel Roberts Noble Foundation, Ardmore, Oklahoma). Organs analysed included leaves, stems, flowers, and nodules, as well as several samples of a time course for pods and seed development (Table 4). Plant growth and harvest conditions were similar to those used for the construction of the Medicago Gene Expression Atlas (Benedito *et al.*. 2008). The plant materials were harvested 3 hours after 'dawn' from plants grown under long day conditions. RNA isolation, probe preparation, array hybridisation and normalisation of the data were also carried out as described by Benedito *et al.*, 2008.

Organ	Description
Leaf	Trifolia without their petioles from 28 d old plants
Petiole	Petioles from 28 d old plants
Stem	Stems from 28 d old plants
Flower	Fully developed flowers
Root	Roots from 28 d old plants
Nod0d	N-starved roots at 0 dpi (control for nodules)
Nod21d	Mature N-fixing nodules at 21 dpi
Pod10d	Seed pod, 10 dap (late embryogenesis)
Pod14d	Seed pod, 14 dap (accumulation of storage compounds)
Pod20d	Seed pod, 20 dap (mature seed, onset of dessication)
Seed10d	Developing seeds, 10 dap (late embryogenesis)
Seed12d	Developing seeds, 12 dap (transition between embryogenesis and seed filling)
Seed14d	Developing seeds, 14 dap (accumulation of storage compounds)
Seed16d	Developing seeds, 16 dap (accumulation of storage compounds)
Seed20d	Developing seeds, 10 dap (physiologically mature seeds, onset of dessication)

Table 4. Description of the organs analysed using the Lotus Gene Expression Atlas.
Microarray data (Affymetrix) for the *L. japonicus* Gene Expression Atlas were generated by Andry Andriankaja and Michael Udvardi (personal communication; Samuel Roberts Noble Foundation, Ardmore, Oklahoma). Abbreviations: d, days; dpi, days post inoculation; dap, days after pollination.

Data available from the 'Lotus Gene Expression Atlas' corresponded to absolute, normalised transcript levels. Normalization was performed by the authors as described in Benedito et al. (2008). These data were processed into an excel file as follows: when several probe sets could be attributed to a single gene, or when a gene had several corresponding clones or LjSGA sequences, a median value was calculated, so that each gene had only one transcript level value. An extreme case could be observed for *LjGWD1* (Chr4.LjT08E06.100.nc) that corresponded to five different probe sets on the chips. Levels of expression of these probe sets varied significantly from one to another. Other genes with multiple probe sets were LDA (four probsets), GWD3 (three probe sets) and APL1, APL2, SS1, SS2, BAM1, BAM3, BAM7, DPE2, PHS2 (two probe sets each). A table of

correspondence between the Lotus starch metabolism genes and their probe sets and the probe sets' absolute transcript levels can be found in Table A1. Graphs were drawn using both absolute transcript values and log2 transformed values. Based on analysis of the whole data set values, the threshold under which the the expression level was considered as background/noise signal was determined to be ca. 60 in case of the absolute transcript values and ca. 6 in case of the log2 transformed values.

2.9. Gene mapping and identification of the mutations isolated from forward genetic screens

2.9.1. Mapping population generation and genomic DNA samples preparation

In this study, mapping populations were created for each of the mutant lines from crosses between mutants (in the Gifu background) and the WT ecotype *L. japonicus* MG-20. F1 plants were allowed to self-pollinate and mutant plants were selected in the F2 generation based on iodine-staining of leaves (see section 2.4). Genomic DNA from these plants was isolated as described above (see section 2.6.1). Mapping techniques employed for the identification of the mutations in this study are presented below.

2.9.2. Rough genetic mapping

Rough mapping was carried out initially by bulk segregant analysis (Michelmore et al., 1991) using microsatellite Simple Sequence Repeat (SSR) markers on at least two pools of eight genomic DNA samples of mutants isolated from F2 segregating populations from a cross with MG-20. Markers were designed at Kazusa DNA Research Institute and ordered from Sigma-Genosys. An exhaustive list of all SSR markers designed by the Kazusa DNA research institute can be found in the Miyakogusa database (http://www.kazusa.jp/lotus/index.html). Typically, the size of the PCR products using these SSR markers was about 100-200 bp length and the difference of size between MG-20 and Gifu varied from 2 bp to 40 bp. PCR products with a size difference of more than 20 bp were separated with a 2.5-3% agarose gel. For lower size differences, 5% acrylamide gel electrophoresis was used (Wang et al., 2003).

Three to four SSR markers were selected for each of the six chromosomes of *Lotus japonicus*. This selection was based on two main criteria: a) their position on the chromosome: markers were selected so that they were as much as possible equidistant to each other and allowed a full coverage of each chromosome; and b) the sequence

polymorphism between MG-20 and Gifu: markers giving PCR products with large size difference between the two accessions were privileged so as to facilitate the scoring A list of these selected markers can be found in Table 5.

Thus identified, the rough chromosomal interval where the mutation mapped was confirmed on the mutant individuals. For each of the mutant lines, further rough mapping (up to an interval of about 5 cM) was carried out using additional SSR markers, generally on a larger population of mutants. PCR and PCR product electrophoresis for this mapping was performed as described above (section 2.6.4).

Marker	Chr.	Map position
TM0193	1	20.1
TM0438	1	42.6
TM0143	1	66.2
TM0065	2	14.0
TM0076	2	46.0
TM0002	2	67.3
TM0080	3	12.5
TM0005	3	34.0
TM0049	3	55.1
TM0616	3	70.4
TM0182	4	8.8
TM0030	4	32.2
TM0046	4	53.8
TM0034	5	4.8
TM0048	5	27.6
TM0036	5	49.7
TM0302	6	14.0
TM0013	6	36.9
TM0336	6	57.6

Table 5. Microsatellite SSR markers used for rough mapping of mutant phenotypes from the forward genetic screen.
The SSR markers selected were designed by the Kazusa DNA research institute (http://www.kazusa.jp/lotus/index.html). Map positions are in cM and correspond to the location of the markers on the genetic linkage map of *Lotus japonicus* from a cross between the accession Gifu and MG-20 (maternal and paternal parents, respectively).

2.9.3. Fine genetic mapping

For several of the mutant lines finer mapping was performed on a large set of mutant individuals isolated from F2 segregating populations (see Chapter 4). This mapping was performed using SSR markers designed either at Kazusa DNA Research Institute or with the Simple Sequence Repeat Identification Tool (SSRIT; Temnykh et al., 2001). SSR markers within the target regions were PCR amplified and fluorescently labelled (Schuelke, 2000). The method used multiplex PCR amplification and automated capillary electrophoresis

analysis, using an ABI 3730xl 96-capillary DNA Analyzer (M. Groth, LMU; unpublished) and GeneMapper® software (Applied Biosystems). This mapping was performed by Andreas Brachmann (Biozentrum der LMU München, Germany).

2.9.4. Mapping data analysis

For each individual, and for each marker, discrimination between homozygous MG-20, homozygous Gifu, and heterozygotes, was performed by PCR gel electrophoresis as mentioned above. Scoring was based on the size of the PCR product(s) that were revealed by ethidium bromide (rough mapping) or by their fluorescent signals (fine mapping). Data were entered and processed in Excel files. The mapped interval was determined as the region where no recombination occurred.

2.9.5. Physical mapping and mutation identification

Mapping was coupled to the candidate-gene approach so that any strong candidate gene (i.e. genes known to play a key role in starch metabolism in other plant species; see Chapter 3) located in the mapped region was sequenced to establish whether its sequence carried a mutation potentially responsible for the mutant phenotype. Such genes (referred as the core set of starch metabolism genes) were mapped according to the results of gene prediction analyses and the information made available from the Miyakogusa database. Relatively recently (May 2008), this database has been updated to include a comprehensive list of all the predicted genes and encoded protein sequences. Before the update, genome sequences were retrieved and the gene and protein prediction were performed manually as described above (section 2.7).

In cases where the mapped interval defined for a particular mutant line did not contain any of these strong candidate genes, finer mapping was performed, and the candidate-gene approach was extended as follows: once the mapping interval was reduced to a relatively small chromosomal region (generally less than 10 cM), the corresponding genome sequence (physical map) was examined for putative candidate genes using the Miyakogusa database. Genes were designated as good candidates when they were likely, based on their annotation and the information available in the literature, to be responsible for the phenotype of the mutant in question, if mutated. This included all genes putatively, or known to be involved in the metabolism of starch or its regulation according to the results of extensive literature searches. Following analysis of their gene structures and the design of primers, the whole predicted coding region of such genes was sequenced.

The possible effects of the mutations thus identified on the protein function was predicted using the PARSESNP program (Project Aligned Related Sequences and Evaluate SNPs; http://www.proweb.org/parsesnp/) in combination with SIFT (Sorting Intolerant From Tolerant) as set up on the CODDLE web page. A SIFT score smaller than 0.05 and a PSSM (Position-Specific Scoring Matrix) difference score above 10 indicates a deleterious effect.

2.10. Targeted Induced Local Lesions in Genomes (TILLING)

2.10.1. Gene sequence analysis using CODDLE and primer design

TILLING was carried out to isolate mutants for genes known to be involved in starch metabolism in other plant species. Primers were designed using the Primer3 program in the region identified by CODDLE as having the maximum likelihood of producing deleterious alleles following EMS mutagenesis. The targeted region ranged from about 1 kb to 1.5 kb in length. Gene-specific primers used for TILLING are listed in Table 2.

2.10.2. Screening for polymorphisms

TILLING was carried out using the general TILLING population and the plant population of starch metabolism mutants from the forward screen (Perry et al., 2003 and 2009). TILLING for the genes *LjPGM1*, *LjAPS1*, *LjAPL2*, and *LjGWD1* was performed as follows: genomic DNA isolated from these populations was quantified and diluted to 5 ng μl^{-1}. Normalized DNA was pooled 4-fold and 1 µl pooled DNA was used in a 10 µl PCR reaction. In total, up to 4908 individuals from the general population were screened for each of the primer pairs. Heteroduplexes were digested with Cel1 from fresh celery (prepared at JIC), filtered though a Sephadex G50 column, concentrated, and loaded as previously described (Colbert et al., 2001; Till et al., 2001). Samples were run on either ABI 377 or LI-COR 4300 DNA analyzer using gene-specific primers that were either labelled with the fluorescent dyes 6-carboxy-fluorescein (6-FAM) and 4,7,2,7-tetrachloro-6-carboxy-fluorescein (TET) for analysis with an ABI 377 sequencer, or with the IRD 700 and IRD 800 labels for analysis with LI-COR 4300 sequencer as previously described (Perry et al., 2003 and 2009; Colbert et al., 2001). TILLING on the genes *LjPGM1*, *LjAPS1*, *LjAPL2* was carried out by Jodie Pike and Tracey Welham (TSL and JIC, respectively, Norwich, UK). I carried out TILLING on the GWD1 gene (two regions targeted). TILLING for *LjGWD3* was carried out by *RevGen*UK (http://revgenuk.jic.ac.uk/) on an ABI 3730xl 96-capillary DNA Analyzer following the method of Le Signor et al. (2009).

2.10.3. Mutation identification and PARSESNP analysis

Individuals from pools yielding cleavage products were analysed individually to confirm the presence of the mutation and identify the mutant line containing it. The point mutations thereby detected were confirmed and identified by sequencing. The severity of their effects on protein function was predicted using the PARSESNP program in combination with SIFT, as done for the forward screen mutations identified and described above. A SIFT score smaller than 0.05 and a PSSM (Position-Specific Scoring Matrix) difference score above 10 indicate a deleterious effect.

Mutations which resulted in the loss of a splicing-site or a premature stop codon and those with a PSSM (Position-Specific Scoring Matrix) difference score greater than zero, or likely to have an effect according to my own bioinformatics analysis (multiple sequence alignments; see section 2.7), were selected for further analysis. M3 seeds of mutant lines carrying such mutations were sown and their phenotype analysed. When mutations were heterozygous at M2, which was the case for the majority of selected lines, homozygous mutants were selected from the heterozygous and homozygous WT segregants by genotyping.

2.11. Protein analysis methods

2.11.1. Protein extraction and quantification

Protein extracts for immunoblots, starch binding assay, and native polyacrylamide gel electrophoresis (PAGE) of starch-metabolising enzyme activities were prepared by homogenizing 0.2-0.4 g of leaf material in 1 mL of cold extraction buffer containing 100 mM HEPES, pH 7.5; 1 mM EDTA; 1 mM DTT, 0.1% (w/v) polyvinylpolypyrrolidone (PVPP), and 10% (v/v) glycerol prior to centrifugation at 10,000 g for 10 min at 4 °C.

The total protein content in the supernatant of each extract was determined using the Bradford method (Bradford, 1976). This assay was performed on a 96-well microtitre plate and the absorbance of the samples was read at 595 nm using a microtitre plate reader (Spectra Max 340 PC and software SoftMax Pro; Molecular Devices Inc., Sunnyvale, USA) according to Bradford solution manufacturer's instructions (Sigma-Aldrich Co., St Louis, USA). Bovine serum albumin (BSA) solutions of 0.1 to 1 $mg.mL^{-1}$ were used for the standard curve.

2.11.2. Denaturing polyacrylamide gel electrophoresis (PAGE), Western blotting, and protein immunodetection

For the detection of GWD1 (SEX1) and SEX4 proteins in *L. japonicus*, antiserum to the SEX4 protein of *A. thaliana* (Niittylä et al., 2006) and a polyclonal antibody to the R1 protein (GWD1) of potato (Lorberth et al., 1998) were used. Soluble extracts of leaf soluble proteins were obtained as mentioned above (section 2.11.1). Depending on the experiment, 25 µg to 100 µg of protein was separated by SDS-PAGE. Briefly, equal amounts of protein from the mutant and corresponding WT were diluted with 2X SDS-PAGE sample loading Buffer (Laemmli Loading dye; 62.5 mM TrisHCl pH 6.8, 10% glycerol, 2% (w/v) SDS, 0.01% (w/v) Bromophenol blue, 5% (v/v) β-mercaptoethanol), heated at 95 °C for 5 min, cooled, and then loaded onto the gels. Protein sample separation by denaturing SDS-PAGE was carried out using a Mini-protean II apparatus (Biorad Laboratories). Gels (1 mm thick; 6% acrylamide in the resolving gel for GWD1 protein separation, 10% for SEX4; 4% in the stacking gel) were prepared and run in Tris-Glycine buffer (25 mM Tris, 192 mM Glycine, 0.1% SDS, pH 8.3) according to Laemmli (1970). The ProSieve™ pre-stained colour protein markers (BMA, Rockland, USA) or Precision Plus Protein™ standards (Biorad Laboratories) were used as molecular mass standards. When required, proteins on gels were visualised by staining with Coomassie blue (BioSafe™ Coomassie G-250 stain, Biorad Laboratories).

Proteins were transferred onto nitrocellulose membrane (PROTRAN BA 85; Schleicher & Schnell, Dassel, Germany) by transfer for 90 min at 100 V and 4 °C using the Mini Trans-blot Cell (Biorad Laboratories) in a buffer of 25 mM Tris, 192 mM glycine, 20% methanol, and 0.1% SDS.

After blocking for 15 min in PBS Buffer (150 mM NaCl; 75 mM Na_2HPO_4; 25 mM NaH_2PO_4) with 2% milk powder (w/v), the membrane was incubated ON at 4°C in presence of the primary antibody diluted 1:5000 in PBS buffer. After incubation, the membrane was rinsed several times in PBS buffer with and then without 0.5% Triton-X100, blocked again, and incubated 1 h at RT in presence of the second antibody (anti-rabbit IgG; Sigma-Aldrich) diluted 1:1500 in PBS buffer. Finally, immunodetection was carried out by using an Alkaline Phosphatase chromogen (BCIP/NBT) according to the manufacturer's instructions (Sigma-Aldrich; SIGMAFAST™ BCIP/NBT tablets).

2.11.3. Starch-binding assays

In vitro and *in vivo* starch-binding assays were carried out to assess the capacity of endogenous GWD1 proteins extracted from *gwd1-1* and WT plants to bind starch. Starch-

binding assays were performed with a protocol modified from Ritte et al. (2000) and Kotting et al. (2005) that had been scaled down. Leaf starch granules were isolated as follow: leaf material was harvested two to four hours after the end of the light period from plants grown in the glasshouse under short day conditions, and immediately frozen in liquid nitrogen. 1.5 to 3g of leaf material was homogenised in mortar with 5 mL of extraction buffer that consisted of 100 mM HEPES, pH 7.5; 1 mM EDTA, pH8; 1 mM DTT, 0.1% (w/v) polyvinylpolypyrrolidone (PVPP), and 0.05% (v/v) Triton X-100. The resulting homogenate was passed through Miracloth prior to centrifugation for 5 min at 10,000 g. The supernatant was discarded and the pellet resuspended in 2 mL extraction buffer following several washes. The resuspended pellet was then filtered through a syringe filled with cotton wool. The recovered filtrate was layered on top of a 2 mL cushion of 95% Percoll® (Sigma-Aldrich Co., St Louis, USA) and 5% 0.5 M HEPES-KOH (pH 7.5). Following centrifugation at 2000 g for 15 min, the pelleted starch was washed twice with extraction buffer, and then dried. If not used immediately, this starch was stored at -20 °C.

Analysis of *in vivo* starch-associated proteins was carried out as follows: dry starch extracted as described above was resuspended in SDS-PAGE loading buffer (ca. 10 µL per mg of dry starch). Bound proteins were solubilized by incubating the starch granules with this buffer for 15 min at RT with shaking. After centrifugation, the supernatant was heated for 5 min at 95 °C and then loaded onto SDS-PAGE gel (6% acrylamide).

For *in vitro* binding assays, commercial starch from potato and corn (Sigma-Aldrich Co., St Louis, USA) was used. This starch was washed with dH_2O prior to resuspension in soluble protein extract (ca. 500-1000 µg of protein for 5 mg of dry starch). The suspension was incubated for 30 min at 4 °C under shaking, and then placed on top of a 4 mL cushion of 95% Percoll® (Sigma-Aldrich Co., St Louis, USA) and 5% 0.5 M HEPES-KOH (pH 7.5). Following centrifugation, the pelleted starch was washed twice with extraction buffer. Finally, the proteins bound to the surface of the starch granule were released by incubation in SDS-PAGE loading buffer at RT.

Soluble protein extracts, SDS-PAGE gel electrophoresis, western blotting, immunodetection, and Coomassie staining were carried out as described above (sections 2.11.1 and 2.11.2).

2.12. *In vitro* enzyme activity assays

2.12.1. ADP-glucose pyrophosphorylase (AGPase) assay

AGPase activity was assayed in the direction of ADP-glucose synthesis (ATP + glucose-1-P → ADP-glucose + PPi) using a protocol modified from Ghosh and Preiss (1966). Briefly, leaf material (0.2-0.3 g) was harvested on ice, extracted in 3 mL of 50 mM HEPES (pH 7.4), 1 mM EDTA, 2 mM $MgCl_2$, 1 mM DTT, and clarified by centrifugation at 4°C. Each assay contained 10 µL soluble extract in 190 µL of 50 mM HEPES (pH 7.4), 15 mM $MgCl_2$, 15 mM 3-phosphoglycerate (PGA), 1.5 mM ATP, 0.5 $mg.mL^{-1}$ BSA, 0.5 mM Glc-1-P, 0.5 mM [U-^{14}C] Glc-1-P at 1 MBq $mmol^{-1}$, and 12.5 $U.mL^{-1}$ inorganic pyrophosphatase (from yeast, Roche Diagnostics). After incubation for 10 min at 37 °C, samples were processed by treatment with DEAE cellulose discs according to Ghosh and Preiss (1966) and the ADP-glucose product measured by liquid scintillation counting.

2.12.2. Phosphoglucose-isomerase (PGI) assay

PGI activity was assayed spectrophotometrically, using a protocol modified from Jones et al. (1986). Briefly, leaf material was extracted in ice-cold buffer consisting of 0.1 M HEPES, pH 7.5, 1 mM EDTA, and of 50 $\mu g.mL^{-1}$ of the serine protease inhibitor phenylmethanesulfonyl fluoride (PMSF; previously dissolved in ethanol), and 1 mM DTT. Homogenates were centrifuged at 10,000 g for 5 min at 4 °C and the supernatant used for the assay. The extracts were heated at 50°C for 10 min to inactivate the plastidial isoform. The reaction mix contained 150 mM Tris, pH 8.3; 1.5 mM NAD; 5 mM fructose-6-phosphate (Fru-6-P); 2 $U.mL^{-1}$ glucose-6-phosphate dehydrogenase (G6PDH); 5 µL of extract. PGI activity was determined by monitoring the production of NADH at 340 nm using a microtitre plate reader. Contribution of the cytosolic and plastidial isoforms to the total PGI activity was estimated by heating the extracts at 50 °C for 10 min, as described in Jones et al. (1986).

2.12.3. Native PAGE of starch-metabolising enzyme activities

Native PAGE of starch-metabolising enzyme activities (also called a zymogram or activity gel) was performed with a method modified from Shaw and Prasad (1970) for PGI and PGM activities, and as described in Delvalle et al. (2005) for other starch-modifying activities (i.e. starch synthase, branching and debranching enzymes, amylases, and starch phosphorylases). Samples of 100 µg of protein extracts, prepared as described above (section 2.11.1), were mixed with native-PAGE sample loading buffer (20 mM TrisHCl pH 6.8, 12% (v/v) glycerol, 0.025% (w/v) Bromophenol blue) and then loaded onto a native polyacrylamide gel (either 5, 6, or 7.5% acrylamide used in the resolving gel; 3.75% in the stacking gel). Electrophoresis was carried out for 3 h at 15 $V.cm^{-1}$, at 4 °C.

Native PAGE gels for the detection of PGM and PGI activities contained 1% (w/v) potato starch (Sigma-Aldrich). Following electrophoresis, gels were incubated for 30 min to 1 h at 37 °C in 100 mM Tricine (pH 8), 10 mM $MgCl_2$, 0.25 mM NADP, 1 mM MTT (3-4,5-Dimethylthiazol-2-yl)-2,5-diphenyltetrazolium bromide), a trace of Meldola's blue (Sigma-Aldrich), 1 $U.mL^{-1}$ Glc-6-P dehydrogenase from *Leuconostoc mesenteroides* and either 7 mM of Glc-1-P (PGM activity) or 8 mM of Fru-6-P (PGI activity). Once the enzyme activity bands were clearly visible, the development was stopped by transferring the gel into dH_2O.

Native PAGE gels for the detection of SBE, DBE, AMY and BAM enzyme activities contained 0.3% (w/v) of potato or corn starch (Sigma-Aldrich), amylopectin (from potato; Sigma-Aldrich), or β-limit dextrin (from potato; Sigma-Aldrich). Following electrophoresis, gels were incubated a minimum of 2 h at 37 °C in a developing buffer containing: 100 mM Tris-HCl, pH 7, 1 mM $MgCl_2$, 1 mM $CaCl_2$, 1 mM DTT. Following this step, gels were stained with Lugol's solution.

Native PAGE gels for the detection of starch phosphorylase and starch synthase enzyme activities contained 1% (w/v) of glycogen (from oyster; Sigma-Aldrich). Following electrophoresis, gels were incubated for 2 h at 37 °C in a buffer containing 100 mM sodium citrate and 20 mM Glc-1-P for starch phosphorylase activities (PHS1 and 2), and 50 mM glycylglycine - NaOH, pH 9, 100 mM ammonium sulphate, 5 mM 2-mercaptoethanol, 5 mM $MgCl_2$, 0.25 gL^{-1} BSA, and 1 mM ADP-Glc for starch synthase activities (SSI and III). Following this development, gels were stained with Lugol's solution.

2.13. Metabolite quantification

2.13.1. Starch extraction and quantification

Starch extraction and quantification was performed with a method modified from Smith and Zeeman (2006) by Alexander Graf (JIC, personal communication). Briefly, 50-200 mg of tissue were harvested into pre-weighed 2 mL Eppendorf tubes and rapidly frozen in liquid nitrogen. Samples were then homogenized on dry ice using a pulverizing mill (MM300; Retsch GmbH, Haan, Germany). One mL of 0.7 M perchloric acid was added to each sample and 0.4 mL of the resulting homogenate was transferred to a 96-well microtitre plate. After centrifugation for 10 min at 3200 g, the pellet was washed twice with 100 and 80% ethanol (centrifugation for 5 min at 3200 g between each wash). The starch-containing pellet (colourless) was finally re-suspended in 150 µL dH_2O and incubated at 95 °C for 15-30 min. The pellet was then washed with 100% ethanol, air-dried and re-suspended in 300 µl dH_2O. Three hundred µL of 0.2 M sodium acetate (pH 4.8) and 10 µL of 9:1 amyloglucosidase:α-

amylase (from *Aspergillus niger;* 10 $\mu g.\mu l^{-1}$; Roche Diagnostics) were then added to each sample, and the samples incubated at 37 °C for between two hours and ON. Following this step, samples could be stored at -20 °C until used. A control plate of samples was simultaneously processed which differed only by the addition of 10 µL dH_2O instead of the enzyme mix.

The starch content was assayed enzymatically by measuring the amount of glucose thus released. Performed on 96-wells microplates, this assay consisted of the conversion of glucose to 6-phosphogluconate by G6PDH and hexokinase (HK) with a concomitant reduction of NAD to NADH. Samples were vortexed and centrifuged 10 min at 5800 g. One to 20 µL of supernatant were added to 50 µL of reaction buffer containing 100 mM HEPES, 4 mM $MgCl_2$, 2.2 mM ATP, 1.6 mM NAD and 8 $U.mL^{-1}$ of HK (from yeast overproducer; Roche Diagnostics). The reaction was started by adding 0.4U of G6PDH (from *Leuconostoc mesenteroides*; Roche Diagnostics) to each sample. The production of NADPH was followed spectrophotometrically at 340 nm. Values were subtracted from those of control samples in which the enzymes amyloglucosidase and α-amylase were replaced by dH_2O (10 µL). Glucose concentration was determined using a standard curve and the linearity of the assay was checked with NADH standards.

2.13.2. Soluble sugar extraction and quantification

To quantify soluble sugars, plant tissues were immediately frozen in liquid nitrogen and extracted in perchloric acid (0.7 M). After homogenisation and centrifugation, the supernatant was used for sugar measurements and the pellet for starch assays. Starch was assayed as described above. The supernatant containing free sugars was adjusted to pH 7 by the addition of ice-cold neutralizing solution (2 M KOH, 0.4 M MES and 0.4 M KCl). Precipitated potassium perchlorate was pelleted by centrifugation (10 min, 3000 g, 4 °C), and the soluble fraction (containing the soluble sugars and MOS) was stored at -20 °C until used.

Sucrose, glucose and fructose contents were determined spectrometrically by reading absorbance at 340 nm. Twenty five µL of sample were mixed with dH_2O (up to 200 µL) and 50 µL of sugar assay cocktail (100 mM HEPES, 4 mM $MgCl_2$, 2.2 mM ATP, 1.6 mM NAD and 8 $U.mL^{-1}$ of HK and placed in a microtitre plate. Glucose, fructose, and sucrose were determined by the successive additions of the enzymes G6PDH (from *Leuconostoc mesenteroides*, 1 $U.\mu L^{-1}$; Roche Diagnositics), phosphoglucose isomerase (PGI; from yeast, 10 $\mu g.\mu L^{-1}$; Roche Diagnositics), and β-fructosidase (Roche Diagnositics)

2.13.3. Malto-oligosaccharide (MOS) analysis by HPLC

Leaf tissue (0.3 g approximately) was harvested and frozen in liquid N_2. The material was powdered and extracted in 1.5 mL of 0.7 M perchloric acid. After centrifugation (3000 g, 5 min, 5 °C), 1 mL of supernatant was adjusted to pH 5 with the following neutralizing solution: 2 M KOH, 0.4 M MES and 0.4 M KCl). The potassium perchlorate precipitate was removed by centrifugation (10,000 g, 10 min, 4 °C), and the soluble fraction (containing the MOS) was stored at -20 °C until use.

For the analysis of MOS by High Performance Anion Exchange Chromatography with Pulsed Amperometric Detection (HPAEC-PAD), 100 µL of extracts were purified through sequential 1.5 mL columns of Dowex® 50 and Dowex® 1 resins (Sigma-Aldrich). The compounds were eluted with water, lyophilized by freeze-drying and then re-dissolved in HPLC-grade water. Metabolites were assayed by HPAEC-PAD using a HPLC machine (DIONEX®; Dionex Co., Sunnyvale, USA). Peaks were identified by adding known amounts of MOS standards. Peak areas were determined using the Chromeleon® software (Dionex) and compared to standard curves.

2.14. Acetylene reduction assay

Acetylene reduction assays were performed by Tracey Welham (JIC, Norwich, UK) to determine the symbiotic nitrogen fixation capacity of the nodules of several of the *Lotus japonicus* mutants and their corresponding WTs. Plants were grown and inoculated with *Mesorhizobium loti* strain *Tono* as mentioned above (section 2.1.3). Four weeks after inoculation, the whole root system was placed in a 35 mL tube and sealed with rubber lid. A volume of 0.5 mL acetylene was injected, and the samples incubated for one to two hours at RT. The amount of ethylene produced was quantified by comparison with an ethylene standard using a gas chromatogram equipped with a hydrogen flame ionization detector as described by Horst et al. (2007).

2.15. Statistical analyses

All physiological analyses were performed with a minimum of three biological replicates as stated in the text for each experiment. The Student's t test ($p<0.05$) was used to analyse statistical significance of the differences obtained between genotypes or treatments. Phenotyping data were subjected to Chi-square (χ^2) statistical analyses to test the goodness-of-fit of the observed to expected ratio. A ratio of 1:2:1 (homozygous

mutant:heterozygous:homozygous WT) was expected for a phenotype conferred by a single recessive mutation. Chi-square analysis was also performed on the results of the genetic mapping to test for significant ($p<0.05$) linkage between the SSR markers and the mutant gene. These were considered as assorting independently when the ratio of individuals from a F2 segregating population from a backcross between a homozygous mutant in Gifu and MG-20 was not statistically significantly different from 25% scoring homozygotes Gifu (Gifu/Gifu), 50% heterozygotes (Gifu/MG-20), and 25% homozygotes MG-20 (MG-20/MG-20). In contrast, the more linked were the SSR marker and the mutated locus (i.e. toward case of co-segregation), the lower was the recombination frequency, and the higher was the proportion of individuals scoring homozygous Gifu for this marker.

CHAPTER 3

The metabolism of starch in *Lotus japonicus*

The cure for boredom is curiosity. There is no cure for curiosity

Dorothy Parker

CHAPTER 3: The metabolism of starch in *Lotus japonicus*

3.1 Introduction

3.1.1. Rationale for studying the metabolism of starch in *L. japonicus*

Studies in *A. thaliana* have greatly enhanced our knowledge about pathways of transitory starch metabolism (Smith et al., 2005; Zeeman et al., 2007; Chapter 1, section 1.3). These studies have also revealed the important role that starch turnover plays in the productivity of the plant by assuring the supply of carbon skeletons to sustain its energy metabolism and growth during the dark period. Mutants of *A. thaliana* unable to synthesize transitory starch, or with reduced rates of starch degradation at night, generally have a reduced rate of growth and a delayed flowering time relative to wild-type plants under most conditions (Caspar et al., 1985; Caspar et al., 1991; Eimert et al., 1995; Corbesier et al., 1998; Smith and Stitt, 2007). However, it is not known whether information about the nature and importance of starch turnover in *A. thaliana* is widely applicable. Plant species differ considerably in the extent to which starch is stored in leaves at night, and in diurnal patterns of growth and metabolic demand (Smith et al., 2005; Chapter 1, section 1.6). Furthermore, the metabolism of starch can vary widely with plant organs and environmental conditions. The function and regulation of starch metabolism in heterotrophic organs and its importance in major physiological and developmental processes such as perenniality, vegetative re-growth, symbiotic nitrogen fixation, and the accumulation of seed storage reserves, cannot be easily studied in *A. thaliana* and remain largely unknown. These processes represent traits of agronomic value in legumes, a family that includes some of the most agriculturally important forage (e.g. alfalfa and clover) and grain (e.g. pea, common bean, and soybean) crops.

Some information is already available about storage starch metabolism in pea and other legume crops (e.g. Wang et al., 1998 and references therein). However, characteristics including large genome sizes and recalcitrant transformation and regeneration have limited progress on these species. To date, there is insufficient information to allow either an overview of the nature and importance of transitory and storage starch metabolism in legumes, or a meaningful comparison with the detailed picture emerging for *A. thaliana*. The recent development of both *L. japonicus* and *M. truncatula* as legume model systems, and the wide range of genetic and genomic resources generated for them, offer the opportunity for a systematic analysis.

3.1.2. Phylogenetic relationship of the genes involved in starch metabolism and their expression pattern

Phylogenetic and expression pattern analyses can provide useful information for the design of reverse genetic studies and to understand the phenotype of mutants and transgenic plants with decreased or increased expression of a particular gene or set of genes of interest. The presence of several close homologs, for instance, is predictive of possible gene function redundancy. Phylogenetic analyses of gene families across several different species can also reveal interesting conservation and divergence that can help predict the importance and/or role of genes in a biological process of interest. Similarly, knowing the expression pattern of a particular gene at the tissue, cell-type, and/or subcellular level can provide insight into its function. Lastly, the study of genes sharing the same expression pattern as a gene of interest (often referred as 'co-expression analysis') can help identify new genes involved in the same biological process, predict the function of unknown genes and/or identify novel function for already characterised genes.

The nature and functionality of phylogenetically-related genes may be different from one species to another due to the occurrence of evolutionary events such as gene duplication. Gene duplication is generally considered as a major evolutionary source of new protein function. The genomes of most eukaryotes have undergone whole genome duplication (WGD) events during their evolutionary history. In addition to WGD (also referred as segmental duplication), small local events can also generate duplicated genes. Following one or another of these events, the duplicated gene can accumulate deleterious mutations and become non-functional or be lost. Alternatively, both duplicated genes can be maintained if the presence of both copies is advantageous. Over time, the function of these duplicated genes can diverge from the ancestral gene, and their expression patterns change. This can occur via sub- and/or neo-functionalization. In the case of sub-functionalisation, the functions of the original single-copy gene are partitioned between the duplicates, whereas in the case of neo-functionalization, one or both of the copies acquire a novel function (Force et al., 1999).

The metabolism of starch involves genes of many different gene families, most of which have been the subject of phylogenetic analyses (Chapter 1, section 1.6). Overall, these analyses have revealed relatively complex phylogenetic relationships for most of the starch metabolism gene families due to the presence of duplicate copies of several genes arising from both WGD and local, independent, duplication events. To add to the complexity, these duplication events after speciation appear to have often occurred in several plant species in parallel, resulting in homologous groups of genes. In some cases, the homologous genes

have undergone convergent evolution while in other cases, divergence of their expression and function occurred between plant species (e.g. phylogenetic relationship and expression pattern of the GBSS and SS genes; Edwards et al, 2002; Pan et al., 2009). Most of the *A. thaliana* starch genes have now been studied in detail (Chapter 1, section 1.3 and reference therein). Information about the homologs of these genes and their functionality in several model and crop species, including legume species, however, is lacking.

3.1.3. Information about the relationship between carbohydrate metabolism and plant growth from QTL analysis

As a complementary approach to the study of laboratory induced-mutants (aka artificially-generated genetic variation), natural diversity provides a rich source of naturally occurring change-of-function alleles that can be harnessed to identify the loci underlying complex, quantitative, physiological processes such as flowering time and plant growth (reviewed in Koornneef et al., 2004). Quantitative Trait Locus (QTL) analyses generally use natural genetic variation of immortal mapping populations such as Recombinant Inbred Lines (RILs) and Near Isogenic Lines (NILs). QTLs for many polygenic traits have been identified in several plant species including *L. japonicus* (e.g. Yano and Sasaki, 1997; Alonso-Blonco and Koornneef, 2000; Gondo et al., 2007). Genes responsible for differences in traits can then be identified by candidate gene searches and positional cloning. In addition, QTL analysis can also be used to reveal correlations between several traits and provide insight into the structure of metabolic and regulatory networks.

QTL analysis has recently been employed in studies aiming at determining the importance of carbohydrate metabolism in several plant growth and development processes, and at discovering interactions between this metabolism and other metabolic pathways (El-Lithy et al., 2004 and 2005; Calenge et al., 2006; Sulpice et al., 2009). A study carried out by Calenge et al. (2006) focused on traits related to the interaction between carbon (C) metabolism and nitrogen (N) availability. Using the *A. thaliana* Bay-0 x Shahdara Recombinant Inbred Lines (RIL) population, these authors identified 39 QTLs for starch, glucose, fructose, and sucrose contents. Their analysis also revealed colocalizations of the QTLs related to carbohydrate metabolism with traits for other physiological processes including nitrogen- and senescence-related traits, and traits for flowering time and water status. El-Lithy et al. (2005) used natural allelic variation in a set of 123 *A. thaliana* accessions to study photosynthetic performance and sugar and starch accumulation in combination with flowering and growth-related traits. A large variation was observed in carbohydrate levels and their diurnal patterns. In general, plant growth was found to be more closely linked with transitory starch levels than with soluble sugar levels. No correlation,

however, was observed between the patterns of sugar and starch accumulation and the geographical origin of the different accessions. This suggests that parameters other than photo-climatic conditions may play a major role in determining the pattern of carbohydrate accumulation. Furthermore, their study also revealed that photosynthetic rate is a highly conserved trait among all the *A. thaliana* accessions analysed that varies only under severe selective pressure (e.g. atrazine). Lastly, using recombinant inbred lines derived from the cross between Landsberg *erecta* and Kondara the authors also performed QTL analysis for carbohydrate-related traits and plant growth. Correlation and co-localisation of the QTLs revealed a complex relationship between carbohydrate content and plant growth- and flowering-related traits.

3.1.4. Carbon partitioning and plant growth strategies

Fast-growing plant species in general tend to maximize resource acquisition, whereas slow-growing species or accessions rather maximize the conservation of resources. With regard to the metabolism of carbohydrates, this means that faster-growing plants are expected to hold less carbohydrate in reserve as starch that would allow them to cope with unexpected changes in their environmental conditions. This hypothesis is supported by the fact that plants growing in favourable habitats often have an inherently high Relative Growth Rate (RGR), whereas those from less favourable environments have an inherently low RGR, even when grown in the same favourable conditions (Grime and Hunt, 1975; Poorter et al., 2005). This idea is also consistent with the results of a study carried out by Cross et al. (2006) in which variation in growth parameters, metabolite levels and activities of key enzymes involved in C and N metabolism were measured across 24 accessions of *A. thaliana*. Their results revealed differences in the extent to which starch is exhausted in a regular light/dark cycle among the accessions. Faster-growing accessions had a lower level of starch at the end of the night than their slower-growing counterparts. Interestingly, their results also indicated that increased growth was related to increased fluxes driven by a higher catalytic activity of enzymes in central C and N metabolism rather than increased levels of starch, sugars, and other metabolites. Meyer et al. (2007) performed large scale metabolite profiling on a Col-0 x C24 RIL population. Levels of most of the metabolites they analysed also showed a negative rather than a positive correlation with the plant growth rate. Taken together, these results indicate that faster growth is driven by faster fluxes, themselves driven by higher enzyme activities rather than a higher level of central metabolites.

Recently, the analysis carried out by Cross et al. (2006) was extended to the metabolic profiling of all major classes of metabolites in 94 *A. thaliana* accessions (Sulpice et al.,

2009). In agreement with the results of the study of Cross et al. (2006), a high negative correlation was observed between starch level and biomass production (R = −0.54). Rosette biomass also showed a significant, but lower, correlation to protein (R = −0.37), chlorophyll (R = −0.31), and several low-molecular-weight metabolites (sucrose, total amino acids, glycine, alanine, glutamate, threonic acid, benzoic acid, sinapic acid). Correlations were nonsignificant with other metabolites. Importantly as well, this analysis identified starch as a central component coordinating metabolism with growth. However, since starch is a polymer of carbon without known regulatory activities, it is likely that regulators of starch metabolism or signals derived from starch, rather than starch itself, act as integrators of the metabolic network regulating plant growth.

The possibility of using biomarkers to predict biomass production in plants is of interest for crop improvement. In this context, Sulpice and collegues (2009) also generated a correlation network combining transcript levels, metabolite levels, and biomass data. Doing so, they identified two genes, Kelch repeat F-box protein (At1g23390), and a myo-inositol-1-phosphate synthase 1 (IPS1; At4g39800), whose transcript level significantly correlated with rosette biomass (R = 0.65 and -0.62 and P = 0.0016 and 0.0026, respectively) and were also significantly associated with starch. These two genes therefore represent good candidate genes to modulate biomass production in crops. It is worth noting, however, that all studies presented above have been carrried out in *A. thaliana* and in controlled environments. It remains to be determined if these finding are widely applicable to other plant species and to field grown plants.

3.1.5. Morphological and physiological traits of the *L. japonicus* accessions Gifu and MG-20

Gifu (B-129) and Miyakojima (MG-20) are the two experimental accessions most commonly used for research in *L. japonicus*. Gifu originates from the central region of the Japanese mainland whereas Miyakojima comes from the most southern part of Japan. These two accessions display a high level of polymorphism (over 4%) with each other - the highest level of polymorphism relative to Gifu amongst 15 accessions of *L. japonicus* collected across the whole of Japan (Kawaguchi et al., 2001). This polymorphism at the genomic DNA level is reflected in phenotypic differences at the whole plant level. In particular, MG-20 plants grow faster and flower earlier than Gifu (generation time of 2-3 months for MG-20 versus 3-4 months for Gifu; flowering time around 6 weeks and 8 weeks, for MG-20 and Gifu, respectively; Kawaguchi et al., 2001). Further, MG-20 flowers readily under white fluorescent light, while Gifu flowers less and with delay under these conditions. MG-20 plants also have several other distinguishing characteristics such as larger leaves and a lower

anthocyanin content that is reflected in the colour of the stem and petiole (green for MG-20, rather purple in case of Gifu). Gifu plants have many trichomes on their leaves, especially around the sepals whereas MG-20 plants possess very few (Kawaguchi et al., 2001). Other characteristics thus far not reported in the literature that I noted when growing the plants in many different conditions for this study included a much higher susceptibility of MG-20 relative to Gifu to several plant diseases including fungal infection (in particular mildew), and diseases carried by insects or damage caused by them (e.g. infection by *Impatiens Necrotic Spot Virus*; thrips). In addition, senescence-like symptoms after seed setting in MG-20 were more pronounced than in Gifu. Lastly, Gifu plants generally have darker-green leaves and produce more tillers than MG-20 plants.

3.1.6. Aims and Approaches

In contrast to *A. thaliana*, almost nothing is known about the metabolism of starch in the model legume *L. japonicus*, and only very little about its nature and importance in legumes and perennial plants in general. The limited amount of literature on starch in *L. japonicus* available thus far only concerned seeds and nodules (Chapter 5, section 5.1.1 and 5.1.2). I present here the results of extensive bioinformatic analyses aiming at identifying the set of genes involved in the synthesis and degradation of starch in the genome of *L. japonicus*, and generate the first molecular-function map for starch metabolism in this species. I also formulate hypotheses about the functionality of these genes in the pathway of transitory and storage starch metabolism through the analysis of publicly available microarray data resources. Furthermore, I carried out starch and sugar measurements across organs, at several developmental stages, and in different growth conditions to characterise the accumulation and turnover of starch in the two *L. japonicus* accessions MG-20 and Gifu. Conservation and divergence with the metabolism of starch in other species, and in *A. thaliana* in particular, is also discussed in this Chapter. Lastly, I suggest future experiments to characterise further the metabolism of starch in *L. japonicus* and to test the hypothesis that variation in starch metabolism may correlate with differences of biomass production in this species.

3.2. Results

3.2.1. *In-silico* identification of genes involved in starch metabolism in *L. japonicus* and their genome location

In order to identify genes involved in starch synthesis and degradation in *L. japonicus*, and to determine their position on the genetic linkage map, I first compiled a list of the *A. thaliana* genes involved in the metabolism of leaf starch (Table 6). This included genes involved in the partitioning of photoassimilates into starch, in the synthesis and degradation of starch, and in the subsequent metabolism of maltose (Smith et al., 2005; Zeeman et al., 2007; Fulton et al., 2008; Kötting et al., 2009). Recent progresses in EST and genome sequencing projects in *L. japonicus* allowed me to identify the homologs of these genes in this species as described in Materials and Methods (Chapter 2, section 2.7.2). Briefly, candidate genes were identified by searching the Miyakogusa genome database using the gene names as keywords and/or by peforming Blastp searches using the protein sequences of their *A. thaliana* homologs. Blastn or tBlastn searches were also performed against the LjEST database. Sequences of all the hits retrieved were submitted to multiple sequence alignments to determine whether they indeed corresponded to the *L. japonicus* homolog of the *A. thaliana* gene in question.

My investigation revealed a certain number of mis-annotations within the Miyakogusa genome database (Sato et al., 2008). For instance, two of three clones (namely chr1.CM0982.220.nd, chr1.CM0982.370.nd, and chr1.LjT29N14.30.nd) that were annotated as encoding plastidial isoforms of PGI (PGI1) corresponded in fact to putative cytosolic isoforms of the enzyme (PGI2). Similarly, the clones LjT28H07.90.nc and chr6.CM0114.50.nc could not be conclusively confirmed as the homolog of *AtPHS2* in *L. japonicus*. Two other clones, LjT22N06.110.nd and chr3.LjT02C24.30.nd, were also most likely to have been mis-annotated as the homologs of *AtSS3* and *AtDPE2*, respectively, given their low percentage of identity at the amino acid level. Likewise, a certain number of the LjSGA sequences were also most likely mis-annotated as starch metabolism genes. Results of this examination are presented in (Table 6). In an attempt to facilitate any future comparative analyses, all starch metabolism genes identified in *L. japonicus* were given the same name as their homologs in *A. thaliana*.

My bioinformatic analysis also aimed at determining whether the translated sequences given in the database were complete and correctly predicted. When this was not the case (i.e. amino acid sequence incomplete or mis-predicted), I carried out additional analyses that included manual gene and protein sequence predictions. Doing so, I was able to correct the predicted protein sequence of LjAPL3, LjGWD1, LjGWD3, LjAMY1, LjBAM1, and LjBAM3. Unfortunately, in several cases, the complete protein sequence could not be obtained either because the programs I used failed to predict the correct intron-exon structure, or because the corresponding genomic DNA sequence was only partially sequenced (Table A2). In case of *LjGWD1*, the prediction of the full coding region was difficult due to the presence of a retroelement in the last intron. The complete translated

sequence, however, could be obtained by using EST sequence information retrieved from the DCFI gene index database gene. A retroelement insertion (LTR-RT; 4594 bp) was also found within the genomic sequence of *LjGWD3* (see Chapter 5, section 2.7.1 for more details). The genomic sequence lengths of these two genes and their introns were significantly bigger in *L. japonicus* than in *A. thaliana*, even when not taking the presence of the retro-transposon into account (*LjGWD1*: 16785 bp, 33 exons versus *AtGWD1*: 9010 bp, 32 exons; *LjGWD3*: 12913 bp, 18 exons *versus AtGWD3*, 7372 bp, 31 exons). This was also true of most other genes I analysed and is consistent with the difference of intron length and gene density between these two plant species at the whole genome level: the average lengths of genes and introns are 2917 versus 1918 bp, and 395 versus 157 bp in *L. japonicus* and *A. thaliana*, respectively. The average gene density in *L. japonicus* was estimated to be one gene in every 10.2 kb versus one gene in every 4.5 kb in *A. thaliana* (Sato et al., 2008).

Whenever possible these genes were mapped onto the genetic linkage map of *L. japonicus* using information provided by the Miyakogusa genome database. The position of the genes whose sequences corresponded to an LjSGA rather than a clone sequence could not be determined since LjSGA sequences are not anchored to the genome (Sato et al., 2008). This affected the genes *LjAMY2*, *LjBAM1*, and *LjBAM6*. The resulting molecular function map for genes involved in starch metabolism in *L. japonicus* is presented in Figure 6. The use of this map for identifying the affected genes in the mutants with altered starch metabolism is discussed in the next chapter (Chapter 4, section 4.2.2).

3.2.2. Comparative genomic analysis of the starch metabolism genes in *L. japonicus* and other plant species

I was able to identify *L. japonicus* genes encoding all classes of enzymes involved in starch metabolism in *A. thaliana*, but there were several differences in isoform representation. First, several homologs of starch metabolic genes or their corresponding cDNA sequence could not be identified either in the genome or in the EST database of *L. japonicus*. For instance, I could not find *L. japonicus* sequences homologous to *A. thaliana* genes encoding the glucan, water dikinase AtGWD2 and the β-amylases AtBAM2 and AtBAM4 (Table 6). For several other *A. thaliana* genes (namely *SS3, SS4, SBE2, SBE3, ISA3, SEX4, PHS1*), clones, LjSGA, and/or EST sequences of candidate genes could be identified, but could not be confirmed with certainty as being their *L. japonicus* homolog. Conversely, I found a number of duplications of starch metabolism genes in *L. japonicus*, including *APL2*, *SS2*, *GBSS*, *AMY3*, *BAM3*, and *PHS2*.

			in *A. thaliana*			in *L. japonicus*					
Enzyme	**EC number**	**CAZy family**	**Gene name**	**Locus**	**Accession**	**Gene name**	**Predicted gene(s)**		**Clone name**	**Chr**	**Map position**
Phosphoglucoisomerase, plastidial	5.3.1.9	n/a	PGI1	At4g24620	Q8H103	PGI1	chr1.LjT29N14.30.nd		LjT29N14	1	0,0
Phosphoglucomutase, plastidial	5.4.2.2	n/a	PGM1	At5g51820	Q9SCY0	PGM1	chr5.CM0953.200.nc		LjT17N13	5	44,9
ADPglucose pyrophosphorylase Small subunit	2.7.7.27	n/a	APS1/ADG1/GLGS	At5g48300	P55228	APS1	chr2.CM0191.60.nc		LjT45D07	2	72.1-72.5
ADPglucose pyrophosphorylase Large subunit 1	2.7.7.27	n/a	APL1/ADG2/GLGL1	At5g19220	P55229	APL1	chr4.CM0387.180.nc		LjT31N09	4	48,2
ADPglucose pyrophosphorylase Large subunit 2	2.7.7.27	n/a	APL2/GLGL2	At1g27680	P55230	APL2a	chr1.LjT34C24.40.nc		LjT34C24	1	17,7
						APL2b	chr5.CM0077.680.nc		LjT08B03	5	0,8
ADPglucose pyrophosphorylase Large subunit 3	2.7.7.27	n/a	APL3/GLGL3	At4g39210	P55231	APL3	chr1.CM0113.470.nd		LjT55F02	1	42,6
ADPglucose pyrophosphorylase Large subunit 4	2.7.7.27	n/a	APL4/GLGL4	At2g21590	Q9SIK1	APL4	chr3.CM0216.100.nd		LjT44D07	3	75,6
ADPglucose pyrophosphorylase Large subunit 5	2.7.7.27	n/a	n/a	n/a	n/a	APL5	LjB06P23.100.nc		LjB06P23	0	
Starch synthase I	2.4.1.21	GT5	ATSS1/SSY1	At5g24300	Q9FNF2	SS1	LjT38J19.80.nd	LjT38J19.60.nd	LjT38J19	0	
Starch synthase II	2.4.1.21	GT5	ATSS2	At3g01180	Q9MAC8	SS2b	chr1.CM0141.60.nd	chr1.CM0141.220.nd	LjT58F09	1	29.3-29.7
						SS2a	CM1835.140.nc			0	
Starch synthase III	2.4.1.21	GT5	ATSS3	At1g11720	Q9SAA5						
Starch synthase IV	2.4.1.21	GT5	ATSS4/SSIV	At4g18240	Q0WVX5						
Starch synthase V/Glycogen synthase-like	2.4.1.21	GT5	putative SSV	At5g65685	Q8GWC5	SS5	chr2.CM0177.660.nc		LjT10N22	2	48,5
Granule-bound starch synthase	2.4.1.21	GT5	putative GBSS	At1g32900	Q9MAQ0	GBSS	chr3.CM0208.40.nd		LjT11A16	3	49.4-52.7
							chr5.LjT41L03.30.nd		LjT41L03	5	19,2
Starch branching enzyme, class I	2.4.1.18	n/a	n/a	n/a	n/a	SBE1	chr1.CM0178.250.nc		LjT29P11	1	20,1
Starch branching enzyme, class II	2.4.1.18	n/a	SBE2.2	At5g03650	NP_195985						
	2.4.1.18	GH13, CBM48	BE3/SBE2.1	At2g36390	O23647						
Starch branching enzyme, class III	2.4.1.18	GH13, CBM48	BE1	At3g20440	Q8GWK4						
Starch debranching enzyme: Isoamylase I	3.2.1.68	GH13, CBM48	ATISA1/ISA1	At2g39930	O04196	ISA1	chr4.CM0004.550.nc		LjT15D01	4	65,6
Starch debranching enzyme: Isoamylase II	3.2.1.68	GH13, CBM48	ATISA2/DBE1/BE2	At1g03310	Q9ZVT2	ISA2	LjSGA_028198.1				
Starch debranching enzyme: Isoamylase III	3.2.1.68	GH13, CBM48	ATISA3/ISA3	At4g09020	Q8RWW6						
Starch debranching enzyme: Pullulanase/Limit dextrinase	3.2.1.41	GH13, CBM48	ATLDA/ATPU1/PU1	At5g04360	Q8GTR4	LDA	chr5.CM0909.690.nc		LjT34P16	5	34.8-36.8
Glucan, water dikinase 1	2.7.9.4	CBM45	GWD1/SEX1/SOP1/R1	At1g10760	Q9SAC6	GWD1	chr4.LjT08E06.100.nc		LjT08E06	4	24,2
Glucan, water dikinase 2	2.7.9.5	CBM45	ATGWD2/GWD2	At4g24450	Q9STV0						
Glucan, water dikinase 3/phosphoglucan water dikinase	2.7.9.5	CBM20	ATGWD3/PWD/OK1	At5g26570	Q6ZY51	GWD3	chr5.LjT42F22.140.nc	chr5.LjT42F22.160.nc	LjT42F22	5	56,1
Phosphoglucan phosphatase	3.1.3.-	CBM48	ATPTPKIS1/SEX4	At3g52180	Q9FEB5						
Alpha-amylase 1	3.2.1.1	GH13	ATAMY1/AMY1	At4g25000	Q8VZ56	AMY1	chr5.CM0852.300.nc		LjT30K21	5	0,4
Alpha-amylase 2	3.2.1.1	GH13	ATAMY2/AMY2	At1g76130	Q8LFG1	AMY2	LjSGA_020916.1				
Alpha-amylase 3	3.2.1.1	GH13, CBM45	ATAMY3/AMY3	At1g69830	Q94A41	AMY3b	chr2.CM0608.610.nc		LjT38H08	2	40,3
						AMY3a	chr1.CM0410.400.nd		LjT26M18	1	31,3
Beta-amylase 1	3.2.1.2	GH14	BAM1/BMY7	At3g23920	Q9LIR6	BAM1	LjSGA_011445.1	LjSGA_032725.2			
Beta-amylase 2	3.2.1.2	GH14	BAM2/BMY9	At4g00490	O65258						
Beta-amylase 3	3.2.1.2	GH14	BAM3/BMY8/CT-BMY	At4g17090	Q9SMW0	BAM3b	chr2.CM0021.1220.nd		LjT16A17	2	60,9
						BAM3a	chr2.CM0021.1150.nd	chr2.CM0021.1290.nd	LjT16A17	2	60,9
Beta-amylase 4	3.2.1.2	GH14	BAM4/BMY6	At5g55700	Q9FM68						
Beta-amylase 5	3.2.1.2	GH14	BAM5/BMY1/RAM1	At4g15210	P25853	BAM5	chr3.CM0152.120.nc		LjT45C16	3	64,8
Beta-amylase 6	3.2.1.2	GH14	BAM6/BMY5	At2g32290	Q8L762	BAM6	LjSGA_030993.1				
Beta-amylase 7	3.2.1.2	GH14	BAM7/BMY4	At2g45880	Q0WU61	BAM7	LjT34L14.60.nc		LjT34L14	0	
Beta-amylase 8	3.2.1.2	GH14	BAM8/BMY2	At5g45300	Q9FH80	BAM8	chr2.CM0803.520.nc		LjT10G21	2	49.3-50.1
Beta-amylase 9	3.2.1.2	GH14	BAM9/BMY3	At5g18670	Q8VYW2	BAM9	chr6.LjT15B19.140.nd		LjT15B19	6	49,9
Disproportionating enzyme/D enzyme	2.4.1.25	GH77	DPE1	At5g64860	Q9LV91	DPE1	chr1.CM0032.500.nc		LjT07E21	1	1,6
Transglucosidase	2.4.1.25	GH77, CBM20	DPE2	At2g40840	Q8RXD9	DPE2	LjSGA_007380.1	LjSGA_011298.1	LjT05B14	1	56,6
Alpha-glucan phosphorylase, plastidial	2.4.1.1	GT35	PHS1	At3g29320	Q9LIB2						
Alpha-glucan phosphorylase, cytosolic	2.4.1.1	GT35	ATPHS2/PHS2	At3g46970	Q9SD76	PHS2a	LjB08M07.80.nc		LjB08M07	0	
						PHS2b	chr2.CM0373.1170.nd		LjT47H03	2	17,7
Maltose transporter	n/a	n/a	MEX1/RCP1	At5g17520	Q9LF50	MEX1	chr3.CM0127.650.nc		LjT44D21	3	82,4

Table 6. Homologs in *L. japonicus* of the core set of genes encoding enzymes of starch metabolism in *A. thaliana*. Continued on next page.

Table 6. Homologs in *L. japonicus* of the core set of genes encoding enzymes of starch metabolism in *A. thaliana*. Continued.
The core set of *A. thaliana* genes was taken from information in Smith et al. (2004; 2005), Zeeman et al. (2007), Fulton et al. (2008) and Kötting et al. (2009). Candidate genes in *L. japonicus* were retrieved by searching the Miyakogusa genome database developed by the Kasuza DNA Research Institute (http://www.kazusa.jp/lotus/index.html; Sato et al., 2008), then manually analyzed at the level of predicted amino acid sequence. The table shows only the gene sequences retrieved with coverage greater than 30% and greater than 50% identity at the amino acid level with the *A. thaliana* homologous sequence. In cases where the translated sequence was found to be incomplete or mispredicted, the gene and protein prediction were performed manually. Protein sequences of all the predicted genes mentioned in this table can be found in annexe (Table A4). The map positions (in cM) are from the *L. japonicus* genetic map from a cross between MG-20 and Gifu. All markers are SSR markers, except those marked with an asterisk (*), which are dCAPS markers. The map position and markers that are underlined are the closest to the gene. Genes located on Selected Genome Assembly (LjSGA) sequences are unmapped (corresponding chromosome given as 0) since these sequences are not anchored to the genome. Additional information on the clones, including the corresponding contig, its accession number and marker sequences, is given in the Miyakogusa database (under 'Clone list'). No clones, LjSGA or EST sequence hits could be obtained in *L. japonicus* for three of the *A. thaliana* genes: *GWD2*, *BAM2* and *BAM4*. Several sequence hits could be identified for the genes *SS3, SS4, SBE1, SBE3, ISA3, SEX4, and PHS1*, but they could not be attributed as their homologs in *L. japonicus* with good confidence. Details of the bioinformatic analyses performed to generate this table are in Chapter 2, section 2.7.2. Abbreviations: EC number, Enzyme Commission number; CAZy family, describes the family of the functional domains (structurally-related catalytic and carbohydrate-binding modules) of the enzymes as given in the CAZy database; GH, Glycoside Hydrolases; GT, Glycosyl-Transferases; CBM, Carbohydrate-Binding Modules; Chr, Chromosome.

In order to confirm the correct annotation of the *L. japonicus* starch metabolism genes thus identified, and examine their phylogenetic relationship with other members of their gene family, I carried out a comprehensive phylogenetic analyis of all the starch gene families (Figure A2). For this, I performed an exhaustive search for homologous genes in fully sequenced plant genomes. This included the three eudicot species *A. thaliana*, *Vitis vinifera* (grapevine), and *Populus trichocarpa* (poplar), and the two monocot species *Oryza sativa* (rice), and *Sorghum bicolor* (sorghum). The rationale for restricting this analysis to fully sequenced genomes was to obtain a clear view of the extent of similarities and divergence existing between higher plant species in terms of isoform representation for each starch gene family, and to avoid the uncertainty as to whether a gene may be present in some species but absent in others because it is in a region of their genome not yet sequenced. I completed this analysis with subcellular localisation prediction of the protein sequences used to draw the phylogenetic trees. This was carried out using the two programs TargetP and Predotar (Chapter 2, section 2.7.1; Table A3). In some cases, I also performed careful examination of the multiple protein sequence alignment to investigate the likelihood, based on the conservation or not of key residues, that some genes may be pseudogenes or functional copies (Figure A3).

As expected, LjPGI1 and LjPGM1 clustered closely with AtPGI1 and AtPGM1, respectively (Figure A2A and Figure A2B), and were predicted to be plastidial (Table A3). Interestingly, I could identify two copies of the PGI1 gene in rice, both predicted to be

plastidial. Two copies of the PGM1 gene were also found in poplar although one of them (XP_00322433) was not predicted to be plastidial, most likely due to misprediction of its sequence in the N-terminal region (Figure A2A and Figure A2B, Table A3). Supprisingly, no distinct clades of plastial and non-plastidial isoforms could found for PGM, while the two phylogenetic clades observed for PGI clearly corresponded to plastidial genes in one clade, and to non-plastidial genes in the other (Figure A2A and Figure A2B).

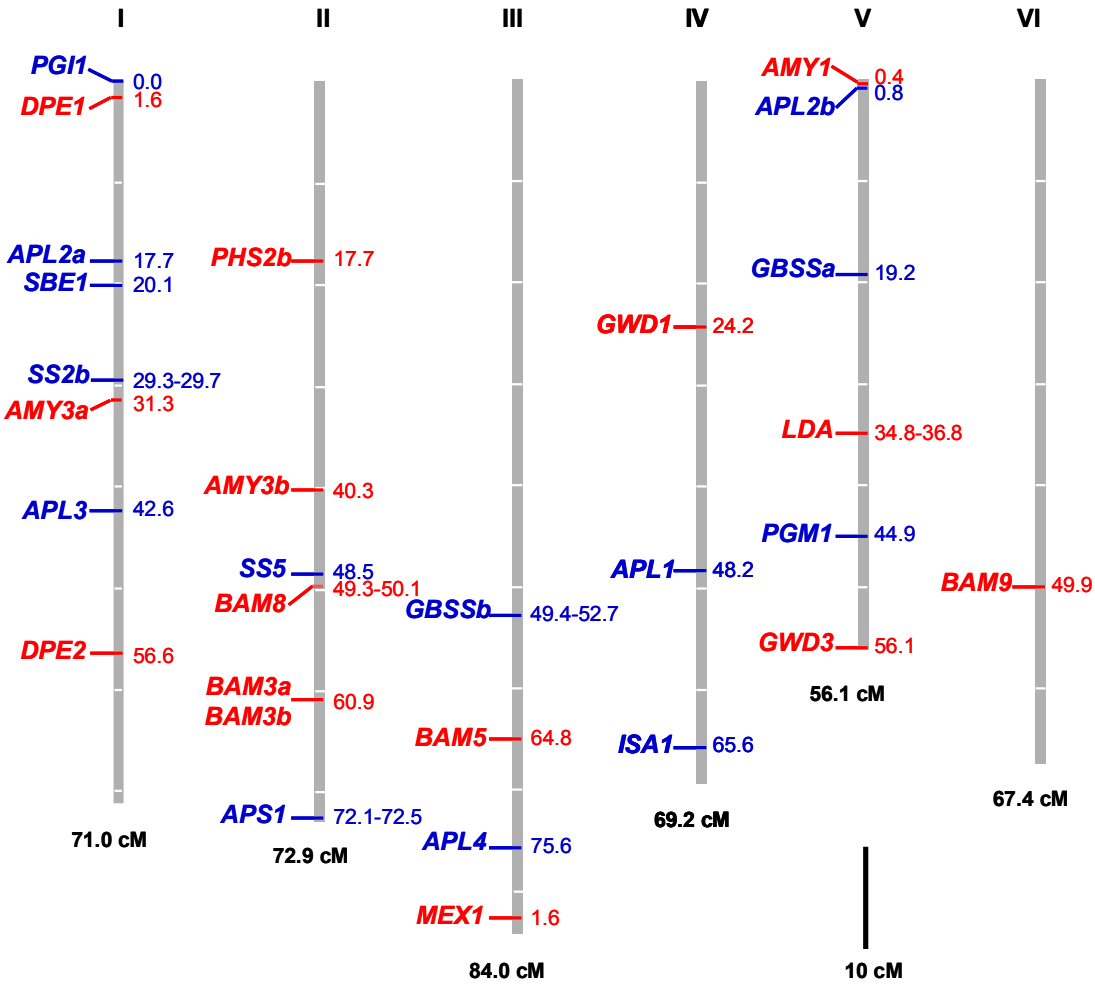

Figure 6. Molecular function map for starch metabolism in *L japonicus*.
Genetic linkage map of *L. japonicus* from a cross between the accessions Gifu and MG-20 (maternal and paternal parents, respectively) showing the position of the annotated starch metabolism genes listed in Table 6. The number and genetic distance in cM of each of the 6 linkage groups of *L. japonicus* are given at their top and bottom, respectively. Names of the genes involved in the starch synthesis and degradation pathway (in blue and red, respectively) are given on the left side of each chromosome and their position (in cM) are given on the right side.

I identified one gene encoding an AGPase small subunit (APS1) and six genes encoding the AGPase large subunit isoforms in the genome of *L. japonicus*. Interestingly, two copies of the gene encoding the AGPase large subunit isoform 2 (APL2) could be identified in *L. japonicus* and in poplar (Figure A2C). Duplicate copies of the *APL2* gene have thus far not been reported in other plant species (Georgelis et al., 2007 and 2008). Examination of the AGPase multiple sequence alignment revealed the absence of conservation, in LjAPL2b, of several amino acid residues very conserved across all other sequences analysed (Figure A3A). Some of these residues have been identified in previous studies to be crucial for the activity of the enzyme (Jin et al., 2005; Greene et al.,, 1998; Kavalki et al., 2001; Chapter 5, section 5.2.1 and reference therein). This suggests that LjAPL2b may not be a functional copy. It is also interesting to note that proteins belonging to this APL2 group were present in all eudicot species analysed (*A. thaliana*, poplar, grapevine, and *L. japonicus*) but absent from the genome of the two monocot species rice and sorghum (Figure A2C).

While only four large subunit (LS) isoforms have been identified in *A. thaliana*, five of them could be identified in *L. japonicus*. Homologs of LjAPL5 could also be found in the genomes of grapevine, poplar, and rice (Figure A2C). The existence of this fifth LS isoform of AGPase has only recently been mentioned in the literature (Georgelis et al., 2007) and its function has not yet been studied. Analysis of the conservation of the key residues in APL5 revealed that LjAPL5 may not be functional, in contrast to its homologs (Figure A3A).

All but one species analysed encoded two proteins homologous to AtAPL3/AtAPL4. Grapevine was the only species to encode only one. Overall, there was a higher level of identity at the amino acid level between LjAPL3 and LjAPL4 on one hand, and AtAPL3 and AtAPL4 on the other (82 and 84% identity, respectively), than between LjAPL3 and AtAPL3, and between LjAPL4 and AtAPL4 (69 and 68% identity, respectively). This was also the case for poplar (Figure A2C). This observation suggests that the duplication event in these eudicot species took place after their speciation. The closest homologs of these AGPase isoforms in rice and sorghum formed a separate clade (named 'monocot APL3/4') with two members in each species (Figure A2C). Lastly, two small subunit (SS) *APS1* genes were identified in rice and in sorghum. Homologs of the *A. thaliana* pseudogene *APS2* were also found in poplar (two *APS2* gene copies), and in grapevine. No homologs of this gene could be identified in the genome of monocots.

Six classes of starch synthase have been identified in plants: GBSS, SS1, SS2, SS3, SS4, and SS5. Two *GBSS* and two *SS2* genes could be identified in the genome of *L. japonicus*. Poplar, grapevine, rice, sorghum, wheat (*Triticum aestivum*), barley (*Hordeum vulgare*), and several legume species including pea (*Pisum sativum*) also have two GBSS genes (Figure A2D; Edwards et al, 2002; Pan et al., 2009). Three *SS2* genes have been identified in several cereal species including rice, sorghum, wheat, and maize (Pan et al., 2009). In eudicots, most

other members of the legume family have two *SS2* genes (Pan et al., 2009), and so do other eudicot species including poplar and grapevine (Figure A2D; Pan et al., 2009). An homolog of the *AtSS5* gene was present in all the plant genomes analysed except sorghum. The function of the enzyme encoded by these *SS5* genes is still unknown (Deschamps et al., 2008b). The predicted AtSS5 protein is truncated at the C-terminus while OsSS5 is truncated at the N-terminus in comparison to their SS5 homologs; therefore, these two proteins are likely to be pseudogenes unless their sequence has been mispredicted (Figure A3B). Lastly, while only one *SS3* and one *SS4* gene were found in the genome of each eudicot species, two copies of SS3 and two copies of SS4 could be identified in the genome of sorghum and rice, respectively (Figure A2D; Yan et al., 2009).

The *L. japonicus* genome contains two genes for each of the starch degrading enzymes AMY3 and BAM3. Two copies of *AMY3* and *BAM3* are also present in the genome of grapevine and poplar, respectively (Figure A2H and Figure A2I). In contrast, the genome of *A. thaliana* contains only one AMY3 and one BAM3 gene. The copy number for the other AMY and BAM genes also varies from one species to another. Thus, the poplar and grapevine genomes have two copies of *AMY1* while other species have only one. Poplar also has two copies of *BAM1*. In contrast, only one homolog of the *A. thaliana* and *L. japonicus* *BAM5* and *BAM6* genes could be identified in the genome of grapevine, poplar, rice, and sorghum. Similarly, the *BAM4* gene could only be identified in *A. thaliana* and grapevine, and no homolog of *BAM7* could be found in monocot genomes or the genome of poplar. I also identified a large, monocot-specific group of genes encoding AMY1-like proteins constituted of seven members in rice, and five in sorghum that clustered apart from the eudicot AMY1 group. Most proteins of these two groups are predicted to be secreted (Table A3). This localisation in the secretory pathway was experimentally demonstrated in case of the AtAMY1 protein (Doyle et al., 2007). Both LjBAM5 and AtBAM5 are also predicted to be part of the secretory pathway (Table A3).

Two copies of PHS2 could be identified in the genome of *L. japonicus*. This duplication event was not seen in any other plant species genome analysed in this study. However, grapevine and poplar possesses two copies of *PHS1*. In addition, the phylogenetic analysis I performed identified a putative new PHS isoform group consisting of a sequence from each of poplar and grapevine. To the best of my knowledge, neither of these two proteins has yet been characterised and their functions remain unknown.

3.2.3. Analysis of the expression pattern of the starch metabolism genes across organs in *L. japonicus*

To get insight into the relative levels and patterns of expression of of all the starch metabolism genes I identified in *L. japonicus*, I analysed their transcript levels using existing microarray data obtained from several different organs including leaves, stems, flowers, and nodules, as well as several samples of a time course for pod and seed development. The Affymetrix microarray data used for this study were obtained from the 'Lotus Gene Expression Atlas' assembled by Andry Andriankaja and Michael Udvardi (personal communication; Samuel Roberts Noble Foundation, Ardmore, Oklahoma). Transcript level analysis was carried out as described in Chapter 2, section 2.8. A detailed description of the organs analysed is presented in Table 4 and a list of correspondence between probesets and gene names is given in Table A1. Results of the analysis of the expression pattern of the core set of starch metabolism genes in these different organs are presented in Figure 7.

The *LjPGI1*, *LjPGM1* and *LjAPS1* genes were expressed in all the organs analysed. *LjAPL1* was the main LS isoform expressed in leaves, with lower expression in petiole, stem, and flowers, and very little to no expression in roots, nodules, pods and seeds. In contrast, *LjAPL3* exhibited the highest expression level among the LS genes in all organs, except in leaves and petiole where its expression level was lower than that of *LjAPL1*. *LjAPL2a* was only very weakly expressed in leaves, but it was the second most highly expressed LS isoform in every other tissue. In contrast, the second gene copy of *LjAPL2* (*LjAPL2b*) and *LjAPL5* did not display any significant level of expression in any of the organs analysed suggesting they may not be functional. Transcript level of *LjAPL4* was at the threshold of detection across all organs analysed. It is interesting to note that the expression of *LjPGM1, LjAPS1, LjAPL2a, and LjAPL3* was up-regulated in nodules in comparison to inoculated roots.

Both the *LjSS1* and *LjSS2a* genes were expressed in all the organs analysed. Transcript level of *LjSS1* was higher than that of *LjSS2a* in leaves, petioles, stems, flowers and pods while the opposite was found in roots, nodules and seeds. In contrast, *LjSS2b* was very weakly expressed, and only in leaves. Both copies of the *LjGBSS1* gene were significantly expressed across all organs, except in roots where the transcript level of *LjGBSS1b* was very low. In all organs, the expression level of *LjGBSS1a* was much higher than that of *LjGBSS1b*. An interesting pattern of expression could be seen for the *LjSS5* gene. Transcripts of this gene were present in leaves, petiole, stem, pods, and seeds, but not in roots or flowers. Across all organs, its transcript level was the highest in nodules at 21 days post inoculation (dpi). Its absolute transcript level in this tissue was over 15 times higher than in inoculated roots at 0 dpi. The expression of *LjGBSS1a, LjGBSS1b* and *LjSBE2* were also higher in nodules than in inoculated roots.

Figure 7A

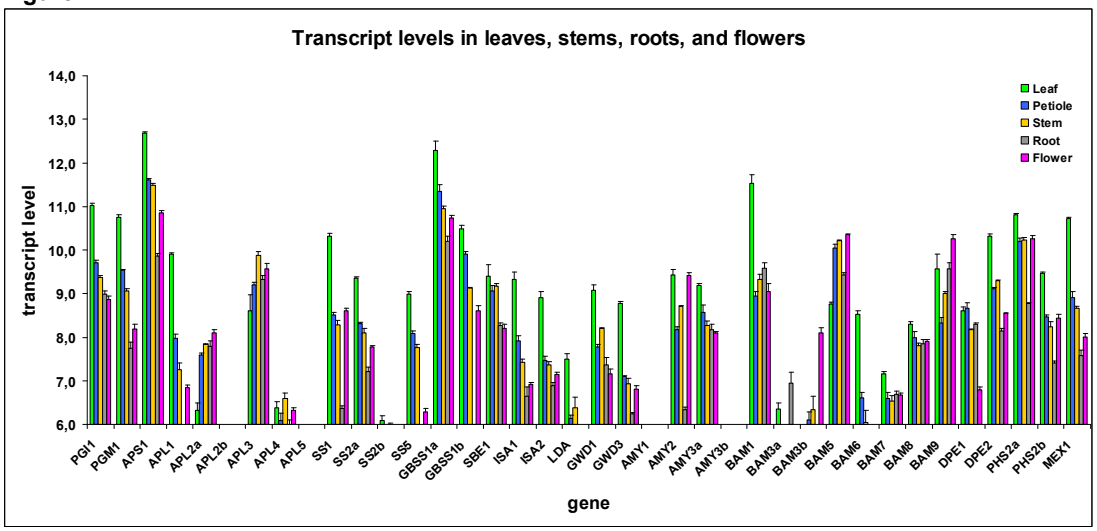

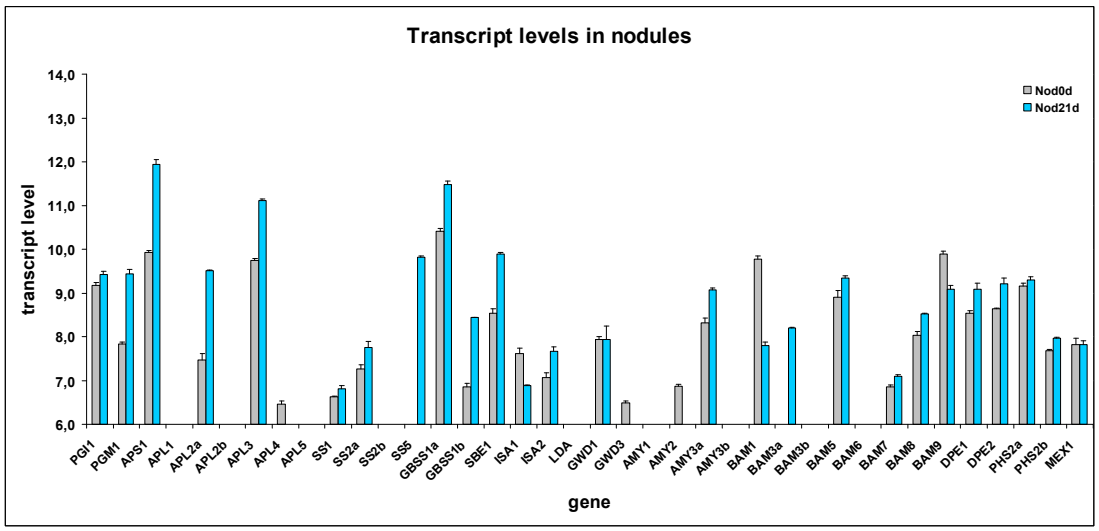

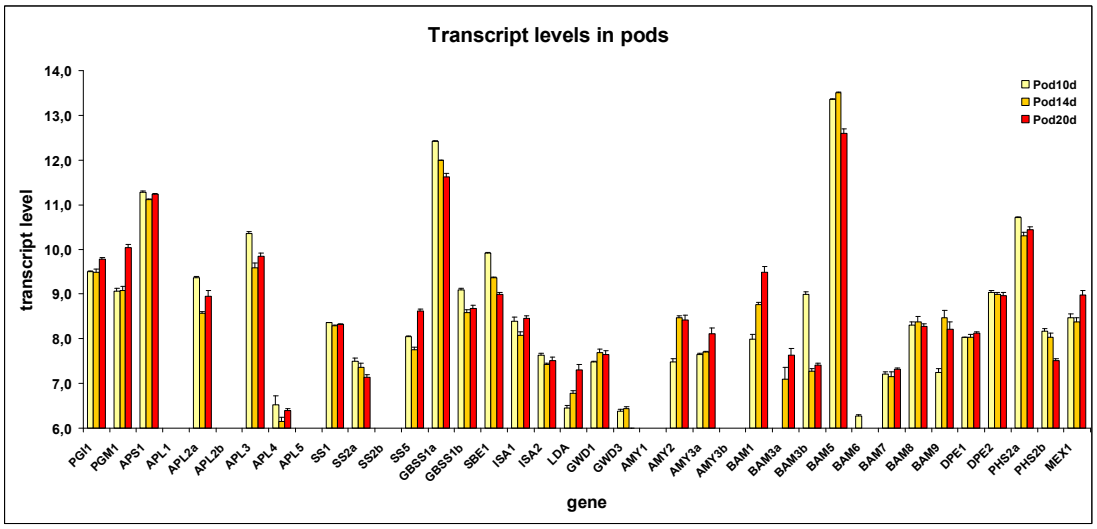

Figure 7. Transcript levels of the core set of starch metabolism genes in different organs of *L japonicus.*

Continued on next page.

Figure 7A continued

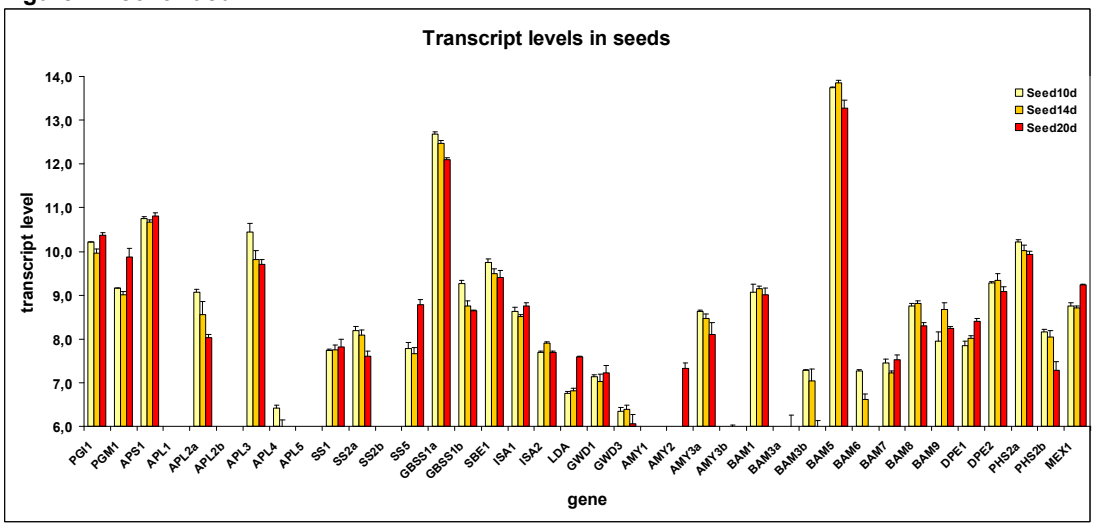

Figure 7B

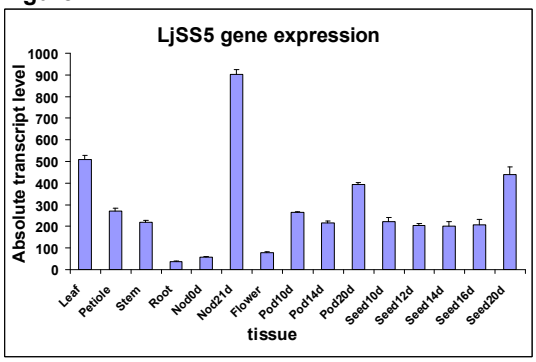

Figure 7. Transcript levels of the core set of starch metabolism genes in different organs of *L japonicus.* Continued
A. Log2 transformed transcript levels of the starch metabolism genes across tissues derived from Affymetrix gene chip data, and **B.** Expression pattern of *LjSS5* across tissues. Transcript level values were retrieved from the 'Lotus Gene Expression Atlas' assembled by Andry Andriankaja and Michael Udvardi (personal communication; Samuel Roberts Noble Foundation, Ardmore, Oklahoma), and processed as described in Chapter 2, section 2.8. A correspondence between the Lotus starch metabolism genes and their probe sets and the probe sets' absolute transcript levels is given in Table A1. For each gene, bars from left to right correspond to its transcript levels in each of the organs mentioned in the title of the graph (same order). Abbreviations: A description of the organs analysed can be found in Table 4 (Chapter 2). The plant materials were harvested 3 hours after 'dawn' from plants grown under long day conditions. RNA isolation, probe preparation, array hybridisation and normalisation of the data were also carried out as described by Benedito *et al.*, 2008. Values are means ± SE of three biological replicates.

LjGWD1 transcript was present at a significant level in all organs. Levels of *LjGWD3* transcript were similar to those of *LjGWD1* in leaves, but lower in all other organs, especially in root and nodules. Members of both *BAM* and *AMY* gene families had organ-specific patterns of expression. At the time point used in this study, *LjBAM1* was the main *BAM* isoform expressed in leaves, where it was highly expressed, whereas *LjBAM5* was the main isoform expressed in petioles, stems, seeds, and pods. In seeds and pods, its level of expression was very high. *LjBAM6* was only significantly expressed in leaves while

LjBAM7, LjBAM8, and *LjBAM9* were expressed in all organs. The expression of *LjBAM3a* and *LjBAM1* were up- and down-regulated, respectively, in nodules in comparison to inoculated roots. *LjAMY1* and *LjAMY3b* transcript levels were low across all the organs analysed while the genes *LjDPE1, LjPHS1a, LjPHS1b*, and *LjMEX1* were significantly expressed in all organs.

To validate the robustness of this analysis, the transcript level of four of the six members of the sucrose synthase gene family in *L. japonicus* (*LjSUS1, LjSUS2, LjSUS3, and LjSUS4*) was also analysed the same way (Table A1 and Figure 8). The pattern and level of expression thus obtained for these genes were compared to the one obtained by qRT-PCR by Horst et al. (2007). Results from these analyses were very similar: *LjSUS1* was the main isoform expressed in leaves, stem and flowers whereas *LjSUS3* was the most highly expressed isoform in roots and nodules. Further, the expression of *LjSUS3* was enhanced in nodules in comparison to its expression level in all the other organs. Consistent with this expression pattern, *LjSUS3* was shown to be important for nodule function (Horst et al., 2007).

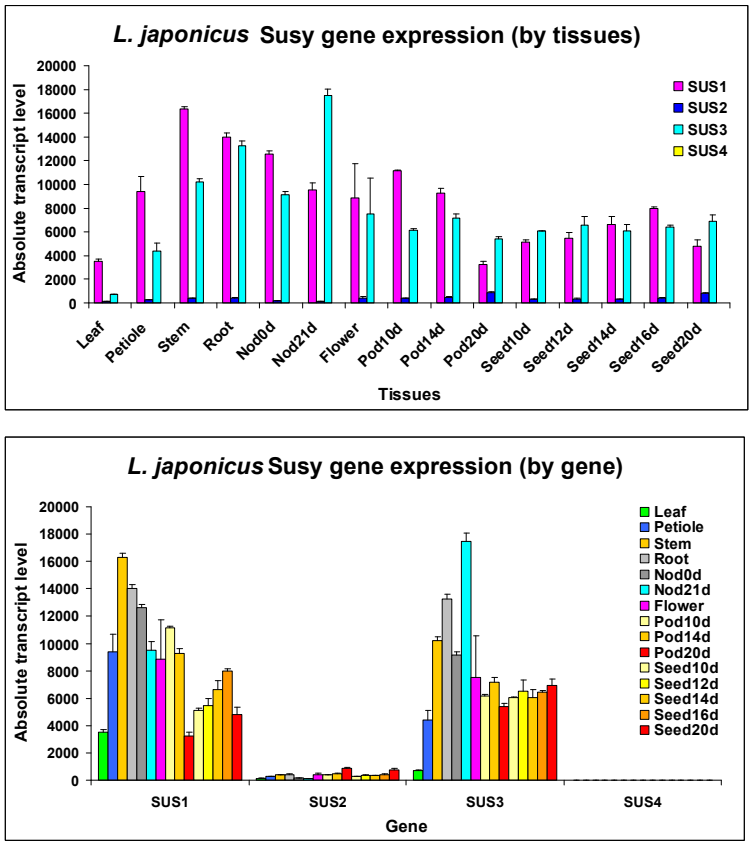

Figure 8. Transcript levels of the sucrose synthase genes *LjSUS1* to *LjSUS4* across organs.
These genes for which the pattern of expression has been determined by qRT-PCR in a previous study (Horst et al., 2007) were used as controls to validate the relevance and reliability of the starch metabolism gene expression analysis carried out using the Lotus Gene expression Atlas.

3.2.4. Diurnal turnover of leaf starch in MG-20 and Gifu accessions of *L. japonicus*

To examine the extent of diurnal starch turnover in leaves of *L. japonicus*, starch contents was measured at the end of the day and the end of the night at two week intervals during the growth of plants of the WT MG-20 and Gifu B-129. Measurements were made on fully-expanded leaves harvested from plants grown in a controlled-environment chamber with 12 h light, 12 h dark. Results of iodine staining showed an increase in leaf starch content in MG-20 and Gifu plants as they matured (Figure 9). This was confirmed by quantification of starch content (starch assays done by Marilyn Pike, JIC). For the first six weeks of growth, the two accessions showed similar, strong diurnal changes in starch content, with a starch content at the end of the day in excess of 7.5 mg starch g^{-1} fresh weight and a content at the end of the night of less than 0.6 mg g^{-1} fresh weight (Figure 10). As the *L. japonicus* plants matured, a gradual accumulation of transitory starch was observed in their leaves, both at the end of day and at the end of the night. At eight weeks, the diurnal amplitude of change in starch content remained the same, but leaves had a starch content at the end of the day of approximately 14 mg g^{-1} fresh weight and retained approximately 5 mg starch g^{-1} fresh weight in their leaves at the end of the night. Between eight and ten weeks there was a dramatic increase in leaf starch content. In Gifu, a diurnal turnover of about 10 mg starch g^{-1} fresh weight was maintained but starch content at the end of the night was 20 mg g^{-1} fresh weight. In MG-20 ten week-old plants, starch content was over 50 mg g^{-1} fresh weight throughout the diurnal cycle.

I completed this analysis by the measurement of leaf starch in MG-20 and Gifu plants grown under two different growth conditions. A clear accumulation of starch in leaves as the plant matured was also observed in other growth conditions (Figure 11). In addition, I carried out starch content measurements on fully-expanded leaves of eight week old plants, in a controlled-environment chamber, under two different photoperiod lengths: 'short day' (12 h light, 12 h dark) and 'long day' (16 h light, 8 h dark) conditions. Leaf starch contents were higher in plants grown in 16 h than in 12 h photoperiod (Figure 12). The leaf starch content was much higher in MG-20 than in Gifu in both photoperiods. The amount of transitory starch diurnally turned over was ca. 50 mg starch g^{-1} fresh weight in MG-20 plants grown in a 12h photoperiod. In contrast, in 16 h photoperiod, only the accession Gifu showed a clear diurnal turnover of starch. Under this photoperiod length, the amount of starch measured in leaves of MG20 was extremely high and was maintained at about the same level throughout the diurnal cycle (ca. 180 mg starch g^{-1} fresh weight at the end of the day and at the end of the night; Figure 12). However it is worth nothing that such differences in the pattern of starch accumulation and turnover between MG-20 and Gifu plants were not seen under all growth conditions. When grown in a glasshouse under natural light conditions

and not supplemented with any artificial lighting, both accessions accumulated similarly high amount of starch in their leaves, and no significant diurnal remobilisation of starch was observed in either accession (Figure 13 and Figure 14).

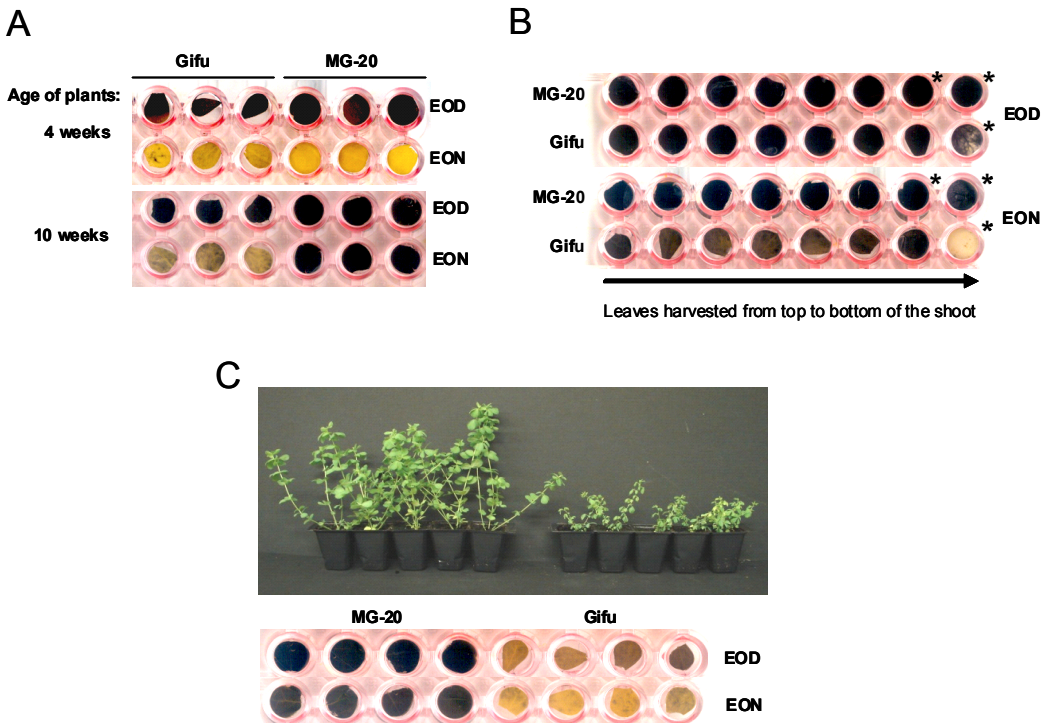

Figure 9. Iodine staining of leaves of MG-20 and Gifu plants.
A. Iodine staining of leaflets of four and ten week-old *L. japonicus* MG20 and Gifu plants harvested at the end of the day (EOD) and the end of the night (EON), at the same time as the samples for the quantitative measurements of starch content shown in Figure 10. Each leaflet is from a different plant. **B.** Iodine staining of leaflets of ten week-old plants harvested from the top to the bottom of the shoot. Senescing leaves (i.e. Leaves close to abscission that displayed chlorosis symptoms) are indicated by an asterisk. **C.** Eight week-old plants of MG-20 and Gifu, at the time of harvesting of the leaf samples for the quantitative measurements of starch content shown in Figure 12, and iodine staining of leaflets of the two accessions at the end of the day (EOD) and the end of the night (EON) in 12h light, 12h dark. Each leaflet is from a different plant.

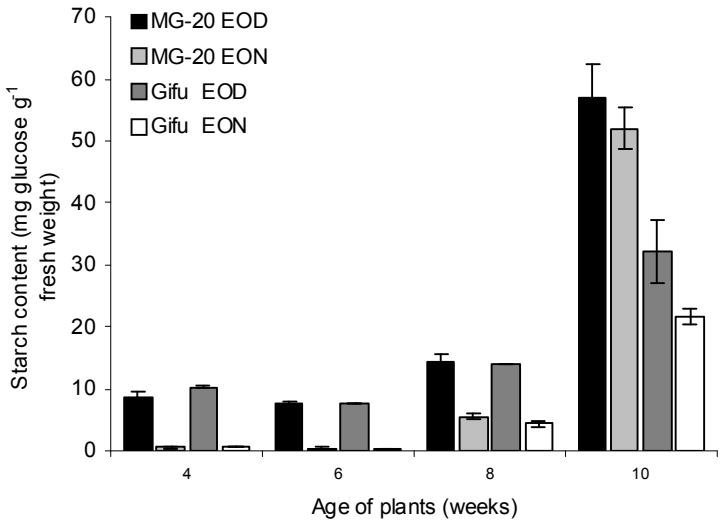

Figure 10. Diurnal changes in leaf starch content through development in *L. japonicus* MG-20 and Gifu plants.
Plants were grown in 12 h light, 12 h dark in a controlled environment chamber. Mature leaves were harvested at the end of the day (EOD) and the end of the night (EON) and assayed for starch content at the indicated times after germination (four to ten week-old plants). Values are means ± SE of measurements on six samples, each of which consisted of 3 fully expanded leaves taken from the top of the shoot of two plants.

3.2.5. Pattern of starch and sugar accumulation across organs in MG-20 and Gifu accessions of *L. japonicus*

Starch and soluble sugar contents were also quantified across organs. Measurement of starch (and soluble sugars) content were performed on samples harvested at the end of a 16 h photoperiod from six and ten week-old MG-20 plants grown in a CER, and from eight week old MG-20 and Gifu plants grown in greenhouse. Leaves were found to contain the highest amount of starch in both conditions (Figure 11 and 13). Stems and pods had relatively low starch contents but had a much higher levels of soluble sugar (sucrose, glucose and fructose) than in leaves (Figure 11). In roots, the starch content was also low in comparison to leaves with most of the starch accumulating in its upper part (crown and primary root). Similar levels of starch across organs, including leaves, were found for MG-20 and Gifu plants grown in natural light, long day conditions (Figure 13).

One difficulty of studying the metabolism of starch in a legume species such as *L. japonicus* is its upright stature and tendency of the stem to lodge and the plant to become bushy when getting older, resulting in different level of exposure of the leaves to light, some being shaded by others. Possibly, this may well have an effect on the amount of starch being accumulated from one leaf to another. In additions, differences in the metabolism of starch may also exist between younger and older leaves. For these reasons, iodine staining and starch quantification of *L. japonicus* leaves were always performed, unless otherwise

indicated, on fully developed leaves from the top of the plant. However, results of preliminary analysis in which leaves of different maturation stage were harvested from different height of the stem of MG-20 and Gifu plants and stained with iodine did not reveal any strong difference in terms of starch content and its diurnal turnover (Figure 9). Nevertheless, a remobilization of the carbon stored as starch before leaf abscission was observed by iodine staining in only one of the two *L. japonicus* accessions analysed. Leaves of MG-20 ready to abscise (i.e. oldest leaves at the bottom of the shoot, characterised by senescence symptoms such as decrease in chlorophyll content) still contained large amount of starch, at a level that appeared similar to those found in mature, non-senescing leaves. In contrast, Gifu leaves close to abscission contained less starch than the others, suggesting that starch in these leaves was being remobilised and the carbon derived from it exported elsewhere in the plant prior to abscission (Figure 9).

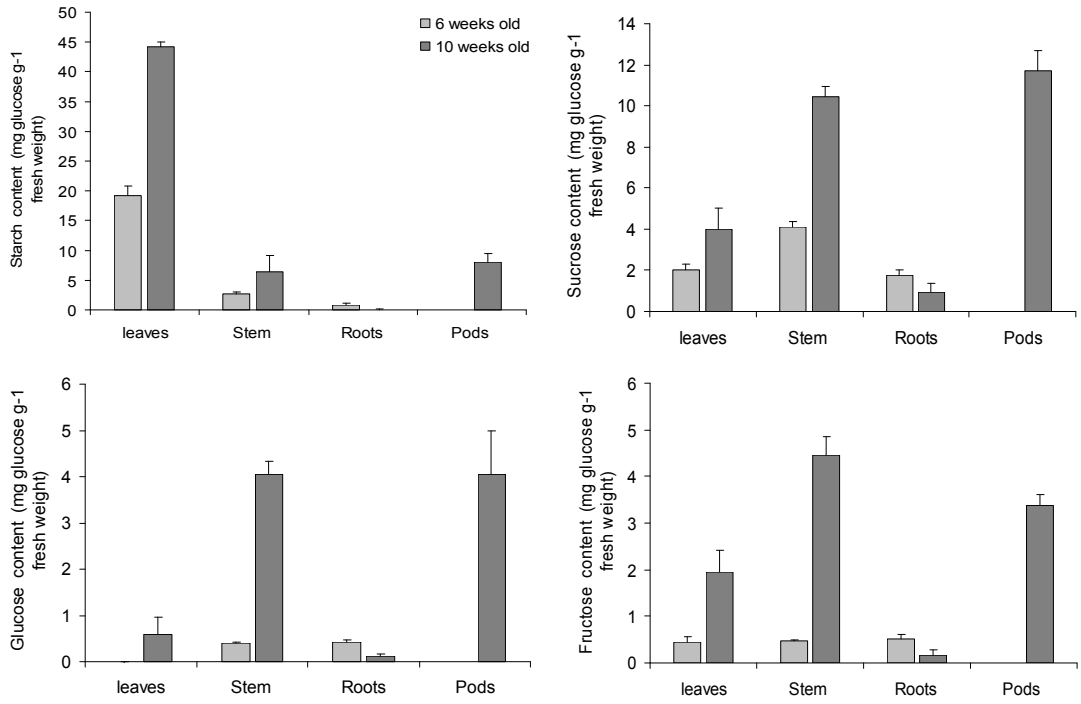

Figure 11. Starch and soluble sugar content across organs and through development in *L. japonicus* MG-20 plants.
MG-20 plants were grown in compost, in a controlled environment room (CER) in 16 h light, 8 h dark. Samples were harvested at the end of the day from six and ten weeks-old plants. In these growth conditions, and at the time of the harvesting of the samples, six weeks-old plants had just started to flower while ten week old plants were bearing green pods. Values are means ±SE of measurements on three biological replicates of sample, each from a different plant.

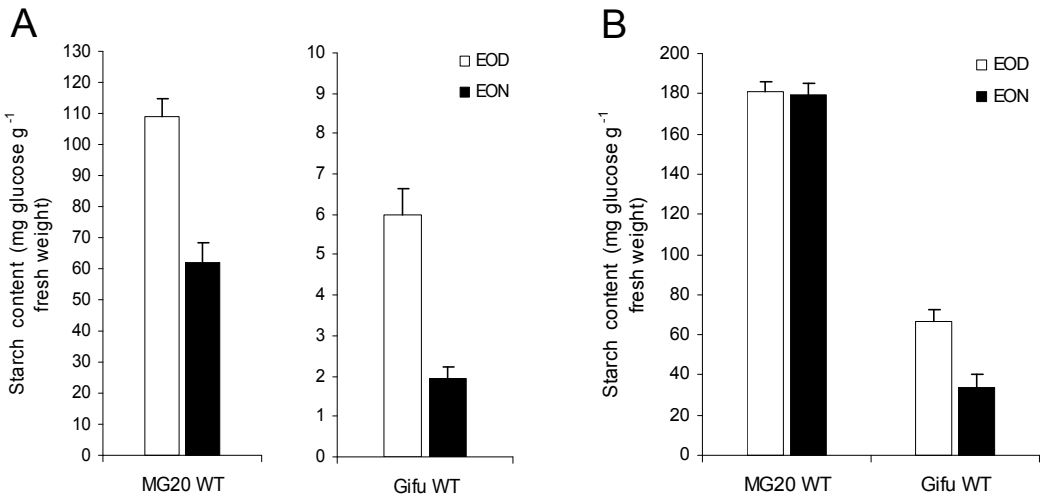

Figure 12. Diurnal changes in leaf starch content of eight-week old *L. japonicus* MG-20 and Gifu plants grown under two different photoperiods.
Plants were grown in a controlled environment chamber, either in 12 h light, 12 h dark (A) or in 16 h light, 8 h dark (B). Starch content (mg Glc equivalents g^{-1} fresh weight) was measured in leaves harvested at the end of the day (EOD) and the end of the night (EON). Values are means ±SE of measurements on six samples, each from a different plant. Each sample consisted of 4 to 8 fully-expanded leaves taken from the upper part of the shoot. MG-20 plants growing in the 16 h photoperiod were flowering at the time of the sample harvesting.

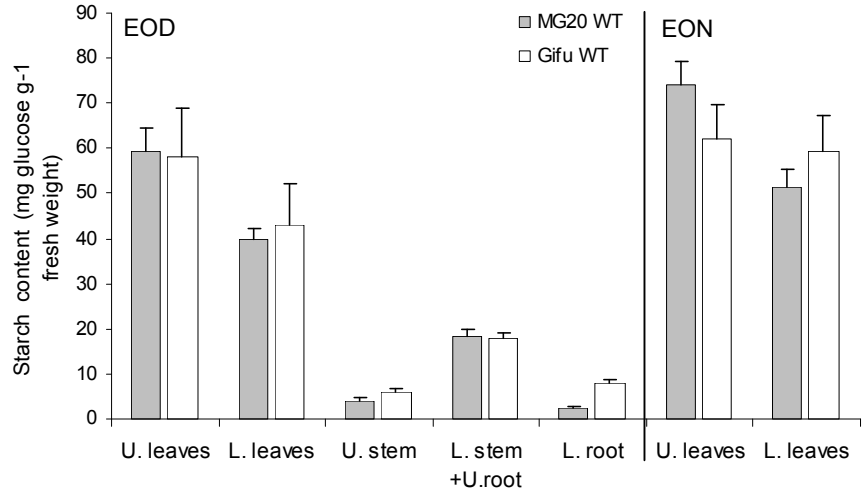

Figure 13. Starch content diurnally and across organs in eight week-old Lotus japonicus MG-20 and Gifu plants.
Plants were grown in a greenhouse in natural light, long day conditions (ca. 16h light/8h dark photoperiod, from April to June 2007). Plants were grown in perlite:vermiculite (1:1) and fed twice a week with a nutrient solution (composition given in Chapter 2) following germination of the seeds in compost. Under these growth conditions, MG20 plants had just started to flower at the time the samples were harvested. Values are means ±SE of measurements on four biological replicates, each of which consisted of samples taken from two plants. Abbreviations: EOD, end of day; EON, end of night; U., upper; L., lower. Upper and lower leaves refer to the first 3 to 5 leaves from the top and bottom of the shoot of the plants, respectively. Lower stem and upper roots correspond to the crown root and the first ca. 2 cm of stem at the base of the shoot. Lower roots consisted mostly of secondary roots.

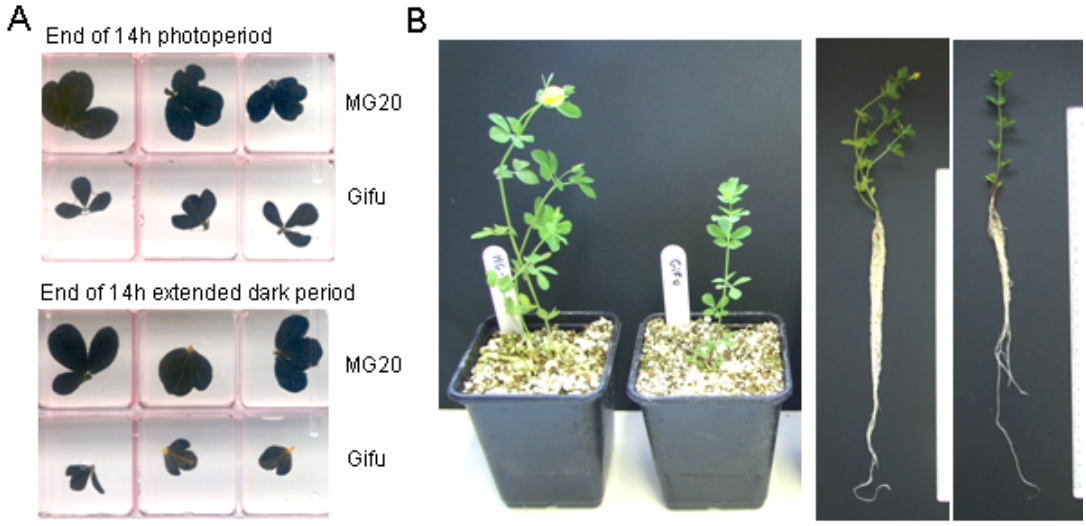

C

	MG20		Gifu	
	mean	SE	mean	SE
Shoot height	16,6	0,2	9,1	0,7
Root length (average)	21,4	0,6	16,0	0,4
Root length (maximum)	30,5	3,4	22,8	1,9
Shoot and root length	37,9	0,5	25,1	0,7
Leaves FW	0,564	0,083	0,164	0,015
Number of leaves	14,75	0,63	11,50	1,44
Average leaf FW	0,038	0,005	0,015	0,002
Stem FW	0,307	0,049	0,046	0,007
Shoot FW	0,945	0,118	0,262	0,014
Root FW	0,935	0,146	0,299	0,024
Shoot and root FW	1,917	0,272	0,581	0,037
Shoot and root DW	0,244	0,029	0,087	0,005
Dry weight/FW in %	12,89	0,44	14,94	0,15
Shoot:Root ratio	1,04	0,07	0,89	0,05

Figure 14. Phenotype and growth parameters of *L. japonicus* MG-20 and Gifu plants, and iodine staining of their leaves.
A. Iodine staining of leaves of four week-old MG-20 and Gifu plants at the end of the day (EOD) and the end of an extended night (EON). Each leaf is from a different plant. **B.** Phenotype of eight week-old MG-20 and Gifu plants representative of several biological replicates. **C.** Growth parameters of eight week-old plants of the two genotypes. Values are means ± SE of four biological replicates. Plants were grown in perlite:vermiculite (1:1) in a greenhouse under natural light, long day conditions. Shoot and root height/length are in cm; fresh weights (FW) and dry weights (DW) are in g.

3.3. Discussion

3.3.1. *L. japonicus* and *A. thaliana* share similar starch metabolism gene families but also display interesting divergences

I investigated the extent to which the genes known to be important for starch metabolism in *A. thaliana* and other plant species are conserved in the model legume *L. japonicus*. Recent progresses in EST and genome sequencing in *L. japonicus* allowed me to identify the

starch metabolism genes in this species. Genes encoding members of all class of enzymes known to be involved in the pathway of starch metabolism in *A. thaliana* and other species were found in *L. japonicus*. However, new members of the different starch gene families will certainly continue to be identified as more genome sequences become available. In total, 38 starch metabolism genes were detected in the *L. japonicus* genome that covered all the starch gene families encoded by 41 genes in *A. thaliana* (Table 6). The *L. japonicus* homologs of 30 of these genes could be identified with good confidence (Table 6). Overall, results of my bioinformatic analyses revealed a high level of conservation between genes involved in starch metabolism in *L. japonicus* and *A. thaliana* and other higher plant species (Figure A2).

All but eight of the 38 genes I identified could be anchored to the genetic linkage map of *L. japonicus*. This core set of starch metabolism genes were mapped according to the results of gene prediction analyses and the information made available from the Miyakogusa database. Relatively recently, this database has been updated (May 2008) to include a comprehensive list of all the predicted genes and encoded protein sequences. Before then, genome sequences were retrieved and the gene and protein prediction were performed manually as described above (Chapter 2, Section 2.7.2). My work created the first *L. japonicus* molecular function-map for starch metabolism. Use of this information for a candidate gene approach aiming at identifying the mutations isolated from forward genetic screens for altered starch metabolism is presented in the next chapter (Chapter 4, Section 4.2.2). In the future, the information given here could also accelerate the identification of genes underlying QTLs in *L. japonicus* for the study of starch metabolism-related traits and their interaction with other traits.

Genes encoding the glucan, water dikinase GWD2 and the β-amylases BAM2 and BAM4 could not be found in the genome of *L. japonicus* (Table 6) and no sequences could be attributed with good confidence as encoding the *L. japonicus* homolog of SS3, SS4, SBE2, SBE3, ISA3, SEX4, and PHS1. Three main hypotheses can be advanced to explain this. Firstly, these genes may be present, but in a region of the genome not yet sequenced (to date 67% of the *L. japonicus* genome representing about 93% of the gene space has been sequenced; Sato et al., 2008). Secondly, these genes could be expressed at too low a level for their transcripts to be detected and represented in the EST collection. Lastly, there may be differences in the composition of some of the gene families between the two species, and these genes may simply be absent from the genome of *L. japonicus*. One analysis that could be carried out to help rule out one or other of these possibilities would be to search for homologs in the genome and EST database of other plant species, including other legume species (e.g. soybean, *Medicago*). If such genes cannot be identified in the genome of other (legume) species, then it is possible to speculate they may simply be absent. AtGWD2 for instance does not play a crucial role for starch degradation in *A. thaliana*, and its presence in

the plant kingdom appears to be restricted to a small number of eudicot species (Figure A2G). Indeed, homologs of AtGWD2 could only be identified so far in the genome of *Ricinus communis* (XP_002527361) and *Citrus clementina* (Glaring et al., 2007). It is entirely possible, therefore, that GWD2 genes may have been lost through evolution in *L. japonicus* as in other species by lack of selective pressure to maintain them. In contrast, the genes encoding SEX4, ISA3, SS3 and SS4 are more likely to be present in the *L. japonicus* genome, but in a region not yet sequenced, since these enzymes have been shown to be essential for starch metabolism in *A. thaliana* (Edner et al., 2007; Zeeman et al., 2007a and b; Kotting et al., 2009; and references therein). Similarly, homologs of SBE2, SBE3, BAM2, and PHS1 are most likely present in the genome of *L. japonicus* given their widespread occurrence among higher plant species (Figure A2).

Some genes known to be present in single copy in *A. thaliana* were found in multiple copies in *L. japonicus*. This was the case for the genes encoding APL2, SS2, GBSS, AMY3, BAM3, and PHS2 (Table 6; Figure A2). In *L. japonicus*, one gene encoding for each for the following AGPase subunits - APS1, APL1, APL3, APL4, and APL5 - has been identified. In contrast, two genes were found to code for the APL2 isoform (Figure A2C). It appears that a duplication of this gene also occurred in poplar. This is the first time, to the best of my knowledge, that a duplication of this gene in higher plant species is reported. However, analysis of their protein sequence for the conservation of key residues for activity suggests that the *LjAPL2b* gene may not be a functional copy (Figure A3A).

In contrast to the genome of *A. thaliana* that encodes only four LS isoforms, genes encoding a fifth LS isoform (named APL5) could be identified in *L. japonicus* as well as in grapevine, poplar, and rice. To the best of my knowledge, none of these APL5 protein have yet been characterised and their functions remain unknown. LjAPL5 lacks several conserved amino acid residues, suggesting that this isoform may not be functional. In contrast, there is no evidence to suggest that its homologs in grapevine, poplar, and rice are non-functional (Figure A3A).

Homologs of both *LjAPL3* and *LjAPL4* genes are present in other eudicot species including *A. thaliana*, grapevine and poplar. In contrast, only one homolog of these two genes has thus far been identified in pea (Patron and Keeling, 2005; Georgelis et al., 2007; Yan et al., 2009; Figure A2C). Two possibilities can be advanced to explain the presence of these two closely related isoforms in some plant species and not others. First, the full genome sequence is not yet complete for several of the plant species mentioned above, and these genes may be found later. Second, the duplicated gene copies could have originated from a whole genome duplication (WGD) event, and then have been lost in several species, but conserved in other. Differences in tissue or developmentally specific expression (sub-functionalisation) could explain why some of the duplicated genes would have been lost and other retained.

Alternatively, tandem duplication events could have occurred independently in some plant species but not in others after their speciation. Results of the analyses I performed reveal that the two *APL3* and *APL4* homologs in *A. thaliana, L. japonicus*, and poplar are more closely related with each other than with their closest homolog in the other species (Figure A2C). This strongly suggests that the duplication event occurred after their speciation. This also seems to be the case in wheat, but not in maize and rice. In these species, *APL3* and *APL4* seem to have arisen from a WGD event that occurred prior to their speciation (Patron and Keeling, 2005; Yan et al., 2009; Figure A2C).

Overall, evolutionary analyses reveal a complex phylogenetic relationship for members of the AGPase gene family. This is particularly true for the LS that has undergone a larger number of duplications than the SS genes. Interestingly, the inclusion of the AGPase genes identified in genome of the moss *Physcomitrella patens* (seven LS and four SS genes) into the phylogenetic analysis carried out by Georgelis et al. (2008) suggests that the earliest duplication in the LS occurred prior to the divergence of angiosperms and mosses, more than 400 million years (Mya) ago. The SS shows a much higher level of conservation among species than the LS. Nonetheless, the two subunits exhibit similar sensitivities to activity-altering amino-acid changes, at least when expressed heterogously in bacteria (Georgelis et al., 2007). To explain this higher evolutionary rate seen for the plant AGPase LS than for the SS, Smith-White and Preiss (1992) suggested that the SS has more selective constraints than the LS. Georgelis et al. (2007) further hypothesized that this more intense evolutionary constraint could be due to the fact that the SS is less tissue-specific, and therefore must form enzyme complexes with different LSs. Studies of the expression pattern of AGPase genes in several plant species, including *A. thaliana*, rice, potato, tomato, and barley have indeed shown that the expression of the LS genes is tissue-specific while the SS is more broadly expressed (La Cognata et al., 1995; Park et al., 1998; Akihiro et al., 2005; Ohdan et al., 2005; Rosti et al., 2006; Crevillen et al., 2005).

Six classes of starch synthase genes have been identified in plants. One SS1 and one SS5 gene and two *GBSS* and *SS2* genes could be identified in the genome of *L. japonicus*. Previous studies had also identified two different *GBSS1* genes in the legume species pea (Denyer et al., 1997). The results of a recent study (Pan et al., 2009) show that these two *GBSS1* genes (namely, *GBSS1a* and *b*) are present in many other legume species, including the two starchy-seeded legumes cowpea (*Vigna unguiculata*) and mung bean (*Vigna radiata*), and the three oilseed legume species alfalfa (*Medicago sativa*), soybean (*Glycine max*), and *L. japonicus*. Phylogenetic analysis performed on the starch synthase gene family also indicates that the *SS2* duplicate genes (*SS2a* and SS2*b*) have been retained in several legume species (Senoura et al., 2004; Pan et al., 2009). However, in contrast to the *GBSS* duplicates that were found in all the species studied by Pan and colleagues (2009), only the

legume species kidney bean, cowpea, mung bean, and *L. japonicus* had retained the *SS2* duplicates. SS2b was shown to be non-functional in soybean (Pan et al., 2009). Furthermore, an homolog of the AtSS5 gene could be identified in *L. japonicus* and all the other plant species genomes analysed with the exception of sorghum. The role of this starch synthase isoform in starch synthesis is not yet known.

Taken together, my analyses of the starch gene families identified several interesting duplication events and divergence of isoform representation between *L. japonicus* and other higher plant species including *A. thaliana.* In the future, it would be interesting to explore the function and importance for starch metabolism of these different gene copies and isoforms yet uncharacterised. In particular, the function of the APL5 and SS5 genes would merit to be investigated. While these two genes are either absent or likely to be pseudogene in *A. thaliana*, they are present and likely to be functional in several other higher plant species (Figure A2 and Figure A3A and B). Therefore, their analysis could reveal new starch enzyme functions and interesting differences with the metabolism of starch in *A. thaliana*.

Most proteins encoded by the AMY1 group of genes were predicted to be secreted (Table A3) and their localisation in the secretory pathway have been experimentally confirmed for a few of them, including AtAMY1 (Doyle et al., 2007). Evidence suggests that the AtAMY1 enzyme may play a role in starch degradation during cell death (Doyle et al., 2007), however, the role of these secreted alpha-amylases in starch degradation remains elusive. Recently, it was shown than the rice α-amylase isoform I-1 (AmyI-1) that contain a signal peptide for translocating the ER membrane, but no plastid targeting signal, still had a plastidial localisation (Kitajima et al., 2009). More particularly, the authors were able to show that AmyI-1 was synthesised in the ER lumen and transported to the Golgi apparatus before being targeted to the plastid (Kitajima et al., 2009). This suggests that α-amylases lacking a predicted transit peptide for platidial localisation may still be targeted to the plastid and be functionally active there following a transit through the secretory pathway.

3.3.2. Transcript profiling of the starch metabolism genes across organs in *L. japonicus*

The synthesis and degradation of starch occurs in both photosynthetic and non-photosynthetic organs and requires the participation of many enzymes. These processes are known to vary between species, to be dependent on environmental conditions, and controlled in a tissue- and developmentally-specific manner, therefore suggesting the involvement of a highly complex regulation. Very little is known so far about the set of enzymes important for the synthesis of starch in each particular tissue of the plants, and the regulatory mechanism involved in turning on or off the expression of the genes encoding these enzymes. In addition, more information is needed to generate hypotheses regarding the function of the

duplicate copies of starch metabolism genes I identified in the genome of *L. japonicus*. To shed light on these questions, I investigated the spatial and developmental expression pattern of the core set of *L. japonicus* starch metabolism genes by using the transcriptomic data of the 'Lotus gene expression atlas' generated and made available by Andry Andriankaja and Michael Udvardi (personal communication; Samuel Roberts Noble Foundation, Ardmore, Oklahoma). Results of the analysis I performed using this resource provided new insights into the potential involvement of these genes and gene copies in starch metabolism in the different organs of the plant. Interesting tissue-specific patterns of expression as well as differences and similarities with their known pattern of expression in other species could also be identified.

The *LjPGI1*, *LjPGM1* and *LjAPS1* genes were significantly expressed in all organs analysed (Figure 7 and Table A1B). Their level of expression in leaves is consistent with the central role that these genes play in the synthesis of starch in this tissue in other plant species (Chapter 1, section 1.3 and references herein). The relatively high level of expression of *LjPGM1* and *LjAPS1* in non-photosynthetic organs including root and seeds, however, contrasts with the results of recent analyses carried out in *A. thaliana* and in rice (Tsai et al., 2009). In these species, *PGM1* and *APS1* transcripts and enzyme activities could be detected in leaves but not in roots, consistent with the fact that roots of these two plant species are starch-free with the exception of the root cap cells. The relatively high expression of these two genes in roots of *L. japonicus* is consistent with the observation that this species accumulates significant amount of starch in its roots, as shown by the results of my starch content analyses (Chapter 3, section 3.2.5, and Chapter 4, section 4.2.3).

The expression of Lj*PGI1* was also found to be relatively high in both leaves and sink, non-photosynthetic, organs such as roots (Figure 7 and Table A1B). Similarly, the PGI1 enzyme was shown to be active in both leaves and roots in *A. thaliana* and in rice (Tsai et al., 2009). It has been hypothesised that the expression and activity of PGI1 in these organs may reflect its biological role in pathways other than the synthesis of starch (e.g. the production of NADPH through the oxidative pentose phosphate pathway; ap Rees, 1980 and 1985).

This transcriptome analysis also provided new information regarding the different isoform and duplicate copies of genes identified in *L. japonicus*. Thus, *LjSS2a* was constitutively expressed in all organs analysed while *LjSS2b* was very weakly expressed only in leaves. The transcript levels of *LjAPL2b*, *LjAPL5*, *LjAMY1*, and *LjAMY3b* were too low to be considered as being expressed in all the organs analysed, suggesting that they may be pseudogenes (Figure 7 and Table A1B). Alternatively, it is possible that the expression of these genes is turned on under specific environmental conditions, or expressed in tissues or at a particular developmental stage not analysed in this study. It is also possible that these

genes could be expressed in a very cell-specific manner. Expression could be masked if this particular cell type is of minor abundance in the tissue analysed (for instance, transcript level of a gene specifically expressed in guard cells would be low on a whole-leaf basis since this organ is mostly constituted of other cell types). Detailed analysis of the protein sequence encoded by *LjAPL2b* and *LjAPL5*, and in particular, of the conservation of the residues known to be crucial for the AGPase enzymatic activity, suggests that these genes are indeed likely to be non-functional in *L. japonicus* (Figure A3A). In contrast, the relatively high transcript level of *LjAPL3* and *LjAPL2a* in all the organs analysed with the exception of leaves (in this organ, *LjAPL1* is the main LS AGPase gene expressed) suggests that these two genes may play a role in starch synthesis in non-photosynthetic tissues of the plants.

Tissue-specific expression patterns could also be observed for members of several gene families. Thus transcript level of *LjSS1* was higher than that of *LjSS2a* in leaves, petioles, stems, flowers and pods whereas the opposite was found in roots, nodules and seeds. *LjSS5* was significantly expressed in leaves, petiole, stem, pods, and seeds, but not in roots nor in flowers. *LjBAM1* was the main *BAM* isoform expressed in leaves whereas *LjBAM5* was the main isoform expressed in petioles, stems, seeds, and pods. In seeds and pods, its level of expression was very high. *LjBAM6* was only significantly expressed in leaves while *LjBAM7, LjBAM8,* and *LjBAM9* were expressed in all organs. *LjDPE1* and *LjDPE2*, *LjPHS2a* and *LjPHS2b*, and *LjMEX1* genes were constitutively and ubiquitously expressed, suggesting that the encoded enzymes may be involved in starch degradation in all the organs of the plants.

The expression of several genes was up-regulated in nodules (21 dpi) in comparison to inoculated roots (0 dpi), suggesting that the encoded proteins may be involved in starch metabolism in this organ. This was the case for the starch synthesis genes *LjPGM1, LjAPS1, LjAPL2a, and LjAPL3* as well as *LjGBSS1a, LjGBSS1b, LjSS5,* and *LjSBE2*. The expression of *LjSS5,* in particular, was highly nodule-enhanced: across all the organs analysed, its expression was the highest in nodules (Figure 7). It would be interesting to investigate the putative contribution of this enzyme to nodule starch metabolism and function. Transcript levels of several genes involved in starch degradation also significantly differed between nodules and roots. Thus *LjBAM3a* gene expression was up-regulated in nodules whereas the expression of *LjBAM1* was down-regulated in comparison to roots.

There was little change in the expression pattern of the starch synthesis and degradation genes through pod and seed development. In addition, the expression profiles were very similar between pod and seeds. However, it is important to stress that transcript levels were analysed at only one time during the day in this study. Expression of some genes encoding starch-degrading enzymes is known to fluctuate diurnally to a large extent in source leaves, and significant diurnal fluctuations could also occur in sink tissues. More generally, one

must be careful when interpreting the results of transcript expression analysis as illustrated by studies carried out on the diurnal transcriptome of starch metabolism-related genes (Smith et al., 2004; Lu et al., 2005; Gibon et al., 2006). Despite marked and coordinated changes seen in the transcripts of several enzymes involved in starch degradation, the amounts of the corresponding enzymes did not change substantially. This suggests a complex relationship between transcript levels, protein levels, enzyme activities, and carbon fluxes, and underlines the importance of combining the analysis of transcript and metabolite with measurements of enzyme activities (Smith and Stitt, 2007). Nevertheless, the analysis of gene expression can provide insights into the function of genes and help identify candidates for reverse genetic studies.

One obvious way of gaining compelling evidence about which genes are important for a particular pathway of interest and deciphering their function is to generate and characterise mutants and/or transgenic plants down-regulating or over-expressing them. We undertook such strategy in *L. japonicus* to determine the genes important for transitory and storage starch metabolism in this model legume species. Details of this approache and its results are presented in the next chapter.

3.3.3. The metabolism of starch in *L. japonicus*

Overall, the results of the analyses I performed on the accumulation and turnover of starch in *L. japonicus* revealed that this species accumulates starch and is able to remobilize it in leaves at night. Large variation in the amount of starch accumulated and its turnover were observed that depended on the environmental conditions as well as on the genotype of the plants. These discoveries and their significance are discussed in detail in this section and the next.

When grown under artificial, low light in a controlled environment chamber, both the level of starch and its diurnal turnover in both MG-20 and Gifu young plants (about four to eight weeks-old) were very similar to that seen for *A. thaliana* plants grown under similar growth conditions (e.g. Yu et al., 2001, Baunsgaard et al., 2005; Yu et al., 2005, Fulton et al., 2008; Figure 10). However, starch levels increased both at the end of the day and at the end of the night as the plant matured (Figure 10). Plants of the accession MG-20 in particular, accumulated an increased amount of starch in their leaves and significant differences in the amount of starch accumulated during the days and remaining at the end of the night could be seen between MG-20 and Gifu plants at eight and ten weeks of growth. Reasons for these variations in the amount of starch accumulated and its level of diurnal turnover between the accessions are unclear but could include intrinsic differences in carbon partitioning and storage, differences in the extent of nodulation, and differences in developmental stage at the

time of harvest (Figure 10). Ten week old MG-20 plants had started to flower, which was not the case of the Gifu plants. It seems possible, therefore, that a change in carbohydrate metabolism triggered by this transition of developmental stage in MG-20 could be partly responsible for the difference in diurnal starch turnover observed between MG20 and Gifu at this particular time point.

In several other of the growth conditions tested, MG-20 only (Figure 10 and Figure 12) or both MG-20 and Gifu plants (Figure 13) also accumulated large amount of carbon as starch in their leaves as they aged, of which only a small fraction was remobilized at night. The physiological significance of this large amount of starch being accumulated and not diurnally turned over is still unknown and remains to be discovered. It may be hypothesised that the accumulation of this larger amount of starch in leaves may represent a conservative strategy of growth that would allow the plants to sustain their growth and energy metabolism in a range of stress or unfavourable environmental conditions. Hence, it would be interesting to determine whether and to what extent the large amount of leaf starch remaining at the end of the night would be remobilized under stress conditions to avoid carbon starvation. Measuring the fluxes of carbon in plants submitted to periods of extended dark, in low CO2, or with reduced nutrient supply could help determine how much the plants rely on these starch reserves and other carbon sources when unable to produce any new photoassimilates from photosynthesis. Comparative analyses could be made with other natural variants or plant species that strictly remobilize all the starch accumulated during the day at night.

Transitory starch synthesis can be 'programmed' or serves as an 'overflow' mechanism (Stitt et al., 1996; Lin et al., 1988b; Schulze et al., 1991; Huber and Hanson, 1992). In the programmed model, transitory starch is synthesised as a source of carbon to maintain growth and energy metabolism of the plant during the night. This model is supported by the ability of leaves of several plant species to synthesise starch constitutively, even when photosynthetic rates are low, such as under low CO_2 and light intensity conditions. In contrast, in plant species in which the overflow mechanism applies, the rate of photosynthesis and the assimilation of its product exceed the demand for sucrose during the day and at night. In this case, starch constitutes an overflow product of the newly assimilated carbon, and only a fraction of the starch accumulated during the day will be remobilized at night. These two models are not mutually exclusive and their relative importance in a given plant species is likely to be dependent on both intrinsic differences in metabolism (e.g. genotype and the developmental stage of the plant) and the environmental growth conditions. Results of my analysis suggest that both models are operative in *L. japonicus*.

I also investigated the accumulation and turnover of starch in leaves of different maturation stages. Results of iodine staining did not reveal any significant difference in the amount of starch accumulated between younger and older leaves in MG-20 and Gifu plants

(Figure 9). This seems to differ from tobacco plants in which a strong diurnal pattern of starch turnover was observed in younger leaves whereas much less of the starch was diurnally turned-over, and its level progressively increased, in older leaves (Chapter 1, section 1.6). Variation in light quality and intensity, temperature, humidity, and nutrient availability could be some of the factors that could explain the differences observed. In several species including tobacco and soybean, starch stored in leaves is remobilized before their abscission (Chapter 1, section 1.6; Matheson and Wheatley, 1962 and 1963; Egli et al., 1980). A remobilization of the starch prior leaves abscission was visible by iodine staining in Gifu, but not in MG-20 plants (Figure 9). Increases in leaf starch content with leaf and/or plant age have been observed in several other species, including tobacco (Matheson and Wheatley 1962; Ölçer et al., 2001) and soybean (Ainsworth et al., 2006).

Very little is known about the metabolism of starch through development and across environmental conditions in most plant species studied to date. The metabolism of starch in *A. thaliana*, for instance, has so far been exclusively studied on ca four week old plants (i.e. before bolting) grown in controlled environment chambers and under a very limited number of growth conditions. Nevertheless, the partitioning of the products of photosynthesis into starch has been shown to be both finely regulated and highly flexible, and the amount of carbohydrate stored as starch is known to be dependent on the environmental conditions. Consistent with this idea, large differences in the pattern of starch accumulation and degradation were found between *L. japonicus* plants grown in different growth conditions. Firstly, *L. japonicus* plants growing in 16 h photoperiod conditions accumulated larger amounts of starch in leaves than those growing in shorter days (12 h photoperiod). In addition, more leaf starch was left at the end of the night in 16 h than in 12 h photoperiod (Figure 12). These results are in agreement with previous studies of the metabolism of starch in other plant species. In *A. thaliana*, the accumulation of starch in leaves was faster in plants growing in short days (SD; 8 h light, 16 h dark) than in those growing in long days (LD; 16 h photoperiod). This faster rate of accumulation, however, could not totally compensate for the shorter photoperiod, so that plants growing in LD accumulated more starch than plants growing in SD. Similarly there was more starch left at the end of the night in leaves of plants grown in LD than in SD, even so their rate of starch degradation was faster (Lu et al., 2005). Likewise, in tomato plants, the amounts of starch and hexose sugars increased with an increase in the length of the light period at any given time (Logendra et al., 1990).

Significant differences were also found between plants grown in the same photoperiod, but in different growth conditions. Hence, the level of starch measured in eight week-old MG-20 and Gifu plants was significantly different between the results of two experiments in which plants were grown in a controlled environment chamber at a similar light intensity (ca. 100

μmol m^{-2} s^{-1}) but the chamber used for the first experiment was fitted with both white and red fluorescent tubes and did not have humidity control while the chamber used for the second experiment was fitted with white fluorescent tubes only, and the humidity level was set to 75% (Figure 10 and Figure 12). This suggests that differences in the light quality and in the level of ambient humidity might have differently affected carbon partitioning and be responsible for this variation. In addition, I discovered large variation in the amount of starch accumulated between MG-20 and Gifu under most conditions tested (Figure 10, Figure 12, and not shown). However, it must be mentioned that such differences between the two accessions were not seen when the plants were grown in natural light, in long day conditions. In these conditions, both MG-20 and Gifu accumulated large and similar amounts of starch from an earlier stage (Figure 13 and Figure 14). Differences in the amount of starch accumulated between *L. japonicus* plants growing in a controlled environment chamber and in natural light conditions were important in case of Gifu. It is not yet clear which factors are responsible for such variation. The intensity and quality of light, the temperature, the CO_2 level, the availability of nutrients, and the extent of nodulation could be some of the factors that could affect significantly the metabolism of transitory starch.

Significant differences in growth rate, flowering and generation time exist between MG-20 and Gifu. The extent of this physiological difference varies depending on the conditions of growth. Thus, the faster growth rate of MG-20 plants relative to Gifu was less pronounced when grown in a glasshouse than when grown in a controlled environment chamber or room. This could be linked or due to differences in photosynthetic efficiency, in carbon partitioning, or in light perception. In this respect, it is interesting to note that the growth rate and biomass production of Gifu plants and their leaf starch accumulation was significantly higher when grown in a glasshouse in natural light, and even more so in a glasshouse supplemented with lighting high in red light (incandescent light bulbs) than when grown in a controlled environment chamber or room (lighting assured with fluorescent tubes with a low proportion in red/far-red light). Hence, there is good reason to suspect that not only the intensity of light, but also its quality (e.g. the proportion of white versus red/far red radiation) are at least partially responsible for the differences observed (Chapter 3, section 3.2.4). More particularly, white, fluorescent light appeared to promote growth and starch accumulation in MG-20 while it has the opposite effect in Gifu. In contrast, in Gifu, growth and starch accumulation appeared enhanced by the presence of red:far red wavelengths in the irradiance (Figure 10, Figure 12, and Figure 13). Such plant response is likely to be phytochrome-mediated. One experiment that could be performed to explore the importance of the quality of light over plant productivity and starch accumulation in *L. japonicus* would be to grow MG-20 and Gifu plants in controlled environment chambers varying only in the

source of light used (i.e. white light in one condition, and white light plus far-red light in the other).

Taken together, the results of my analyses showed important differences in the level of leaf starch accumulation and its turnover depending on the plant age, genetic differences between MG-20 and Gifu, and the environmental conditions of growth. More particularly concerning this later factor, the results suggested an important control exerted by the nature of light over plant growth and development in *L. japonicus* as observed for other plant species (Keiller and Smith, 1989). This illustrates the high level of plasticity and complexity of the metabolism of starch in plants and highlights the difficulty of extrapolating the results of experiments performed in controlled environmental conditions and on very young plants, to what may happen in natural growth conditions, and throughout the life of the plant. Although providing novel information on the metabolism of starch in *L. japonicus* and interesting insight into its regulation, the analyses I performed are preliminary and additional experiments would be needed to determine precisely the factors that control the pattern of starch accumulation and degradation in *L. japonicus*.

3.3.4. Carbon partitioning and plant growth strategy in *L. japonicus*

In addition to variation in the accumulation and turnover of leaf starch, plants of the accessions *L. japonicus* MG-20 and Gifu differed significantly in growth vigour, with MG-20 plants showing faster growth and higher biomass production than Gifu plants (Figure 9). It is potentially of great interest to determine whether a significant correlation exists between starch content and plant productivity and to identify the genes controlling the important differences observed between MG-20 and Gifu for these two traits. In *A. thaliana*, starch content and growth have been shown to be inversely correlated (Sulpice et al., 2009). It is not yet known whether this negative correlation holds true through the developmental stage of the plants, for other plant species and/or in other environmental conditions than in a controlled environmental chamber, in relatively low light. However, this model may not apply, for instance, to plant species in which the amount of assimilated carbon from photosynthesis largely exceeds the amount of starch they need to remobilize to avoid carbon starvation at night. The results of my analyses suggest that it may not be the case in *L. japonicus*. This species therefore represents an excellent system in which to test the wider applicability of the finding of Sulpice et al. (2009).

Further, it would be interesting to perform QTL analysis on leaf starch content and biomass production in *L. japonicus* so as to discover novel regulators of these two traits. Together with their high level of polymorphism, the large genetic variation observed for both starch metabolism and growth in Gifu and MG-20 accessions make them excellent

candidates to use as parents for these QTL analyses. Such analyses could be done on recombinant lines (RIL) from a cross between these two accessions. Once the QTLs are identified, the corresponding region on the genome can be searched for putative candidate genes controlling the synthesis of starch in *L. japonicus*. These genes and their mode of action could then be further characterised by carrying out complementation analysis and/or by generating additional variants (mutant alleles) of these genes via TILLING or other techniques. A set of RILs (187 lines) has already been developed by the Kasuza DNA research institute, and can be ordered from the 'Legume base' (http://www.shigen.nig.ac.jp/lotusjaponicus/index_e.html). This resource has already been used with success in several studies (e.g. Sandal et al., 2006; Gondo et al., 2007).

QTL analysis on the plant traits mentioned above could simply consist in quantifying leaf starch content at the end of the day and night, together with the measurement of an indicator of biomass production and growth. This is typically achieved by calculating the Relative Growth Rate (RGR), a comprehensive parameter able to take into account, to a large extent, plant performance and fitness that have been shown to vary among plant species, with environmental growth conditions, and developmental changes (e.g. onset of flowering or the formation of storage organs). RGR calculation is generally based on dry weight measurements (Hoffmann and Poorter, 2002) which are destructive, hence requiring a large number of plants to analyse growth in time. For *A. thaliana*, which in its vegetative phase grows as a rosette with limited leaf overlap, a non destructive system based on image analysis of leaf area has been developed (Leister et al., 1999), and is now widely used as an effective and reliable way of determining plant growth rate. Unfortunately, thus far, no equivalent methods have yet been developed for the measure of growth rate in *L. japonicus*. From the results of the preliminary analyses I performed, the difference between MG-20 and Gifu was the largest in terms of both starch accumulation and plant growth rate when grown in growth cabinet or in CER fitted with low white light. However, it may be preferable to use more natural growth conditions if the aim is to transfer the knowledge from model species to crops. In any cases, pilot experiments would need to be performed to confirm this before setting up any large scale experiments. The conditions of growth in terms of nutrient supply is another important factor to consider (e.g. C and N limiting or not limiting conditions) when setting up such experiment. Alternatively, or in addition to QTL analysis using RILs, the wild accessions of *L. japonicus* available from the 'Legume base' could also be used to explore the existence of correlations between carbon metabolism and growth in this species.

CHAPTER 4

Isolation of starch metabolism mutants of *Lotus japonicus*

One never notices what has been done; one can only see what remains to be done

Marie Curie

CHAPTER 4: Isolation of starch metabolism mutants of *Lotus japonicus*

4.1. Introduction

4.1.1. Reverse genetic approaches in plants

Whole genome sequencing and transcriptome analyses have provided very valuable information on genes and their expression in a continually increasing number of species. Genetic approaches, however, remain of central importance in determining the function of genes. Forward and reverse genetics are two highly complementary approaches to investigate gene function. Reverse genetics consists of isolating mutants in which the function of a gene of interest is altered. In higher plants, targeted gene disruption methods are not yet fully established and alternative methods are needed to obtain mutants. Reverse genetic strategies generally employed include insertional mutagenesis using either T-DNA or transposons, fast neutron and chemical mutagenesis, e.g. using ethyl methane sulfonate (EMS) or N-ethyl-N-nitrosourea (ENU) combined with TILLING, and RNA interference (RNAi; Mansoor et al., 2006).

Insertional mutagenesis addresses gene function through the identification of tagged loci and the analysis of the mutant phenotypes. This typically results in complete loss of function of the gene of interest due to the disruptive nature of the technique. Advantages of fast neutron and chemical mutagenesis include the ease of generating large mutant populations and their almost universal applicability. Hence they can be used on organisms that are not easily transformable or in which active transposons have not yet been characterised. Radiation induced deletions can be readily detected by PCR (Li et al., 2001), but the number of such deletions that the genome can tolerate is limited. In contrast, chemical agents such as EMS induce point mutations randomly that can be tolerated at high density, thereby permitting near saturation and good coverage of the genome with a manageable number of mutant individuals (Henikoff et al., 2004). However, the risk associated with this high density of mutations per genome is that background mutations can cause phenotype(s) that may be attributed wrongly to the candidate gene. Hence, several backcrosses to the WT plants are necessary to attribute the phenotype to the mutation with good confidence. For each F2 generation resulting from these crosses, the Mendelian ratio (i.e. the segregation ratio of homozygous mutants versus heterozygous and homozygous WTs) can be used as an indicator of the nature of the mutation. F2 segregating populations can also be analysed to

check that the mutation thought to be responsible for the mutant phenotype segregate with it. Hence, misattribution problems can only occur when the background mutation is closely linked to the mutation causing the phenotype and does not segregate following backcrossing. This risk decreases as the number of backcrosses increases. Performing several backcrosses, isolating several deleterious mutant alleles affecting the candidate gene, and doing complementation analyses are generally used to exclude the possibility of wrong mutation-phenotype assignment. Alternatively, if several alleles are available, complementation tests can be performed.

EMS induces point mutations that are G/C to T/A transitions in more than 99% of the cases (Greene et al., 2003). An advantage of the use of this type of chemical agent is that it generates a wide range of mutations (e.g. missense, splicing and stop codon mutations). This offers the potential to recover not only strongly affected or knockout alleles, but also alleles with subtle changes in gene functionality such as partial loss-of-function alleles (hypomorphic mutations), novel-function alleles (neomorphic mutation) or gain-of-function alleles (hypermorhic mutations). These weaker alleles are especially beneficial in cases where the complete disruption of the gene function would be lethal for the plant. The proportion of truncations (premature stop codon and splice site junction mutations) versus missense and silent changes vary between species, but generally truncations occur in the range of ca. 3 to 5%, and 30 to 50% are missense changes (Greene et al., 2003; Perry et al., 2009; Till et al., 2004; Slade et al., 2005). From this last class of mutation, only about 50% are thought to be deleterious for the protein function (Till et al., 2004)

Large EMS-mutagenised populations can be used in a high throughput, reverse genetic strategy called TILLING (Targeting Induced Local Lesions IN Genomes; McCallum et al., 2000; Comai and Henikoff, 2006). TILLING is based on chemical mutagenesis combined with screening for mutations in genes of interest in a large population of mutant individuals. This technique is based on the detection of mismatches caused by point mutations in heteroduplex DNA by an endonuclease such as CEL1 (Till et al., 2004a) that allows the detection of a single mutant allele in a pool of WT alleles (Colbert et al., 2001). Details of the TILLING process are provided in Chapter 2, section 2.10, and in Figure 15 and 16. Briefly, this involves the amplification of region(s) of the gene of interest (generally 1 to 1.5 kb in length) by PCR on pooled WT and mutant DNA with fluorescently labelled primers. Mismatched heteroduplexes are generated between the WT and mutant DNA by melting and re-annealing the PCR products. Annealed products are then incubated with the endonuclease that cleaves at mismatches. The resulting cleavage products are normally separated by gel electrophoresis (Figure 16).

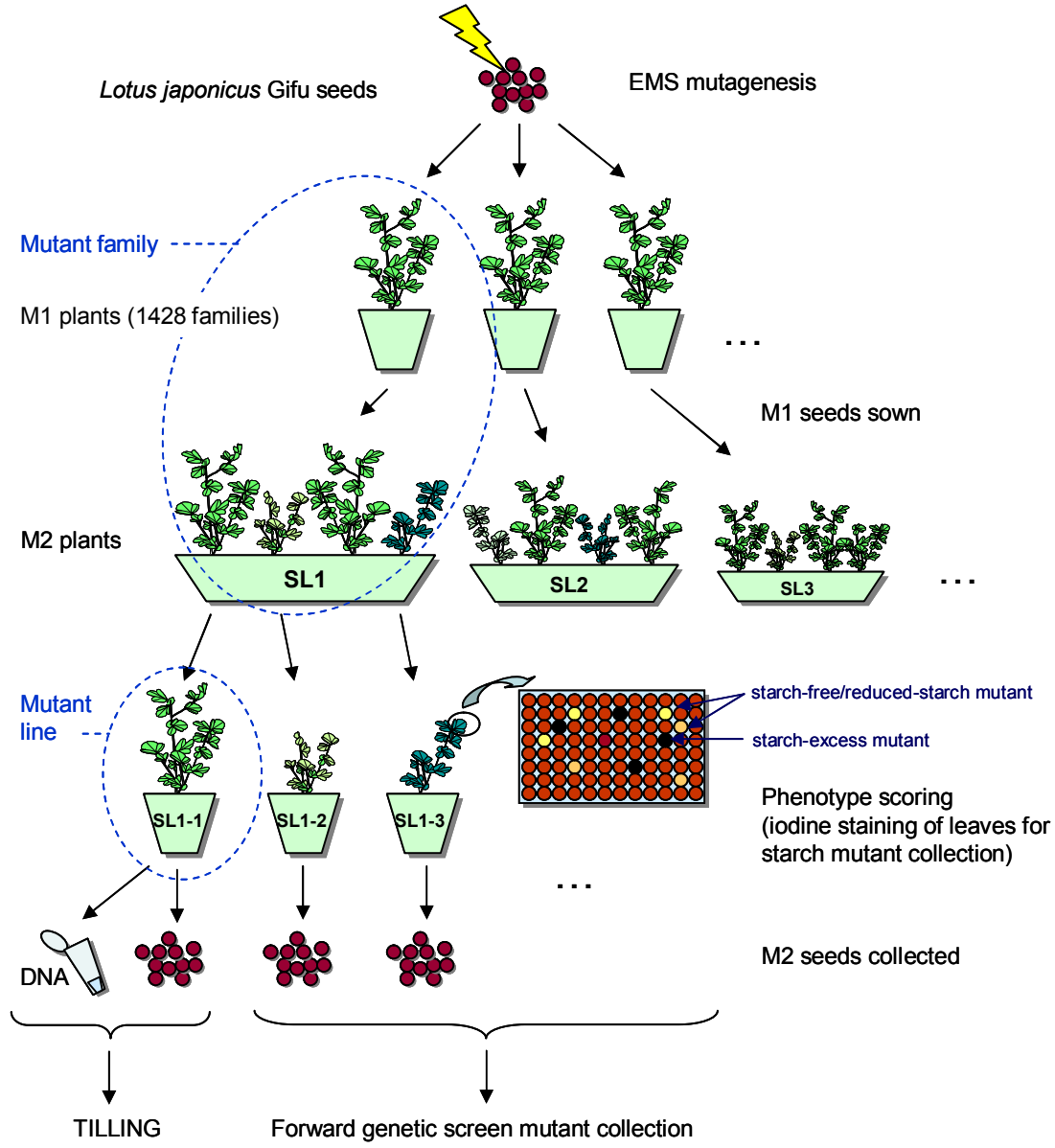

Figure 15. Generation of the population of TILLING and forward screen mutants.
Seeds of *Lotus japonicus* Gifu were EMS-mutagenenized and seeds were harvested from the resulting M1 plants. M1 seeds were sown and the M2 plants were scored for defective root nodules and several plant morphological characters. M2 plants were also screened for altered starch metabolism phenotypes (cf. Perry et al., 2003). All mutants altered in starch synthesis and degradation used in this study came from this original screen. For each family (designed with the SL number), a single healthy-looking plant (designed with SLxxxx-n, where n identifies the sibling; referred to as a mutant line thereafter) was chosen for the general TILLING population. Genomic DNA was extracted and seeds were harvested from these plants, individually. Seeds were also harvested from the selected mutant lines that displayed a mutant phenotype of interest (forward screen mutant collection).

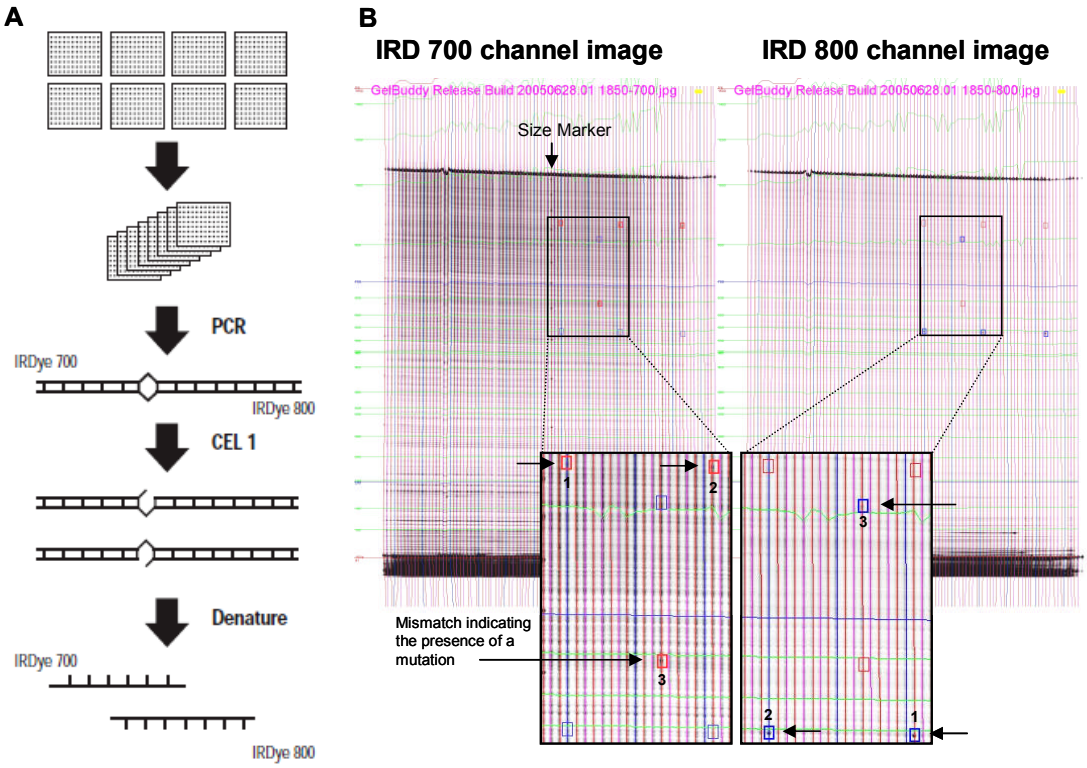

Figure 16. TILLING workflow and example of EMS-induced mutations identified by TILLING in *L. japonicus*.
A. Typical TILLING workflow (modified from a LI-COR brochure). A population of TILLING mutants is generated from seeds that have been mutagenised, using EMS, to induce point mutations in the genome as described in Figure 15. DNA samples from these mutant plants are collected in 96-well plates. Up to eight plates are pooled into one and the samples subjected to PCR with the forward and reverse gene specific primers labelled with two different fluorescent dyes (IRDyes™ 700 and 800 for TILLING performed using a LI-COR 4300 DNA analysis system). The resulting PCR products are heated and then cooled, allowing the formation of heteroduplex between the wild-type and mutant samples. The CEL1 nuclease is then used to cleave the DNA at the mismatches. Lastly, samples are denatured and electrophoresed on the LI-COR sequencer. **B**. An example of TILLING results obtained for *LjGWD1* in *L. japonicus.* The image for the IRD700 primer is shown on the left, and for the IRD800 primer is shown on the right. CEL1-cleaved heteroduplexes appear as dark bands/spots (circled in red for IRD700 and in blue for IRD800) that indicate the presence of a mutation. Mutations can be distinguished from PCR artifacts by the appearance of cleavage products in both the IRD700 and the IRD800 channel images, and at reciprocal sizes that add up to the full length of the PCR product. After detection of a mutation in a DNA sample pool (corresponds to a lane), each individual DNA sample of this pool is screened so as to determine which of them carry the mutation. The DNA sample of the mutated individual is then sequenced, leading to the identification of the mutation.

In addition to its ease of use, relative low cost, and high throughput nature, TILLING is widely applicable and particularly well suited for species with few genomic resources, where insertion mutagenesis and other reverse genetic techniques remain difficult. First described by McCallum and collegues (2000) in *A. thaliana*, this strategy has since be applied to many other plant species including *L. japonicus* (Perry et al., 2003), maize (*Zea mays*; Till et al., 2004b), wheat (*Triticum aestivum*; Slade et al., 2005), rice (*Oryza sativa*; Till et al., 2007), soybean (*Glycine max*; Cooper et al., 2008), pea (*Pisum sativum*; Dalmais et al., 2008),

common bean (*Phaseolus vulgaris*; Porch et al., 2009), and *Medicago truncatula* (Le Signor et al., 2009). Apart from being a powerful approach for gene function analysis, TILLING can also be used for DNA polymorphism assessment, and plant improvement. Hence, TILLING and EcoTILLING can be used in plant breeding for identifying allelic variation in genes that correlate with phenotypes of interest, and for establishing allelic series at these genetic loci by screening germplasms and/or induced mutant populations (Wang et al., 2006). Furthermore, the use of TILLING has also been proposed as a suitable alternative to genetic engineering technology for the development of new plant varieties with improved traits since the use of such induced mutations has a much wider public acceptance and does not face the same level of regulatory restrictions as those imposed on genetically modified material since they do not involve the introduction of foreign DNA into the plant genome (Tadege et al., 2009).

4.1.2. Approaches for the identification of mutants from forward genetic screens in higher plants

In addition to their use in reverse genetics, EMS-mutagenised populations are also used in forward genetics, a well suited approach to uncover unknown genes involved in a particular biological process. This approach consists in screening the population for mutant phenotypes of interest followed by the identification of the genetic basis of these phenotypes. Identifying single point mutations in an EMS-mutagenised population is technically challenging. This is generally achieved through map-based cloning (also referred as positional cloning or gene mapping). Briefly, this approach involves two main steps: genetic mapping and physical mapping. Genetic mapping uses linkage analysis and relies on natural polymorphisms occurring between different ecotypes of the same species. For *L. japonicus*, the most widely used ecotypes for this analysis are MG-20 and Gifu because of their high level of polymorphism (Kawaguchi et al., 2001) and the availability of markers for linkage analysis (SSR and AFLP; http://www.kazusa.jp/lotus/index.html).

The principle of positional cloning in plant species with sequenced genomes is as follows: a plant homozygous for the mutant allele of interest in one particular ecotype is crossed with a WT individual of a second ecotype (or species). The resulting F1 generation plants are allowed to self-pollinate, which leads to recombination events during meiosis between the genomes of the two parents. Plants of the next generation (segregating F2 population) are screened for the mutant phenotype of interest. The genomic DNA of these plants is then submitted to genetic mapping. This consists of looking for linkage to genetic markers based on the principle that the mutated locus will always retain its original genetic background, and that the recombination frequency will be low for the genetic markers in the vicinity of

the mutation. From this, a rough chromosomal region (ca. 5 cM) containing the mutation is defined (Figure 17). This mapped interval is further reduced with the selection and use of additional markers within it. Once this region is small enough (generally less than 0.1 cM), physical mapping is used to determine the absolute position of the mutation on the genome and identify the gene mutated. This is followed by cloning and testing of the candidate gene (Remington et al., 2001).

Major advances including genome sequencing, the availability of large sets of markers and improvements to the methods used to detect DNA polymorphisms, have made this process easier and significantly faster in *A. thaliana* and some other plant species (Jander et al., 2002). Historically, physical mapping involved the screening of large insert genomic libraries (e.g. BAC) and a procedure termed chromosomal walking. For model plant species for which the genome has been sequenced, however, it is possible to speed up the process of identifying the mutation by following a candidate gene approach which consists of searching for genes that could be responsible for the phenotype, once the mapped interval is small enough to do so. Further, advances recently made in sequencing techniques (so called next-generation sequencing technology) now allow effective gene mapping by a process involving whole-genome resequencing (Huang et al., 2009). Such an approach, however, can only be used for species for which the genome is completely sequenced, of good quality, and of relatively small size (e.g. *A. thaliana* genome, ca. 125 Mb). For other plant species such as *L. japonicus* (genome size of ca. 472 Mb), next-generation sequencing technology can still be used to accelerate the identification of the mutated gene once the interval where the mutation maps is restricted to a relatively small genomic region (less than 500 kp). Use of this technology (referred to as targeted resequencing) could prove particularly useful and cost effective in cases, for instance, where the mutated gene causes a weak phenotype, therefore causing difficulties in the final stages of the map-based cloning approach.

4.1.3. Functional genomic tools in *L. japonicus*

L. japonicus is a valuable model species for research into several physiological and developmental processes (Chapter 1, section 1.7.2). This species has a small diploid genome, is self fertile, can be transformed easily and is therefore amenable for forward and reverse genetics and functional genomics. In addition to EST sequence libraries, high resolution genetic linkage maps and a sequenced genome, a wide range of functional genomics tools has been developed for this species. These include populations of mutants, TILLING, and RNA interference.

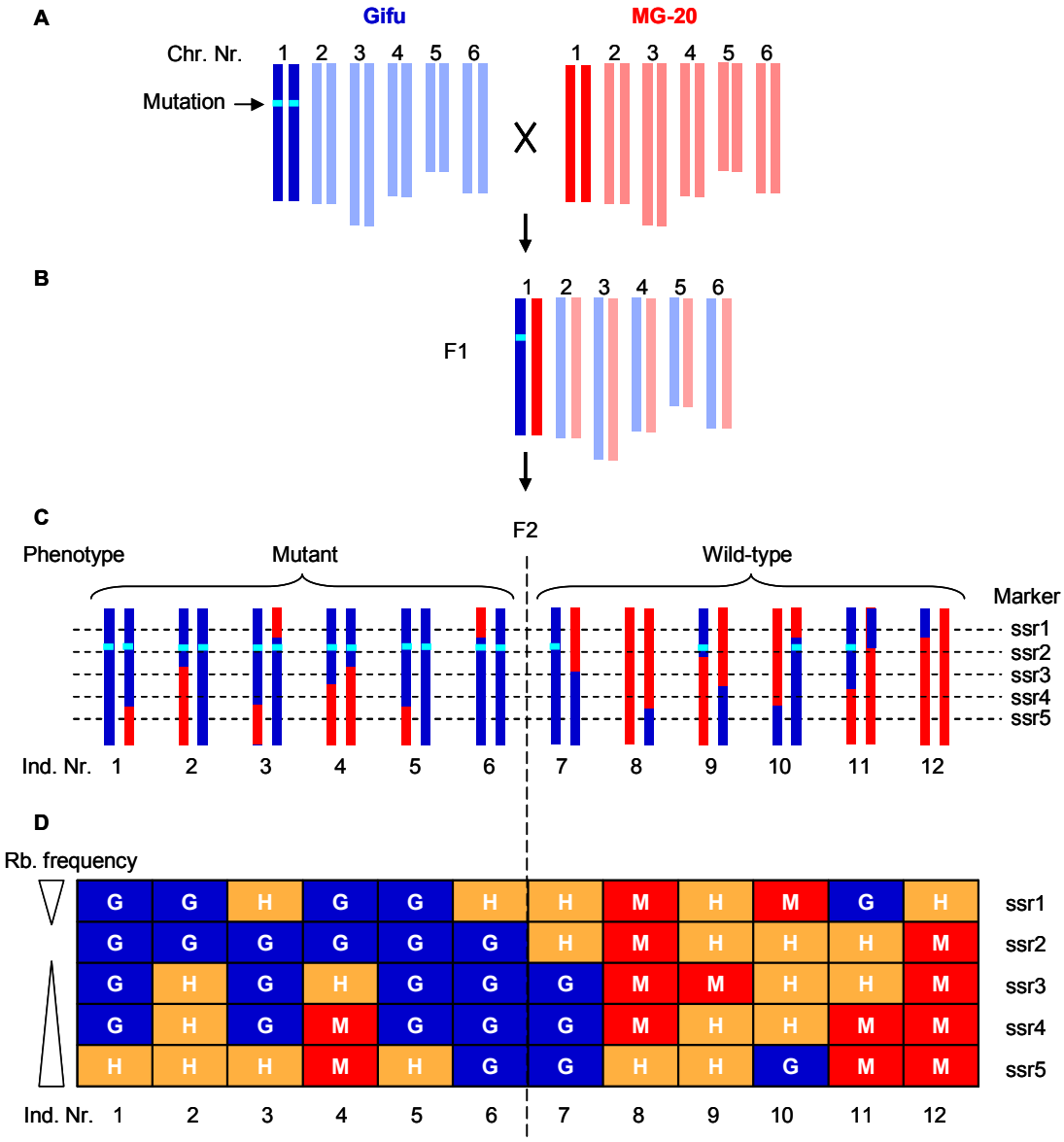

Figure 17. Principle of gene mapping.
In this example, the mutant phenotype is caused by a single recessive mutation in the genome of the *L. japonicus* accession Gifu. The mutation identification process starts by crossing this accession with another accession, in this case MG-20 (A). These two plant accessions show a high level of polymorphism at the DNA sequence level. Plants of the F1 generation that are heterozygous for the mutation are allowed to self-fertilise (B), and the F2 progeny are phenotyped to distinguish the mutants from their WT segregants. Cross-over events during meiosis allow fragments of DNA from the parents to segregate independently. The DNA region at the mutant locus, however, will stay homozygous Gifu in the population of mutants (C). Polymorphism markers (microsatellites SSR markers in this example) are used to identify this region according to the frequency of recombination (Rb. frequency). Here, the mapping analysis (rough mapping) locates the mutation, that co-segregates with the ssr2 marker, in the interval flanked by the ssr1 and ssr3 markers (D). Use of additional markers in this mapped interval (finer mapping) allow the interval to be reduced, until it is small enough to carry out physical mapping and candidate gene searches. Abbreviations: G, Gifu; M, MG20; H, heterozygote; ssr, simple sequence repeat; Ind. Nr., individual's number.

Mutagenesis using T-DNA, transposons, or retro-transposon insertions that disrupt gene function have been used in both model legumes *L. japonicus* and *M. truncatula*. In *M. truncatula*, insertion mutagnesis using Tnt1 has been developed and about 15,000 independent lines have been generated to date. It has been estimated that this population size should provide a very high probability of tagging any average-sized, single copy gene (Tadege et al., 2009). So far in *L. japonicus*, T-DNA and transposon insertions have only been used to a limited extent (Schauser et al., 1998; Schauser et al., 1999). In contrast, the use of EMS mutagenesis for TILLING in *L. japonicus* is already well established. A *Lotus* TILLING facility has been available to the research community since 2003 (Perry et al., 2003). This TILLING resource comprises a general structured population of M2 progeny of 4904 EMS-mutagenized M1 embryos, each representing an independent family, that was generated in the ecotype Gifu. Thematic populations for nitrogen-fixing root nodule symbiosis, development, and starch synthesis and degradation have also been assembled (Perry et al., 2003 and 2009). The phenotypes can be searched using the following web-based database: http://www.lotusjaponicus.org. In addition, a new population of approximately 3500 mutagenized mutant lines of the ecotype MG-20 is being assembled (Tadege et al., 2009). This Lotus TILLING facility can be accessed at http://revgenuk.jic.ac.uk.

Based on the analysis of subsets of genes, the mutation load of the original population has been estimated to be one per 502 kb. This is equivalent to approximately 940 mutations per genome (Perry et al., 2009). In earlier estimates, an average mutation frequency of six mutations per 2.3 Mb of sequences (equivalent to 2.6 mutations per Mb) suggested that each genome bears ca. 1300 point mutations caused by EMS (Perry et al., 2003), a value similar to that reported for the *A. thaliana* TILLING (McCallum et al., 2000). The mutation types identified in the GENEPOP population for all the genes analyzed by TILLING to date consisted of 3.5% truncations (of which 2.8% were premature stop codons and 0.7% affected splice site junctions), 47.7% missense changes, and 48.8% silent changes (of which 28.3% were silent because they were located in an intronic region, and 20.5% were silent because they did not result in an amino acid change; Perry et al., 2009). Hence, a disadvantage of carrying out TILLING on an EMS mutagenised population is that the proportion of knockouts among the mutant alleles recovered is low (ca. 3.5% on average in *L. japonicus*). A major advantage, however, is that it generates allelic series with alleles differing in strength. This offers the potential of providing more detailed information on protein function.

Forward genetic screens using the same EMS-mutagenized population as the one used for TILLING have also been successfully carried out in *L. japonicus*, notably for identifying nodulation-defective mutants (Perry et al., 2003). Lastly, a series of transcriptomic,

proteomic, metabolomic tools and resources have also been developed for this species (e.g. Wienkoop and Saalbach, 2003; Desbrosses et al., 2005). A more exhaustive review on the functional genomics tools developed for *L. japonicus* and other legume species can be found in the reviews of Udvardi et al. (2005) and Tadege et al. (2009).

4.1.4. Aims and Approaches

In order to elucidate the pathway of starch synthesis and degradation in legumes and provide resources for future experimentation, an EMS-mutagenized population of *L. japonicus* was screened for mutants altered in transitory starch metabolism. Positional mapping together with a candidate gene and candidate enzyme approaches were used to identify their mutations. In addition, TILLING was also used to confirm that the mutations identified were indeed responsible for the mutant phenotype and to obtain additional mutations in genes known to affect leaf starch content in other species. Results of this work are presented below. In total, several deleterious mutations affecting seven genes encoding key enzymes of the starch metabolism pathway were identified. Mapping was also performed for several other starch synthesis and degradation mutants from forward genetics. The mutations responsible for these mutant phenotypes still remain to be identified. Candidate gene searches in the mapping interval identified in these mutants suggest that the mutations they carry are likely to affect novel proteins involved in starch metabolism. Methods and strategies followed to achieve these results and the approaches that could be employed for the identification of the yet uncharacterised mutations are also discussed in this chapter.

4.2. Results

4.2.1. Forward genetic screens to isolate mutants affected in starch metabolism

Prior the start of this research project, and in order to identify mutants affected in leaf starch metabolism, a forward genetic screen was performed on 1428 M2 families (17,100 plants) from a batch of seeds of *L. japonicus*, ecotype Gifu, mutagenized with EMS (Perry et al., 2003). This population was screened in the laboratory of Dr. Trevor Wang (JIC) for mutants displaying either a low or a high content of starch in leaves relative to the WT. Initial screening and isolation of the mutant lines were carried out by Trevor Wang and collegues (JIC) as described below and presented in Figure 15. Starch content was estimated by staining decolorized leaves with iodine solution. This staining with iodine provided a

quick, easy, robust, and high throughput way of estimating the starch content in leaves of the mutants of this collection. As starch is synthesised during the day and degraded at night, screening was performed on leaf samples harvested at the end of the day in order to identify starch synthesis mutants (reduced-starch or starch-free phenotype), and at the end of the night in order to identify starch degradation mutants (starch-excess phenotype). Because leaf starch was generally not completely degraded at the end of a normal night, and the content varied with growth conditions and the age of the plants, screening for degradation mutants was usually performed on young plants (about 4 weeks old) in the glasshouse under long day, natural light conditions and after subjecting them to an extended dark period of up to 44 h. From this first screen, a set of eleven synthesis and ten degradation mutants was selected by Tracey Welham (JIC). I then performed a second screen in which several of the mutants that were not fertile and did not present a clear and reproducible mutant phenotype were not analysed further. This resulted in a selection of a set of ten synthesis and six degradation mutants to characterise.

The selected mutant lines were backcrossed at least once to the WT accession MG-20 (Table 7; performed with the help of Tracey Welham). Confirmation that the F1 plant resulted from a true cross was obtained by marker analysis that was performed as described in Material and Methods (Chapter 2, section 2.1.2). With the exception of SL5272-11, segregation ratios in the F2 progeny indicated a recessive monogenic mode of inheritance for the starch mutant phenotypes, consistent with the nature of such mutations in other species.

Some allelism tests were also carried out by Tracey Welham (JIC) and myself on the mutants selected for further analysis. We made 16 different combinations of crosses for the synthesis mutants and six in the case of the degradation mutants. Results suggested that the mutations defined at least five loci for the synthesis mutants, and four loci for the degradation mutants (Table 8). Three of the starch synthesis mutants, namely SL4308-12, SL4715-2 and SL5069-2, were shown to be allelic.

4.2.2. Gene mapping and TILLING as complementary approaches to identify mutations affecting starch metabolism

To discover genes necessary for starch metabolism in *L. japonicus*, two approaches were undertaken: gene mapping, to identify the mutations responsible for the phenotypes of the starch synthesis and degradation mutants from the forward screen; and TILLING, to identify mutations in genes encoding enzymes known to be necessary for starch metabolism in other plant species (Chapter 3; Table 6). TILLING was also used to identify additional mutant alleles of genes for which only one mutant allele had been isolated from the forward genetic screen.

Table 7A. Starch synthesis mutants from forward screen

Mutant Line name	Allele name	Backcrossing stage (most advanced)
SL4715-2	*pgi1-1*	B3F2
SL4308-12	*pgi1-2*	B2F2
SL5069-2	*pgi1-3*	B3F2
SL4725-4	*pgm1-4*	B3F2
SL4867-11	*pgm1-5*	B2F2
SL5127-5	*apl1-1*	B3F1
SL5074-12	n/a	B2F2
SL5249-3	n/a	B3F1
SL4618-12	n/a	B1F3
SL5143-3	n/a	B2F1

Table 7B. Starch degradation mutants from forward screen

Mutant Line name	Allele name	Backcrossing stage (most advanced)
SL5215-2	*gwd1-1*	B2F2
SL5358-3	*gwd1-1*	B2F1
SL5104-12	*gwd3-1*	B3F1
SL4841-4	*n/a*	B3F2
SL5035-7	n/a	B3F2
SL5272-11	n/a	B2F1

Table 7C. Starch synthesis mutants from TILLING

Mutant Line name	Allele name	Backcrossing stage (most advanced)
SL4490-1	*pgm1-1*	B2F2
SL0755-1	*pgm1-2*	M4/M5
SL1837-1	*pgm1-3*	B1F3
SL0933-1	*apl2-1*	B1F2
SL0443-1	*apl2-2*	B1F2
SL0501-1	*apl2-3*	B1F2
SL4318-1	*apl2-4*	B1F2
SL0529-1	*aps1-1*	B3F1
SL4504-1	*aps1-2*	M3
SL5072-1	*aps1-3*	B2F1
SL4723-1	*aps1-4*	M3

Table 7D. Starch degradation mutants from TILLING

Mutant Line name	Allele name	Backcrossing stage (most advanced)
SL1833-1	*gwd1-2*	B1F2
SL4958-1	*gwd1-4*	M3
SL3001-1	*gwd1-3*	B1F2
SL0176-1	*gwd1-5*	M3
SL5535-1	*gwd1-6*	M3
SL0692-1	*gwd3-2*	M3
SL0639-1	*gwd3-4*	M3
SL4648-1	*gwd3-3*	M3

Table 7. Most advanced backcrossing stage of the forward screen and TILLING mutant lines selected for further analyses.

Starch synthesis mutant lines crossed	No. of F1 pods obtained	Complementation (starch synthesis restored)
SL4725-4xSL4308-12	6	yes
SL4725-4xSL4308-12	2	yes
SL4725-4xSL5069-2	5	yes
SL4308-12xSL4715-2	10	no
SL4308-12xSL5069-2	4	no
SL5069-2xSL4715-2	4	no
SL4618-12xSL5074-12	1	yes
SL4618-12xSL5249-3	3	yes
SL4618-12xSL4867-11	3	yes
SL4618-12xSL5127-5	1	yes
SL5074-12xSL5249-3	2	yes
SL5074-12xSL4867-11	3	yes
SL5074-12xSL5127-5	none	n/a
SL5249-3xSL4867-11	3	yes
SL5249-3xSLSL5127-5	none	n/a
SL4867-11xSL5127-5	3	yes

Starch degradation mutant lines crossed	No. of F1 pods obtained	Complementation (starch degradation restored)
SL4841-4xSL5035-7	4	yes
SL4841-4xSL5215-2	4	yes
SL5215-2xSL5035-7	2	yes
SL5104-12xSL4841-4	4	yes
SL5104-12xSL5035-7	4	yes
SL5104-12xSL5215-2	3	yes

Table 8. Results of complementation analyses (allelism tests) performed on several of the starch synthesis and degradation mutants from the forward screen.

I initially carried out rough mapping on the forward screen mutant lines by bulk segregant analysis (Michelmore et al., 1991), using genomic DNA from at least two pools of eight mutants from F2 populations from crosses with MG-20. Microsatellite SSR markers evenly distributed over the arms of each of the six chromosome pairs of *L. japonicus* (three to four SSR markers per chromosome) were selected from the markers developed by the Kazusa DNA Research Institute (http://www.kazusa.jp/lotus/index.html; Table 9). The mapping interval thus identified was confirmed by further mapping on the mutant individuals. An example of mapping results is given in Figure 18. Using information from the genome sequence of *L. japonicus*, mapping was coupled to a candidate-gene approach so that any strong candidate gene (i.e. genes known to play a key role in starch metabolism in other plant species) located in the mapped region was sequenced. The molecular function-map for starch metabolism in *L. japonicus* I had established (Chapter 3, Figure 6) was used to facilitate this strategy. In the absence of any strong candidate gene within the mapped interval, searches were extended to consider other potential candidate genes. Synteny with the genomes of the legume species soybean (http://www.phytozome.net/soybean) and *M. truncatula* (http://www.medicago.org/genome/) was also used in some cases where the *L. japonicus* genome sequence was not available.

Marker	Chromosome	Map position
TM0193	1	20,1
TM0438	1	42,6
TM0143	1	66,2
TM0065	2	14,0
TM0076	2	46,0
TM0002	2	67,3
TM0080	3	12,5
TM0005	3	34,0
TM0049	3	55,1
TM0616	3	70,4
TM0182	4	8,8
TM0030	4	32,2
TM0046	4	53,8
TM0034	5	4,8
TM0048	5	27,6
TM0036	5	49,7
TM0302	6	14,0
TM0013	6	36,9
TM0336	6	57,6

Table 9. Microsatellite SSR markers used for rough mapping of the forward screen mutations.
The map positions are in cM and correspond to the location of the markers on the genetic linkage map of *L. japonicus* (Figure 19).

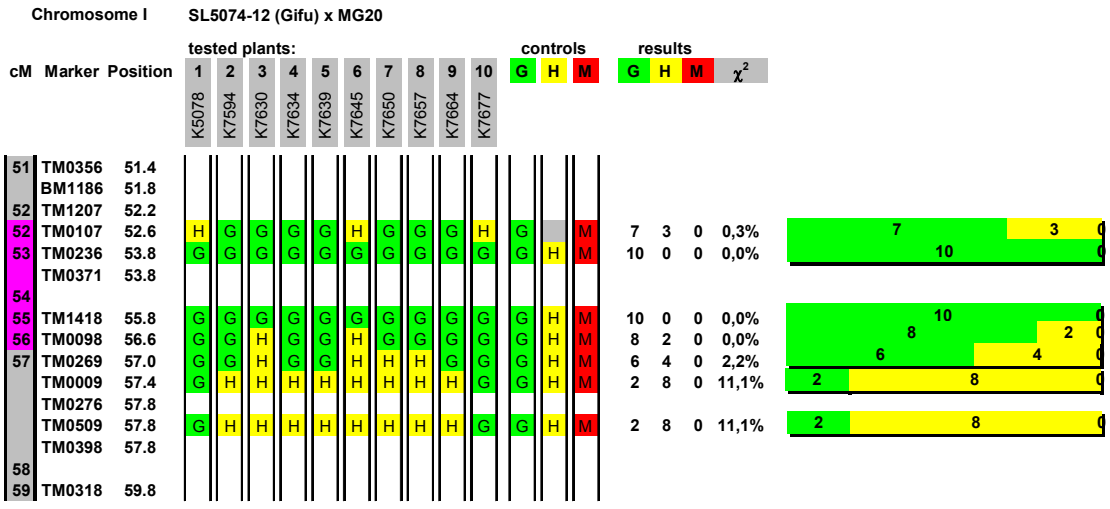

Figure 18. Example of mapping results.
Individuals of a F2 segregating population from a cross between the mutant line SL5249-3 and MG-20 that displayed a mutant phenotype were analysed for mapping. For each SSR marker, the plants scored as either homozygous Gifu (G, in green), homozygous MG-20 (M, in red), or heterozygous (H, in yellow). Only mutant plants that were recombinants in the region of the genome where the mutation map according to previous rough mapping analyses are shown here; all other tested F2 mutant plants scored Gifu with these markers. Molecular markers and phenotypic data were subjected to Chi-square (χ^2) statistical analyses to test the goodness-of-fit of the observed to expected ratio (shown on the left; see Chapter 2, section 2.15). In this particular example, the mutation maps on chr1, between the markers TM0107 at position 52.6 cM and TM0098 at position 56.6 cM as shown by the recombination frequency and the breakpoint in recombination. The mutation is said to co-segregates with TM0236 (53.8 cM) and TM1418 (55.8 cM) since no recombination events are seen for none of the mutant samples analysed with these markers.

When sequencing of candidate genes (primers are given in Table 2) revealed mutations, biochemical and genetic approaches were used to check rigorously that the mutations were indeed responsible for the starch phenotype. As described in the following sections, this strategy led to the identification of the mutated genes in six out of the ten synthesis mutants, and three out of the six degradation mutants. Results of this mapping are presented in Figure 19 and Table 10.

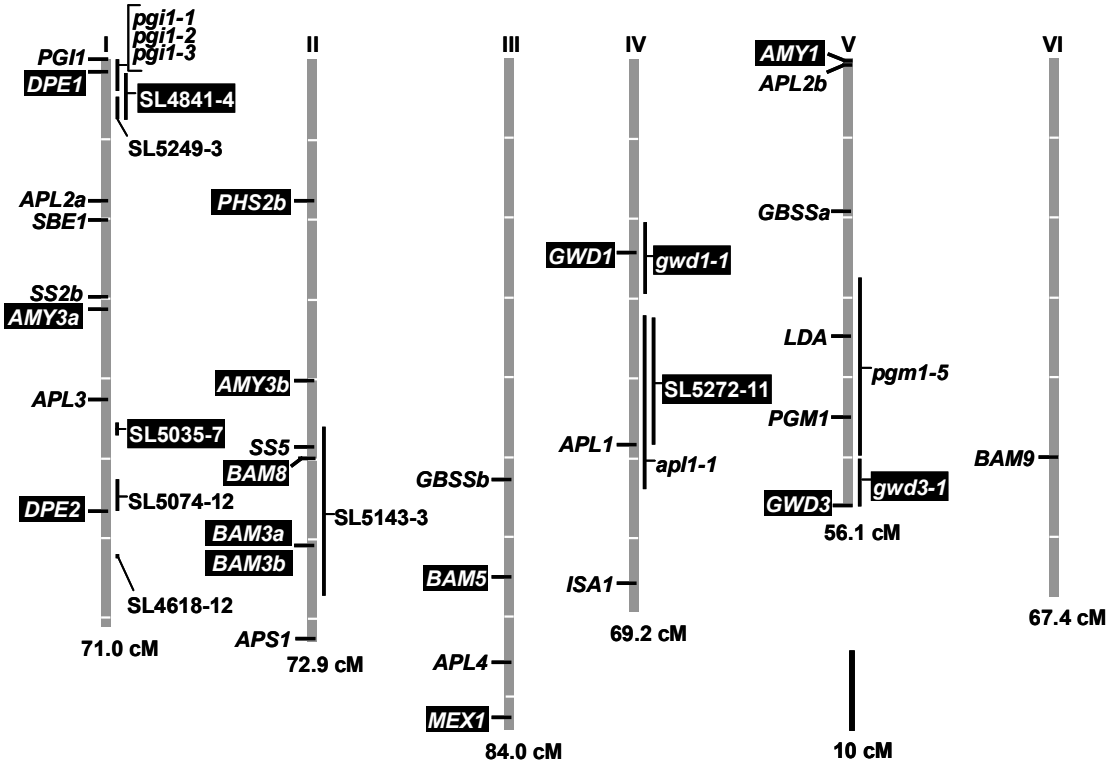

Figure 19. Chromosomal location of the starch metabolism genes of *L. japonicus* and mapped position of the mutations discovered in the forward genetic screen.
Genetic linkage map of *L. japonicus* derived from a cross between the ecotypes Gifu and MG-20 (maternal and paternal parents, respectively). For each chromosome, the number is given at the top and the size (in cM) at the bottom (data from http://www.kazusa.or.jp/lotus/index.html). Genes involved in the synthesis and degradation of starch (lettered in white and black, respectively) are shown on the left of each chromosome. Mutations from the forward genetic screen are shown on the right of each chromosome. Identified mutations are labelled with allele numbers; mapped intervals of the mutations yet to be characterised are labelled with the SL number of the mutant lines. The starch metabolism genes are listed in Table 6. Full details of the mutant alleles identified are given in Tables 10 and 15.

Mutant line	Mutant class	Chromosome	Mapped interval	Flanking markers	Recombination frequency
SL4308-12	synthesis	1	0,0	TM0102-TM0192	7/19
SL4715-2	synthesis	1	0.0-1.2	TM0102-TM0039	6/13
SL5069-2	synthesis	1	0.0-4.0	TM0058-TM0094	9/17
SL4725-4	synthesis	-	-	-	-
SL4867-11	synthesis	5	27.6-49.7	TM0048-TM0366	n/a
SL5127-5	synthesis	4	32.2-53.8	TM0030-TM0046	n/a
SL5074-12	synthesis	1	52.6-56.6	TM0107-TM0098	4/112
SL5249-3	synthesis	1	4.8-7.6	TM0063-TM0982	5/75
SL4618-12	synthesis	1	62,2	TM2089-BM1994	6/286
SL5143-3	synthesis	2	46.0-67.3	TM0076-TM0002	4/24
SL5215-2	degradation	4	20.5-29.4	TM283-TM0500	5/19
SL5358-3	degradation	4	21.3-32.2	TM0131-TM0030	4/24
SL5104-12	degradation	5	50.1-56.1	TM0703-TM1948	1/24
SL4841-4	degradation	1	1.6-7.6	TM0032-TM0982	11/87
SL5035-7	degradation	1	45.4-47.0	TM0989-TM0001	8/131
SL5272-11	degradation	4	32.2-47.8	TM0030-TM0387	5/16

Table 10. Mapped interval and flanking microsatellite markers of the forward screen mutations.
Mutant class was determined by iodine staining of leaflets at the end of the day (revealing synthesis mutants) and the end of the night (revealing breakdown mutants). The mapped interval corresponds to the upper and lower limit (given in cM) of the interval in which the mutation maps. The map positions are from the *L. japonicus* linkage map (see Figure 19). Recombination frequencies are the number of recombinants obtained with both flanking markers divided by the total number of mutants analyzed. The mutation in line SL4725-4 was not mapped because the mutated gene was successfully identified by a candidate gene approach based on the starch-free phenotype of the plant.

TILLING was carried out using DNA isolated from plants that originated from the same population of EMS-mutagenized *L. japonicus* seeds used for the forward genetic screen (Perry et al., 2003 and 2009; Figure 15). The genes targeted and the mutations identified are described below and the gene-specific primers used for this TILLING are listed in Table 2. TILLING on the genes *LjPGM1*, *LjAPS1*, *LjAPL2* was carried out by Jodie Pike and Tracey Welham (The Sainsbury Laboratory and JIC, respectively, Norwich, UK). I carried out the full TILLING process on the *LjGWD1* gene for which two different regions of the gene were targeted, and the whole population (4904 individuals) screened for both. TILLING for *LjGWD3* was carried out by *RevGen*UK (http://revgenuk.jic.ac.uk/). Selection of the region of this gene to TILL, primer design and results analysis were carried out by myself. An illustration of the TILLING workflow followed and the TILLING results obtained can be found in Figure 15 and 16.

For each of the gene regions targeted by TILLING, several mutant alleles with non-silent mutations were identified (Table 11). Only the mutations predicted to be deleterious (PSSM score given by the PARSESNP program >10) or shown to result in a mutant phenotype are discussed in the following sections. However, all the variants identified for the *LjGWD1* and *LjGWD3* genes, including those with a silent mutation (i.e. mutation not causing an amino acid change or mutation located within intron) are listed in Table 12 and Table 13. Mutants

were screened for either a reduced-starch or a starch-excess phenotype. Most of the mutants isolated were heterozygous at the M2 generation, so homozygous mutant, heterozygous, and WT segregant plants in the M3 generation were identified by sequencing (primers are given in Table 2 and Table 3). As carried out for the forward screen mutants, the TILLING mutants thus identified with an altered starch phenotype and selected for further analyses were out- and successively back-crossed to MG-20 to reduce the numbers of background mutations introduced by EMS mutagenesis (Table 7). Whenever possible, and unless otherwise indicated, mutant characterisation was carried out on both homozygous mutants and their WT segregants (or their progeny) to allow a more accurate mutant *versus* WT comparison since the number of background mutations would be similar between the two, as would be the genome background.

Table 11A. Starch synthesis mutants from forward screen

Mutant Line	Gene	Allele	Nucleotide change	Effect	PSSM difference	SIFT score
SL4715-2	PGI1	*pgi1-1*	C917T	Q200*	n/a	n/a
SL4308-12	PGI1	*pgi1-2*	G3602A	W360*	n/a	n/a
SL5069-2	PGI1	*pgi1-3*	G5047A	Splice junction	n/a	n/a
SL4725-4	PGM1	*pgm1-4*	G1233A	Splice junction	n/a	n/a
SL4867-11	PGM1	*pgm1-5*	G377A	G95D	17.1	0.00
SL5127-5	APL1	*apl1-1*	C4408T	S400L	21.2	0.00

Table 11B. Starch degradation mutants from forward screen

Mutant Line	Gene	Allele	Nucleotide change	Effect	PSSM difference	SIFT score
SL5215-2	GWD1	*gwd1-1*	G4633A	E566K	6.6	0.00
SL5358-3	GWD1	*gwd1-1*	G4633A	E566K	6.6	0.00
SL5104-12	GWD3	*gwd3-1*	G7871A	Splice junction	n/a	n/a

Table 11C. Starch synthesis mutants from TILLING

Gene	Mutant line	Allele	Nucleotide change	Effect	PSSM difference	SIFT score
PGM1	SL4490-1	*pgm1-1*	G6413A	D436N	19.4	0.00
	SL0755-1	*pgm1-2*	G6848A	W467*	n/a	n/a
	SL1837-1	*pgm1-3*	G6932A	W495*	n/a	n/a
	SL4532-1		G6924A	E493K		
	SL4619-1		G7194A	G533D		
APL2	SL0933-1	*apl2-1*	G1104A	D236N	8.7	0.12
	SL0443-1	*apl2-2*	G1471A	G275E	23.6	0.00
	SL0501-1	*apl2-3*	C2369T	P383S	11.1	0.12
	SL4318-1	*apl2-4*	G2453A	Splice junction	n/a	n/a
APS1	SL0529-1	*aps1-1*	G1059A	A111T	20.5	0.00
	SL4504-1	*aps1-2*	G1129A	S134N	19.7	0.00
	SL5072-1	*aps1-3*	G2379A	A359T	22.9	0.00
	SL4723-1	*aps1-4*	C1077T	L117F	3.6	0.18
	SL4543-1		G1203A	A159T		
	SL4799-1		G1215A	G163S		
	SL0553-1		G1216A	G163D		
	SL4827-1		G1219A	G164E		
	SL4638-1		G1842A	R289K		

Table 11. List of mutations isolated from forward screen and TILLING in several starch synthesis and degradation genes in *L. japonicus*. Continued on next page.

Table 11D. Starch degradation mutants from TILLING

Gene	Mutant line	Allele	Nucleotide change	Effect	PSSM difference	SIFT score
GWD1	SL1833-1	*gwd1-2*	G3303A	W303*	n/a	n/a
SBD2	SL3001-1	*gwd1-3*	G3994A	W456*	n/a	n/a
	SL4958-1	*gwd1-4*	G3491A	R324K	5.7	1.00
	SL0176-1	*gwd1-5*	C4236T	P497L	1.9	1.00
	SL5791-1		G3559A	G347R	-4.0	0.39
	SL0133-1		G3745A	E409K		0.22
	SL6221-1		G3745A	E409K		0.22
	SL1752-1		G3748A	E410K		0.24
	SL3333-1		G3748A	E410K		0.24
	SL4545-1		G3748A	E410K		0.24
	SL4704-1		G3932A	D436N		0.54
	SL6904-1		G3932A	D436N		0.54
	SL1523-1		C4173T	P476L		0.07
	SL1651-1		C4173T	P476L		0.07
	SL1786-1		C4173T	P476L		0.07
	SL1981-1		C4173T	P476L		0.07
	SL4826-1		C4173T	P476L		0.07
	SL0672-1*		C4239T	S498F	12.5	0.01
	SL6859-1*		G4582A	G549S	12.0	0.64
GWD1	SL5535-1	*gwd1-6*	G9912A	A968T	6.4	0.16
PHD	SL0897-1		G9769A	S920N		0.83
	SL6392-1		G9774A	D922N		0.52
GWD3	SL0692-1	*gwd3-2*	G16648A	G890E	10.2	0.02
	SL4648-1	*gwd3-3*	C17437T	P1153L	28.9	0.02
	SL0639-1	*gwd3-4*	G16918A	G980E		0.02
	SL4691-1		G16666A	G896E	-1.2	0.12
	SL1185-1		C16702T	T908I		0.10
	SL1335-1		C16801T	S941F		0.02
	SL1603-1		C16948T	P990L		0.09
	SL2714-1		C16956T	P993S		0.41
	SL5713-1		G16962A	V995I		0.08
	SL1840-1		G17052A	E1025K		0.16
	SL0489-1		G17094A	D1039N		0.10
	SL0528-1		G17163A	A1062T	-0.4	0.04
	SL1002-1		G17277A	E1100K		0.28
	SL6581-1		G17286A	V1103I		0.30
	SL6084-1		G17313A	E1112K		0.90
	SL0326-1		G17316A	V1113I		0.36
	SL6298-1		C17322T	R1115C		0.00
	SL4584-1		C17349A	P1124T		0.37
	SL1795-1		C17382T	L1135F		0.06

Table 11. List of mutations isolated from forward screen and TILLING in several starch synthesis and degradation genes in *L. japonicus*. Continued.
A and **B**, mutations from forward screen; **C** and **D**, mutations from TILLING. For mutations identified by TILLING (C and D), the tables show only non-silent mutations, e.g. Mutations giving rise to alterations at splice sites, to stop codons (*), or to missense changes. Variants identified by TILLING with silent mutation (i.e. mutation not causing an amino acid change or mutation located within intron) have been ignored here. The positions of the nucleotide changes given are their position from the start codon of the corresponding gene. The asterisk (*) indicates that no seeds were available (seed bags missing from TILLING seed collection) and that therefore the phenotype of the mutants of these lines could not be analyzed. A SIFT score smaller than 0.05 and a PSSM (Position-Specific Scoring Matrix) difference score above 10 indicates a deleterious effect. The variant displayed is colored according to the severity of its effect, as given by the PARSESNP program: changes to a stop codon and splice junction changes are colored red, and silent changes are colored black. If a missense change is in a Block, it is colored according to its PSSM difference score: if the score is less than 0, indicating that variant residue is more similar to the corresponding column of the Blocks alignment than the reference residue, then the change is colored green; if it is greater than 10, it is colored red, otherwise it is colored black. Missense changes outside of a Block are also colored black.

Table 12A. GWD1 TILLING - SBD2 domain

#	Line	Nucleotide Change	Effect	PSSM Difference	SIFT Score	Zygosity
1	SL1833-1	G3303A	W303*			Het
2	SL4958-1	G3491A	R324K	5.7	1.00	Het
3	SL5791-1	G3559A	G347R	-4.0	0.39	Hom
4	SL5039-1	G3591A	L357=			Het
5	SL4627-1	C3609T	F363=			Het
6	SL5060-1	G3744A	K408=			Hom
7	SL0133-1	G3745A	E409K		0.22	Het
8	SL6221-1	G3745A	E409K		0.22	Hom
9	SL1752-1	G3748A	E410K		0.24	Het
10	SL3333-1	G3748A	E410K		0.24	Het
11	SL4545-1	G3748A	E410K		0.24	Het
12	SL4704-1	G3932A	D436N		0.54	Het
13	SL6904-1	G3932A	D436N		0.54	Het
14	SL3001-1	G3994A	W456*			Het
15	SL1523-1	C4173T	P476L		0.07	Het
16	SL1651-1	C4173T	P476L		0.07	Het
17	SL1786-1	C4173T	P476L		0.07	Het
18	SL1981-1	C4173T	P476L		0.07	Het
19	SL4826-1	C4173T	P476L		0.07	Het
20	SL0176-1	C4236T	P497L	1.9	1.00	Het
21	SL0672-1	C4239T	S498F	12.5	0.01	Hom
22	SL6859-1	G4582A	G549S	12.0	0.64	Het

Table 12B. GWD1 TILLING - PHD domain

#	Line	Nucleotide Change	Effect	PSSM Difference	SIFT Score	Zygosity
1	SL6491-1	G9637A	Non-coding			Hom
2	SL0122-1	C9729T	Non-coding			Het
3	SL0836-1	C9729T	Non-coding			Het
4	SL0897-1	G9769A	S920N		0.83	Het
5	SL6392-1	G9774A	D922N		0.52	Het
6	SL5293-1	C9830T	L940=			Het
7	SL0511-1	C9891T	L961=			Het
8	SL5535-1	G9912A	A968T	6.4	0.16	Het
9	SL6027-1	C9924T	Non-coding			Het
10	SL5936-1	C10448T	Non-coding			Het
11	SL1027-1	G10490A	Non-coding			Het
12	SL6040-1	C10605T	Non-coding			Het

Table 12. List of the mutations identified in the regions of *LjGWD1* and *LjGWD3* genes targeted by TILLING.
Continued on next page.

Table 12C. GWD3 TILLING

#	Line	Nucleotide Change	Effect	PSSM Difference	SIFT Score	Zygosity
1	SL0692-1	G16648A	G890E	10.2	0.02	Het
2	SL4691-1	G16666A	G896E	-1.2	0.12	Het
3	SL1185-1	C16702T	T908I		0.10	Het
4	SL1335-1	C16801T	S941F		0.02	Het
5	SL0639-1	G16918A	G980E		0.02	Het
6	SL6226-1	C16937T	P986=			Het
7	SL1603-1	C16948T	P990L		0.09	Het
8	SL2714-1	C16956T	P993S		0.41	Het
9	SL5713-1	G16962A	V995I		0.08	Hom
10	SL4942-1	C16998T	L1007=			Het
11	SL6423-1	C16998T	L1007=			Het
12	SL0688-1	G17048A	Q1023=			Het
13	SL0137-1	G17048A	Q1023=			Het
14	SL1164-1	G17048A	Q1023=			Hom
15	SL1840-1	G17052A	E1025K		0.16	Het
16	SL0489-1	G17094A	D1039N		0.10	Het
17	SL0528-1	G17163A	A1062T	-0.4	0.04	Het
18	SL1002-1	G17277A	E1100K		0.28	Het
19	SL2727-1	C17283T	L1102=			Het
20	SL6581-1	G17286A	V1103I		0.30	Hom
21	SL6084-1	G17313A	E1112K		0.90	Het
22	SL326-1	G17316A	V1113I		0.36	Het
23	SL6298-1	C17322T	R1115C		0.00	Het
24	SL4584-1	C17349A	P1124T		0.37	Het
25	SL1795-1	C17382T	L1135F		0.06	Het
26	SL4648-1	C17437T	P1153L	28.9	0.02	Het

Table 12. List of the mutations identified in the regions of *LjGWD1* and *LjGWD3* genes targeted by TILLING. Continued.
The positions of the nucleotide changes given are their position from the start codon of the corresponding gene. Hom corresponds to homozygotes and Het to heterozygotes. The variant displayed is colored according to the severity of its effect, as given by the PARSESNP program: changes to a stop codon and splice junction changes are colored red, and silent changes are colored black. If a missense change is in a Block, it is colored according to its PSSM difference score: if the score is less than 0, indicating that variant residue is more similar to the corresponding column of the Blocks alignment than the reference residue, then the change is colored green; if it is greater than 10, it is colored red, otherwise it is colored black. Missense changes outside of a Block are also colored black.

	GWD1-SBD2		GWD1-PHD		GWD3	
	Obtained	Predicted	Obtained	Predicted	Obtained	Predicted
Percentage of						
Non silent changes	86.4	52.1	25	45.1	73.1	53.9
Truncation changes	9.1	6.4	0	5.2	0.0	3.9
Nonsense	9.1	4.4	0	3.6	0.0	3.7
Splice junction	0.0	2.0	0	1.6	0.0	0.2
Missense changes	77.3	45.7	25	39.8	73.1	50.0
Predicted deletorious	9.1	6.0	8.3	15.4	7.7	7.0
Predicted non deletorious	68.2	41.7	16.7	24.4	65.4	43.0
Silent changes	13.6	47.9	75	54.9	26.9	46.1

Table 13. Statistics on the mutations identified by TILLING in the targeted regions of the *LjGWD*1 and *LjGWD3* genes.
Continued on next page.

	GWD1-SBD2	GWD1-PHD	GWD3
Ratio Hom:Het (in %)	18.2	8.3	11.5
G to A transition (in %):	63.6	41.7	57.7
C to T transition (in %):	36.4	58.3	42.3
Targeted region length (in bp)	1578	1183	1299
Number of mutations obtained	22	12	26
Number of mutation per kb	13.9	10.1	20.0
Number of			
Duplicate mutation	2	1	1
Triplicate mutation	1	0	1
Quadruple mutation	0	0	0
Quintuple mutation	1	0	0

Table 13. Statistics on the mutations identified by TILLING in the targeted regions of the *LjGWD*1 and *LjGWD3* genes. Continued.
The predicted percentages of the different categories of mutations are those given by the CODDLE program. Nonsense changes refer to mutation leading to premature stop codons. Abbreviations: Hom, homozygote; Het, heterozygote. SBD2 stands for Starch Binding Domain and PHD for Phospho-Histidine Domain.

4.2.3. Identification of several mutant alleles of the starch synthesis genes PGI, PGM, and AGPase

Taking advantage of the knowledge gained from *A. thaliana* (Chapter 1 and Table 6), I examined with Tracey Welham (JIC) whether the starch-free and reduced-starch mutants selected in the forward screen lacked PGI1, PGM1, or AGPase by coupling the genetic linkage mapping with a candidate gene and enzyme approach. Doing so, we were able to determine that the mutations affecting these three enzymes accounted for the phenotypes of six of the ten synthesis mutants, as described below. In addition, additional mutant alleles of genes coding for PGM1 and two different subunits of AGPase were also generated via TILLING.

4.2.3.1. PGI1 mutant alleles

Three of the synthesis mutants from the forward screen (SL4308-12, SL4715-2 and SL5069-2) had leaf starch contents that were only 10% of WT values (Figure 20 and Table 14), but their embryo and root starch contents were indistinguishable by iodine staining from those of WT plants (Figure 20). This pattern of starch distribution is also seen in the *A. thaliana pgi1* mutant (Yu et al., 2000). The three mutants were shown by crossing to be allelic, and the mutations in all three mapped to the same interval at the top of chromosome I (Figure 19, Table 6 and Table 10). The *LjPGI1* gene is located in this interval. Sequencing of the *PGI1* gene in the three mutants revealed two mutations that create stop codons (*pgi1-1*, SL4715-2; *pgi1-2*, SL4308-12) and one (*pgi1-3*, SL5069-2) at a splice-site junction (Figure 21 and Table 15).

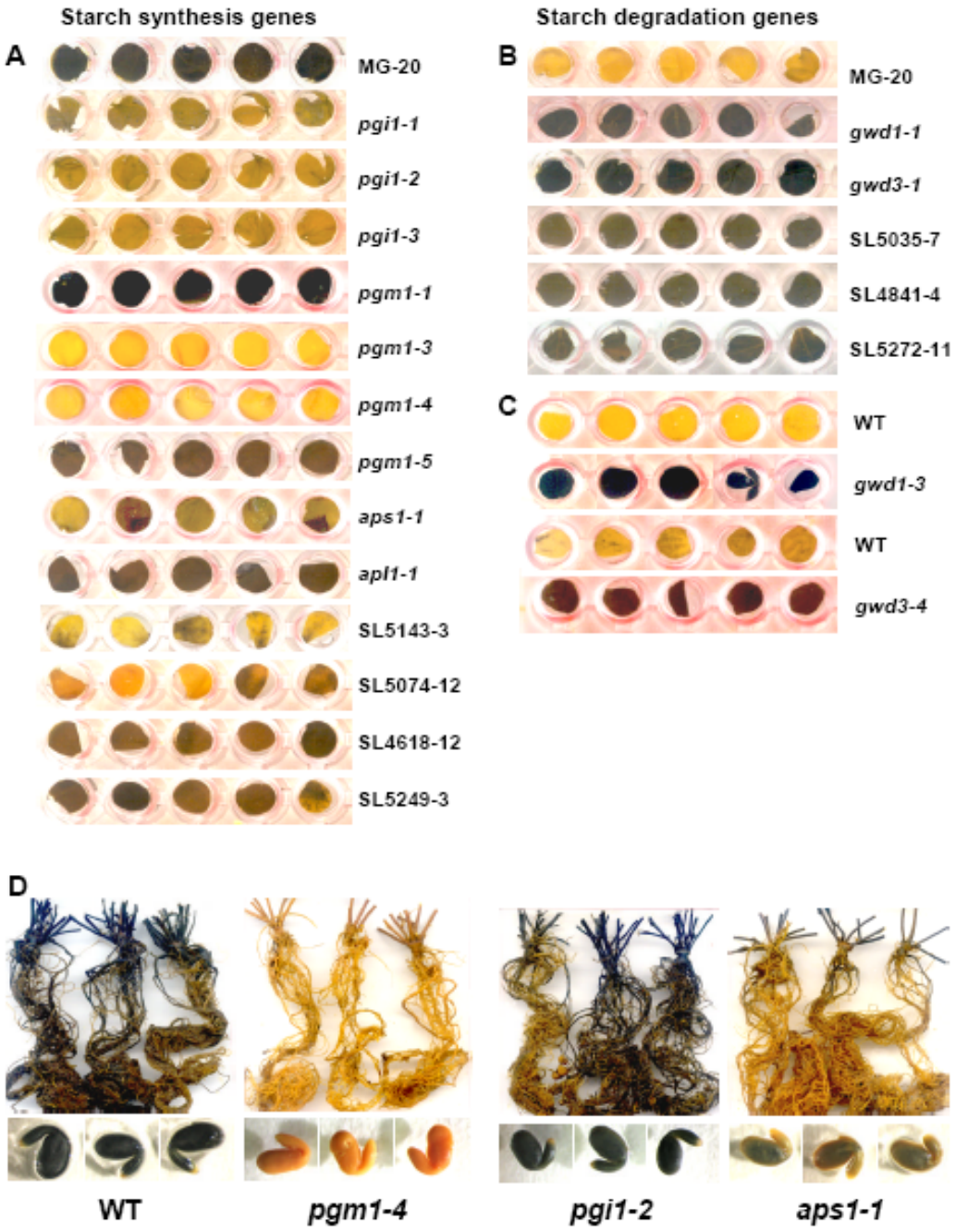

Figure 20. Iodine staining of starch synthesis and degradation mutants.
A-C. Iodine staining of leaves of mutants obtained from the forward genetic screen and from TILLING. All mutant lines shown here except *gwd1-3* and *gwd3-4* were derived from outcrosses of the original mutant with MG-20. Each leaflet is from a different plant. Plants were grown in 16-h light, 8-h dark and were ca. four weeks old at the time of harvest. The name of the mutant allele is given where this is known (Table 15). **A.** Mutants in starch synthesis from the forward genetic screen and TILLING. Leaflets were harvested at the end of the day. **B** and **C.** Mutants from the forward genetic screen (B) and TILLING (C). Leaf phenotype of the *gwd1-3* and *gwd3-4* TILLING mutants is shown in comparison to those of their segregating WT. Leaflets were harvested at the end of an extended night of up to 44 h. **D.** Starch contents of roots and embryos of WT and starch synthesis mutant plants. Plants were harvested when approximately 3 months old. Roots and embryos were decolorized prior to staining with iodine solution. Note that roots and embryos of WT plants have high starch contents, those of *pgm1-4* have no detectable starch, those of *aps1-1* mutant have drastically reduced starch contents, and those of *pgi1-2* (SL4308-12) mutant appear very similar to WT.

[a]Genotype	Starch content (mg Glc equivalents g^{-1} fresh weight)	
	Wild-type	Mutant
PGM1		
pgm1-3	25.3 ± 6.4	[b] n.d.
pgm1-4	20.1 ± 4.8	[b] n.d.
pgm1-5	29.7 ± 6.2	6.1 ± 1.3
PGI1		
pgi1-1	17.2 ± 5.9	1.83 ± 0.35
pgi1-2	50.6 ± 4.7	4.56 ± 1.90
APS1		
aps1-1	47.0 ± 4.1	3.73 ± 1.29
APL1		
apl1-1	59.6 ± 10.5	12.7 ± 2.0

Table 14. Starch content at the end of the day in leaves of mutants with starchless or low-starch phenotypes.
Values are means ± SE of measurements on six samples, each consisting of fully-expanded leaves from the upper part of the shoot of a single plant. [a]For each genotype, F3 homozygous mutant and wild-type plants for analysis were selected by genotyping individual plants in a single F2 population derived from a cross between the original mutant in Gifu and MG-20. Plants were grown for 7 weeks, as described for starch quantification in Chapter 2, section 2.13.1. [b]n.d., not detected.

I performed native PAGE followed by activity staining on protein extracts from WT leaves that revealed two bands of PGI activity. From equivalent studies on other species, these are likely to be attributable to the cytosolic and plastidial isoforms of the enzyme. One of these two bands was missing in extracts of mutant leaves. Assuming that the relative mobilities of these isoforms are the same in *L. japonicus* as in the other species studied to date - with the plastidial isoform always migrating faster (Shaw and Prasas, 1970; Weeden and Gottlieb, 1982) - the missing band was attributable to the plastidial isoform (Figure 22). As a further check on the identity of these mutants, I assayed leaf extracts for PGI activity. In several species including *A. thaliana*, spinach (*Spinacia oleracea*), cauliflower (*Brassica oleracea*) and *Clarika xantiana*, it has been shown that the activity of the cytosolic and plastidial isoform can be separately estimated by measurement before and after heat treatment of the extract, because the plastidial isoform is much more heat sensitive than the cytosolic isoform (Weeden and Gottlieb, 1982; Jones et al., 1986). For extracts of MG-20, activity was reduced by heat treatment 10 min at 50°C (8.9 ± 0.4 before heat, 7.1 ± 0.5 after heat) whereas there was no decline after heat treatment in extracts of *pgi1-1* (8.9 ± 0.1 before heat, 9.5 ± 0.2 after heat; all values are μmol min^{-1} g^{-1} FW and means ± SE from 3 plants), suggesting that the *pgi1-1* mutant was indeed lacking plastidial PGI enzyme activity. However, careful examination of the PGI activity in *L. japonicus* MG-20 and Gifu WT plant extracts before

and after heat treatment by native PAGE gels revealed that, in contrast to all the other species mentioned above, the cytosolic PGI isoform of *L. japonicus* is also sensitive to heat treatment (Figure 23). Nevertheless, the results of the native PAGE gels of PGI enzyme activity clearly show the specific loss of the plastidial isoform of PGI in the *pgi1-1* mutant (Figure 22).

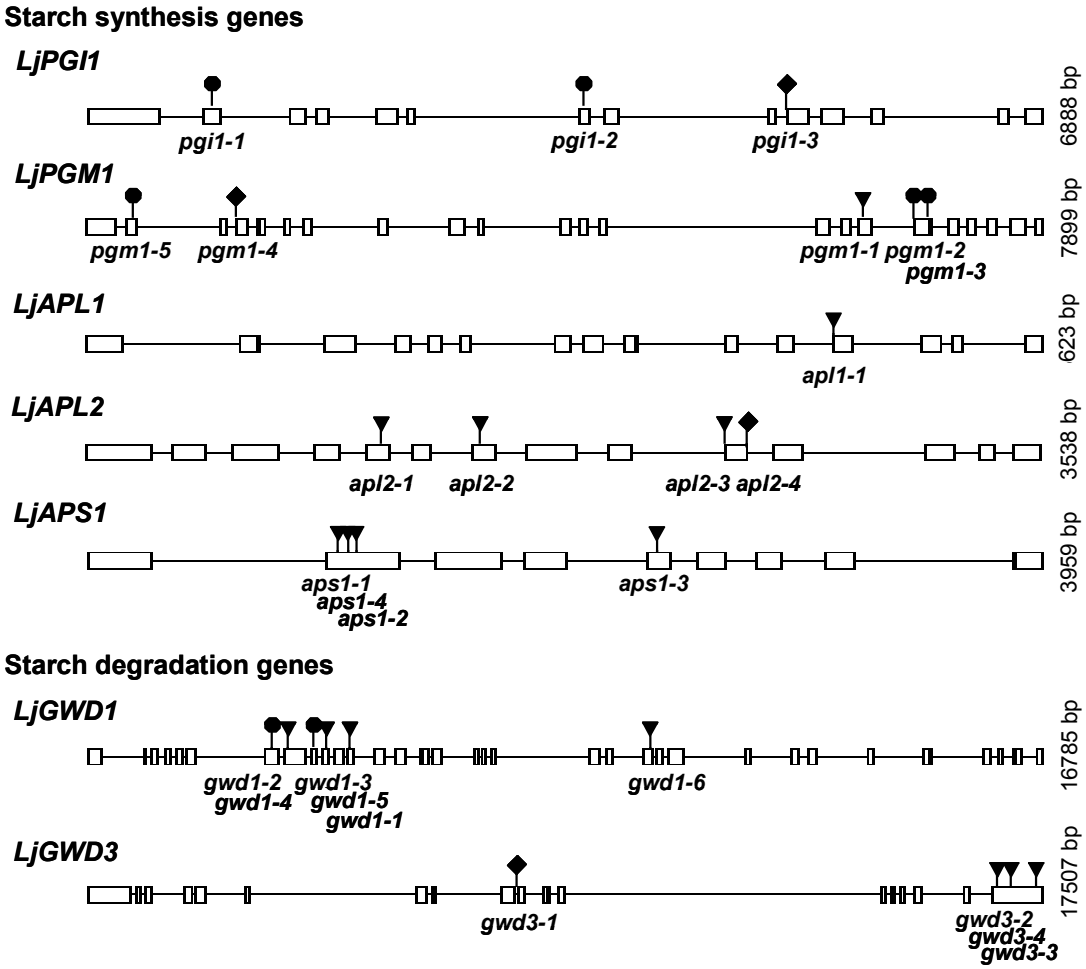

Figure 21. Structures of the starch metabolism genes and positions of the non-silent mutations discovered in the forward genetic screen and by TILLING.
Boxes and lines indicate exons and introns, respectively. Only the TILLING mutations leading to a starch phenotype and/or predicted by the PARSESNP program to have PSSM values >0 are shown. The length of the gene sequence (in base pair, bp) is given on the right. The symbols above the gene specify the mutation type and position. Octagons, stop codons; diamonds, splice site junction mutations; triangles, amino acid changes. Details on the nature and position of the mutations are given in Table 15.

Gene	Mutant line	Allele name	Nucleotide change	Effect of the mutation	Source of the mutation
LjPGI1	SL4715-2	*pgi1-1*	C917T	Q200*	Forward screen
	SL4308-12	*pgi1-2*	G3602A	W360*	Forward screen
	SL5069-2	*pgi1-3*	G5047A	Splice-site junction	Forward screen
LjPGM1	SL4725-4	*pgm1-4*	G1233A	Splice-site junction	Forward screen
	SL4867-11	*pgm1-5*	G377A	G95D	Forward screen
	SL4490-1	*pgm1-1*	G6413A	D436N	TILLING
	SL0755-1	*pgm1-2*	G6848A	W467*	TILLING
	SL1837-1	*pgm1-3*	G6932A	W495*	TILLING
LjAPL1	SL5127-5	*apl1-1*	C4408T	S400L	Forward screen
LjAPL2	SL0933-1	*apl2-1*	G1104A	D236N	TILLING
	SL0443-1	*apl2-2*	G1471A	G275E	TILLING
	SL0501-1	*apl2-3*	C2369T	P383S	TILLING
	SL4318-1	*apl2-4*	G2453A	Splice-site junction	TILLING
LjAPS1	SL0529-1	*aps1-1*	G1059A	A111T	TILLING
	SL4504-1	*aps1-2*	G1129A	S134N	TILLING
	SL5072-1	*aps1-3*	G2379A	A359T	TILLING
	SL4723-1	*aps1-4*	C1077T	L117F	TILLING
LjGWD1	SL5215-2	*gwd1-1*	G4633A	E566K	Forward screen
	SL5358-3	*gwd1-1*	G4633A	E566K	Forward screen
	SL1833-1	*gwd1-2*	G3303A	W303*	TILLING
	SL3001-1	*gwd1-3*	G3994A	W456*	TILLING
	SL4958-1	*gwd1-4*	G3491A	R324K	TILLING
	SL0176-1	*gwd1-5*	C4236T	P497L	TILLING
	SL5535-1	*gwd1-6*	G9912A	A968T	TILLING
LjGWD3	SL5104-12	*gwd3-1*	G7871A	Splice-site junction	Forward screen
	SL0692-1	*gwd3-2*	G16648A	G890E	TILLING
	SL4648-1	*gwd3-3*	C17437T	P1153L	TILLING
	SL0639-1	*gwd3-4*	G16918A	G980E	TILLING

Table 15. Mutant alleles of genes encoding enzymes of starch metabolism in *L. japonicus*.
For mutations identified by TILLING, the table shows only those giving rise to alterations at splice sites, to stop codons (*), or to missense changes leading to a starch phenotype, or with PSSM values given by PARSESNP >0.

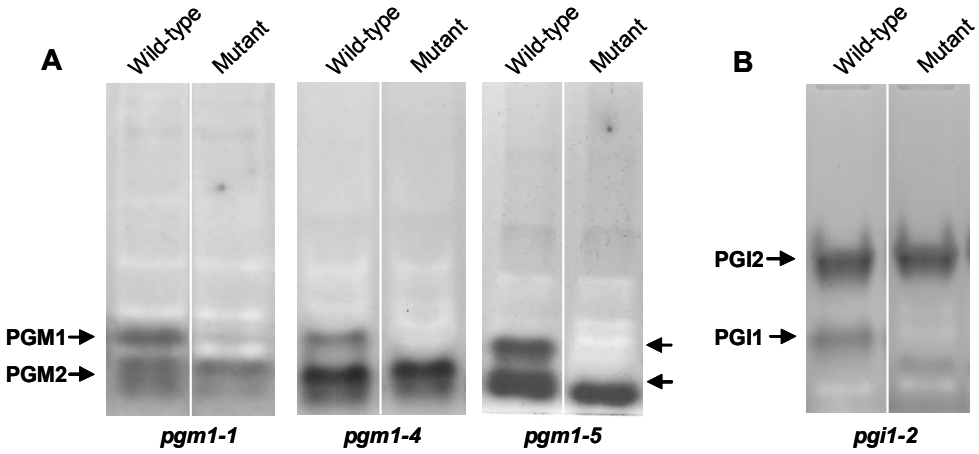

Figure 22. Separation of PGM and PGI isoform activities by native gel electrophoresis.
The positions of bands corresponding to the activity of the plastidial (PGM1, PGI1) and cytosolic (PGM2, PGI2) isoforms of the enzymes are indicated by arrowheads. The experiment was repeated on three different mutant and segregating wild-type plants for each genotype; representative results are displayed for one plant of each genotype. For each genotype, wild-type and mutant lanes are from the same gel. **A.** gels treated to reveal PGM activity. Each lane contained 100 µg of protein from a soluble extract of leaves. **B.** gel treated to reveal PGI activity. Each lane contained 50 µg of protein from a soluble extract of leaves.

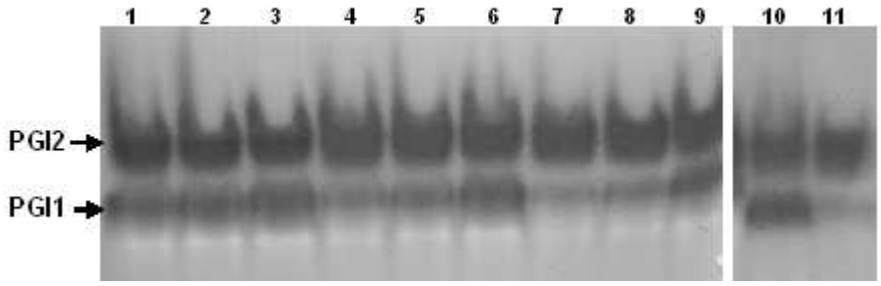

Figure 23. Heat sensitivity of the activity of the plastidial (PGI1) and cytosolic (PGI2) isoforms in *L. japonicus*.
50 µg of protein from soluble WT extracts of leaves of *L. japonicus* (1-9) and *A. thaliana* (10, 11) that had been or had not been heat-treated were subjected to PAGE followed by activity staining.1-3 and 10, WT extract not heated; 4-6 and 11, heat treated for 10 min at 50°C; 7-8, heat treated for 20 min at 50°C. The positions of bands corresponding to the activity of the PGI1 and PGI2 isoforms of the enzymes are indicated by arrowheads. Each lane contained 50 µg of protein from a soluble WT extract of leaves.

4.2.3.2. PGM1 mutant alleles

One of the synthesis mutants, SL4725-4, appeared from iodine staining to lack starch in leaves, roots, and embryos, suggesting that it might be a *pgm1* mutant (Figure 20). Consistent with these iodine staining results, quantitative measurements of starch content failed to detect any starch above the detection limit of the assay in any of the organs

analysed, including leaves, roots and stem (Table 14 and not shown). *A. thaliana*, tobacco, and pea mutants lacking PGM1 are starch-free in all plant parts examined (Caspar et al., 1985; Hanson and McHale, 1988; Harrison et al., 1998). The phenotype of this mutant is described in more detail in Chapter 5, section 5.2.2. Another mutant from forward screen, SL4867-11, had strongly reduced starch content relative to WT plants in all organs examined (Figure 20 and Table 14). I mapped the mutation accounting for its phenotype to an interval of about 10 cM on chromosome V, in which the *LjPGM1* gene is located (Figure 18, Table 6 and Table 10). *PGM1* genes of these two mutants were sequenced. The *PGM1* gene in SL4725-4 contained a mutation affecting a splice-site junction, and the gene in SL4867-11 contained a mutation predicted to result in the amino acid change G95D. These mutants are referred to as *pgm1-4* and *pgm1-5*, respectively (Figure 21 and Table 15). To investigate the lack or reduction of PGM1 activity in the mutants, I carried out native PAGE followed by activity staining on protein extracts from leaves. This revealed two bands of PGM activity in the WT extract. Assuming that the relative mobilities of the PGM isoforms are the same in *L. japonicus* as in *A. thaliana* and in pea (Caspar et al., 1985; Harrison et al., 1998), the upper and lower bands are attributable to the plastidial (PGM1) and cytosolic (PGM2) activities, respectively. The band attributable to the plastidial isoform was missing from extracts of *pgm1-4* and *pgm1-5* mutants, confirming that plastidial PGM activity is strongly reduced or absent in both cases (Figure 22).

In parallel to this forward genetic approach, TILLING was also performed on the *PGM1* gene. The program CODDLE was used to identify the region(s) of the gene most likely to contain mutations deleterious for the function of the encoded protein. The TILLING mutant population (about 5000 individuals) was then screened for mutations in the targeted region of the gene thus selected as described in Chapter 2, section 2.10. This TILLING resulted in the isolation of lines homozygous for three additional mutant alleles of the PGM1 gene (Figure 21 and Table 15). Two of these alleles named *pgm1-2* and *pgm1-3* contained mutations creating stop codons. Mutants of both lines (SL755-1 and SL1837-1, respectively) appeared from iodine staining to lack starch in all plant parts and were identical in phenotype to *pgm1-4* (Figure 20). The mutation in the third allele, *pgm1-1* (SL4490-1), was predicted to result in the amino acid change D436N. Activity of the plastidial isoform of PGM was reduced in *pgm1-1*, as assessed by native gel electophoresis (Figure 22) but no reduction in starch content of the plant was apparent from iodine staining (Figure 20).

4.2.3.3. AGPase mutant alleles

I used similar approaches to identify the mutation accounting for the phenotype of another synthesis mutant, SL5127-5, in which leaf starch content at the end of the day in plants

grown in growth cabinet was reduced by about 80% (Table 14). Following a candidate enzyme approach, I assayed the AGPase activity in extracts of the WT and mutant leaves. Activity was 93% lower in this mutant than in WT extracts (Table 16). Activity in extracts made from mixtures of WT and mutant leaves was 98.5% of that predicted from separate extracts of the two genotypes, hence the large difference in activity is likely to result from loss of AGPase function in the mutant rather than the presence of inhibitory substances in the mutant leaf. No visible reduction of starch content could be observed by iodine staining in the roots or embryos of this mutant (data not shown).

AGPase in higher plants is a heterotetramer composed of two small (APS) and two large (APL) subunits. As described in earlier chapters, many species possess one or two *APS* genes and several *APL* genes that are differentially expressed between organs (e.g. Crevillen et al., 2003; 2005; and citations therein). One *APS* gene and six *APL* genes could be identified in the *L. japonicus* genome (Table 6). In *A. thaliana*, loss of the small subunit (in the *adg1* mutant) almost eliminates AGPase activity and starch synthesis and loss of the major leaf isoform of the large subunit (in the *adg2* mutant) reduces activity by 95% and starch synthesis by 60% (Lin et al., 1988b; Wang et al., 1997). To discover whether a mutation in one of the AGPase subunit genes was indeed responsible for the starch phenotype of this mutant, I carried out mapping and gene sequencing. The mutation mapped to an interval on chromosome IV encompassing a gene encoding a large subunit of AGPase, APL1 (Figure 19, Table 6 and Table 10). Sequencing revealed a single mutation in the *APL1* gene of SL5127-5, predicted to result in the amino acid change S400L. A detailed structure-function analysis of the AGPase protein is presented in the next chapter.

To understand further the importance of AGPase subunits in *L. japonicus*, TILLING was used to identify mutations in one of the two copies of the second large subunit gene, *APL2a* (hereafter referred to simply as APL2), and in the single small subunit gene identified in the genome of *L. japonicus*, *APS1*. For APL2, four allelic variants containing mutations predicted to have a deleterious effect on activity of the encoded protein could be identified. The iodine staining I performed revealed that none of these had a clear effect on starch content in any of the organs examined, including leaves, roots, and embryos (not shown). One of the four mutant alleles identified for APS1, *aps1-1*, contained a mutation predicted to bring about the amino acid change A111T (Figure 21 and Table 15). In contrast to the APL2 mutants, mutants of this line (SL0529-1) displayed a strong reduction in starch content in leaves, roots and embryos (Figure 20). AGPase activity in leaves of this mutant grown in a growth cabinet was about 70% lower than in WT leaves (Table 16), and leaf starch content was reduced by up to 90% (Table 14).

[a]Genotype	AGPase activity (nmol min-1 g^{-1} fresh weight)
MG-20	[b]1457 ± 41
Gifu	1367 ± 140
apl1-1	105 ± 9
apl1-2	1166 ± 166
apl2-1	1844 ± 32
apl2-3	1996 ± 63
apl2-4	1364 ± 174
aps1-1	439 ± 10
aps1-2	1376 ± 160
aps1-3	1412 ± 168

Table 16. AGPase activities in leaves of the apl and aps synthesis mutants of *L. japonicus*.
[a]Plants were grown in a greenhouse as described in Chapter 2, and harvested 10 h into the 16 h light period when seven to 12 week-old. [b]Values are means ± SE of measurements on three plants.

4.2.4. Identification of several mutant alleles of the starch degradation genes *GWD1* and *GWD3*

In order to identify the mutations responsible for the starch-excess phenotypes of the degradation mutants, I followed a similar strategy to that for the synthesis mutants, and coupled the map-based cloning to a candidate gene approach. Thus far, the mutations in three of them have been identified. The mutations in lines SL5215-2 and SL5358-3 mapped to the same interval on chromosome IV, and the mutation in SL5104-12 mapped to the top of chromosome V (Figure 19 and Table 10). These two intervals encompass genes encoding *GWD1* (Ritte et al., 2002) and *GWD3* (aka *PWD*; Baunsgaard et al., 2005; Kötting et al., 2005), respectively (Figure 19 and Table 6). In *A. thaliana*, the *gwd1* (aka *sex1*) mutant has a severe starch-excess phenotype, and reduced growth under short-day conditions (Caspar et al., 1991; Yu et al., 2001). The *gwd3* (aka *pwd*) mutant (Baunsgaard et al., 2005; Kötting et al., 2005) also has a starch excess phenotype, although less severe than that of *gwd1*. Sequencing revealed that SL5215-2 and SL5358-3 both carry a mutation in *GWD1*, while SL5104-12 has a mutation in *GWD3*. Although SL5215-2 and SL5358-3 were independently selected, they carry the same mutation in *GWD1*, predicted to result in the amino acid change E566K (Figure 21 and Table 15). Plants carrying this mutation are referred to as *gwd1-1* mutants. The mutation in *GWD3* affects a splice-site junction and results in the nucleotide change G7871A (Figure 21 and Table 15). Results of detailed molecular analyses performed on these mutations are presented in the next chapter (Chapter 5, section 5.2.1). In addition, leaf starch granule microscopy of plants carrying these mutant alleles was also carried out (Figure A4)

Since only one mutant allele was isolated from the forward screen for *GWD1* and *GWD3*, the *L. japonicus* TILLING population was screened for additional mutant alleles of these two genes. Isolation of these additional allelic variants was needed to gain compelling evidence that the forward screen mutations in *GWD1* and *GWD3* are indeed responsible for the starch-excess phenotypes. The TILLING I performed on the *GWD1* gene targeted two regions of the genes, one encoding part of the phospho-histidine domain of the enzyme (PHD; Yu et al., 2001), and one encompassing the sequence encoding the second of the two putative starch binding domains of the protein (SBD, CBM45 family; Mikkelsen et al., 2006). Only one missense change could be isolated from the TILLING of the region of the gene encoding the PHD domain of the enzyme. In contrast, two changes leading to premature stop-codon sequences and nine different missense changes, of which two were predicted to be deleterious, were obtained for the region coding for the SBD-2 domain of GWD1. As expected, mutants of the two lines isolated by TILLING that had point mutations in *GWD1* leading to stop-codons (SL1833-1 and SL3001-1, *gwd1-2* and *gwd1-3,* respectively; Figure 21 and Table 15) had altered starch metabolism (Figure 20). Leaves of M3 homozygous mutant plants of both lines displayed a very strong starch-excess phenotype, stronger than that of *gwd1-1* (Figure 20). With the help of Tracey Welham (JIC) starch quantifications were performed that confirmed very high levels of starch in the *gwd1-2* mutant (end of night values WT 0.9±0.3, *gwd1-2* 43.1±3.3 mg g^{-1} fresh weight, mean±SE of at least five replicates; see also Figure 24). Immunoblotting (carried out by Tracey Welham; JIC) with an antiserum to GWD1 from potato revealed that an immuno-reactive protein of the expected mass was present in extracts of WT plants, but missing in extracts of the *gwd1-2* mutant (Figure 24). Mutants of these two lines were also strongly impaired in growth and reproduction. Functional analysis of their phenotypes is described in more detail in Chapter 5, section 5.2.2.

Several other mutant alleles were identified by TILLING, of which two (SL0672-1 and SL6859-1) were predicted to have a deleterious effect on the enzyme function. Unfortunately, both M2 and M3 seeds of these mutant lines were reported missing from the seed stock, and therefore, could not be further analysed. None of the other mutant alleles identified were predicted by the PARSESNP program to have a deleterious effect on enzyme function and leaves of the homozygous mutants did not have a starch excess phenotype (data not shown).

TILLING performed on GWD3 targeted the region encoding the nucleotide binding domain involved in the dikinase activity of the enzyme (NB domain; Kötting et al., 2005). A suite of 19 mutant alleles with missense change mutations was identified. Only two of them were predicted by the PARSESNP program to have a deleterious effect on the protein function (PSSM score greater than ten), but their homozygous mutants did not display any

clear starch excess phenotype. In contrast, homozygous mutants for another allele, *gwd3-4* (SL0639-1; Figure 21 and Table 15) had a clear starch excess phenotype in leaves (Figure 20).

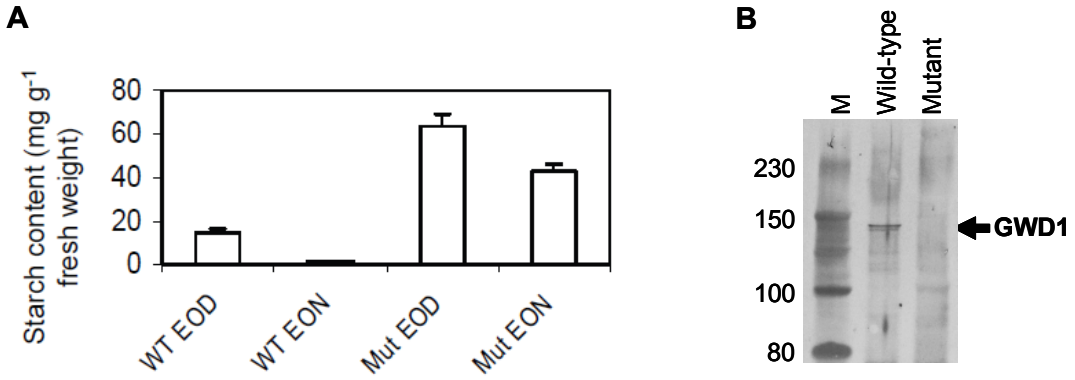

Figure 24. Starch content phenotype and western blot of of *gwd1-3* TILLING mutant.
A. Elevated starch content of leaves in *gwd1-2* leaves at end of day (EOD) and end of night (EON). Values are means ± SE of measurements on at least five, 4 week old plants. Plants were from lines derived by outcrossing to MG-20 and selfing F2 segregants. **B**. Absence of GWD1 protein in *gwd1-3* leaves. Samples of 10 µg protein from soluble extracts of leaves of the *gwd1-3* mutant and its WT segregant were subjected to electrophoresis on a 4-12% gradient polyacrylamide-SDS gel, electroblotted onto a nitrocellulose membrane, and probed with rabbit serum containing antibodies to potato GWD1 at a dilution of 1/1000. M is molecular mass markers, values in kD.

4.2.5. Phenotype of the uncharacterised mutants and map positions of their mutations

4.2.5.1. Phenotype of the mutants yet to be characterised

The starch synthesis mutants isolated from the forward screen displayed much variation in their phenotypes (from slight reduction to a completely starch-less phenotype). Differences in starch-excess phenotypes among the class of starch degradation mutants isolated from forward genetics were much less apparent (Figure 20). However, it was clear from the screening results that all were capable of some starch degradation. Although most of these mutants did not show any significant differences in growth rate or flowering time relative to the WT, two of the synthesis mutants - SL5074-12 and SL5249-3 - displayed severely impaired growth as well as delayed flowering, and a reduction in fertility. Mutants of SL5249-3 also had pale green leaves suggesting a reduction in chlorophyll content. These traits consistently co-segregated with the reduced leaf starch content of the mutants of these two lines, suggesting that a single mutation was responsible for all the phenotypic traits observed. However, analysis of segregating populations from several independent F1 crosses would be required to confirm this.

Another of the starch synthesis mutants of *L. japonicus*, SL4618-12, that had mildly reduced leaf starch content, also displayed some degree of impairement in growth and

flowering (Figure 20). The effect of the mutation in this line was developmentally dependent: as the plant matured, the reduced-starch phenotype became less clear. However, when reaching maturity, the plants could then be relatively well distinguished from the WT by a significant delay in flowering (ca. two to four weeks).

4.2.5.2. Candidate enzyme approach employed for the identification of the mutations

In an attempt to identify the mutations responsible for the phenotypes of the starch synthesis and degradation mutants from the forward screen, I initially followed a candidate enzyme approach. This approach consisted in performing a series of biochemical assays for well characterised enzymes known to be important for starch metabolism (Figure 25, Figure 26, and Figure 27). For the starch synthesis mutants, I assayed for the activity of PGM, PGI and AGPase. As described above, this helped in the characterisation of two of the mutant lines, SL4715-2 and SL5127-5, as *pgi1* and *apl1* mutants, respectively. From this analysis, it seemed unlikely that a mutation in one of these three enzymes could be responsible for the phenotypes of any of the starch synthesis mutants that remained uncharacterised (Figure 25). This was further confirmed by the results of the genetic linkage mapping (Figure 19 and Table 10).

Although the degradation of starch is less well characterized and more complex than the synthesis of starch, I also followed a candidate enzyme approach for the unidentified degradation mutants. Firstly, I performed quantification of malto-oligosaccharides (MOS) in order to determine whether any of the degradation mutants could be mutated in either *MEX1* or *DPE2*. The *A. thaliana mex1* and *dpe2* mutants accumulate very high levels of maltose (up to 100-fold greater than in the WT; Chia et al., 2004; Lu and Sharkey, 2004; Niittylä et al., 2004) as well as displaying a starch-excess phenotype in leaves. Althrough the analysis revealed an altered diurnal pattern of MOS accumulation and degradation for some of the starch degradation mutants, none of them had an increased maltose level similar to the one found in the *mex1* and *dpe2* mutants of *A. thaliana* (Figure 26). Secondly, I also carried out a western blot for the proteins SEX1 and SEX4, loss of either of which is likely to give rise to a strong starch excess phenotype. Polyclonal antibodies directed again the potato SEX1 and the *A. thaliana* SEX4 protein were used to assess whether the LjSEX1 and SEX4 proteins were present in crude protein extracts. Western blot of SEX1 revealed that the protein was present at a WT level in all the starch degradation mutant lines tested. However, since the protein may still be present but inactive, the possibility that one or some of these mutants may be a *sex1* mutant could not be excluded from this experiment. Antiserum against AtSEX4, unfortunately, failed to detect the protein in blots of WT extracts (Figure 26).

In addition, I also performed native PAGE followed by activity staining for the several starch metabolizing enzyme activities, including starch branching enzymes, starch

debranching enzymes, β-amylase 5, and starch phosphorylases (Figure 27). This was directed at determining whether the starch phenotype of any of the unidentified mutants was caused by a lack or deficiency in one of these enzymes. Depending on the enzyme activity tested, polyacrylamide gels contained starch, amylopectin or glycogen. Bands corresponding to the enzyme activities mentioned above could be found in the extracts of both the unidentified mutants and the WT, suggesting that none of these mutants were affected in these enzymes. From the results presented in Figure 27A and B, it appeared that mutants of the line SL5035-7 may lack or have reduced isoamylases and starch branching enzyme activities, however this was not confirmed in subsequent analyses (Figure 27D and data not shown).

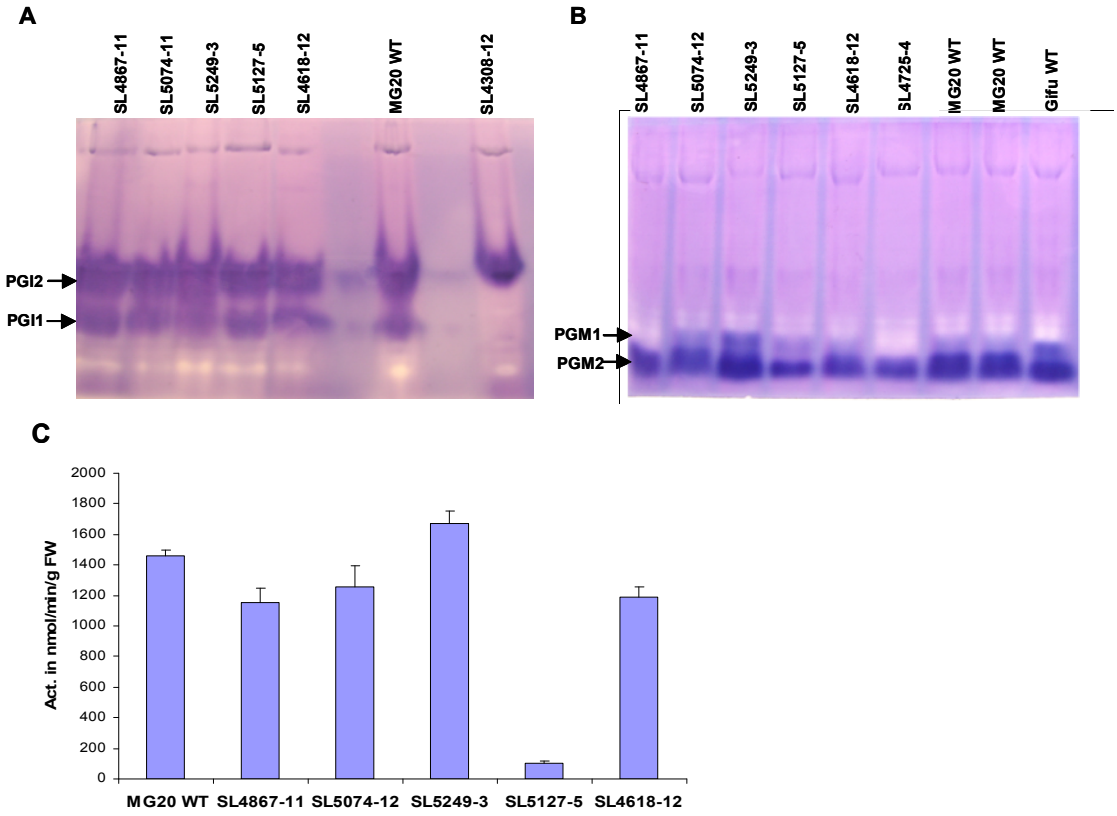

Figure 25. Results of the candidate enzyme approach performed for the synthesis mutants from forward screen.
A-C. PGI, PGM, and AGPase activity assays performed on leaf extracts of the synthesis mutants in comparison to the WT MG-20. **A** and **B.** PGI1 (plastidial) and PGI2 (cytosolic) isoform activity in leaf extracts of the synthesis mutants in comparison to the WT MG-20. The positions of bands corresponding to the activity of the plastidial and cytosolic isoforms of the enzymes are indicated by arrowheads. Approximately 100 µg of protein from soluble extracts of leaves from three plants were loaded into each lane. **A.** Native gel electrophoresis followed by PGI activity staining. SL4308-12 (*pgi1-2*) was used as control. **B.** Native gel electrophoresis followed by PGM activity staining revealing a strong reduction in PGM1 enzyme activity in mutants of the line SL4867-11 (*pgm1-5*). Mutants of SL4725-4 (*pgm1-4*) were used as controls. **C.** In vitro AGPase enzyme activity assay on leaf extracts of the starch synthesis mutants in comparison to the WT MG-20. For each genotype, the assay was performed on three biological replicates and each of them was assayed in triplicate. Values are mean ± SE of measurement on three plants. A dramatic reduction in AGPase enzyme activity was found in the mutant line SL4618-12 (*apl1-1*). FW, fresh weight.

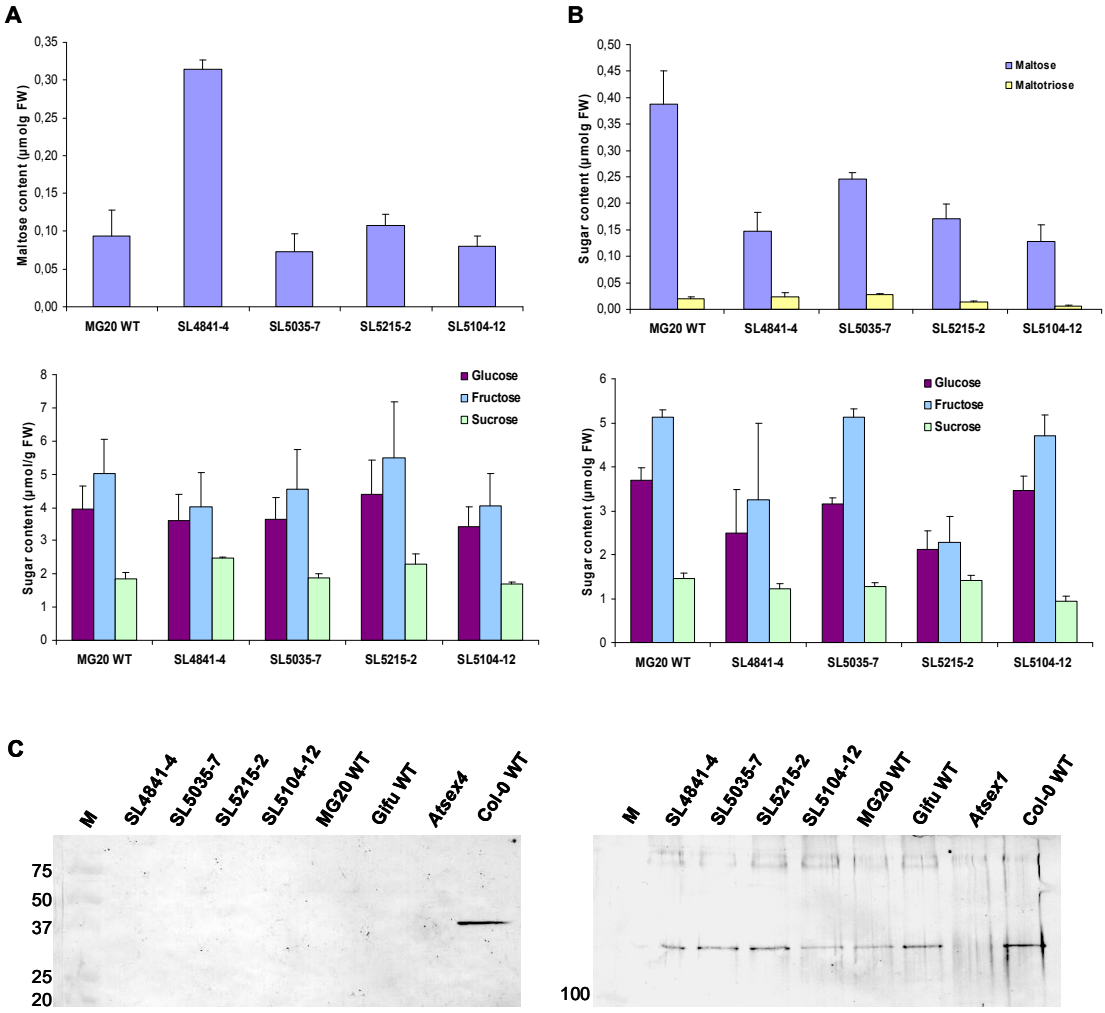

Figure 26. Results of the candidate enzyme approach performed for the degradation mutants from forward screen.
A and **B.** Measurements of maltose, maltotriose, and soluble sugars contents in leaf extracts of the degradation mutants in comparison to the WT MG-20. Plants were grown in 16 h light, 8 h dark photoperiod. Measurements were done at two different time points: at the end of the 16 h photoperiod (A) and at the middle of the dark period (B). Sugar contents were quantified by HPLC (HPAEC-PAD) as described in Chapter 2, section 2.13.3. Values are mean ± SE of measurement on three plants. FW, fresh weight. **C.** Western blots of SEX1 and SEX4 proteins performed on leaf extracts of the degradation mutants in comparison to the *L. japonicus* WT MG-20 and Gifu. The *A. thaliana* mutant *sex4* and WT col-0 were used as controls. Twenty-five µg of protein were loaded in each lane. M indicates molecular mass markers; values are in kDa. The blots were probed using StSEX1 or AtSEX4 antisera at a dilution of 1:5000.

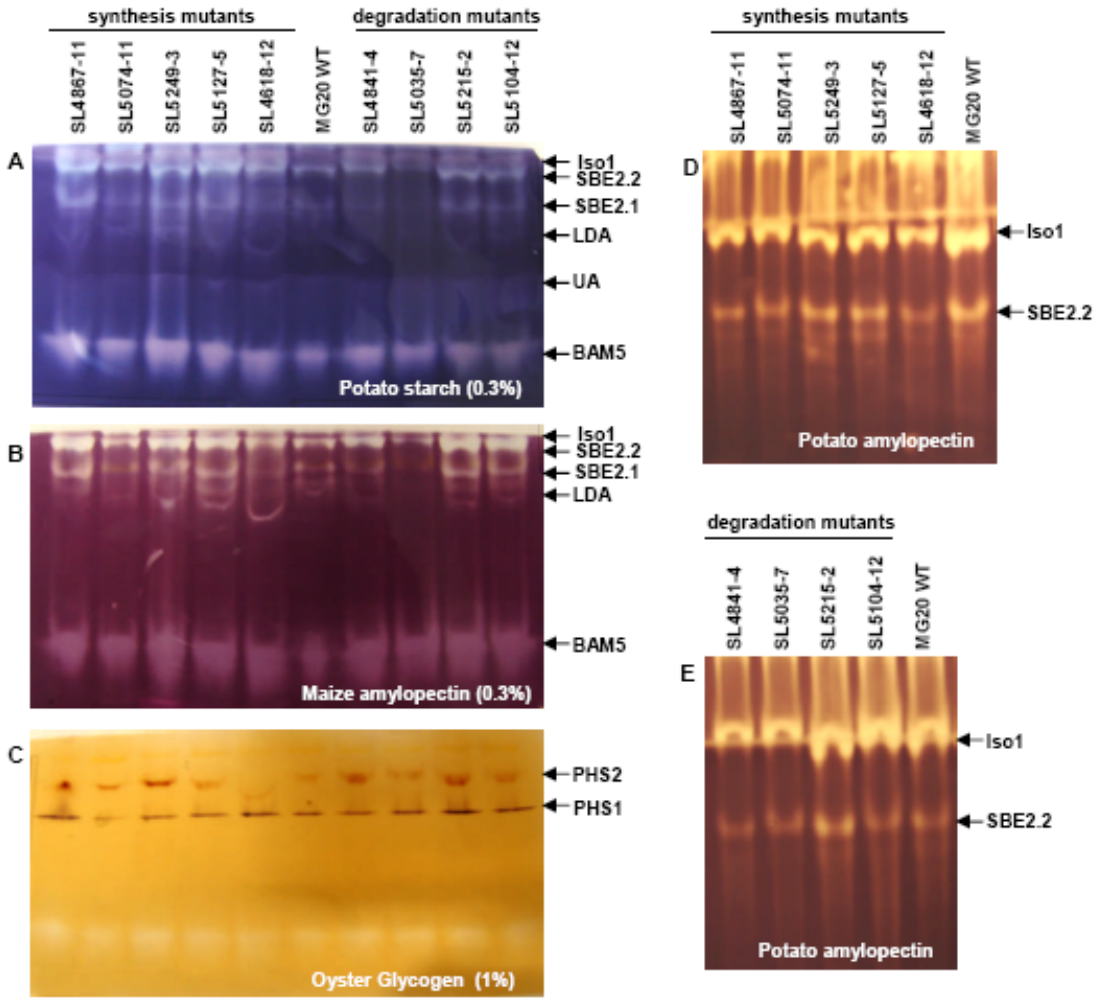

Figure 27. Zymograms of starch-metabolizing enzyme activity in several of the forward screen mutants in comparison to the WT MG-20.
Native PAGEs followed by activity staining (aka zymograms) were performed on leaf extracts of the synthesis and degradation mutants from the forward screen, in comparison to the WT MG-20 (candidate enzyme approach). Approximately 100 µg of proteins from soluble extracts of leaves from three plants was loaded onto poylacrylamide gels containing different subtrates. **A**, starch; **B**, **D**, and **E**, amylopectin; **C**, glycogen. After migration and incubation in the appropriate buffer (Chapter 2, section 2.12.3), starch-enzyme activities were revealed by iodine staining. On the right of each gel, a putative attribution of the enzyme activities corresponding to the bands is made according to the annotation given for equivalent analyses in *A. thaliana* (Zeeman et al., 1998; Wattebled et al., 2005 and 2008; Dumez et al., 2006; Delvallé et al., 2005). Identification of the different bands in *A. thaliana* was established following the analysis of mutant plants defective in each of the specified activity. Abbreviations: WT, wild-type; Iso1, isoamylase; SBE2.2, starch-branching enzyme 2.2; SBE2.1, starch-branching enzyme 2.1; LDA, limit-dextrinase, BAM5, β-amylase 5, PHS1 and 2, starch phosophorylase 1 and 2. Detailed information on these enzymes, including their corresponding locus name and accession number can be found in Table 6.

Taken together with the results of the mapping presented above, results of this candidate enzyme approach suggested that none of the unidentified mutants was likely to be affected in most of the core set of enzymes involved in the pathways of starch synthesis and degradation. However, not all the starch enzymes - including several that may have been responsible for the phenotype of some of the mutants (e.g. ISA2, ISA3, SS3, SS4, DPE2)-

could be mapped onto the genetic map. Further, the activity of several starch synthases, β-amylases, ISA3, DPE1 and DPE2 known to play an important function in starch synthesis or degradation remain to be tested for this set of uncharacterised mutants.

4.2.5.3. Map position of the mutations yet to be identified

In collaboration with Andreas Brachmann (LMU, Munich), I mapped the mutations responsible for the mutant phenotype of the remaining four synthesis mutants (SL5249-3, SL5143-3, SL5074-12 and SL4618-12) and three degradation mutants (SL4841-4, SL5035-7 and SL5272-11) from the forward screen. To date, mutations of four of the mutants have been mapped to intervals of less than 5 cM (synthesis mutants SL5249-3 and SL4618-12 and degradation mutants SL4841-4 and SL5135-7; Figure 19 and Table 10). This mapping was coupled to the candidate gene approach so that any strong candidate gene (i.e. genes known to play a key role in starch metabolism in other plant species) located in the mapped region was sequenced. In agreement with the results of the candidate enzyme approach, however, no strong candidate genes could be identified within the mapped region of any of these seven yet uncharacterised mutants. Hence, the search for candidate genes was extended to genes known to be, or potentially, involved in carbohydrate metabolism and its regulation.

Several putative candidate genes could be identified for some of these mutant lines, and were sequenced (Table 17). This included genes encoding proteins possibly involved in carbohydrate metabolism or its regulation, including 14-3-3 proteins and protein phosphatases. Analysis of the coding sequence of all these genes, however, did not identify any mutations other than Single Nucleotide Polymorphisms (SNPs) between MG-20 and Gifu. Taken together, this suggests that the mutated genes responsible for the phenotypes of these mutants are likely to encode previously-undiscovered components or regulators of the pathways of starch metabolism.

The presence of several recombinants for the flanking markers of these mapped regions means it could still be possible to shorten the interval where the mutation maps without the need to isolate more mutants. Unfortunately for most of the mutations, the presence of gaps in the genome sequence in these regions rendered difficult any comprehensive candidate gene approach as well as the design and use of additional markers for finer mapping. In one particular instance, however, namely the mutant line SL4618-12, the mutation could be mapped to an interval of less than 0.1 cM. Finer mapping and strategy employed for the identification of this mutation are presented in more detail below.

4.2.5.4. SL4618-12 fine mapping and mutation identification by next generation sequencing

For SL4618-12, mapping by bulk segregant analysis originally mapped the mutation close to the marker TM0143, at the bottom of chromosome 1 (Figure 19 and Table 10). This position was later confirmed and refined by finer mapping (Figure 28). At first, this finer mapping was performed on the mutants only (120 individuals with reduced-starch phenotype isolated from F2 segregating populations), and thereafter on a whole F2 population of 802 segregants (200 mutants, 602 WT) in collaboration with Dr. Andreas Brachmann (LMU Munich, Germany). This segregating population consisted of F2 plants from three independent F1 crosses to check the robustness of the phenotyping and genotyping results. Interestingly, it was found that this mutant line had a particularly high recombination rate compared to all the other lines of our collection as well as many published results of map-based cloning in *L. japonicus*. Further, it became apparent from the mapping of whole population of 802 F2 that the frequency of recombination in the mapped region of this mutant line was significantly higher for the mutants than it was for its WT segregants (five recombinants out of 200 mutants were identified with the markers TM2089 and BM1994, while only four recombinants out of about 600 WT and heterozygous plants could be identified with the same markers).

From this fine mapping, the mapped interval containing the mutation could be refined to a 150 kb region on the physical map (less than 0.1 cM on the genetic linage map) that contained 22 predicted genes (Figure 28). Three putative candidate genes, namely an adenosine kinase, a thioredoxin-like fold protein, and an unknown plastidial protein were identified among them (Table 17). Sequencing of their coding sequence, however, did not identify any point mutation that could have led to affected protein function.

After having envisaged different approaches for the identification of the mutation of this line, an attempt to identify the mutation in SL4618-12 was made by massively parallel sequencing (so called next generation sequencing) using the Illumina® Solexa sequencing technology (Illumina Inc., San Diego, USA). Such approach can be divided into the following three main steps: 1) Genomic DNA extraction, primer design and long range PCR; 2) Sequence data generation by Illumina genome analyzer; and 3) Sequence data analysis. Such an approach has recently been employed in *A. thaliana* on one occasion (Sturre et al., 2009) but has not yet been attempted in any other plant species.

The strategy I chose to follow consisted of amplifying long DNA fragments overlapping each other, and covering the whole region of interest, followed by the use of the Illumina® Solexa sequencing technology (massively parallel sequencing) and the subsequent *de novo* assembly of the short sequences. For this approach, the original homozygous mutant in Gifu background was backcrossed with a wild type plant of the ecotype Gifu (instead of MG-20), and the resulting F2 segregating population was screened for plants displaying the mutant phenotype. Ten of the homozygous mutant plants together with 10 biological replicates of

the Gifu WT were isolated to be further used for the identification of the mutation by massively parallel sequencing. Genomic DNA extraction was performed on leaf material harvested from each of these individuals, as described above (Chapter 2, section 2.6.1).

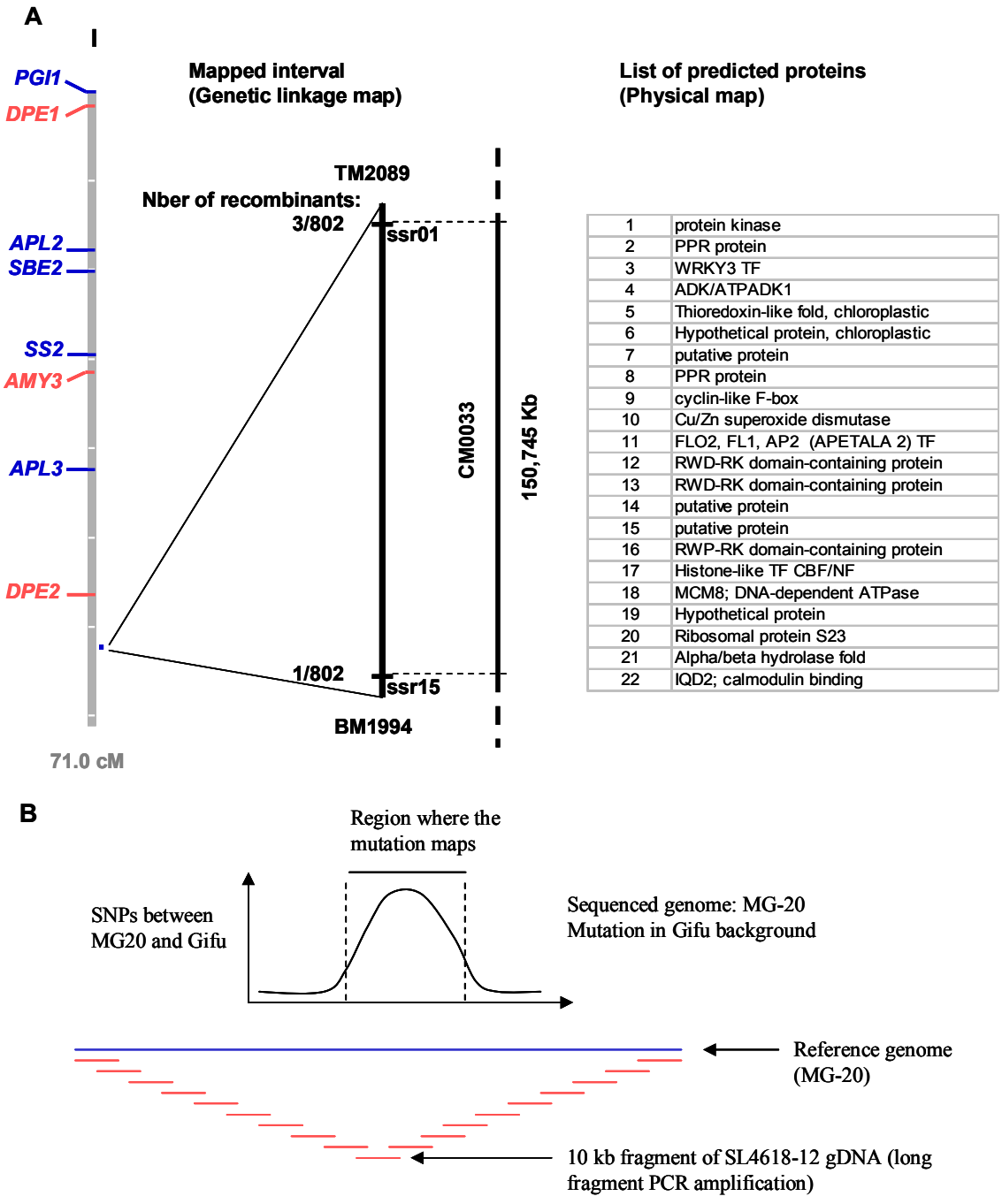

Figure 28. Fine mapping and mutation identification strategy of the mutation responsible for the mutant phenotype of the forward screen mutant line SL4618-12.
A. Results of the final step of fine mapping of the mutation of the starch synthesis mutant from forward screen SL4618-12. The mutation could be restricted by mapping to a ca. 150 kb genomic interval delimited by the SSR markers ssr01 and ssr15. Twenty two genes are predicted in this genomic region (annotation shown on the right). **B.** Illustration of the strategy chosen for the identification of the mutation responsible for the mutant phenotype of SL4618-12 using the Illumina® Solexa sequencing technology (massively parallel sequencing).

Mutant line	Locus name	Description	Best At hit
SL5249-3	chr1.CM0982.360.nd, CM0982.410.nd	14-3-3 protein (GRF)	AT5G65430.2
	chr1.CM0036.130.nc	Photosystem II oxygen evolving complex protein (PsbP)	AT2G28605.1
SL5074-12	chr1.CM0104.280.nc	Trehalose-6-phosphate phosphatase (TPP)	AT1G35910.1
	chr1.CM0104.340.nd, CM0104.350.nd	Thioredoxin family protein (TRX), chloroplastic	AT1G08570.1
SL5143-3	chr2.CM0177.660.nc	Starch synthase V (SS5)	AT5G65685.1
SL4841-4	chr1.CM0032.500.nc	Disproportionating enzyme (DPE1)	AT5G64860.1
	chr1.LjT27C19.160.nd	RSW3 (radial swelling 3) hydrolase	AT5G63840.1
	chr1.CM0982.360.nd, CM0982.410.nd	14-3-3 protein (GRF)	AT4G24620.2
	chr1.CM0248.240.nd	Dual specificity protein phosphatase (DSP)	AT3G10940.1
SL5035-7	chr1.LjT36l17.120.nd	glycosyl hydrolase family 17 protein (GH17)	AT3G07320.1
SL4618-12	chr1.CM0033.220.nd	Adenosine kinase (ADK/ATPADK1)	AT2G37250.1
	chr1.CM0033.230.nd	Thioredoxin-like fold (TRX), chloroplastic	AT2G37240.1
	chr1.CM0033.240.nd	Unknown protein, chloroplastic	AT3G53470.2

Table 17. List of putative candidate genes identified and sequenced for the yet uncharacterised forward screen mutants.
For each of the gene listed, the full predicted coding region was sequenced using gene specific primers. Sequences of these genes were retrieved from the Miyakogusa database (http://www.kazusa.or.jp/lotus/). In each case, the sequence was submitted to the program COODLE to check the correctness of this prediction, determine the gene structure (introns and exons) and the region of the gene most likely to contain deleterious mutations. Multiple protein sequence alignment using the program Clustal W2 was also carried out with sequences of their homologs from other plant species to verify that the sequence was correctly predicted. In case of the DSP gene (chr1.CM0248.240.nd), the predicted sequence was only partial (marked with an asterisk). Coding sequences of all candidate genes but the ones of chr1.CM0104.280.nc and chr1.CM0104.340.nd were sequenced. Several point mutations (not listed) were identified. However, systematic sequencing of the gene sequence of both MG-20 and Gifu WT parents in comparison to the mutant revealed they were Single Nucleotide Polymorphisms (SNPs; natural variants) between the two parents. No point mutation likely to arise from the EMS mutagenesis and to be responsible for the mutant phenotype was identified in the coding sequence of any of these candidate genes. Single nucleotide changes corresponding to silent changes (e.g. either located in introns or not leading to amino acid changes) were ignored. chr1.CM0982.360.nd and CM0982.410.nd; chr1.CM0036.130.nc; chr1.CM0982.360.nd and CM0982.410.nd; and chr1.CM0248.240.nd are currently located outside of the mapped interval.

Table 18A

name	position	Forward primer (5'-3' sequence)	Reverse primer (5'-3' sequence)
TM2089	1	CAGCTCCATTAACTTCCACC	AACCTGAAAGAAGATGCCAC
ssr01	7353	CTCAATCACCACACGATGCT	TGGGGTTTTTCCGACCAAAA
ssr02	26995	AGTTTGTGCTATTCTTGTATATGTTT	AGTCAGATATGGAGTTCATAAGTT
ssr11	35814	TACCTGCAAAAGATAGCGGG	GCTATAGCTTAAGTTAATTTGTTCA
ssr03	40666	GAGGGCTAAAGTTGGGGAAC	TCCAATCCAAGAGAAGCAAACA
snp01	43754	TTGACCACCAAGTCAATGTC	ACTTGTTGTGCTCCATTCTC
ssr12	54427	TTGGTTCCTCCATTGTCACC	GGAGGAGAGGGTAAAGGTGT
snp02	75206	AATGATGGCAGGAATTGCAT	AATGTTGGTGAGAGAAGGGA
ssr04	83603	TGGTTACCCAAGGACTACACT	ACGTTAGCACCGCATAACTG
ssr05	89894	TGGAACCGAAATGTTTGACAGA	TGGCTGCTTCTTCTTTTGGG
ssr06	90201	AAAGGCATCCGGAAAAACCA	TAGGCACCTGACTTTGGAGT
ssr07	105277	TGCATAAACCTGCTTGGTCA	ATTTCGTACAAGGACTAGAAAAGA
ssr08	113260	TGCTGTGTAATATATTGGTGTGTG	TCATTGGCTCATTACTATTGTTTCT
ssr13	123704	TCATCTCACTCACTCGCTCT	GTGGACGGAACCCTAATCTG
ssr09	125311	CCCCTTTCCTTTGAAAAGCC	AGATGTTTGTGTGTAGGGGG
snp03	126519	GTGGTAATCACGTGTGTTCT	TAATCAACCCACCAACATCG
ssr14	140362	ACGGCCTCGTTTCTTTTTGA	TTCACACAACACTTCCCCTC
snp04	141516	CGCCAAGACCGTCATTATTA	TGTGCTTTATCAGTTCGAGG
snp05	148348	CACCAAGATTCAGGTCAGTC	TCCTTCTCAACCCCTTCAAT
ssr10	152273	AGGGTTTCAATCTTCCTTTCGT	AAACCTTCAGGATGCAGAGC
snp06	154239	TTTAACTGTACCACCGAAGC	TACGTAAGTGTGAGGGGAAA
ssr15	158098	GAGAAAACAAACCCAACCGT	CCGTGGGACTACAGTACAATC
BM1994	168887	AAACATGGATGGGGTCATAG	CATGTTTAGCTTGAGAACCG

Table 18. List of primers designed for the identification of the mutation responsible for the mutant phenotype of SL4618-12 using the Illumina® Solexa sequencing technology.
Continued on next page.

Table 18B

name	position	5'-3' sequence
1F'	6365	CCTCTCCCAAGAGACATTCTGCTC
1R_nested	11859	GGGAATAGGTGGTTAGTGACATGC
1F_nested	11412	GGCTCTGCTAAACCTTCCTCTGAT
1R'	17210	GTAACAAGGTAGCCGCACTGGAAG
2F	16851	TGGACCAAACCTGCACTATACACC
2R-nested	22360	GACGGAGAGTGGGTGACTTGATCT
2F_nested	21924	CCCGACGCCTTACAGAACTTAGTG
2R	27669	GGTGGTCGCTGATACCTTATTGGA
3F	27018	TCTCGCCGGTAATGGAGAACTT
3R_nested	32754	GAGGAAAAACACATCGGAGTGGTC
3F_nested	31954	ATCAGTATGAGAACCTGGCCTTGG
3R	37653	GTGGCAGAGATGGAGATCATTGTC
4F	36759	GGACTTTCTCCACCCCAACTCA
4R_nested	42250	GACAGGACACAGTACCAGCTCTTGA
4F_nested	41726	AACCCTTGAGGCTTGAGGTAAGGT
4R	47396	ATCCAATGAACCTGTGGTGTCCTC
5F	46476	AGATGGACTGTTTGAGGCTTGGAG
5R_nested	52359	GCTACATTTAGGCCCAGTTTGG
5F_nested	51396	CGCTCCTCTTCACGATCACAAA
5R	57161	ACTTCGTTGCAGAGAGGTGAAGGA
6F	56532	CCCATGCGAAACATGTAGACACCT
6R_nested	62167	TCGCCTCCTCACGTATGATGAAAG
6F_nested	60748	TGATACCCAGTACCATGCAA
6R	66725	GTGTTATTTGACCCCACGGTATGG
7F	66273	GAACCACTAAGGCTCTCCCAATGA
7R_nested	71799	GCCTCCTCGCAGAAGATGATTAC
7F_nested	71231	TCCAGGACTGAACAACGTAACCTG
7R	77109	TCTTCCCGTCCTCCGATAGAAAGT
8F	76145	TTGTCATCACCACTCCCTCTCCTT
8R_nested	81877	TGGGAGGTTTGCGGAGAAAATG
8F_nested	81004	TTTAGCTCCCCTTGCCCTCAC
8R	86943	TGTCTCTCGATCTCGCCCTAAAAC
9F	86138	GTTTACACGACACGCCACATCAC
9R_nested	91922	GTTGGACATTGAAGCCAGCCTCT
9F_nested	90940	CTCAATCTCACATCGGCAGCAA
9R	96717	CTCTGCAGTTTATGACCCCCAAAC
10F	95976	CATGCAACAGCTGCCTGTGAAA
10R_nested	101602	GCAGGGAAGTCTACGAGCAAAGC
10F_nested	101267	TTTGCTTCATCAGCCGTCTCAG
10R	106905	AACAGGGTAGATGGCAAGCAAGAG
11F	106334	CTACAGCCCCGACCGATAACAG
11R_nested	112019	GTTAGCCAACCTCTGGTGCCTCT
11F_nested	111338	ACCGGTGCTTCACGTACAGAGATT
11R	117073	AGGGCGATCTATTGTCCATTACCC
12F	116640	CACTGGTGGGATATGAGCAAAGTG
12R_nested	122618	TTGGTTTGTTGACGCACGAC
12F_nested	121654	TTCCATATGCCAAGCGTGAACC
12R	127378	GCATGTCAACCCCTATCCTTGGTA
13F	126928	TGTCGAGCACCTTATCGTATGACC
13R_nested	132429	TTTCGGCCAAACTTTCACG
13F_nested	131628	ACTTCCGGGTTGGCTATTGTTG
13R	137260	CCTGGTCAACTCCTTCGCAAATAC
14F	136426	GTTGACTCATACCCCCACTTCGAC
14R_nested	142037	GCCACATTGCCCACATAAGTTACC
14F_nested	140964	GGCCAAGTTTGGGTTGGTTTAGAG
14R	146673	GACCATCGTCGTTACAGTCGTCAT
15F	146262	TCTCACGCCCATGACATCTAGTTC
15R_nested	151984	ACCCGTGGCAATGAATCCATGTAG
15F_nested	151467	GACTGATGGCAGCTTCTCAGGTAA
15R	157113	CACACTCCATCTTCTCCGATTTCC
16F	156241	GCCTACGGTGAGACATCAGCTTG
16R_nested	161843	GCCTCTGGTTTGACACTTCTTCTG
16F_nested	161190	GTTTCCTGTCTCCCATGCTT
16R	166732	CTGTTCAGGCAGCAGTTGTTAGGA

Table 18. List of primers designed for the identification of the mutation responsible for the mutant phenotype of SL4618-12 using the Illumina® Solexa sequencing technology. Continued.
The positions (in base pair; bp) given correspond to the position from the 5' of the SSR marker TM2089 that is located at the position 56849 from the start of the complete sequence of the contig CM0033. Sequence of this contig was retrieved from the Miyakogusa database. The primers ssr01 to ssr15 designed for fine mapping of the mutation and listed in **A** were designed by Andreas Brachmann (LMU, Munich) using the program SSRIT. Primers for the identification of the mutation by Illumina® Solexa sequencing technology are listed in **B.** These primers were designed using the program Primer3 as described in Chapter 2, section 2.6.3.

PCR primers were designed using the Primer3 program with the criteria generally recommended for the amplification of large amplicons: GC content above 50%, matched melting temperature above 60 °C, and primer sequence close to 24 nucleotides in length. Furthermore, primers pairs were designed to assure a minimum of 300 bp overlap between each amplified fragment. First, trials were made to determine the optimal size of DNA fragments and the most efficient polymerase enzyme to use for their amplification. Genomic *Lotus* DNA was amplified in a range of 5 to 15 kb DNA fragments. Different high fidelity DNA polymerases were tested for the amplification of these fragments. This included the TaKaRA Ex Taq™ polymerase (TaKaRA Biotechnology), the Expand Long Template PCR system (Roche Diagnositics GmbH, Mannheim, Germany), the LongAmp Taq DNA polymerase (New England Biolabs), the SequalPrep™ Long PCR Kit (Invitrogen), and the Phusion™ high-fidelity DNA polymerase (Finnzymes OY, Espoo, Finland). In each case, PCR was performed according to the manufacturers' instructions. PCR products were then subjected to electrophoresis on a 0.5-1% agarose gel to check for specificity and yield of the amplification products. The purification step of the PCR products was tested using several PCR purification kits according to the manufacturers' instructions. This included the kits PureLink™ PCR Micro Kit (Invitrogen), the Nucleospin® extract II (Macherey-Nagel GmbH, Düren, Germany), and the QIAquick PCR purification kit (QIAGEN). Performance of the purification kits was assessed by measuring the DNA concentration using a Picodrop™ spectrophotometer.

At first, primers were designed to allow the amplification of PCR products 10 kb long. However, robust amplification of such long DNA fragments proved to be difficult to obtain for all the primers pairs with any of the polymerase enzymes tested above. In the meantime, new advances in the use of the Illumina® Solexa sequencing technology made possible the use of DNA fragments of any size instead of the previous requirement of 10 kb-long fragments. Taking advantage of this, additional, nested PCR primers were designed for the coverage of the whole 150 kb region by a series of overlapping 5 kb fragments. In total, this corresponded to the design of 32 primers pairs (Table 18) and the amplification of 640 PCR products. The most efficient and robust amplification could be obtained using the Phusion™ high-fidelity DNA polymerase (Finnzymes). Highest DNA recovery and purity of the PCR products were obtained with the QIAquick PCR purification kit (QIAGEN).

4.3. Discussion

4.3.1. Forward and reverse genetics to isolate starch metabolism mutants in *L. japonicus*

In order to elucidate the pathway of starch synthesis and degradation in legumes and discover its importance for plant growth and development in these species, a collection of forward genetic mutants of the model legume *L. japonicus* was generated. This forward genetic approach with map-based cloning was coupled with a reverse genetic approach using TILLING. TILLING in model and crop legume species has largely been used so far for functional genomics research, either to generate new mutants of genes encoding enzymes of a pathway of interest and investigate their function (e.g. Horst et al., 2007; Welham et al., 2009), or to confirm the effect of mutations identified in forward screen mutants and carry out structure-function studies (e.g. Perry et al., 2009; Hofer et al., 2009). In this study, TILLING was employed with success both to confirm the identity of forward screen mutations thought to be responsible for the starch mutant phenotype, and to generate mutants for additional genes encoding enzymes known to be involved in starch metabolism in other species.

Put together, this work led to the characterisation of multiple mutations affecting five enzymes of starch synthesis and two enzymes of starch degradation. In addition several more mutants with altered starch metabolism from the forward screen remain to be characterised. Arguably, this set of characterised forward screen mutants constitutes the most comprehensive resource developed so far for the study of transitory and storage starch metabolism in a species other than *A. thaliana*. These results illustrate the power of using the forward and reverse genetic approaches employed in this study and the usefulness of combining these two complementary approaches for the identification of mutants with alteration in a biological process of interest.

Screening of the forward screen mutants for starch content was typically done by iodine staining, however, quantitative measurements of starch content were also made during their characterisation. Results obtained by both methods and the conclusions that could be drawn from them correlated well with each other. For instance, organs of mutants that displayed a clear yellowish colour following iodine staining always had starch content in these organs below the level detectable by enzymatic assays. Hence, iodine staining constitutes a method suitable, sensitive and robust enough for the screening of large population of mutants with reduced starch content. However, the fact that the staining is saturated above a certain level represents a major drawback for its use in screening mutants with starch excess phenotype in species in which the basal starch content is naturally high (the case of *L. japonicus* plant over six weeks old; Chapter 3, sections 3.2.4 and 3.3.5). Above this level, the organ or tissue appears totally black and a starch-excess phenotype can no longer be detected visually. However, it might be possible in this situation to screen the plants when still very young, or

to develop a screen with diluted iodine, or following decolourisation for a specific time in water.

Screening for an alteration in leaf starch content was chosen over screening of other organs because it was easy to perform, non destructive of the plant, and because we were interested in identifying mutants altered in transitory leaf starch metabolism. However, it would be interesting to extend this screen to alteration in starch content not only in leaves, but also in other organs of the plants, such as the roots. Very little is known to date about the pathway of starch accumulation and turnover in roots but there is evidence to suggest that significant differences exist between the pathway of transitory and storage starch metabolism, and between organs and tissues of the plants (Chapter 1 and references therein). Performing the screen in roots may lead to the discovery of genes specifically important for the metabolism of root starch and provide information for manipulating the metabolism of root/storage starch to improve yield in crops.

Since the characterisation of the mutants required to generate progenies and backcrossing, only mutant plants that were not too strongly affected in growth and development and were fertile were selected for further analyses. Hence, the selection process was biased in favour of mutant alleles conferring a starch phenotype without any strong deleterious effect on growth and reproduction. It was not possible within the period of this study to characterise mutant alleles that strongly affected growth and fertility. However, it is likely that, in the future, technological advances, particularly those being made in sequencing technology, would facilitate the characterisation of forward screen mutants strongly impaired in growth and reproductive capacity by reducing the size of plant population required to identify forward screen mutations.

4.3.2. Advantages and disadvantage of using EMS mutagenesis to generate mutant collections

In this study, an EMS mutagenised population of *L. japonicus* was used for both forward and reverse genetic approaches to isolate mutants altered in starch metabolism. Mutagenesis with EMS offers several advantages as mentioned earlier (section 4.1.1). One main advantage is that it can creates large number of point mutations per genome (the mutation load is dependant of the EMS mutagen concentration used to generate the population), therefore allowing the saturation of the genome to be achieved with a relatively small population. The degree of saturation is an important criterion for effective mutagenesis and TILLING since the mutation frequency is what determines the likelihood of obtaining deleterious mutant alleles for any gene of interest. It has been estimated that the EMS mutagenised population in *L. japonicus* contains, on average, over 900 mutations per

genome in addition to the mutations in specific genes of interest (Perry et al., 2009). The size of this population (ca. 5000 independent M2 mutant lines) is sufficient for the saturation of the *L. japonicus* genome with mutants (Perry et al., 2003). Another major advantage of EMS is that it allows a range of allele strengths to be generated. An illustration of this can be found in the collection of *PGM1* mutants of this study; no plastidial PGM activity at all could be detected in the starch-free mutants SL1837-1 and SL4725-4 (*pgm1-3* and *pgm1-4*; stop-codon and splice-site junction mutations, respectively) whereas a significant reduction in enzyme activity and starch content could be observed for the intermediate mutant allele SL4867-12 (*pgm1-5;* amino-acid change), and to a lesser extent for SL4490-1 (*pgm1-1;* amino-acid change) (Figure 20 and Figure 22). Hence, the degree of loss of starch correlated well with those of PGM enzyme activity and was consistent with the nature of the mutation carried by these mutants.

One major disadvantage of using EMS mutagenesis, however, is that backcrosses are necessary to minimise the number of these background mutations (Henikoff et al., 2004). Given that the generation time of *L. japonicus* is about three months (Handberg and Stougaard, 1992), and that several rounds of backcrossing are needed, backcrossing of the mutant plants is time consuming. This is generally circumvented by including WT plants from the segregating population into the analysis so as to minimize problems related to background mutations, or by using one of the other alternatives mentioned in section 4.3.3. The selected mutants in Gifu background were out-crossed and then successively backcrossed at least once to the WT accession MG-20 (Table 7). These crosses were performed for several reasons. Firstly, crossing was needed to reduce the number of background mutations generated by EMS, and eliminate their possible effect on the mutant phenotype. Theory suggests that, in the absence of heterosis, the genome of one mutant line should be pure (i.e. almost completely homozygous for either one or the other parental marker) at the F6 stage (i.e. after six successive backcrossings; Jiang and Gresshoff, 1997). Secondly, out-crossing with another ecotype was needed to establish a mapping population for the identification of the forward screen mutations. MG-20 was chosen as crossing partner because it had been shown to have the highest level of polymorphism relative to Gifu (over 4%) among all the *L. japonicus* accessions analysed, a well as several desired phenotypic traits. Furthermore, a genetic linkage map from a cross between these two accessions was already well established at the start of this study (Kawasaki and Murakami, 2000; Hayashi et al., 2001). Thirdly, crossing with MG-20 was performed because this accession is easier to grow under most conditions, and has a relatively fast generation time as mentioned earlier (Chapter 3, section 3.1.5).

This backcrossing had been initiated before the start of this PhD project, and was pursued during it so that each mutant line had reached the second or third backcross stage (Table 7).

However, backcrossing resulted in the random segregation of the starch content trait in the progeny, most likely to due to the large difference in the metabolism of starch I identified in the course of this study between the two parents MG-20 and Gifu (Chapter 3, sections 3.2.4 and 3.2.5). Hence, backcrossing complicated the further characterisation of the mutants. To circumvent this problem as well as minimize the problem of the background mutations, the experiments reported in this study included, whenever possible, the WT plants from the same segregating population as the mutants. More specifically, analyses were carried out either by comparing the progeny (F3) of homozygous mutants and WT isolated from the same segregating population, or by comparing the mutant, WT, and heterozygous segregants of the same segregating population (F2). Yet, some differences in starch metabolism and in growth and development independent of the mutation were still observed between genotypes in the first case. Larger biological variation and the need to genotype large populations of plants represented a major hurdle in the second case. Hence, outcrossing to an accession different from the one mutagenised should be restricted to cases in which the trait of interest is very similar in both parents and to the establishment of population for genetic mapping. Preferably, alternative strategies to the use of backcrossing should be chosen to gain compelling evidence that the mutation identified is indeed the one responsible for the mutant phenotype. Such strategies are discussed below (section 4.3.3).

4.3.3. Approaches employed for the characterisation of *L. japonicus* mutants

A candidate enzyme approach was employed first to try and identify the mutations isolated from the forward screen. This helped in the identification of the mutation responsible for the starch phenotype of three of the mutant lines (*pgm1-4*, *pgm1-5*, *apl1-1*). Genetic linkage mapping was then employed for the identification of the remaining mutations. I first performed rough mapping of the forward screen mutations. This step could be successfully achieved and fastened by carrying out bulk segregant analysis (Michelmore et al., 1991). I then combined the results of this genetic linkage mapping with a candidate gene search and the establishment of a molecular-function map of starch metabolism in *L. japonicus*. Use of these methods allowed the rapid identification of five of the mutants isolated from forward screen (namely, *pgi1-1*, *pgi1-2*, *pgi1-3*, *gwd1-1*, and *gwd3-1*). In addition, this mapping was also used to validate the mutant loci I had identified via the candidate enzyme approach (*pgm1-5, apl1-1*). More cost and time effective than following the candidate enzymes approach and allelism tests, such a strategy also allowed me to determine whether mutants of a collection were likely or not to carry mutations affecting the same gene (i.e. mutations of independant mutant lines mapping in the same genome region) and/or to affect any key genes already known to be involved in the physiological process in question (i.e. mutation

mapping in a region where a strong candidate gene – for starch metabolism in the case of this study – is present). This therefore constitutes an excellent strategy to follow as a first step toward the identification of mutations responsible for forward screen mutant phenotypes in a species such as *L. japonicus* for which genome sequences are available.

Direct, compelling evidence that the mutation identified in these mutants is indeed responsible for their mutant phenotype is required. Several strategies can be used for this purpose. A first genetic test would be to analyse co-segregation between the genotype and phenotype in a population segregating for the mutation. If complete co-segregation occurs, the mutation causing the phenotype is likely to be identical to the mutation genotyped. A second, more widely used, strategy consists of over-expressing a full-length cDNA of the WT gene in the mutant plants. If transgenic plants containing the transferred DNA construct are like the WT rather than the mutant plants (mutant phenotype complemented), then the mutation identified is considered to be responsible for the mutant phenotype. Root transformation by *Agrobacterium rhizogenes* can be very easily achieved in *L. japonicus* (Jiang and Gresshoff, 1997), and is therefore largely used as a method to complement mutants with altered nodule function. Complementation analysis at the whole plant level in *L. japonicus* using *Agrobacterium tumefaciens*-mediated transformation, however, is much more difficult to achieve and a more lengthy procedure. A third approach is to generate multiple mutant alleles in the gene under study. Confirmation that the phenotype observed is indeed caused by the initial mutation identified is obtained if several independent alleles of the same gene result in a similar phenotype. Complementation analysis between such mutants is also generally performed for further confirmation. If no complementation occurs, the statistical chance that the mutant plants carry a second site mutation responsible for the phenotype is dramatically reduced.

To confirm that the mutations thus identified was indeed responsible for the mutant phenotype, the strategy I employed in this study consisted in generating additional mutant alleles of the gene by TILLING coupled with a series of analyses and assays at the genetic, transcript, protein, and enzyme activity level. In addition, backcrossing was also performed and, whenever possible, the phenotype of the mutants was compared with segregating WT siblings with similar mutation load, so as to control the influence of the background mutations generated by EMS. Altogether, this provided strong evidence that the mutations identified were indeed the ones causing the mutant phenotype of interest.

Although the candidate gene approach proved very useful for the identification of several of the forward screen mutants, it had limitations. One was that the genome of *L. japonicus* is not yet fully sequenced. At the start of this study, the Miyakogusa database (http://www.kazusa.or.jp/lotus/) was not up to date and less than half of the genome sequences were available. Since May 2008, this database has been updated and the sequence

information has expanded. To date 67% of the genome of *L. japonicus* covering 91% of the gene space has been sequenced (Sato et al., 2008). A second limit to this knowledge-based strategy is that mutations responsible for the starch-less or starch-excess phenotypes may also result from a secondary or pleiotropic changes. Indeed, one cannot exclude the possibility that the change in starch content may be a pleiotropic effect of a mutation directly affecting a different process. Possibly also, the mutated gene could encode a regulator (e.g. transcription factor) able to control the metabolism of starch as well as other pathways. This means that mutation in an unexpected rather than a strong candidate gene could be responsible for the mutant phenotype. To avoid setting up time-consuming map-based cloning in such cases or to provide help toward their characterisation, a metabolite profiling approach may be performed beforehand. Such an approach has already been successfully undertaken in *A. thaliana* by Messerli et al. (2007). By performing metabolite profiling (using GC-MS) the authors were able to determine whether unknown mutants with altered starch content were most likely to be genuinely affected in the starch metabolism pathway rather than in the function of a protein with pleiotropic effects. Another alternative to map-based cloning would be to perform transcript-based cloning using microarray technology (Mitra et al., 2004; Gong et al., 2004). Such a strategy, however, is expected to have little success for the characterisation of EMS mutants since only a small percentage of the mutations generated by this mutagen result in null alleles.

4.3.4. Strategies for the identification of the uncharacterised mutations from the forward screen

Mutations conferring the starch metabolism phenotypes of seven of the forward screen mutants remain to be identified. Mutations of these uncharacterised mutants have been mapped to regions of the *L. japonicus* genome ranging from 10 to less than 0.1 cM. Since no strong candidate genes were identified in these regions, these mutations may affect the function of novel proteins involved in the metabolism of starch. Candidate gene searches were extended to any gene involved in carbohydrate metabolism and/or likely to have an effect on starch metabolism according to the literature. The coding sequence of putative candidate genes was sequenced (Table 17) but no mutations could be identified in any of them. However, as mentioned above, the genome of *L. japonicus* is not yet fully sequenced, and gaps are still present in most of these regions where the mutations map. Therefore, comprehensive candidate gene searches could not be performed for these intervals.

For one of the mutant lines, SL4618-12, the mutation was mapped to a small interval of less than 0.1 cM (150 kb). The sequence in this interval was complete and twenty-two genes were predicted to be present (Figure 28). No strong candidate gene could be identified in this

region and none of the putative candidate genes sequenced to date carried a point mutation that could have affected gene function and led to the mutant phenotype (Table 16). Since the sequenced genome of *Lotus* is MG-20, and the mutation is in the Gifu background, my approach to discover the mutated gene using the next generation, massively parallel sequencing technology (Illumina® Solexa) was to sequence both the genome of the homozygous mutant in Gifu background, and the WT Gifu, using the genome of MG-20 as reference. Alternatively, homozygous mutants isolated from the progeny of crosses with MG-20 could have been used for the mutant genome. I reasoned, however, that the first strategy was best since it allowed comparison of the genome of the WT Gifu with that of the mutant without having to discriminate the point mutation of interest caused by EMS from the numerous single nucleotide polymorphisms (SNPs) likely to be present between the genome of the ecotypes Gifu and MG-20 (i.e. induced *versus* natural variation). More precisely, the strategy I developed with the advice of Dr. Eric Kemen (Sainsubury Laboratory, Norwich, UK) involved the independent amplification of the 10 biological replicate samples with each primer pair, and for each of the two genotypes. Following amplification, PCR products from the 10 biological replicate samples would be pooled at equimolar concentration before being purified and submitted to the next steps of the procedure. Amplification by PCR of this genomic region by overlapping 10 kb long fragments proved problematic to obtain robustly. Promising results, however could be obtained when amplifying 5 kb fragments. Unfortunately due to lack of time, amplification of all these PCR fragments and their sequencing using the Solexa technology could not be completed within the time frame of this PhD research project. Identification of the mutation of this mutant line is currently being pursued in the laboratory of Dr. Trevor Wang. Alternative strategies could include the sequencing of the whole mapped region (ca. 150 kb) by amplifying 1 to 2 kb fragments using classical sequencing technologies. Alternatively, finer mapping using larger segregating populations could be carried out in an attempt to restrict further the mapped interval. In addition, comparison of the expression between the mutants and WT segregants of each candidate gene in the interval could help identify the mutated locus. This integration of linkage mapping with gene expression profiling has, for instance, recently been employed in plants to identify genes underlying drought resistance in maize (Marino et al., 2009).

The apparent enhanced recombination frequency observed in the mutants of SL4618-12 is potentially very interesting as it suggests that the gene affected by the mutation in this line may have a function in genome stability, and more particularly an anti-recombination meiotic effect. To date, only one example of such gene in higher plant has been reported (Emmanuel et al., 2006). The identification of genes having this function could potentially

lead to crop improvement applications by promoting gene transfer between distant plant species.

4.3.5. Nature of the mutations identified in the starch metabolism mutants from forward screen and TILLING

It is interesting to note that several of the mutant alleles of the *PGI1* and *PGM1* genes, and one allele affected the AGPase enzyme could be recovered from forward screen while none of the mutation identified so far affected any of the other enzymes known to be essential for starch granule formation (e.g. SS3 and SS4; Chapter 2 and reference therein). Likewise, out of the three starch degradation mutants characterised, two had mutations in GWD1 and one in GWD3. ISA3, DPE2, and MEX1 are three other enzymes that have been shown to be essential for starch degradation (Chapter 2 and reference therein). Results of the candidate enzyme approach and mapping I performed on the forward screen mutant yet uncharacterised show that none of them are likely to be affected in either DPE2 or MEX1. However, it is still possible that one of them could be affected in the gene ISA3 since its sequence has not yet been anchored to the genome (Table 6). A hypothesis that could be advanced to explain the over-representation of forward screen mutants affected in *PGI1* and *PGM1* genes is that selecting only the mutants that were fertile introduced a bias in the screen. Hence, strong forward screen mutant alleles leading to defects in starch metabolism as well as impaired growth and development such as the *gwd1-2* and *gwd1-3* alleles identified by TILLING would not have been retained for further analyses.

Several observations could be made regarding the nature of the mutations identified both in the forward and reverse screens, and in particular from the results of the TILLING of the targeted regions of the *LjGWD1* and *LjGWD3* genes. Although this analysis was based on only three targets as opposed to 84 analysed in Perry et al. (2009), several interesting differences could be noted. Firstly, the number of mutations obtained per kb varied significantly from one targeted region to another, ranging from ca. 10 to 20 mutations per kb. On average for the three targeted regions of these two genes, the number of mutations identified per kb was ca. 14.7 (60 mutations obtained for a total fragment length of 4 kb). This is much higher than the average of 5.8 mutation per kb obtained so far with the general TILLING population of *L. japonicus* (576 mutations obtained for a total fragment length TILLed of 100 kb; Perry et al., 2009) and could simply reflect a better, more careful selection of the region of the gene of interest targeted by TILLING in the case of this study. The percentage of silent and non silent changes, and of the different categories of non-silent changes were also highly variable from one targeted region to another. In addition, the range of changes obtained and their proportion were significantly different from the predictions

given by the CODDLE program. For instance, only three missense changes could be detected in one of the targeted region of the *LjGWD1* gene (PHD; 1183 bp) apart from silent mutations (i.e. mutation not causing an amino acid change or mutation located within intron). In contrast, two truncation changes (stop-codon mutations) and nine missense changes, of which two were predicted to be deleterious, were obtained for the other targeted region of the same gene (SBD2; 1578 bp). In both cases, this corresponded to a significant deviation from the theoretical values (many fewer non-silent changes than expected identified in the first case, and significantly more in the second case; Table 12 and Table 13).

Of the detected mutations, 100% were G/C to T/A transitions typically induced by EMS (Greene et al., 2003). In addition, the G to A and C to T transitions were on average almost equal in number among the mutant alleles, as expected for a random distribution. However, a distorted ratio of homozygous versus heterozygous mutants of 12.7% on average was found for the three targeted regions analysed (percentage ranging from ca. 8 to 18%; Table 12 and Table 13). This is in agreement with the result of the analysis done by Perry et al., 2009 on a larger set of the mutants of the *L. japonicus* TILLING population. In their study, a ratio of 1:10 was observed between homozygous and heterozygous mutations in the M2 progeny. This profoundly differs from the 1:2 homozygous to heterozygous ratio observed *in A. thaliana* (Greene et al., 2003) and reveals a difference in germline genetics between these two species, indicative of a difference in the number of genetically effective cells (Perry et al., 2009). Interestingly, results of analyses performed by the authors also revealed a significant bias for the replacement of glycine residues in functionally defective alleles. Perry et al. (2009) suggested that this over-representation of amino acid changes affecting glycine in defective mutant alleles could be explained by the propensity of this residue to adopt exceptional conformations that are sterically forbidden for other amino acids. The massive alteration in protein structure resulting from this is likely to lead to impaired protein function. In the work presented here, missense change of a glycine residues to another or a stop codon represented 15.6% of all the non-silent changes (10 out of 64 changes affected a glycine residue) and 20.0% of the mutations predicted to be deleterious by the CODDLE program (PSSM difference > 10; four out of 20 affected glycine) that could be identified from both forward screen and TILLING across all the genes studied (splice junction mutation excluded from the calculation; Table 11). This figure is very similar to the one obtained by Perry et al. (2009): out of 47 potentially causative alleles of the NODPOP population, 11 affected a glycine residue (i.e. 23.4%).

Several replicates of mutations (i.e. an identical mutation present in several independent mutant lines) were identified among the forward screen and TILLING populations. In the forward screen mutants, an identical mutation (E566K) was identified in the two mutant lines SL5215-2 and SL5358-3 (*gwd1-1* mutant allele). Similarly, some mutations were

identified in several independent mutant lines by TILLING, the most common being duplicate mutations (Table 12 and Table 13). In an extreme case, the same mutation was identified in five independent mutant lines (GWD1-PHD targeted region; Table 12 and Table 13). A possible explanation for this would be seed contamination (and/or DNA in case of the TILLING population). Alternatively, the replication could be the result of the presence of 'hot spots' in the genomic sequence that would be affected preferentially by the mutagen. The results of TILLING would tend to support this hypothesis since significant differences between theoretical and obtained values were observed for the mutation load of the targeted regions (Table 13). These mutation 'hot spots' may be explained by differences in epigenetic changes (e.g. methylation) from one genomic region to another.

As mentioned earlier, the CODDLE program was used for the selection of the target region to be TILLed since it allows one to determine the region most likely to bear deleterious mutations when mutagenised. In addition to assessing the probability of obtaining deleterious mutations, this program and the PARSESNP programs were used to predict the effect of the mutations identified. A SIFT score smaller than 0.05 and a PSSM (Position-Specific Scoring Matrix) difference score above 10 indicates a deleterious effect. My results indicate that, although very useful, the accuracy of the predictions given by these programs did not match the results obtained experimentally. For example, several of the mutations from both the forward screen and TILLING that generated a PSSM < 10 still led to a mutant phenotype, and, conversely, some mutations with a PSSM > 10 did not lead to a phenotype (Table 11). Overall, the results of this analysis suggests that caution should be exercised when using the results from these programs, and that, ideally, the phenotype of all the mutations identified, or at least all the ones with a PSSM > 0 should be analysed to reduce the risk of missing functionally defective mutant alleles. Furthermore, while mutations in introns and silent mutations were automatically classed as non deleterious by these programs, recent evidence in the literature suggests that such mutations may have an effect on gene expression. For instance, a mutation located at an exon-intron junction could lead to aberrant splicing and have an effect on protein function (e.g. Brand et al., 1996; Pohjanvirta et al., 1998; Miné et al., 2003). In fact, evidence shows that even synonymous mutations can have an effect on protein function, although one may expect their effect to be relatively mild. Synonymous substitutions and mutations affecting noncoding DNA are collectively known as silent mutations, and the change is often assumed to be neutral. Several pieces of evidence, however, suggest that this type of mutation may not be neutral. One reason is that certain codons are translated more efficiently than others (Carlini et al., 2003). Another is the fact that coding sequences at the vicinity of exon-intron borders function as RNA splicing signals. If this splicing signal is destroyed by a synonymous mutation, an exon of the final protein is skipped, resulting in the synthesis of a trunctated form of the protein. For

example, about a quarter of synonymous variations affecting exon 12 of the cystic fibrosis transmembrane conductance regulator gene result in that exon being skipped (Pagani et al., 2005). Finally, synonymous mutations have also been shown to affect the stability of the mRNA secondary structure in mammals (Chamary and Hurst, 2005). These discoveries may have implications for the design of algorithms aimed at predicting the effect of point mutations. Likewise, the recent discovery of the bias towards the amino acid changes affecting glycine in deleterious mutant alleles (Perry et al., 2009) could also be used for improving the algorithm for these programs.

4.3.6. The significance of the starch metabolism mutants of *L. japonicus*

The metabolism of starch is of central importance in plant growth and development. Yet, very little is known to date about the metabolism in legumes. Previously, I provided evidence that *L. japonicus* is a starch accumulating species and outlined our collection of mutants. The analyses I carried out on this collection indicated that the pathways of starch metabolism in *L. japonicus* are largely conserved with those of *A. thaliana*. Nevertheless, some novel findings were made. In addition, some substantial difference between the two species in the nature and the importance of this pathway for plant growth and development were identified and are discussed below.

The reduced starch content of the *pgi* mutants was observed and/or measured in leaves but not in embryos or roots (Figure 20). This suggests that the synthesis of starch in seed embryos and roots is not dependent on PGI activity. The fact that none of the mutants affected in seed starch accumulation that were isolated from extensive mutant screening in cereals were shown to be deficient in the PGI activity (Yu et al., 2001) tends to suggest that the absence of effect of the loss of PGI activity seen on seed starch content in *L. japonicus* is common to other plant species. In contrast, the analyses of the starch content of the *pgm1-4* mutant showed that this mutant is completely starch-free in all the tissues and organs analysed, including leaves, stem, roots, seed embryos, and nodules (Figure 20 and following chapter). This means that this plastidial isoform of the enzyme is essential for the synthesis of starch in all these tissues and organs. The crucial role of this enzyme for the synthesis of starch in leaves and embryos had already been reported in other species, including *A. thaliana* and pea (Caspar et al., 1985; Harrison et al., 2000), but its importance for starch synthesis in nodules constitutes a novel finding. Results of my analysis revealed that starch in *L. japonicus* accumulates in all the root tissues. In contrast, in roots of *A. thaliana* and rice WT plants starch is only found in the root cap cells (Yu et al., 2001; Tsai et al., 2009). Further, in *A. thaliana*, starch is absent in the root cap cells of the *pgm1* mutant, but present in those of the *pgi1* mutants (Yu et al., 2001). Similary in *L. japonicus*, results of my

analyses showed that the loss of LjPGM1, but not of LjPGI1 activity affected the accumulation of starch in roots.

The *apl1-1* mutant had a reduced-starch phenotype specifically in leaves, but no visible reduction of starch accumulation in the embryos or in roots (Figure 20 and data not shown). This strongly suggests that, as in *A. thaliana*, APL1 in *L. japonicus* is the main large subunit isoform involved in the activity of the AGPase heterotetrameric enzyme in leaves. In contrast, the starch content of the *aps1-1* mutant was strongly reduced in all organs analysed including leaves, roots, and embryos while none of the *apl2* mutant lines displayed any clear defect in starch content in any of the organs of the plant analysed, including leaves, roots, and embryos suggesting that this large subunit isoform may not play a crucial role in starch synthesis, at least under the growth conditions used. These results are in agreement with the results of the characterisation of their homologs in *A. thaliana* (Lin et al., 1988a; Lin et al., 1988b; Crevillen et al., 2003 and 2005) and are consistent with the tissue specific pattern of expression found for these AGPase isoforms in *L. japonicus* (Chapter 3, section 3.2.3). Since neither the loss of LjAPL1 and LjAPL2 led to a reduction in starch content in seeds, it is likely that other isoforms encode the large subunit of AGPase in this organ. Results of the analysis of transcript levels presented in Chapter 3 (section 3.2.3) suggest that *LjAPL3* may be the large subunit isoform responsible for the AGPase activity in association with LjAPS1 in this organ as well as in roots (*LjAPL3* is the most highly expressed large subunit isoform in these organs). Lastly, it is worth noting that the effect of the mutations identified in the *aps1-1* and *apl1-1* mutants on starch content was found to be quite variable depending on the growth conditions according to the results of iodine staining (data not shown). This suggests that isoforms of the large subunit may, to a certain extent substitute for each other and contribute to the AGPase activity under some specific conditions.

The leaf starch-excess phenotypes of all the defective mutant alleles of both GWD1 and GWD3 strongly suggest that both these enzymes play an important role in the degradation of starch in leaves of *L. japonicus*. It seems likely, therefore, that these two enzymes act synergistically to phosphorylate the starch granule as a prerequisite for its degradation as in *A. thaliana* (Kötting et al., 2005; Baunsgaard et al., 2005). Starch content in plants of the two GWD1 null mutant alleles, *gwd1-2* and *gwd1-3,* was altered in most organs analysed including leaves, roots and nodules, albeit a much more pronounced effect in leaves than in other organs (Figure 20 and following chapter). By comparison, an increase in starch content could only be observed in leaves in the weaker *gwd1-1* mutant plants (and in the *gwd3* mutants), probably due to the difficulty of visualizing the starch-excess phenotype.

The characterisation of these starch synthesis and degradation mutants of *L. japonicus* shows that their starch phenotypes are largely similar to those of the equivalent mutants in *A. thaliana*, indicating that the pathways of starch metabolism are well conserved between the

two species. However, their characterisation also revealed some interesting differences, in particular relative to their importance in plant growth and development. These results are presented and discussed in detail in the next chapter.

It would be interesting in the future to complete this collection by isolating mutants affected in the other enzymes/proteins known to play a crucial role in leaf starch degradation in *A. thaliana*. In particular it would be valuable to have mutants lacking BAM3, BAM4, ISA3, DPE2, and MEX1 so that one could determine more precisely the degree of conservation of the pathway of starch degradation between *L. japonicus* and *A. thaliana*.

Interestingly, no strong candidate genes were identified in the map regions of the unknown mutants. Hence, this series of mutants provides the basis for the discovery of novel proteins involved in the metabolism of starch. Moreover, the mutants covered in this study were selected from a larger population of putative mutants impaired in starch metabolism. Investigation of the full collection may allow the discovery of further novel proteins.

Put together this suite of mutants provides a strong platform for further investigations of the partitioning of carbon and its importance for traits of agronomic importance in legumes including symbiotic nitrogen fixation, seed storage product accumulation, and perenniality and re-growth. Results of experiments aiming at exploring the importance of starch in such traits together with novel information on some of the starch enzymes are presented and discussed in the next two chapters as an illustration of the wealth of new information that may be obtained from this collection of mutants.

CHAPTER 5

Functional characterisation of the mutants

I am a great believer in luck, and I find the harder I work, the more I have of it

Thomas Jefferson

CHAPTER 5: Functional characterisation of the mutants

5.1. Introduction

5.1.1. Importance of carbohydrate metabolism for plant growth and reproduction, and seed development

As discussed earlier (Chapter 1), the extent to which starch accumulates in leaves differs between species. In *A. thaliana*, transitory starch is the major storage carbohydrate that accumulates during the day and is degraded at night. Its importance for plant growth is reflected in the phenotype of *A. thaliana* mutants unable to synthesize or to degrade it fully. Hence, growth of the starch synthesis-deficient mutants *pgm1, pgi1,* and *adg1* is impaired under short day conditions in comparison to wild-type plants (Caspar et al., 1985; Lin et al., 1988; Yu et al., 2000). Growth of the *sex1* mutant that has reduced capacity to mobilize starch in leaves at night is similarly affected unless it is grown under continuous light (Caspar et al., 1991). In several plant species, starch also appears to be of importance in aspects of flowering and reproduction. Hence, several *A. thaliana* mutants with defects in leaf starch metabolism are late flowering (Caspar et al., 1985; Eimert et al., 1995; Yu et al., 2000).

Recently, starch degradation has also been shown to be vital for normal pollen development and germination in tomato plants (Nashilevitz et al., 2009). Pollen grains develop in the anther where they are initially surrounded by the tapetum, a short-lived tissue which mediates their growth and nutrition (Pacini and Viegi, 1995). Sugars supplied to the pollen grains can either be rapidly utilized as energy source, or temporarily stored as starch in the plastids. Depending on the species, one or two cycles of amylogenesis and amylolysis occurs during pollen development. In addition, mature pollen grains are either starchy or starchless (Pacini and Franchi, 1988; Franchi et al., 1996; Pacini, 1996). In tomato (*Lycopersicon esculentum*), starch is synthesised at early stages of pollen development before being hydrolysed at later stages, so that the mature pollen grain is starchless (Pacini and Franchi, 1988). In contrast, the pollen of a wild tomato relative *L. pennelli* is starchy, whereas in *A. thaliana* pollen, starch is only partially hydrolyzed (Pacini and Franchi, 1988; Franchi et al., 1996). A knockout of the *LeGWD1* gene by transposon insertion in tomato led to a starch-excess phenotype and a reduced level of sugars in the mature pollen grain that was associated with a reduction in pollen germination, gametophytic lethality and male

sterility (Nashilevitz et al., 2009). This suggests that in species in which starch accumulates and is fully remobilized during pollen development, the processes of starch phosphorylation and its degradation are of central importance for the reproductive capacity of the plant. In contrast in *A. thaliana,* no defect in pollen fertility has been reported for starch mutants, including the *gwd1* mutant *sex1* (Caspar et al., 1991). Nevertheless, it was recently shown that a deficiency in the plastidial glycolytic glyceraldehyde-3-phosphate dehydrogenase led to male sterility in *A. thaliana* (Munoz-Bertomeu et al., 2010), suggesting a critical role played by the metabolism of carbohydrates for pollen viability in this species.

In seeds, very different patterns of reserve accumulation are observed among legume species. In pea seeds, the major component is starch (50% of the dry weight). In contrast, starch content is very low (less than 1%) in mature seeds of several species, including soybean, *L. japonicus,* and *M. truncatula* (Dam et al., 2009). In seeds of these species, starch is either not synthesised in large amounts, or is completely degraded during seed maturation, probably to provide carbon skeletons for the synthesis of other compounds (Gallardo et al., 2008). Instead, these species have seeds with high protein contents (between 30 and 40% depending on the species and genotypes; Djemel et al., 2005; Gallardo et al., 2008; Dam et al., 2009). Levels of lipids, the third major component of mature legume seeds, also vary significantly between species (ca. 20% in soybean, 7% in *L. japonicus*, and ca. 2% in pea; Dam et al., 2009)

Thus far, what is known of the metabolism of carbohydrates in seeds largely comes from studies carried out in pea. In this species, a suite of mutants in which starch synthesis is reduced in developing seeds has been isolated. These are the *rug4* (Susy), *rug3* (plastidial PGM), *rug5* (SS2), *r* (SBE), and *rb* (AGPase) mutants (Bogracheva et al., 1999). In each case, reduced flux of carbon into starch has extensive consequences for many other aspects of seed metabolism and development. These include elevated level of sugars and reduced sugar uptake, elevated level of lipids, altered ratios of storage protein, and wrinkled appearance of the mature seeds (Wang et al., 2003). For instance, in the SBEI mutant (*r* mutant) where the seed starch content is reduced by ca. 50%, the sucrose level is elevated by 180%, and the rate of sucrose uptake is reduced (Wang and Hedley, 1991; Edwards and ap Rees, 1986). This tuning of the sucrose uptake fluxes by the size of the intracellular sugar pool involves sugar transporter activities whose contribution to cotyledon growth rate and biomass gain has been shown to be important (Patrick and Offler, 2001; Rosche et al., 2002; Zhou et al., 2009). In addition, seeds of the starch synthesis mutants lacking SBEI and AGPase (aka *r* and *rb* mutants, respectively) that display a reduced starch content were found to have increased protein and lipid contents (Hughes et al., 2001; Wang et al., 1990). This stimulative effect of a reduction in AGPase activity and starch accumulation on the storage protein synthesis and fatty acid metabolism in pea embryos has recently been

confirmed by Weigelt et al. (2009). Decreased starch synthesis also led to an increased sugar accumulation that appeared to stimulate cytokinin-mediated cell proliferation pathways (Weigelt et al., 2009).

In contrast, in *A. thaliana*, an oil-seed species, a decreased rather than increased lipid accumulation was observed in the seeds of the starch-free *pgm1* mutant (40% reduction in oil content in the mutant that lack starch completely compared with that of WT; Periappuram et al., 2000). Similarly, an embryo-specific reduction of the AGPase activity in *Brassica napus* (rape) seeds caused a marked decrease in lipid synthesis at the onset of oil accumulation. This influence of AGPase on fatty acid accumulation, however, was largely compensated for in the late stages of seed development (Vigeolas et al., 2004). This could be explained by the fact that in *A. thaliana* and oilseed rape, starch accumulates only transiently during early development. Starch is then hydrolyzed during phases of oil accumulation, and is absent from mature seeds. Confirmation that clear, yet complex, interactions occur between the pathway of starch metabolism and lipid synthesis in these oilseed species come from the analysis of an *A. thaliana* mutant, *sse1* (shrunken seed 1) whose reduced rate of fatty acid synthesis was shown to lead to an increased accumulation of both starch and sugars (Lin et al., 2006).

In comparison, very little is known about the importance of starch for seed metabolism and development in seeds of legume species other than pea. Given the storage product composition of seeds of soybean, *L. japonicus,* and *M. truncatula* described above, it may be hypothesized that alteration of starch synthesis and turnover would lead to effects similar in several respects to those observed in *A. thaliana* and oilseed rape, rather than to those observed in pea. However, there is not yet any experimental evidence available on this. Further, the nature of the starch metabolism pathway in seeds of these legume species still remains to be determined.

5.1.2. Importance of carbohydrate metabolism for symbiotic nitrogen fixation

Symbiotic nitrogen fixation (SNF) requires a supply of carbon from the plant to the bacteroids in the root nodules. Nodules represent strong carbon sinks since they need assimilates for N_2 fixation and ammonium assimilation (between 12 and 17 g of carbohydrate are needed per gram of nitrogen fixed; Vance and Gantt, 1992) as well as for maintenance and growth. Several lines of evidence support an important role for the metabolism of carbohydrate in this process. In pea, the *rug4* mutant deficient in sucrose synthase (Susy) activity is severely impaired in SNF (Gordon et al., 1999; Craig et al., 1999). Consistent with this observation, the corresponding Susy gene was found to be a member of a class of genes called nodulins that are uniquely or highly expressed in nodules

(Thummler and Verma, 1987). Mutants lacking this isoform of Susy (referred as nodule-enhanced Susy) have since been studied in several other legume species, and the crucial role of this enzyme in nodulation confirmed in every case (Horst et al., 2007; Baier et al., 2007). Sucrose is required for nodulation not only as a source of energy for nodule metabolism including the fixation of atmospheric nitrogen, but also as a source of carbon skeletons for the assimilation of ammonium and its export from nodules. In addition to its role in the provision of carbon skeletons to the nodules, the control of Susy gene expression may be a way of regulating N_2 fixation by acting on the supply of carbohydrate (Gordon et al., 1997). In support of this hypothesis, it has been found that the gene encoding nodule-enhanced Susy is quickly down-regulated in response to stresses that simultaneously reduce N fixation in soybean (Gonzalez et al., 1995; Gordon et al., 1997). A high correlation between a decline in N_2 fixation and sucrose synthase downregulation is also observed under water stress (Galvez et al., 2005). Alternatively, a decreased Susy expression and activity could be a response to decreased N fixation.

Together with sucrose, starch represents the principal carbohydrate accumulated in nodules (Kouchi and Yoneyama, 1984; Gordon et al., 1985; Walsh et al., 1987). Uninfected cells of nodules tend to contain large starch granules while infected cells generally have few, if any starch granules. Despite its widespread presence in most, if not all, root nodules of rhizobial symbioses studied to date, very little is known about the importance of nodule starch for SNF. It may be hypothesized that the formation of starch in nodules simply represents an overflow for photosynthates supplied by the plant, or that conversion of incoming sucrose to starch maintains the sink strength of the nodule. Alternatively, starch degradation may play a crucial role in maintaining N_2 fixation under normal conditions, during dark periods, and/or during prolonged periods of cold during winter, or under stresses (e.g. nutrient, drought, salt).

Results of analyses performed in soybean pointed toward a role for nodule starch under stress conditions only. Walsh et al. (1987) examined the location and nature of the carbon pool supporting the nodule activity under non-photosynthetic conditions, following the observation that soybean nodules are able to maintain a constant rate of N_2 fixation during the night, if the temperature is held constant (Walsh and Layzell, 1986; Williams et al., 1982). The starch pool in soybean leaves and roots showed diurnal fluctuations but the pool in nodules and stems showed no variation. In this species, starch stored in leaves appeared to be the major carbon pool used to support nodule function under normal, non-photosynthetic conditions. The results of leaf excision, stem girdling, and stem chilling studies in soybean further demonstrated that nodule respiration and nitrogenase activity were highly dependent upon a constant supply of photosynthates from the shoot, and that, when forced to draw upon its own reserves by stem girdling, soluble sugar pools in the nodule were initially

rapidly consumed (58% decrease over ca. 3 h). From 3 to 26 h after stem girdling, however, the pool of soluble sugars was relatively stable, and the starch reserves declined to 47% of their initial size (Walsh et al. 1987). Similarly, nodules of chickpea plants kept in the dark for 48 h still possessed 40 and 74% of their initial soluble sugar and starch content, respectively, and 69% of their rate of nitrogen fixation (measured by acetylene reduction assay; Swarej et al., 1986). Put together, these results suggest that, at least in these species, nodule carbohydrate reserves are only remobilized under severe stress conditions in which external, phloem-supplied carbohydrates are severely restricted. When soybean plants were maintained under continuous light, nodule starch and sugars accumulated but the rate of nitrogenase activity was not significantly higher than in the control plants. This suggests that under normal growth conditions, nodule activity is limited by the intrinsic nodule metabolism (i.e. its ability to utilize the available photosynthates) rather than the supply of carbohydrates by the plant (Walsh et al. 1987).

Important differences in the metabolism of nodule starch seem to exist between legume species. Thus, while nodule carbohydrate levels fluctuated very little during light and dark periods in soybean (Walsh et al., 1987), a significant diurnal variation was found in carbohydrate levels in the nodules of other species (e.g. white clover, Gordon et al., 1986 and 1987; cowpea, Rainbird et al., 1983; pea, Michin and Pate, 1974). In white clover in particular, both sucrose and starch increased during the 12 h light period and declined during the subsequent dark period. Sucrose accumulation and degradation was completely in phase with the light and dark period whereas starch turnover was out of phase by about 3-4 h (Gordon et al., 1986 and 1987). It was estimated that this reserve of sugar and starch accumulated during the photoperiod would be sufficient to maintain N_2 fixation at the time rates as during the day for three quarters of the dark period (Gordon et al., 1987). Furthermore, in white clover, in contrast to soybean where the large majority (80%) of the total carbon stored during the light period was as starch in the leaves (Kerr et al., 1985), half of the starch accumulated in organs other than leaves. The continued export of the stored carbon from these organs contributed to the uninterrupted nodule nitrogen fixation during darkness (Gordon et al., 1987). Interestingly in white clover plants acclimated to a 12 h photoperiod, shortening the light period by only a few hours caused an abrupt decline in nodule metabolism toward the end of the dark period (Ryle et al., 1988). This suggests that plants of this species are unable to accumulate sufficient reserves in either the nodules or other organs to sustain SNF under unexpected change of conditions.

Evidence that starch may also play a role in nodules under non-stress growth conditions in some plant species comes from the results of gene expression analyses. Transcript profiling using cDNA arrays has been performed in *L. japonicus* (Colebatch et al., 2002 and 2004) to help identify nodule-induced genes (also called nodulins) that are likely to play a critical role

during the SNF process. Primary metabolism constitutes the functional category containing the largest number of nodule-induced genes. Interestingly, AGPase (APS1) was mentioned as a nodule-induced metabolic gene by Colebatch et al., 2002 (ratio of expression level nodule/root of 2.3); and starch phosphorylase (PHS1) and SEX1/GWD1 were also among the nodule-induced genes (expression nodule/root ratio of 3.7 and 8.6, respectively). By comparison, ESTs of the sucrose synthase genes encoding isoforms LjSUS1 and LjSUS3 known to be important for nodule function had a nodule/root ratio of expression of 3.9 and 8.3, respectively.

In an attempt to determine whether starch plays a role in nodule cold tolerance and winter dormancy, seasonal changes in starch and soluble sugars were studied in the perennial root nodules of beach pea (*Lathyrus japonicus*; Chinnasamy and Bal, 2003). Results revealed an increase in starch reserves during the summer and a dramatic depletion (60%) during winter in this species. It is believed that this remobilization of starch reserves plays a role in keeping constant, elevated reducing sugar levels to help maintain high osmolarity in cells, and thus prevent the dormant nodule from freezing during prolonged periods of cold during winter.

Taken together, these results support the idea that storage carbohydrates in root nodules should be considered as necessary rather than simply as excess photosynthates. However, the means of ensuring continuous nitrogen fixation under photosynthetic and non-photosynthetic conditions appears to be species dependent. Furthermore, it is clear from examples described above that the importance of nodule starch metabolism and its regulation under normal growth conditions varies from one species to another. In contrast, the results of several studies all support an important role played by nodule starch as a source of carbon under stress conditions and as a long term form of stored carbon.

Atypically high levels of starch are generally observed in nodules infected by different mutant bacteria. For example, nodules infected by bacteroids with a deficiency in the transport of dicarboxylic acids have high levels of starch and undergo premature senescence (Finan et al., 1983). Similarly, both pea nodules infected by bacteroids defective for aspartate amino transferase or for amino acid import/export (Lodwig et al., 2003) and alfalfa nodules with bacteroids defective in glutathione synthesis (Harrison et al., 2005) were found to accumulate high levels of starch. A common feature in these three examples is the fact that bacteroids are not fully differentiated and have deficiencies in the import and processing of carbon skeletons, amino acids, and antioxidants. As a consequence, nitrogen-fixing activity is severely reduced or even abolished, and the photosynthates imported to the nodule are stored as starch in the symbiosome instead of being metabolised. Consistent with these observations, the activities of the carbon metabolism enzymes starch synthase (SS) and phosphoenolpyruvate carboxylase (PEPC) were altered in these cases.

The commonly observed correlation between high starch accumulation and senescence is still unclear, but the results presented above suggest that the accumulation of high level of starch is more likely to be a result of an impaired nodule function and premature senescence rather than the other way around (i.e. high level of starch causing a premature senescence).

5.1.3. Properties and structure-function relationships in three key enzyme of starch metabolism: AGPase, GWD1, and GWD3

The AGPase enzymes from bacteria and cyanobacteria (involved in glycogen synthesis) are homotetrameric. Conversely, AGPase in higher plants is a heterotetramer (α2 β2) composed of two small (APS, α2) and two large (APL, β2) subunits (Okita et al., 1990). Most plants possess one or two APS genes and several APL genes. In *A. thaliana*, one functional *APS* gene (*APS1*) and four functional *APL* genes (*APL1, APL2; APL3, APL4*) have been identified. *A. thaliana* also has another *APS* gene (*APS2*) that is a pseudogene. Gene expression profiling of AGPase isoforms has been performed in several plant species (Crevillen et al., 2005; Hirose et al., 2006; Ohdan et al., 2005). These studies have revealed that the AGPase genes in plants are differentially expressed between tissues and organs (Chen et al., 1998a and 1998b; Kim et al., 2001; Crevillen et al., 2005). In addition to this tissue-specific pattern of expression, different APL isoforms have been shown to confer distinct kinetic and regulatory properties to the heterotetrameric enzyme (Crevillen et al., 2003).

Because AGPase catalyzes the first committed step in the starch biosynthetic pathway and has long been thought to be rate limiting for starch synthesis, extensive studies have been carried out on this enzyme. In particular, the mode of regulation of the plant AGPase enzyme has received considerable attention, and many analyses of the catalytic and regulatory properties of the different subunits, and of variants in a range of plant species and organs have been performed (Chapter 1 and reference therein). Moreover, several extensive phylogenetic analyses have also been performed for this enzyme as discussed earlier (Chapter 3 and references therein).

Three main mechanisms have been shown to modulate its activity: allosteric regulation, reductive activation, and thermal inactivation. Further, many residues important for the overall activity of the AGPase enzyme or more specifically for its regulatory properties, heat stability, and for the interaction between subunits have been determined (e.g. Ballicora et al., 1998; Cross et al., 2005; Kim et al., 2007; Georgelis et al., 2009; Boehlein et al., 2008 and 2009).

As mentioned earlier, phosphorylation of starch is essential for its normal degradation at night. Two isoforms of α-glucan water, dikinase (GWD) are known to be involved in the phosphorylation of starch: GWD1 (aka SEX1 or R1 protein) and GWD3 (aka PWD). The importance and role of these enzymes in starch degradation has been detailed earlier (Chapter 1 and reference therein). Briefly, GWD1 catalyses the phosphorylation of the C6 position of glucose units of starch while GWD3 phosphorylates at the C3 position of the glucose units (Ritte et al., 2006). The activity of GWD3 is dependent on starch being phosphorylated by GWD1. Evidence also suggests that both dikinases work in cooperation with the glucan phosphate phosphatase SEX4 in a cycle of phosphorylation and dephosphorylation events occurring at the surface of the starch granules to allow its degradation.

Both GWD1 and GWD3 proteins contain a C-terminal region homologous to a dikinase activity domain (PPDK), consisting of a phospho-histidine and a nucleotide binding motif. This domain is responsible for the transfer of the β-phosphate of ATP to the glucan substrate. The two enzymes also possess a putative Starch Binding Domain (SBD) located at the N terminus that allows them to bind to the surface of the starch granule. In GWD3, this domain belongs to the well characterised Carbohydrate Binding Module (CBM) family 20 (CBM20) defined by the CAZy database (http://www.cazy.org). The N terminal region of GWD1 contains two starch binding domains, SBD-1 and SBD-2, that have recently been classified into a newly defined CBM family 45 (CBM45) in the CAZy database. Modules belonging to this family are found in an extra-plastidial glucan, water dikinase of unknown function (GWD2; Glaring et al., 2007) and in plastidial α-amylases. However, in contrast to the GWD1 protein that possesses a tandem repeat of SBD, the α-amylases contain only one copy of SBD in their N-terminal region. Expression of an N-terminally truncated form of the *A. thaliana* plastidial α-amylase AMY3 has established that this module is not required for the catalytic activity of this enzyme (Yu et al., 2005).

Many mutant alleles of GWD1 have been described in *A. thaliana*. All mutations identified affected the dikinase activity domain only (i.e. deleterious amino acid/truncation change or T-DNA insertion located in the C-terminal region of the protein; Yu et al., 2001) and, consequently, not much is known about the function of the putative SBD and its importance for the activity of the enzyme. The first evidence suggesting that this SBD may be required for efficient starch phosphorylation comes from a study by Mikkelsen et al. (2006). The authors performed limited proteolysis of the potato tuber GWD1 (StGWD1) with trypsin, thereby producing two stable fragments. One corresponded to the N-terminal region containing the first SBD only (termed SBD fragment) and the other (termed N11) contained the remaining sequence (SBD-2 and C-terminus of StGWD). *In-vitro* starch phosphorylating activity of the N11 fragment was altered (two fold higher specific activity) compared to the

WT StGWD1. Furthermore, deletion of the N-terminal region containing the first SBD motif resulted in an enzyme with a higher preference for phosphorylating shorter amylopectin chains. Information about the contribution of the second SBD to the substrate specificity and the activity of starch phosphorylation is lacking.

5.1.4. Aims and Approaches

In the previous chapter, I described the isolation of mutants of *L. japonicus* with altered starch synthesis or degradation. I showed that the suite contained allelic series for several key enzymes of starch metabolism. This comprehensive collection of starch metabolism mutants should provide a useful resource for further studies on the metabolism of transitory and storage starch and the roles of starch in legumes (e.g. in nitrogen symbiotic fixation and in seed storage product accumulation), and may also help to uncover new facets of the metabolism of starch. To illustrate this, I present here the results of some phenotypic and molecular analyses carried out on the mutants and show that they provide new information about the structure-function relationships of the AGPase and glucan, water dikinase (GWD) enzymes. In addition, functional analyses of the phenotypes of the *pgm1-4* and *gwd1-2/3* mutants of *L. japonicus* offer new insights into the metabolism of starch and its importance for plant growth and development in legumes.

5.2. Results

5.2.1. Molecular characterisation of selected starch mutants

5.2.1.1 APL1 mutant alleles

In Chapter 3, I identified one gene encoding the small subunit isoform (named *LjAPS1*) and five genes encoding the large subunit ioforms (named *LjAPL1* to *LjAPL5*) in the genome of *L. japonicus*. In addition, a duplicated copy of the *APL2* gene (*LjAPL2b*) was also found. Results of the gene expression and protein sequence analyses suggested that *LjAPL2b* and *LjAPL5* genes may not be functional (Chapter 3, sections 3.2.2 and 3.2.3). As described in the previous chapter, several mutants for the *LjAPS1* and *LjAPL2a* gene were isolated by TILLING. In addition, one of the mutants from the forward screen carried a mutation in the *LjAPL1* gene.

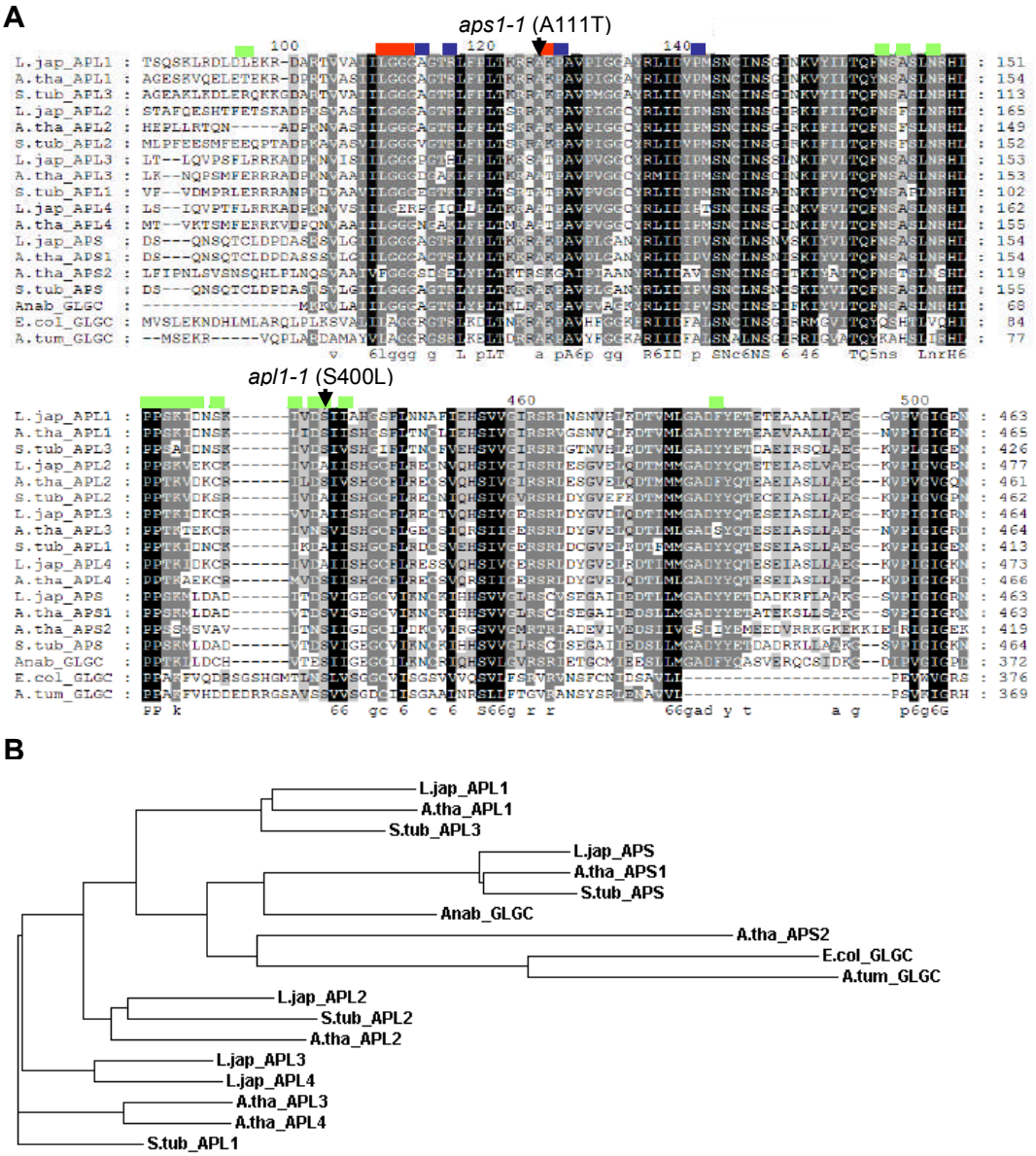

Figure 29. Comparison of the amino acid sequences of *L. japonicus* AGPase subunits with those of other species.
A. Comparison of two regions of the small and large subunits from *L. japonicus* (L.jap) genes carrying the mutations *aps1-1* and *apl1-1* with homologs from species including bacteria [*E. coli* (E.col) and *A. tumefaciens* (A.tum)], cyanobacteria [*Anabena* sp. (Anab)] and plants [*Arabidopsis thaliana* (A.tha) and *S. tuberosum* (S.tub)]. GLGC is the single gene product responsible for AGPase activity in bacteria and cyanobacteria. The alignment was made with the programs Clustal W2 (default settings) and GeneDoc. Strictly conserved residues are highlighted in black, less conserved residues are in grey. The positions of the *aps1-1* and *apl1-1* mutations are indicated by arrows. Residues marked in red interact with the substrates ADPGlc and/or ATP in the *S. tuberosum* APS protein (Jin et al., 2005); those marked in blue may be important in the regulatory properties of the enzyme (Kavakli et al., 2001; 2002). Residues marked in green are those involved in subunit interactions according to Jin et al. (2005) Note that in this alignment the residue in the potato APS protein equivalent to *L. japonicus* S400 is S401. Jin et al. (2005) numbered this residue as S331; their numbering is used in Figure 30. The 55 amino-acid motif identified by Cross et al. (2005) as being critical for interaction between the small and the large subunit corresponds to amino acids 368-468 in the potato APS sequence on our alignment. An alignment of the full amino acid sequences is given in Figure A4. Accession numbers for the sequences are: A.tha APL1, P55229; A.tha APL2, P55230; A.tha APL3, P55231; A.tha APL4, Q9SIK1, S.tub APL1, Q00081 ; S.tub APL2, P55242; S.tub APL3, P55243; A.tha APS1, P55228; A.tha APS2, Q7YKW3; S.tub APS, P23509; E.col GLGC, P046V1; A.tum GLGC, P39669: Anab GLGC, P30521. **B**. Guide tree made with the Clustal W2 program, showing the phylogenetic relationships between the AGPase proteins.

The mutation identified in the starch deficient mutant *Ljaps1-1* (from SL529-1; Chapter 4, section 4.2.3) results in a change of an amino acid adjacent to a highly conserved residue of the small subunit of AGPase, known to interact with the substrate (Figure 29). It is therefore not surprising that this mutation has an effect on the enzyme activity and leads to low starch content in the mutant relative to the WT. Conversely, the nature of the mutation identified in the *LjAPL1* gene of the forward screen mutant line SL5127-5 was unexpected in the light of our present understanding of the structure-function relationships of the enzyme. Leaves of this mutant, *Ljapl1-1*, had only 7% of the AGPase activity of wild-type leaves (Table 16, Chapter 4), suggesting that the mutation was likely to be a truncation change (i.e. splice-site or stop-codon mutation) or to affect one of the residues involved in the catalytic and/or the regulatory activity of the enzyme. The mutation identified in *Ljapl1-1* however, led to an amino acid change (S400L) not previously shown to be important for the AGPase enzyme activity (Figure 29).

The crystal structure of the AGPase small subunit homotetramer from potato tubers has been solved, both free and in complex with ATP and ADPGlc (Jin et al., 2005). Together with mutagenesis studies (Ballicora et al., 1998; Greene et al., 1998; Kavakli et al., 2002), analysis of its structure has enabled the identification of residues important for either substrate affinity or sensitivity of the subunits to the allosteric effectors inorganic phosphate (Pi) and 3-phosphoglycerate (3-PGA) (Figure 29 and Figure A4). No crystal structure of the heterotetrameric enzyme is currently available. However, the strong sequence similarity between the small and large subunits of AGPase (48% identity at the amino acid level between LjAPL1 and StAPS) allowed the use of the crystal structure of the small subunit homotetramer for analysing the impact of the mutation on LjAPL1.

The mutated residue (S400; equivalent to S331 in the potato small subunit) is positioned at the interface between monomers (Figure 30), suggesting that this residue is crucial for AGPase activity because it is involved in the interaction between the subunits. Consistent with this finding, the residue equivalent to S400 in the potato large subunit has been predicted to be involved in subunit interaction by homology modelling of the heterotetrameric structure of the potato AGPase (Tuncel et al., 2008). Furthermore, Cross et al. (2005) identified a 55-amino acid region of the potato small subunit including S331 that is critical both for the catalytic and the allosteric properties of the enzyme by modulating interaction between the subunits. This important role played by the residues at the interfaces between the large and small subunits for the catalytic and allosteric properties of AGPase has since been confirmed in several more recent studies (Georgelis et al., 2009; Boehlein et al., 2009). However, the preliminary *in silico* analysis I carried out indicated that the change from serine to leucine at this position is unlikely to affect subunit interaction (Figure 30, and personal communication with Dr Faridoon Yousafzai, JIC); the backbone, rather than the

side-chain, of the residue at this position is involved in subunit interaction. Instead, the side-chain of the serine S400 interacts with other amino acids in the β-helix domain in which it is located. These interactions are lost when a leucine is substituted for this serine residue (Figure 30). Hence, it may be hypothesized that the effect that the mutation identified in *Ljapl1-1* has on the activity of the enzyme results from a disruption of the heterotetramer stability as a whole, rather than from a disruption of the interaction between subunits.

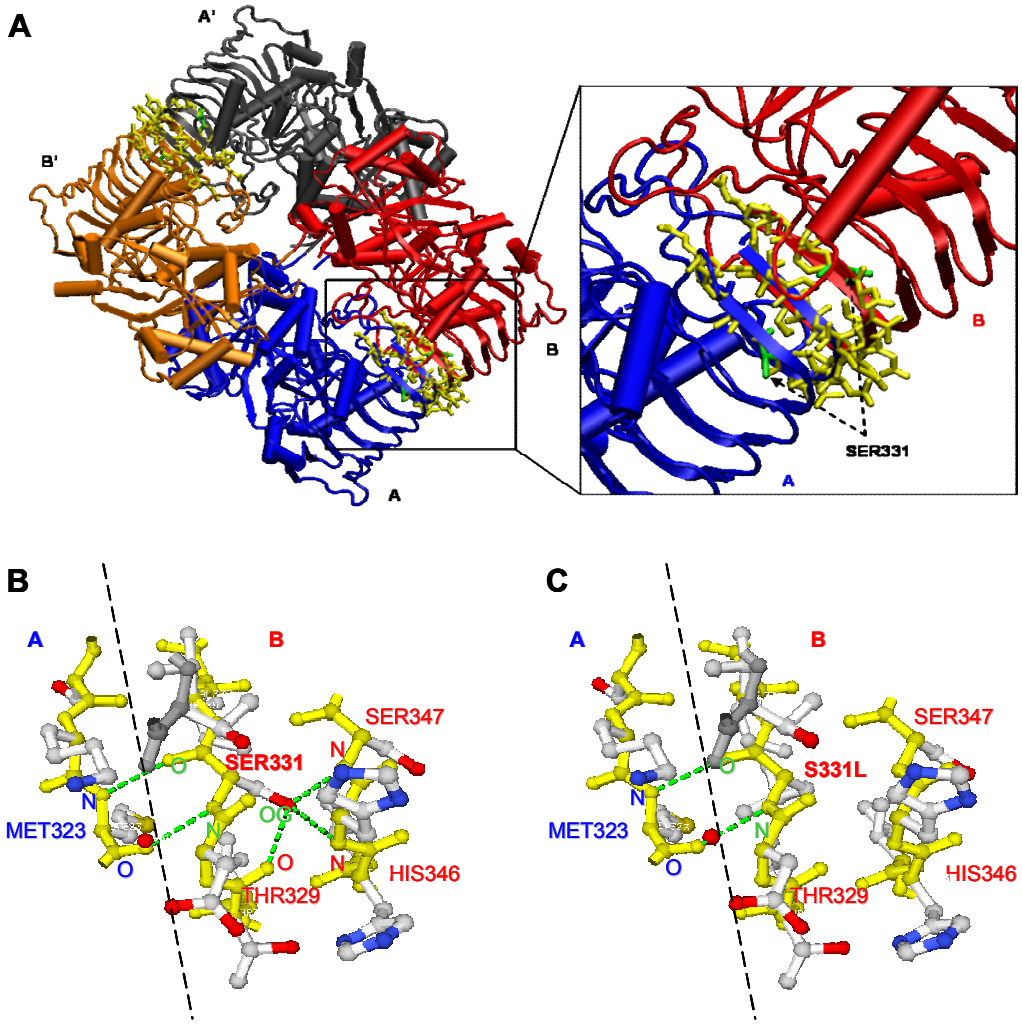

Figure 30. Predicted effect on AGPase function of the S400L amino acid change in the large subunit found in the *L. japonicus* mutant *apl1-1*.
A. Position of S331, the residue equivalent to S400 of the *L. japonicus* APL1, in the three dimensional structure of the small subunit of the potato tuber AGPase. The representation was generated by the VMD program from the crystallographic structure obtained by Jin et al. (2005), entered on the RCSB PDB databank with the PDB ID 1YP2. The residues at the interface between monomer A and B of the small subunit homotetramer are highlighted in yellow and enlarged on the right. The residue S331 is highlighted in green and indicted by arrows. **B**. Closer view of residues at the interface between subunits. **C**. *In silico* mutagenesis of S331 using the program Swiss PDB Viewer. The serine 331 residue was replaced by a leucine residue to simulate the effect of the mutation identified in *apl1-1*. The change brings about a disruption of the interaction of the side chain of this residue with other residues of the β-helix domain, suggesting a possible effect of the amino acid change S400L on the stability of this domain.

5.2.1.2 GWD1 mutant alleles

The *Ljgwd1-1* mutation identified in two of the starch-excess mutant lines from the forward screen (SL5215-2 and SL5358-3; see Chapter 4, section 4.2.4) leads to an amino acid change, E566K, in the second of the two starch-binding domains (SBD-1 and SBD-2) located in the N-terminal region of the GWD1 protein (Figure 31; Mikkelsen et al., 2006). The importance of this second starch binding domain for GWD1 enzyme activity, and therefore the phosphorylation and degradation of starch, has thus far not been studied. The starch excess phenotype of the *Ljgwd1-1* mutant was mild compared to those of *Ljgwd1-2* and *Ljgwd1-3* (premature stop codon mutants) isolated from TILLING (Chapter 4, section 4.2.4). Nevertheless, the starch-excess phenotype of the *Ljgwd1-1* mutant strongly indicated that the SBD-2 module plays an important role in the *in vivo* function of the enzyme. More specifically, it may be hypothesized that the mutation in *Ljgwd1-1* prevents the encoded protein from binding to starch, and that the binding of GWD to the surface of the starch granule is important for the activity of the enzyme, and hence for starch degradation in leaves.

Multiple sequence alignment with GWD1 homologs shows that the glutamate residue at position 566 is conserved at the equivalent position in GWD1 from other species, and lies in a generally conserved region. (Figure 31). This conserved region (an alpha-helix domain) is predicted to contain a coiled-coil domain according to the results of secondary structure prediction (Figure 32). *In silico* mutation analysis on this secondary structure of LjGWD1 shows that the replacement of a glutamate residue by a lysine at position 566 affects the predicted coiled-coil motif in which it lies (Figure 32). This suggests that this motif may be important for the binding of GWD1 to starch and that the *Ljgwd1-1* mutation may have an impact on starch degradation by disrupting it. In order to explore this hypothesis, I carried out *in vitro* and *in vivo* starch binding assays using crude protein extracts from leaves. Despite several attempts, however, no clear band corresponding to the GWD1 protein bound to starch could be detected by western blot even in the WT control (data not shown).

To further explore the hypothesis that the SBD2 domain of GWD1 is important for its activity on starch, I also attempted to isolate lines carrying additional mutations deleterious for this domain by TILLING. As detailed in the previous chapter, one mutant allele with the change G549S (from SL6859-1) predicted to be deleterious and located within this SBD2 domain (amino acids 505-602) was identified. Unfortunately, plants carrying this mutant allele could not be analysed since seeds of this mutant line were not available.

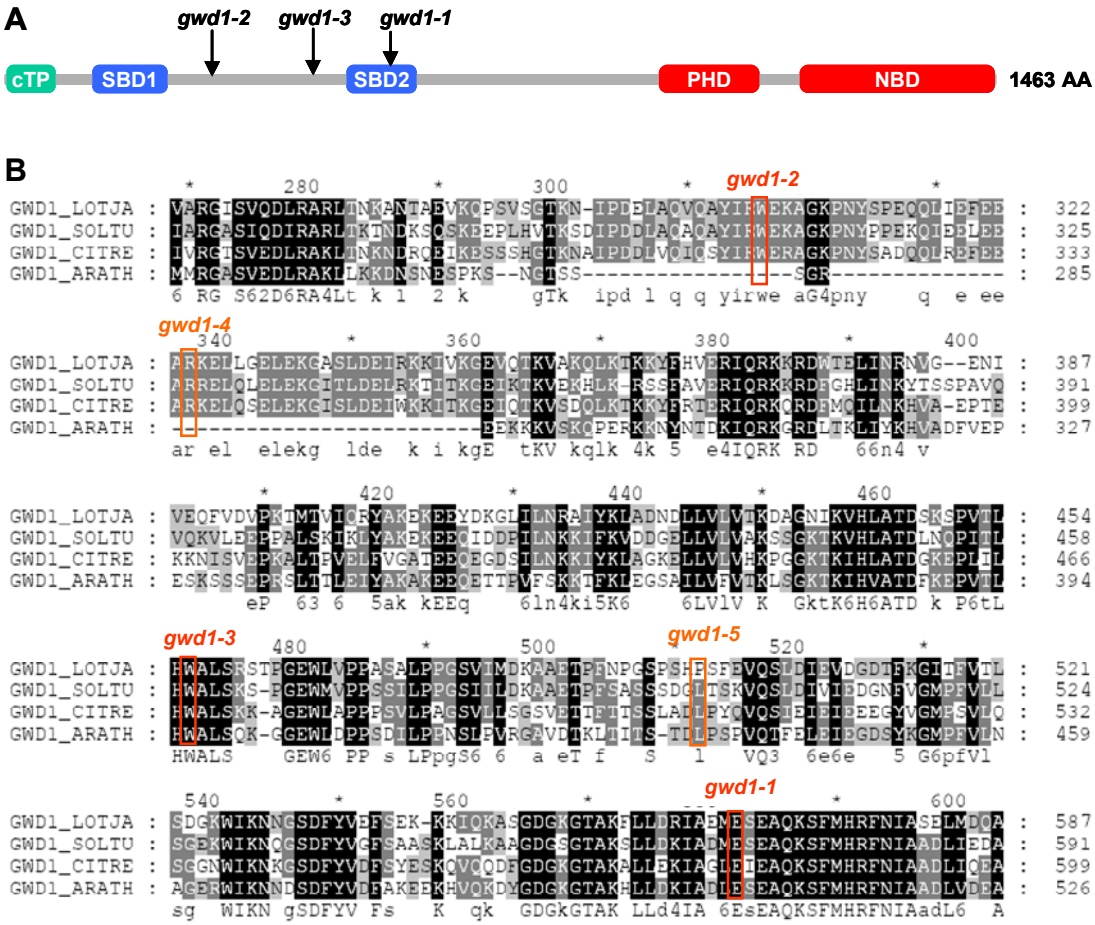

Figure 31. Protein domains of the LjGWD1 and comparison of its amino acid sequence with those of other species.
A. Location of the putative protein domains of LjGWD1 as defined by Yu et al. (2001) for its homolog in *A. thaliana*. cTP, chloroplast Transit Peptide (amino acids 1-75); SBD, Starch Binding Domain (amino acids 132-247 and 505-602); PHD, Phospho-Histidine Domain (amino acids 963-1112); NBD, Nucleotide Binding Domain (amino acids 1164-1462). **B**. Comparison of the region of GWD1 of *L. japonicus* carrying the *gwd1-1*, *gwd1-2* and *gwd1-3* mutations with the corresponding amino acid sequence in *Solanum tuberosum* (GWD1_SOLTU; Q9AWA5), *Citrus reticulata* (GWD1_CITRE; Q8LPT9), and *A. thaliana* (GWD1_ARATH; Q9SAC6). The alignment was made with the programs Clustal W2 (default settings) and GeneDoc. Strictly conserved residues are highlighted in black, less conserved residues are in grey. Amino acids changed in plants carrying the *gwd1-1, gwd1-2 and gwd1-3* alleles and their equivalent residues in the GWD1 proteins of other species are boxed in red. It is interesting to note that the *gwd1-2* mutation (W303*) lies within a region predicted to be coding for *GWD1* from *L. japonicus*, *S. tuberosum* (potato) and *C. reticulata*, but non-coding for *GWD1* from *A. thaliana*. The fact that in *L. japonicus* this mutation leads to a strong degradation phenotype, indistinguishable from the phenotype produced by another stop-codon mutant allele (*gwd1-3*; W456*) demonstrates that, at least for this species, the region is indeed translated.

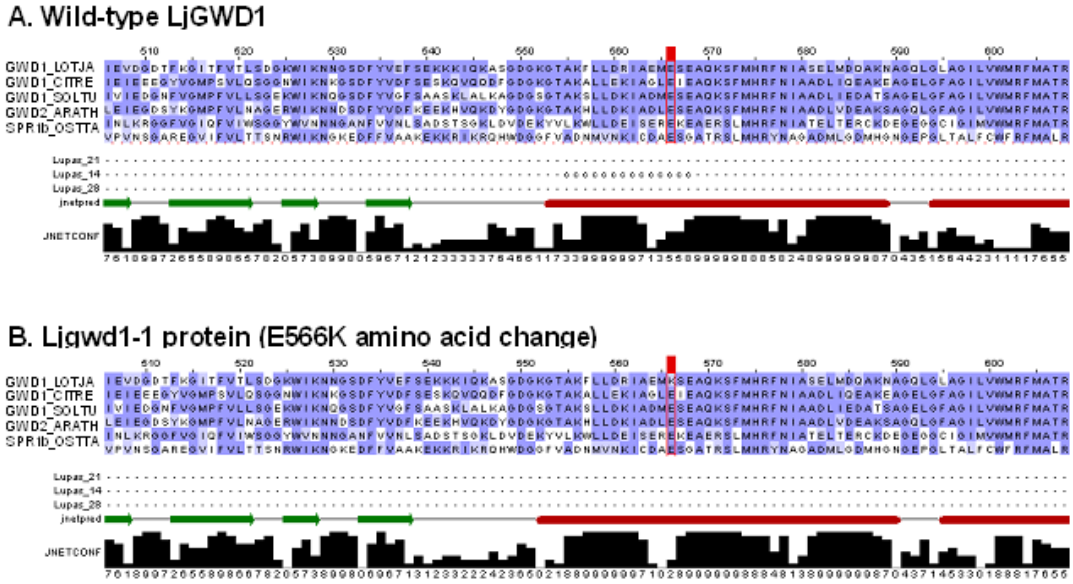

Figure 32. Predicted effect of the gwd1-1 mutation on the secondary structure of LjGWD1.
A. Effect of the *Ljgwd1-1* mutation on the secondary structure of LjGWD1 predicted *in silico* by the program Jpred (http://www.compbio.dundee.ac.uk/www-jpred/). The region of WT GWD1 protein of *L. japonicus* (panel A) was aligned with those of other species and its predicted secondary structure was compared to those given for the LjGWD1 protein carrying the E566K mutation (panel B; *gwd1-1* mutant allele; boxed in red). Note that the predicted coiled coil motif (indicated by a succession of the letter C below the alignment) is lost when the glutamic acid (E) at position 566 was replaced by a lysine (K). In this analysis, LjGWD1 (GWD1_LOTJA) was aligned with its homologous sequences in *Solanum tuberosum* (GWD1_SOLTU, Q9AWA5), *Citrus reticulata* (GWD1_CITRE, Q8LPT9), *Arabidopsis thaliana* (GWD1_ARATH, Q9SAC6). Homolog sequences of the *A. thaliana* GWD2 (GWD2_ARATH, Q84W86) and *Ostreococcus tauri* SPR1b (SPR1b_OSTTA; Q6PYX7) were also included.

5.2.1.3 GWD3 mutant alleles

As described earlier (Chapter 4, section 4.2.4), I identified a point mutation in *LjGWD3* (*Ljgwd3-1*; SL5104-12). This mutation (G7871) affects the 3' acceptor site of the splice site junction between the 9th and 10th exon of the gene (Figure 33). I performed bioinformatic analyses that suggested the mutation may lead to two different splicing variants, one resulting from the skipping of the 10th exon (117 nt shorter, 3' splice site acceptor site of the downstream exon 11 used instead), the other resulting from the use of an alternative 3' splicing site (21 nt longer, a cryptic site within the intron just upstream the mutation; Figure 33).

To determine experimentally the effect of this splice-site junction mutation on the *GWD3* transcript, I carried out RT-PCR analysis on total RNA preparations of homozygous mutant, heterozygous and homozygous WT segregants of a F2 population of the *Ljgwd3*-1 mutant. RT-PCR primers were designed on both sides of the mutation (sequence from exon 7 to exon 14 covered) and were intron-spanning in order to avoid co-amplification of genomic DNA. As predicted, RT-PCR results revealed the expression of at least one splicing variant

as a result of the mutation (Figure 33). Analysis of the RT-PCR product size suggested the main splicing variant expressed in the mutant segregants was the result of the skipping of exon 10. This was confirmed by sequencing the RT-PCR products of the homozygous mutant, WT and heterozygote. RT-PCR results also showed that this variant was expressed at a significantly lower level than the WT *GWD3* transcript (Figure 33). Abolition of the transcription of the exon 10 would lead to an in-frame deletion of 39 amino acids in the encoded protein. Although these residues do not belong to any particular functional domain of the protein, such a deletion is most likely to affect the functionality of the protein.

Furthermore, it seems that the mutation also leads to a second splicing variant that would correspond to the use of an alternative 3' splicing site within the intron located upstream the mutation and would give rise to an abnormal protein, 7 amino acids longer (Figure 33). The very low level of expression of this transcript variant, however, did not allow for its sequence to be successfully confirmed by sequencing despite several attempts.

Analysis of the genomic sequence of *GWD3* in MG-20 revealed the insertion of a LTR-retroelement (about 4.6 kb long) within the intron sequence in between exon 12 and 13 (Figure 33). PCR primers were designed to determine if this retrotransposon was also present in Gifu. PCR results showed that this was not the case (data not shown). However, the results of the RT-PCR analysis I performed on the *GWD3* transcript of MG-20 and Gifu, showed this insertion had no significant effect on its nature or expression level (Figure 33).

As already mentioned in Chapter 4, TILLING was also performed on *LjGWD3* to obtain additional mutant alleles of this gene. The targeted region contained the nucleotide binding domain involved in the dikinase activity of the enzyme (NB domain; Kötting et al., 2005). Out of the 19 mutant alleles identified, only one, *gwd3-4* (from SL0639-1), had a clear starch excess phenotype in leaves (Chapter 4, section 4.2.4). Consistent with this observation, the mutation in this line is predicted to affect a residue (amino acid change G980E) that is identical across all the predicted protein homologs of *LjGWD3* I analyzed, and lies within a conserved motif (GWD3_ARATH, Q6ZY51; GWD3_ORYSJ, NP_001066613; putative homologs in *Vitis vinifera*, XP_002265211; *Ricinus communis*, XP_002518612, and *Sorghum bicolor*, XP_002453659; Figure 34).

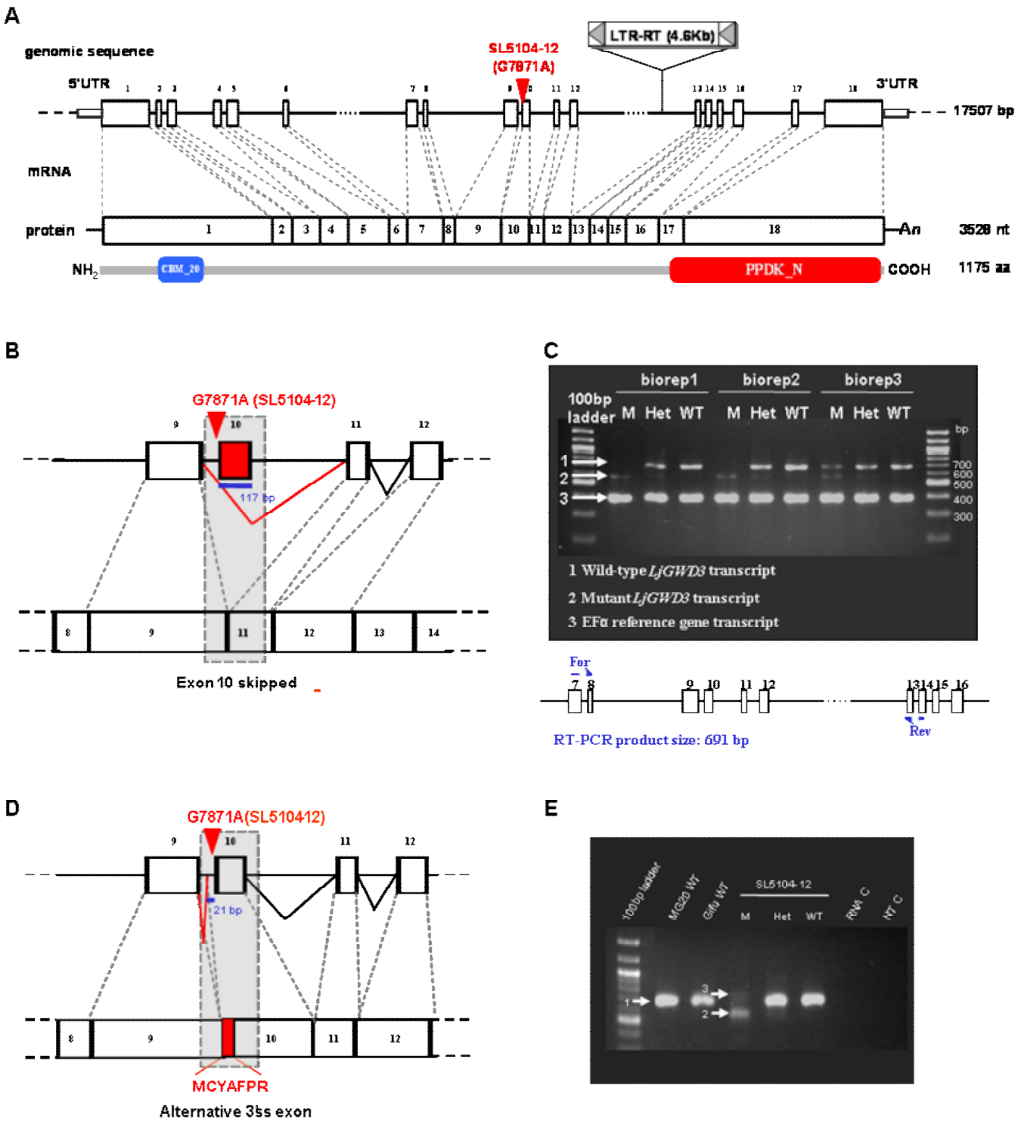

Figure 33. Predicted effects of the *gwd3-1* splice-site junction mutation on LjGWD3 function.
A. Gene structure and protein domain of LjGWD3. **B** and **C**. Sequence analysis revealed that the *gwd3-1* mutation leads to the production of a splicing variant in which the 10th exon is skipped (B). Production of this splicing variant as a result of the mutation was confirmed by RT-PCR analysis and sequencing of the RT-PCR product. Results of the RT-PCR analysis of the *LjGWD3* transcript expression in homozygous mutant, homozygous WT, and heterozygous segregants of the forward screen mutant line SL5104-12 (*Ljgwd3-1* mutant allele; splice-site junction mutation G7871A) are shown in C. For each genotype, three biological replicates from three individual plants were analysed. The WT, mutant, and reference gene (EF-α) transcripts are indicated by arrows (annotated 1, 2, and 3, respectively). Note that this variant was expressed at significantly lower level than the WT *LjGWD3* transcript. It must be mentioned, however, that such results were not so clear for the third biological replicate of the mutant for which it seems the normal transcript could also be detected (Panel C). This is surprising since this individual undoubtedly scored WT and not heterozygous according to the genotyping that had been performed twice, both by sequencing and restriction analysis. Sequences of the primers used for this RT-PCR analysis can be found in Table 2C. Sequence analysis predicted the expression of another splicing variant in the *gwd3-1* mutant plants that resulted from the use of a cryptic splicing site at position 7853 from the start codon on the genomic sequence (Transcript 21 bp longer; panel D). A very faint band at about the expected size for this putative splicing variant was observed but could not be sequenced (band indicated by an arrow labelled 3 in E). Note that a retroelement is inserted within the *LjGWD3* genomic sequence (panel A). PCR analysis using gene-retroelement spanning primers revealed that this retroelement is present in MG-20 but not in Gifu WT (data not shown). However, RT-PCR analyses suggested that this retroelement does not have any impact on the nature and level of expression of the *LjGWD3* transcript (band of identical size and intensity obtained in MG-20 and Gifu WT; panel E). Abbreviations: biorep, biological replicate; EF-α, elongation factor alpha; RNA C, control using the RNA sample as template; NTC, no template control.

Figure 34. Comparison of the amino acid sequence of LjGWD3 with those of other species.
Comparison of the region of GWD3 of *L. japonicus* carrying the *gwd3-4* mutation with the corresponding amino acid sequence in *Arabidopsis thaliana* (GWD3_ARATH, Q6ZY51), *Orysa sativa* (GWD3_ORYSA, NP_001066613); *Vitis vinifera* (GWD3-VITVI, XP_002265211; *Ricinus communis* (GWD3_RICCO, XP_002518612, and *Sorghum bicolor* (GWD3_SORBI, XP_002453659). The alignment was made with the programs Clustal W2 (default settings) and GeneDoc. Strictly conserved residues are highlighted in black, less conserved residues are in grey. Amino acids changed in plants carrying the *gwd3-4* mutant allele (starch excess phenotype) and their equivalent residues in the GWD3 proteins of other species are boxed in red, those of the *gwd3-2* and *gwd3-3* (PSSM>0; no starch excess phenotype) are boxed in orange.

5.2.2. Physiological analysis of selected mutants

5.2.2.1 PGM1 mutants

I analysed the starch content of the *pgm1-4* mutant by iodine staining and starch quantification. This mutant is completely starch-free in all the tissues and organs analysed, including leaves, stem, roots, seed embryos, and nodules (Chapter 4, Figure 20 and Figure 35). Interestingly, despite its inability to synthesis starch, the growth rate of this mutant was indistinguishable from that of the WT, both under long days (16/8 h light dark period) and under a 12 h photoperiod. This is consistent with the phenotype of the equivalent mutant in

pea (*rug3*; Harrison et al., 2000), but contrasts with the near- or completely starch-free mutants of *A. thaliana* and other plant species whose growth is impaired under 12 h photoperiod (Caspar et al., 1985; Hanson and McHale, 1988; Lin et al., 1988).

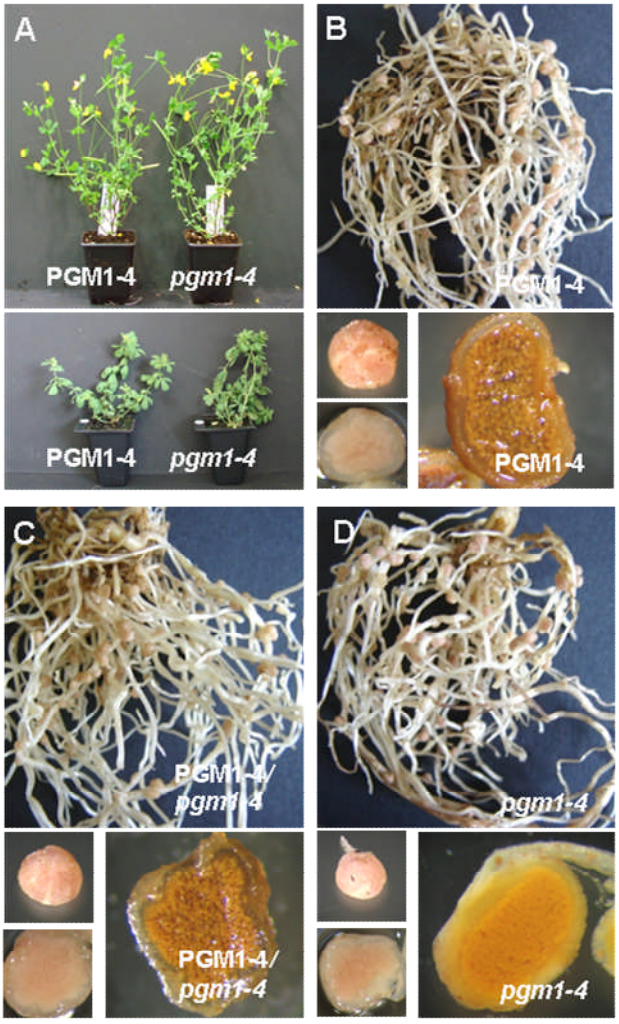

Figure 35. Phenotypes of the *pgm1-4* mutant of *L. japonicus*.
A. Plants grown in 16 h light, 8 h dark (top) and 12 h light, 12 h dark (bottom). **B-D**. Root systems and nodules of 3 month-old plants grown in 16 h light, 8 h dark and inoculated with *Mesorhizobium loti* at 6 weeks. Nodules are shown either whole (top left), cut open (bottom left) or cut open and stained with iodine (right). The cortical zone and non-infected cells in WT nodules contain starch. Mutant nodules contain no starch.

There is little information about the importance of starch stored in nodules for the rate of Symbiotic Nitrogen Fixation (SNF). Given the normal growth of starchless *L. japonicus* plants, I decided to examine specifically whether a lack of starch affected nitrogen fixation in *Rhizobium*-containing root nodules under nitrogen free conditions. As described above, legume nodules generally contain starch in cortical cells and non-infected cells within the infected zone (Gordon et al., 1992; Gordon and James, 1997; Szczyglowski et al., 1998). In

pgm1-4 mutants of *L. japonicus* inoculated with *Mesorhizobium loti (M. loti)*, nodules had a normal pink colour, and their size and number per root system were similar to those of wild-type segregants (Figure 35B-D). In spite of the lack of starch in the nodules, assays for nitrogen fixation (acetylene reduction) performed by Tracey Welham (JIC, Norwich, UK) revealed no statistically significant differences (Student's t-test p-value of 0.05) between mutant, heterozygote and wild-type plants 36 days after inoculation with *M. loti* (0.57 ± 0.06, 0.75 ± 0.11, and 0.67 ± 0.20 μmol ethylene h^{-1} root $system^{-1}$, respectively; means ± SE of 5 root systems).

5.2.2.2 GWD1 mutants

Iodine staining of the complete loss of function mutants *gwd1-2* and *gwd1-3* revealed a very strong starch-excess phenotype in their leaves compared to those of the WT. A clear starch excess phenotype was also visible in nodules, roots and pollen of the mutants, although less pronounced than in leaves and nodules (Figure 20 and Figure 36A-D). Mutants of both lines also showed severe-growth defects including an impaired growth, chlorosis and premature senescence symptoms, and an almost complete failure to produce seeds (Figure 36H-J and Figure A6). Across all batches of segregating populations analysed, only a small fraction of the mutant plants survived to maturity and produced flowers (ca. 20%), and did so about two months later than wild-type plants in Gifu background (Table A4). Further, most of these flowers did not produce pods, and when they did, pods and embryos aborted at early stages of development, at what seemed to correspond to the beginning of the seed filling stage. These characteristics were present regardless of the day length under which the plants were grown. A similar phenotype was observed in the progeny plants of an outcross with the wild-type accession MG-20 (Figure A6).

I explored further the causes of the loss of fertility in *gwd1*-2 and *gwd1*-3 mutants. In the progeny of plants heterozygous for *gwd1-2* (in Gifu background; SL1833-1 mutant line), segregation did not follow the Mendelian ratio of 1:2:1 mutant:heterozygote:WT. From 219 plants, 13 were mutants, 116 were heterozygotes and 90 were WT. Similarly for the mutant line SL3001-1 (*gwd1-3* mutant allele), I identified 15 mutants, 98 heterozygotes and 89 WT out of a segregating population of 202 plants (Table A4). Three hypotheses can be advanced to explain this low proportion (6-7%) of homozygous mutant plants: either (1) loss of GWD1 is lethal at the gametophyte stage, or (2) homozygous mutant embryos generally do not survive to maturity, or (3) mutant seeds do not germinate as well as the heterozygous and WT ones. In tomato, loss of GWD1 leads to pollen with an abnormally high starch content that fails to germinate (Nashilevitz et al., 2009). However, two lines of evidence suggested that pollen from *L. japonicus gwd1* mutants is at least partially viable despite its high starch content. First, heterozygote plants could be obtained in the F1 progeny of reciprocal crosses

made between heterozygote and WT plants – it should be mentioned, however, that a paternal transmission ratio different to the 1:1 expected ratio of heterozygote:WT in the F1 progeny of the cross ♂GWD1-3/gwd1-3 x ♀MG-20 WT was observed, suggesting a possible case of partial gametophytic lethality (Table A5). Second, staining the pollen with acetocarmine, a dye used to assess whether pollen grains have matured, showed no differences between WT, heterozygote, and homozygous mutants (Figure 36E. Similarly, staining with FDA, another dye used to access pollen grain viability did not reveal any visible difference between the WT and heterozygote (Figure 36F). Further, an *in vitro* germination assay of the pollen grains was also performed that revealed the mutant pollen grains with starch excess phenotype were still able to produce pollen tubes (Figure 36G). Thus, in *L. japonicus* starch accumulation in pollen does not appear to prevent pollen viability or germination, and may not account, at least fully, for the loss of fertility observed in the *gwd1-2* and *gwd1-3* mutants.

Most *gwd1-2/3* mutant flowers did not produce pods, and when they did, pods and embryos usually aborted at an early stage of development (Figure 36K). However, fully developed pods and seeds could be obtained from the mutants by detaching flowers and placing the peduncles in MS liquid medium supplemented with 3% sucrose (Figure 36L). These results suggested that the effect of the mutation on the production of viable seed was maternal rather than due to a defect in embryo development. To examine this idea further, I analyzed embryos and seeds from 40 pods each of wild-type (*GWD1-2/GWD1-2*) and heterozygous (*GWD1-2/gwd1-2*) plants from the same segregating population (Table A4). Both the number of seeds per pods and the average weight of the seeds produced were very similar for the two lines (average number of seeds per pod and average seed weight were 9.1 and 1.0 mg for the heterozygote, and 10.2 and 1.0 mg for the WT, respectively). Similarly, for the *gwd1-3* mutation analysis of 20 pods gave an average number of seeds per pod and seed weights of 15.9 and 1.0 mg, respectively, for the heterozygote (GWD1-3/*gwd1-3*), and 15.1 and 1.1 mg for WT (*GWD1-3/GWD1-3*), supporting the idea that reduced production of viable seeds on homozygous mutant plants is a maternal effect. However, genotyping of each individual mature embryo in pods from heterozygous plants (*GWD1-2/gwd1-2* and *GWD1-3/gwd1-3*) was not wholly consistent with a maternal effect. Out of 63 mature seeds analysed, only seven contained homozygous mutant embryos (one in nine rather than the expected one in four; Table A4). Thus mutant embryos were disadvantaged whether in mutant or heterozygote pods.

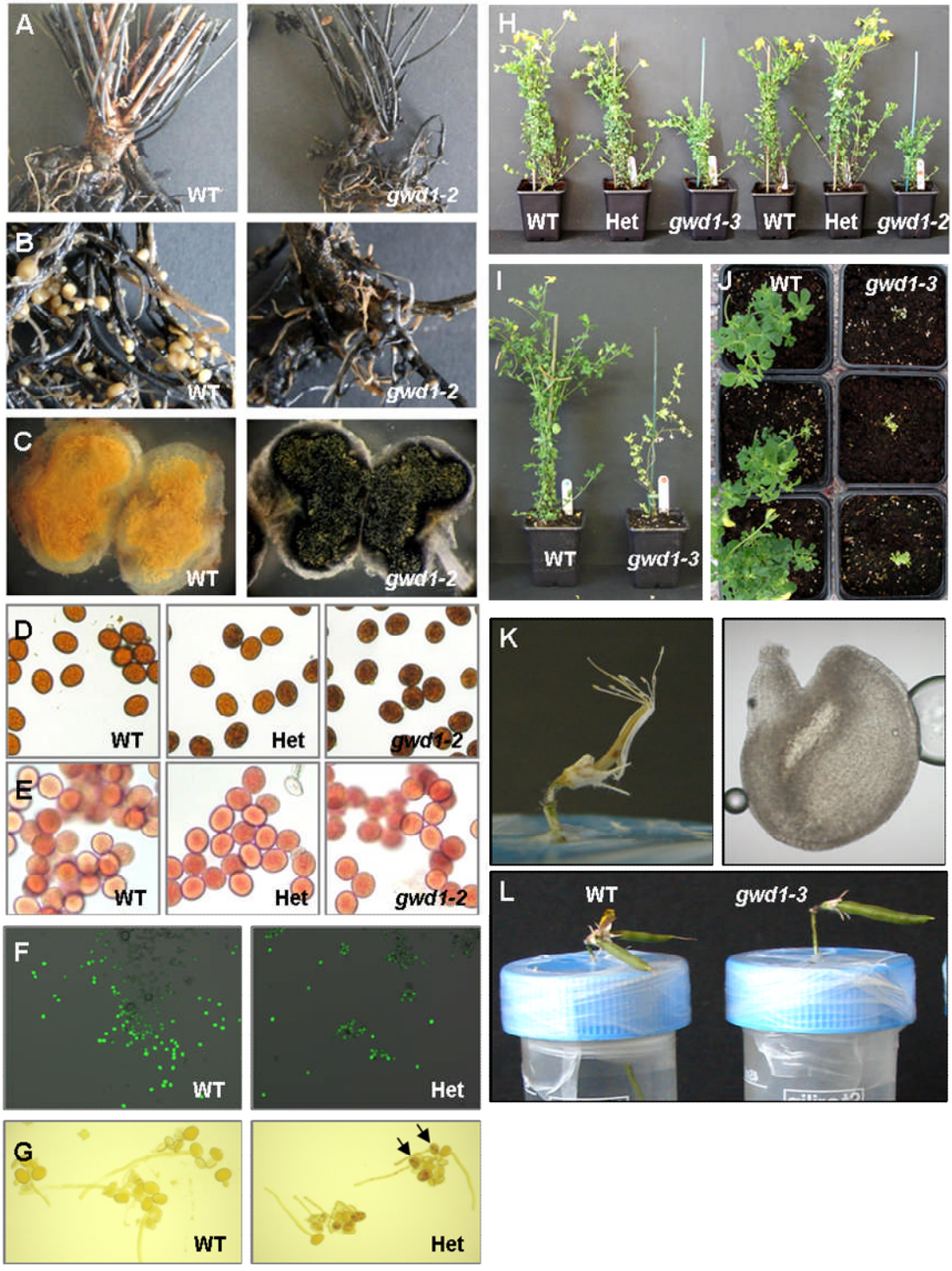

Figure 36. Phenotypes of the *gwd1-2* and *gwd1-3* mutants of *L. japonicus*.
Continued on next page.

Figure 36. Phenotypes of the *gwd1-2* and *gwd1-3* mutants of *L. japonicus*. Continued.
A-C. Iodine staining of root systems and of the interior of a nodule of the *gwd1-2* mutant (right) and WT segregant (left). Plants were grown in 16 h light, 8 h dark and were 6 months old. **D** and **E**. Pollen grains from WT, heterozygote, and gwd1-2 mutant plants stained with iodine (D) and acetocarmine (E). The mutation increases the starch content of pollen, but does not affect its viability. **F** and **G**. Pollen grains from the heterozygote and WT segregant of the mutant line *gwd1-2* harvested at anthesis and stained with FDA (F), and with iodine following *in vitro* germination (G). Note that mutant pollen grains from the heterozygote plant (ones with a starch excess phenotype; indicated with an arrow) were capable of germinating *in vitro* as indicated by the production of a pollen tube. Pollen grains from the homozygous mutants were not available at the time this experiment was performed, and therefore could not be analysed together with the pollen grains of the heterozygote and WT segregants. **H**. Three month-old WT, heterozygote and mutant segregants for *gwd1-3* (left three plants) and *gwd1-2* (right three plants) grown in a controlled environment chamber. **I**. Phenotype of four month old *gwd1-3* mutant (right) and WT segregant (left) plants grown in a greenhouse with supplemental lighting. **J**. Phenotype of 2 to 3 month old *gwd1-3* mutant (right) and WT segregant (left) plants grown in a greenhouse under natural light conditions. **H-J**. Plants were grown under long day conditions (ca. 16 h photoperiod). Detailed phenotypes of the *gwd1-2* and *gwd1-3* in Gifu and MG-20 background, including photographs of the chlorosis and premature senescence symptome and of their root system and nodules is shown in Figure A6. **K-L**. Nodule phenotype. **K**. Example of aborted pod and embryo of the *gwd1-2/3* mutants. **L**. *In vitro* culture of pods. Mature flowers were taken and their peduncles sterilised with 10% bleach. Following several washes in sterile water they were placed in liquid Murashige and Skoog medium supplemented with 3% sucrose, and cultured as described in Chapter 2 (section 2.1.4) for ca. 4 weeks to produce mature seeds.

In order to determine if the embryo of the mutants had a starch excess phenotype that may, at least partially, explain their impaired development, I stained the embryos and seeds of GWD1-*2/gwd1-2* and *GWD1-3/gwd1-3* heterozygous pods and compared their starch content to those of the homozygote WT segregants, as well as to seed embryos of homozygote mutants of the forward screen mutant lines SL5215-2, SL5358-3 (*gwd1-1* mutant allele) and SL5104-12 (*gwd3-1*.mutant allele). A few of the embryos or seeds isolated from pods of GWD1-2/*gwd1-2* and GWD1-3/*gwd1-3* heterozygote plants displayed a clear starch excess phenotype (Figure 37). Unfortunately, since iodine staining and genotyping could not be carried out on the same individual embryo and no embryos could be obtained from homozygous mutants plant for this starch content analysis, I could not obtain compelling evidence that the mutation indeed confers a embryo starch excess phenotype. However, embryos of the *gwd1-1* and *gwd3-1* mutants displayed a very weak, but consistent starch excess phenotype in comparison to their WT segregants (Figure 37).

Since root nodules of the *gwd1-2* and *gwd1-3* mutants also presented a strong starch excess phenotype in comparison to their WT segregants (Figure 36C), I examined, with the help of Tracey Welham (JIC) whether the lack of starch turnover in these organs affected nitrogen fixation. At two stages of nodule development, nodules on *gwd1-2* plants contained about 15 times more starch than nodules on wild-type plants (Figure 38A). Nonetheless, mutant nodules were capable of nitrogen fixation. In one batch of plants, nitrogen fixation (acetylene reduction) was comparable in *gwd1* mutants and their segregating wild-type and heterozygous lines. In two further batches fixation was reduced in mutants relative to wild-

type and heterozygous plants but was above the threshold for detection in this assay (Figure 38B).

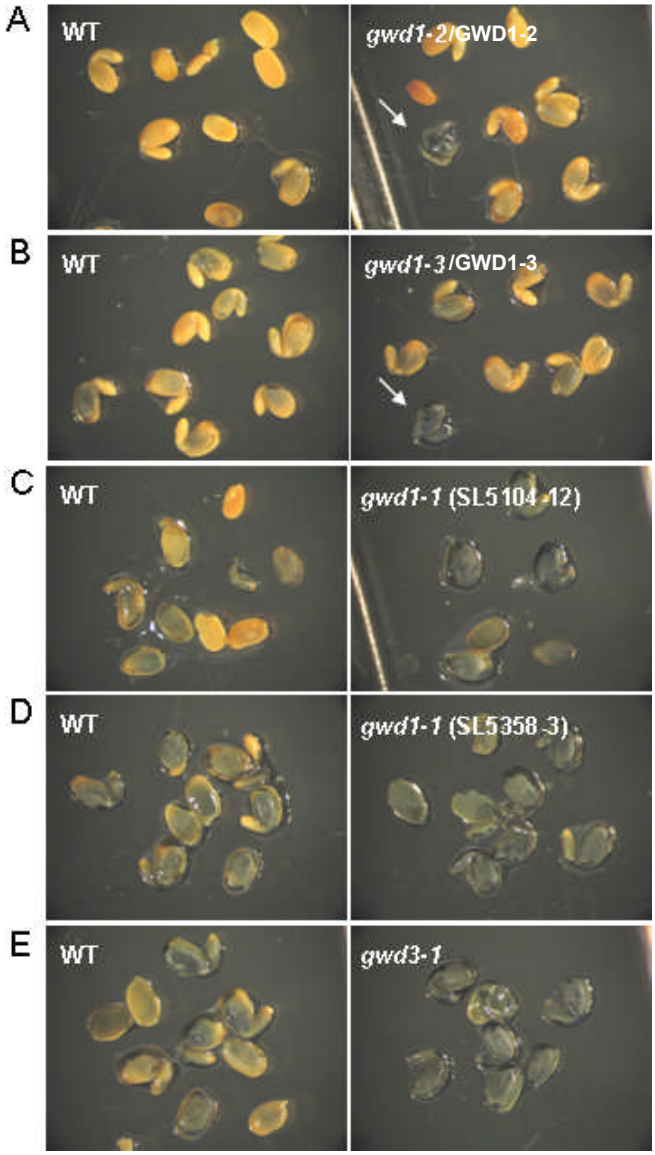

Figure 37. Iodine staining of the seed embryos of the *gwd1-1* and *gwd1-2/3* mutants.
Embryos of the heterozygote of the *gwd1-2/3* mutant lines (A and B) and of the *gwd1-1* (B and C) and *gwd3-1* mutants (left panels) in comparison to their WT segregants (right panels). Embryos were extracted from dry seeds (the testa and endosperm were removed) and left to soak in water for some time before they were decolorized and stained with iodine as described in Chapter 2, section 2.4. Stained embryos were observed with a Leica MZ8 binocular (x10). Note that a few of the embryos (indicated with an arrow) from a pod of a heterozygous plant of the *gwd1-2* and *gwd1-3* mutant lines presented a starch excess phenotype. These embryos would need to be genotyped to test the hypothesis that embryos with a starch excess phenotype correspond to those of gwd1-2/3 mutants. The fact that embryos of the *gwd1-1* and *gwd3-1* mutants also appeared to have a slight starch excess in comparison to WT segregants tends to favor this hypothesis.

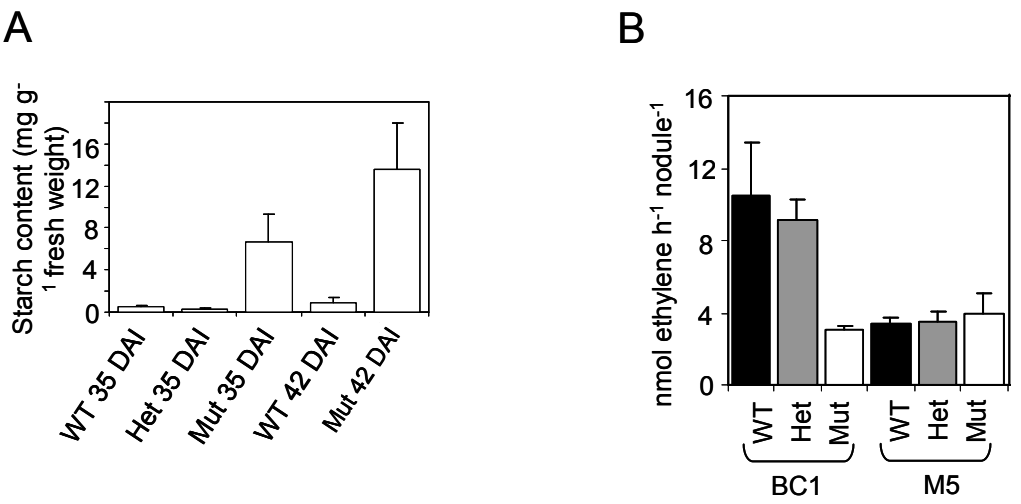

Figure 38. Nodule phenotype of *Ljgwd1* TILLING mutants.
A. Elevated starch contents of *gwd1-2* nodules. Nodules were harvested from individual *gwd1-2* plants and segregating heterozygous and wild-type plants from the first outcross to MG-20 at 35 and 42 days after inoculation (DAI) with *Mesorhizobium loti*, and assayed for starch content. Values are means ± SE of measurements on five plants, except for WT at 42 DAI for which four plants were used. **B**. Ethylene released in an acetylene reduction assay for nitrogenase activity on root systems of *gwd1-2* mutants and their wild-type and heterozygous segregants. Plants were from lines derived either by outcrossing to MG-20 (BC1), or directly from the original mutant in Gifu (M5).

5.3. Discussion

5.3.1. Functional characterisation of the mutants

The amino acid change identified in the *apl1-1* mutant was unexpected given the marked change in enzyme activity brought by the mutation. Since the mutated residue (S400; equivalent to S331 in the potato small subunit) is positioned at the interface between monomers (Figure 30), it is tempting to speculate that this residue has a dramatic impact on the AGPase activity because it is crucial for the interaction between the subunits. However, this did not appear to be the case from the analysis of the homotetrameric structure. Instead, it appeared that this residue along with some other residues are important for the integrity of the β-helix domain and that a disruption in this domain may affects its interaction with the substrate binding domain, resulting in an almost complete loss of activity (Figure 30, and personal communication with Dr Faridoon Yousafzai, JIC).

Results of genetic (mapping), biochemical and bioinformatic analysis combined with recent literature evidence strongly suggest that mutation identified in APL1 gene is indeed responsible for the mutant phenotype (chapter 4, section 4.2.3). However, additional analyses would need to be performed to gain a better understanding of the molecular mechanism by which the S400L amino acid change is able to disturb so drastically the

activity of the enzyme. More precisely, it would be useful to obtain a series of mutant alleles affecting other residues of the β-helix domain involved in maintaining its integrity and determine whether these mutations lead to a loss of activity and a mutant phenotype similar to the one observed for *Ljapl1-1*. This may be achieved via site-directed mutagenesis or TILLING. In addition, modelling of the heterotetramer and *in-silico* site-directed mutagenesis would help determine the importance of the S400 residue to the stability of the β-helix domain. Such analyses may also rule out the possibly that the mutation affects the enzyme activity through a disruption of the interaction between subunits. Native PAGE gel and western blot analysis could also be performed to explore the impact that the *apl1* mutation has on the conformation of the AGPase heterotramer, since one may expect a change in the migration of the protein if folding is altered or there is a loss of subunit interaction.

I have reported here the isolation and characterisation of two *Lotus japonicus gwd1* mutants that have a starch-excess phenotype in leaves. Interestingly, the mutation identified in *GWD1* as being responsible for the mutant phenotype led to a single amino acid change (E566K) in the second putative starch binding domain (SBD2) of the protein (Figure 31). This suggests an important role for this domain in the activity of the enzyme and the phosphorylation of starch and, consequently, its normal degradation. Moreover, this suggests that the residue E566 of SBD2 is crucial for the starch binding capacity of the enzyme. Neverthless, the effect that the mutation in *Ljgwd1-1* has on the functionality of the LjGWD1 protein remains to be further investigated. In order to explore the effect that this mutation could have on the functionality of the SBD2 domain, I carried out secondary structure predictions. The results suggested that the mutation identified in LjGWD1 is located within and may affect a predicted coiled-coiled motif of an alpha-helix domain (Figure 32). However, generation of the three dimensional structure of this domain and *in silico* mutagenesis would need to be performed to decipher the impact that the mutation has on the LjGWD1 enzyme functionality. Unfortunately, the crystallographic structure of CBM45 from GWD1 or any other member of this family of starch binding domains has yet to be solved (http://www.cazy.org). By default, homology modelling of the CBM45 domain using CBM20 as template was attempted, but the similarity of sequence between the two was too low to obtain any satisfactory models.

Since the mutation identified in *Ljgwd1-1* was located in SBD2 it may be hypothesized that the starch-excess phenotype of this mutant results from an impaired capacity of its GWD1 mutant enzyme to bind starch. In an attempt to gain such evidence, *in vitro* and *in vivo* starch binding assays were carried out, but failed to generate any clear results. The

generation and use of a recombinant LjGWD1 protein (native and mutant versions) rather than crude protein extracts may help obtain clearer results from such assays in the future.

Lastly, one approach that could be used to explore the impact of the mutation on GWD1 enzyme activity would be to measure the phosphate content of the starch. Unfortunately, such measurements have proven to be difficult to achieve in the past (Alison Smith, JIC, personal communication). A radiolabelling assay to quantify the starch-phosphorylating enzyme activity in crude extracts of plant tissues has been established (Ritte et al., 2003) that could be tried in the future. Alternatively, measuring β-amylase activity and the release of maltose could be another, although indirect, way of measuring the effect of the mutation on the functionality the GWD1 protein. Indeed, using purified recombinant enzymes, Edner et al. (2007) were able to show that BAM1 and BAM3 activities are strongly stimulated by the phosphorylation of the starch granule by GWD1. Hence, one may expect the activity of these BAM enzymes to be decreased in this assay when using a mutated version of the recombinant GWD1 protein with a reduced or a complete lack of GWD1 activity. More particularly, it would be interesting to perform such assay on a GWD1 protein carrying an equivalent mutation to E566K. One could envisage also testing in a same way the effect of mutating other conserved residues of the SBD1 and SBD2 domains of GWD1.

Starch constitutes a major component of the human diet and an important material for many industrial processes (Jobling, 2004). Chemical modification of starch, including phosphorylation is often needed for these applications. Increasing the phosphate content in starch in crops plants is therefore highly desired as it reduces the need for environmentally unfriendly and expensive industrial processes (Blennow et al., 2002). Production of recombinant GWD protein with enhanced dikinase activity and/or stronger binding on starch could be a way to increase the level of starch phosphorylation. Hence, it would be of interest, by using recombinant DNA technology and *in vitro* assays, to explore the phosphorylation capacity, substrate specificity and binding capacity of the GWD1 enzyme either carrying both, one of the two, and/or none of the two SBDs. Of great interest also would be to determine if the two SBD have distinct, complementary or synergistic roles. Potentially interesting as well from a biotechnological point of view would be to identify the residues determinant for the properties mentioned above. Structure-function analyses including site-directed mutagenesis may help achieve this. Lastly, the introduction into plants via transformation of modified forms of GWD with different binding affinities for starch would need to be performed to determine the effect of the SBDs of GWD1 on the starch content and the fitness of the plant (e.g. does a weaker/stronger GWD1-starch interaction have a beneficial effect on plant productivity?).

Further mutant alleles conferring a starch-excess phenotype, namely *gwd3-1* and *gwd3-4*, were isolated during this study. Their characterisation indicated that another enzyme, LjGWD3, played an important role in the degradation of starch in leaves of *L. japonicus.* Hence, it seems likely that, as in *A. thaliana*, LjGWD3 acts in synergy with LjGWD1 to phosphorylate the starch granule as a prerequisite for degradation (Kötting et al., 2005; Baunsgaard et al., 2005). The mutation identified in *Ljgwd3-1* affected the 3' acceptor site of the splice site junction between the 9th and 10th exon of the gene (Figure 33). Splice site junction mutations generally result in the production of an aberrant protein through the lost of exon(s) or the retention of intron(s) and are therefore most likely to be deleterious. Furthermore, when the mRNA does not encode a functional protein, non-sense mediated decay of the transcript can occur (Chang et al., 2007). In the case of the *Ljgwd3-1* mutant, results of the RT-PCR analysis I carried out revealed that the mutation led to the production of at least one splice-site variant. Most likely, the protein resulting from this splice-site variant would not be functional, however, this remains to be experimentally tested. Firstly, the presence and expression level of the GWD3 protein could be monitored by western blot – unfortunately, antibodies against the GWD3 protein were not available and could not be generated within the time frame of this study. Secondly, measurement of the phosphorylation at the C3 positions of the glucose moieties of starch could be performed to indirectly measure the activity of the GWD3 enzyme in the mutant in comparison to the WT (Ritte et al., 2006).

Analysis of the genomic sequence of *GWD3* in MG-20 revealed the insertion of a LTR-retroelement (about 4.6 kb long) within the intron in between exon 12 and 13 (Figure 33). Retrotransposons (RT) are mobile genetic elements that are ubiquitous in plants and constitute the most abundant and widespread class of eukaryotic transposable elements (TE). In several instances, the insertion of a retroelement has been shown to disturb gene regulation and result in altered gene expression e.g. in the maize *waxy* gene it has been shown to result in tissue-specific expression of alternatively-spliced transcripts (Marillonnet and Wessler, 1997). However, the results of the RT-PCR I performed on the *GWD3* transcript revealed that this insertion had no significant effect on its expression (Figure 33).

5.3.2. Importance of starch metabolism for plant growth and its regulation in legumes

The starchless phenotype of the *pgm1-4* mutant (Figure 16 and Figure 35) indicates that plastidial PGM (PGM1) is necessary for starch synthesis throughout the plant. Interestingly, despite its inability to synthesize starch, this mutant grows normally even under relatively short days (12 h light, 12 h dark; Figure 35). This is also true of the equivalent mutant in pea (*rug3*; Harrison, 1996). In contrast, although the almost starchless *pgm1* mutant of *A.*

thaliana grows at approximately the same rate as the wild type under continuous light, it grows much more slowly under 12-h light, 12-h dark conditions (Caspar et al., 1985). Thus, complete loss of starch seems to have no deleterious consequences for the growth of *L. japonicus* plants under normal conditions in contrast to the situation in *A. thaliana*. This suggests that either a compensation mechanism exists in *L. japonicus*, or that the impairement in growth seen in the starch-free mutant of *A. thaliana* but not in *L. japonicus* is the result of difference in signalling or regulation between the two species, rather than the direct consequence of the lack of starch. The *pgm1* mutant of *A. thaliana* accumulates increased level of soluble sugars during the day in comparison to the WT (Caspar et al., 1985). This soluble sugar pool is rapidly consumed during the subsequent night, when photosynthesis cannot take place. Under short day conditions, however, these reserves of sugars are not sufficient to sustain growth and energy metabolism of the plant during the entire dark period. This phase of carbon starvation is believed to be the cause of the impaired growth of the *pgm1* mutant of *A. thaliana* when grown under 12 h photoperiod and even more so under shorter days/longer night cycles (Caspar et al., 1985; Gibon et al., 2004).

Compensatory mechanisms that could explain the capacity of the *pgm1* mutant of *L. japonicus* to cope with the absence of carbon stored as starch even under short day conditions may involve similar, but more pronounced, responses to the ones seen in the *pgm1* mutant of *A. thaliana*. Thus, it may be hypothesized that *Ljpgm1* is able to compensate for the lack of starch by an increased accumulation of soluble sugars during the day in comparison to the WT to serve as a supply of carbon during the night. This increased sugar accumulation could potentially be fuelled by an increased rate of photosynthesis. If this model is true, one would expect the *pgm1* mutant of *L. japonicus* to be at least partially impaired in growth under very short day conditions and/or under very low irradiance. Such hypotheses remain to be tested.

Another feature of *L. japonicus* that contrasts with *A. thaliana* is provided by the stop-codon mutant lines SL1833-1 and SL3001-1 (carrying the mutations *gwd1-2* and *gwd1-3*, respectively), which had a very strong starch-excess phenotype in leaves, roots, stems, nodules and pollen (Figure 16 and Figure 36). These mutants showed severe growth defects including leaf chlorosis, premature leaf senescence and, although showing some variation, all the mutants isolated had a very impaired reproduction capacity (very poor or no seed set). Only a small proportion of mutant plants in a given batch produced flowers, and did so about two months later than WT plants. These characteristics were present regardless of the day length under which the plants were grown. This is in contrast to the situation in *A. thaliana*, in which *gwd1* (*sex1*) knockout mutants display almost no growth phenotype under long days although retaining very high starch contents, and can reproduce even under short days

when growth is significantly retarded (Caspar et al., 1991). Thus loss of GWD seems to have much more serious consequences for *L. japonicus* than for *A. thaliana*. It is possible that the variation observed in the *Ljgwd1-2* and *Ljgwd1-3* phenotypes might be caused by the retrotransposon inserted at the 3' end of the genomic sequence encoding the GWD1 gene, however this would require further investigation.

The starch-excess mutants show that the phosphorylation of starch via the glucan, water dikinases GWD1 and GWD3 is essential for normal starch degradation in *L. japonicus*, and that this, in turn, is crucial for normal growth. Remarkably, these mutants - together with the growth phenotype of the *pgm1-4* mutant – also show that while *L. japonicus* plants are able to grow well in the absence of starch, they are very impaired in growth when not able to degrade it. It is not clear why growth rates are reduced in some mutant plants impaired in leaf starch synthesis or degradation, or why mutations in homologous starch metabolism genes have different consequences for growth in *L. japonicus* and *A. thaliana*. Poor plant growth may be due to a sequestration of carbon into starch preventing its use during the dark period. Hence, in *A. thaliana*, genetic and environmental factors that reduce carbohydrate availability at night can also cause temporary cessation of growth (Smith and Stitt, 2007; Graf and al, 2010). Alternatively, plant growth may be restricted directly by the accumulation of starch itself (e.g. physical impairment of the normal chloroplast function). Lastly, a signalling mechanism compelling the plant to limit its growth more than it would theoretically need to due to the lack of available starch may also take place. The fact that the starch-free *pgm1* mutant of *L. japonicus* does not show any impairment in growth and development even when grown under 12 h photoperiod tends to support this last hypothesis. Further, it may be hypothesised that the putative signalling that would lead to restricted growth in case of failure to degrade starch involves a sensing of the phosphate status of starch. The fact that a restricted growth is observed in most of the starch-excess mutants of *A. thaliana*, however tends to rule out this possibility. In respect of this signalling and sensing model, it is interesting to note that SnRK1, a SNF1-related protein kinase that plays a key role in the global control of plant carbon metabolism, was found to interact with SEX4 (Fordham-Skelton et al., 2002). In the future, the identification of interactors of GWD1 and other key starch degrading enzymes by yeast-two-hybrid (Y2H) or other protein-protein interaction analysis methods may be carried out that would help shed light on the putative signalling mechanism involved in regulating the plant growth response to carbon availability.

5.3.3. Importance of starch for seed metabolism and development in legumes

Since *L. japonicus* seeds accumulate very little starch, it is unlikely that altering the synthesis of this storage carbohydrate would have as much effect in *L. japonicus* as it does in pea (Chapter 5, section 5.1.1 and references therein). In agreement with this, no visible impairment in seed development including seed morphology, seed weight, germination capacity, or early seedling growth could be observed in the starch-free *pgm1-4* mutant of *L. japonicus* in comparison to the WT, but these observations would need to be confirmed. It cannot be ruled out that, as in leaves, the effect of the lack of starch in this organ may be masked by some compensatory mechanisms (e.g. increase synthesis and storage of soluble sugars). In this respect, analysis of other starch mutants of the collection, and in particular of the mutants unable to degrade starch may prove very useful in determining the importance played by starch in seed metabolism and development.

Segregation ratios in the offspring of a heterozygous plants of the two starch excess mutant lines SL1833-1 and SL3001-1 did not follow the Mendelian ratio of 1:2:1 mutant:het:WT (Table 8), suggesting a possible case of homozygote or gametophytic lethality. Recently, it has been shown that the lack of GWD1 activity causes male gametophytic lethality in tomato (Nashilevitz et al., 2009) but not in *A. thaliana* (Caspar et al., 1991). In *L. japonicus*, the mutants were essentially infertile. Results of the *in vitro* pod culture I performed suggested that the effect of the mutation on the seed production was maternal rather than intrinsic to the development of the embryo. However, genotyping of the mature embryos in pods from heterozygous plants revealed a segregation ratio significantly different from the expected Mendelian ratio for a single recessive mutation. Reciprocal crosses were preformed that suggested a possible case of partial gametophytic lethality. Failure to transmit the mutant alleles by the paternal parent can be caused by defects in pollen viability, germination, pollen tube growth, and fertilization (Nashilevitz et al., 2009). Several analyses of the pollen grains were performed that included iodine, acetocarmine and FDA staining as well as *in vitro* germination assays. Results of these preliminary analyses did not reveal any clear impairment in the viability and germination capacity of the mutant pollen grains in comparison to the WT. However, more extensive, quantitative analyses such as germinating pollen grain number and pollen tube growth length between the mutant, heterozygote and WT would need to be carried out to fully assess and define the extent of the male gamete- and maternal-specific defects. Overall, the effect of the lack of GWD1 activity on the fertility of *L. japonicus* plants appears to be complex, the data indicating that pollen, embryos, and/or germinating seeds bearing mutant alleles may be at a competitive disadvantage to those with WT alleles. Thus, gametophytic, maternal, and embryo effects may all be involved.

5.3.4. Importance of starch metabolism for nodule function and SNF in legumes

Comprehensive studies on sucrose synthase in several legume species have clearly demonstrated the important role played by primary carbon metabolism in nodulation (Gordon et al., 1999; Craig et al., 1999; Horst et al., 2007; Baier et al., 2007). Yet, with the exception of this enzyme, remarkably little is known about the importance of the other enzymes of carbohydrate metabolism in nodule function. In addition, the importance that the supply and storage of carbon to/in the nodule may have in regulating the rate of N_2 symbiotic fixation remains to be determined. In particular, relatively little is known about the physiological role of starch in the SNF process despite several observations made on its accumulation in root nodules. The importance and regulation of nodule starch metabolism both under normal and stress conditions is still unclear, but seems to differ significantly from one legume species to another (Chapter 5, section 5.1.2 and references therein). Almost nothing is known to date about the metabolism of root nodule starch in the two model legumes *L. japonicus* and *M. truncatula*. Firstly, identification of the enzymes involved in this metabolism is needed. Secondly, the role of nodule starch metabolism in the SNF process in *L. japonicus* and other legume species, both under normal and stress conditions need to be established.

The functional characterisation I carried out on the starch metabolism mutants of *L. japonicus* identified LjPGM1 and LjGWD1 as two important enzymes for the synthesis and degradation of starch in *L. japonicus* leaves. Since analysis of the nodule starch content of the *pgm1-4* and *gwd1-2*/*gwd1-3* mutants revealed a clear nodule starch-free and starch-excess phenotype, respectively, I tested the hypothesis that the inability to synthesize starch or to degrade it in root nodules could lead to impaired nodule function and to a decrease in SNF efficiency. Acetylene reduction assays revealed no statistically significant difference in the capacity to reduce acetylene into ethylene between the starch-free *pgm1-4* mutants and the WT segregants. Similarly, measurements done on the nodules of *gwd1-2*/*gwd1-3* mutant plants that were strongly impaired in their capacity to degrade starch revealed they were able to fix nitrogen. Taken together, these data indicate that starch storage and normal starch metabolism are not essential for nodule function under the growth conditions used. In case of the nodules of *gwd1-2/gwd1-3* mutants, the N2 fixation was found strongly reduced for two of the three batches of plants analysed, however, because of the poor growth of the plants, it is not possible to say whether this is a root starch nodule-specific effect, or an effect of poor C supply from the plant to the nodule and organic N utilisation in the plant as a whole that could be dependant on the plant genotype/growth conditions. In the future, grafting experiments or RNA silencing of LjGWD1 by hairy root transformation could be performed to help determine to what extent high starch/low turnover in nodule does directly prevent N2 fixation.

The regulation of the supply of carbohydrate to the nodule and the metabolism of nodule starch may constitute an interesting area of research to explore further with respect to increasing the rate of SNF. The fact that non-functioning nodules of alfalfa (Chapter 5, section 5.1.2 and references therein) generally accumulate high levels of starch suggests two things. The first is that starch is normally being turned over in functioning nodules. The second is that the supply of carbon from the plant to the nodule is not tightly regulated nor is it dependent on a demand from the nodule. It remains to be determined, however, if such a model applies to all legume species, including *L. japonicus*. In this respect, it would be interesting to determine the main organs from which starch is remobilized to supply the nodule with carbon during the dark period in this species. More importantly, one needs to determine whether the limiting factor in SNF is the supply of carbon or the intrinsic metabolism of the nodule, as it has been established for soybean (Walsh et al., 1987). This may be tested in *L. japonicus* by measuring the SNF efficiency (nitrogenase activity) of root nodules fed with increased amount of carbon.

CHAPTER 6

Importance of starch for perenniality and re-growth in *Lotus*

The best way to have a good idea is to have a lot of ideas

Linus Pauling

CHAPTER 6: Importance of starch for perenniality and re-growth in *Lotus*

6.1. Introduction

6.1.1. Plant life form strategies and allocation of resources

Annual and perennial habits are two major strategies by which plants adapt to seasonal environmental changes (Hu et al., 2003). Meristem indeterminacy and programmed senescence have been suggested to be the two major determinants of perenniality (Chapter 1, section 1.10.2 and reference therein). More particularly, the regulation of the duration of flowering, the separation of reproductive development from whole-plant senescence, and the conservation of viable axillary meristems following flowering and seed setting represent key factors of perennial growth (Battey and Tooke, 2002; Munné-Bosh et al., 2008; Figure 39).

The partitioning of nutrient reserves may also be an important determinant of perenniality. Indeed, in contrast to annual plants that tend to remobilize all their resources during seed production, herbaceous perennials are believed to split their resources between sexual reproduction (flowering and seed setting) and storage in persistent organs (e.g. root, bulbs, rhizomes, stolons, or tubers) to sustain the vegetative re-growth and reproduction the following season (Figure 39). The partitioning of carbon and nitrogen resources, in particular, are expected to play an important role in this process, In support of this hypothesis, starch content in roots was found to be higher in perennial than in annual cotton (*Gossypium hirsutum L.*; De Souza and Da Silv, 1987). Interestingly as well, resprouting shrubs accumulated more root starch than 'obligate seeding' shrubs (plants killed by fire) in fire-prone environments (Knox and Clarke, 2005). However, whether perennials across species and plant families generally store more carbon as starch below ground than their annual counterparts remains to be investigated.

So far, most experiments on the importance of root N and C reserves for re-growth vigour in perennial species have been carried out in alfalfa (*Medicago sativa L.*), and in response to defoliation. Some contradictory results between these studies and their interpretations render it difficult to draw conclusions.

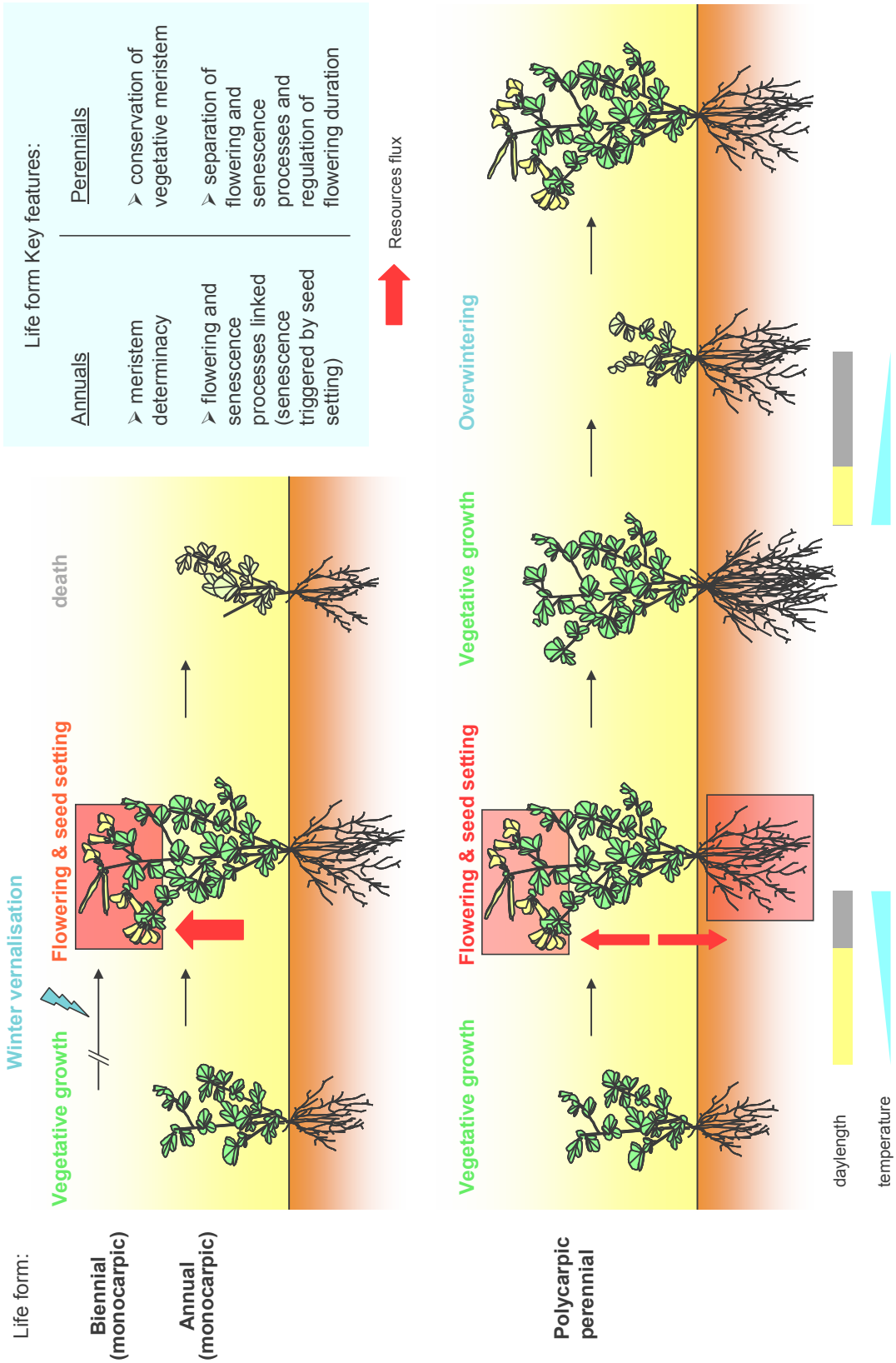

Figure 39. Proposed model of the partitioning of carbon resources in monocarpic annual/biennial and polycarpic perennial species.
Continued on next page.

Figure 39. Proposed model of the partitioning of carbon resources in monocarpic annual/biennial and polycarpic perennial species. Continued.
Meristem determinacy and the control of flowering time and senescence are key factors of the plant life form strategy. Monocarpic plants flowers, set seeds, and then die. With the exception of monocarpic perennials, these are short lived. In contrast in polycarpic perennials, flowering and seed production occurs many times during their life and over many years, interspersed by period of vegetative growth. Notably, the regulation of the flowering duration is different between the two. Evidence suggests that the allocation of resources may also play an important role in assuring the success of the plant life form strategy. While resources are mostly directed toward to reproduction in annual species, part of them is also allocated to long-lived storage organs (e.g. roots) in perennials so as to assure the re-growth and reproduction of the plant the following season.

The fact that starch degradation increased while shoot re-growth resumed during spring in alfalfa (Volenec et al., 1991) suggests that root starch reserves may be important for re-growth. In addition, the accumulation, after autumn harvest(s), of N reserves (in the form of free amino acids and soluble proteins), of starch and of total non-structural carbohydrates in the roots was found to be positively correlated to spring re-growth vigour in field-grown alfalfa (Dhont et al., 2002 and 2006).

However, it was also found that shoot yield during re-growth in afalfa was higher in plants with the highest N content and lowest level of starch content in the roots (Ourry et al., 1994). The authors of this study concluded from this result that root N reserves are the major factor that initiates and sustains new shoot growth and that, in contrast, there is no direct relationship between starch accumulation in root tissues and shoot production during early re-growth. Similarly Boyce and Volenec (1992) and Frankauser and Volenec (1989) concluded from analyses done in alfalfa that root total non-structural carbohydrates may not be the major source of energy for shoot re-growth.

Besides, although the apparent decline in root N reserves is generally small compared with that of non-structural carbohydrate (Kim et al., 1993), several authors have suggested that the decline in root carbohydrates during shoot re-growth may be primarily due to the use of carbohydrates in the roots (Ta et al., 1990; Avice et al., 1996; Schnyder and De Visser, 1999). In a study by Avice et al. (1996), the flow of ^{15}N and ^{13}C from organs remaining after defoliation to regrowing tissues as well as ^{13}C losses through root and shoot respiration were assessed by pulse-chase labelling during re-growth in alfalfa. A total of 73% of labelled C and 34% of labelled N were remobilized in source organs within 30 days. Although all the ^{15}N from source organ was recovered in the re-growing tissue, much of the ^{13}C was lost, mainly as CO_2 respired from the root (61%). Likewise, C and N steady state labelling was performed to access the actual contribution of reserve-derived C and N to re-growth following defoliation in plants of perennial ryegrass (*Lolium perenne* L.; Schnyder and De Visser, 1999). It was concluded by the authors that carbohydrate reserves were an insignificant source of C for tiller growth although these carbohydrates may have contributed

indirectly to tiller re-growth via energy supply in shoot respiration and maintenance of root integrity and function.

In summary, although the re-growth of perennial plants after grazing, cutting-back or winter die-back must require a supply of carbon and nitrogen reserves for energy and biosynthesis until the photosynthetic capacity of the plant has been restored, direct evidence about the quantitative importance of the storage and remobilization of starch and other resources for the vegetative re-growth capacity and the perennial lifestyle are still lacking. An important approach to this problem, which has not been included in any studies so far, would be to include the analysis of mutants impaired in the accumulation and/or remobilization of root starch or nitrogen reserves. In addition, little use has been made so far of natural variation. At best, natural variant analyses in alfalfa have involved only two different cultivars (Dhont et al., 2002 and 2006). Therefore, it is still not clear to what extent the mobilisation and flux of C and N reserves from storage organs to the new shoot are controlling its re-growth capacity and vigour in perennial plants following either overwintering or enforced re-growth.

6.1.2. Importance of the perenniality trait in agriculture: perennial to annuals, and now back to perennials?

The world's terrestrial biomes are primarily made up of a mixture of perennial plants. In contrast, more than two-thirds of the land covered by crops consists of monocultures of annual species (Cox et al., 2006). This is the result of intense and long term selection for high yielding crops, favouring annual species (with an increased allocation of photoassimilates to seeds) over their relatively low-seed yielding perennial counterparts. However, with longer growing seasons, more extensive root systems (Figure 40), better access to resources, and more conservative use of nutrients, perennial plants display many desired characteristics. They have a higher efficiency in water management and nutrient-use and provide more protection against soil erosion than annual crops. They also yield more biomass above-ground, store more carbon below-ground, and are in general more resistant to biotic and abiotic stresses than their annual relatives (Cox et al., 2006; Glover, 2005 and 2007). In addition, perennial crops are expected to be less detrimentally affected by climate change (Brown et al., 2000; Glover et al., 2007) and their net values for global warming potential are negative while those for annual crops are positive. Hence, through a greater carbon storage, lower need for applied chemicals, and the possibility to grow them on marginal lands that do not support the long term use of annual crops because of severe erosion risk, perennial species offer the opportunity of a more sustainable agriculture system

(Cassman et al., 2003; Glover et al., 2010). For these reasons, perennial crops are currently attracting attention from researchers and breeders.

Figure 40. Illustration of the annual versus perennial strategy.
From Cox et al. (2006). Root system of an annual wheat (on the left in each panel) and its wild perennial relative, intermediate wheatgrass (Thinopyrum intermedium; on the right in each panel) at four times of the year. The longer growing season, and consequently the greater access to resources of the perennial variety, results in a greater below- and above-ground biomass production than in its annual counterpart, which tends to give higher seed yield in a single year.

Breeding programs aiming at developing perennial grain crops have been initiated in several species including wheat, wheatgrass, sorghum, rice, and sunflower. Some of the grain crops – including rye, sorghum, and rice – can be hybridized with close perennial relatives to attempt to transfer the pool of genes able to confer the perenniality trait into annual, cultivated species. However, in other crops such as wheat, maize, soybean, and sunflower, hybridization with more distantly related perennial species is required. Lastly, some perennial species with relatively high grain yield are candidates for direct domestication. This includes wheatgrass (*Thinopyrum intermedium*), Wildrye (*Leymus racemosus*), Maximilian sunflower (*Helianthus maximiliani*), and Indian ricegrass (*Oryzopsis hymenoides*). Programs on these perennial crops aim at developing new cultivars able to produce high seed yields (Cox et al., 2002). Indeed, the major drawback of perennials is their inability to yield as much seed as annual varieties. This may be because carbohydrates produced by the plant are needed by the root system to survive the dormant period in perennials while they normally end up in the grain in annuals. Therefore, the first

challenge for plant breeding consists of allocating more carbon to grain production. A major difficulty, however, resides in the fact that the perenniality trait is expected to be multigenic and to involve complex interactions with the environment. Annuality and perenniality, indeed, have been proposed to be quantitative traits (Thomas et al., 2000). Evidence for this comes from studies of crosses between annuals and perennials. In all the species studied to date (e.g. rye, triticale, sorghum, maize and soybean), it is generally observed that plants derived from inter-specific hybrids tend to be perennial only if 50% or more of their genes are inherited from a perennial parent (Cox et al., 2002). This, along with a lack of success so far in introducing a single gene or chromosome conditioning perenniality into an annual crop genotype, attests to the complexity of the trait and suggests that perenniality is likely to be governed by multiple loci. However, one exception to this can be found in the literature: a single chromosome addition from a perennial wheat species was able to confer a polycarpic, perennial growth habit to an annual wheat relative (Lammer et al., 2004). More recent evidence suggests that the life form could be determined by a small number of genes as mentioned earlier (Chapter 1, section 1.10.2).

As discussed above, breeding programs have thus far mainly concentrated on developing perennial grain crops in grass varieties. However, perennial grasses such as *Miscanthus* and switchgrass are also of great interest as feedstocks for the production of biofuels. Further, because of their ability to perform symbiotic nitrogen fixation and their conservative growth strategy, perennial legume grain and forage crops such as chickpea and alfalfa also offer the opportunity to develop more sustainable agricultural systems. They are of current and potential agronomic importance for forage, grain production and the production of biofuels.

6.1.3. Aims and Approaches

The genus *Lotus* comprises both annual and perennial species, several of which are cultivated for forage (e.g. *L. corniculatus*, *L. glaber* and *L. uliginosus*). These species are similar in structure and growth characteristics to more important forage legumes such as alfalfa and clover. Recent development of genetic and genomic tools in the perennial legume *L. japonicus* allows the study of the importance of carbon allocation to vegetative re-growth and the perenniality trait. Almost nothing is known thus far about the importance of carbon reserves in perenniality and vegetative re-growth. The capacity for vigorous re-growth represents a key trait for the use of perennial plant species as forage crops. The collection of starch metabolism mutants of *L. japonicus* presented in the previous chapters provides an ideal resource for testing the hypothesis that starch storage in the roots is important for vegetative re-growth in perennial species. If root starch turnover is indeed necessary and limiting, re-growth in crops may be improved by manipulating this process.

In this chapter, I describe the use of both natural and induced genetic variation to investigate the role of root starch accumulation and remobilization for vegetative re-growth and perenniality in the genus *Lotus*. In a first series of experiments, I used the collection of starch metabolism mutants of the perennial species *L. japonicus* - the isolation and characterisation of which has been presented in the previous chapters - to explore the importance of starch for the capacity of the plant to re-grow after cutting-back. I show that, although mutants of *L. japonicus* with strongly altered root starch content grow relatively normally prior to cutting-back, they are impaired in their capacity to regenerate after a harvest in which the photosynthetic parts of the plant are removed. In a second set of analyses, I explored the hypothesis that root starch content may play an important role both for re-growth vigour and the perenniality trait using a collection of perennial and annual species of *Lotus*. Results of this analysis revealed a good correlation between their root starch content and their ability to re-grow post cutting-back. The significance of this finding in term of potential agricultural applications is also discussed.

6.2. Results

6.2.1. Mutants of *L. japonicus* with altered root starch content are impaired in their ability to re-grow following cutting-back

As mentioned earlier, perenniality in plants refers to the capacity of the plants to persist across seasons and over several years. In herbaceous perennial plant species such as *L. japonicus*, this generally involves the ability of the plants to grow back following overwintering. Given the difficulty of studying such phenomenon and the relatively short time frame of this study, I chose instead to study the enforced re-growth capacity of the plants and developed an assay in which the vegetative re-growth of *L. japonicus* plants was monitored after cutting-back all the leafy shoots at the base of their stems. Hence, the term 're-growth capacity' and 're-growth vigour' mentioned later on in this chapter refer to the capacity and vigour of the plant to regenerate after a harvest in which all the photosynthetic parts of the plants are removed. Such analyses are referred to as cutting-back experiments elsewhere in the text. As well as mimicking grazing, I reasoned that this experiment would be a good indicator of the perennial status and capacity of the plant to re-grow following overwintering. Such cutting-back experiments were carried out on several of the starch metabolism mutants of *L. japonicus* whose isolation and characterisation have been described in the previous chapters (Chapter 4 and Chapter5).

One of these mutants, the *pgm1-4* mutant does not accumulate any starch in any of its organs and tissues (Chapter 4, Figure 20; Chapter 5, Figure 35). I hypothesized that, if carbon allocation - and in particular starch accumulation - is indeed important for re-growth in *L. japonicus*, this starch-free mutant would be expected to struggle to re-grow following cutting-back. Similarly, starch excess mutants deficient in starch degradation in roots would also be expected to struggle to re-grow because of their inability to remobilise the carbon stored as starch. In contrast, the *pgi* mutant that displays a starch-free phenotype in leaves but still accumulates starch in its root system may be expected to re-grow normally. To test these hypotheses, I first carried out a preliminary analysis with plants of the *pgm1-4* and *pgi1-1* mutants and the two WT accessions Gifu and MG-20. Importantly, and as presented earlier (Chapter 4, section 5.2.2), neither the *pgm1-4* nor the *pgi1-1* mutant plants displayed any impairment in growth under normal conditions. Under enforced vegetative re-growth, however, the starch-free *pgm* mutant was severely impaired in its ability to re-grow in comparison to the *pgi* mutant and the WTs (Figure 41), suggesting that root starch storage and remobilisation may play an important role in vegetative re-growth.

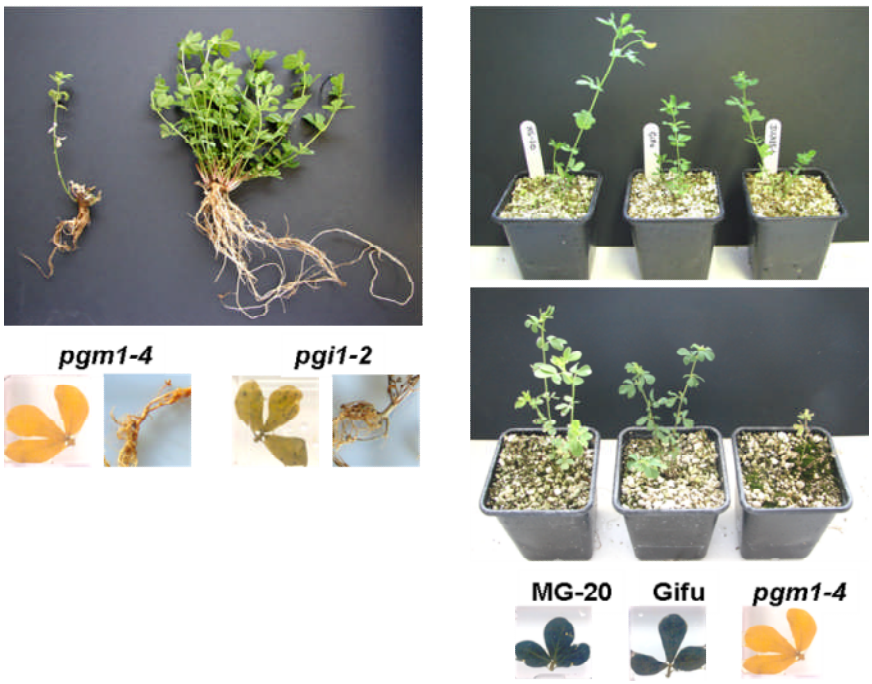

Figure 41. Pilot cutting-back experiments performed on the *L. japonicus* starch mutants *pgm1-4* and *pgi1-2*.
A. Results of cutting-back experiment performed on four month old mutant plants (B1F3 generation) of the mutant lines *pgm1-4* and *pgi1-2*. Plants were grown under long day conditions in a greenhouse supplemented with artificial light. Pictures of the plants were taken ca. 6 weeks post cutting. Root and shoot samples of plants carrying the mutant alleles stained with iodine are displayed on the bottom panels. **B**. Cutting-back experiment performed on the *pgm1-4* mutants (B1F3 generation) in comparison to the MG-20 and Gifu wild-types. Cutting-back was performed on three month old plants grown in a greenhouse under natural light conditions between April and August 2007. A representative biological replicate of each genotype photographed prior to cutting (top panel) and ca. six weeks post cutting (middle panel). On the bottom panel is shown the results of iodine staining of the leaves of each genotype.

To further explore this finding, and discover whether the starch stored in roots is not only necessary but also limiting as a source of carbon supply during re-growth, several cutting-back experiments were performed on larger populations of mutant and WT segregants of multiple mutant alleles of the *PGM1* gene as well as mutants of several other starch metabolism genes that displayed variation in the degree of alteration of their starch content. The starch synthesis and degradation mutant alleles used for these cutting-back experiments were *pgi1-1, pgm1-1, pgm1-3, pgm1-4, pgm1-5, aps1-1, apl1-1, gwd1-1,* and *gwd3-1*. Unless otherwise indicated, these experiments were carried out on homozygous mutants, WT, and heterozygous segregants of F2 segregating populations. Homozygous mutants, heterozygous and homozygous WT plants were identified among the segregating population by genotyping individual plants (either by sequencing or restriction analysis) as described in Chapter 2, section 2.6.7. Some pilot cutting-back experiments were also performed on plants of the generation F3. However, cases of hybrid vigour/heterosis with randomly segregated, significant effects on their root and shoot biomass as well as starch content could be observed in the progeny of outcrosses between Gifu (mutants were isolated in this background) and MG-20. Hence, segregants from an F2 population were analysed in most subsequent experiments in order to minimise this issue. Unless otherwise indicated, cutting-back was performed on mature plants ca. 4-5 months old that were flowering and setting seeds. Plants were cut at about 2 cm from above the base of the stem and the shoot fresh weight measured. Following cutting-back, shoots of the cut plants were allow to re-grow for ca. 6 to 7 weeks and fresh weight was measured again. Some root fresh weight measurements and iodine staining were also performed before and after cutting-back. Details on the protocol employed for these experiments are given in Chapter 2, section 2.2.

The results of this experiment showed that some of mutants had a strongly-reduced capacity for re-growth following cutting-back (Figure 42). More particularly, statistically significant differences in re-growth ratio (fresh weight of the new growth divided by the FW of the initial growth, i.e. the shoots of mature plants measured just prior cutting-back) could be observed between the *pgm1-4, pgm1-3*, *pgm1-5, aps1-1* mutants and their WT segregants. In addition, the heterozygotes of the mutant line *pgm1-4* also displayed a reduced re-growth capacity in comparison to the WT segregants. Hence, an overall correlation was found between the lower amount of starch in the roots of the mutant plants and their reduced capacity and vigour to re-growth in comparison to the WTs. Further, it is interesting to note that significant difference in re-growth ratio was also observed between plants of the WT accessions MG-20 and Gifu which also presented a clear difference in their root starch content before cutting according to the results of iodine staining (Figure 42). More particularly, and in agreement with the results presented above for the mutant lines, their amount of root starch positively correlated with their extent of re-growth.

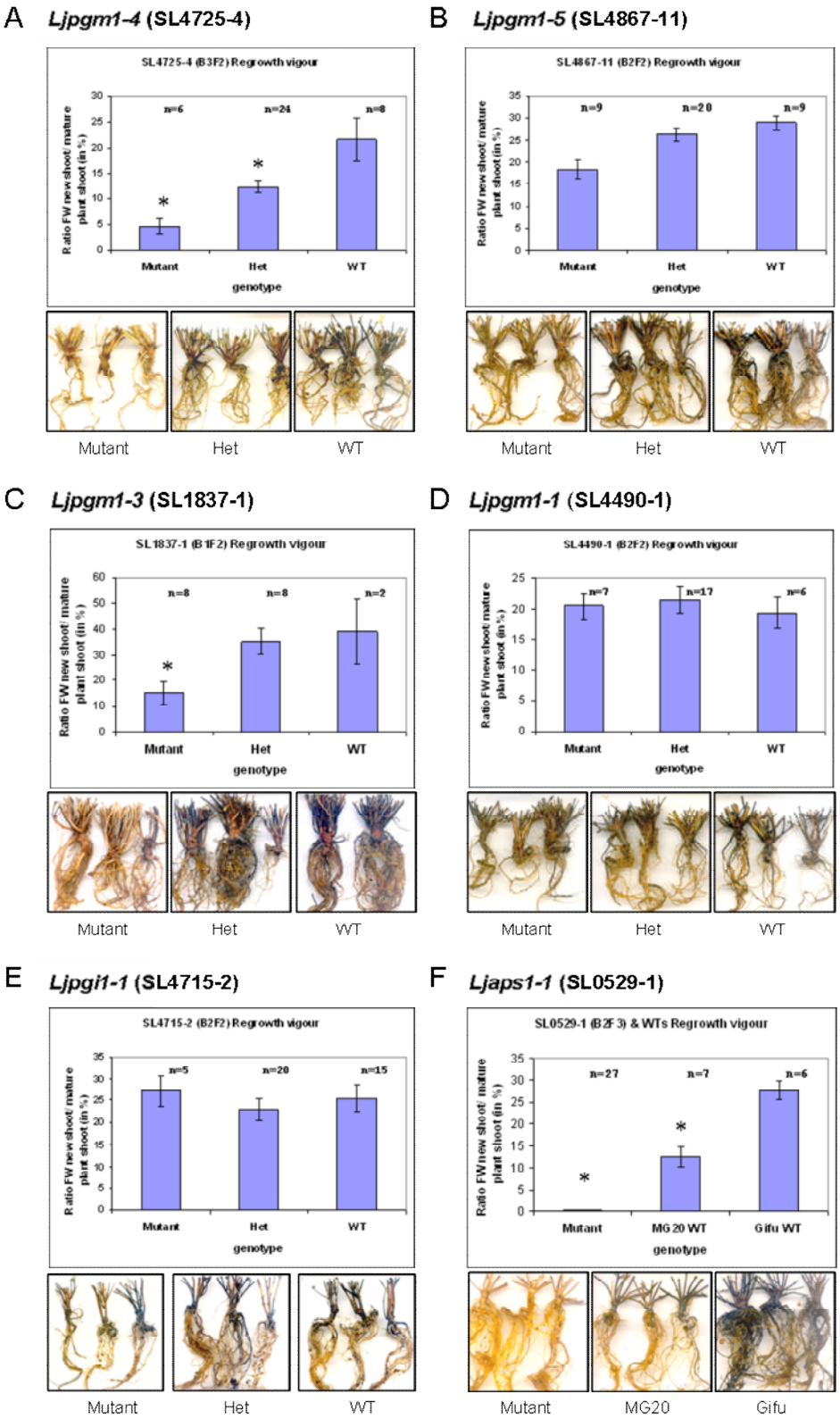

Figure 42. Cutting -back experiment performed on the collection of *L. japonicus* starch metabolism mutants.
Continued on next page.

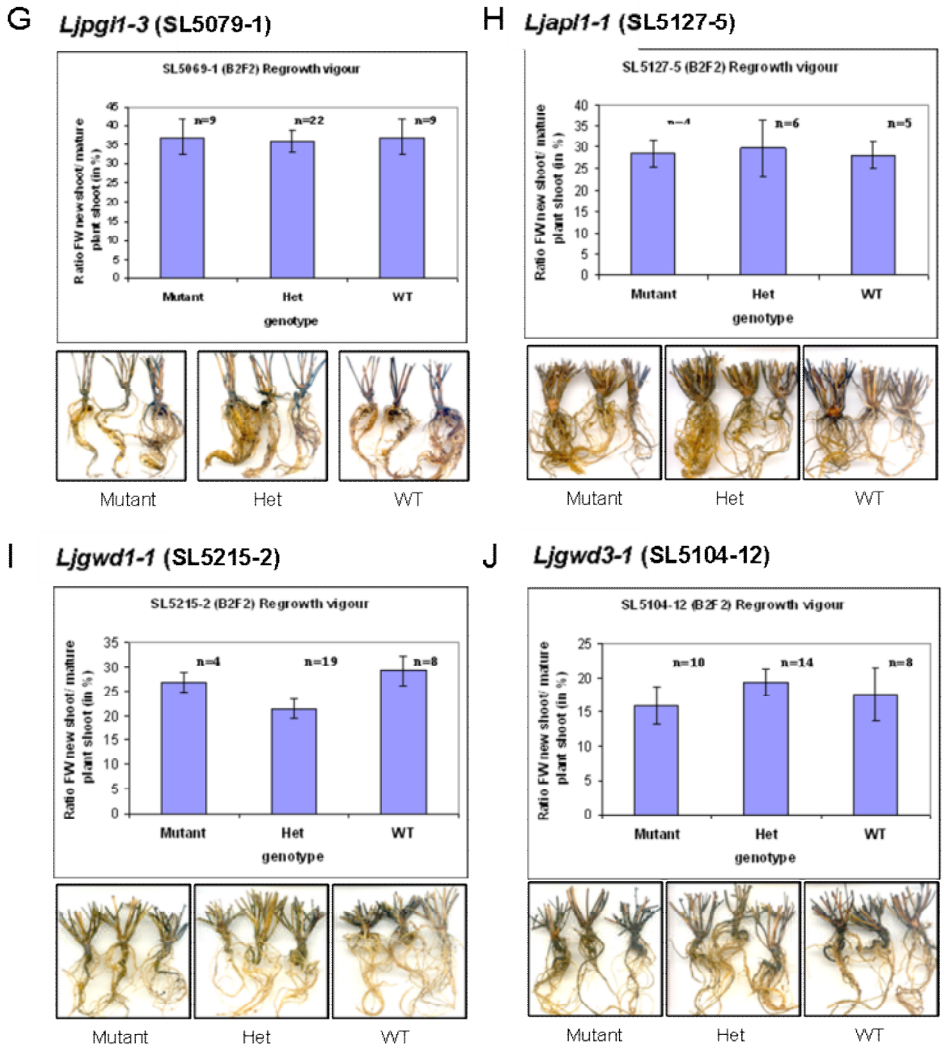

Figure 42. Cutting -back experiment performed on the collection of *L. japonicus* starch metabolism mutants. Continued.
Root starch content and re-growth vigour were examined in a set of starch synthesis (**A-H**) and degradation (**I, J**) mutants of *Lotus japonicus*. Plants of the mutant lines *pgm1-4, pgm1-5, pgm1-1, aps1-1, gwd1-1*, and *gwd1-3* were grown in a greenhouse from December until May 2008, supplemented with artificial light until April, and were 4 to 5 months old at the time of cutting. Plants of the mutant lines *pgi1-1* and *pgi1-3* that were ca. 4 months old at the time of cutting were grown under natural light conditions (from April until August 2008). Plants of the two lines *pgm1-3* and *apl1-1* were also grown in a greenhouse under natural light conditions and were ca. 10 months old at the time of cutting. Re-growth biomass measurements were performed 6 weeks post cutting. The re-growth ratio (in %) is defined as the fresh weight (FW) of the new growth (i.e. new shoot including stems and leaves) divided by the FW of the shoot of mature plants measured just prior cutting. The values given are mean values +/- standard error of mean. Student's t tests (95% confidence interval) were performed that revealed statistically significant difference (marked by an asterisk) of re-growth ratio between the *pgm1-4, pgm1-3*, *pgm1-5* mutants and their WT segregants. Difference of re-growth ratio was also statistically significant between the *aps1-1* mutants and the WT MG-20 and Gifu plants, and between plants of these two WT accessions. Root and stem base starch contents were visualised by iodine staining 6 weeks post cutting, with the exception of *aps1-1* mutants and the WT MG-20 and Gifu whose root starch content were examined at the time of cutting (harvesting at the end of the day from biological replicates that were representative of the whole set in term of re-growth vigour). A net reduction in the root starch content in the mutants compared to the heterozygotes and WTs can be observed for plant carrying the mutant alleles *pgm1-4, pgm1-3, aps1-1*, and to a lesser extent, *pgm1-5*. For all mutant lines, the analysis was performed on mutants, heterozygotes (abbreviated 'Het' on the figure), and WT segregants of a F2 population, with the exception of *aps1-1* for which F3 mutants were compared to plants of the two WT accessions MG20 and Gifu. Further, plants of all the genotypes analysed were from a second cross of the mutant in Gifu background with MG-20, except for plants of the mutant lines *pgm1-4* and *pgm1-3* which were at the B3 and B1 backcrossing stage, respectively.

It should be mentioned here that when this experiment was repeated under other growth conditions, the roots of the *aps1-1* mutant plants were not starch-free according to the results of iodine staining (instead, their root starch content phenotype was similar to that of the *pgm1-5* mutant), and consistently, their re-growth capacity was much less impaired (data not shown). Concerning the other mutants analysed, including the starch degradation mutants *gwd1-1* and *gwd3-1*, neither any root starch excess/reduced starch phenotypes nor any significant impairment in the vegetative re-growth capacity of the mutants were observed in comparison to their heterozygous and WT segregants.

The re-growth vigour of the *pgm1-4* mutant and heterozygote in comparison to their WT segregants was analysed in more detail in relation to their starch content and PGM1 enzyme activity. Interestingly, an intermediate phenotype (case of incomplete dominance) between the *pgm1-4* mutants and the PGM1-4 WT could be seen for the *pgm1-4*/PGM1-4 heterozygote, in terms of re-growth vigour (measured as a ratio of the fresh weight of shoot prior and post cutting-back), leaf starch content, and enzyme activity (Figure 43). Leaf rather than root starch contents were measured for this analysis, however, the results of iodine staining across all the organs of these plants strongly suggest that the same is true for roots (i.e. intermediate content of starch in the root of the heterozygous plants in comparison to its mutant and WT segregants).

Overall, the results of all these analyses revealed a good correlation between root starch content and vegetative re-growth capacity and vigour. It must been noted, however, that when the cutting-back experiment was repeated in other greenhouses with different lighting systems and light quality, and/or at other times of the year, the effect of the lack of root starch on re-growth was much less clear (data not shown). Use of different greenhouses and growth conditions from one experiment to another were mostly dictated by issue of availability of space for plant growth. The clearest correlations between root starch content and re-growth vigour were observed when the plants were grown in a greenhouse supplemented with artificial lighting to give a photoperiod of ca.. 16 h (see Chapter 2, section 2.1.3 for more details). Under these growth conditions, *Lotus japonicus* plants produced more shoot and root biomass, and flowered later than when grown under natural, long day conditions.

Lastly, the developmental stage of the plants seemed to be important. All experiments mentioned above were performed on mature plants that were ca 4-5 months old. However, pilot experiments were also performed on younger plants for several of the mutant lines (*pgm1-1, pgm1-3, pgm1-4, pgm1-5, aps1-1, apl1-1, gwd1-1,* and *gwd3-1*). Interestingly, no clear impairment in re-growth was seen for the mutants versus their WT segregants when the experiment was performed on younger plants (ca 2 months old) that had not yet or only just started to flower, and had not yet set seeds (data not shown).

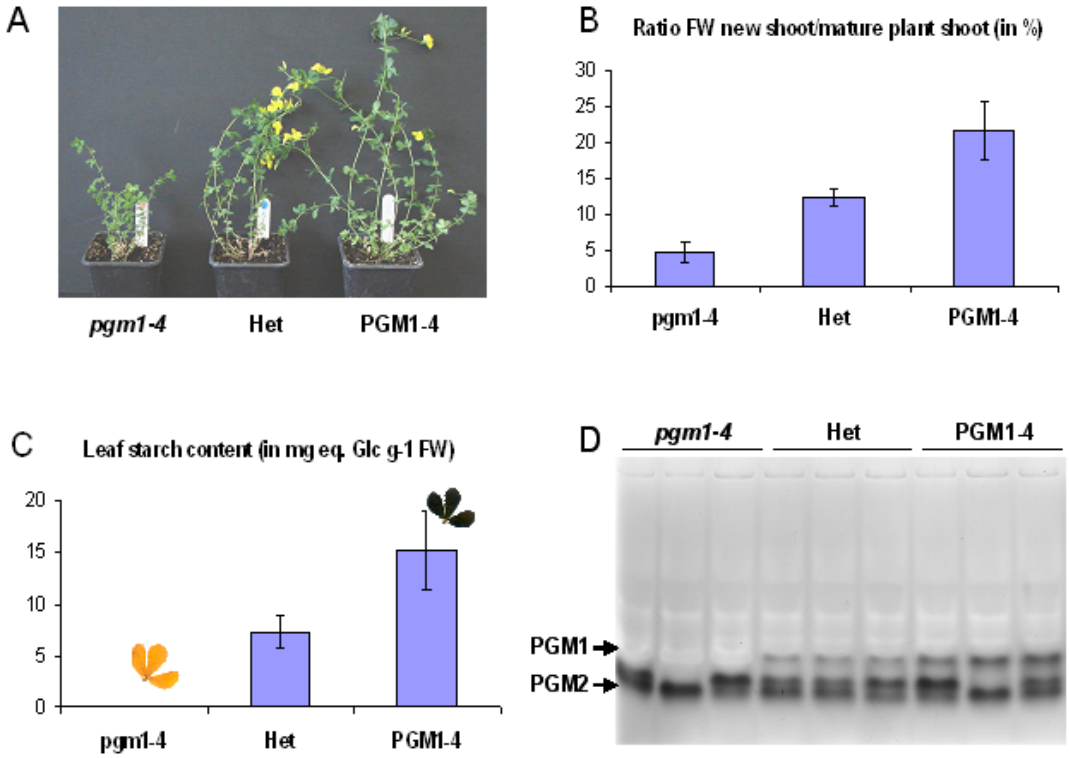

Figure 43. Correlation between re-growth vigour following cutting-back, starch content, and enzyme activity for the mutant line *pgm1-4*.
Cutting-back experiment was carried out as described in the legend of Figure 42. **A**. Phenotype of the *pgm1-4* mutant, heterozygous and WT segregants (only one individual representative of the one of at least 6 biological replicates for each genotype is shown here) during re-growth, ca. six weeks post cutting. **B**. Re-growth biomass measurement and ratio of re-growth as defined in the legend of Figure 42. **C**. Leaf starch content (in mg. eq. glucose per g of fresh weight) and **D**. Native PAGE of PGM1 (plastidial PGM isoform) and PGM2 (cysosolic PGM isoform) activity in leaves of the mutant, heterozygote, and WT of *pgm1-4*. Notes that a clear, positive correlation is observed between the PGM1 enzyme activity, the starch content, and the re-growth vigour across the three genotypes, with the heterozygotes displaying an intermediate phenotype between those of wild types and homozygous mutants. Interestingly, a difference in migration could be seen for the PGM2 isozyme (two lowest bands) between the wild-type MG-20 and Gifu that segregated in the progeny from a cross between the two accessions as illustrated in D.

6.2.2. Re-growth vigour positively correlates with root starch content in natural genetic variants of *Lotus*

The results presented above indicated that the capacity of the plant to store and remobilize its carbon stored as starch in the roots may determine its vegetative re-growth vigour following cutting-back. If starch stored in roots indeed plays an important role for re-growth vigour and the perenniality trait, I hypothesized that a good correlation would exist between the root starch content of perennial species of *Lotus* and their capacity for re-growth post cutting-back. In addition, since resources in annual species are mostly directed to reproduction while they are also directed to storage organs in perennials, perennial species would be expected to store more starch below ground than their annual counterparts. Lastly,

I hypothesized that if re-growth capacity following cutting-back was indeed a good indicator of the perenniality trait (i.e. seasonal re-growth), annual species would not be expected to re-grow following cutting-back, while perennials would.

In order to test these hypotheses, I established and used a unique collection of annual and perennial *Lotus* species (Table 1 and Table 19). This collection consisted of 14 and 10 species recorded as annuals and perennials, respectively, in the USDA plant database (GRIN NPGS, http://www.ars-grin.gov/npgs/). Apart from the recorded growth habit of the accessions, other criteria including the phenotype, geoclimatic origin, and the phylogenetic relationship of the accessions (Table 19 and Figure 44) were also taken into account so as to generate a collection of natural variants with a high level of polymorphism. I rationalized there would be a high chance that large variations in both root starch content and re-growth vigour would exist among the species in such a collection. Cultivated species of *Lotus* were also added to this suite of natural variants. Lastly, MG-20 and Gifu, the two most used accessions for research in *L. japonicus,* were also included in this collection.

These plant species/accessions were submitted to phenotypic and physiological analyses that included records on shoot and root height/length and biomass, taproot morphology, length and diameter, extent of nodulation, flowering time and senescence as well as leaf, stem, and root starch content estimation by iodine staining. Two sets of annual and perennial species of *Lotus* were analysed. The first set that comprised the species *L. arabicus, L burtii, L. corniculatus var. corniculatus, L. edulis, L. glinoides, L. ornithopodioides, L. parviflorus, L. peregrinus, L. subbiflorus, L. tenuis,* and *L. uliginosus* was grown from November until March in a greenhouse supplemented with artificial light to give a light period of approximately 16 h ((see Chapter 2, section 2.1.3 for more details). The second set of *Lotus* species, that included the species *L. collinus, L. conimbricensis, L. denticulatus, L. gebelia, L. halophilus, L. mearnsii, L. palustris, L. unifoliolatus,* and *L. weilleri* were grown in a greenhouse under natural light from May until September. *L. japonicus* MG-20 and Gifu were grown in both sets.

Phenotypic analysis of the different *Lotus* species indicated that several of them (in particular *L. parviflorus, L subbiflorus, L. glinoides,* and *L. unifoliolatus*) may have been misclassified with regard to their growth habit (i.e. annual versus perennial). This is entirely possible as the information on the species growth habit (aka life form) entered into GRIN is generally based on the literature available for the species rather than from experimental determination (personal communication from Stephanie Greene, USDA-GRIN germplasm curator of the *Lotus* collection since 1995). Besides, it is believed that perennial and annual habits can be different not only from one species to another within a genus, but also from one ecotype/cultivar to another within a species (personal communication from Stephanie Greene, USDA-GRIN). Hence, mis-annotations may have occurred. I therefore undertook

the experimental determination of the growth habit of all these species. For this analysis, plants (at least five biological replicates of each genotype) were grown for ca. nine months during which they were subjected to a winter period. Following this, plants that had died versus those that were still alive and produced new basal branches were recorded. Since some of the species did not flower and/or set seeds, the life form could not be attributed with certainty to all of them. Nevertheless, this experimental testing clearly confirmed some cases of wrong assignment of the growth habit of the species given by the USDA database. A new, most likely correct classification is presented in Table 19. Further analysis and interpretation of the results were carried out following this new classification.

Cutting-back experiments on the *Lotus* plant species were performed on ca. 3 month old plants. Surprisingly, all *Lotus* species, both annual and perennial, were able to re-grow at first (emergence of few leaves after only a couple of days post cutting-back) but this new shoot growth stopped after a few days and eventually dried out and died for some of the species. After about two weeks post cutting-back, large differences in re-growth vigour were visible among the species (Figure 45). The results of root starch staining with iodine prior to cutting-back and of shoot biomass measurement revealed a clear, positive correlation between the amount of starch stored in the roots and the re-growth vigour (ratio of FW of the new shoot/FW mature plant shoot expressed in %). On average, the re-growth ratios 15 days post cutting-back of the annual species were 2.42 and 0.41 for the first and second set of the species analysed respectively, versus 10.62 and 8.61 for the perennial species.

A clear correlation was also observed between the growth habit on one side, and the root starch content and re-growth vigour following cutting-back on the other. Perennial species generally had both higher root starch content and higher re-growth vigour than their annual counterparts (Figure 45). A trend toward a higher root to shoot biomass ratio in the perennial versus the annual species was also observed (Table A6). Apart from this, no clear differences between the annual and perennial species were observed for any of the other parameters measured/calculated that included the fresh weight and height/length of the shoots and roots of the species as well as their specific root length (SRL; Table A6).

Root starch staining 15 days post cutting-back showed that a significant amount of starch had been remobilized during re-growth in most of the species although careful examination of the results revealed that some of the species had remobilized a larger amount of their root starch during re-growth than others (e.g. *L. burtii* compared to *L. glinoides*). Overall, a good correlation could be seen between the amount of starch remobilized in the species and their re-growth vigour (Figure 45A). Hence, not only initial root starch content but also the ability of the plant to remobilize it may be important for determining the re-growth vigour. This reduction of root starch (estimated by iodine staining) was also accompanied by a net reduction of the root biomass for most species (visible on Figure 45A).

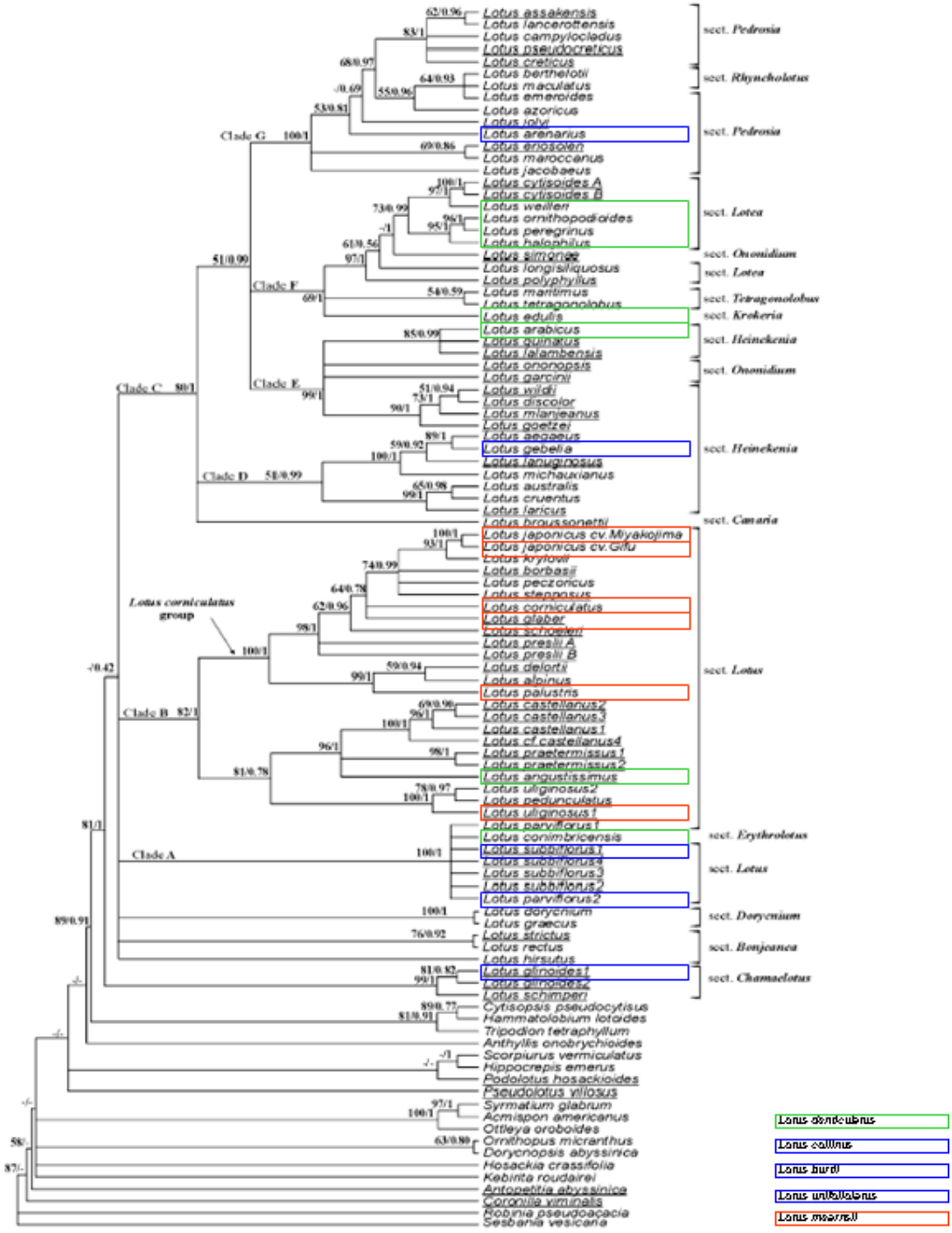

Figure 44. Phylogenetic relationship of the species of the genus *Lotus* and their life form.
Modified from Degtjareva *et al.* (2006). *Lotus* species that were analysed in this study are framed. Annual species are framed in green, perennial in red, and species for which the life form is uncertain are in blue. Species included in my collection but not included in the phylogenetic analysis of Degtjareva *et al.* (2006) are mentioned on the left bottom of the Figure. The annual and perennial species are largely intermixed, suggesting that the switch of one life form to another may not require major genetic changes.

Scientific name and synonyms	Common name	Comment	Clastidic group	USDA ID	Origin (collection place)	USDA Life form	Curated Life form	Analysed set
Lotus angustissimus	Slender Bird's-foot-trefoil		OW	PI 368894	Israel	annual	annual	2
Lotus arabicus			OW	PI 214109	Spain (?)	annual	annual	1
Lotus arenarius			OW	PI 319020	Spain (cadiz)	annual	perennial?	2
Lotus burtii			OW	n/a	Pakistan (?)	perennial	annual?	1
Lotus collinus			OW	PI 641351	Morocco (Oujda)	annual	perennial	2
Lotus conimbricensis			OW	PI 308033	Solvakia (Pruhonice)	annual	annual?	2
Lotus corniculatus var. corniculatus (aka L. filicaulis)	Common Bird's-foot-trefoil	Agriculturally important	OW	PI 464684	Turkey (Ankara)	perennial	perennial	1
Lotus denticulatus	Riverbar Bird's-foot-trefoil		NW	PI 236862	Canada (british Columbia)	annual	annual	2
Lotus edulis		Edible seedpods	OW	PI 244281	Spain (?)	annual	annual	1
Lotus gebelia			OW	PI 464824	Turkey (Agri)	perennial	annual?	2
Lotus glinoides			OW	PI 246736	Spain	annual	perennial	1
Lotus halophilus (aka L. pusillus)	Greater Bird's-foot-trefoil		OW	PI 300237	Greece (Crete)	annual	annual	2
Lotus japonicus, ecotype B-129 (aka Gifu)			OW	n/a	Japan (Gifu)	perennial	perennial	1,2
Lotus japonicus, ecotype MG-20 (aka Miyakogusa)			OW	n/a	Japan (Miyakojima)	perennial	perennial	1,2
Lotus mearnsii	Mearns' Bird's-foot-trefoil		NW	PI 226275	United States (?)	perennial	perennial	2
Lotus ornithopodioides	Southern Bird's-foot-trefoil		OW	PI 442514	Belgium (Antwerp)	annual	annual	1
Lotus palustris (aka L. lamprocarpus)			OW	PI 311427	Spain (?)	perennial	perennial	2
Lotus parviflorus (aka L. hispidus)	Small flower Bird's-foot-trefoil		OW	PI 415815	Portugal	annual	perennial	1
Lotus peregrinus (aka L. carmeli)			OW	PI 368905	Israel (Ahiturd)	annual	annual	1
Lotus subbiflorus (aka L. hispidus)	Hairy Bird's-foot-trefoil	Agriculturally important	OW	PI 631785	Morocco (khemisset)	annual	perennial	1
Lotus tenuis (aka L. glaber)	Narrow-leaf Bird's-foot-trefoil	Agriculturally important	OW	PI 302922	Spain (?)	perennial	perennial	1
Lotus uliginosus (aka L. pedunculatus)	Big trefoil/Greater Bird's-foot-trefoil	Agriculturally important	OW	W6 20479	United States (Washington)	perennial	perennial	1
Lotus unifoliolatus (aka L. purshianus; L. americanus)	American Bird's-foot-trefoil		NW	PI 338644	United States (?)	perennial	annual	2
Lotus weilleri			OW	PI 196332	Morocco (?)	annual	annual	2

Table 19. List of natural variants of the genus *Lotus* analysed in this study. Continued on next page.

Table 19. List of natural variants of the genus *Lotus* analysed in this study. Continued.
Seeds of all the annual and perennial species analysed in this study were ordered from the USDA GRIN germaplasm with the exception of *L. burtii* and *L.japonicus* ecotypes Gifu and MG-20 which were from the JIC seed store (Zopra dababase). The Clastidic group designed 'OW' refers to Old World species, and 'NW' are New World species as determined in Arambarri et al., 2000a and 2000b. The 'UDSA life form' is the life form of the species according to the UDSA database (not experimentally determined). The 'curated Life form' correspond to a consensus of its experimental determination and on information from several plant species databases. The life form was experimentally tested by recoding the phenotype (i.e. senescence/death and capacity to keep producing new tillers) of the *Lotus* species grown in glasshouses over a period of at least nine months. Seeds of the *Lotus* species were sown in November 2007 for the first set analysed, and in May 2008 for the second set analysed.

A relatively important variation between species was also observed in the extent to which starch had disappeared and from which part of the root it had disappeared. For instance, in species such as *L. peregrinus*, *L. ornithopodioides*, and *L. edulis*, a clear reduction of starch content in the crown root and stem base could be seen between prior and two weeks post cutting. In contrast, a clear reduction in starch content in *L. glinoides* and *L. parviflorus* was visible in secondary roots, but not in the crown root and stem base. The re-growth vigour appeared to correlate better with the amount of starch present in secondary roots (and stolon-like structures as well, e.g. *L. uliginosus*) than with the amount of starch at the base of the stem and in the crown root/primary root, although, as mentioned above, this starch too can be remobilized (Figure 45A).

6.3. Discussion

6.3.1. Correlation between root starch content and re-growth vigour in starch metabolism mutants of *L. japonicus*

I tested the hypothesis that starch stored in roots is necessary for re-growth in *L. japonicus*. Consistent with this hypothesis, the *pgm1-3, pgm1-3*, *pgm1-5* and *aps1-1* mutants with reduced root starch content displayed a significant impairment in their capacity to re-grow following cutting-back in comparison to their WT segregants. In contrast, no significant reduction in vegetative re-growth capacity could be observed in the starch degradation mutants, including the two starch degradation mutant lines *gwd1-1* and *gwd3-1*. Roots of these mutants, however, did not display any visible reduced starch or starch-excess phenotype. Hence, mutants more strongly affected in their capacity to degrade root starch would need to be analysed to test the hypothesis that incapacity of the plant to remobilize the carbon stored as starch in roots also affects its capacity to re-grow.

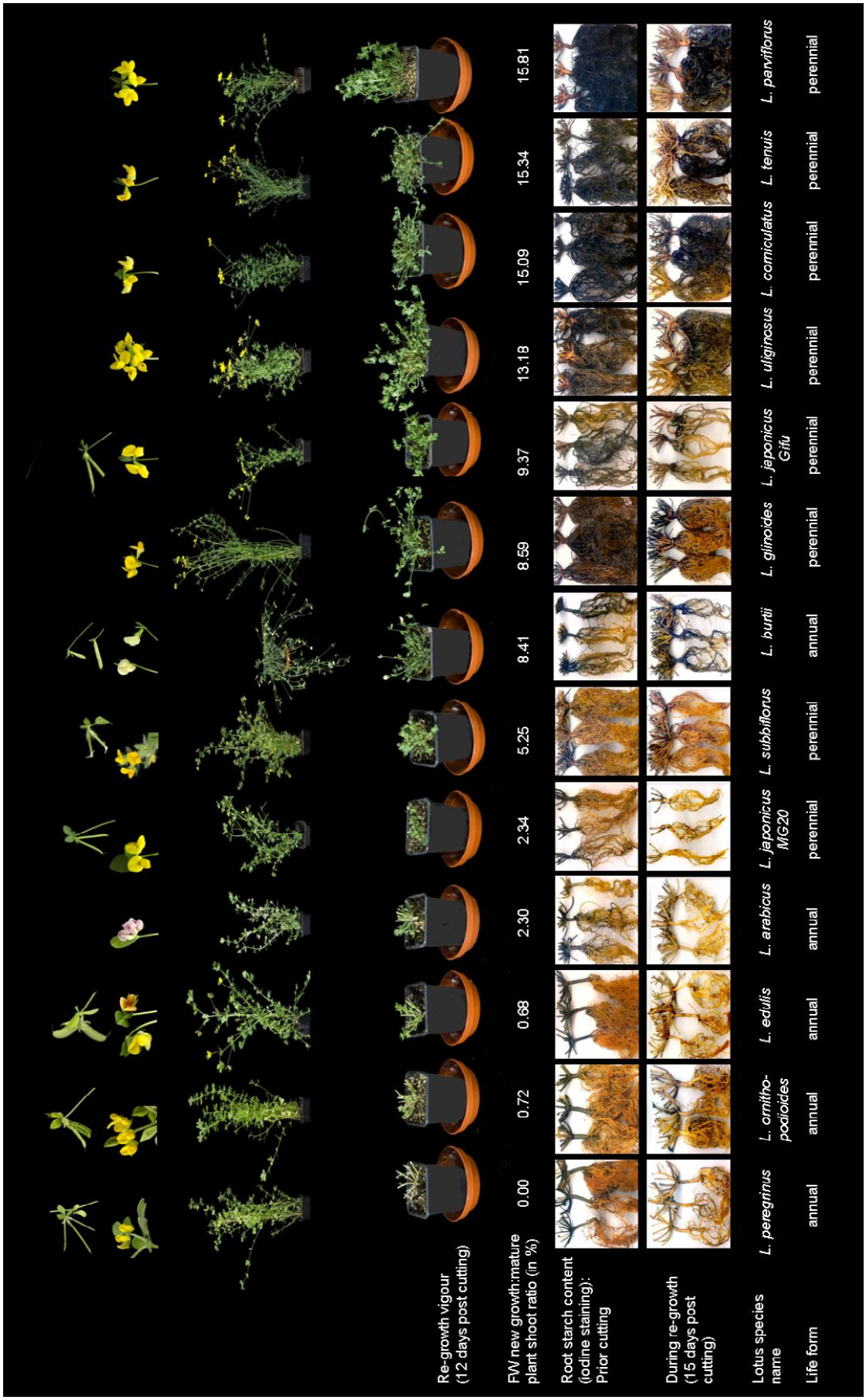

Figure 45A. Cutting-back experiment performed on a collection of 24 natural variants of the genus *Lotus*. Continued on next page.

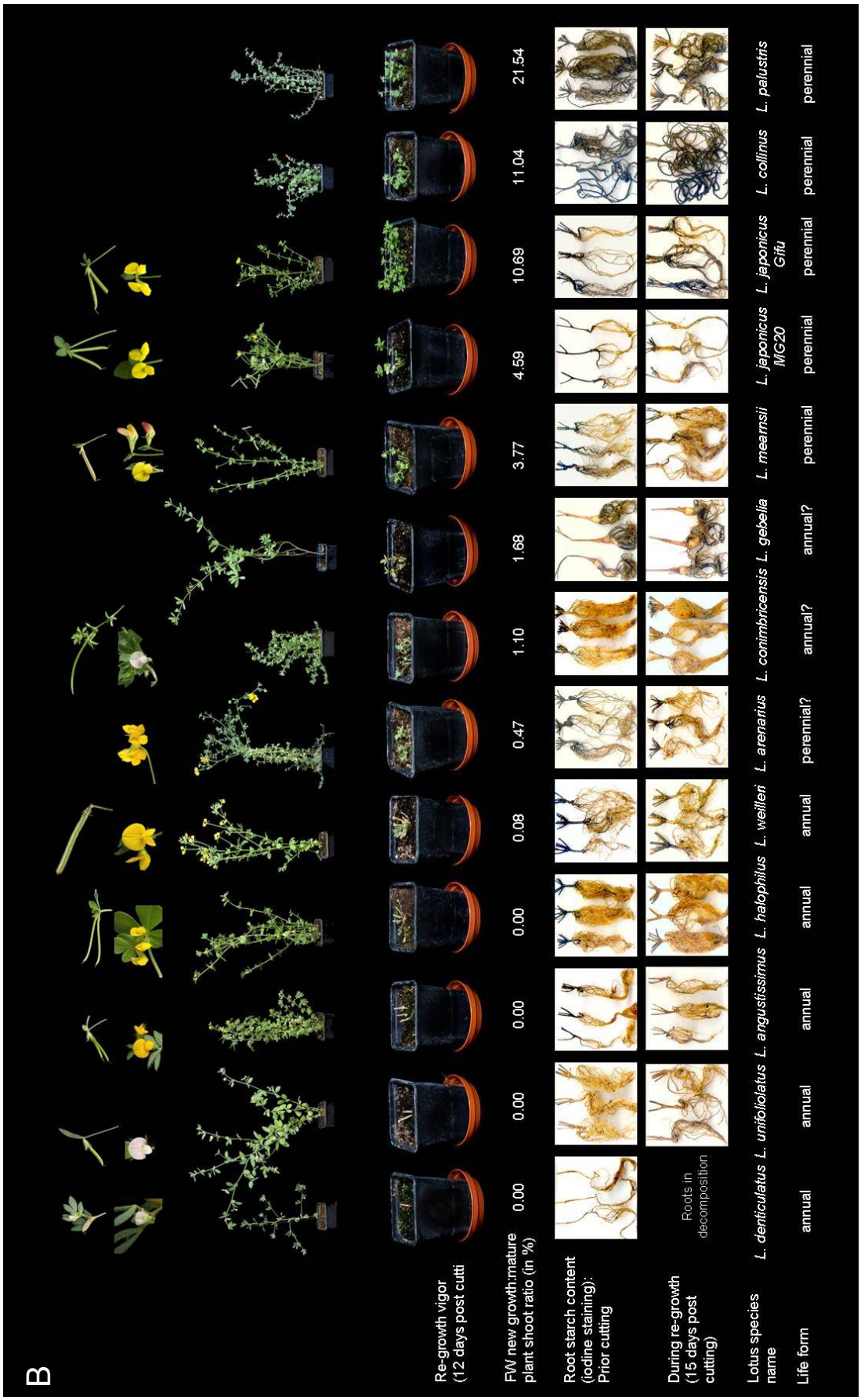

Figure 45B. Cutting-back experiment performed on a collection of 24 natural variants of the genus *Lotus*. Continued on next page.

Figure 45. Cutting-back experiment performed on a collection of 24 natural variants of the genus *Lotus*. Continued.
Root and shoot biomass measurement, and iodine staining of the roots were performed both prior and post cutting. Plants were grown in the greenhouse, under LD conditions and the analyses were performed on ca. 3 month-old plants. Unless otherwise indicated, 4 to 5 biological replicates that were good representatives of a set of about 20 plants were used for each species/accessions and for each measurement. As for the cutting-back experiment performed on the starch metabolism mutants of *L. japonicus*, plants were cut off at about 2 cm from the base of the tillers and re-growth was recorded over time. 15 d (A and B) or 30 d (C) post cutting. Dry and fresh weights of the new shoots (leaves and stems) were measured and the ratio of the new shoot to mature plant shoot biomass was calculated. Another three biological replicates were used for iodine staining of the root. Details of the results obtained, including the SE values are given in Table A6. **A**. Cutting-back experiment on this first set of *Lotus* species was carried out on plants grown from November 2007 until March 2008 in a greenhouse supplemented with artificial light (long day conditions). **B.** Plants of this second set of Lotus species were grown in a greenhouse under natural light conditions, from May until September 2008. Note that *L. arabicus, L arenarius, L. corniculatus, L. glinoides, L. parviflorus, L. tenuis,* and *L. uliginosus* flowered but did not set seeds. *L. colllinus, L. gebellia*, and *L palustris* did neiher flower nor set seeds. The root architecture of *L. gebelia* differs so significantly from the other Lotus species that there is doubt as to whether this accession truly belongs to the species *L. gebelia* and the *Lotus* genus.

The capacity for strong, rapid re-growth is a particularly important trait in perennial crops grown for silage, forage and the production of biofuel. It has been speculated that stores of starch in roots, rhizomes and stems provide the carbon necessary for re-growth. However, information about the importance of starch turnover in this process was lacking thus far. Results of the cutting-back experiments I carried out on the collection of starch metabolism mutants show that - at least under some growth conditions - the accumulation of root starch and its remobilization are necessary for vegetative re-growth following cutting-back in a perennial legume species such as *L. japonicus*. This constitutes an important new finding as it suggests that, although meristem activity is crucial for the initiation of vegetative re-growth as previously mentioned, the storage of carbon as starch in the roots is necessary to sustain it.

Additional experiments could be performed to explore further this finding. First, the quantification of starch on root samples of the mutant, heterozygous, and WT segregants harvested prior and post cutting-back would need to be performed and the resulting starch content data used for a correlation analysis with the shoot and new shoot biomass prior and post cutting-back. Roots samples for these quantitative measurements have been harvested that are waiting to be processed. Second, labelling experiments using C^{13} or C^{14} isotopes may be performed to monitor the flux of carbon from the roots to the new shoots being produced during re-growth. Lastly, it would be interesting to confirm that the re-growth impairment seen for some of the starch synthesis mutants is caused by the lack of sugars derived from the degradation of starch. If the failure of the mutants to regenerate a new shoot after cutting-back is indeed caused by the lack of sugars from starch degradation, one

would expect their altered re-growth capacity to be rescued upon the exogenous supply of sugars.

As well as determining whether root starch is necessary for re-growth, it is also important to determine whether starch is limiting for re-growth, and if so, to what extent. Results of the analyses I performed strongly suggest that the accumulation of root starch and its remobilization are both necessary and limiting for the vegetative re-growth vigour in *L. japonicus* since both an intermediate root starch content and re-growth phenotype could be observed for the *pgm1-4*/PGM1-4 heterozygous plants, and the *pgm1-5* mutants (reduced starch content) in comparison to the *pgm1-4* mutants (starch-free) and the WTs. However, this finding would need to be further explored. If starch turnover is indeed necessary and limiting, manipulation of this process might offer an important route for the improvement of re-growth characteristics in perennial crops. To explore further the control that root starch exercises over the rate and extent of re-growth, both the root (and above-ground) starch content and the shoot and root biomass prior cutting-back and during re-growth would need to be quantified on a series of mutant alleles with different levels of root starch content. From this, a control coefficient for starch content against re-growth could be calculated. Performing this control analysis should allow determination of the extent to which root starch content is important to the capacity and vigour of re-growth. More particularly, this should help determine to what extent the carbon remobilized from starch degradation in the roots accounts for the shoot biomass gain. Indeed, if root starch is sustaining the shoot growth, then a quantitative relationship should exist between the amount of carbon lost from root starch and the gain of new shoot biomass, at least in the early stages of re-growth.

Large variations of the effect of mutations on vegetative re-growth were observed, depending on the age of the plant and the growth conditions used. Thus, no significant differences in re-growth vigour were observed between the mutant and the WT when the cutting-back experiment was performed on younger plants, before flowering and seed setting. Therefore, flowering induction and seed production too may play a role in the vegetative re-growth and perenniality trait by modifying the allocation of resources at the whole plant level. The important change in starch storage in leaves observed around the transition to flowering time in MG-20 and Gifu plants (Chapter 3, sections 3.2.4 and 3.2.5) tends to support this hypothesis. It also seems likely that large changes in temperature and/or day length and light quality influence the partitioning of the resources, and hence the vegetative re-growth capacity of perennial plants. The analyses I performed would need to be reproduced in field conditions to understand the extent to which my findings are relevant to an agricultural situation.

Re-growth vigour might also be influenced by the number of basal branches (aka tillers). A higher number of basal branches will be associated with a higher number of axillary buds

from which to initiate re-growth. In *Lotus*, meristematic sites (i.e. sites of re-growth giving rise to new basal branches) could be observed both at the base of the branches (i.e. crown root) and on the few cm of stems remaining after cutting-back. Plants of the accession Gifu that had higher root starch content than MG-20 also had a significantly higher number of basal branches at the time of cutting-back (visible on Figure 42B). Such characteristics might have played a role in determining their more vigorous re-growth capacity compared to MG-20 counterparts. Analysis of the mutants and their corresponding WT which only varied in their starch content, however, suggest that this factor is unlikely to have been a major determinant of the amount of new shoot biomass measured. In future, it would be necessary to distinguish more precisely the contribution made by meristem activity from the contribution made by root starch content in vegetative re-growth vigour. Most likely, meristem activity is crucial for the initiation of re-growth following overwintering or under enforced re-growth (e.g. cutting-back) while root starch is necessary, possibly with other nutrient reserves, to sustain re-growth. This would be in agreement with the suggestion made by Munné-Bosh et al. (2007) that growth in herbaceous perennials results from the activity of apical meristems sustained by the nutrients found in underground organs.

6.3.2. Correlation between root starch content and re-growth vigour and the perenniality trait in annual and perennial species of *Lotus*

Analysis of natural genetic variation for root starch content and re-growth vigour in *Lotus* revealed a clear, positive correlation between root starch content and the rate and extent of re-growth, suggesting that starch turnover is both necessary and limiting in this process. Further, there was considerable variation between species in how much and from where the starch had disappeared during their re-growth. Several had strikingly lost starch from the crown root and stem base (e.g. *L. peregrinus*, *L. edulis*, *L. tenuis*) but remobilization of this starch was apparently not correlated with the capacity for re-growth. Instead, re-growth vigour correlated best with remobilization of starch in the secondary roots. Other species such as *L. burtii* had a relatively high amount of root starch, but little of it appeared to have been allocated to re-growth, and accordingly capacity of the plants of this species to re-grow was limited (Figure 45A). This suggests that not only the capacity of the plant to accumulate carbon reserves as starch in the roots, but also its capacity to remobilize it efficiently is important in determining the re-growth vigour.

It must be mentioned, however, that some exceptions could be seen to this overall good correlation between root starch and re-growth vigour following cutting-back. For example, *L. subbiflorus* re-grew a reasonable amount while it was not clear that much of its root starch had disappeared. Hence, other factors than root starch such as the accumulation of soluble

sugars and the metabolism of nitrogen, for instance, could also be important in determining the vegetative re-growth capacity of the plants, the extent to which may be dependent of the genotype (e.g. species, ecotypes) and the environmental conditions.

A good correlation was also found between root starch content and re-growth vigour on one side, and the life form of the species/accession on the other (Figure 45). That is to say, the perennial species of *Lotus* tended to have higher root starch content and a better re-growth capacity following cutting-back than their annual counterparts. More specifically, annual species generally had low root starch and were not able to sustain enforced re-growth so that they died several days after cutting-back. This suggests that, at least for plants of the genus *Lotus*, the re-growth capacity of mature plants following cutting-back (i.e. under enforced re-growth) represents a good indicator of the perenniality trait.

Following this finding, it remains to be determined whether the capacity of the plants to accumulate and remobilize their carbohydrate reserves stored in the roots is what governs their life form strategy, or is rather a consequence of it. Evidence suggests that the partitioning of reserves in plants differs between perennial and annual species with resources generally directed mostly toward reproduction in annual species and toward the storage of carbohydrate reserves in perennial species (De Souza and Da Silva, 1987). More generally, it has been proposed that annual species tend to maximize resource acquisition, whereas perennials rather maximize the conservation of resources (Aerts and Chapin, 2000; Poorter and Garnier, 1999). In this regard, it would be interesting to perform a grafting experiment in which the root system of a perennial accession – with a capacity to store high levels of carbon reserves - would be grafted to the shoot of an annual relative - with high seed yield. This may help establish whether a higher storage of carbon in the roots leads to an increased life-span of the resulting graft plant in comparison to the shoot donor species. Of course, this would be conditional on whether the roots of the perennial plant will still maintain their capacity to store large amounts of carbon when grafted with the annual plant. Conversely, it is not known whether the shoot of the annual will partition its carbon into the root to the same extent that the perennial would. Ultimately, the aim is to develop high seed yielding, perennial cultivars. A better knowledge of both the factors determining carbon sink/source strength (including capacity to store carbon as starch) and the factors controlling the fluxes of carbon between vegetative and reproductive organs would certainly help achieve this goal.

In addition to performing a cutting-back experiment, I also examined the possibility that a correlation may exist between root starch content and/or re-growth vigour, and the geoclimatic origin of the *Lotus* species I analysed. More specifically, I aimed to test the hypothesis that the capacity of the plant to store a large amount of starch may be of

competitive advantage under some environmental conditions. If this is the case, a positive correlation may be expected between the root starch content of the accessions and more extreme climate/harsher environments characterised notably by longer period of winter dormancy. No clear correlations, however, could be seen between their root starch content, re-growth vigour, and growth habit on one side, and their geoclimatic origin on the other (Figure 46). This is consistent with the results of an earlier study performed by Suginobou and collegues (1998) on different species of *Lotus* and different ecotypes of *L. japonicus*. In this study, natural variation for a certain number of phenotypic traits including plant height and weight, flowering time, autumn vigour and re-growth were analysed. No correlation was found between the geographical distribution of the accessions and their phenotypes and the degree of polymorphism between them. Similarly, a natural variation study performed on a set of *A. thaliana* accessions revealed no correlation between their pattern of carbohydrate accumulation in leaves and their geographical origin (El-Lithy et al., 2005), suggesting that climatic conditions may not play a major role in driving evolutionary change in the carbon allocation and life form strategy. However, it must be mentioned that in these studies, the geoclimatic origin of the accessions were correlated with parameters measured in a set of invariant, controlled conditions. Hence, these studies did not assess the ability of carbon storage to respond to significant environmental changes and challenges.

It would be interesting in the future to examine the capacity of the mutants deficient in starch turnover and/or natural variants for root starch content to regenerate after over-wintering and compare these results with the results of the cutting-back study presented above. This may give insight into the importance of change in temperature and photoperiod conditions (eg; requirement of dormancy period) on the allocation of resources and the perenniality trait. More generally, environmental factors may be important determinants of root starch storage. It may be hypothesised, for instance, that some species would use their capacity to store a large amount of root starch only when the environmental conditions require it, while in some others the accumulation of storage starch in their roots may be more constitutive. Reciprocal transplant experiments and measurements of phenotype under different environments such as cold treatments could be performed to determine the phenotypic plasticity of root starch storage capacity and identify trait x environment interactions.

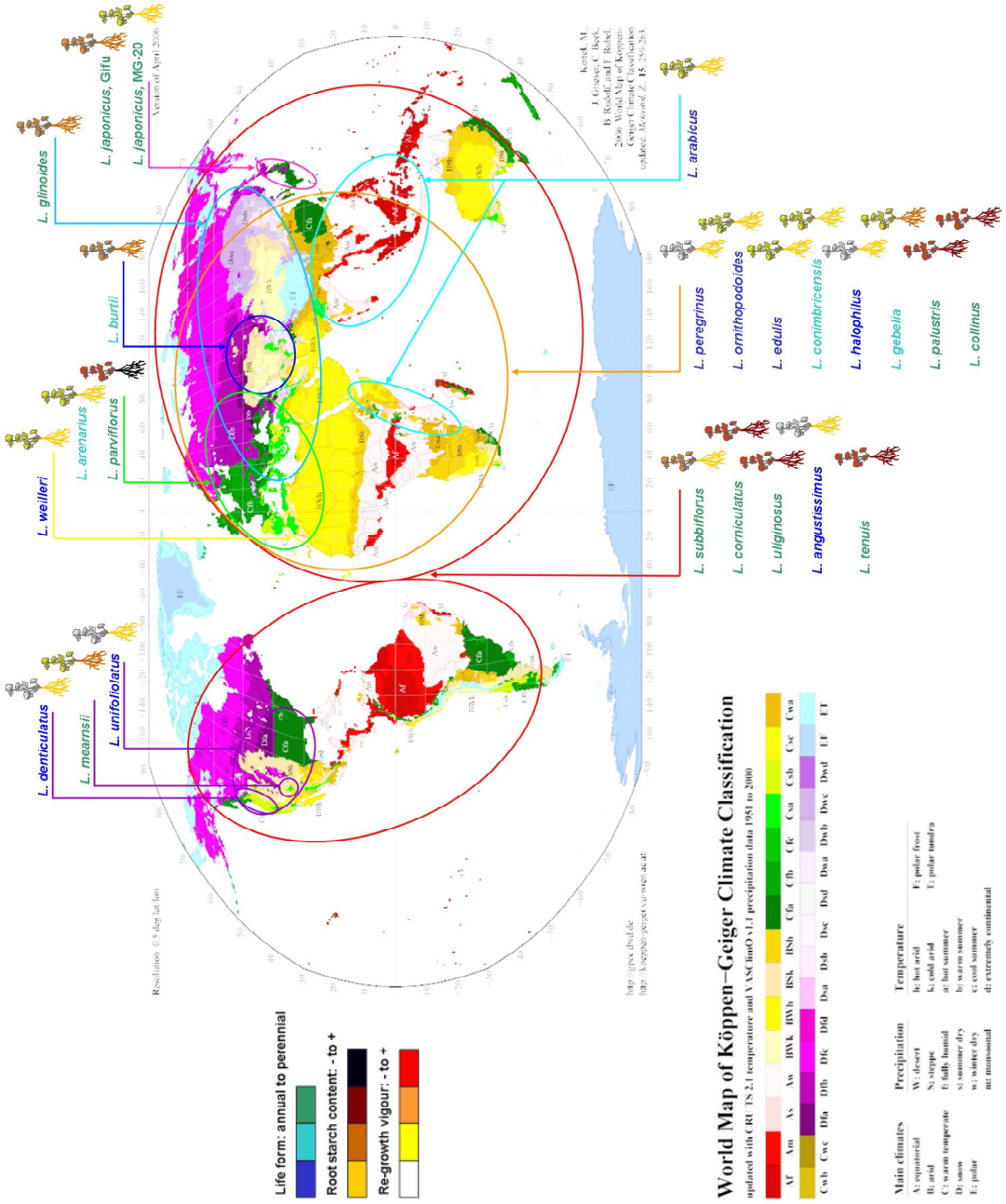

Figure 46. Root starch content, re-growth vigour, life form, and geoclimatic origin of the Lotus natural variants.
Geoclimatic origin (geographic origin as given by the USDA GRIN database), life form, root starch content, and re-growth vigour following cutting of the the annual and perennial species of *Lotus* analysed in the cutting-back experiment. Scores were attributed to the *Lotus* natural variants for their root starch content and re-growth vigour based on results of biomass measurements and root iodine staining as described in Figure 45. This allowed their classification into classes as shown in the legend displayed on the left of the Figure.

6.3.3. Study of the importance of starch for re-growth and perenniality in other legumes and non-legume plant species

In the future, it would be interesting to determine whether, as observed in *Lotus*, variation in root starch content correlates well with variation in vegetative re-growth vigour and the growth habit in other annual and perennial species of legumes or even of other plant families (e.g. grasses). More particularly, it would be interesting to determine whether the control observed for root starch over re-growth in *Lotus* is restricted to the genus *Lotus* or rather conserved across the plant kingdom. Ultimately, this may help the design of strategies aimed at developing new crops with perennial characteristics in which the stored reserves of starch would be made more available to reproductive tissues.

To this end, I also established a collection of both annual and perennial species of the *Medicago* genus. In total, seeds of 24 species of *Medicago* were ordered from the USDA-GRIN germplasm. Lists of the species selected and their phylogenetic relationship are presented in Table 1 and Figure 47. It is interesting to note that whatever the plant genus studied, annual and perennial species were found intermixed on the phylogenetic tree (Figure 44 and 39). This suggests that a change from a life form habit to another requires little genetic innovation. This idea is consistent with the results of recent studies performed in *A. thaliana* and tomato (Chapter 1, section 1.10.2 and references therein). A preliminary analysis of root starch content was also performed on the annual and perennial species belonging to the same genus as *A. thaliana* (Table 1 and Figure 48). Seeds of eight species of *Arabidopsis* were ordered from the NASC database and grown in a growth cabinet for ca one month prior iodine staining their shoot and roots. In contrast to plants of the genus *Lotus*, neither the annual nor the perennial *Arabidopis* species accumulated significant amounts of root starch (Figure 49).

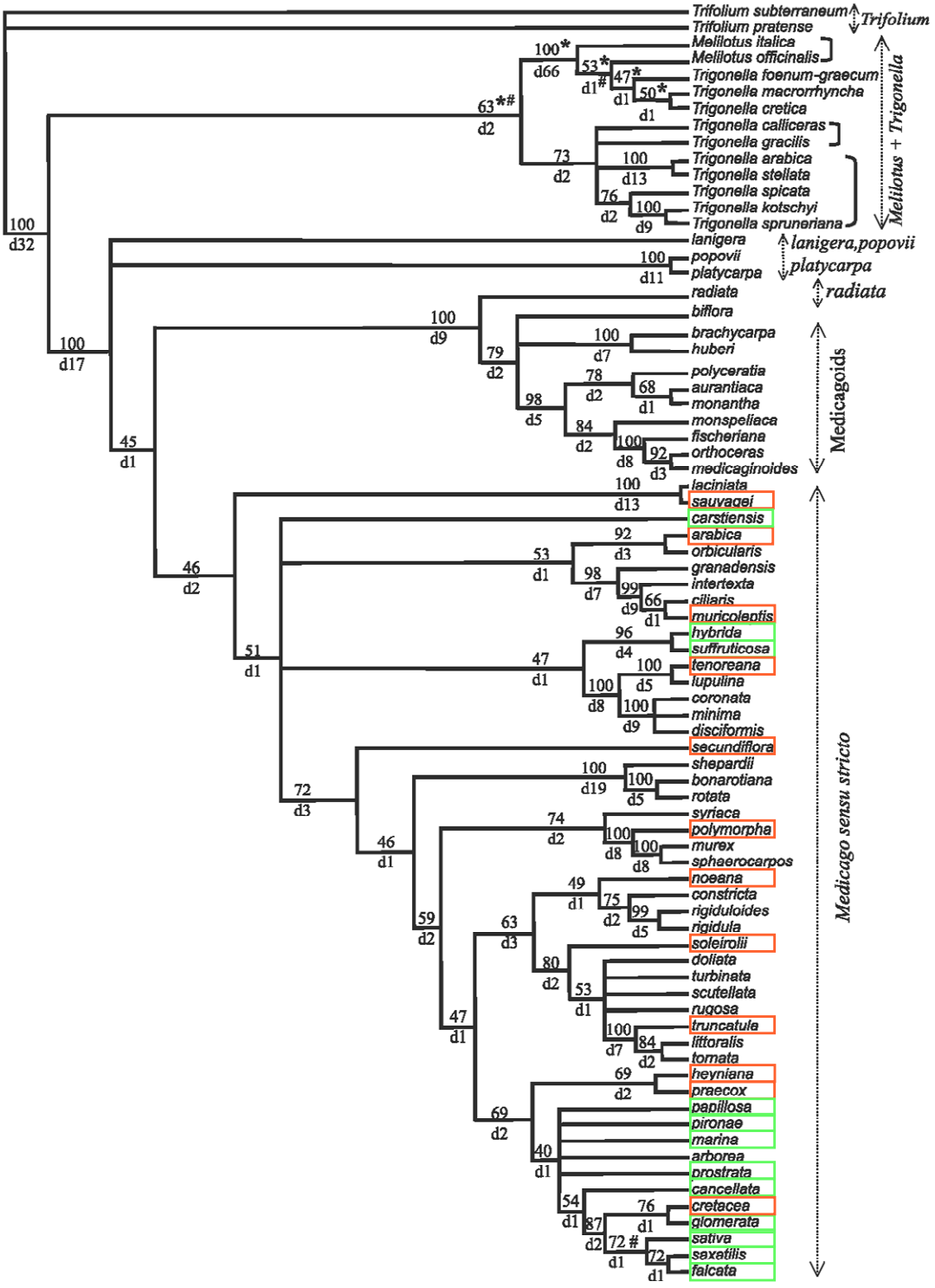

Figure 47. Phylogenetic relationship of the species of the genus *Medicago* and their life form. Modified from Bena *et al.* (2001). Annual species are framed in green and perennial species in red (Life form as given by the USDA database). As observed for the *Lotus* species (Figure 44), the annual and perennial species of *Medicago* genus are intermixed, suggesting that the switch of one life form to another may not requires major genetic changes.

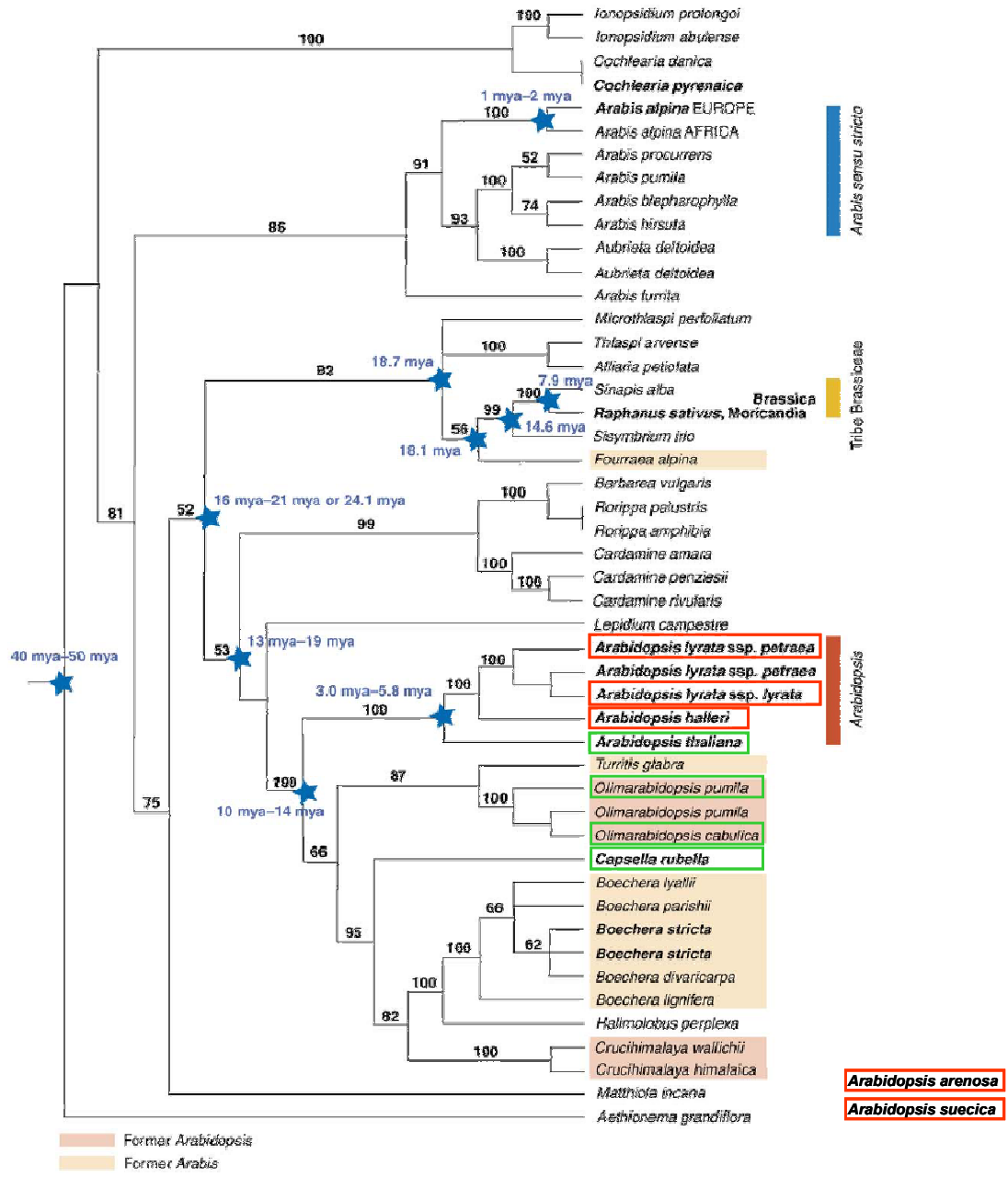

Figure 48. Phylogenetic relationship of the *Arabidopsis* species and their life form.
Modified from Clauss and Koch (2006). Annual species are framed in green and perennial species in red, according to the life form information given in Al-Shehbaz and O'Kane (2002) and Clauss and Koch (2006). *Arabidopsis arenosa* is closely related to *Arabidopsis lyrata*. *Arabidopsis suecica* (Sue1) is derived from an *Arabidopsis thaliana* x *Arabidopsis arenosa* hybridization (Al-Shehbaz and O'Kane; 2002)

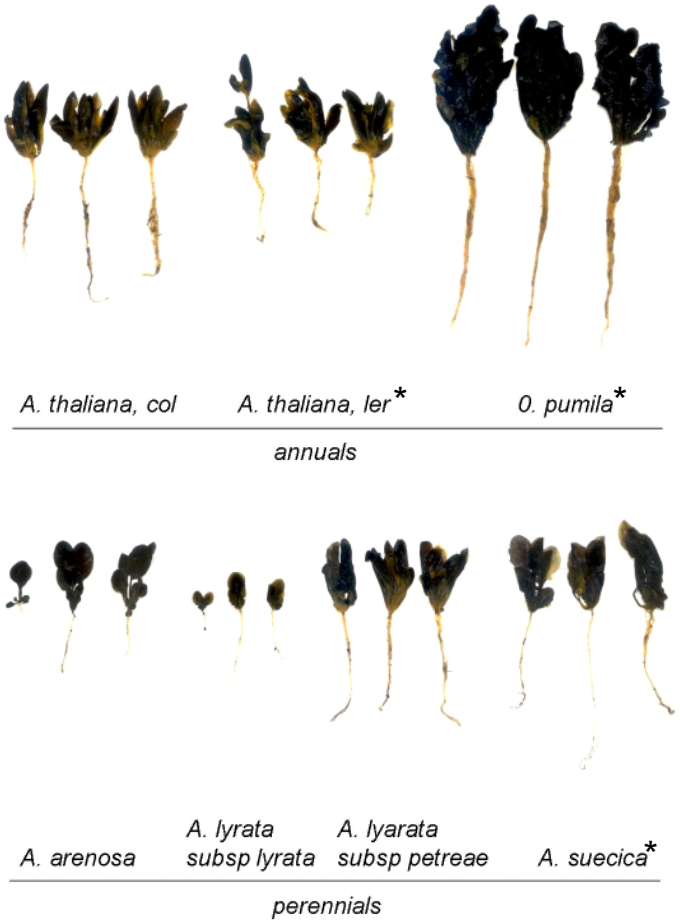

Figure 49. Iodine staining of the shoot and root starch of annual and perennial species of *Arabidopsis*. Iodine staining was performed at the end of day on ca 1 month old plants grown in a controlled environment chamber, in a 16 h light, 8 h dark cycle. Bolting had started at the time this analysis was performed in the species indicated with an asterisk (*). Results showed no visible variation in root starch content between the species.

6.3.4. Genetic determinants of vegetative re-growth vigour and the perenniality trait in Legumes

Analysis of the *Lotus* species revealed large variation in term of root starch content. In the future, it would be interesting to try identifying the gene(s) responsible for such differences. This may be achieved, for instance, by performing cross-species microarray transcript profiling using the GeneChips available for *L. japonicus*.

Further study of the perennial species *L. parviflorus* (USDA accession PI 415815) is of great potential interest. This species out-performed all the others studied, including the *Lotus* species currently cultivated for forage (*L. uliginous, L. corniculatus, and L. glaber*) both for the amount of starch stored in its roots (assessed by iodine staining only) and its re-growth vigour following cutting-back (Figure 45). In addition, this species presented the highest root biomass of all the species analysed and, together with *L. glinoides*, bore a high number of naturally occurring nodules in comparison to all the other plant species grown under the

same conditions (Table A6). These characteristics make it not only a very interesting accession to study further in regard to the importance of starch for re-growth vigour and the perenniality trait, but also a promising species in term of agricultural use for forage and pasture, and as a rotation legume crop.

Lastly, the results of the analysis I performed showed that MG-20 has a faster growth rate than Gifu, but its re-growth rate is slower (Chapter 6, section 6.2.1). QTL for vegetative re-growth vigour and root starch content could be studied using the Recombinant Inbred (RI) Lines available from a cross between the *L. japonicus* accessions MG-20 and Gifu (187 RI lines available to date; http://www.shigen.nig.ac.jp/bean/lotusjaponicus/top/top.jsp). If root starch content indeed plays a central role for re-growth vigour in *Lotus*, a positive correlation should be observed between these two traits and the QTL for both should co-localize. The resulting mapped QTL regions could then be searched for candidate genes and the genes responsible for the variation eventually identified as described in Chapter 3, section 3.3.4.

CHAPTER 7

Conclusions and perspectives

The important thing is not to stop questioning

Albert Einstein

CHAPTER 7: Conclusions and perspectives

7.1. The metabolism of leaf starch in the model legume *L. japonicus*

Almost nothing was known about the metabolism of starch in the model legume *L. japonicus* at the start of this PhD research project. Taking advantage of the new information derived from the sequencing of its genome, I provided detailed information on the genes involved in starch metabolism and generated the first molecular-function map for starch metabolism in this species. The analyses I performed revealed a large conservation, but also some significant differences with the metabolism of starch in *A. thaliana* and its regulation. Results of this work set the basis for future experiments aiming at identifying key genes controlling the metabolism of starch in *L. japonicus.*

In addition, I carried out starch and sugar measurements across organs, at several developmental stages, and in different growth conditions to characterise the accumulation and turnover of starch in the two *L. japonicus* accessions MG-20 and Gifu. My analyses revealed significant differences in the metabolism of starch between plants of MG-20 and Gifu, the two accessions of *L. japonicus* most commonly used for research. Plants of these two accessions also displayed large differences in several other traits, including biomass production. This finding is particularly interesting in the light of the recent demonstration that rates of starch turnover are positively, causally linked to productivity in *A. thaliana* (Sulpice et al., 2009). *L. japonicus* appears to be an excellent system with which to test the wider applicability of this finding.

7.2. A Suite of *Lotus japonicus* Starch Mutants Reveals Both Conserved and Novel Features of Starch Metabolism

Prior the start of this PhD research project, an EMS mutagenised population had been set up and screened for mutants impaired in the synthesis and degradation of starch in *L. japonicus*. I identified the mutations for several of these mutants from the forward screen by genetic mapping. For mutations not yet identified, their positions on the genetic map coupled with the results of candidate gene searches suggest that they are likely to affect novel proteins involved in the metabolism of starch. In addition, TILLING was used to confirm that the mutations identified were indeed responsible for the mutant phenotype and to obtain additional mutations in genes known to affect leaf starch content in other species. During the

course of this research project, I linked the characterisation of these forward and reverse genetic mutations and the mutant phenotypes. In total, several deleterious mutations affecting seven genes encoding key enzymes of the starch metabolism pathway were identified. Arguably, this represents the most comprehensive collection to date of forward and reverse genetic mutants impaired in the synthesis and degradation of transitory starch in any species other than *A. thaliana.*

This unique collection of mutants represents a significant resource for uncovering new information about the properties of starch-metabolising enzymes. As an illustration, I discovered new information about the structure-function relationships of two key enzymes: ADP-glucose pyrophosphorylase (AGPase) and glucan, water dikinase (GWD1) from the study of the mutations affecting them. Further, this collection of mutants also constitutes a valuable new resource for further studies on the metabolism of transitory and storage starch in general, and on its importance in legumes in particular.

Characterisation of the mutant phenotypes I performed revealed that, although the main components of the pathways of starch metabolism in leaves of *L. japonicus* are similar to those in *A. thaliana* leaves, the role and importance of leaf starch accumulation and turnover clearly differs between the two species. Whereas the inability to synthesise starch has much less effect in *L. japonicus* than in *A. thaliana*, loss of the capacity for starch degradation has much more profound consequences for plant growth and development. Whereas starchless *A. thaliana* plants lacking plastidial phosphoglucomutase (PGM1) grow slowly relative to wild-type plants, the equivalent mutant of *L. japonicus* grows normally even in short days. In contrast, the loss of glucan water dikinase 1 (GWD1), required for starch degradation, has a far greater effect on plant growth and fertility in *L. japonicus* than it does in *A. thaliana*. Further investigation of these differences may lead to a better understanding of the regulatory mechanisms linking the metabolism of starch with plant growth. Characterisation of these mutants also provided insight into the nature of the pathway and importance of starch for symbiotic nitrogen fixation in *L. japonicus*.

These results highlight the limit of extrapolating findings gained from study of *A. thaliana* to other plant species, and illustrate the importance of performing comparative and translational studies of important plant processes in several other model species, and in crops. Species of legumes that include important crop plants exhibit several traits of agronomic importance that cannot be studied in *A. thaliana*: they possess the capacity to assimilate nitrogen and phosphorus via symbiosis with rhizobia and arbuscular mycorrhiza, respectively (Oldroyd and Downie, 2008). In addition, they also have certain aspects of their biology that are unique to them. This include some aspect of their development (e.g. floral patterning and seed biology; Dong et al., 2005 and Le et al., 2007), primary and secondary metabolism (e.g. Horst et al., 2007; Dixon and Sumner, 2003), and disease resistance

(Frugoli et al., 2001). The collection of starch metabolism mutants of the model legume *L. japonicus* I characterised offers the opportunity to examine the partitioning of carbon in relation to several legume crop traits of agronomic importance including symbiotic nitrogen fixation, seed metabolism and filling, and perenniality and re-growth.

7.3. Carbon allocation, re-growth vigour and perenniality in *Lotus*

Plants possess a highly plastic metabolism that allows them to cope with an environment under constant change (day-length, temperature, availability of nutrients, pathogen attack, etc). Among the major strategies used by plants to adapt to seasonal environmental conditions are annual and perennial habits. With longer growing seasons, perennials have higher above-ground biomass and have a more extensive root systems than their annual relatives. Furthermore, perennials also generally have better access to resources, a more conservative use of nutrients and tend to be more resistant to biotic and abiotic stresses than annual crops (Cox et al., 2006). Because of these characteristics, perennial crop species are expected to be less detrimentally affected by climate change and the development of their cultivation offers the opportunity of a more sustainable agriculture systems.

The capacity for a vigorous re-growth is also an important trait for the use of perennial crops as forage or for the production of biofuels. Meristem determinacy and processes of cell death have been suggested to be major determinants of perenniality (Thomas et al., 2000). The allocation of resources may also play an important role in determining the lifespan and the capacity for vegetative re-growth in perennial plants. This hypothesis has received little attention so far and no conclusive evidence has been presented to support it. In this study, I tested the hypothesis that the partitioning of carbon, and more particularly the storage of starch in roots, may play an important role for re-growth and the perenniality trait in perennial legume species. For this, I used both the collection of starch metabolism mutants of *L. japonicus* mentioned above and a unique collection of annual and perennial species of the genus *Lotus* that displayed large variation in root starch content and re-growth vigour.

I was able to show that, although mutants of *L. japonicus* with strongly reduced root starch content grow normally prior to cutting, they are impaired in their capacity to regenerate after a harvest in which the photosynthetic parts of the plant are removed. The results I obtained also revealed a good correlation between the amount of root starch and the vigour of re-growth as well as the annual versus perennial growth habit, suggesting that root starch reserves may be necessary and limiting for re-growth vigour in *Lotus*.It would be interesting in the future to identify the genetic basis of such variation (i.e. identification of the genes responsible for high root starch content and re-growth vigour).

Last but not least, the analyses I carried out also identified *L. parviflorus* (USDA accession PI 415815) as a very promising *Lotus* species to develop and use as legume crop for forage and pasture given its outstanding re-growth vigour and capacity to store large amounts of root starch. The imposing root system and the large numbers of naturally occurring nodules found in its roots in the growth conditions tested also suggest that this accession may be highly resistant to unfavourable growth conditions and stresses such as drought as well as particularly efficient in performing symbiotic nitrogen fixation.

Appendix 1

List of Figures

List of Tables

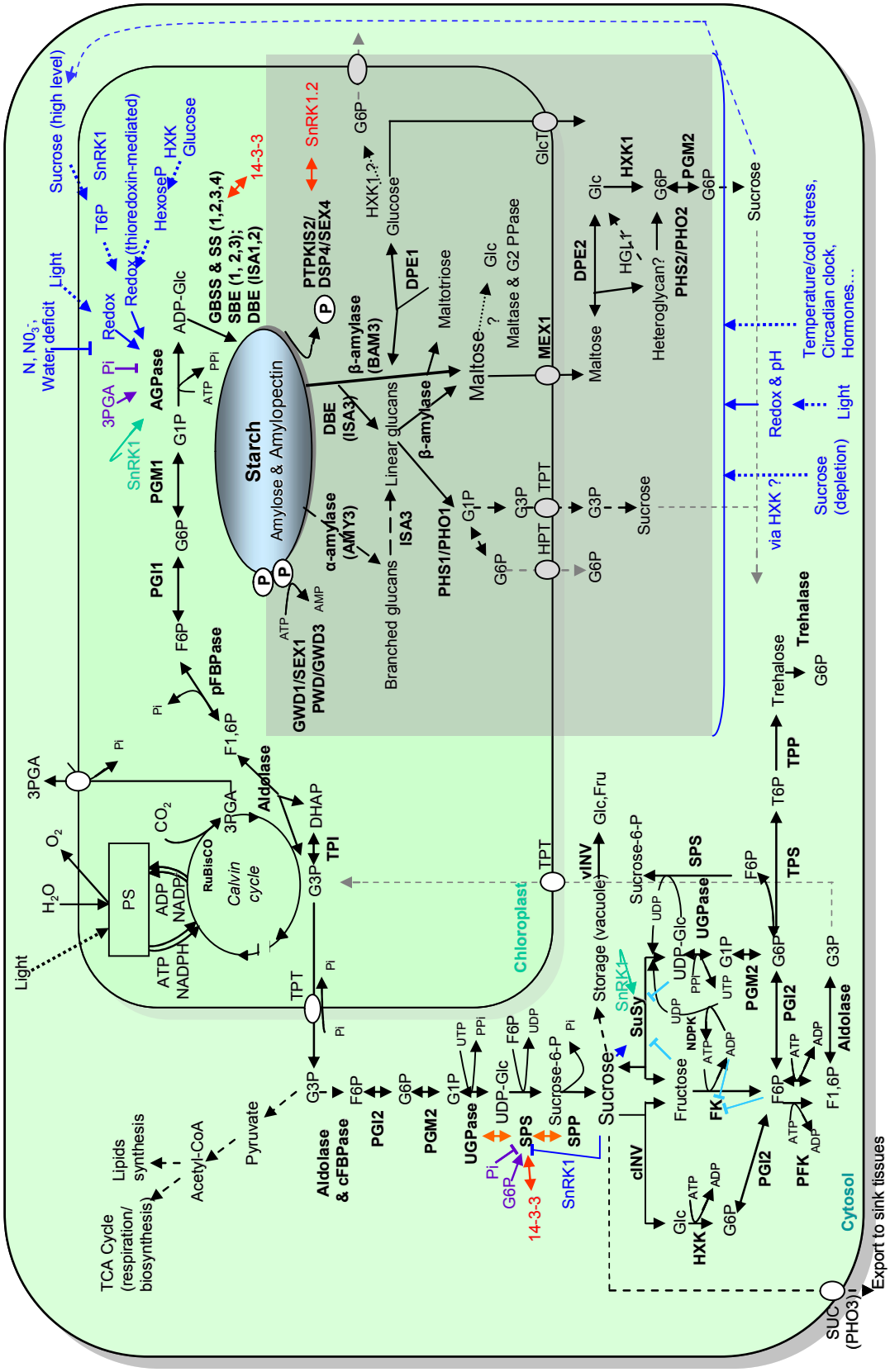

Figure A1. Detailed pathways of transitory starch metabolism in *A. thaliana*
Proposed pathways of starch synthesis and degradation *in A. thaliana* leaves. Factors involving in the regulation of these pathways are in blue or pruple (post-translational regulations) and in green (regulation at the transcriptional and/or translational level); known protein interactions are in red.

Table A1.A
Starch metabolism genes

Gene name	Gene locus	Probeset	Name	Leaf	Petiole	Stem	Root	Nod0d	Nod21d	Flower	Pod10d	Pod14d	Pod20d	Seed10d	Seed12d	Seed14d	Seed16d	Seed20d
PGI1	chr1.LjT29N14.30.nd	chr1.TM0454.3_at	PGI1	2094,1	838,1	661,6	508,5	578	684,1	465,4	726,1	717,9	876,6	1189,3	1086,5	1000,1	1039,5	1329,1
PGM1	chr5.CM0953.200.nc	chr5.CM0953.28_at	PGM1	1716,2	746,2	536,8	215,1	227,4	693,3	293	533,9	543,6	1048,2	571,4	581,3	517,2	512,6	938,2
APS1	chr2.CM0191.60.nc	chr2.CM0191.7_at	APS1	6582,8	3132,6	2854,7	930	969,8	3922,6	1860,2	2492,4	2223,3	2400,9	1719,5	1765,7	1638,8	1722,9	1799,3
APL1	chr4.CM0387.180.nc	Ljwgs_085946.1_at	APL1	1038,6	285,4	153,9	13,9	13,2	12,9	110,9	61,2	48,2	37,5	25,3	23,7	17,5	18,1	19,1
APL1	chr4.CM0387.180.nc	Ljwgs_118248.1_at	APL1	877,6	220,2	151,9	19,9	17,5	21,1	117,5	50,9	44,1	28,2	30	28,9	31,1	27,7	29,3
			APL1	958,1	252,8	152,9	16,9	15,35	17	114,2	56,05	46,15	32,85	27,65	26,3	24,3	22,9	24,2
APL2	chr1.LjT34C24.40.nc	chr1.TM0952.12_at	APL2a	80,1	193,5	227,9	222,7	176,3	733,4	273,9	657,6	381,4	492,5	536,6	458,5	376,7	303,1	259,9
APL2	chr5.CM0077.680.nc	chr5.CM0077.28_at	APL2b	7,5	7,5	7	6,9	6,4	6,5	7,7	8	7,2	8,1	8,7	8,5	8,3	7,6	7,9
APL2	chr5.CM0077.680.nc	Ljwgs_024431.1_s_at	APL2b	13	12	11,6	11,3	11,2	12,7	13,6	12,3	13,3	12	15,6	14,3	13,8	15,1	13,7
			APL2b	10,25	9,75	9,3	9,1	8,8	9,6	10,65	10,15	10,25	10,05	12,15	11,4	11,05	11,35	10,8
APL3	chr1.CM0113.470.nd	chr1.CM0113.51.1_at	APL3	387,5	586,8	938,4	640,6	859,4	2219,2	760,5	1308,8	772,7	920,5	1393,9	1128,8	899,4	816	838,6
APL4	chr3.CM0216.100.nd	chr3.CM0216.12_at	APL4	83,5	67,9	97,2	59,5	87,8	56	80,3	91,9	70,7	83,9	85,4	70,2	60,6	56,3	43,5
APL5	LjB06P23.100.nc	Ljwgs_037383.1.1_at	APL5	21,2	48,1	54,3	23,1	21,9	19,4	17,5	25,4	18,2	18,4	16,3	16,2	15,9	15,9	20,3
SS1	LjT38J19.80.nd	TM0720.10_at	SS1_1	1502,6	467,2	391,6	97,5	115,2	147,9	492,1	475,7	437,5	483,7	290,7	304,4	281,1	305,4	330,6
SS1	LjT38J19.60.nd	TM0720.8_at	SS1_2	1048,9	264,3	229,3	66,8	81,6	75,2	287,9	179,5	189	152,5	137,8	149,4	152,6	148,3	119,8
			SS1	1275,75	365,75	310,45	82,15	98,4	111,55	390	327,6	313,25	318,1	214,25	226,9	216,85	226,85	225,2
SS2	CM1835.140.nc	Ljwgs_042679.1_at	SS2a	653,5	318,6	273,7	147,9	153,4	215	218,5	180,7	164,6	140,4	294,1	330,4	271,8	290,6	193,8
SS2	chr1.CM0141.60.nd	chr1.CM0141.6.1_at	SS2b_1	88,4	28,5	51,7	29,7	20,4	11,8	15	11,2	17,4	11,6	10,6	10,7	10,6	10	11,7
SS2	chr1.CM0141.220.nd	chr1.CM0141.21_at	SS2b_2	48	16,4	18,3	11,8	10,2	8,6	10,9	10,6	13,8	9,6	10,8	9,8	9,3	10,4	10
			SS2b	68,2	22,45	35	20,75	15,3	10,2	12,95	10,9	15,6	10,6	10,7	10,25	9,95	10,2	10,85
SS5	chr2.CM0177.660.nc	chr2.CM0177.77.1_at	SS5	508,8	270,5	218	35,4	59,4	903,5	78	263,8	215,2	393,5	221,4	204,3	201,8	208,3	438,1
GBSS	chr5.LjT41L03.30.nd	chr5.TM0431.23_at	GBSS1a	4990,2	2620,3	1985,7	1172,8	1369,4	2845,6	1708,3	5454,8	4084,5	3150,4	6559,2	5894,1	5663,2	5351,2	4383,7
GBSS	chr3.CM0208.40.nd	chr3.CM0208.4_at	GBSS1b	1439,5	958,9	557,6	62,7	115,3	346,3	389,5	548,4	383,4	410,4	617,9	522,1	429,8	366,3	399,3
SBE2	chr1.CM0178.250.nc	chr1.CM0178.37_at	SBE1	674	533,4	574,4	307,9	370,4	947,8	296,4	969,4	656,8	510,4	858,2	783,1	718,7	658	674
ISA1	chr4.CM0004.550.nc	chr4.CM0004.43_at	ISA1	641,8	241,6	172,2	99,6	197	117,9	120,5	336,9	270,7	351,1	396,6	369	363,8	334,8	430,8
ISA2	LjSGA_028198.1	Ljwgs_028198.1_at	ISA2	483,4	178	165,4	118,7	134,6	202,1	142,7	198,2	170,7	182,6	207,1	206	238,7	249,4	207,6
LDA	chr5.CM0909.690.nc	Ljwgs_019774.1_at	LDA	172,2	58,1	67,6	26,9	31,3	38,4	41,6	63,5	86,6	105,1	78,2	88,4	86,9	100,8	100,2
LDA	chr5.CM0909.690.nc	Ljwgs_032265.1.1_at	LDA	329,3	186,5	193,7	88,2	90,2	124,4	106,9	224,4	247,3	391,6	239,3	257	263,3	270	504,6
LDA	chr5.CM0909.690.nc	Ljwgs_083649.1_at	LDA	188,4	83,4	100,2	38,4	37,9	75,3	55,9	111,9	133	210,2	137,1	135,4	138,9	141,9	284,7
LDA	chr5.CM0909.690.nc	Ljwgs_112747.1_at	LDA	88,1	30	33,4	19,4	21,1	22,3	25,4	31,3	34,3	30,4	41,8	44,5	44,8	44,1	28,4
			LDA	180,3	70,75	83,9	32,65	34,6	56,85	48,75	87,7	109,8	157,65	107,65	111,9	112,9	121,35	192,45
GWD1	chr4.LjT08E06.100.nc	chr4.TM0296.16_at	GWD1	542,8	218,5	296,1	164,7	244,3	245	149,8	179	206,5	202,8	140,9	143,4	130,7	135,6	160,4
GWD1	chr4.LjT08E06.100.nc	Ljwgs_024041.1_at	GWD1	6,8	6,7	6,2	7	7,4	6,8	6,9	7	6,7	7,3	7	7,2	7,3	7,2	6,6
GWD1	chr4.LjT08E06.100.nc	Ljwgs_024041.1_s_at	GWD1	1207,1	485,6	649,7	394,3	580,5	606,4	332,1	511,5	501,5	540,8	345	338,9	314,5	302,2	321,7
GWD1	chr4.LjT08E06.100.nc	Ljwgs_084383.1_s_at	GWD1	685	259,1	353,2	245,6	366,4	286,1	143,8	209,5	237,8	200,6	157,9	165,2	144,6	156,8	149,4
GWD1	chr4.LjT08E06.100.nc	Ljwgs_104904.1_s_at	GWD1	313,8	88,1	122,2	91,1	168,5	113,3	45,4	43,7	63,6	41,2	53,3	56	49,7	53,5	30,1
			GWD1	542,8	218,5	296,1	164,7	244,3	245	143,8	179	206,5	200,6	140,9	143,4	130,7	135,6	149,4
GWD3	chr5.LjT42F22.160.nc	Ljwgs_017560.1_at	GWD3_1	425,5	102,5	112,1	75,9	83,9	34,4	90,8	37,7	54,8	35,2	48	64,1	57,5	66,3	40,7
GWD3	chr5.LjT42F22.160.nc	Ljwgs_028662.1_at	GWD3_1	437,9	138,1	122,8	75,7	90,1	46,7	112,8	82,9	86,5	63	81,4	91,7	84,1	93	66,7
GWD3	chr5.LjT42F22.140.nc	Ljwgs_138786.1_at	GWD3_2	983,2	337,8	305,8	176,1	199	129,2	289,3	271,4	259,5	278,1	246,2	269,3	253,3	249,6	239,8
			GWD3	437,9	138,1	122,8	75,9	90,1	46,7	112,8	82,9	86,5	63	81,4	91,7	84,1	93	66,7

Table A1. *L. japonicus* starch metabolism genes and their corresponding probe sets and absolute transcript level values. Continued on next page.

Table A1.A continued

Starch metabolism genes

Gene name	Gene locus	Probeset	Name	Leaf	Petiole	Stem	Root	Nod0d	Nod21d	Flower	Pod10d	Pod14d	Pod20d	Seed10d	Seed12d	Seed14d	Seed16d	Seed20d
AMY1	chr5.CM0852.300.nc	Ljwgs_014622.1_at	AMY1	42,8	37,7	25,8	31,7	31	39	29,9	35,2	35,2	34,9	30,5	28,2	36,2	33,8	37
AMY2	LjSGA_020916.1	Ljwgs_020916.1_at	AMY2	694,4	289,1	420,6	81,2	117,6	48,9	687,2	178,5	353,7	343,6	51	60,6	51,8	59,7	160,5
AMY3	chr1.CM0410.400.nd	chr1.CM0410.51_at	AMY3a	580,2	382,7	309,4	290,7	320,8	537,4	274,1	200,5	208,3	276,8	395,4	402,4	354,6	323,8	275,5
AMY3	chr2.CM0608.610.nc	chr2.TM1534.12_at	AMY3b	34,8	29,4	41,6	42,9	50,5	31,1	34,3	37,6	48,2	55,9	59	73,8	61,4	78,2	52,3
BAM1	LjSGA_011445.1	Ljwgs_011445.1_at	BAM1_1	3956,5	717,5	928,7	1056,6	1203,4	344,8	773	428,3	703,2	1219,4	851,6	929,8	879	839,7	870
BAM1	LjSGA_032725.2	Ljwgs_032725.2_at	BAM1_2	1967,3	267,1	350,3	473,7	547	102,8	289,8	81,1	171,1	212,3	223,5	275,1	251,3	235,7	159,6
			BAM1	2961,9	492,3	639,5	765,15	875,2	223,8	531,4	254,7	437,15	715,85	537,55	602,45	565,15	537,7	514,8
BAM3	chr2.CM0021.1150.nd	chr2.CM0021.54_at	BAM3a_1	88,3	46,3	49,7	132,4	35,5	254,9	39,2	49,3	114,5	123,7	41,7	54,3	51,5	46,3	61,4
BAM3	chr2.CM0021.1290.nd	chr2.CM0021.61_at	BAM3a_2	74,9	23,3	32,4	116	17,5	329,6	19,8	25,6	157,3	274,3	27,3	27,6	26,5	30	56,6
			BAM3a	81,6	34,8	41,05	124,2	26,5	292,25	29,5	37,45	135,9	199	34,5	40,95	39	38,15	59
BAM3	chr2.CM0021.1220.nd	chr2.CM0021.56_at	BAM3b	36,8	68,9	81,2	33,4	42	35,1	273,9	508	154,8	169,2	155,9	148,9	131,6	91,2	60,4
BAM5	chr3.CM0152.120.nc	chr3.CM0152.11_at	BAM5	430,9	1058,8	1192,8	690,2	477,8	650,5	1300,8	10493,6	11607,2	6200,8	13779,5	14572,2	14730,5	13734,2	9890
BAM6	LjSGA_030993.1	Ljwgs_030993.1_at	BAM6	369,5	98,4	65,8	21,1	18,9	22,4	35,2	77,5	48,7	28,4	154,9	145,3	98,3	78,9	40,9
BAM7	LjT34L14.60.nc	Ljwgs_014587.1_at	BAM7	134,1	107,8	96,9	110,8	116,5	158	112,8	184,7	172,8	217,1	208,5	197,7	170,9	164,4	234,9
BAM7	LjT34L14.60.nc	Ljwgs_015904.1_at	BAM7	152,6	86,3	89,5	96	114,3	116,9	90,6	112,8	112,9	101,8	143,2	138	129,2	124,8	134,6
			BAM7	143,35	97,05	93,2	103,4	115,4	137,45	101,7	148,75	142,85	159,45	175,85	167,85	150,05	144,6	184,75
BAM8	chr2.CM0803.520.nc	chr2.CM0803.65_at	BAM8	313,3	255,7	223,1	230,3	261,7	367	238,3	315,9	333	310,9	429	455,4	448,4	417,9	313,6
BAM9	chr6.LjT15B19.140.nd	chr6.TM0756.17_at	BAM9	758	321,2	514,8	763,8	947,1	540,8	1232,7	151,6	355,4	296	246,4	355,8	408,1	361,4	301,4
DPE1	chr1.CM0032.500.nc	chr1.CM0032.64_at	DPE1	390,8	406,9	288,8	315,7	371,9	542,6	111	262,1	262,9	278	228,8	266,3	256,7	298	337,2
DPE2	LjSGA_011298.1	Ljwgs_011298.1_at	DPE2_1	514,1	124,4	156	103,9	156,9	162,5	110,2	83,9	106,4	61,6	113,1	140,7	125,2	131,1	59,9
DPE2	LjSGA_007380.1	Ljwgs_007380.1_at	DPE2_2	2057,8	981,5	1096,5	461,6	639,7	1022,6	645,2	970,6	914,7	931,5	1129,2	1174,4	1167	1061	1029,5
			DPE2	1285,95	552,95	626,25	282,75	398,3	592,55	377,7	527,25	510,55	496,55	621,15	657,55	646,1	596,05	544,7
PHS2	LjB08M07.80.nc	Ljwgs_039850.1_at	PHS2a	1498,5	805,7	814,5	330,7	452,9	447	859,1	899,3	736,2	565,1	746,3	769,1	642,4	639	465
PHS2	LjB08M07.80.nc	Ljwgs_046632.1_s_at	PHS2a	2088,6	1554	1593,3	540,9	687	808,7	1581,5	2453,7	1803	2212,1	1647,7	1618,9	1445,7	1299,6	1496,1
			PHS2a	1793,55	1179,85	1203,9	435,8	569,95	627,85	1220,3	1676,5	1269,6	1388,6	1197	1194	1044,05	969,3	980,55
PHS2	chr2.CM0373.1170.nd	chr2.TM1491.23_at	PHS2b	703,1	352,3	302,8	169,4	205,6	250,7	346,3	288,4	262,3	182,8	285,4	301,4	263,8	272,2	156,6
MEX1	chr3.CM0127.650.nc	chr3.CM0127.49_at	MEX1	1688,9	481,3	405,9	191	225,3	225	258,5	353,7	331,1	500,9	431,6	471,1	419,8	416,5	602,7

Sucrose synthase genes

Gene name	Gene locus	Probeset	Name	Leaf	Petiole	Stem	Root	Nod0d	Nod21d	Flower	Pod10d	Pod14d	Pod20d	Seed10d	Seed12d	Seed14d	Seed16d	Seed20d
SUS1	chr6.CM0013.290.nc	chr6.CM0013.38_s_at	SUS1	3547	9362,4	16322,5	14008,9	12599,8	9508,3	8877,3	11128,5	9270,7	3245,7	5114,7	5444,2	6651,2	7976,5	4788,9
SUS2	chr1.LjT30M08.30.nd	chr1.TM1573.7_at	SUS2	141,5	274	397,6	431,4	185,6	101,8	393,1	415,5	481,5	883,4	313	369,4	324,9	410,9	782,6
SUS3	chr4.CM0006.600.nc	BM1684.10_at	SUS3	714,6	4420,5	10221,1	13266,7	9139,9	17506,3	7509,3	6175,1	7173,7	5388	6052,8	6536	6061	6443,8	6892,8
SUS4	chr5.CM0239.870.nd	chr5.CM0773.16_at	SUS4	13,9	15,4	14,9	13,7	12,3	15,3	15,3	14,2	16,6	15,6	14,4	16,8	17,3	19,2	16,4

Table A1. *L. japonicus* starch metabolism genes and their corresponding probe sets and absolute transcript level values. Continued on next page.

Table 1A.B
Absolute transcript levels

Name	Leaf	Petiole	Stem	Root	Nod0d	Nod21d	Flower	Pod10d	Pod14d	Pod20d	Seed10d	Seed12d	Seed14d	Seed16d	Seed20d
PGI1	2094,1	838,1	661,6	508,5	578	684,1	465,4	726,1	717,9	876,6	1189,3	1086,5	1000,1	1039,5	1329,1
PGM1	1716,2	746,2	536,8	215,1	227,4	693,3	293	533,9	543,6	1048,2	571,4	581,3	517,2	512,6	938,2
APS1	6582,8	3132,6	2854,7	930	969,8	3922,6	1860,2	2492,4	2223,3	2400,9	1719,5	1765,7	1638,8	1722,9	1799,3
APL1	958,1	252,8	152,9	16,9	15,35	17	114,2	56,05	46,15	32,85	27,65	26,3	24,3	22,9	24,2
APL2a	80,1	193,5	227,9	222,7	176,3	733,4	273,9	657,6	381,4	492,5	536,6	458,5	376,7	303,1	259,9
APL2b	10,25	9,75	9,3	9,1	8,8	9,6	10,65	10,15	10,25	10,05	12,15	11,4	11,05	11,35	10,8
APL3	387,5	586,8	938,4	640,6	859,4	2219,2	760,5	1308,8	772,7	920,5	1393,9	1128,8	899,4	816	838,6
APL4	83,5	67,9	97,2	59,5	87,8	56	80,3	91,9	70,7	83,9	85,4	70,2	60,6	56,3	43,5
APL5	21,2	48,1	54,3	23,1	21,9	19,4	17,5	25,4	18,2	18,4	16,3	16,2	15,9	15,9	20,3
SS1	1275,75	365,75	310,45	82,15	98,4	111,55	390	327,6	313,25	318,1	214,25	226,9	216,85	226,85	225,2
SS2a	653,5	318,6	273,7	147,9	153,4	215	218,5	180,7	164,6	140,4	294,1	330,4	271,8	290,6	193,8
SS2b	68,2	22,45	35	20,75	15,3	10,2	12,95	10,9	15,6	10,6	10,7	10,25	9,95	10,2	10,85
SS5	508,8	270,5	218	35,4	59,4	903,5	78	263,8	215,2	393,5	221,4	204,3	201,8	208,3	438,1
GBSS1a	4990,2	2620,3	1985,7	1172,8	1369,4	2845,6	1708,3	5454,8	4084,5	3150,4	6559,2	5894,1	5663,2	5351,2	4383,7
GBSS1b	1439,5	958,9	557,6	62,7	115,3	346,3	389,5	548,4	383,4	410,4	617,9	522,1	429,8	366,3	399,3
SBE1	674	533,4	574,4	307,9	370,4	947,8	296,4	969,4	656,8	510,4	858,2	783,1	718,7	658	674
ISA1	641,8	241,6	172,2	99,6	197	117,9	120,5	336,9	270,7	351,1	396,6	369	363,8	334,8	430,8
ISA2	483,4	178	165,4	118,7	134,6	202,1	142,7	198,2	170,7	182,6	207,1	206	238,7	249,4	207,6
LDA	180,3	70,75	83,9	32,65	34,6	56,85	48,75	87,7	109,8	157,65	107,65	111,9	112,9	121,35	192,45
GWD1	542,8	218,5	296,1	164,7	244,3	245	143,8	179	206,5	200,6	140,9	143,4	130,7	135,6	149,4
GWD3	437,9	138,1	122,8	75,9	90,1	46,7	112,8	82,9	86,5	63	81,4	91,7	84,1	93	66,7
AMY1	42,8	37,7	25,8	31,7	31	39	29,9	35,2	35,2	34,9	30,5	28,2	36,2	33,8	37
AMY2	694,4	289,1	420,6	81,2	117,6	48,9	687,2	178,5	353,7	343,6	51	60,6	51,8	59,7	160,5
AMY3a	580,2	382,7	309,4	290,7	320,8	537,4	274,1	200,5	208,3	276,8	395,4	402,4	354,6	323,8	275,5
AMY3b	34,8	29,4	41,6	42,9	50,5	31,1	34,3	37,6	48,2	55,9	59	73,8	61,4	78,2	52,3
BAM1	2961,9	492,3	639,5	765,15	875,2	223,8	531,4	254,7	437,15	715,85	537,55	602,45	565,15	537,7	514,8
BAM3a	81,6	34,8	41,05	124,2	26,5	292,25	29,5	37,45	135,9	199	34,5	40,95	39	38,15	59
BAM3b	36,8	68,9	81,2	33,4	42	35,1	273,9	508	154,8	169,2	155,9	148,9	131,6	91,2	60,4
BAM5	430,9	1058,8	1192,8	690,2	477,8	650,5	1300,8	10493,6	11607,2	6200,8	13779,5	14572,2	14730,5	13734,2	9890
BAM6	369,5	98,4	65,8	21,1	18,9	22,4	35,2	77,5	48,7	28,4	154,9	145,3	98,3	78,9	40,9
BAM7	143,35	97,05	93,2	103,4	115,4	137,45	101,7	148,75	142,85	159,45	175,85	167,85	150,05	144,6	184,75
BAM8	313,3	255,7	223,1	230,3	261,7	367	238,3	315,9	333	310,9	429	455,4	448,4	417,9	313,6
BAM9	758	321,2	514,8	763,8	947,1	540,8	1232,7	151,6	355,4	296	246,4	355,8	408,1	361,4	301,4
DPE1	390,8	406,9	288,8	315,7	371,9	542,6	111	262,1	262,9	278	228,8	266,3	256,7	298	337,2
DPE2	1285,95	552,95	626,25	282,75	398,3	592,55	377,7	527,25	510,55	496,55	621,15	657,55	646,1	596,05	544,7
PHS2a	1793,55	1179,85	1203,9	435,8	569,95	627,85	1220,3	1676,5	1269,6	1388,6	1197	1194	1044,05	969,3	980,55
PHS2b	703,1	352,3	302,8	169,4	205,6	250,7	346,3	288,4	262,3	182,8	285,4	301,4	263,8	272,2	156,6
MEX1	1688,9	481,3	405,9	191	225,3	225	258,5	353,7	331,1	500,9	431,6	471,1	419,8	416,5	602,7
SUS1	3547	9362,4	16322,5	14008,9	12599,8	9508,3	8877,3	11128,5	9270,7	3245,7	5114,7	5444,2	6651,2	7976,5	4788,9
SUS2	141,5	274	397,6	431,4	185,6	101,8	393,1	415,5	481,5	883,4	313	369,4	324,9	410,9	782,6
SUS3	714,6	4420,5	10221,1	13266,7	9139,9	17506,3	7509,3	6175,1	7173,7	5388	6052,8	6536	6061	6443,8	6892,8
SUS4	13,9	15,4	14,9	13,7	12,3	15,3	15,3	14,2	16,6	15,6	14,4	16,8	17,3	19,2	16,4

SE absolute transcript levels

Name	Leaf	Petiole	Stem	Root	Nod0d	Nod21d	Flower	Pod10d	Pod14d	Pod20d	Seed10d	Seed12d	Seed14d	Seed16d	Seed20d
PGI1	63,2	37,8	21,4	26,2	27,2	37,1	24,4	3,9	36,6	22,3	6,5	21,1	61,5	9,6	42,8
PGM1	73,7	4,2	14,3	19,7	7,1	45,9	22,2	21,2	29,8	55,2	3,0	27,6	27,5	31,4	130,7
APS1	130,1	54,9	96,0	42,6	28,4	287,1	47,9	44,3	15,7	32,6	58,4	27,5	40,8	21,8	88,1
APL1	22,0	14,7	15,2	0,4	0,5	0,3	5,8	1,1	0,7	1,9	0,9	1,1	1,7	0,7	1,4
APL2a	8,8	6,1	3,5	18,6	18,1	5,0	14,9	16,0	5,7	43,7	23,9	28,3	74,2	46,2	13,4
APL2b	0,3	0,1	0,4	0,4	0,3	0,4	0,3	0,3	0,4	1,0	0,7	0,2	0,7	0,5	0,0
APL3	106,6	25,0	60,7	41,4	26,7	55,5	60,2	41,4	53,5	47,2	171,2	164,2	123,2	21,3	53,1
APL4	8,4	8,2	7,3	9,0	4,9	5,4	3,0	13,2	4,2	2,8	4,1	4,8	8,8	8,3	2,3
APL5	0,8	5,0	3,9	1,9	0,7	0,5	1,4	1,9	1,7	1,9	0,4	0,6	0,8	0,6	1,8
SS1	65,4	15,0	24,7	4,1	1,3	5,8	14,9	1,3	2,6	4,5	4,9	8,1	14,3	4,2	27,1
SS2a	17,9	7,9	21,2	11,5	10,7	21,3	5,5	9,8	9,8	6,0	15,8	22,6	22,9	0,7	16,9
SS2b	5,5	9,0	22,6	3,8	0,7	0,3	0,6	0,2	1,4	0,6	0,6	0,6	0,5	0,7	0,6
SS5	18,5	13,2	9,9	4,9	1,8	20,8	4,4	3,3	9,6	9,4	20,0	9,7	20,2	24,1	38,1
GBSS1a	741,7	264,9	78,5	105,3	48,1	162,8	65,6	61,0	12,3	159,9	205,8	147,6	251,3	143,4	113,9
GBSS1b	71,5	48,6	9,8	1,2	6,5	2,6	33,3	8,6	16,6	20,9	32,4	15,9	35,3	43,7	6,0
SBE1	130,1	43,5	29,8	13,0	27,5	20,0	17,1	7,1	7,6	15,3	44,7	53,3	53,5	18,0	85,1
ISA1	75,0	21,5	8,3	14,8	15,1	1,6	4,2	19,6	13,4	13,5	23,3	18,6	13,5	5,7	21,3
ISA2	47,9	10,8	8,4	5,6	9,2	14,5	4,0	6,5	3,5	8,9	3,6	6,3	6,7	1,8	4,7
LDA	16,6	3,7	12,5	3,0	2,7	2,5	1,5	2,9	4,8	13,7	4,2	3,1	4,0	11,5	1,6
GWD1	43,6	10,9	3,7	18,4	12,2	47,4	10,8	0,9	9,9	12,7	4,6	12,9	15,3	0,9	17,2
GWD3	13,1	0,7	9,8	1,6	2,8	7,2	6,1	3,0	2,5	0,9	5,0	7,6	5,3	8,3	9,4
AMY1	6,0	5,2	0,8	0,2	1,5	3,4	1,0	3,0	3,2	3,2	0,7	2,2	3,6	4,3	6,3
AMY2	53,8	13,3	3,3	2,7	2,9	4,7	29,3	9,4	11,8	23,1	1,5	5,5	3,9	6,3	12,9
AMY3a	20,6	44,5	20,2	22,6	21,7	16,2	6,8	3,9	3,1	24,7	10,3	41,7	24,2	7,7	46,4
AMY3b	2,0	0,9	3,1	1,4	1,0	4,4	1,4	3,2	2,4	6,4	2,7	7,0	4,1	3,3	10,8
BAM1	424,4	35,7	60,6	70,1	47,7	12,0	62,0	16,7	11,7	68,7	72,6	55,4	23,8	29,2	54,8
BAM3a	7,8	2,7	6,0	18,8	0,7	4,6	0,9	3,1	22,9	18,4	2,2	8,9	2,4	2,0	16,9
BAM3b	3,4	9,3	15,1	2,5	1,2	1,3	22,5	21,0	5,8	5,6	1,6	3,3	25,4	16,9	8,8
BAM5	18,2	70,0	7,8	26,6	53,7	22,9	13,6	158,4	167,8	440,7	21,4	362,0	599,2	421,2	1284,3
BAM6	19,0	7,7	11,4	0,6	1,1	1,4	2,0	1,6	3,4	2,4	2,9	4,2	8,0	2,2	4,8
BAM7	4,9	9,5	7,7	5,2	3,4	2,5	3,7	3,9	9,2	3,9	10,1	12,5	4,0	6,0	14,1
BAM8	14,6	23,3	11,3	16,0	16,8	5,6	7,4	15,0	27,0	12,4	19,1	24,8	17,9	5,9	18,2
BAM9	171,8	26,1	15,1	75,0	39,1	33,1	75,2	8,6	35,5	34,4	39,5	51,9	47,1	47,4	11,4
DPE1	25,4	32,9	4,7	6,0	13,6	49,5	5,0	0,7	10,0	7,7	16,7	6,0	12,1	17,1	15,4
DPE2	35,6	10,2	5,4	12,4	4,1	54,0	1,0	11,6	14,8	30,4	12,1	69,2	65,3	14,9	37,5
PHS2a	51,1	61,7	46,2	5,9	24,5	33,3	70,1	20,3	65,5	58,9	34,4	85,8	81,1	4,4	46,8
PHS2b	20,6	12,1	23,3	5,3	3,1	2,6	22,6	11,5	16,1	5,2	13,4	13,0	26,7	8,3	21,0
MEX1	39,6	46,2	12,6	16,5	22,3	14,8	13,7	21,1	22,5	36,0	20,4	65,6	11,2	9,5	6,3
SUS1	176,91	1303,19	257,01	319,46	233,06	620,81	2551,06	104,80	375,40	257,24	191,34	530,73	637,04	165,07	572,40
SUS2	16,48	25,40	20,71	10,91	3,37	12,41	107,14	14,24	45,52	48,22	7,84	19,24	7,83	50,11	102,34
SUS3	31,52	662,68	281,35	358,94	250,86	532,37	2893,84	120,62	328,44	225,18	58,27	790,53	579,93	127,59	507,10
SUS4	0,91	1,56	0,70	1,45	0,49	1,84	1,84	0,80	0,38	0,27	0,58	0,47	2,08	0,89	0,50

Table A1. *L. japonicus* starch metabolism genes and their corresponding probe sets and absolute transcript level values.
Continued on next page.

Table 1A.C
Log2 transcript levels

Name	Leaf	Petiole	Stem	Root	Nod0d	Nod21d	Flower	Pod10d	Pod14d	Pod20d	Seed10d	Seed12d	Seed14d	Seed16d	Seed20d
PGI1	11,0	9,7	9,4	9,0	9,2	9,4	8,9	9,5	9,5	9,8	10,2	10,1	10,0	10,0	10,4
PGM1	10,7	9,5	9,1	7,7	7,8	9,4	8,2	9,1	9,1	10,0	9,2	9,2	9,0	9,0	9,9
APS1	12,7	11,6	11,5	9,9	9,9	11,9	10,9	11,3	11,1	11,2	10,7	10,8	10,7	10,8	10,8
APL1	9,9	8,0	7,3	4,1	3,9	4,1	6,8	5,8	5,5	5,0	4,8	4,7	4,6	4,5	4,6
APL2a	6,3	7,6	7,8	7,8	7,5	9,5	8,1	9,4	8,6	8,9	9,1	8,8	8,6	8,2	8,0
APL2b	3,4	3,3	3,2	3,2	3,1	3,3	3,4	3,3	3,4	3,3	3,6	3,5	3,5	3,5	3,4
APL3	8,6	9,2	9,9	9,3	9,7	11,1	9,6	10,4	9,6	9,8	10,4	10,1	9,8	9,7	9,7
APL4	6,4	6,1	6,6	5,9	6,5	5,8	6,3	6,5	6,1	6,4	6,4	6,1	5,9	5,8	5,4
APL5	4,4	5,6	5,8	4,5	4,5	4,3	4,1	4,7	4,2	4,2	4,0	4,0	4,0	4,0	4,3
SS1	10,3	8,5	8,3	6,4	6,6	6,8	8,6	8,4	8,3	8,3	7,7	7,8	7,8	7,8	7,8
SS2a	9,4	8,3	8,1	7,2	7,3	7,7	7,8	7,5	7,4	7,1	8,2	8,4	8,1	8,2	7,6
SS2b	6,1	4,5	5,1	4,4	3,9	3,4	3,7	3,4	4,0	3,4	3,4	3,4	3,3	3,4	3,4
SS5	9,0	8,1	7,8	5,1	5,9	9,8	6,3	8,0	7,7	8,6	7,8	7,7	7,7	7,7	8,8
GBSS1a	12,3	11,4	11,0	10,2	10,4	11,5	10,7	12,4	12,0	11,6	12,7	12,5	12,5	12,4	12,1
GBSS1b	10,5	9,9	9,1	6,0	6,8	8,4	8,6	9,1	8,6	8,7	9,3	9,0	8,7	8,5	8,6
SBE1	9,4	9,1	9,2	8,3	8,5	9,9	8,2	9,9	9,4	9,0	9,7	9,6	9,5	9,4	9,4
ISA1	9,3	7,9	7,4	6,6	7,6	6,9	6,9	8,4	8,1	8,5	8,6	8,5	8,5	8,4	8,8
ISA2	8,9	7,5	7,4	6,9	7,1	7,7	7,2	7,6	7,4	7,5	7,7	7,7	7,9	8,0	7,7
LDA	7,5	6,1	6,4	5,0	5,1	5,8	5,6	6,5	6,8	7,3	6,8	6,8	6,8	6,9	7,6
GWD1	9,1	7,8	8,2	7,4	7,9	7,9	7,2	7,5	7,7	7,6	7,1	7,2	7,0	7,1	7,2
GWD3	8,8	7,1	6,9	6,2	6,5	5,5	6,8	6,4	6,4	6,0	6,3	6,5	6,4	6,5	6,1
AMY1	5,4	5,2	4,7	5,0	5,0	5,3	4,9	5,1	5,1	5,1	4,9	4,8	5,2	5,1	5,2
AMY2	9,4	8,2	8,7	6,3	6,9	5,6	9,4	7,5	8,5	8,4	5,7	5,9	5,7	5,9	7,3
AMY3a	9,2	8,6	8,3	8,2	8,3	9,1	8,1	7,6	7,7	8,1	8,6	8,7	8,5	8,3	8,1
AMY3b	5,1	4,9	5,4	5,4	5,7	5,0	5,1	5,2	5,6	5,8	5,9	6,2	5,9	6,3	5,7
BAM1	11,5	8,9	9,3	9,6	9,8	7,8	9,1	8,0	8,8	9,5	9,1	9,2	9,1	9,1	9,0
BAM3a	6,4	5,1	5,4	7,0	4,7	8,2	4,9	5,2	7,1	7,6	5,1	5,4	5,3	5,3	5,9
BAM3b	5,2	6,1	6,3	5,1	5,4	5,1	8,1	9,0	7,3	7,4	7,3	7,2	7,0	6,5	5,9
BAM5	8,8	10,0	10,2	9,4	8,9	9,3	10,3	13,4	13,5	12,6	13,8	13,8	13,8	13,7	13,3
BAM6	8,5	6,6	6,0	4,4	4,2	4,5	5,1	6,3	5,6	4,8	7,3	7,2	6,6	6,3	5,4
BAM7	7,2	6,6	6,5	6,7	6,9	7,1	6,7	7,2	7,2	7,3	7,5	7,4	7,2	7,2	7,5
BAM8	8,3	8,0	7,8	7,8	8,0	8,5	7,9	8,3	8,4	8,3	8,7	8,8	8,8	8,7	8,3
BAM9	9,6	8,3	9,0	9,6	9,9	9,1	10,3	7,2	8,5	8,2	7,9	8,5	8,7	8,5	8,2
DPE1	8,6	8,7	8,2	8,3	8,5	9,1	6,8	8,0	8,0	8,1	7,8	8,1	8,0	8,2	8,4
DPE2	10,3	9,1	9,3	8,1	8,6	9,2	8,6	9,0	9,0	9,0	9,3	9,4	9,3	9,2	9,1
PHS2a	10,8	10,2	10,2	8,8	9,2	9,3	10,3	10,7	10,3	10,4	10,2	10,2	10,0	9,9	9,9
PHS2b	9,5	8,5	8,2	7,4	7,7	8,0	8,4	8,2	8,0	7,5	8,2	8,2	8,0	8,1	7,3
MEX1	10,7	8,9	8,7	7,6	7,8	7,8	8,0	8,5	8,4	9,0	8,8	8,9	8,7	8,7	9,2
SUS1	11,8	13,2	14,0	13,8	13,6	13,2	13,1	13,4	13,2	11,7	12,3	12,4	12,7	13,0	12,2
SUS2	7,1	8,1	8,6	8,8	7,5	6,7	8,6	8,7	8,9	9,8	8,3	8,5	8,3	8,7	9,6
SUS3	9,5	12,1	13,3	13,7	13,2	14,1	12,9	12,6	12,8	12,4	12,6	12,7	12,6	12,7	12,8
SUS4	3,8	3,9	3,9	3,8	3,6	3,9	3,9	3,8	4,1	4,0	3,8	4,1	4,1	4,3	4,0

SE Log2 transcript levels

Name	Leaf	Petiole	Stem	Root	Nod0d	Nod21d	Flower	Pod10d	Pod14d	Pod20d	Seed10d	Seed12d	Seed14d	Seed16d	Seed20d
PGI1	0,0	0,1	0,0	0,1	0,1	0,1	0,1	0,0	0,1	0,0	0,0	0,0	0,1	0,0	0,0
PGM1	0,1	0,0	0,0	0,1	0,0	0,1	0,1	0,1	0,1	0,1	0,0	0,1	0,1	0,1	0,2
APS1	0,0	0,0	0,0	0,1	0,0	0,1	0,0	0,0	0,0	0,0	0,0	0,0	0,0	0,0	0,1
APL1	0,0	0,1	0,2	0,0	0,0	0,0	0,1	0,0	0,0	0,1	0,0	0,1	0,1	0,0	0,1
APL2a	0,2	0,0	0,0	0,1	0,2	0,0	0,1	0,0	0,0	0,1	0,1	0,1	0,3	0,2	0,1
APL2b	0,0	0,0	0,1	0,1	0,1	0,1	0,0	0,0	0,1	0,1	0,1	0,0	0,1	0,1	0,0
APL3	0,4	0,1	0,1	0,1	0,0	0,0	0,1	0,0	0,1	0,1	0,2	0,2	0,2	0,0	0,1
APL4	0,1	0,2	0,1	0,2	0,1	0,1	0,1	0,2	0,1	0,0	0,1	0,1	0,2	0,2	0,1
APL5	0,1	0,2	0,1	0,1	0,0	0,0	0,1	0,1	0,1	0,2	0,0	0,1	0,1	0,1	0,1
SS1	0,1	0,1	0,1	0,1	0,0	0,1	0,1	0,0	0,0	0,0	0,0	0,1	0,1	0,0	0,2
SS2a	0,0	0,0	0,1	0,1	0,1	0,1	0,0	0,1	0,1	0,1	0,1	0,1	0,1	0,0	0,1
SS2b	0,1	0,5	0,9	0,3	0,1	0,0	0,1	0,0	0,1	0,1	0,1	0,1	0,1	0,1	0,1
SS5	0,1	0,1	0,1	0,2	0,0	0,0	0,1	0,0	0,1	0,0	0,1	0,1	0,1	0,2	0,1
GBSS1a	0,2	0,1	0,1	0,1	0,0	0,1	0,1	0,0	0,0	0,1	0,0	0,0	0,1	0,0	0,0
GBSS1b	0,1	0,1	0,0	0,0	0,1	0,0	0,1	0,0	0,1	0,1	0,1	0,0	0,1	0,2	0,0
SBE1	0,3	0,1	0,1	0,1	0,1	0,0	0,1	0,0	0,0	0,0	0,1	0,1	0,1	0,0	0,2
ISA1	0,2	0,1	0,1	0,2	0,1	0,0	0,1	0,1	0,1	0,1	0,1	0,1	0,1	0,0	0,1
ISA2	0,1	0,1	0,1	0,1	0,1	0,1	0,0	0,0	0,0	0,1	0,0	0,0	0,0	0,0	0,0
LDA	0,1	0,1	0,2	0,1	0,1	0,1	0,0	0,0	0,1	0,1	0,1	0,0	0,1	0,1	0,0
GWD1	0,1	0,1	0,0	0,2	0,1	0,3	0,1	0,0	0,1	0,1	0,0	0,1	0,2	0,0	0,2
GWD3	0,0	0,0	0,1	0,0	0,0	0,2	0,1	0,1	0,0	0,0	0,1	0,1	0,1	0,1	0,2
AMY1	0,2	0,2	0,0	0,0	0,1	0,1	0,0	0,1	0,1	0,1	0,0	0,1	0,1	0,2	0,2
AMY2	0,1	0,1	0,0	0,0	0,0	0,1	0,1	0,1	0,0	0,1	0,0	0,1	0,1	0,1	0,1
AMY3a	0,1	0,2	0,1	0,1	0,1	0,0	0,0	0,0	0,0	0,1	0,0	0,1	0,1	0,0	0,3
AMY3b	0,1	0,0	0,1	0,0	0,0	0,2	0,1	0,1	0,1	0,2	0,1	0,1	0,1	0,1	0,3
BAM1	0,2	0,1	0,1	0,1	0,1	0,1	0,2	0,1	0,0	0,1	0,2	0,1	0,1	0,1	0,2
BAM3a	0,1	0,1	0,2	0,2	0,0	0,0	0,0	0,1	0,3	0,1	0,1	0,3	0,1	0,1	0,4
BAM3b	0,1	0,2	0,3	0,1	0,0	0,1	0,1	0,1	0,1	0,0	0,0	0,0	0,3	0,3	0,2
BAM5	0,1	0,1	0,0	0,1	0,2	0,0	0,0	0,0	0,0	0,1	0,0	0,0	0,1	0,0	0,2
BAM6	0,1	0,1	0,3	0,0	0,1	0,1	0,1	0,0	0,1	0,1	0,0	0,0	0,1	0,0	0,2
BAM7	0,0	0,1	0,1	0,1	0,0	0,0	0,1	0,0	0,1	0,0	0,1	0,1	0,0	0,1	0,1
BAM8	0,1	0,1	0,1	0,1	0,1	0,0	0,0	0,1	0,1	0,1	0,1	0,1	0,1	0,0	0,1
BAM9	0,3	0,1	0,0	0,1	0,1	0,1	0,1	0,1	0,2	0,2	0,2	0,2	0,2	0,2	0,1
DPE1	0,1	0,1	0,0	0,0	0,1	0,1	0,1	0,0	0,1	0,0	0,1	0,0	0,1	0,1	0,1
DPE2	0,0	0,0	0,0	0,1	0,0	0,1	0,0	0,0	0,0	0,1	0,0	0,1	0,2	0,0	0,1
PHS2a	0,0	0,1	0,1	0,0	0,1	0,1	0,1	0,0	0,1	0,1	0,0	0,1	0,1	0,0	0,1
PHS2b	0,0	0,0	0,1	0,0	0,0	0,0	0,1	0,1	0,1	0,0	0,1	0,1	0,2	0,0	0,2
MEX1	0,0	0,1	0,0	0,1	0,2	0,1	0,1	0,1	0,1	0,1	0,1	0,2	0,0	0,0	0,0
SUS1	0,07	0,22	0,02	0,03	0,03	0,10	1,34	0,01	0,06	0,12	0,05	0,14	0,14	0,03	0,16
SUS2	0,16	0,14	0,07	0,04	0,03	0,18	0,93	0,05	0,14	0,08	0,04	0,07	0,04	0,17	0,20
SUS3	0,06	0,22	0,04	0,04	0,04	0,04	1,45	0,03	0,07	0,06	0,01	0,17	0,14	0,03	0,10
SUS4	0,09	0,15	0,07	0,15	0,06	0,17	0,39	0,08	0,03	0,02	0,06	0,04	0,17	0,07	0,04

Table A1. *L. japonicus* starch metabolism genes and their corresponding probe sets and absolute transcript level values.
Continued on next page.

Table A1. *L. japonicus* starch metabolism genes and their corresponding probe sets and absolute transcript level values. Continued.
A. Genes and the name and transcript levels of their corresponding probe sets. Gene names followed by '_#' (e.g. SS1_1, SS1_2 correspond to partial sequences of the same gene locus) while gene names followed by 'a' or 'b' correspond to different isoforms. In cases where multiple probe sets corresponded to a unique gene locus (highlighted in pale yellow), or when a gene had several corresponding clones or LjSGA sequences, and therefore multiple corresponding probe sets (highlighted in yellow), a median value (written in red) was calculated. **B**. Absolute transcript levels and their associated standard error (SE) values (n=3). Coloured in grey are transcripts whose expression is too low (below ca. 60) to be considered as significant. Above this threshold, transcripts with weak (values between 60 and 200), medium (between 200 and 1000) and high level of expression (above 1000) are highlighted in white, yellow, and red, respectively. **C**. Absolute transcript levels and their associated SE. Coloured in grey are transcripts whose expression is considered as background signal (below ca. 6).

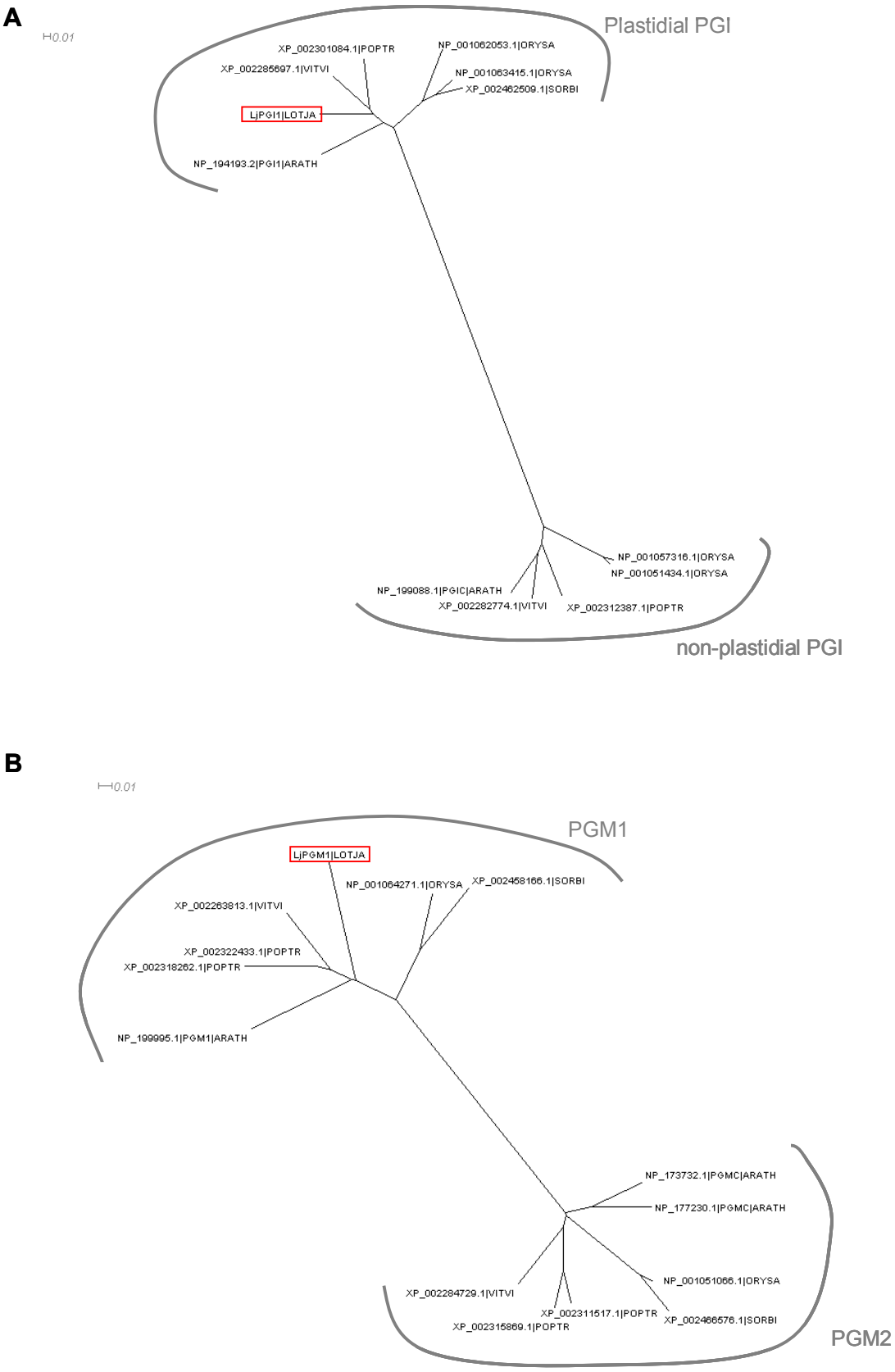

Figure A2. Phylograms of starch metabolism genes families in several plant species, including *L. japonicus*.
Continued on next page.

E

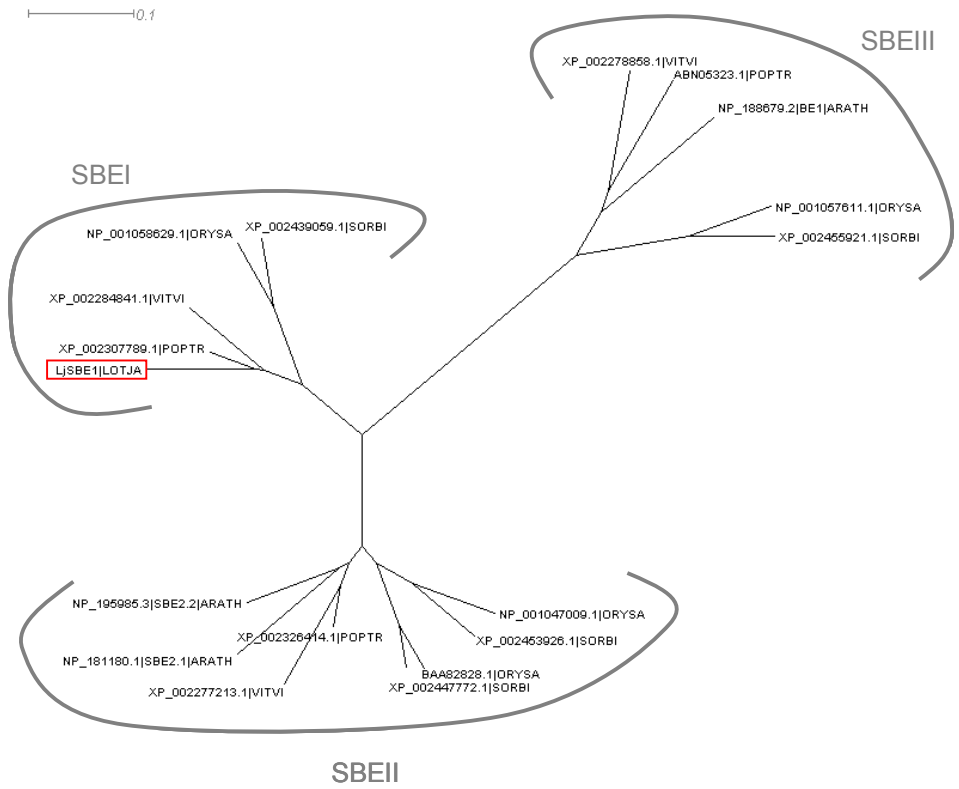

F

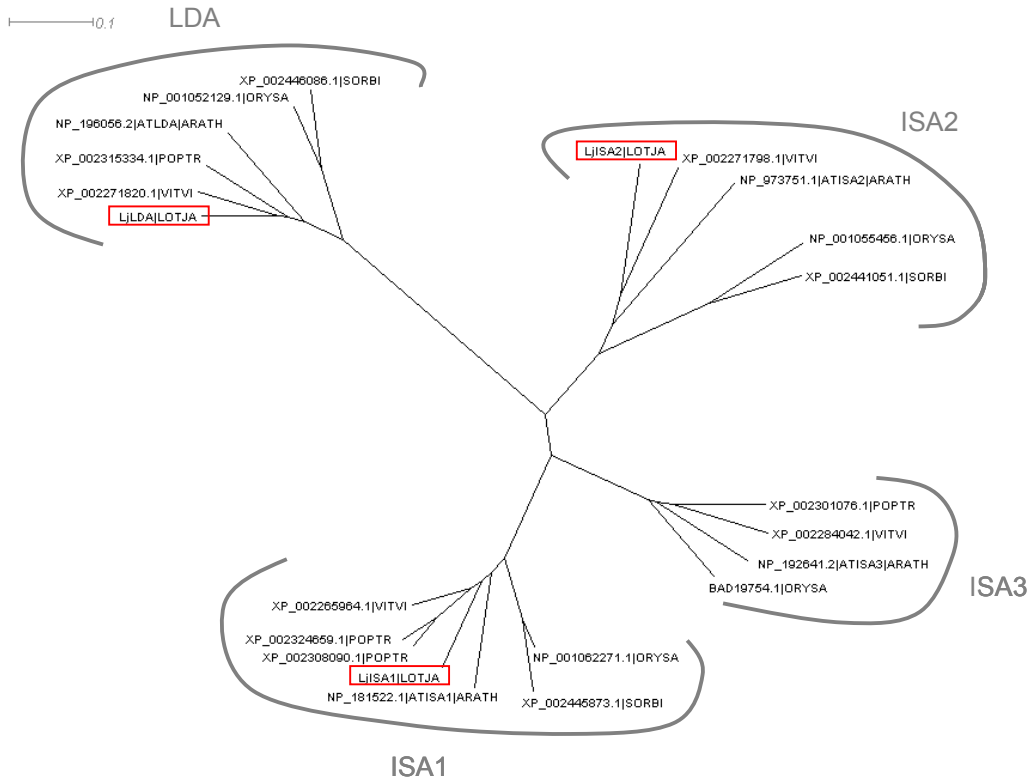

Figure A2. Phylograms of starch metabolism genes families in several plant species, including *L. japonicus*.
Continued on next page.

Figure A2. Phylograms of starch metabolism genes families in several plant species, including *L. japonicus*.
Continued on next page.

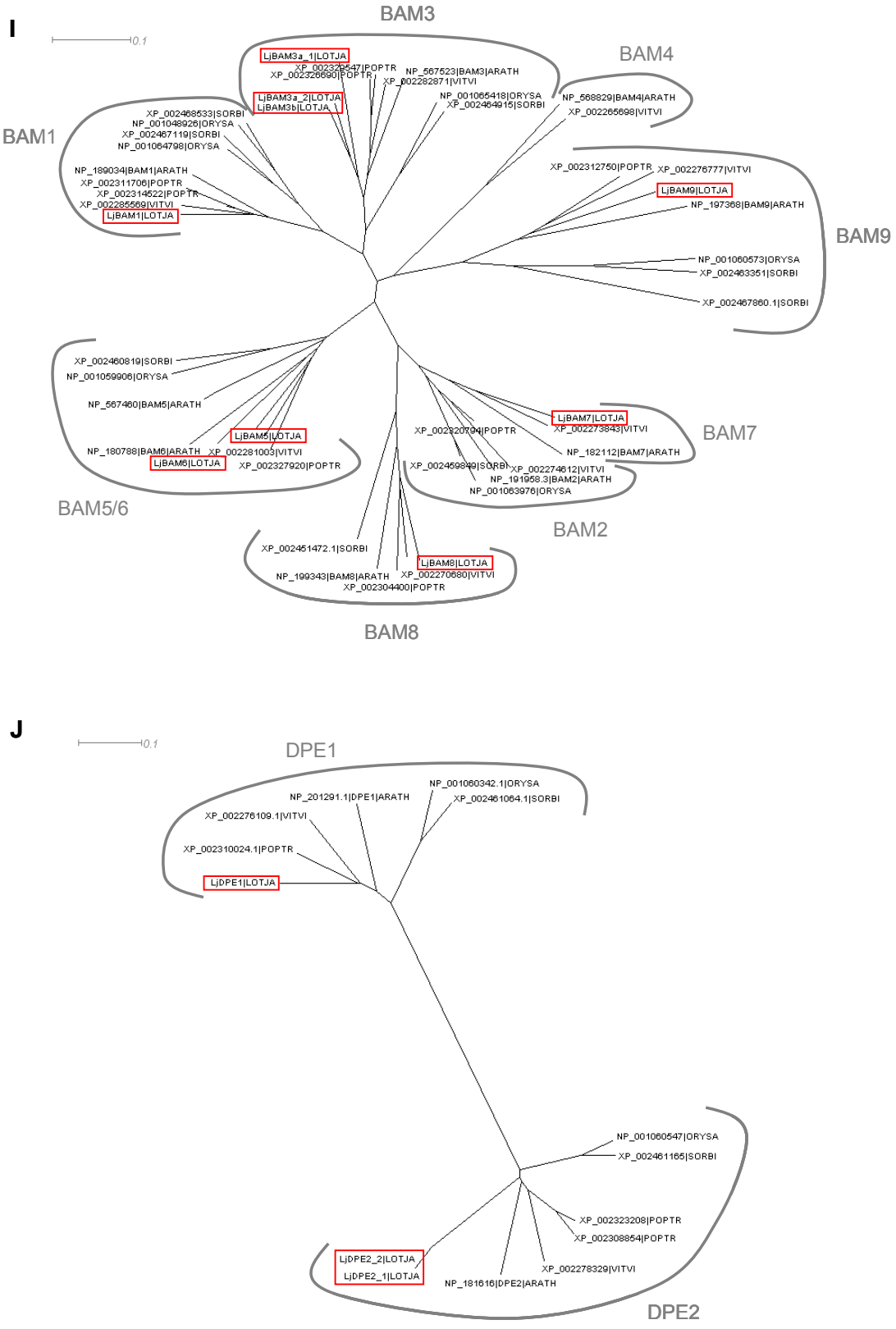

Figure A2. Phylograms of starch metabolism genes families in several plant species, including *L. japonicus*.
Continued on next page.

K

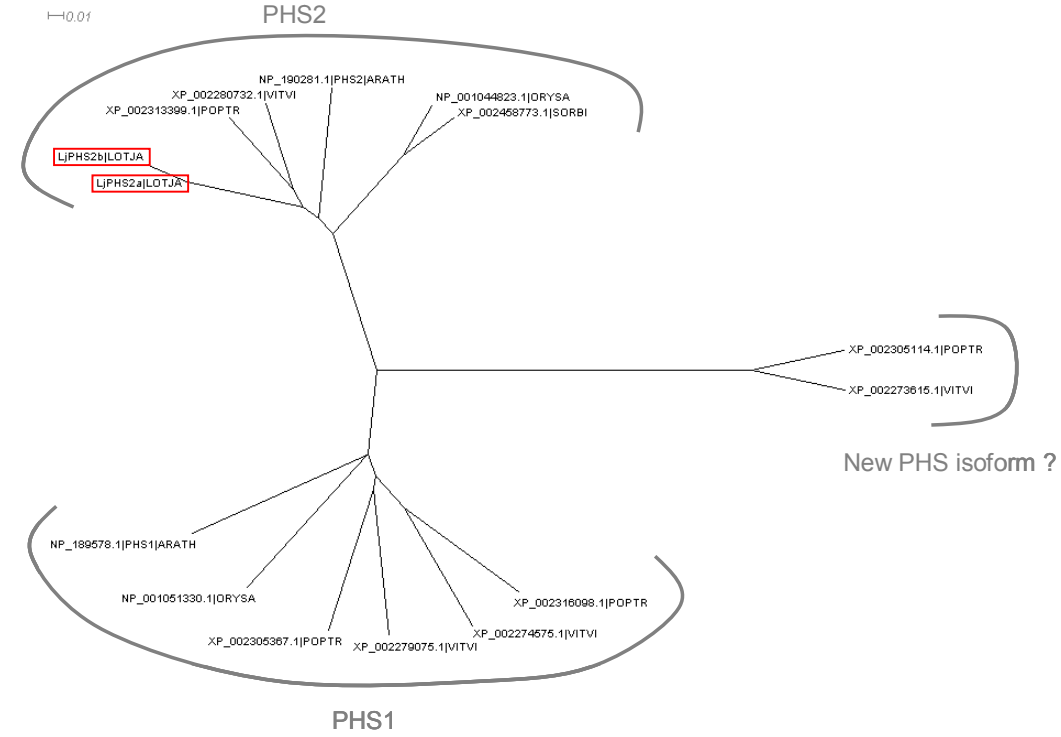

L

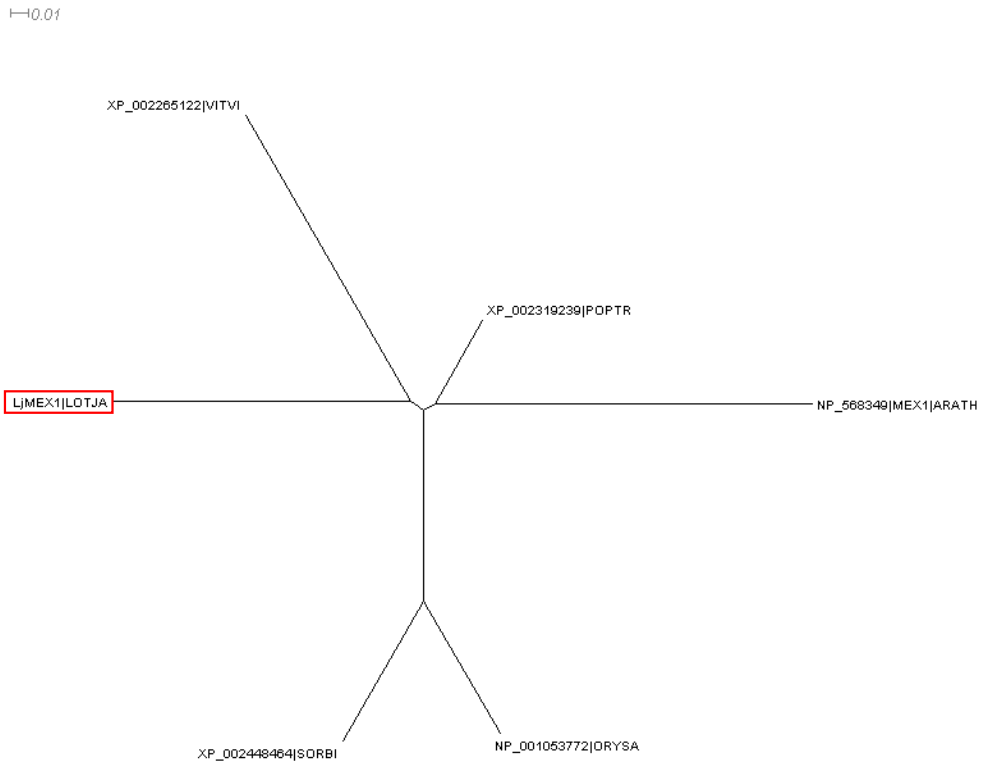

Figure A2. Phylograms of starch metabolism genes families in several plant species, including *L. japonicus*.
Continued on next page.

Figure A2. Phylograms of starch metabolism genes families in several plant species, including *L. japonicus*. Continued.
Protein sequences were retrieved from NCBI and aligned using the program Clustal W2. The phylogenetic trees were drawn using Dendroscope. Phylograms were drawn for of all the families of starch metabolism genes for which homologs could be identified in the genome of *L. japonicus* (framed in red). The name given for each sequence corresponds to the protein accession number followed by the organism name. Their corresponding protein sequence, gene name and sequence together with other links and depository informations can be readily obtained from browsing the NCBI database with the accession number given on the phylograms. Genes and the name and transcript levels of their corresponding probe sets. Gene names followed by '_#' (e.g. SS1_1, SS1_2 correspond to partial sequences of the same gene locus) while gene names followed by 'a' or 'b' correspond to different isoforms. **A**. PGI, phosphoglucoisomerase; **B**. PGM, phosphoglucomutase; **C**. AGPase, ADP-glucose pyrophosphorylase; **D**. SS, starch synthase; **E**. SBE, starch branching enzyme; **F**. DBE, starch debranching enzyme; **G**. GWD, glucan, water dikinase; **H**. AMY, alpha-amylase; **I**. BAM, beta-amylases; **J**. DPE, disproportionating enzyme/transglucosidase; **K**. PHS, alpha-glucan phosphorylase; **L**. MEX1, maltose transporter 1. Abbreviations of the plant species names: ARATH, *Arabidopsis thaliana*; VITVI, *Vitis vinifera*; POPTR, *Populus trichocarpa*; LOTJA, *Lotus japonicus*; ORYSA, *Orysa sativa*; SORBI, *Sorghum bicolor*.

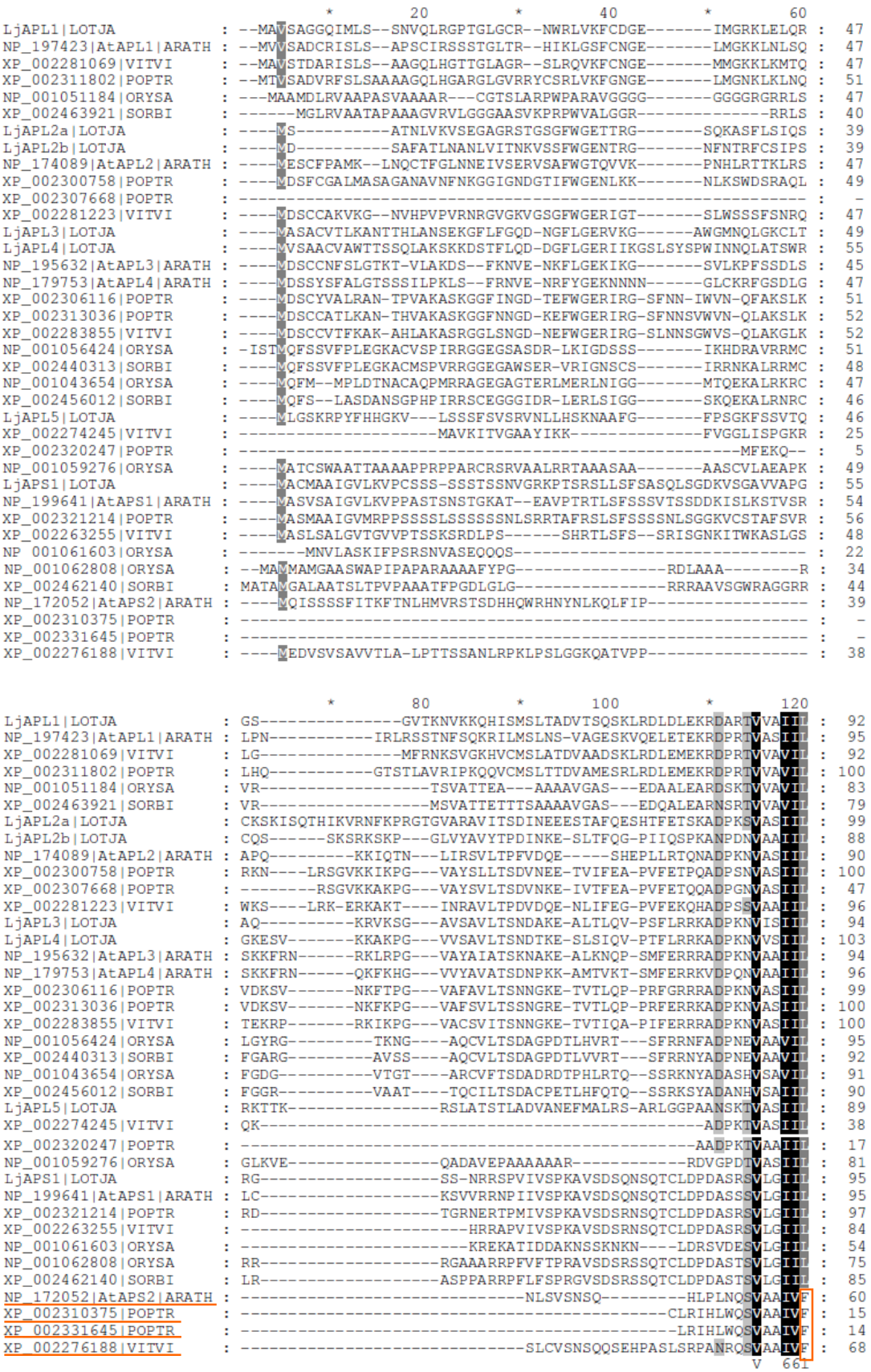

Figure A3. Comparison of the amino acid sequences encoded by *L. japonicus* AGPase subunits and SS5 genes with those of other species.
Continued on next page.

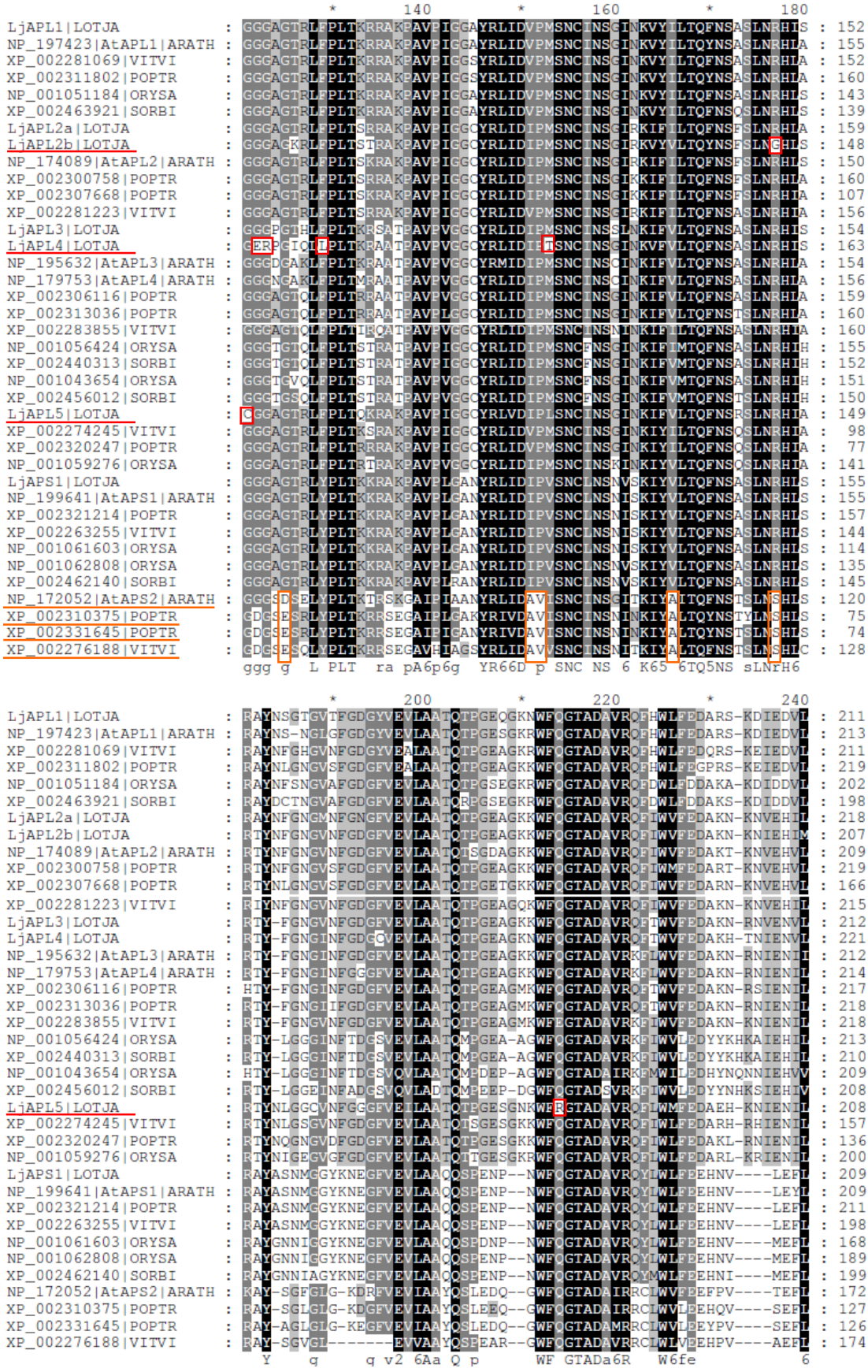

Figure A3. Comparison of the amino acid sequences encoded by *L. japonicus* AGPase subunits and SS5 genes with those of other species.
Continued on next page.

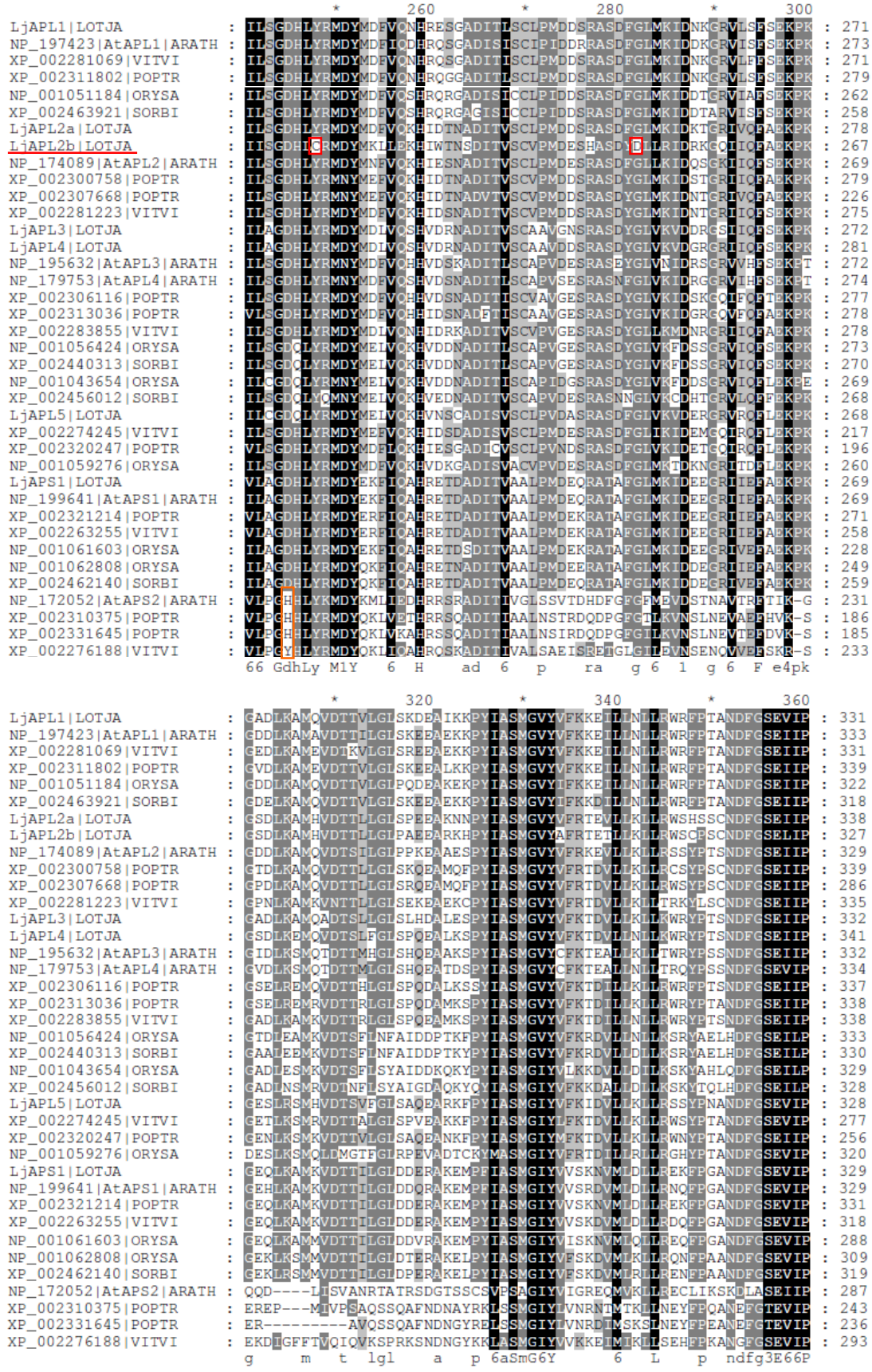

Figure A3. Comparison of the amino acid sequences encoded by *L. japonicus* AGPase subunits and SS5 genes with those of other species.
Continued on next page.

Figure A3. Comparison of the amino acid sequences encoded by *L. japonicus* AGPase subunits and SS5 genes with those of other species.
Continued on next page.

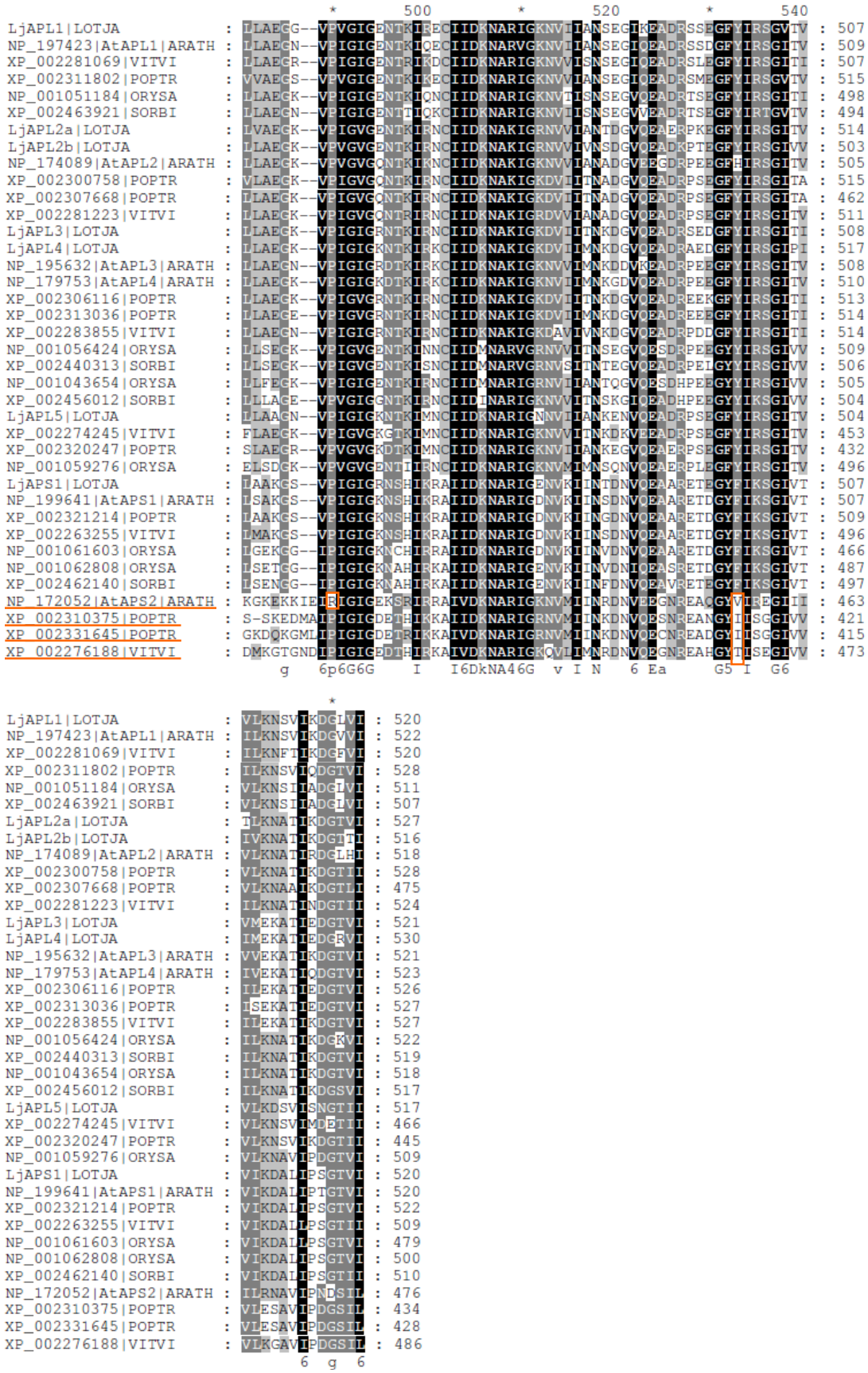

Figure A3. Comparison of the amino acid sequences encoded by *L. japonicus* AGPase subunits and SS5 genes with those of other species.
Continued on next page.

B

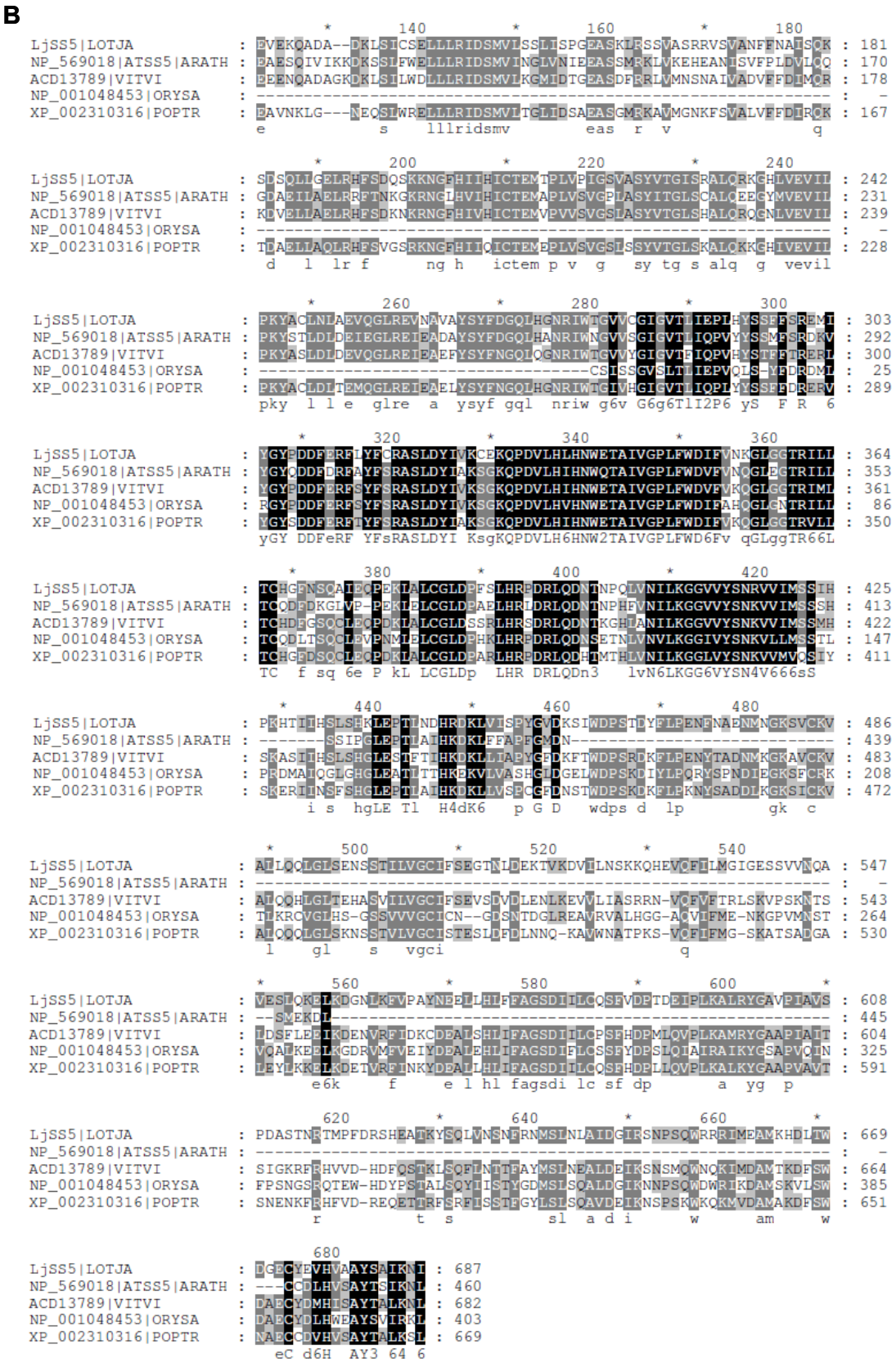

Figure A3. Comparison of the amino acid sequences encoded by *L. japonicus* AGPase subunits and SS5 genes with those of other species.
Continued on next page.

Figure A3. Comparison of the amino acid sequences encoded by *L. japonicus* AGPase subunits and SS5 genes with those of other species. Continued.
A. AGPase proteins sequence alignment. The alignment was made with the programs Clustal W2 (default settings) and GeneDoc. Stricly conserved residues are highlighted in black, less conserved residues are in grey. Residues framed in red are residues that are not conserved in a unique or small group of protein sequences (their corresponding name on the left is highlighted in red) while showing a high level of conservation across all other protein sequences analysed. Several of these residues have been shown in previous studies to be important for the AGPase enzyme activity as described in Chapter 4, and their change to another residues is likely to lead to a lost of protein function. **B**. Alignment of the SS5 protein sequence of several plant species showing the absence of predicted amino acid sequence in 3' and 5' of the *A. thaliana* and *Orysa sativa* proteins in comparison to those of the other species analysed. Abbreviations: ARATH, *Arabidopsis thaliana*; VITVI, *Vitis vinifera*; POPTR, *Populus trichocarpa*; LOTJA, *Lotus japonicus*; ORYSA, *Orysa sativa*; SORBI, *Sorghum bicolor*.

Protein	Clone/LjSGA accession	Status	Sequence
LjPGI1	chr1.LjT29N14.30.nd	Complete	MASISGICSSSPTLNKYQNQTPSSTSFSIRRRTHLLPTFPTRTKLPLTRSVAREAPADLS AVTKHRLEKNPAALWQRYVDWLYQHKDLGLYIDVSRVGFTDEFLLEMEPRFQAAFRAMAE LEKGAIANPDEGRMVGHYWLRDSTRAPNSFLKAKIDDTLDAICRFADDIVSGKIKPPSSP EGRFTQILSVGIGGSALGPQFVAEALAPDNPPLKIRFIDNTDPAGIDHQIAQLGSELAST LVIVISKSGGTPETRNGLLEVQKAFREAGLSFPKQGVAITQENSLLDNTARIEGWLARFP MFDWVGGRTSEMSAVGLLPAALQSIDIREMIAGASLMDEATRSTVIRNNPAALLALCWYW ATDGVGSKDMVILPYKDSMLLFSRYLQQLVMESLGKEFDLDGNRVNQGLSVYGNKGSTDQ HAYIQQLREGVHNFFATFIEVLRDRPPGHDWELEPGVTCGDYLFGMLQGTRSALYANDRE SITVTVQEVTPRSVGALIALYERAVGIYASIVNINAYHQPGVEAGKKAAGEVLALQKRVL TVLNEASCKEPVEPLTLEEVADRCHAPEDIEIIYKIIAHMAANDRALIAEGSCGSPRSIK VFLGECNVDELYA
LjPGM1	chr5.CM0953.200.nc	Complete	MAFSSSSRLDHFNIISAFKPQNSILPPSLKPSSYLPSSSFKFRNLLPFRIRYASTIRATS SSSSPSSPSTTIDQSDDGIKINSIPTKPIEGQKTGTSGLRKKVKVFMEENYLANWIQALF NSLPPEDYKNGVLVLGGDGRYFNKEAAQIIIKIAAGNGVGKILVGKEGVLSTPAVSAVIR KRKANGGFIMSASHNPGGPEYDWGIKFNYSSGQPAPESITDKIYGNTLSISEIKIADIPD VYLSNVGVTEFGSFSVEVIDPVSDYLELLETVFDFQLIKGLLSRPDFRFIFDAMHAVTGA YAKPIFVDKLGASPDSILNGIPLEDFGHGHPDPNLTYAKDLVNILYAENGPDFGAASDGD GDRNMILGRSFFVTPSDSVAVIAANAKEAIPYFKNGVNGLARSMPTSGALDRVAEKLNLP FFEVPTGWKFFGNLMDAGKLSICGEESFGTGSDHIREKDGIWAVLAWLSIIAHRNKDKKP EEKLISVSDVMMEYWATYGRNFFSRYDYEECESEGANKMIAYLRETVSNSKPGDKYGSYV LQFADDYTYTDPVDGSVVSKQGVRFVFTDGSRIIYRLSGTGSAGATVRVYIEQFEADVSK HDVDAQIALKPLIDLALSVSKLKDFTGREKPTVIT
LjAPS1	chr2.CM0191.60.nc	Complete	MACMAAIGVLKVPCSSSSSSTSSNVGRKPTSRSLLSFSASQLSGDKVSGAVVAPGRGSSN RRSPVIVSPKAVSDSQNSQTCLDPDASRSVLGIILGGGAGTRLYPLTKKRAKPAVPLGAN YRLIDIPVSNCLNSNVSKIYVLTQFNSASLNRHLSRAYASNMGGYKNEGFVEVLAAQQSP ENPNWFQGTADAVRQYLWLFEEHNVLEFLVLAGDHLYRMDYEKFIQAHRETDADITVAAL PMDEQRATAFGLMKIDEEGRIIEFAEKPKGEQLKAMKVDTTILGLDDERAKEMPFIASMG IYVVSKNVMLDLLREKFPGANDFGSEVIPGATSIGMRVQAYLYDGYWEDIGTIEAFYNAN LGITKKPVPDFSFYDRSSPIYTQPRYLPPSKMLDADITDSVIGEGCVIKNCKIHHSVVGL RSCVSEGAIIEDTLLMGADYYETDADKRFLAAKGSVPIGIGRNSHIKRAIIDKNARIGEN VKIINTDNVQEAARETEGYFIKSGIVTVIKDALIPSGTVI
LjAPL1	chr4.CM0387.180.nc	Complete	MAVSAGGQIMLSSNVQLRGPTGLGCRNWRLVKFCDGEIMGRKLELQRGSGVTKNVKKQHI SMSLTADVTSQSKLRDLDLEKRDARTVVAIILGGGAGTRLFPLTKRRAKPAVPIGGAYRL IDVPMSNCINSGINKVYILTQFNSASLNRHISRAYNSGTGVTFGDGYVEVLAATQTPGEQ GKNWFQGTADAVRQFHWLFEDARSKDIEDVLILSGDHLYRMDYMDFVQNHRESGADITLS CLPMDDSRASDFGLMKIDNKGRVLSFSEKPKGADLKAMQVDTTVLGLSKDEAIKKPYIAS MGVYVFKKEILLNLLRWRFPTANDFGSEVIPASAAEFYMKAYLFNDYWEDIGTIRSFFEA NLALTEHPSKFSFYDAAKPMYTSRRNLPPSKIDNSKIVDSIIAHGSFLNNAFIEHSVVGI RSRINSNVHLKDTVMLGADFYETETEAAALLAEGGVPVGIGENTKIRECIIDKNARIGKN VIIANSEGIKEADRSSEGFYIRSGVTVVLKNSVIKDGLVI
LjAPL2a	chr1.LjT34C24.40.nc	Complete	MSATNLVKVSEGAGRSTGSGFWGETTRGSQKASFLSIQSCKSKISQTHIKVRNFKPRGTG VARAVITSDINEEESTAFQESHTFETSKADPKSVASIILGGGAGTRLFPLTSRRAKPAVP IGGCYRLIDIPMSNCINSGIRKIFILTQFNSFSLNRHLARAYNFGNGMNFGNGFVEVLAA TQTPGEAGKKWFQGTADAVRQFIWVFEDAKNKNVEHILILSGDHLYRMDYMDFVQKHIDT NADITVSCLPMDDSRASDFGLMKIDKTGRIVQFAEKPKGSDLKAMHVDTTLLGLSPEEAK NNPYIASMGVYVFRTEVLLKLLRWSHSSCNDFGSEIIPSAVSDHNVQAYLFNDYWEDIGT IKSFFDANLALTEHPPKFEFYDPKTPFFTSPRFLPPSKVEKCKIVDAIISHGCFLRECNV QHSIVGIRSRLESGVELQDTMMMGADYYQTETEIASLVAEGKVPIGVGENTKIRNCIIDK NAKIGRNVVIANTDGVQEAERPKEGFYIRSGITVTLKNATIKDGTVI
LjAPL2b	chr5.CM0077.680.nc	Complete	MDSAFATLNANLVITNKVSSFWGENTRGNFNTRFCSIPSCQSSKSRKSKPGLVYAVYTPD INKESLTFQGPIIQSPKANPDNVAAIILGGGAGKRLFPLTSTRAKPAVPIGGCYRLIDIP MSNCINSGIRKVYVLTQYNSFSLNGHLSRTYNFGNGVNFGDGFVEVLAATQTPGEAGKKW FQGTADAVRQFIWVFEDAKNKNIEHIMIISGDHLCRMDYMKLLEKHIWTNSDITVSCVPM DESHASDYDLLRIDRKGQIIQFAEKPKGSDLKAMHVDTTLLGLPAEEARKHPYIASMGVY AFRTETLLKLLRWSCPSCNDFGSELIPSALRDHKVQAYLFRDYWKDIGTIKSFFDANLDL TGQNPKFELYDSKTPFFTSPRFLPPTKVVKSKIVDAIISHGCFLSECSVQRSIVGVRSRL ESGADLQDTMMMGADYYQTDSEVKSLLAEGKVPVGVGENTKIRNCIIDKNAKIGRNVVIV NSDGVQEADKPTEGFYIRSGIVVIVKNATIKDGTTI
LjAPL3	chr1.CM0113.470.nd	Corrected	MASACVTLKANTTHLANSEKGFLFGQDNGFLGERVKGAWGMNQLGKCLTAQKRVKSGAVS AVLTSNDAKEALTLQVPSFLRRKADPKNVISIILGGGPGTHLFPLTKRSATPAVPVGGCY RLIDIPMSNCINSSLNKIFVLTQFNSASLNRHISRTYFGNGVNFGDGFVEVLAATQTPGE AGKKWFQGTADAVRQFTWVFEDAKNRNVENVLILAGDHLYRMDYMDLVQSHVDRNADITV SCAAVGNSRASDYGLVKVDDRGSIIQFSEKPKGADLKAMQADTSLLGLSLHDALESPYIA SMGVYVFKTDVLLKLLKWRYPTSNDFGSEIIPSAVKEYDVQSYIFRDYWEDIGTIKSFYD ANLALTEESPKFKFYDPKTPIFTSPGFLPPTKIDKCRVVDAIISHGCFLRECTVQHSIVG ERSRLDYGVDLQDTIMMGADYYQTESEIASLLAEGKVPIGIGRNTKIRNCIIDKNAKIGK DVIITNKDGVQEADRSEDGFYIRSGITIVMEKATIEDGTVI

Table A2. Predicted protein sequences of the core set of starch metabolism enzymes in *L. japonicus.* Continued on next page.

LjAPL4	chr3.CM0216.100.nd	Complete	MVSAACVAWTTSSQLAKSKKDSTFLQDDGFLGERIIKGSLSYSPWINNQLATSWRGKESV KKAKPGVVSAVLTSNDTKESLSIQVPTFLRRKADPKNVVSIILGERPGIQLLPLTKRAAT PAVPVGGCYRLIDIPTSNCINSGINKVFVLTQFNSASLNRHISRTYFGNGINFGDGCVEV LAATQTPGEAGKNWFQGTADAVRQFTWVFEDAKHTNIENVLILAGDHLYRMDYMDLVQSH VDRNADITVSCAAVDDSRASDYGLVKVDGRGRIIQFSEKPKGSDLKEMQVDTSLFGLSPQ EALKSPYIASMGVYVFKTDVLLNLLKWRYPTSNDFGSEIIPAAVKEYNVQGYFFGDYWED IGTIKSFYDANMALTEENPMFKFYDPKTPIYTSPRFLPPTKIDKCRIVDAIISHGCFLRE SSVQHSIVGERSRLDYGVELRDTIMMGADYYQTESEIASLLAEGKVPIGIGKNTKIRKCI IDKNAKIGKDVIIMNKDGVQEADRAEDGFYIRSGIPIIMEKATIEDGRVI
LjAPL5	LjB06P23.100.nc	Complete	MLGSKRPYFHHGKVLSSSFSVSRVNLLHSKNAAFGFPSGKFSSVTQRKTTKRSLATSTLA DVANEFMALRSARLGGPAANSKTVASIILCGGAGTRLFPLTQKRAKPAVPIGGCYRLVDI PLSNCINSGINKIFVLTQFNSRSLNRHIARTYNLGGCVNFGGGFVEILAATQTPGESGNK WFRGTADAVRQFLWMFEDAEHKNIENILILCGDQLYRMDYMELVQKHVNSCADISVSCLP VDASRASDFGLVKVDERGRVRQFLEKPKGESLRSMHVDTSVFGLSAQEARKFPYIASMGI YVFKIDVLLKLLRSSYPNANDFGSEVIPMAAKDFNVQACLFSGYWEDIGTIKSFFDANLA LMDQPPKFQLYDQSRPIFTSPRFLPPSKMEKCQVLNSLISDGCFLRECSVEHSIVGIRSK IDSGVQLKDTLMMGADYYQTEAEIAALLAAGNVPIGIGKNTKIMNCIIDKNARIGNNVII ANKENVQEADRPSEGFYIRSGITVVLKDSVISNGTII
LjSS1_1	LjT38J19.80.nd	Pseudo/partial (encodes for C-term.)	MVWSTGMGVP*LGKGACS*HG*SCQLFEGAVVTADTDCNK*ARVIRGR*QLVKVDMVCMN Y*AAEKVFSVVCL*TIFWITNGIDITEWDPSSDEHIACSYSADDLSGKVKCKIALQKELG LPVRPDIPLIGFIGRLDYQKGIDLIREAIPELMEYDVQFVMLGSGSSIYEDWMRAAESSY RDKFRGWVGFNVPVSHRITAGCDILLMPSIFEPCGLNQLYAMRYGTIPVVHETGGLRDTV QSFNPFAEGGNAEGTGWTFSPLSKESMLVGLRHAIKTYTEYKSCWEGLMKRGMNRDYTWV KAATQYEQIIEWAFMDPPY
LjSS1_2	LjT38J19.60.nd	Pseudo/partial (encodes for N-term.)	MESLQLGSPLLLRHPRTPAQAYANSRLMKIAQLGFPSFLKRAAKNANLRAFPVDNEGGVA ASQDDPFAFEDEQVKALPLSTEMDDFGSIVGFHLGSENGKITEEDSTSDGVEEKAKARVC YNIVFVTSEAAPYSKTGGLGDVCGSLPIALAARGHRVMVVSPRYIHGTPGDSKFSGAIDL ERRINVPCFGGAQEVGFFHECREGVDWVFVDHPSFHRPGNPYGDKNGPFGDNQFRFTLLC YAACEAPLVLHLGGLTYGEKCLFIVNDWHASLVPVLLAAKYRPHGVYKDARSVLVIHNIA HQVN
LjSS2a	CM1835.140.nc	Complete	MASLSSAPFLVETHADTTVLLLHTSNLKIPVKFSTINASVFTRGFDRGRLKHRCSRGLLC PWGTKHIRALGKSSGTSEEDKDESEDRIKATIAKGQKALALQRELLQQIAEGKKLVSSIS SESIPEPDGNSVSYEPSGKSLSSDSDPQKASASRDKSFENQRGGIALTDYGNSRKKEIRK VSSVSIDQDSDEADGEDNKFSPAEMTSSKQYFFDKGKEEGDKFSPAEVTSSKQYFNEQLK TKRYEENSPKNLPNDRRNSIDSSSLKVESLKGVSQPNLKDVANDAESEGEKSPPLAGANV MNVILVAAECAPWSKTGGLGDVAGSLPKALARRGHRVMIVAPRYGNYAEAQDMGVRKRYK VDGQDMEVTYFHAYIDGVDFVFIDSPIFRHLEQNIYGGNRVDILRRMALFCKAAAEVCWH VPCGGVCYGDGNLVFIANDWHTALLPVYLKAYYRDHGLMQYTRSVLVIHNIAHQGRGPLD DFRIVDLPENYMDLFKFYDPLGGEHFNIFAAGLKTADRIVTVSHGYAWELKTSEGGWGLH GIINENDWKFRGIVNGIDSKDWNPQFDVHLTSDGYTNYTLETLHSGKRQCKAALQKELGL PVREDVPLIGFIGRLDHQKGVDLIAEAIPWMMDQDVQLIMLGTGRPDLEQMLRQFESQHR DKVRGWVGFSVKTAHRITAGVDILLMPSRFEPCGLNQLYAMNYGTVPVVHAVGGLRDTVQ AFNPFEESGLGWTFDSAEADKLIHALGNCLWTYREYKKSWEGLQKRGMSQDLSWDNAAQQ YEEVLVAAKYQW
LjSS2b_1	chr1.CM0141.60.nd	Pseudo/partial*	GLGDVAGSLPKALARRGHRVMVVAPRYGNYAEPQDTGVRKTYSVDGHDMEVQYFQAYIDG VDFVFIESPIFHHLDNNIYGGSRLDILKRMVLFCKAAVEVPWHVPCGGVCYGDGNLVFIA NDWHTALLPVYLKAYYRDQGLMKYTRSVLVIHNIAHQGRGPVDDFFFVDLPEYYMDIFKL YDPVGGEHFNIFAAGLKAADRVVTVSHGYAWELKTSEGGWGLNGIINDNGWKLRGIVNGI DNKEWNPMHDVHLKSDGYTNYSLETLPVGKAQCKAALQKELGLPVNEDVPVIGFIGRLDN QKGVDIIGEAIPWMMGQDVQLVMLGTGRPDLEHMLRQFENQHNDKIRGWVGFSVKMAHRI TAGVDILLMPSRFEPCG*TNSMP*SMDKSSCTSCGG
LjSS2b_2	chr1.CM0141.220.nd	Pseudo/partial*	YCAAF*SFQ*SRLGWTFDSAESGKLIHALGNCLLTYREHKKSWEGIQRRGMMQDLSWDNA AQLYEEVLVAAKYQ
LjSS5	chr2.CM0177.660.nc	Complete	MAAMGTFFMPLTLRLPLPSSSSSSSISKPKHTAPNNSPLFCLRNSGDAKGLHKKRLEDSK NEDMSKPISGDHQNKKRGNIWQLFREAQQNILYLNNQRLVAIEELNKTNEENQLLLNKIK KLEVEKQADADKLSICSELLLRIDSMVLSSLISPGEASKLRSSVASRRVSVANFFNAISQ KSDSQLLGELRHFSDQSKKNGFHIIHICTEMTPLVPIGSVASYVTGISRALQRKGHLVEV ILPKYACLNLAEVQGLREVNAVAYSYFDGQLHGNRIWTGVVCGIGVTLIEPLHYSSFFSR EMIYGYPDDFERFLYFCRASLDYIVKCEKQPDVLHLHNWETAIVGPLFWDIFVNKGLGGT RILLTCHGFNSQAIEQPEKLALCGLDPFSLHRPDRLQDNTNPQLVNILKGGVVYSNRVVI MSSIHPKHTIIHSLSHKLEPTLNDHRDKLVISPYGVDKSIWDPSTDYFLPENFNAENMNG KSVCKVALLQQLGLSENSSTILVGCIFSEGTNLDEKTVKDVILNSKKQHEVQFILMGIGE SSVVNQAVESLQKELKDGNLKFVPAYNEELLHLFFAGSDIILCQSFVDPTDEIPLKALRY GAVPIAVSPDASTNRTMPFDRSHEATKYSQLVNSNFRNMSLNLAIDGIRSNPSQWRRRIM EAMKHDLTWDGECYEVHVAAYSAIKNI

Table A2. Predicted protein sequences of the core set of starch metabolism enzymes in *L. japonicus.* Continued on next page.

LjGBSS1a	chr5.LjT41L03.30.nd	Pseudo/partial*	MATVTASSYAVSRSACLNRHGRTDSAAAKVNSVTLGGHALVYDGLRSLNKLHVRSARAVK GLSSTASDGGAARGKASGEVVCGMNLVFVGAEVGPWSKTGGLGDVLGGLPPALAGNGHRV MTVSPRYDQYKDAWDTNVTVEVKVGDRVETVRFFHCYKRGVDRVFVDHPMFLEKVWGKTG SKLYGPTAGVDYEDNQLRFSLLCQAALEAPRVLNLNSSKYFSGPYGEDVVFIANDWHTAL LPCYLKSMYKSRGIYQNAKVAFCIHNIAYQGRNAFSDFSQLNLPNQFKSSFDFTDGYDKP VKGRKINWMKAAILESNRVFTVSPYYAQELVSGEDRGVELDNIIRKTGITGIVNGMDIRE WSPETDKFIDVHYDATTVTEAKSLLKEALQAEVGLPVDRNIPLIGFIGRLEEQKGSDILV EAIPEFIDQNVQIIVLGTGKKIMEKQIEQLEETYPDKAIGVAKFNAPLAHKIIAGADFIV IPSRFEPCGLVQLHAMPYGTVPIVSSTGGLVDTVKEGYTGFHTGAFNVECETVDPADVDK LATTVKRALQTYGTPVLKEMIQNCMAQDFSWKGPAKQWKRRY*A*RLLVVKLE*MGKRLL LLRRR
LjGBSS1b	chr3.CM0208.40.nd	Pseudo/partial*	MNLIFLGTEVGPWSKTGGLGDVLGGLPPALAANGHRVMTIAPRYDQYKDAWDTSVTIEVK VGDKTEKVGFFHCHKRGVDRVFVDHPIFLEKVWGKSGTKLYGPTAGEDYQDNQLRFSLFC QAALEAPRVLNLTSNKYFSGPYGEDVIFIANDWHTALIPCYLKSMYQSIGIYKNARVVYC IHNIAYQGRFAFADFQLLNLPDQFKSSFDFLDGHVKPVIGRKTNWMKAGILESDLVLTVS PYYAEELVSGPDKGVELDNIIRRTGITGIVNGMDVQEWNPSTDKYLTVKYNASTVVEGKA LLKEALQAEVGLPVDRNIPLIGFIGRLEEQKGSDILVAAIPQFIKENIQIVALGTGKKQM EKQLEQLEIAYPDKARGVAKFNVPLAHMIIAGADFILIPSRFEPCGLIQLQAMRYGTVPI VASTGGLVDTVKEGFTGFQMGSFNVECEAVDPADVDALAKTVKRALAVHGTLAFTEIIKN CMAQDLSWKGPAKRWEEVLLSLGVPGSEAGIEGEEIAPQAKENLATP
LjSBE1	chr1.CM0178.250.nc	Pseudo/partial	MITSFSLQSFNIASTAHNSRNKQDLAKQNSVELVLGYRNPKGCNRFSFGSRRSIHERVST GFKGVAVITDNKSAMSATEEDLENIGILHIDPAIKPFKDHFKCRLKRYIDQKKLIEEYEG GLEEFAQGYLKFGFNREEGGIVYREWAPAAQEAQIIGDFNEWNGSNHPMEKNQFGVWSIK IPDVAGNPAIPHNSRVKFRFRHGGVWADRIPAWIKYATVDPTKFAAPYDGVYWDPPLSER YQFKYPRPPKPKAPRIYEAHVGMSSSEPRINSYKEFADDILPRIRANNYNTVQLMAVMEH SYYASFGYHVTNFFAVSSRSGTPEDLKYLIDKAHSLGLHVLMDVVHSHASNNVTDGLNGF DVGQVSQESYFHTGDRGYHKLWDSRLFNYANWEVLRFLLSNLRWWLEEFKFDGFRFDGVT SMLYHHHGVNIAFSGDYNEYFSEATDVDAVVYLMLANSLIHNILPDATVIAEDVSGMPGL GRPISEVGIGFDYRLAMAIPDKWIDYLKNKKDHEWSMKEISLSLTNRRYSEKCVSYAESH DQSIVGDKTFSFLLMDEEIYSGMSCLADASPTIERGIALHKMIHFITMSLGGEGYLNFMG NEFGHPEWIDFPREGNGWSYEKCRRQWSLVDTDHLRYKFMNAFDKAMNLLDDKFSFLAST KQIVSSTNEEDKVIVFERGDLVFVFNFHPETTYEGYKVGCDLPGKYRVALDSDAREFGGH GRVGHNVDHFTAPEGIPGVPESNFNNRPNSFKILSPPRTCVVYYRVDESQEENSISNLVG VQETSTAADIVANIPDGSSASKEREVSNFNWTMETLAAANADVAKIPDELVPAAENEVFQ DEVEDADE
LjISA1	chr4.CM0004.550.nc	Complete	MSILTFTHISSPPNLTFSLFPHSDSQCRVSLSKRVSEKHKSICSTTKILATGNGSGFETE TTLVVDKPQLGGRFQVSRGYPAPFGATVRDGGVNFAIYSLNAVSATLCLFTLSDFQDNQV TEYITLDPLMNKTGSVWHVFLKGDFGDMLYGYKFDGKFSPIEGHYYDSSLILLDPYAKAV ISRGEFGSLGPDGNCWPQMAGMVPSNDDEFDWEGDLPLKYPQKDLIIYEMHVRGFTKHES SKTKFPGTYLGVVEKLDHLKELGVNCIELLPCHEFNELEYFSYNSVQGDYRVNFWGYSTV NYFSPMIRYSSAGIQNCGRDGINEVKFLIKEAHKRGIEVIMDVVFNHTVEGNENGPIISF RGVDNSIYYMIAPKGEFYNYSGCGNTLNCNHPVVRQFIVDCLRYWVTEMHVDGFRFDLAS IMTRSSSLWNGVNVFGTSIEGDLLATGTPLVSPPLIDLISNDPILHGVKLIAEAWDAGGL YQVGTFPHWGIWSEWNGKYRDTVRQFVKGTDGFAGAFAECLCGSPNVYQGGGRKPWNSIN FVCTHDGFTLADLVTYNNKHNLPNGEDNNDGENHNNSWNCGQEGEFASSSVKKLRKRQMR NFFLSLMVSQGVPMIYMGDEYGHTKGGNNNTYCHDNYLNYFQWDIKEESSSDFFRFCCLM TKFRYECESLGLDDFPTSDRLQWHGHFPGKPDWSETSRFVAFTMVDSVKREIYIAFNTSH LPVTITLPERPGYRWEPLVDTGKSAPYDFLTPDLPGRDIAIQQYAQFLDANLYPMLSYSS IILLRTPDENA
LjISA2	LjSGA_028198.1	Pseudo/partial	**QWCGEACFGALIWILMSIGQATSGMSRLRVPGLL*DTVIASEELFGVGSMKNLGRLGQ EPAFDWGDDYHLDLPMEKLVVYRLNVKRFTEHESSQLPSDLAGTFSGLAKKLQHFKDLGV NAVLLEPVFTFDKEKGPYFPCHFFAPTSAYGPSSGPVSTITSMKEMVKAMHANGIEVLME VVFSNTAEMAALQGIDDSSYYYDNGVGNLKLHNALNCNFPIVQNLILDSLRHWVTEFHID GFSFINASHLLKGFHGEYLSRPPLVEAIAFDPVLSKTKIVADCWDPHGIAVAKENPFPHW MRWAEINTKFCDDVRNFLRGENLLSNLATRLCGSGDMFSDGRGPAFSFNYISRNSRLSLV DLVSFSNGDLAAELSWNCGEEGPTNNTTVLERRLKQIRNFLFILFVSLGVPVLNMGDESG QSSGGSPAYGDIKPFNWSALKTGFGKQTMQFISFLTSLRIRRSDVLQSRCFLKEKNIEWS GSDQALPKWEDPSCKFLAMTLKAEKLEFPENSTICDDGSGDLFIAFNADDKPETVVLPLL PEGMSWYRLVDTALPFPGFFSTNGEFVPEQASGLTVYQMKSYSCTLFEVKHST
LjLDA	chr5.CM0909.690.nc	Pseudo/partial	TSILESFPADSDQQQALITAIQNVDAYNWGYNPVLWGVPKGSYASNPNGPYRIIEFRKMI QALNRTGLRIVLDTVYNHLQGSGPFDDHSVLDKIVPGYYLRRNTDGFIENSTCMNNTASE HFMVERLILDDLVHWAVNYKIDGFRFDLMGHIMKSTMVKAKNALHCLRKEKDGVDGSSIY IYGEGWDFGEVANNGRGINASQFNLSGTQIGSFNDRIRDAILGGSPFGHPLQQGFVTGLL LQPNGHDHGTEANAKSMLATSMDHIQVGMAANLKDFVLTNSKGEEVKGSEVLTYGGTPVA YASCPTDTINYVSAHDNETLFDIVSLKTPMDINVAERCRINHLATSIIALSQGIPFFHSG DEILRSKSLDRDSYNSGDWFNRLDFTYNSNNWGVGLPPQEKNEKSWPLIKPRLADPSFKP QKINILAALDNFLNLLRIRYSSPLFRLRTANAIQQRVCFHNTGPSLVDGVIVMSIEDGHE GFPGLPQLDPIYSFIVVVVNAGPEEVSFVSPSLQSRSLQLHPILVTSSDELVKSSTYEAS SGCFVVPRRTTAVFVEPRG

Table A2. Predicted protein sequences of the core set of starch metabolism enzymes in *L. japonicus.* Continued on next page.

LjGWD1	chr4.LjT08E06.100.nc	Corrected	MSHSIFHQTLLCQTQTVAEHQSKVSSRGSTLFPALSVSKGKKLVLSTNLRGNRLCLRKRR FAMGRNRNTVAIPRAVLTSNAASELSGKFNLDGNIELQVGVSSSGPGGATQVDIQVSNKS GSLILHWGVLHESQGKWVLPSRHPDGTQVYKNRALRTPFVKSGSGSFLKIEIDDPAAQAI EFLILDESQNKWFKNNGENFHIKLPGKDEGVQQGSVPEDLVQVQAYLRWERNGKQMYTPE KEKEEYEAARQDLLKEVARGISVQDLRARLTNKANTAEVKQPSVSGTKNIPDELAQVQAY IRWEKAGKPNYSPEQQLIEFEEARKELLGELEKGASLDEIRKKIVKGEVQTKVAKQLKTK KYFHVERIQRKKRDWTELINRNVGENIVEQFVDVPKTMTVIQRYAKEKEEYDKGLILNRA IYKLADNDLLVLVTKDAGNIKVHLATDSKSPVTLHWALSRSTPGEWLVPPASALPPGSVI MDKAAETPFNPGSPSHPSFEVQSLDIEVDGDTFKGITFVTLSDGKWIKNNGSDFYVEFSE KKKIQKASGDGKGTAKFLLDRIAEMESEAQKSFMHRFNIASELMDQAKNAGQLGLAGILV WMRFMATRQLIWNKNYNVKPREISQAQDRLTDLLQDAYTSYPQYRELVRMILSTVGRGGE GDVGQRIRDEILVIQRKNECKGGMMEEWHQKLHNNTSPDDVVICQALIDYINNDFDIGVY WKTLNDNGITKERLLSYDRAIHSEPNFRRDQKEGLLRDLGNYMRTLKAVHSGADLESAIT NCLGYKSEGQGFMVGVQINPVSGLPSGFPQQLVQFVMEHVEVKYVEPLLEGLLEARQELR PSLNKSQSRLKDLLFLDVALDSTVRTAVERGYEELNNAGPEKIMYFIFLVLENLALSSDN NEDLIYCLKGWEIALSMCKSKDTHWALYAKSVLDRTRLALATKSEEYHNILQPSAEYLGS LLGVETWAVEIFTEEIIRAGSAASLSALLNRLDPVLRKTANLGSWQVISPVETIGYVVVV DELLSVQNKSYERPTILIAKSVRGEEEIPDGAVAVLTPDMPDVLSHVSVRARNSKVCFAT CFDPSILADLESKKGKLLSLKPTSAEVVYSEVNEGELIDEKSSHLNEVGSVPSISLVKKQ FSGRYAVSSEEFTGEMVGAKSRNISYLKGKVPSWIGIPTSVALPFGVFEHVLSDKSNQVV AEKVNVLKRKLTEGDFSALKDIRETVLQLNAPPQLVEELKTKMKSSGMPWPGDEGEQRWE QAWKAIKKVWGSKWNERAYFSTRKVKLDHDYLSMAVLVQEVVNADYAFVIHTTNPSSGDS SEIYTEVVKGLGETLVGAYPGRALSFICKKHDLDSPQVLGYPSKPIGLYIRRSIIFRSDS NGEDLEGYAGAGLYDSVPMDEEEKVVLDYSSDPLIVDGSFRKSILSSIARAGNAIEELYG SPQDIEGVIRDGKVYVVQTRPQM
LjGWD3	chr5.LjT42F22.140.nc and chr5.LjT42F22.160.nc	Corrected	MIRSGSRKKEKQLGGSSSSSSFSIHHLCRHTPHPLLLHRPKTVPHISAVSSTSTQTREER NNKKKNKVRLRLRLNHQVEFGDHVVISGSAKELGSWKKPVPLDWTQEGWACYLDFQGSQQ LEFKFIIVDKDNTLLWEAGDNRLLNLPEEGHFEMVATWNATRENMDLQPLELDFDGGEIQ QEKDFSDAATNDAPLSQSEEPSPFVGQWQGNTVTFMQSNQHRTHETERKWDTTGLQGLPL KLVQGDQNARNWWRKLDIVREIIAESLLGKDPLEALIYSAIYLKWINTGQITCFEDGGHH RPNRHAEISRLIFRELERHTSQKDISPQEVLIVRKIHPCLPSFKAEFTASVPLTRIRDIA HRNDIPHDLKTQIKHTIQNKLHRNAGPEDLVATEAMLAKITKNPGEYSETFVEQFKIFHR ELKDFFNAGSLSEQLESIRESMDKYGISSLDSFLQCKQTMDSAADSTPGVEQEIKLLFKT MESLIALRETFVKGLESGLRNDAPDSAIAMRQKWRLCEIGLEDYSFVLLSRFINVLEAMG GAHWLAANLQSKNVNSWNDPLGALTIGVHQLKLSNWKPEECGAIENELIAWSARGLSERE GNEDGKMIWALRLKATLDRSKRLTDEYTEELLKIFPQKVQTLGKALGIPENSVRTYTEAE IRAGVIFQVSKLCILLLKAVRSTLGSDGWDVLVPGAVLGTLVQVERIVPGSLPSSVEGPI ILLVNRADGDEEVTAAGRNIVGVILQQELPHLSHLGVRARQEKVAFVTCEDDEKIADVKS LIGSCVRLDASAASVTLKLSSSVDSNGSFSVERASDDSFSGVEVPAFSAGGISNSNQDAS SGGVILLPDAETQTSGAKAAACGRLSSLSAVSDKVYSDQGVPASFQVPSGAVLPFGSMEL ELEKSNSTETFRSILDKIETAKLEGGELDGLCHQLQELVCSLKPSKDVIESIGRIFPSSA CLIVRSSANVEDLAGMSAAGLYESIPNVSPSNPTVFGNAVSRVWASLYTRRAVLSRRAAG VPQKEASMAILIQEMLSPDLSFVLHTVSPTNQDSNTVEAEIACGLGETLASGTRGTPWRI SSGKFDGVVQTLAFANLSEELLVRGAGPADGEVIRLTVDYSKKPLTVDPVFRRQLGQRLC AVGFFLERKFGSPQDVEGCLVGKDIYIVQTRPQPN
LjAMY1	chr5.CM0852.300.nc	Corrected	MDSLSWLSLFCLSFSHFPLFSSSALLFQGFNWESSGKGGWYNSLKNSIPDLANAGITHVW LPPPSQSVASQGYLPGRLYDLDASKYGSKDELKSLIAAFHDKGIKCLADIVINHRTAERK DGRGIYCIFEGGTPDASLDWGPSFICRDDTAYSDGKGNLDSGEGYDAAPDIDHLNPQVQR ELSDWMNWLRNEVGFDGWRFDFVKGYAPSITKIYMEKTSPDFAVGEYWNSLSYGQDGKPN FNQDAHRGELVNWVQSAGGAVNAFDFTTKGILQAAVQGELWRLKDSNGKPPGMIGVKPEN AVTFVDNHDTGSTQRTWPFPDDKVMLGYVYILTHPGHPTIFYDHYIEWGLMEPIKKLTEI RKRNGIKPTSTVNILAAEADLYMAEIDNKIITKIGPKQDLGNLLPPNVQVATSGQDYAVW ERK
LjAMY2	LjSGA_020916.1	Pseudo/partial	YEFQSQSYIHDPVASMHCLFQGKPDTGAIFQGFPNIDHTQDFVRKDIIGWLRWLRYNIGF QDFRFDFAKGFSPKYVKEYIEEAKPLFSVGEYWDSCNYKGSALDYNQDSHRQRIINWIDG TGQLSTAFDFTTKGILQEAVKGQFWRLRDPQGKPPGVVGWWPSRSVTFIDNHDTGSTQAH WPFPKDHIMEGYAYILTHPGTPTVFYDHFYDWGNSFRNEIVKLIDIRKRQGIHSRSPIRI LEANDNLYSAIIGEKVCMKIGDGSWCPSGREWTLSTCGYNYAVWQTVVALI
LjAMY3a	chr1.CM0410.400.nd	Pseudo/partial	FQAFNWESWRRSWYLELSSKAADLSQCGVTAVWLPPPTNSVSPQGYMPSDLYNLNSSYGS VEELKSCIEEMHSQDLVVLGDAVLNHRCAQKQSPNGVWNIFGGKLAWGPEAIVCDDPNFQ GRGNPSSGDIFHAAPNIDHSQDFVRKDIKGWLNWLRNDIGFDGWRLDFVRGFSGTYVKEY IEASNPVFAIGEYWDSLAYEHGSLCYNQDAHRQRIVNWINATGGTSSAFDITTKGILHSA LHNEYWRLIDPQGKPTGVMGWWPSRAVTFLENHDTGSTQGHWPFPRDKLMQGYAYILTHP GTPVIFYDHFYDFGIHDVITELIEARRRAGIHCRSSIKIIHAHNEGYVAQVGDALVMKLG HFDWNPSKENQLEGSWQKFVDKGQDYQVWLR

Table A2. Predicted protein sequences of the core set of starch metabolism enzymes in *L. japonicus*. Continued on next page.

LjAMY3b	chr2.CM0608.610.nc	Complete	MSTVALEPLFFHLRRRETPIHLSKQNPFRPFFLISASSNLNLNLNASFTFRQPRMPALAA SLTDTPIIDPLQCSDTFFTNTFPINTTQTVEGKVFVRLDHRKDLRDLELTVSCNLPGKWI LHWGVTHGDDVGREWDQPSHDMIPPGSVSIKDCAIETPLMKSLLSTESDTFHEVRIDLKP NNEISAINFVLKDEESGAWYRNQGRDFRVPLVNYLKADTNMIGTKRGFSLWPENLGQMPK MFLKSKSGQDGSSKTRDPKQENTQPEGFYVEIPITKEVSINNFIRVSIKKCFESEAVKNL LCLETDLPGDIVLHWGVCRDDSRKWEVPPAPYPPETITFKDKSLRTRLQPRGSGKGSSVL ITLGEEFSGFLFVLKQNEKTWFKQMRNDFYIPLSSSGSLPIDGNREDQSGVQREAAEEAS QGTSFFSFTDGIINEIRNLVTDNSSEKSRKTKSKKAQESILQEIERLAAEAYIFFKTSIP YFSEATIAEPEAPIAEPEAASESEALALDPEICSGTGTGYEILCQGFNWESHKTGRWYME LKEKASELASLGFTVVWLPPPTESVSPEGYMPKDLYNLNSRYGNTDELKDLVKRLHQVGI RALGDAVLNHRCAHCQNQNGIWNIFGGRLNWDDCAVVADDPHFQGRGNNSSGDNFHAAPN IDHSQEFVRKDLKEWLCWLRNEIGYDGWRLDFVRGFWGGYIKDYLDASEPYFAVGEYWDS LSYTYGEMDCNQDAHRQRIVDWIKATNGTAGAFDVTTKGILHSALERCEYWRLSDQQGKP PGVVGWWPSRAVTFIENHDTGSTQGHWRFPSGKEMEGYAYILTHPGTPSVFFDHIFSHYK NEIASLVSCRKRNKIHCRSTVQICKAERDVYAAMIDEKIAMKIGPGHFEPPTGSHRWSLA IGGRDYKIWEAL
LjBAM1	LjSGA_011445.1 and LjSGA_032725.2	Corrected	MALSMTHQIGSLAGTPVTSESGSGETTASVSAAAVWKSPAMNLRCQVTRSEGATADGLSP PMSPCRSPALRADLSAACQAFETAVVEKEHGTGAKGEGKGTGVPVYVMMPLDSVTMGNTV NRRKAVNAAMAALRSAGVEGIMMDVWWGLVEREAPGEYNWGGYAELLEMAKKHGLKVQAV MSFHQCGGNVVICTIPLPKWAVEEIEKDPDLAYTDQWGRRNYEYISLGCDTLPVLKGRTP VQCYADFMRAFRDNFKHLLGDTVVEIQVGMGPAGELRYPSYPEQNGTWRFPGIGAFQCYD KYMLSSLKAAAEAEGKQEWGSTGPTDAGEYNNWPEDTAFFRREGGGWDSHYGEFFLTWYS QMLLDHGERILTSAKSIFDSTGVKISVKVAGIHWHYGTRSHAPELTAGYYNTRFRDGYLP IAQMLARHGAVFNFTCIEMRDHEQPQDALCAPEKLVNQVALATQKAQVPLAGENALQRYD EHAHEQILKSAQLNDDTEMCAFTYLRMNPQLFQPDNWRKFVSFVKKMKEGKGTHKCWEQV EREAEHFVHVTRPLVQEAALM
LjBAM3a_1	chr2.CM0021.1150.nd	Pseudo/partial (encodes for N-term.)	GNTLRSAILR*QQRNQSF*LRSYKVVSFQK*KHHSSPSKEFHTRSTLEKQEWEEVHHAPL VIHAPLVVHEHSDSKRVPVFVMLPLETVTVGGTLNKPRAMNASLMALKSAGVEGVMVDVW WGLVEKDGPLNYNWEGYAELFQMVQKHGLKVQVVMSFHQCGGNVGDSCSIPLPPWVLEEI GKNPDLVYTDRSGRRNPEYISLGCDSMPVLRGRSPLQVYSDYMRSFRDSFGDYMGSVIRL QVGLGPCGERET
LjBAM3a_2	chr2.CM0021.1290.nd	Pseudo/partial (encodes for C-term.)	EVQVGLGPCGELRYPSYPESEGTWRFPGIGEFQCYDKYMKASLEASAEAIGKKDWGRSGP HDSGQYNQFPEDTGFFKREGTWNTEYGHFFLEWYSNKLLEHGESILVAAKGIFQDSGVKL SAKVAGIHWHYRARSHASELNAGYYNTRFHDGYLPIAQMFARHGVVLNFTCMEMKDREQP EHANCSPEGLVHQVKNATTSAGAELAGENALERYDAGAFGQVLSTSNSGSGLGAFTYLRM NKRLFEGDNWRHFAGFVRSMSEGGQRQRLPVSDSFGIKLYVGHIKGIEQKQDQEAALV
LjBAM3b	chr2.CM0021.1220.nd	Pseudo/partial	MAEAPITLEKIHAPLAVHGLSDSKSVPSFVMLPLDTVTVGGTLNKPRVMNVSLMALKSAG VEGVMVDVWWGLVEKDGPFKYNWEGYAELFQMVQKHGLKLQVVMSFHQCGGNVGDSCSIP LPPWVLEEISENPDLVYTDRSGRRNPEYISLGCDSMPVLRGRTPLQEVQVGLGPCGELRY PSYPESEGTWRFPGIGEFQCYDKYMRASLEASAEAIGKKDWGRSGPHDSGQYNQFPEDTG FFKKEGTWNTEYGHFFLNWYSHKLLGHGDKILLSAKAIFQLTGVKLSAKVAGIHWHYKAR SHATELTAGYYNTRFHDGYLPIAQMLARHGAVFNFTCMEMKDREQPEHANCSPEGLVHQV QMAARTAGVELAGENALGRYDAGAFAQVLSTRNSVDGLGAFTYLRMNKRLFEGDNWRHFV DFVRSMSEGGLIERLPEADSFGTDLYVGHIIKEIEKKKNQEAILV
LjBAM5	chr3.CM0152.120.nc	Complete	MATSERNMLLNYVPVFVMLPLGVVSVSNVFEDPAGLKEQLLQLRAAGVDGVMVDVWWGIT EQKGPKQYDWGAYRSLFQLIQECGLKLQAIMSFHQCGGNVGDAVNIPIPQWVLDIGESNP DIFYTDISGTRNKEYLTVGVDNERIFHGRTAIELYSDYMKSFRENMSDFLKSELIIDIEV GLGPAGELRYPSYPQSQGWEYPGIGEFQCYDNYLKADFKAAATRAGHPEWELPDDAGKYN DVPQSTEFFRSNGTYLTEKGKFFLTWYSNKLLNHGDQILDEANKAFLGCKVKLALKVSGI HWWYKSESHAAELTAGYYNLGNRDGYRPIARMLSRHHAILNFTCLEMRDSEQRSDVDSGP EELVQQVLSGGWREHIEVAGENALSRYDATAYNQIILNARPQGVNKDGPPKFRMYGVTYL RLSDDLLQQSNFDIFRKFVQKMHADQDYCADPGKYGHIIPPLKRSGPKIPDDVLLKATEP MPPFPWDSETDMEVDG
LjBAM6	LjSGA_030993.1	Pseudo/partial	MADFLESELMIDIEVGLGPAGELRYPSYSYCTGWKFPGIGEFQCYDKYLEAQFKGAVAAL GHPEWELPDNAGECNSTPESTEFFRSQGTYLTDQGIIFLTWYSSILVMHGDAIMDEANKA FVGCKVKLAAKVSGIHWWYRTENHAAELTAGYYNLNYRDGYRPIARMLNRHGAILNFTCL EMRNCEQVEEAKSGPQELVQQVLSTGWRENLEVAGENALPRYDREAYNQILLNARPNGVN RHSPPKLRMYGVTYLRLTDELFQETNFQLFKTFVRRMHANQDYCSDPERYCHYTFPMQRS KPYLGTLTHGTEPVLQPYPWNNETDMSIEGPGFFADIVAFIWRIFCNKKR
LjBAM7	LjT34L14.60.nc	Complete	MIEIDDGNGIQTAPGDNRFQQHQQFQELEEPGGGARRSRPLEEKERTKLRERRRRAITAR ILAGLRRHGNYNLRVRADINDVIAALAREAGWVVLPDGTTFPSRSQGQRPDGGNSAPVTS SSQVPSQQTPSASLRGVASGYGSPLEYNACQMKGVFMPAPSPYDLSSSSRSQTSIVGDGE TQRDNIPGIGGSMNSVDEKQIADMPPRLPERDLAGTPYVPVYVMLPLGVINIKCELVDPD GLLKQLRVLKSINVDGVMVDCWWGIVEAHAPQEYNWNGYKRLFQMVRELKLKLQVLMSFH ECGGNFGDDVCIPLPHWVAEIGRSNPDIFFTDREGRHNPECLSWGIDKERVLRGRTAVEV YFDFMRSFRVEFDEYFEDGFISMIEVGLGPCGELRYPSCPVKHGWRYPGIGEFQCYDQYM LKSLRKAAEIRGHSIWARGPDNVGTYNSQPHETGFFCDGGDYDSFYGRFFLNWYSQVLVD HGNRVLSLAKLAFEGSCIAAKLSGIYWWYKTASHAAELTAGYYNPCNRDGYASIMTMLKR NGVSLNIPCVDLQTLNQHEGFPETFADPEGLVWQVLNAGWDVGLPVVSENALPCLNRVSY NKVLDNAKPMNDPDGRHFSSFAYPRLSPLLMERQNFIEFERFVKRMHGKFNG

Table A2. Predicted protein sequences of the core set of starch metabolism enzymes in *L. japonicus*. Continued on next page.

LjBAM8	chr2.CM0803.520.nc	Complete	MKNTNDDVSAQDLDPQSDHSSDYLAHSHQLSQPQPRRPRGFAAAAAGVNSAGKGKKEREK EKERTKLRERHRRAITSRMLAGLRQYGNFPLPARADMNDVLAALAREAGWVVDADGTTYR QCPPPSHMGSFAAARSVETQLSAGSLRACSVKETLENQPPVLRIDECLSPASIDSVVLAE RDSKSRKFASASPIDSVDCLEADQLMQVMHTGVHENDFTGTPYVPVYIKLPVGIINKFCQ LIDPEGIRQELIHIKSLNIDGVVVDCWWGIVEGWSPQKYVWSGYRELFNIIREFKLNLQV VMAFHECGGSDSSDALISLPQWVLDIGKDNQDIFFTDREGRRNTECLSWGIDKERVLKGR TGIEVYFDMMRSFRTEFDDLFAEGLISSVEIGLGASGELKYPSFSERMGWRYPGIGEFQC YDKYLQHSLRRAAKLRGHSFWARGPDNAGHYNSMPHETGFFCERGDYDNYYGRFFLHWYS QTLVDHADNVLSLASLAFEETQIIVKVPAVYWWYKTPSHAAELTAGYHNPTNQDGYSPVF EVLKKHAVTMKFVCLGFHLSSQEANESLVDPEGLSWQVLNSAWDRGLIAAGENALLCYDR EGHKRLVEMAKPRNDPDRRHFSFFVYQQPSLLQGNPCLSELDFFIKCMHGEMTGDL
LjBAM9	chr6.LjT15B19.140.nd	Complete	MEVSVIGSSQAKLGKSDLVTREQGFCFVKESCRIENNRVSFGGNMRWKKDGLRFSLRAVH HAEPVLEKKKKKSHSGSGTGSSNSVDGVRLFVGLPLDAVSYDCSSLNHSRAIAAGLRALK LLGVEGVELPVWWGIVEKEAMGEYNWSGYLAIAEMVQKAGLKLHMTLCFHGSEKPNIPLP KWVSKIGESQSSIFFTDRSGQRYNEYLSLAVDNLPVLDGKTPVQVYQSFCESFKSSFSAF MGSTITGISMGLGPEGELRYPSHHHSNGKTQGVGEFQCYDQNMLQLLKQHAEASGNPLWG LGGPHDVPTYDQPPHSNNFFKDGGSWESQYGDFFLSWYSNQLITHGDCLLSLAASTFGDT GVTIHGKIPLMHTWYGTQSHPSELTAGFYNTANREGYEPVAKIFAKNSCKIMLPGLDLSD ANQPSETRSSPESLLAQIMASCRNHGVRVSGQNSSVFGAPEGFDQIKKNLSGDNVLDLFT YPKNGSIFLFSLTLFPLFPKLCSKP
LjDPE1	chr1.CM0032.500.nc	Complete	MALLTPSISVRFPQLQQHQQQWKFKPKPFFPRASSFTSTSLAQLSVGEDLPSNYGDWLPT PDPHLRRRAGILLHPTSFRGPYGIGDLGDEAFRFVDWLHNAGCSLWQVLPLVPPGRKANE EGSPYSGQDANCGNTLLISLQGLVDDGLLEKHELPQPIDAERVDFSVVADLKDPLITKAA ERLISSKGELKTQLENFRKDPNISSWLEDAAYFAAIDDSLNTFSWYNWPEPLRNRHLVAL ENIYEQKRDFINVFIAQQFLFQRQWQKVRDYAQSRGISIMGDMPIYVGYHSADVWANKNQ FSLNRKGFPLLVSGVPPDAFSETGQLWGSPLYDWNAMEKEGYSWWIRRIQRAQNLYDEFR IDHFRGLAGYWAVPSEAKVAMVGKWKVGPGISFFDAIFRAVGKVNIIAEDLGVITEDVVK LRKSIGAPGMAVLQFGFGGGADNPHLPHNHEFNQVVYTGTHDNDTVKGWWEAMNQEEKSK ALSYLSLTGEDDISWVLIQKVLASVAQTAVIPMQDVLGLGNSARMNIPATQFGNWGWRIA SSVSFDNLEREAARLKDMLSMYGRL
LjDPE2_1	LjSGA_011298.1	Pseudo/partial (encodes for N-term.)	MVNLGLFSSNKSVSSVKVTFRIPYFTQWGQSLLVCGSVPLLGSGNVKKGVLLSPSPQGSE LVWSGSITVPRGFQCQYSYYVVDDNKNILRWEMGKKRELNLPEGLQNGQEVEFRDLWQTG SDALPFRSAFKDVVFRQSWDSCITGVDHTNIEPEAESIVVQFKISCPNIEKDTSLCVIGS NTKLGQWKVENGLKLNYFGESVWLAECVMQRSDFPIRYPFWTFHPEQYDELMLSGNSSIE DGPNREVSINSSRNEAKYIFLSDGMMRGTPWRGAGVAIPMFSIRSESDLGVGEFLDLKLL VDWAVASGFHLVQLLPINDTSVHGMWWDSYPYSSLSVCALHPLYLRVQALSENIPEEIKQ EIEKAKQQLDG
LjDPE2_2	LjSGA_007380.1	Pseudo/partial (encodes for C-term.)	IFIFPN*F*FKGDSTPEKKIASKLKTCSESFFLLESEDKMGRNLFDFLQNIVLIQDPEDP RKFYPRFNLEDTSNFQALDDHSKNVLKRLYYDYYFHRQENLWRQNALKTLPALLNSSDML ACGEDLGLIPSCVHPVMQELGLVGLRIQRMPNESDLEFGIPSRYSYMTVCAPSCHDCSPM RAWWEEDEERRQRFFKDVVESDELAPDQCVPEVAHFIIRQHFEAPSMWAIFPLQDLLALK EEYTKRPAAEETINDPTNPKHYWRYRVHVTLESLLKDNELKTSIKNLVRWSGRSFPHEDS QVEASPVSASSVAEAVSDKKIAGAADKIRLPSESNGVQPRDHVAV
LjPHS2a	LjB08M07.80.nc	Complete	MAAKVETNGGGGGGIASPASDKVPAVAHPLAEKPDEIASNISYHAQFSPHFSPFKFELEQ AYYATAESVRDRLIRQWNETYLHFHKVDPKQTYYLSMEFLQGRALTNAIGNLNIQDAYAD ALRKFGLELEEIVEQEKDAALGNGGLGRLASCFLDSMATLNLPAWGYGLRYRYGLFKQKI TREGQEEVPEDWLEKFSPWEVVRHDILYPIRFFGNVEVNPNGSRKWVGGEVVQALAYDVP IPGYQTKNTISLRLWEAKASAEDFNLFLFNDGHHESASVLHSRSEQICAVLYPGDATEGG KLLRLKQQYFLCSASLQDIISRFKERRQGPWNWSEFPTKVAVQLNDTHPTLSIPELMRLL MDDEGLGWDEAWDVTSKTIAYTNHTVLPEALEKWSQPVMWKLLPRHMEIIEEIDRRFIAM ISKTRLDLEGELSTMRILDNNPQKPVVRMANLCVVSAHTVNGVAQLHSDILKAELFANYV SIWPTKFQNKTNGITPRRWLSFCSPVLSRIITKWLKTDQWVTNLDLLTGLRQFADNEDLQ AEWLSAKMANKQRLAQYILQVTGESIDPDSLFDIQVKRIHEYKRQLLNILGVIYRYKKLK EMSPEERKSTTSRTVMIGGKAFATYTNAKRIVKLVNDVGAVVNSDPEVNSYLKVVFVPNY NVTVAEVLIPGSELSQHISTAGMEASGTSNMKFALNGCLIIGTLDGANVEIREEVGEENF FLFGATAEDVPRLRKERENGLFKPDPRFEEAKKFIRSGVFGSYDYNPLLDSLEGNSGYGR GDYFLVGYDFPSYMDAQEKVDEAYRDKKRWLKMSILSTAGSGKFSSDRTISQYAKEIWNI EECRVP
LjPHS2b	chr2.CM0373.1170.nd	Pseudo/partial	RKWVGGEVVQALAYDVPIPGYQTKNTISLRLWEAKASAEDFNLFLFNDGHHESASVLHSR SEQICAVLYPGDATEGGKLLRLKQQYFLCSASLQDIISRFKERRQGPWNWSEFPTKVAVQ LNDTHPTLSIPELMRLLMDDEGLGWDEAWDVTSKTIAYTNHTVLPEALEKWSQPVMWKLL PRHMEIIEEIDRRFIAMISKTRLDLEIELSTMRILDNNPQKPLFGT
LjMEX1	chr3.CM0127.650.nc	Complete	MAKSYYAASLPLHLTQHHHNRNPLHFKYLTFPRPPNISTAHRLFASPRRRHNFSLNALDS DAPRPHQQGSVDIGRDESYQQWDSLTAKFSAAANVPFLLLQMPQILLNARNLAAGNKTAL LAVPWLGMLTSLLGNLSLLSYFAKKKEKEAMVVQTLGVVSTYVVIAQLALAEAMPLPYFL ATSVIVGSGLFLNFMNYFGLLNAGIWSFWEDFITVGGLSVLPQIMWSTFVPFIPNSILPG ATAFVLAVLAVTMARTGKLSEEGVKFVGGISGWTATLLFMWMPVSQMWTNILNPENMKGL SAFSMLLAMLGNGLLLPRALLIRDLMWFIGSSWATLFYGYGNLACLFVLNIISKEFFLAA TVGLVAWIGMAFWRDSAVHGHNSPLASIRDLVFGYRDDKA

Table A2. Predicted protein sequences of the core set of starch metabolism enzymes in *L. japonicus.* Continued on next page.

* Protein sequences of LjGBSSIa, LjGBSSIb,LjSS2a and LjSS2b retrieved from NCBI, from the work of Pan et al., 2009:

```
>gi|170676393|gb|ACB30384.1| granule bound starch synthase Ia precursor [Lotus japonicus]
MATVTASSYAVSRSACLNRHGRTDSAAAKVNSVTLGGHALVYDGLRSLNKLHVRSARAVKGLSSTASDGG
AARGKASGEVVCGMNLVFVGAEVGPWSKTGGLGDVLGGLPPALAGNGHRVMTVSPRYDQYKDAWDTNVTV
EVKVGDRVETVRFFHCYKRGVDRVFVDHPMFLEKVWGKTGSKLYGPTAGVDYEDNQLRFSLLCQAALEAP
RVLNLNSSKYFSGPYGEDVVFIANDWHTALLPCYLKSMYKSRGIYQNAKVAFCIHNIAYQGRNAFSDFSQ
LNLPNQFKSSFDFTDGYDKPVKGRKINWMKAAILESNRVFTVSPYYAQELVSGEDRGVELDNIIRKTGIT
GIVNGMDIREWSPETDKFIDVHYDATTVTEAKSLLKEALQAEVGLPVDRNIPLIGFIGRLEEQKGSDILV
EAIPEFIDQNVQIIVLGTGKKIMEKQIEQLEETYPDKAIGVAKFNAPLAHKIIAGADFIVIPSRFEPCGL
VQLHAMPYGTVPIVSSTGGLVDTVKEGYTGFHTGAFNVECETVDPADVDKLATTVKRALQTYGTPVLKEM
IQNCMAQDFSWKGPAQQWEKALLSLEVAGSEAGIDGEEIAPLAKENVPTP

>gi|170676395|gb|ACB30385.1| granule bound starch synthase Ib precursor [Lotus japonicus]
MAAVAASSNLVSSSSYIHHRSILSYESKAASTGLRSLRQTNTHNGLRILNLVDELLNRTPIQVKAVQARR
KGLQGKNVRPTGVIICGMNLIFLGTEVGPWSKTGGLGDVLGGLPPALAANGHRVMTIAPRYDQYKDAWDT
SVTIEVKVGDKTEKVGFFHCHKRGVDRVFVDHPIFLEKVWGKSGTKLYGPTAGEDYQDNQLRFSLFCQAA
LEAPRVLNLTSNKYFSGPYGEDVIFIANDWHTALIPCYLKSMYQSIGIYKNARVVYCIHNIAYQGRFAFA
DFQLLNLPDQFKSSFDFLDGHVKPVIGRKTNWMKAGILESDLVLTVSPYYAEELVSGPDKGVELDNIIRR
TGITGIVNGMDVQEWNPSTDKYLTVKYNASTVVEGKALLKEALQAEVGLPVDRNIPLIGFIGRLEEQKGS
DILVAAIPQFIKENIQIVALGTGKKQMEKQLEQLEIAYPDKARGVAKFNVPLAHMIIAGADFILIPSRFE
PCGLIQLQAMRYGTVPIVASTGGLVDTVKEGFTGFQMGSFNVECEAVDPADVDALAKTVKRALAVHGTLA
FTEIIKNCMAQDLSWKGPAKRWEEVLLSLGVPGSEAGIEGEEIAPQAKENLATP

>gi|221063674|gb|ACL98481.1| starch synthase IIa precursor [Lotus japonicus]
MASLSSAPFLVETHADTTVLLLHTSNLKIPVKFSTINASVFTRGFDRGRLKHRCSRGLLCPWGTKHIRAL
GKSSGTSEEDKDESEDRIKATIAKGQKALALQRELLQQIAEGKKLVSSISSESIPEPDGNSVSYEPSGKS
LSSDSDPQKASASRDKSFENQRGGIALTDYGNSRKKEIRKVSSVSIDQDSDEADGEDNKFSPAEMTSSKQ
YFFDKGKEEGDKFSPAEVTSSKQYFNEQLKTKRYEENSPKNLPNDRRNSIDSSSLKVESLKGVSQPNLKD
VANDAESEGEKSPPLAGANVMNVILVAAECAPWSKTGGLGDVAGSLPKALARRGHRVMIVAPRYGNYAEA
QDMGVRKRYKVDGQDMEVTYFHAYIDGVDFVFIDSPIFRHLEQNIYGGNRVDILRRMALFCKAAAEVCWH
VPCGGVCYGDGNLVFIANDWHTALLPVYLKAYYRDHGLMQYTRSVLVIHNIAHQGRGPLDDFRIVDLPEN
YMDLFKFYDPLGGEHFNIFAAGLKTADRIVTVSHGYAWELKTSEGGWGLHGIINENDWKFRGIVNGIDSK
DWNPQFDVHLTSDGYTNYTLETLHSGKRQCKAALQKELGLPVREDVPLIGFIGRLDHQKGVDLIAEAIPW
MMDQDVQLIMLGTGRPDLEQMLRQFESQHRDKVRGWVGFSVKTAHRITAGVDILLMPSRFEPCGLNQLYA
MNYGTVPVVHAVGGLRDTVQAFNPFEESGLGWTFDSAEADKLIHALGNCLWTYREYKKSWEGLQKRGMSQ
DLSWDNAAQQYEEVLVAAKYQW

>gi|221063676|gb|ACL98482.1| starch synthase IIb precursor [Lotus japonicus]
MLCHIIFWLLMATSIGSSPFVLETTTSSAQVFVVPESRRNRCLRLGWDWHKRGLLSKNIRAEANGSNGTN
EDEDGSEGVLHATTEKSKKVLAWQSNLLQQIAERKKPISYELIDKFPPNNSSPHNASTSGHNAVENQNGG
IVWRKYVNSSTYSDTIIESEGNSISHEGSNESNQQNGSISRVNAVETQKSGTFVRNYVHSNKGSLEVTSV
GINGGFDEVNEENVKIPTPKMSSSELYFTEQFKGKKYQAIKPDSDTLQAFLANGTETSSIKVENQEGMSE
TRSKLITEESSTVDGEGEISAPLAGTNVMNVILVAAECAPWSKTGGLGDVAGSLPKALARRGHRVMVVAP
RYGNYAEPQDTGVRKTYSVDGHDMEVQYFQAYIDGVDFVFIESPIFHHLDNNIYGGSRLDILKGMVLFCK
AAVEVPWHVPCGGVCYGDGNLVFIANDWHTALLPVYLKAYYRDQGLMKYTRSVLVIHNIAHQGRGPVDDF
FFVDLPEYYMDIFKLYDPVGGEHFNIFAAGLKAADRVVTVSHGYAWELKTSEGGWGLNGIINDNGWKLRG
IVNGIDNKEWNPMHDVHLKSDGYTNYSLETLPVGKAQCKAALQKELGLPVNEDVPVIGFIGRLDNQKGVD
IIGEAIPWMMGQDVQLVMLGTGRPDLEHMLRQFENQHNDKIRGWVGFSVKMAHRITAGVDILLMPSRFEP
CGLNQLYAMNYGTVPVVHAVGGLRDTVQPFDPFNESGLGWTFDSADSGKLIHALGNCLLTYREHKKSWEG
IQRRGMMQDLSWDNAAQLYEEVLVAAKYQW
```

Table A2. Predicted protein sequences of the core set of starch metabolism enzymes in *L. japonicus.* Continued.
Protein sequences were retrieved from the Miyakogusa genome database developed by the Kasuza DNA Research Institute (http://www.kazusa.jp/lotus/index.html; Sato et al., 2008). These sequences were annotated, and in several cases corrected, as described in Chapter 2 (section 2.7.2) and Chapter 3 (section 3.2.1).

TargetP predictions

PGI

Name	Len	cTP	mTP	SP	other	Loc	RC
LjPGI1_LOTJA	613	0.976	0.063	0.009	0.055	C	1
NP_001051434.1_ORYSA	567	0.093	0.090	0.117	0.879	_	2
NP_001057316.1_ORYSA	567	0.094	0.106	0.106	0.852	_	2
NP_001062053.1_ORYSA	615	0.974	0.098	0.012	0.017	C	1
NP_001063415.1_ORYSA	625	0.896	0.429	0.006	0.010	C	3
NP_194193.2_PGI1_ARA	613	0.949	0.105	0.009	0.045	C	1
NP_199088.1_PGIC_ARA	560	0.097	0.069	0.061	0.922	_	1
XP_002282774.1_VITVI	568	0.073	0.073	0.086	0.927	_	1
XP_002285696.1_VITVI	623	0.916	0.167	0.025	0.037	C	2
XP_002285697.1_VITVI	615	0.916	0.167	0.025	0.037	C	2
XP_002301084.1_POPTR	616	0.754	0.273	0.071	0.066	C	3
XP_002312387.1_POPTR	568	0.147	0.075	0.097	0.902	_	2
XP_002462509.1_SORBI	615	0.784	0.469	0.012	0.011	C	4

Predotar predictions

PGI

Sequence	Mitochondr	Plastid	ER	Elsewhere	Prediction
LjPGI1|LOTJA	0.04	0.91	0.00	0.09	plastid
NP_001051434.1|ORYSA	0.01	0.02	0.00	0.97	none
NP_001057316.1|ORYSA	0.01	0.02	0.00	0.97	none
NP_001062053.1|ORYSA	0.01	0.97	0.00	0.03	plastid
NP_001063415.1|ORYSA	0.08	0.97	0.02	0.03	plastid
NP_194193.2|PGI1|ARATH	0.02	0.92	0.01	0.08	plastid
NP_199088.1|PGIC|ARATH	0.01	0.00	0.00	0.99	none
XP_002282774.1|VITVI	0.01	0.05	0.00	0.94	none
XP_002285696.1|VITVI	0.01	0.93	0.00	0.07	plastid
XP_002285697.1|VITVI	0.01	0.93	0.00	0.07	plastid
XP_002301084.1|POPTR	0.15	0.90	0.03	0.08	plastid
XP_002312387.1|POPTR	0.01	0.04	0.00	0.95	none
XP_002462509.1|SORBI	0.20	0.97	0.10	0.02	plastid

PGM

Name	Len	cTP	mTP	SP	other	Loc	RC
LjPGM1_LOTJA	635	0.982	0.015	0.006	0.080	C	1
NP_001051066.1_ORYSA	582	0.032	0.414	0.030	0.891	_	3
NP_001064271.1_ORYSA	609	0.772	0.658	0.011	0.002	C	5
NP_173732.1_PGMC_ARA	583	0.059	0.313	0.077	0.919	_	2
NP_177230.1_PGMC_ARA	585	0.088	0.216	0.074	0.879	_	2
NP_199995.1_PGM1_ARA	623	0.361	0.247	0.014	0.032	C	5
XP_002263813.1_VITVI	614	0.880	0.161	0.013	0.020	C	2
XP_002284729.1_VITVI	583	0.029	0.642	0.019	0.893	_	4
XP_002311517.1_POPTR	582	0.069	0.317	0.020	0.928	_	2
XP_002315869.1_POPTR	582	0.060	0.292	0.029	0.923	_	2
XP_002318262.1_POPTR	631	0.839	0.143	0.001	0.018	C	2
XP_002322433.1_POPTR	551	0.179	0.105	0.085	0.894	_	2
XP_002458166.1_SORBI	608	0.421	0.834	0.005	0.013	M	3
XP_002466576.1_SORBI	649	0.985	0.125	0.002	0.025	C	1

Sequence	Mitochondr	Plastid	ER	Elsewhere	Prediction
LjPGM1|LOTJA	0.01	0.93	0.00	0.07	plastid
NP_001051066.1|ORYSA	0.12	0.02	0.01	0.85	none
NP_001064271.1|ORYSA	0.20	0.54	0.14	0.32	plastid
NP_173732.1|PGMC|ARATH	0.01	0.40	0.00	0.60	possibly plastid
NP_177230.1|PGMC|ARATH	0.01	0.63	0.01	0.36	plastid
NP_199995.1|PGM1|ARATH	0.03	0.95	0.09	0.04	plastid
XP_002263813.1|VITVI	0.04	0.93	0.02	0.06	plastid
XP_002284729.1|VITVI	0.05	0.13	0.00	0.83	none
XP_002311517.1|POPTR	0.01	0.12	0.00	0.87	none
XP_002315869.1|POPTR	0.01	0.08	0.00	0.91	none
XP_002318262.1|POPTR	0.13	0.72	0.01	0.24	plastid
XP_002322433.1|POPTR	0.01	0.01	0.00	0.99	none
XP_002458166.1|SORBI	0.43	0.60	0.04	0.22	plastid
XP_002466576.1|SORBI	0.07	0.54	0.16	0.36	plastid

AGPase

Name	Len	cTP	mTP	SP	other	Loc	RC
LjAPL1_LOTJA	520	0.319	0.181	0.037	0.413	_	5
LjAPL2a_LOTJA	527	0.669	0.123	0.006	0.288	C	4
LjAPL2b_LOTJA	516	0.788	0.030	0.039	0.297	C	3
LjAPL3_LOTJA	521	0.243	0.037	0.030	0.786	_	3
LjAPL4_LOTJA	530	0.222	0.069	0.016	0.614	_	4
LjAPL5_LOTJA	517	0.359	0.393	0.003	0.017	M	5
LjAPS1_LOTJA	520	0.987	0.027	0.004	0.016	C	1
NP_001043654_ORYSA	518	0.282	0.231	0.019	0.629	_	4
NP_001051184_ORYSA	511	0.673	0.228	0.014	0.028	C	3
NP_001056424_ORYSA	522	0.658	0.034	0.060	0.354	C	4
NP_001059276_ORYSA	509	0.745	0.271	0.031	0.083	C	3
NP_001061603_ORYSA	479	0.584	0.119	0.044	0.207	C	4
NP_001062808_ORYSA	500	0.585	0.135	0.022	0.038	C	3
NP_172052_AtAPS2_ARA	476	0.457	0.120	0.021	0.219	C	4
NP_174089_AtAPL2_ARA	518	0.359	0.037	0.030	0.516	_	5
NP_179753_AtAPL4_ARA	523	0.453	0.050	0.083	0.530	_	5
NP_195632_AtAPL3_ARA	521	0.252	0.029	0.023	0.871	_	2
NP_197423_AtAPL1_ARA	522	0.923	0.031	0.003	0.072	C	1
NP_199641_AtAPS1_ARA	520	0.976	0.013	0.008	0.044	C	1
XP_002263255_VITVI	509	0.967	0.043	0.004	0.050	C	1
XP_002274245_VITVI	466	0.028	0.192	0.077	0.628	_	3
XP_002276188_VITVI	486	0.814	0.027	0.024	0.136	C	2
XP_002281069_VITVI	520	0.259	0.202	0.029	0.359	_	5
XP_002281223_VITVI	524	0.401	0.084	0.015	0.631	_	4
XP_002283855_VITVI	527	0.195	0.106	0.025	0.599	_	3
XP_002300758_POPTR	528	0.143	0.033	0.108	0.637	_	3
XP_002306116_POPTR	526	0.103	0.080	0.024	0.833	_	2
XP_002307668_POPTR	475	0.051	0.115	0.246	0.736	_	3
XP_002310375_POPTR	434	0.142	0.291	0.194	0.207	M	5
XP_002311802_POPTR	528	0.241	0.401	0.020	0.044	M	5
XP_002313036_POPTR	527	0.212	0.039	0.016	0.845	_	2
XP_002320247_POPTR	445	0.277	0.102	0.097	0.474	_	5
XP_002321214_POPTR	522	0.975	0.184	0.001	0.010	C	2
XP_002331645_POPTR	428	0.109	0.280	0.109	0.239	M	5
XP_002440313_SORBI	519	0.892	0.036	0.006	0.265	C	2
XP_002456012_SORBI	517	0.738	0.080	0.008	0.525	C	4
XP_002462140_SORBI	510	0.887	0.028	0.007	0.121	C	2
XP_002463921_SORBI	507	0.325	0.459	0.007	0.041	M	5

Sequence	Mitochondr	Plastid	ER	Elsewhere	Prediction
LjAPL1|LOTJA	0.02	0.76	0.00	0.24	plastid
LjAPL2a|LOTJA	0.01	0.24	0.00	0.76	possibly plastid
LjAPL2b|LOTJA	0.01	0.19	0.02	0.80	none
LjAPL3|LOTJA	0.01	0.27	0.00	0.72	possibly plastid
LjAPL4|LOTJA	0.01	0.84	0.00	0.16	plastid
LjAPL5|LOTJA	0.26	0.04	0.03	0.69	possibly mitochondrial
LjAPS1|LOTJA	0.09	0.96	0.02	0.04	plastid
NP_001043654|ORYSA	0.01	0.02	0.00	0.97	none
NP_001051184|ORYSA	0.19	0.58	0.04	0.33	plastid
NP_001056424|ORYSA	Discarding NP_001056424|ORYSA: no terminal Met				
NP_001059276|ORYSA	0.06	0.95	0.02	0.04	plastid
NP_001061603|ORYSA	0.01	0.03	0.00	0.96	none
NP_001062808|ORYSA	0.09	0.89	0.04	0.10	plastid
NP_172052|AtAPS2|ARATH	0.02	0.19	0.01	0.79	none
NP_174089|AtAPL2|ARATH	0.01	0.03	0.00	0.96	none
NP_179753|AtAPL4|ARATH	0.01	0.08	0.00	0.92	none
NP_195632|AtAPL3|ARATH	0.01	0.32	0.00	0.68	possibly plastid
NP_197423|AtAPL1|ARATH	0.03	0.60	0.00	0.39	plastid
NP_199641|AtAPS1|ARATH	0.10	0.92	0.01	0.07	plastid
XP_002263255|VITVI	0.01	0.96	0.03	0.03	plastid
XP_002274245|VITVI	0.57	0.00	0.03	0.42	mitochondrial
XP_002276188|VITVI	0.01	0.36	0.03	0.62	possibly plastid
XP_002281069|VITVI	0.03	0.43	0.00	0.55	possibly plastid
XP_002281223|VITVI	0.01	0.03	0.00	0.97	none
XP_002283855|VITVI	0.01	0.04	0.01	0.94	none
XP_002300758|POPTR	0.01	0.12	0.02	0.85	none
XP_002306116|POPTR	0.01	0.11	0.00	0.89	none
XP_002307668|POPTR	Discarding XP_002307668|POPTR: no terminal Met				
XP_002310375|POPTR	Discarding XP_002310375|POPTR: no terminal Met				
XP_002311802|POPTR	0.01	0.23	0.01	0.76	possibly plastid
XP_002313036|POPTR	0.01	0.05	0.00	0.94	none
XP_002320247|POPTR	0.01	0.00	0.00	0.99	none
XP_002321214|POPTR	0.26	0.96	0.00	0.03	plastid
XP_002331645|POPTR	Discarding XP_002331645|POPTR: no terminal Met				
XP_002440313|SORBI	0.01	0.68	0.01	0.32	plastid
XP_002456012|SORBI	0.01	0.02	0.00	0.98	none
XP_002462140|SORBI	0.03	0.97	0.02	0.03	plastid
XP_002463921|SORBI	0.51	0.48	0.04	0.24	mitochondrial

SS

Name	Len	cTP	mTP	SP	other	Loc	RC
ACB30384.1_LjGBSS1a_	610	0.504	0.326	0.009	0.095	C	5
ACB30385.1_LjGBSS1b_	614	0.878	0.144	0.028	0.034	C	2
ACL98481.1_LjSS2a_LO	792	0.632	0.015	0.179	0.442	C	5
ACL98482.1_LjSS2b_LO	800	0.714	0.013	0.414	0.044	C	4
LjSS1_1_LOTJA	245	0.072	0.080	0.086	0.954	_	1
LjSS1_2_LOTJA	304	0.176	0.815	0.007	0.079	M	2
LjSS5_LOTJA	687	0.808	0.297	0.024	0.033	C	3
NP_001056881.1_ORYSA	641	0.946	0.145	0.006	0.030	C	1
AAL16661.1_ORYSA	810	0.934	0.050	0.100	0.003	C	1
AAK81729.1_ORYSA	694	0.955	0.225	0.008	0.014	C	2
AAK64284.1_ORYSA	749	0.868	0.037	0.008	0.127	C	2
NP_001053933.1_ORYSA	1216	0.864	0.290	0.002	0.027	C	3
NP_001044091.1_ORYSA	972	0.863	0.114	0.042	0.007	C	2
NP_001056142.1_ORYSA	915	0.936	0.466	0.004	0.005	C	3
NP_001048453.1_ORYSA	403	0.035	0.140	0.246	0.719	_	3
NP_001056704.1_ORYSA	609	0.948	0.084	0.005	0.022	C	1
NP_001059450.1_ORYSA	608	0.220	0.291	0.009	0.358	_	5
NP_197818.1_ATSS1_AR	652	0.938	0.165	0.005	0.027	C	2
NP_186767.1_ATSS2_AR	792	0.938	0.162	0.011	0.032	C	2
NP_172637.1_ATSS3_AR	1025	0.818	0.083	0.020	0.124	C	2
NP_193558.3_ATSS4_AR	1040	0.779	0.113	0.051	0.033	C	2
NP_569018.1_ATSS5_AR	460	0.812	0.265	0.035	0.070	C	3
NP_174566.1_ATGBSS_A	610	0.910	0.048	0.006	0.032	C	1

Sequence	Mitochond	Plastid	ER	Elsewhere	Prediction
ACB30384.1|LjGBSS1a|LO	0.08	0.94	0.01	0.06	plastid
ACB30385.1|LjGBSS1b|LO	0.06	0.93	0.00	0.06	plastid
ACL98481.1|LjSS2a|LOTJA	0.01	0.58	0.03	0.40	plastid
ACL98482.1|LjSS2b|LOTJA	0.02	0.04	0.99	0.01	ER
LjSS1_1|LOTJA	Discarding LjSS1_1|LOTJA: no terminal Met				
LjSS1_2|LOTJA	0.04	0.06	0.01	0.90	none
LjSS5|LOTJA	0.04	0.04	0.91	0.09	ER
NP_001056881.1|ORYSA	0.07	0.95	0.02	0.05	plastid
AAL16661.1|ORYSA	0.01	0.83	0.10	0.15	plastid
AAK81729.1|ORYSA	0.01	0.93	0.03	0.06	plastid
AAK64284.1|ORYSA	0.01	0.97	0.00	0.03	plastid
NP_001053933.1|ORYSA	0.02	0.62	0.02	0.37	plastid
NP_001044091.1|ORYSA	0.01	0.88	0.02	0.12	plastid
NP_001056142.1|ORYSA	0.25	0.90	0.03	0.08	plastid
NP_001048453.1|ORYSA	Discarding NP_001048453.1|ORYSA: no terminal Met				
NP_001056704.1|ORYSA	0.03	0.92	0.00	0.08	plastid
NP_001059450.1|ORYSA	0.01	0.25	0.00	0.74	possibly plastid
NP_197818.1|ATSS1|ARAT	0.05	0.95	0.00	0.05	plastid
NP_186767.1|ATSS2|ARAT	0.01	0.95	0.00	0.05	plastid
NP_172637.1|ATSS3|ARAT	0.10	0.01	0.00	0.89	none
NP_193558.3|ATSS4|ARAT	0.10	0.50	0.00	0.45	plastid
NP_569018.1|ATSS5|ARAT	0.20	0.10	0.00	0.72	possibly mitochondrial
NP_174566.1|ATGBSS|AR	0.04	0.92	0.00	0.07	plastid

Table A3. Subcellular localisation prediction of the starch metabolism protein from several higher plant species.

Continued on next page.

XP_002321996.1_POPTR	649	0.244	0.301	0.021	0.540	_	4	XP_002321996.1|POPTR	0.01	0.47	0.00	0.53	possibly plastid
XP_002277372.1_VITVI	633	0.437	0.040	0.129	0.150	C	4	XP_002277372.1|VITVI	0.07	0.53	0.02	0.42	plastid
XP_002278470.1_VITVI	772	0.902	0.098	0.052	0.053	C	1	XP_002278470.1|VITVI	0.04	0.93	0.00	0.06	plastid
XP_002269011.1_VITVI	1140	0.351	0.304	0.019	0.209	C	5	XP_002269011.1|VITVI	0.01	0.21	0.00	0.79	possibly plastid
XP_002274716.1_VITVI	1011	0.907	0.331	0.007	0.012	C	3	XP_002274716.1|VITVI	0.19	0.64	0.00	0.29	plastid
ACD13789.1_VITVI	682	0.722	0.095	0.072	0.405	C	4	ACD13789.1|VITVI	0.01	0.14	0.01	0.85	none
XP_002273608.1_VITVI	614	0.801	0.180	0.012	0.204	C	3	XP_002273608.1|VITVI	0.02	0.69	0.00	0.30	plastid
XP_002279034.1_VITVI	605	0.879	0.073	0.004	0.148	C	2	XP_002279034.1|VITVI	0.02	0.93	0.00	0.07	plastid
XP_002324061.1_POPTR	742	0.787	0.042	0.048	0.591	C	5	XP_002324061.1|POPTR	0.01	0.77	0.00	0.22	plastid
XP_002305571.1_POPTR	1017	0.374	0.344	0.041	0.310	C	5	XP_002305571.1|POPTR	0.03	0.00	0.01	0.96	none
XP_002298514.1_POPTR	887	0.082	0.230	0.049	0.738	_	3	XP_002298514.1|POPTR	Discarding XP_002298514.1|POPTR: no terminal Met				
XP_002310316.1_POPTR	669	0.748	0.116	0.149	0.106	C	3	XP_002310316.1|POPTR	0.01	0.26	0.02	0.72	possibly plastid
XP_002300507.1_POPTR	610	0.845	0.128	0.018	0.185	C	2	XP_002300507.1|POPTR	0.01	0.81	0.00	0.19	plastid
XP_002317054.1_POPTR	585	0.961	0.043	0.012	0.111	C	1	XP_002317054.1|POPTR	0.01	0.86	0.00	0.14	plastid
ACC86844.1_SORBI	743	0.899	0.081	0.054	0.004	C	1	ACC86844.1|SORBI	0.01	0.93	0.04	0.06	plastid
ACC86845.1_SORBI	704	0.951	0.134	0.024	0.002	C	1	ACC86845.1|SORBI	0.01	0.83	0.15	0.14	plastid
ABY27640.1_SORBI	765	0.907	0.025	0.035	0.081	C	1	ABY27640.1|SORBI	0.01	0.81	0.12	0.17	plastid
XP_002443985.1_SORBI	1664	0.492	0.431	0.002	0.038	C	5	XP_002443985.1|SORBI	0.29	0.52	0.22	0.26	plastid
XP_002448557.1_SORBI	1173	0.514	0.743	0.002	0.011	M	4	XP_002448557.1|SORBI	0.14	0.61	0.07	0.31	plastid
XP_002440128.1_SORBI	909	0.966	0.100	0.014	0.010	C	1	XP_002440128.1|SORBI	0.07	0.69	0.01	0.28	plastid
XP_002453009.1_SORBI	277	0.061	0.294	0.026	0.861	_	3	XP_002453009.1|SORBI	0.01	0.00	0.00	0.99	none
XP_002436418.1_SORBI	608	0.688	0.262	0.012	0.042	C	3	XP_002436418.1|SORBI	0.03	0.55	0.00	0.44	plastid
XP_002461889.1_SORBI	607	0.875	0.068	0.005	0.056	C	1	XP_002461889.1|SORBI	0.02	0.91	0.03	0.08	plastid

SBE

Name	Len	cTP	mTP	SP	other	Loc	RC	Sequence	Mitochond	Plastid	ER	Elsewhere	Prediction
LjSBE1_LOTJA	848	0.918	0.064	0.023	0.088	C	1	LjSBE1|LOTJA	0.01	0.96	0.00	0.04	plastid
BAA82828.1_ORYSA	841	0.163	0.488	0.016	0.155	M	4	BAA82828.1|ORYSA	0.17	0.11	0.03	0.71	none
NP_001047009.1_ORYSA	825	0.935	0.178	0.004	0.018	C	2	NP_001047009.1|ORYSA	0.18	0.97	0.01	0.03	plastid
NP_001057611.1_ORYSA	903	0.973	0.135	0.005	0.049	C	1	NP_001057611.1|ORYSA	0.01	0.89	0.00	0.11	plastid
NP_001058629.1_ORYSA	820	0.931	0.029	0.049	0.036	C	1	NP_001058629.1|ORYSA	0.02	0.30	0.01	0.68	possibly plastid
NP_181180.1_SBE2.1_A	858	0.898	0.097	0.003	0.109	C	2	NP_181180.1|SBE2.1|ARA	0.11	0.63	0.01	0.32	plastid
NP_188679.2_BE1_ARAT	869	0.643	0.296	0.034	0.102	C	4	NP_188679.2|BE1|ARATH	0.06	0.33	0.00	0.63	possibly plastid
NP_195985.3_SBE2.2_A	805	0.511	0.427	0.009	0.083	C	5	NP_195985.3|SBE2.2|ARA	0.38	0.10	0.02	0.55	possibly mitochondrial
XP_002277213.1_VITVI	1068	0.180	0.169	0.256	0.113	S	5	XP_002277213.1|VITVI	0.33	0.17	0.14	0.47	possibly mitochondrial
XP_002278858.1_VITVI	866	0.933	0.099	0.019	0.061	C	1	XP_002278858.1|VITVI	0.03	0.89	0.00	0.10	plastid
XP_002284841.1_VITVI	817	0.222	0.272	0.066	0.558	_	4	XP_002284841.1|VITVI	0.01	0.01	0.00	0.98	none
ABN05323.1_POPTR	896	0.692	0.058	0.485	0.009	C	4	ABN05323.1|POPTR	0.02	0.55	0.01	0.44	plastid
XP_002307789.1_POPTR	701	0.098	0.113	0.144	0.884	_	2	XP_002307789.1|POPTR	0.01	0.00	0.00	0.99	none
XP_002326414.1_POPTR	730	0.238	0.072	0.049	0.925	_	2	XP_002326414.1|POPTR	0.01	0.01	0.00	0.99	none
XP_002439059.1_SORBI	668	0.968	0.101	0.009	0.034	C	1	XP_002439059.1|SORBI	0.04	0.58	0.04	0.39	plastid
XP_002447772.1_SORBI	827	0.804	0.220	0.011	0.045	C	3	XP_002447772.1|SORBI	0.20	0.67	0.02	0.26	plastid
XP_002453926.1_SORBI	803	0.685	0.249	0.020	0.096	C	3	XP_002453926.1|SORBI	0.35	0.53	0.02	0.30	plastid
XP_002455921.1_SORBI	906	0.650	0.131	0.005	0.118	C	3	XP_002455921.1|SORBI	0.01	0.21	0.14	0.68	possibly plastid

DBE

Name	Len	cTP	mTP	SP	other	Loc	RC	Sequence	Mitochondr	Plastid	ER	Elsewhere	Prediction
LjISA1_LOTJA	791	0.860	0.067	0.082	0.165	C	2	LjISA1|LOTJA	0.04	0.66	0.00	0.33	plastid
LjISA2_LOTJA	590	0.048	0.285	0.481	0.092	S	5	LjISA2|LOTJA	Discarding LjISA2|LOTJA: no terminal Met				
LjLDA_LOTJA	559	0.106	0.077	0.135	0.835	_	2	LjLDA|LOTJA	Discarding LjLDA|LOTJA: no terminal Met				
BAD19754.1_ORYSA	700	0.209	0.138	0.053	0.864	_	2	BAD19754.1|ORYSA	0.01	0.01	0.00	0.98	none
NP_001052129.1_ORYSA	621	0.384	0.085	0.077	0.653	_	4	NP_001052129.1|ORYSA	Discarding NP_001052129.1|ORYSA: no terminal Met				
NP_001055456.1_ORYSA	817	0.684	0.233	0.040	0.204	C	3	NP_001055456.1|ORYSA	0.03	0.61	0.01	0.38	plastid
NP_001062271.1_ORYSA	700	0.026	0.412	0.198	0.499	_	5	NP_001062271.1|ORYSA	Discarding NP_001062271.1|ORYSA: no terminal Met				
NP_181522.1_ATISA1_A	783	0.659	0.061	0.034	0.232	C	3	NP_181522.1|ATISA1|ARAT	0.02	0.13	0.00	0.85	none
NP_192641.2_ATISA3_A	764	0.976	0.011	0.016	0.112	C	1	NP_192641.2|ATISA3|ARAT	0.01	0.32	0.01	0.67	possibly plastid
NP_196056.2_ATLDA_AR	965	0.903	0.053	0.004	0.023	C	1	NP_196056.2|ATLDA|ARATH	0.31	0.97	0.01	0.02	plastid
NP_973751.1_ATISA2_A	882	0.859	0.069	0.017	0.116	C	2	NP_973751.1|ATISA2|ARAT	0.03	0.85	0.00	0.15	plastid
XP_002265964.1_VITVI	742	0.108	0.170	0.290	0.272	S	5	XP_002265964.1|VITVI	0.01	0.00	0.09	0.90	none
XP_002271798.1_VITVI	882	0.189	0.151	0.175	0.264	_	5	XP_002271798.1|VITVI	0.04	0.11	0.02	0.84	none
XP_002271820.1_VITVI	907	0.007	0.239	0.605	0.557	S	5	XP_002271820.1|VITVI	0.01	0.00	0.30	0.69	possibly ER
XP_002284042.1_VITVI	787	0.680	0.030	0.041	0.384	C	4	XP_002284042.1|VITVI	0.01	0.25	0.01	0.73	possibly plastid
XP_002301076.1_POPTR	819	0.773	0.021	0.153	0.116	C	2	XP_002301076.1|POPTR	0.01	0.06	0.00	0.93	none
XP_002308090.1_POPTR	826	0.666	0.133	0.028	0.184	C	3	XP_002308090.1|POPTR	0.02	0.12	0.00	0.87	none
XP_002315334.1_POPTR	893	0.055	0.274	0.242	0.617	_	4	XP_002315334.1|POPTR	0.01	0.03	0.04	0.93	none
XP_002324659.1_POPTR	801	0.665	0.111	0.025	0.053	C	3	XP_002324659.1|POPTR	0.09	0.27	0.01	0.66	possibly plastid
XP_002441051.1_SORBI	800	0.884	0.318	0.019	0.056	C	3	XP_002441051.1|SORBI	0.02	0.96	0.00	0.04	plastid
XP_002445873.1_SORBI	784	0.672	0.341	0.010	0.033	C	4	XP_002445873.1|SORBI	0.24	0.29	0.03	0.53	possibly plastid
XP_002446086.1_SORBI	966	0.909	0.233	0.007	0.014	C	2	XP_002446086.1|SORBI	0.08	0.76	0.02	0.22	plastid

GWD

Name	Len	cTP	mTP	SP	other	Loc	RC	Sequence	Mitochondr	Plastid	ER	Elsewhere	Prediction
LjGWD1_LOTJA	1463		0.133	0.230	0.681	_	3	LjGWD1|LOTJA	0.01	0.71	0.00	0.29	plastid
LjGWD3_LOTJA	1175		0.749	0.019	0.389	M	4	LjGWD3|LOTJA	0.06	0.00	0.01	0.93	none
NP_001057699.1_ORYSA	1414		0.939	0.015	0.109	M	1	NP_001057699.1|ORYSA	Discarding NP_001057699.1|ORYSA: no terminal Met				
NP_001066613.1_ORYSA	1206		0.677	0.031	0.364	M	4	NP_001066613.1|ORYSA	0.15	0.11	0.04	0.73	none
NP_194176.3_ATGWD2_A	1278		0.104	0.080	0.864	_	2	NP_194176.3|ATGWD2|ARA	0.01	0.00	0.03	0.96	none
NP_198009.3_ATGWD3_A	1196		0.435	0.022	0.716	_	4	NP_198009.3|ATGWD3|ARA	0.01	0.54	0.00	0.46	plastid
NP_563877.1_GWD1_ARA	1399		0.623	0.049	0.408	M	4	NP_563877.1|GWD1|ARATH	0.12	0.04	0.00	0.84	none
XP_002265211.1_VITVI	1188		0.335	0.037	0.719	_	4	XP_002265211.1|VITVI	0.05	0.21	0.00	0.76	possibly plastid
XP_002270485.1_VITVI	1470		0.521	0.058	0.452	M	5	XP_002270485.1|VITVI	0.16	0.03	0.00	0.81	none
XP_002315679.1_POPTR	1477		0.645	0.033	0.484	M	5	XP_002315679.1|POPTR	0.05	0.43	0.00	0.54	possibly plastid
XP_002438419.1_SORBI	1469		0.759	0.084	0.184	M	3	XP_002438419.1|SORBI	0.14	0.90	0.00	0.09	plastid
XP_002453659.1_SORBI	1212		0.695	0.047	0.281	M	3	XP_002453659.1|SORBI	0.01	0.10	0.01	0.88	none

AMY

Name	Len	cTP	mTP	SP	other	Loc	RC	Sequence	Mitochondr	Plastid	ER	Elsewhere	Prediction
LjAMY1_LOTJA	423	0.039	0.005	0.985	0.039	S	1	LjAMY1|LOTJA	0.01	0.03	0.97	0.03	ER
LjAMY2_LOTJA	291	0.065	0.102	0.213	0.867	_	2	LjAMY2|LOTJA	Discarding LjAMY2|LOTJA: no terminal Met				
LjAMY3a_LOTJA	391	0.045	0.580	0.026	0.191	M	4	LjAMY3a|LOTJA	Discarding LjAMY3a|LOTJA: no terminal Met				
LjAMY3b_LOTJA	912	0.595	0.352	0.002	0.167	C	4	LjAMY3b|LOTJA	0.03	0.29	0.01	0.68	possibly plastid
NP_001044062.1_ORYSA	876	0.879	0.226	0.006	0.043	C	2	NP_001044062.1|ORYSA	0.17	0.73	0.05	0.21	plastid
NP_001048220_ORYSA	434	0.002	0.103	0.983	0.034	S	1	NP_001048220|ORYSA	0.01	0.00	0.72	0.27	ER
NP_001052697.1_ORYSA	469	0.056	0.409	0.044	0.619	_	4	NP_001052697.1|ORYSA	0.01	0.00	0.02	0.97	none
NP_001058568_ORYSA	445	0.004	0.099	0.974	0.035	S	1	NP_001058568|ORYSA	0.05	0.00	0.99	0.01	ER
NP_001062023_ORYSA	437	0.006	0.027	0.993	0.013	S	1	NP_001062023|ORYSA	0.01	0.00	0.99	0.01	ER
NP_001062024_ORYSA	476	0.338	0.077	0.066	0.730	_	4	NP_001062024|ORYSA	0.01	0.02	0.00	0.97	none
NP_001063367_ORYSA	440	0.002	0.050	0.994	0.026	S	1	NP_001063367|ORYSA	0.01	0.00	0.99	0.01	ER
NP_001063368_ORYSA	438	0.004	0.033	0.995	0.014	S	1	NP_001063368|ORYSA	0.04	0.00	0.99	0.01	ER
NP_001063369_ORYSA	437	0.003	0.027	0.995	0.024	S	1	NP_001063369|ORYSA	0.01	0.00	0.99	0.01	ER

Table A3. Subcellular localisation prediction of the starch metabolism protein from several higher plant species.
Continued on next page.

NP_177740.1_AMY2_ARA	413	0.166	0.073	0.092	0.923	_	2	NP_177740.1|AMY2|ARATH	0.01	0.00	0.00	0.99	none
NP_564977.1_AMY3_ARA	887	0.916	0.082	0.007	0.043	C	1	NP_564977.1|AMY3|ARATH	0.01	0.47	0.00	0.52	possibly plastid
NP_567714.1_AMY1_ARA	423	0.010	0.010	0.992	0.027	S	1	NP_567714.1|AMY1|ARATH	0.01	0.00	0.99	0.01	ER
XP_002270049.1_VITVI	901	0.796	0.222	0.003	0.124	C	3	XP_002270049.1|VITVI	0.04	0.13	0.01	0.83	none
XP_002282184_VITVI	425	0.039	0.002	0.991	0.078	S	1	XP_002282184|VITVI	0.01	0.01	0.99	0.01	ER
XP_002284805.1_VITVI	459	0.590	0.223	0.016	0.462	C	5	XP_002284805.1|VITVI	0.02	0.01	0.00	0.98	none
XP_002285213_VITVI	424	0.042	0.003	0.980	0.095	S	1	XP_002285213|VITVI	0.01	0.01	0.98	0.01	ER
XP_002301187_POPTR	404	0.073	0.286	0.075	0.510	_	4	XP_002301187|POPTR	0.01	0.11	0.04	0.85	none
XP_002301935.1_POPTR	406	0.052	0.222	0.100	0.862	_	2	XP_002301935.1|POPTR	0.01	0.00	0.00	0.99	none
XP_002327139_POPTR	423	0.008	0.013	0.984	0.025	S	1	XP_002327139|POPTR	0.01	0.01	0.99	0.01	ER
XP_002444507_SORBI	443	0.001	0.135	0.982	0.026	S	1	XP_002444507|SORBI	0.01	0.00	0.99	0.01	ER
XP_002446386.1_SORBI	415	0.193	0.055	0.047	0.915	_	2	XP_002446386.1|SORBI	0.01	0.00	0.00	0.99	none
XP_002452881_SORBI	428	0.006	0.018	0.995	0.024	S	1	XP_002452881|SORBI	0.02	0.00	0.99	0.01	ER
XP_002454601_SORBI	428	0.006	0.019	0.993	0.023	S	1	XP_002454601|SORBI	0.02	0.00	0.99	0.01	ER
XP_002456247.1_SORBI	820	0.023	0.033	0.973	0.081	S	1	XP_002456247.1|SORBI	0.01	0.00	0.99	0.01	ER
XP_002460331_SORBI	437	0.005	0.021	0.996	0.020	S	1	XP_002460331|SORBI	0.01	0.00	0.99	0.01	ER
XP_002460332_SORBI	437	0.005	0.021	0.996	0.020	S	1	XP_002460332|SORBI	0.01	0.00	0.99	0.01	ER
XP_002462321_SORBI	435	0.004	0.088	0.975	0.009	S	1	XP_002462321|SORBI	0.01	0.00	0.99	0.01	ER

BAM

Name	Len	cTP	mTP	SP	other	Loc	RC	Sequence	Mitochondr	Plastid	ER	Elsewhere	Prediction
LjBAM1_LOTJA	561	0.929	0.029	0.012	0.221	C	2	LjBAM1|LOTJA	0.01	0.64	0.00	0.36	plastid
LjBAM3a_LOTJA	249	0.187	0.869	0.003	0.055	M	2	LjBAM3a|LOTJA	Discarding LjBAM3a|LOTJA: no terminal Met				
LjBAM3b_1_LOTJA	465	0.523	0.047	0.158	0.467	C	5	LjBAM3b_1|LOTJA	0.01	0.05	0.01	0.94	none
LjBAM3b_2_LOTJA	298	0.106	0.232	0.119	0.825	_	3	LjBAM3b_2|LOTJA	Discarding LjBAM3b_2|LOTJA: no terminal Met				
LjBAM5_LOTJA	496	0.006	0.052	0.953	0.159	S	2	LjBAM5|LOTJA	0.01	0.00	0.98	0.02	ER
LjBAM6_LOTJA	350	0.154	0.081	0.234	0.785	_	3	LjBAM6|LOTJA	0.01	0.01	0.00	0.99	none
LjBAM7_LOTJA	652	0.409	0.034	0.035	0.903	_	3	LjBAM7|LOTJA	0.01	0.01	0.00	0.99	none
LjBAM8_LOTJA	656	0.168	0.176	0.059	0.809	_	2	LjBAM8|LOTJA	0.01	0.00	0.00	0.99	none
LjBAM9_LOTJA	505	0.211	0.067	0.043	0.698	_	3	LjBAM9|LOTJA	0.01	0.51	0.01	0.48	plastid
NP_001059906_ORYSA	600	0.966	0.221	0.001	0.019	C	2	NP_001059906|ORYSA	0.02	0.93	0.05	0.06	plastid
NP_001063976_ORYSA	533	0.888	0.087	0.006	0.018	C	1	NP_001063976|ORYSA	0.15	0.46	0.38	0.29	plastid
NP_001065418_ORYSA	544	0.791	0.068	0.061	0.171	C	2	NP_001065418|ORYSA	0.01	0.72	0.00	0.28	plastid
NP_180788_BAM6_ARATH	577	0.357	0.181	0.014	0.600	_	4	NP_180788|BAM6|ARATH	0.02	0.75	0.00	0.25	plastid
NP_182112_BAM7_ARATH	691	0.037	0.090	0.045	0.972	_	1	NP_182112|BAM7|ARATH	0.01	0.00	0.00	0.99	none
NP_189034_BAM1_ARATH	575	0.462	0.172	0.035	0.331	C	5	NP_189034|BAM1|ARATH	0.01	0.51	0.00	0.48	plastid
NP_191958.3_BAM2_ARA	542	0.870	0.227	0.031	0.017	C	2	NP_191958.3|BAM2|ARATH	0.36	0.72	0.02	0.17	plastid
NP_197368_BAM9_ARATH	536	0.205	0.228	0.011	0.235	_	5	NP_197368|BAM9|ARATH	0.01	0.61	0.00	0.38	plastid
NP_199343_BAM8_ARATH	689	0.565	0.044	0.009	0.750	_	5	NP_199343|BAM8|ARATH	0.01	0.00	0.00	0.99	none
NP_567460_BAM5_ARATH	498	0.002	0.053	0.974	0.287	S	2	NP_567460|BAM5|ARATH	0.01	0.00	0.91	0.09	ER
NP_567523_BAM3_ARATH	548	0.790	0.087	0.025	0.325	C	3	NP_567523|BAM3|ARATH	0.01	0.25	0.00	0.74	possibly plastid
NP_568829_BAM4_ARATH	531	0.289	0.099	0.003	0.597	_	4	NP_568829|BAM4|ARATH	0.01	0.04	0.00	0.95	none
XP_002265698_VITVI	522	0.085	0.105	0.007	0.860	_	2	XP_002265698|VITVI	0.01	0.00	0.00	0.99	none
XP_002270680_VITVI	670	0.346	0.131	0.034	0.609	_	4	XP_002270680|VITVI	0.01	0.00	0.00	0.99	none
XP_002273843_VITVI	699	0.065	0.070	0.043	0.951	_	1	XP_002273843|VITVI	0.01	0.00	0.00	0.99	none
XP_002274612_VITVI	580	0.957	0.053	0.014	0.007	C	1	XP_002274612|VITVI	0.02	0.85	0.01	0.15	plastid
XP_002276777_VITVI	541	0.091	0.813	0.007	0.088	M	2	XP_002276777|VITVI	0.11	0.93	0.01	0.06	plastid
XP_002281003_VITVI	520	0.023	0.093	0.641	0.725	_	5	XP_002281003|VITVI	0.01	0.00	0.05	0.94	none
XP_002282871_VITVI	543	0.810	0.071	0.010	0.349	C	3	XP_002282871|VITVI	0.10	0.36	0.02	0.56	possibly plastid
XP_002285569_VITVI	573	0.772	0.054	0.018	0.336	C	3	XP_002285569|VITVI	0.02	0.64	0.01	0.35	plastid
XP_002304400_POPTR	701	0.483	0.035	0.005	0.740	_	4	XP_002304400|POPTR	0.01	0.00	0.00	0.99	none
XP_002311706_POPTR	562	0.862	0.036	0.009	0.311	C	3	XP_002311706|POPTR	0.01	0.00	0.00	0.99	none
XP_002312750_POPTR	437	0.028	0.193	0.132	0.725	_	3	XP_002312750|POPTR	Discarding XP_002312750|POPTR: no terminal Met				
XP_002314522_POPTR	472	0.111	0.151	0.180	0.831	_	2	XP_002314522|POPTR	Discarding XP_002314522|POPTR: no terminal Met				
XP_002320794_POPTR	437	0.014	0.036	0.873	0.499	S	4	XP_002320794|POPTR	Discarding XP_002320794|POPTR: no terminal Met				
XP_002326690_POPTR	547	0.683	0.045	0.034	0.381	C	4	XP_002326690|POPTR	0.01	0.49	0.00	0.50	possibly plastid
XP_002327920_POPTR	519	0.009	0.089	0.761	0.686	S	5	XP_002327920|POPTR	0.01	0.00	0.46	0.54	possibly ER
XP_002329547_POPTR	548	0.412	0.392	0.006	0.092	C	5	XP_002329547|POPTR	0.48	0.43	0.02	0.29	mitochondrial
XP_002459849_SORBI	469	0.082	0.142	0.141	0.914	_	2	XP_002459849|SORBI	0.01	0.00	0.00	0.99	none
XP_002460819_SORBI	604	0.923	0.220	0.004	0.031	C	2	XP_002460819|SORBI	0.02	0.55	0.03	0.43	plastid
XP_002464915_SORBI	557	0.760	0.047	0.016	0.266	C	3	XP_002464915|SORBI	0.01	0.91	0.00	0.09	plastid

DPE

Name	Len	cTP	mTP	SP	other	Loc	RC	Sequence	Mitochondr	Plastid	ER	Elsewhere	Prediction
LjDPE1_LOTJA	565	0.761	0.374	0.017	0.052	C	4	LjDPE1|LOTJA	0.16	0.36	0.00	0.53	possibly plastid
LjDPE2_1_LOTJA	343	0.227	0.040	0.173	0.918	_	2	LjDPE2_1|LOTJA	Discarding LjDPE2_1|LOTJA: no terminal Met				
LjDPE2_2_LOTJA	371	0.190	0.200	0.064	0.079	M	5	LjDPE2_2|LOTJA	0.33	0.10	0.04	0.58	possibly mitochondrial
NP_001043271.1_ORYSA	657	0.294	0.261	0.029	0.442	_	5	NP_001043271.1|ORYSA	0.01	0.02	0.01	0.97	none
NP_001060342.1_ORYSA	601	0.772	0.288	0.027	0.028	C	3	NP_001060342.1|ORYSA	0.18	0.72	0.05	0.22	plastid
NP_201291.1_DPE1_ARA	576	0.702	0.261	0.028	0.019	C	3	NP_201291.1|DPE1|ARATH	0.76	0.84	0.06	0.03	plastid
NP_850336.1_DPE2_ARA	658	0.288	0.075	0.115	0.598	_	4	NP_850336.1|DPE2|ARATH	0.01	0.26	0.01	0.72	possibly plastid
XP_002276109.1_VITVI	583	0.644	0.062	0.308	0.086	C	4	XP_002276109.1|VITVI	0.02	0.50	0.04	0.48	plastid
XP_002283436.1_VITVI	659	0.327	0.170	0.167	0.412	_	5	XP_002283436.1|VITVI	0.01	0.02	0.01	0.97	none
XP_002283443.1_VITVI	669	0.232	0.253	0.176	0.451	_	5	XP_002283443.1|VITVI	0.01	0.02	0.01	0.97	none
XP_002310024.1_POPTR	574	0.691	0.047	0.221	0.048	C	3	XP_002310024.1|POPTR	0.19	0.15	0.16	0.58	none
XP_002323217.1_POPTR	661	0.457	0.100	0.115	0.545	_	5	XP_002323217.1|POPTR	0.01	0.01	0.01	0.97	none
XP_002455756.1_SORBI	652	0.206	0.317	0.027	0.419	_	5	XP_002455756.1|SORBI	0.01	0.02	0.01	0.97	none
XP_002461064.1_SORBI	590	0.630	0.732	0.006	0.013	M	5	XP_002461064.1|SORBI	0.43	0.07	0.23	0.41	mitochondrial

PHS

Name	Len	cTP	mTP	SP	other	Loc	RC	Sequence	Mitochondr	Plastid	ER	Elsewhere	Prediction
LjPHS2a_LOTJA	846	0.192	0.081	0.119	0.881	_	2	LjPHS2a|LOTJA	0.01	0.01	0.00	0.98	none
LjPHS2b_LOTJA	226	0.025	0.404	0.146	0.664	_	4	LjPHS2b|LOTJA	Discarding LjPHS2b|LOTJA: no terminal Met				
NP_001044823.1_ORYSA	841	0.369	0.029	0.305	0.636	_	4	NP_001044823.1|ORYSA	0.01	0.01	0.00	0.98	none
NP_001051330.1_ORYSA	629	0.119	0.359	0.033	0.620	_	4	NP_001051330.1|ORYSA	Discarding NP_001051330.1|ORYSA: no terminal Met				
NP_189578.1_PHS1_ARA	962	0.615	0.035	0.015	0.259	C	4	NP_189578.1|PHS1|ARATH	0.01	0.24	0.00	0.76	possibly plastid
NP_190281.1_PHS2_ARA	841	0.124	0.046	0.272	0.840	_	3	NP_190281.1|PHS2|ARATH	0.01	0.00	0.00	0.99	none
XP_002273615.1_VITVI	818	0.050	0.247	0.124	0.803	_	3	XP_002273615.1|VITVI	0.01	0.00	0.00	0.99	none
XP_002274575.1_VITVI	981	0.982	0.072	0.003	0.038	C	1	XP_002274575.1|VITVI	0.01	0.97	0.00	0.03	plastid
XP_002279075.1_VITVI	958	0.967	0.037	0.008	0.061	C	1	XP_002279075.1|VITVI	0.01	0.97	0.00	0.03	plastid
XP_002280732.1_VITVI	843	0.158	0.063	0.376	0.713	_	4	XP_002280732.1|VITVI	0.01	0.00	0.00	0.99	none
XP_002305114.1_POPTR	818	0.049	0.297	0.068	0.868	_	3	XP_002305114.1|POPTR	0.03	0.00	0.00	0.96	none
XP_002305367.1_POPTR	949	0.298	0.234	0.064	0.193	C	5	XP_002305367.1|POPTR	0.05	0.00	0.00	0.95	none
XP_002313399.1_POPTR	853	0.767	0.108	0.167	0.115	C	2	XP_002313399.1|POPTR	0.01	0.79	0.00	0.20	plastid
XP_002316098.1_POPTR	953	0.923	0.147	0.026	0.016	C	2	XP_002316098.1|POPTR	0.05	0.84	0.00	0.15	plastid
XP_002458773.1_SORBI	838	0.208	0.067	0.134	0.820	_	2	XP_002458773.1|SORBI	0.01	0.00	0.00	0.99	none

MEX1

Name	Len	cTP	mTP	SP	other	Loc	RC	Sequence	Mitochondr	Plastid	ER	Elsewhere	Prediction
LjMEX1_LOTJA	400	0.458	0.568	0.009	0.095	M	5	LjMEX1|LOTJA	0.19	0.56	0.04	0.34	plastid
NP_001053772_ORYSA	399	0.803	0.194	0.009	0.057	C	2	NP_001053772|ORYSA	0.34	0.24	0.03	0.48	possibly mitochondrial
NP_568349_MEX1_ARATH	415	0.940	0.046	0.006	0.083	C	1	NP_568349|MEX1|ARATH	0.01	0.29	0.00	0.71	possibly plastid
XP_002265122_VITVI	405	0.694	0.157	0.007	0.093	C	3	XP_002265122|VITVI	0.02	0.64	0.08	0.33	plastid
XP_002319239_POPTR	294	0.005	0.184	0.516	0.305	S	4	XP_002319239|POPTR	0.40	0.24	0.17	0.38	mitochondrial
XP_002448464_SORBI	401	0.819	0.361	0.004	0.039	C	3	XP_002448464|SORBI	0.15	0.37	0.03	0.52	possibly plastid

Table A3. Subcellular localisation prediction of the starch metabolism protein from several higher plant species. Continued on next page.

Table A3. Subcellular localisation prediction of the starch metabolism protein from several higher plant species. Continued.
Predictions were carried using the programs TargetP (left panel) and Predotar (right panel) as described in Chapter 2, section 2.7.1. The sequences of the proteins analysed are given in Table A2. Proteins predicted by both programs to be plastidial are highlighted in green and those predicted to be mitochondrial or secreted are highlighted in pale yellow and pale red, respectively. Abreviations for the results given by TargetP: Name, sequence name; Len, sequence length; cTP, mTP, SP, final score on which the final localisation prediction (Loc) is based: C, Chloroplast (i.e. the sequence contains a cTP, a chloroplast transit peptide), M, Mitochondrion (i.e. the sequence contains a mTP, a mitochondrial targeting peptide, and S, Secretory pathway (i.e. the sequence contains a SP, a signal peptide); the symbol '_' refers to any other location. RC, reliability class (from 1 to 5, where 1 indicates the strongest prediction).

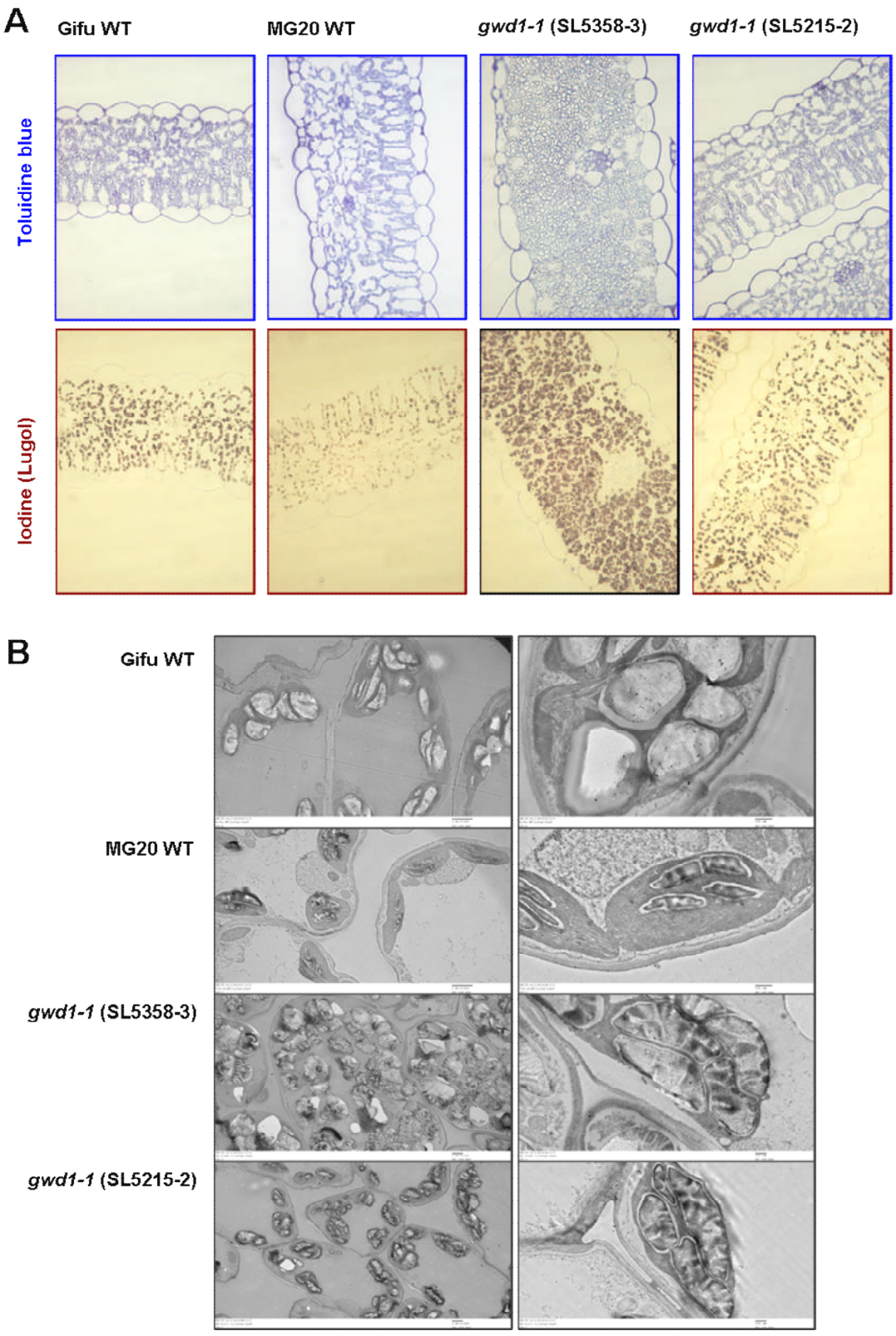

Figure A4. Leaf starch granule micrographs of the *gwd1-1* mutants and the MG-20 and Gifu WTs. **A.** Light microscopy (LM) sections of leaf material (pool of two mature leaves from the top of the plant for each genotype) harvested at the end of the night from plants grown in a greenhouse in LD conditions. LM sections were prepared by Sue Bunnewell (JIC, Norwich, UK). This microscopy sections were then staining with either Toluidine blue or iodine solution prior observation and imaging under a light microscope as described in Chapter 2, section 2.5. **B.** Transmission electron microscopy (TEM) sections performed on the same leaf material than the one used for the LM sections. TEM sections were prepared and micrographs were taken by Sue Bunnewell.

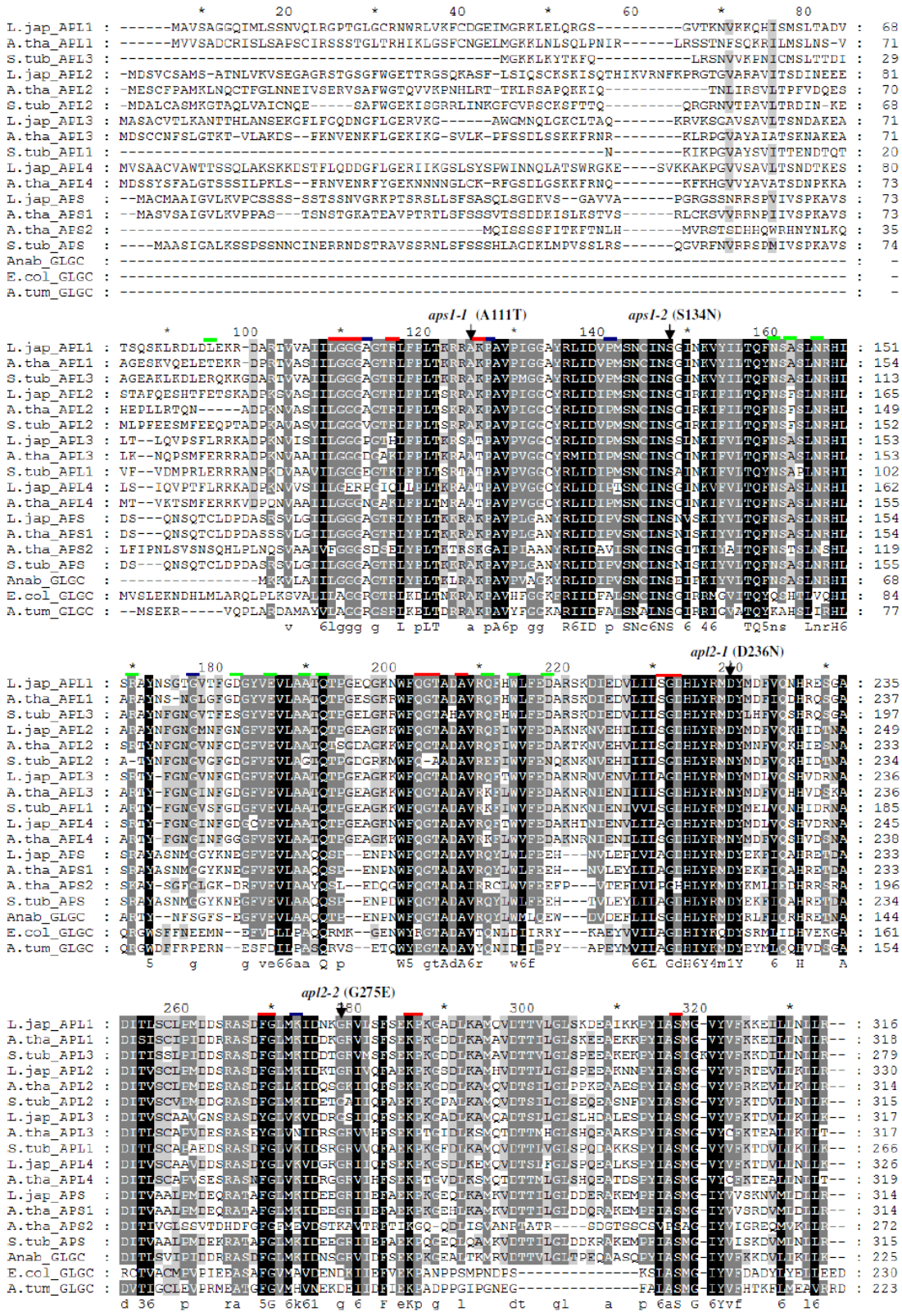

Figure A5. Comparison of the amino acid sequences of *L. japonicus* AGPase subunits with those of other species (full length sequence alignment).
Continued on next page.

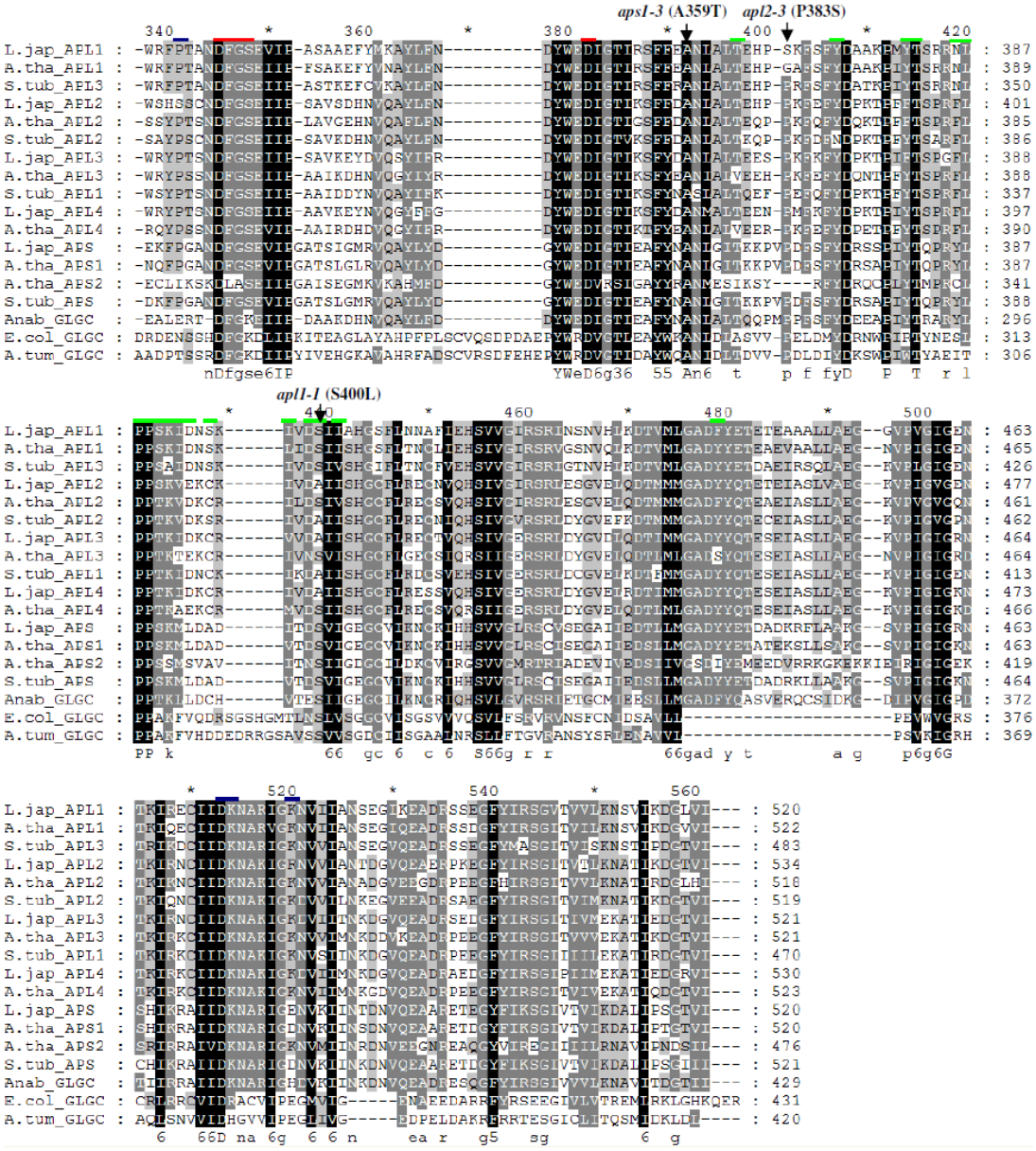

Figure A5. Comparison of the amino acid sequences of *L. japonicus* AGPase subunits with those of other species (full length sequence alignment). Continued.
Comparison of the full length sequence of the small and large subunits from *L. japonicus* (L.jap) genes with homologs from species including bacteria [*E. coli* (E.col) and *A. tumefaciens* (A.tum)], cyanobacteria [*Anabena* sp. (Anab)] and plants [*Arabidopsis thaliana* (A.tha) and *S. tuberosum* (S.tub)]. The alignment was made with the programs Clustal W2 (default settings) and GeneDoc. Strictly conserved residues are highlighted in black, less conserved residues are in grey. The positions of the mutations identified from forward screen and TILLING in LjAPL1 and LjAPS1 are indicated by arrows. Residues marked in red interact with the substrates ADPGlc and/or ATP in the *S. tuberosum* APS protein (Jin et al., 2005); those marked in blue may be important in the regulatory properties of the enzyme (Kavakli et al., 2001; 2002). Residues marked in green are those involved in subunit interactions according to Jin et al. Note that in this alignment the residue in the potato APS protein equivalent to *L. japonicus* S400 is S401. Accession numbers for the sequences are given in Figure 29.

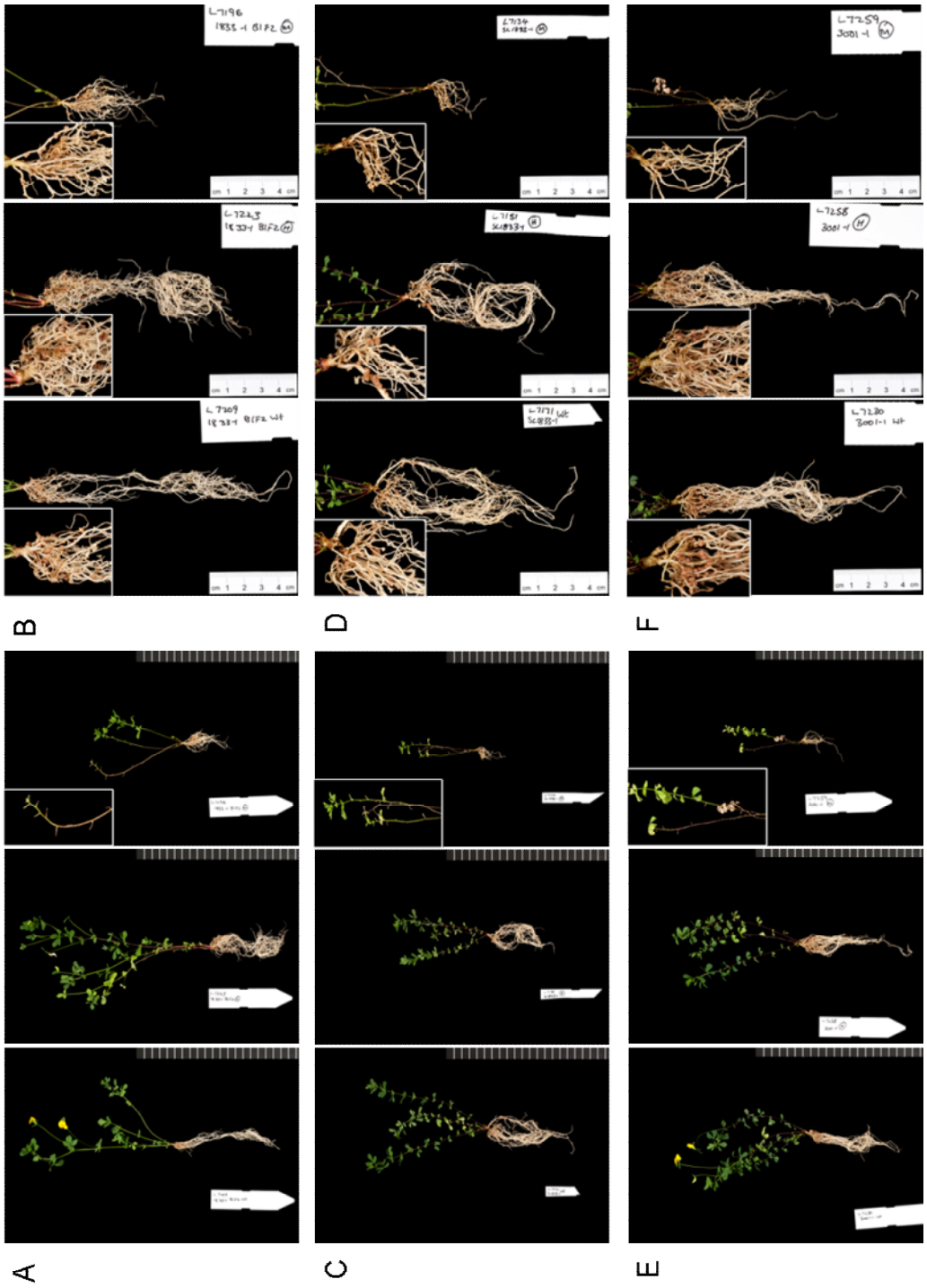

Figure A6. Shoot and root phenotypes of the *gwd1-2* and *gwd1-3* mutants of *L. japonicus*.
A and **B**. Phenotype of the whole plant (A) and root system (B) of the *gwd1-2* mutant from a first outcross to MG-20 (B1F2 generation). **B-F**. Phenotype of the whole plant (C and E) and root system (D and F) of the *gwd1-2* (C, D) and *gwd1-3* (E, F) mutants in the Gifu genotype background (M5). A-F WT, heterozygote, and mutant segregant plants (left, middle, and right, respectively) that were grown in a controlled environment room under long day conditions (16 h light, 8 h dark) and were ca. 3 month old at the time the photographs were taken. A representative plant of a minimum of seven biological replicates are shown for each genotype These plants were grown for an acetylene reduction assay as described in Chapter 2, section 2.1.3. Despite a certain degree of variable expressivity of the mutant phenotype, all the *gwd1-2/3* mutants isolated so far presented a strong impairment in growth and reproduction together with signs of chlorosis and premature senescence (zoom on this phenotype is shown on the left corner of each A-C panel) but were still able to produce nodules and fix atmospheric nitrogen. Plants were grown and genotyped by Tracey Welham, and photographed by Andrew Davis (JIC, Norwich, UK).

Table A4.A

SL1833-1 (*gwd1-2*)

screen #	Class #				
	1	2	3	4	5
1	0	n/a	n/a	n/a	n/a
2	0	n/a	n/a	n/a	n/a
3	0	n/a	n/a	n/a	n/a
4	L1614	no	no	yes	no
	L1643	no	no	no	n/a
	L1644	no	yes	n/a	n/a
5	L2271	no	no	yes	no
	L2272	no	yes	n/a	n/a
	L2308	yes	n/a	n/a	n/a
6	L2899	no	no	no	n/a
	L2914	no	no	no	n/a

ratio: 2/8

in %: 25,0

SL3001-1 (*gwd1-3*)

screen #	Class #				
	1	2	3	4	5
1	0	n/a	n/a	n/a	n/a
2	K9904	yes	n/a	n/a	n/a
3	L2211	yes	n/a	n/a	n/a
	L2212	yes	n/a	n/a	n/a
	L2221	yes	n/a	n/a	n/a
4	L1660	yes	n/a	n/a	n/a
5	L2236	yes	n/a	n/a	n/a
	L2257	no	yes	n/a	n/a
	L2259	no	no	yes	no
	L2263	no	yes	n/a	n/a
	L2267	no	no	no	n/a
6	L2932	no	no	yes	yes (2)

ratio: 2/11

in %: 18,2

Table A4.B

SL1833-1 (*gwd1-2*)

genotype	screen #							Actual ratio	
	1	2	3	4	5	6	7	sum	in %
WT	9	4	0	8	21	11	37	90	41
Het	3	4	0	9	31	31	38	116	53
M	0	0	0	3	3	2	5	13	6
sum	12	8	0	20	55	44	80	219	100

SL3001-1 (*gwd1-3*)

genotype	screen #							Actual ratio	
	1	2	3	4	5	6	7	sum	in %
WT	6	5	6	11	12	12	37	89	44
Het	7	5	8	19	21	11	27	98	49
M	0	1	3	1	5	1	4	15	7
sum	13	11	17	31	38	24	68	202	100

Table A4.C

SL1833-1 (*gwd1-2*)

genotype	Line	pod nber	seed weight (in g)	seed nber	seed nber/pod	average seed weight	seed weight/pod
Het	L2880	20	0,321	318,0	15,9	0,0010	0,016
WT	L2910	20	0,338	301,0	15,05	0,0011	0,017

SL3001-1 (*gwd1-3*)

genotype	Line	pod nber	seed weight (in g)	seed nber	seed nber/pod	average seed weight	seed weight/pod
Het	L2931	20	0,175	167,0	8,35	0,0011	0,009
WT	L2922	20	0,243	216,0	10,8	0,0011	0,012
Het	L2937	10	0,091	92,0	9,2	0,0010	0,009
Het	L2944	10	0,103	104,0	10,4	0,0010	0,010
WT	L2930	10	0,070	87,0	8,7	0,0008	0,007
WT	L2934	10	0,102	104,0	10,4	0,0010	0,010
average	Het	40	0,370	363,0	9,075	0,0010	0,009
	WT	40	0,415	407,0	10,175	0,0010	0,010

Table A4.D

SL1833-1 (*gwd1-2*)

genotype	observed	in %	expected
M	4	11	25
Het	18	49	50
WT	15	41	25
total	37	100	100

CHITEST (df=2): 0,000139829

SL3001-1 (*gwd1-3*)

genotype	observed	in %	expected
M	3	12	25
Het	11	42	50
WT	12	46	25
total	26	100	100

CHITEST (df=2): 1,91522E-06

Average WT:het:M ratio for the two lines

genotype	observed	in %	expected
M	3,5	11	25
Het	14,5	46	50
WT	13,5	43	25
total	31,5	100	100

CHITEST (df=2): 3,06448E-05

Table A4. Results of genotyping and phenotyping of the SL1833-1 andSL3001-1 TILLING mutant lines.

Continued on next page.

Table A4. Results of genotyping and phenotyping of the SL1833-1 andSL3001-1 TILLING mutant lines. Continued.
A. Several screens of segregating populations were performed for the two mutant lines in different growth conditions and the phenotype and genotype of the plants recorded. Screens # 1, 2, and 3 were performed on plants grown in a greenhouse under natural light and long day conditions. Plants of screens #4 and 5 were grown in a greenhouse with supplemental lighting under long day conditions. Lastly, screens # 6 and 7 were performed on plants grown in a controlled environment chamber under a 16 h and 12 h photoperiod, respectively. Classes are as follow: 1. number of mutants isolated per screening; 2. mutants that died when still young (ca or less than one month old); 3. mutants that died before reached maturity (between ca on month and 4 month old); 4. mutants that flowered albeit an important flowering time delay (two to three months) in comparison to the heterozygote and WT segregants; 5. mutants that gave pods. **B.** Results of CHITEST (df=2) reveal that the actual ratio of mutants versus heterozygotes and WTs in the segregating populations analysed is statistically significantly different ($P<0.0001$) from the expected mendelian ratio for a single recessive mutation (mutant:heterozygote:WT ratio of 1:2:1) for both mutant lines. The actual ratios obtained suggest a case of partial gametophytic lethality and/or homozygote mutant lethality (expected ratio between the heterozygote and homozygote WT of 1:1 and 2:1 for these two mode of inheritance, respectively). **C**. Detailed results of the seed weight measurements performed on seeds harvested from pods of heterozygote and WT segregant plants for the *gwd1-2* and *gwd1-3* mutant alleles. **D.** Detailed results of the genotyping of seed embryos from pods of *GWD1-2/gwd1-2* and *GWD1-3/gwd1-3* heterozygote plants. The difference of the mutant:heterozygote:WT actual ratios obtained for each lines and the average of both (43:46:11) were statistically significant to the expected mendelian ratio of 1:2:1 according to the results of CHITEST (df=2). Lxxxx corresponds to the Zopra number attributed to the plant.

A. ♂GWD1-3/*gwd1-3* x ♀MG-20 WT

	1	2	3	4	5
A	80304, 1	80310, 1	80311, 6	80313, 2	80314, 1
B	80305, 1	80310, 2	80311, 7	80313, 3	80315,1
C	80305, 2	80310, 3	80312, 1	80313, 4	80315,2
D	80307, 1	80311, 1	80312, 2	80313, 5	80315,3
E	80307, 2	80311, 2	80312, 3	80313, 6	80315,4
F	80307, 3	80311, 3	80312, 4	80313, 7	80315,5
G	80307, 4	80311, 4	80312, 5	80313, 8	80315,6
H	80308, 1	80311, 5	80313, 1	80313, 9	80315,7

♀GWD1-3/*gwd1-3* x ♂MG-20 WT

	6	7	8	9	10	11	12
A	80315, 8	80318, 2	80319, 1	80319, 9	80321, 3	80323, 1	80323, 9
B	80316, 1	80318, 3	80319, 2	80319, 10	80321, 4	80323, 2	90324, 1
C	80316, 2	80318, 4	80319, 3	80320, 1	80321, 5	80323, 3	90324, 2
D	80316, 3	80318, 5	80319, 4	80320, 2	80321, 6	80323, 4	90324, 3
E	80316, 4	80318, 6	80319, 5	80320, 3	80322, 1	80323, 5	90324, 4
F	80316, 5	80318, 7	80319, 6	80320, 4	80322, 2	80323, 6	90324, 5
G	80317, 1	80318, 8	80319, 7	80321, 1	80322, 3	80323, 7	90324, 6
H	80318, 1	80318, 9	80319, 8	80321, 2	80322, 4	80323, 8	

B. ♂GWD1-3/*gwd1-3* x ♀MG-20 WT

	1	2	3	4	5
A	WT	WT	WT	WT	WT
B	Het	WT	WT	WT	WT
C	WT	WT	WT	WT	n/a
D	Het	WT	WT	WT	WT
E	WT	WT	WT	WT	WT
F	n/a	WT	WT	WT	Het
G	WT	WT	WT	WT	Het
H	WT	WT	WT	WT	n/a

♀GWD1-3/*gwd1-3* x ♂MG-20 WT

	6	7	8	9	10	11	12
A	Het	Het	WT	WT	Het	WT	WT
B	WT	n/a	WT	Het	Het	WT	WT
C	WT	Het	Het	WT	WT	Het	Het
D	Het	WT	WT	Het	WT	Het	WT
E	WT	WT	Het	Het	WT	WT	WT
F	Het	Het	WT	WT	WT	Het	WT
G	Het	Het	Het	Het	Het	Het	WT
H	Het	WT	Het	Het	Het	WT	

Table A5. Results of reciprocal crosses between a heterozygote (GWD1-3/*gwd1-3*) offspring of line SL3001-1 (in Gifu background) and MG-20 WT plants.
A. Because *L. japonicus* is capable of self-fertilisation, the hybrid nature of the F1 progeny from the outcross was checked both using SSR markers (in this case, the SSR markers used were TM0193 and TM0027) and based on the F1 plant phenotype (all plants from an outcross between a Gifu and MG-20 plants should have redish stem according to Kawaguchi et al., 2001; MG-20 plants, in contrast, have fully green stem since they lack anthocyanin pigment in this tissue). This analysis allowed the determination as to whether the F1 progeny originated from a true cross or not (in red and yellow, respectively). The number given correspond to the Zopra number (seed bag number) given for the F1 seeds. Crosses were performed in both directions to test both the paternal and maternal transmission; ♂GWD1-3/*gwd1-3* x ♀MG-20 WT crosses were performed by Tracey Welham, and ♀GWD1-3/*gwd1-3* x ♂MG-20 WT crosses were performed by Cécile Vriet (JIC, Norwich, UK). Note that ambiguous results were obtained for the F1 progeny from the ♂GWD1-3/*gwd1-3* x ♀MG-20 WT cross with some plants originating from a single F1 pod scoring true cross, other not. **B**. The F1 progeny from the reciprocal crosses were genotyped by PCR using gene-specific primers as described in Chapter 2, section 2.6. 29 out of 60 F1 plants obtained from the cross ♀GWD1-3/*gwd1-3* x ♂MG-20 WT scored heterozygote (i.e. maternal transmission close to the expected ratio 1:1). In contrast, when taking into account only unambiguous F1 progeny of this analysis and of a F1 pod previously obtained, only 2 out 11 F1 plants of the cross ♂GWD1-3/*gwd1-3* x ♀MG-20 WT scored heterozygote, suggesting a case of partial gametophytic lethality.

Table A6.A. Initial growth vigour
1st set (continued on next page)

Species name	Life form: Database	Life form: Exp.	Biorep	Height (cm): Shoot	Height (cm): Root	Fresh weight (g): Whole plant	Fresh weight (g): Shoot	Fresh weight (g): Root	Root:shoot ratio (l): height	Root:shoot ratio (l): biomass	SRL(cm/g	Root starch content (starch staining): Stem base	Root starch content (starch staining): Crown-prim. roots	Root starch content (starch staining): Sec. roots	Root starch content (starch staining): Total	Nodulation
L. japonicus-Gifu	Perennial	**P**	1	53	45	21,6	17,97	3,55	0,85	0,20						Yes (1)
			2	52	40	20,2	16,36	3,36	0,77	0,21						No
			3	52	42	13,22	11,78	1,78	0,81	0,15						Yes (1)
			4	55	35	21,83	18	3,25	0,64	0,18						No
			average	53,00	40,50	19,21	16,03	2,99	0,77	0,18	13,57	4	6	4	16	0,5
			SE	0,61	1,82	1,76	1,27	0,35	0,04	0,01						
L. japonicus-MG20	Perennial	**P**	1	42	40	34,61	29,92	3,63	0,95	0,12						No
			2	48	45	26,98	23,12	2,25	0,94	0,10						No
			3	46	35	25,12	22,59	2,65	0,76	0,12						No
			4	42	32	26,01	25,19	1,82	0,76	0,07						No
			average	44,50	38,00	28,18	25,21	2,59	0,85	0,10	14,69	4	5	2	12	0
			SE	1,50	2,86	2,18	1,67	0,39	0,05	0,01						
L. edulis	Annual	**A**	1	60	27	46,54	40,07	5,65	0,45	0,14						No
			2	55	31	40,14	34,97	4,57	0,56	0,13						No
			3	64	31	47,82	43,04	3,82	0,48	0,09						No
			4	60	25	41,06	37	4,22	0,42	0,11						No
			average	59,75	28,50	43,89	38,77	4,57	0,48	0,12	6,24	5	3	1	7	0
			SE	1,60	1,30	1,67	1,53	0,34	0,03	0,01						
L. arabicus	Annual	**A**	1	62	32	24,13	19,9	4,23	0,52	0,21						No
			2	60	33	31,95	23,39	6,38	0,55	0,27						No
			3	50	30	32,88	26,52	4,84	0,60	0,18						No
			4	45	30	21,33	18,71	2,05	0,67	0,11						No
			average	54,25	31,25	27,57	22,13	4,38	0,58	0,19	7,14	5	3	2	7	0
			SE	4,05	0,75	2,86	1,77	0,90	0,03	0,03						
L. parviflorus	Annual	**P**	1	45	28	35,6	27,97	7,32	0,62	0,26						Yes (5-10)
			2	68	32	41,62	31,9	9,57	0,47	0,30						Yes (35-50)
			3	60	39	42,38	30,88	11,55	0,65	0,37						Yes (1-5)
			4	42	26	33,96	23,76	8,3	0,62	0,35						Yes (1-5)
			average	53,75	31,25	38,39	28,63	9,19	0,59	0,32	3,40	3	6	6	18	1
			SE	6,17	2,87	2,12	1,82	0,91	0,04	0,03						
L. uliginosus	Perennial	**P**	1	68	30	34,1	28,39	5,48	0,44	0,19						No
			2	84	28	39,1	33,67	5,3	0,33	0,16						Yes (5-10)
			3	70	21	32,65	29,34	4,57	0,30	0,16						No
			4	48	22	28,4	23,46	4,82	0,46	0,21						No
			average	67,50	25,25	33,56	28,72	5,04	0,38	0,18	5,01	3	4	5	14	0,25
			SE	7,41	2,21	2,21	2,09	0,21	0,04	0,01						
L. burtii	Perennial	**A?**	1	40	43	18,81	16,35	2,38	1,08	0,15						No
			2	45	31	18,25	15,94	2,25	0,69	0,14						No
			3	41	42	17,2	14,8	2,22	1,02	0,15						Yes (1-5)
			4	40	27	18,34	15,9	1,82	0,68	0,11						Yes (1-5)
			average	41,50	35,75	18,15	15,75	2,17	0,87	0,14	16,49	5	6	4	16	0,5
			SE	1,19	3,99	0,34	0,33	0,12	0,11	0,01						

Table A6. Summary of the growth, re-growth, and starch content parameters of a collection of 24 natural variants of the genus *Lotus.*
Continued on next page.

Table A6.A. Initial growth vigour 1st set (continued)

Species name	Life form: Database	Life form: Exp.	Biorep	Height (cm): Shoot	Height (cm): Root	Fresh weight (g): Whole plant	Fresh weight (g): Shoot	Fresh weight (g): Root	Root:shoot ratio (!): height	Root:shoot ratio (!): biomass	SRL(cm/g	Root starch content (starch staining): Stem base	Root starch content (starch staining): Crown-prim. roots	Root starch content (starch staining): Sec. roots	Root starch content (starch staining): Total	Nodulation
L corniculatus	Perennial	**P**	1	61	24	21,02	15,69	5,29	0,39	0,34						No
			2	49	32	29,38	21,4	7,74	0,65	0,36						No
			3	56	27	20,5	15,04	5,74	0,48	0,38						No
			4	45	38	20,99	16,06	4,94	0,84	0,31						No
			average	52,75	30,25	22,97	17,05	5,93	0,59	0,35	5,10	6	6	5	17	0
			SE	3,57	3,07	2,14	1,47	0,63	0,10	0,02						
L. tenuis (glaber)	Perennial	**P**	1	47	36	21,86	18,4	3,49	0,77	0,19						No
			2	46	38	23,3	20,64	4,41	0,83	0,21						No
			3	43	30	26,1	19,74	6,18	0,70	0,31						No
			4	47	40	19,85	17,1	3,07	0,85	0,18						No
			average	45,75	36,00	22,78	18,97	4,29	0,79	0,22	8,40	6	6	5	17	0
			SE	0,95	2,16	1,31	0,77	0,69	0,03	0,03						
L.subbiflorus	Annual (?)	**P**	1	62	25	30,7	26,1	5,3	0,40	0,20						No
			2	50	52	28,02	22,92	4,96	1,04	0,22						No
			3	52	38	29,68	24,41	5,1	0,73	0,21						No
			4	55	16	34,11	30,1	3,5	0,29	0,12						No
			average	54,75	32,75	30,63	25,88	4,72	0,62	0,19	6,95	2	2	2	6	0
			SE	2,63	7,85	1,29	1,55	0,41	0,17	0,02						
L. peregrinus	Annual	**A**	1	62	34	40,94	32,2	8,04	0,55	0,25						No
			2	60	36	29,55	26,7	3,68	0,60	0,14						Yes (1)
			3	62	30	26,15	21,68	4,15	0,48	0,19						No
			4	60	26	30,04	27,8	2,65	0,43	0,10						No
			average	61,00	31,50	31,67	27,10	4,63	0,52	0,17	6,80	4	2	1	5	0,25
			SE	0,58	2,22	3,21	2,16	1,18	0,04	0,03						
L. glinoides	Annual	**P**	1	78	35	44,45	36,4	8,8	0,45	0,24						Yes (10-15)
			2	77	23	49,26	33,03	16,38	0,30	0,50						Yes (50-75)
			3	90	28	34,58	29,04	5,65	0,31	0,19						Yes (1-5)
			4	66	40	31,25	27,48	4,07	0,61	0,15						Yes (1-5)
			average	77,75	31,50	39,89	31,49	8,73	0,42	0,27	3,61	5	6	5	15	1
			SE	4,91	3,75	4,20	2,01	2,73	0,07	0,08						
L. ornithopodioides	Annual	**A**	1	64	30	34,94	32,88	3,74	0,47	0,11						No
			2	67	24	46,4	38,8	7,08	0,36	0,18						No
			3	66	20	35,7	31,2	4,05	0,30	0,13						No
			4	54	20	34,1	31,75	2,38	0,37	0,07						No
			average	62,75	23,50	37,79	33,66	4,31	0,38	0,13	5,45	4	3	1	7	0
			SE	2,98	2,36	2,89	1,75	0,99	0,03	0,02						
Perennials			Average	56,22	33,19	29,45	24,00	5,43	0,63	0,23	7,59	5,50	4,63	4,25	14,38	0,34
			SE	3,94	1,71	2,67	2,08	0,86	0,06	0,03	1,54	0,50	0,56	0,53	1,38	0,16
Annuals			Average	55,85	30,10	31,81	27,48	4,01	0,56	0,15	8,43	3,60	3,00	1,80	8,40	0,15
			SE	3,86	2,02	4,39	4,07	0,46	0,08	0,01	2,04	0,75	0,77	0,58	1,94	0,10

Table A6. Summary of the growth, re-growth, and starch content parameters of a collection of 24 natural variants of the genus *Lotus.*
Continued on next page.

Table A6.A. Initial growth vigour 2nd set (continued on next page)

Species name	Life form: Database	Life form: Exp.	Biorep	Height (cm): Shoot	Height (cm): Root	Fresh weight (g): Whole plant	Fresh weight (g): Shoot	Fresh weight (g): Root	Root:shoot ratio (!): height	Root:shoot ratio (!): biomass	SRL(cm/g	Root starch content (starch staining): Stem base	Root starch content (starch staining): Crown-prim. roots	Root starch content (starch staining): Sec. roots	Root starch content (starch staining): Total	Nodulation
L. japonicus-Gifu	perennial	**P**	1	27	22	6,68	5,21	1,38	0,81	0,26						n/a
Gifu			2	29	43	4,34	3,58	0,76	1,48	0,21						n/a
			3	34	33,5	4,11	3,39	0,7	0,99	0,21						n/a
			4	28,5	34	5,53	4,45	1,05	1,19	0,24						n/a
			5	28	34	7,8	6,02	1,75	1,21	0,29						n/a
			average	29,30	33,30	5,69	4,53	1,13	1,14	0,24	29,52	6	6	4	16	n/a
			SE	1,22	3,34	0,70	0,49	0,20	0,11	0,02						n/a
L. japonicus-MG20	(perennial)	**P**	1	30	28	6,48	5,36	1,04	0,93	0,19						n/a
MG20			2	26	25,7	5,7	4,73	0,96	0,99	0,20						n/a
			3	30,5	23	7,27	6,31	0,96	0,75	0,15						n/a
			4	30	19	6,74	5,64	1,05	0,63	0,19						n/a
			5	34	30	6,27	5,29	0,98	0,88	0,19						n/a
			average	30,10	25,14	6,49	5,47	1,00	0,84	0,18	25,19	6	6	2	14	n/a
			SE	1,05	1,93	0,33	0,33	0,02	0,06	0,01						n/a
L. unifoliolatus	perennial	**A**	1	51	50	13,9	10,77	3,62	0,98	0,34						n/a
uni			2	48,5	53	16,2	12,97	3,15	1,09	0,24						n/a
			3	57	44	13,67	10,33	3,29	0,77	0,32						n/a
			4	65,5	46	14,79	11,43	3,32	0,70	0,29						n/a
			average	55,50	48,25	14,64	11,38	3,35	0,89	0,30	14,42	2	2	1	5	n/a
			SE	3,78	2,02	0,57	0,58	0,10	0,09	0,02						n/a
L. arenarius	annual?	**P?**	1	43	50	12,39	9,42	2,82	1,16	0,30						n/a
are			2	50,5	32	11,52	10,28	1,17	0,63	0,11						n/a
			3	46,5	53	13,45	11,17	2,16	1,14	0,19						n/a
			4	46	37	13,46	10,85	2,4	0,80	0,22						n/a
			average	46,50	43,00	12,71	10,43	2,14	0,94	0,21	20,12	5	5	4	14	n/a
			SE	1,54	5,05	0,47	0,38	0,35	0,13	0,04						n/a
L. conimbricensis	annual	**A?**	1	24	21	12,2	8,27	3,88	0,88	0,47						n/a
con			2	28,5	20	10,78	8,19	2,54	0,70	0,31						n/a
			3	30	23	10,53	8,44	2,08	0,77	0,25						n/a
			4	35	30	9,27	6,76	2,49	0,86	0,37						n/a
			5	29	24	8,25	6,02	2,18	0,83	0,36						n/a
			average	29,30	23,60	10,21	7,54	2,63	0,81	0,35	8,96	5	2	2	9	n/a
			SE	1,57	1,56	0,60	0,43	0,29	0,03	0,04						n/a
L. halophilus	annual	**A**	1	44	32	16,26	12,89	3,34	0,73	0,26						n/a
hal			2	47	29	18,87	12,83	5,94	0,62	0,46						n/a
			3	52,2	24	14,96	12,63	2,29	0,46	0,18						n/a
			4	49	24	18,01	12,96	4,87	0,49	0,38						n/a
			5	41	28	15,02	11,54	3,48	0,68	0,30						n/a
			average	46,64	27,40	16,62	12,57	3,98	0,60	0,32	6,88	6	6	2	14	n/a
			SE	1,94	1,54	0,79	0,26	0,64	0,05	0,05						n/a
L. collinus	annual?	**P**	1	34	34	9,77	4,57	5,15	1,00	1,13						n/a
col			2	30	67	5,75	2,48	2,48	2,23	1,00						n/a
			3	21,5	17	4,34	1,67	1,67	0,79	1,00						n/a
			4	25,5	45	5,8	2,41	2,41	1,76	1,00						n/a
			average	27,75	40,75	6,42	2,78	2,93	1,45	1,03	13,92	5	6	5	16	n/a
			SE	2,71	10,48	1,17	0,62	0,76	0,34	0,03						n/a

Table A6. Summary of the growth, re-growth, and starch content parameters of a collection of 24 natural variants of the genus *Lotus.*
Continued on next page.

Table A6.A. Initial growth vigour
2nd set (continued)

Species name	Life form			Height (cm)		Fresh weight (g)			Root:shoot ratio (!)		SRL(cm/g	Root starch content (starch staining)			Nodulation
	Database	Exp.	Biorep	Shoot	Root	Whole plant	Shoot	Root	height	biomass		Stem base	Crown-prim. roots	Sec. roots	Total	
L. gebelia geb	perennial	**A?**	1	52,5	22	8,68	5,08	3,64	0,42	0,72						n/a
			2	49	27	7,2	4,58	2,62	0,55	0,57						n/a
			3	58	26	11	6,84	4,09	0,45	0,60						n/a
			4	56	26	8,54	5,14	3,31	0,46	0,64						n/a
			average	53,88	25,25	8,86	5,41	3,42	0,47	0,63	7,39	2	4	2	8	n/a
			SE	1,98	1,11	0,79	0,49	0,31	0,03	0,03						n/a
L. angustissimus ang	annual	**A**	1	39	30	13,11	9,84	2,79	0,77	0,28						n/a
			2	40	22,4	9,83	7,77	1,88	0,56	0,24						n/a
			3	38	15,7	6,86	5,63	1,2	0,41	0,21						n/a
			4	46	16,7	5,83	4,66	1,15	0,36	0,25						n/a
			average	40,75	21,20	8,91	6,98	1,76	0,53	0,25	12,08	6	6	2	14	n/a
			SE	1,80	3,28	1,64	1,16	0,38	0,09	0,01						n/a
L. denticulatus dent	annual	**A**	1	26	20	3,72	2,83	0,88	0,77	0,31						n/a
			2	26	23	1,97	1,4	0,57	0,88	0,41						n/a
			3	25,5	28	2,44	1,84	0,59	1,10	0,32						n/a
			4	26	19	2,6	2,09	0,5	0,73	0,24						n/a
			average	25,88	22,50	2,68	2,04	0,64	0,87	0,32	35,43	1	1	2	4	n/a
			SE	0,13	2,02	0,37	0,30	0,08	0,08	0,03						n/a
L. mearnsii mea	perennial	**P**	1	36,5	26	5,9	3,79	1,86	0,71	0,49						n/a
			2	43	23	5,82	4,37	1,44	0,53	0,33						n/a
			3	40	40	5,55	4,16	1,37	1,00	0,33						n/a
			4	49,5	21	7,99	6,27	1,68	0,42	0,27						n/a
			average	42,25	27,50	6,32	4,65	1,59	0,67	0,35	17,32	6	6	4	16	n/a
			SE	2,76	4,29	0,56	0,55	0,11	0,13	0,05						n/a
L. weilleri wei	annual	**A**	1	41	32	16,84	13,28	3,2	0,78	0,24						n/a
			2	44,5	21	12,48	10,85	1,61	0,47	0,15						n/a
			3	52,5	25	14,47	12,48	1,97	0,48	0,16						n/a
			4	44,5	43	9,95	8,21	1,7	0,97	0,21						n/a
			average	45,63	30,25	13,44	11,21	2,12	0,67	0,19	14,27	6	6	4	16	n/a
			SE	2,44	4,82	1,46	1,12	0,37	0,12	0,02						n/a
L. palustris pal	perennial	**P**	1	29	23	8,11	3,78	4,2	0,79	1,11						n/a
			2	29,5	30	6,64	3,4	3,26	1,02	0,96						n/a
			3	18	34	5,92	3,7	2,19	1,89	0,59						n/a
			4	31	46	5,33	2,62	2,68	1,48	1,02						n/a
			average	26,88	33,25	6,50	3,38	3,08	1,30	0,92	10,79	6	6	5	17	n/a
			SE	2,99	4,82	0,60	0,26	0,43	0,24	0,11						n/a
Perennials			Average	33,80	33,82	7,35	5,21	1,98	1,05	0,49	19,48	5,67	5,83	4,00	15,50	n/a
			SE	3,42	2,88	1,08	1,12	0,36	0,12	0,16	2,86	0,21	0,17	0,45	0,50	n/a
Annuals			Average	42,51	28,35	10,76	8,16	2,56	0,69	0,34	14,21	4,00	3,86	2,14	10,00	n/a
			SE	4,31	3,51	1,75	1,43	0,43	0,06	0,05	3,73	0,85	0,83	0,34	1,79	n/a

Table A6. Summary of the growth, re-growth, and starch content parameters of a collection of 24 natural variants of the genus *Lotus.*
Continued on next page.

B. Regrowth vigor (15d post cutting-back)
1st set (continued on next page)

Species name	Life form Database	Exp.	Biorep	FW new shoot (g)	New shoot:shoot biomass ratio	ratio in %
L. japonicus-Gifu	Perennial	**P**	1	1,05		
			2	1,72		
			3	0,98		
			4	1,93		
			5	1,83		
			average	1,50	0,0937	9,37
			SE	0,18		
L. japonicus-MG20	Perennial	**P**	1	0,45		
			2	0,23		
			3	0,94		
			4	1,28		
			5	0,05		
			average	0,59	0,0234	2,34
			SE	0,23		
L. edulis	Annual	**A**	1	0,16		
			2	0,02		
			3	0,97		
			4	0,11		
			5	0,06		
			average	0,26	0,0068	0,68
			SE	0,18		
L. arabicus	Annual	**A**	1	0,05		
			2	0,00		
			3	0,00		
			4	1,79		
			5	0,70		
			average	0,51	0,0230	2,30
			SE	0,35		
L. parviflorus	Annual	**P**	1	6,45		
			2	4,38		
			3	4,06		
			4	4,73		
			5	3,01		
			average	4,53	0,1581	15,81
			SE	0,56		
L. uliginosus	Perennial	**P**	1	5,05		
			2	4,64		
			3	2,86		
			4	2,45		
			5	3,92		
			average	3,78	0,1318	13,18
			SE	0,50		
L. burtii	Perennial	**A?**	1	1,47		
			2	1.5 (?)		
			3	1,69		
			4	0,79		
			5	1,17		
			average	1,28	0,0813	8,13
			SE	0,15		

Table A6. Summary of the growth, re-growth, and starch content parameters of a collection of 24 natural variants of the genus *Lotus.*
Continued on next page.

B. Regrowth vigor (15d post cutting-back)
1st set (continued)

Species name	Life form Database	Exp.	Biorep	FW new shoot (g)	New shoot:shoot biomass ratio	ratio in %
L corniculatus	Perennial	**P**	1	1,22		
			2	2,81		
			3	3,25		
			4	2,89		
			5	2,69		
			average	2,57	0,1509	15,09
			SE	0,35		
L. tenuis (glaber)	Perennial	**P**	1	4,08		
			2	3,60		
			3	2,87		
			4	2,30		
			5	1,70		
			average	2,91	0,1534	15,34
			SE	0,43		
L.subbiflorus	Annual (?)	**P**	1	1,42		
			2	0,49		
			3	1,01		
			4	1,63		
			5	2,24		
			average	1,36	0,0525	5,25
			SE	0,29		
L. peregrinus	Annual	**A**	1	0,00		
			2	0,00		
			3	0,00		
			4	0,00		
			5	0,00		
			average	0,00	0,0000	0,00
			SE	0,00		
L. glinoides	Annual	**P**	1	2,59		
			2	2,71		
			3	3,20		
			4	2,52		
			5	2,51		
			average	2,71	0,0859	8,59
			SE	0,13		
L. ornithopodioides	Annual	**A**	1	0,52		
			2	0,00		
			3	0,00		
			4	0,11		
			5	0,58		
			average	0,24	0,0072	0,72
			SE	0,13		
Perennials			Average	2,49	0,11	10,62
			SE	0,46	0,02	1,79
Annuals			Average	0,46	0,02	2,36
			SE	0,22	0,01	1,49

Table A6. Summary of the growth, re-growth, and starch content parameters of a collection of 24 natural variants of the genus *Lotus.*
Continued on next page.

B. Regrowth vigor (15d post cutting-back)
2nd set (continued on next page)

Species name	Life form Database	Exp.	Biorep	FW new shoot (g)	New shoot:shoot biomass ratio	ratio in %	ratio in %
L. japonicus-Gifu	perennial	**P**	1	4,94	0,48		
Gifu			2	5,84	0,49		
			3	4,72	0,26		
			4	4,45	0,49		
			5	4,69	0,71		
			6	5,2	0,48		
			average*	4,54	0,49	0,1069	10,69
			SE	0,25			
L. japonicus-MG20	perennial	**P**	1	4,49	0,24		
MG20			2	3,63	0,38		
			3	4,63	0,35		
			4	5,05	0,16		
			5	4,97	0,10		
			6	4,86	0,24		
			average*	5,33	0,25	0,0459	4,59
			SE	0,21			
L. unifoliolatus	perennial	**A**	1	12,21	0,00		
uni			2	10,28	0,00		
			3	8,89	0,00		
			4	11,1	0,00		
			5	10,91	0,00		
			6	11,24	0,00		
			average*	11,03	0,00	0,0000	0,00
			SE	0,35			
L. arenarius	annual?	**P**	1	11,28	0,00		
are			2	7,6	0,00		
			3	8,52	0,22		
			4	9,49	0,05		
			5	10,06	0,01		
			6	8,72	0,00		
			average*	9,85	0,05	0,0047	0,47
			SE	0,38			
L. conimbricensis	annual	**A**	1	8,54	0,24		
con			2	7,9	0,03		
			3	9,57	0,05		
			4	7,36	0,10		
			5	7,37	0,07		
			6	5,5	0,00		
			average*	7,39	0,08	0,0110	1,10
			SE	0,36			
L. halophilus	annual	**A**	1	13,18	0,00		
hal			2	16,04	0,00		
			3	7,33	0,00		
			4	8,11	0,00		
			5	12,02	0,20		
			6	11,36	0,00		
			average*	12,11	0,03	0,0028	0,28
			SE	0,73			
L. collinus	annual?	**P**	1	2,31	0,19		
col			2	4,24	0,22		
			3	3,75	0,29		
			4	2,46	0,44		
			5	2,54	0,28		
			6	2,78	0,50		
			average*	2,90	0,32	0,1104	11,04
			SE	0,30			

Table A6. Summary of the growth, re-growth, and starch content parameters of a collection of 24 natural variants of the genus *Lotus.*
Continued on next page.

B. Regrowth vigor (15d post cutting-back)
2nd set (continued)

Species name	Life form Database	Exp.	Biorep	FW new shoot (g)	New shoot:shoot biomass ratio	ratio in %	ratio in %
L. gebelia geb	perennial	**A**	1	3,82	0,02		
			2	4,55	0,02		
			3	4,82	0,12		
			4	4,34	0,21		
			5	4,41	0,02		
			6	5,21	0,11		
			average*	4,97	0,08	0,0168	1,68
			SE	0,26			
L. angustissimus ang	annual	**A**	1	3,77	0,00		
			2	3,31	0,00		
			3	3,36	0,00		
			4	2,35	0,00		
			5	2,62	0,00		
			6	4,23	0,00		
			average*	5,17	0,00	0,0000	0,00
			SE	0,76			
L. denticulatus dent	annual	**A**	1	0,13	0,00		
			average*	0,99	0,00	0,0000	0,00
			SE	0,45			
L. mearnsii mea	perennial	**P**	1	6,65	0,18		
			2	5,62	0,15		
			3	4,5	0,18		
			4	4,14	0,22		
			5	5,24	0,13		
			6	5,68	0,22		
			average*	4,78	0,18	0,0377	3,77
			SE	0,31			
L. weilleri wei	annual	**A**	1	9,79	0,00		
			2	8,03	0,00		
			3	9,77	0,01		
			4	9,61	0,00		
			5	8,54	0,03		
			6	9,46	0,01		
			average*	10,28	0,01	0,0008	0,08
			SE	0,87			
L. palustris pal	perennial	**P**	1	2,43	0,96		
			2	2,83	0,62		
			3	2,45	0,81		
			4	2,23	0,51		
			5	1,63	0,41		
			6	2,81	0,42		
			average*	2,89	0,62	0,2154	21,54
			SE	0,21			
Perennials			Average	5,05	0,32	0,09	8,69
			SE	1,05	0,09	0,03	3,07
Annuals			Average	7,42	0,03	0,00	0,45
			SE	1,51	0,01	0,00	0,25

Table A6. Summary of the growth, re-growth, and starch content parameters of a collection of 24 natural variants of the genus *Lotus.*
Continued on next page.

Table A6. Summary of the growth, re-growth, and starch content parameters of a collection of 24 natural variants of the genus *Lotus.* Continued.
These parameters were measured/recored prior (i.e. during initial growth; in **A**) and post cutting-back (i.e. 15 d post cutting-back; in **B**). Biomass measurements and other physiological analyses including root and shoot biomass measurement, scoring of root iodine staining results were performed prior and post cutting-back on plants grown in the greenhouse, under LD conditions and the analyses were performed on ca. 3 month-old plants. Two sets of annual and perennial species of *Lotus* together with the *L. japonicus* ecotypes MG-20 and Gifu were analysed. Plants of the first set were grown from November 2007 until March 2008 in a greenhouse supplemented with artificial light (long day conditions) while plants of the second set of *Lotus* species were grown in a greenhouse under natural light conditions, from May until September 2008. Life form 'database' corresponds to the life form of the species (i.e. annual, perennial growth habit) as determined by the USDA database. Life form 'Exp.' correspond to the life form of the species experimentally determined in this study as described in the text of Chapter 6. Root starch content values were arbitrarily given from iodine starch staining results. Note that the SRL (specific root length) parameter and the biomass root:shoot and new shoot:shoot ratios were calculed on fresh weight (FW) rather than dry weight (DW), however, preliminary analysis revealed that the DW was consistently equal to ca. 6 to 9% of the FW. Cutting-back experiment was performed as detailed in the text of Chapter 6, and in Chapter 2, section 2.2.

Appendix 2

Parts of the results presented in this PhD thesis have been published in the journal Plant Physiology:

Vriet C, Welham T, Brachmann A, Pike M, Pike J, Perry J, Parniske M, Sato S, Tabata S, Smith AM, Wang TL (2010) A Suite of Lotus japonicus Starch Mutants Reveals both Conserved and Novel Features of Starch Metabolism. Plant Physiology **154:** 643-655

A copy of this publication is given in the following pages.

A Suite of *Lotus japonicus* Starch Mutants Reveals Both Conserved and Novel Features of Starch Metabolism[1][W][OA]

Cécile Vriet, Tracey Welham, Andreas Brachmann, Marilyn Pike, Jodie Pike, Jillian Perry, Martin Parniske, Shusei Sato, Satoshi Tabata, Alison M. Smith, and Trevor L. Wang*

Metabolic Biology, John Innes Centre, Colney, Norwich NR4 7UH, United Kingdom (C.V., T.W., M. Pike, J. Perry, A.M.S., T.L.W.); Faculty of Biology, Genetics, Ludwig-Maximilians-Universität München, 82152 Martinsried, Germany (A.B., M. Parniske); The Sainsbury Laboratory, Colney, Norwich NR4 7UH, United Kingdom (J. Pike); and Kazusa DNA Research Institute, Kisarazu, Chiba 292–0818, Japan (S.S., S.T.)

The metabolism of starch is of central importance for many aspects of plant growth and development. Information on leaf starch metabolism other than in Arabidopsis (*Arabidopsis thaliana*) is scarce. Furthermore, its importance in several agronomically important traits exemplified by legumes remains to be investigated. To address this issue, we have provided detailed information on the genes involved in starch metabolism in *Lotus japonicus* and have characterized a comprehensive collection of forward and TILLING (for Targeting Induced Local Lesions IN Genomes) reverse genetics mutants affecting five enzymes of starch synthesis and two enzymes of starch degradation. The mutants provide new insights into the structure-function relationships of ADP-glucose pyrophosphorylase and glucan, water dikinase1 in particular. Analyses of the mutant phenotypes indicate that the pathways of leaf starch metabolism in *L. japonicus* and Arabidopsis are largely conserved. However, the importance of these pathways for plant growth and development differs substantially between the two species. Whereas essentially starchless Arabidopsis plants lacking plastidial phosphoglucomutase grow slowly relative to wild-type plants, the equivalent mutant of *L. japonicus* grows normally even in a 12-h photoperiod. In contrast, the loss of GLUCAN, WATER DIKINASE1, required for starch degradation, has a far greater effect on plant growth and fertility in *L. japonicus* than in Arabidopsis. Moreover, we have also identified several mutants likely to be affected in new components or regulators of the pathways of starch metabolism. This suite of mutants provides a substantial new resource for further investigations of the partitioning of carbon and its importance for symbiotic nitrogen fixation, legume seed development, and perenniality and vegetative regrowth.

Recent studies in Arabidopsis (*Arabidopsis thaliana*) have greatly enhanced our knowledge about pathways of transitory starch metabolism (Zeeman et al., 2007; Keeling and Myers, 2010; Kötting et al., 2010; Zeeman et al., 2010). The pathway of synthesis is well established for several species, but the degradative pathway is understood only in Arabidopsis. During synthesis, the plastidial isoforms of phosphoglucoisomerase (PGI1) and phosphoglucomutase (PGM1), together with ADP-Glc pyrophosphorylase (AGPase), catalyze the conversion of the Calvin cycle intermediate Fru 6-P to ADPGlc, the substrate for starch synthases (Supplemental Fig. S1). Leaves of mutants lacking any of these three enzymes either have strongly reduced starch contents or lack starch almost completely (Caspar et al., 1985; Hanson and McHale, 1988; Lin et al., 1988a, 1988b; Kruckeberg et al., 1989; Harrison et al., 1998; Yu et al., 2000; Streb et al., 2009). In contrast, the phenotypes of mutants lacking individual enzymes that convert ADPGlc into starch vary between species and are often much less pronounced (starch synthases [Delvallé et al., 2005; Zhang et al., 2005] and starch-branching enzymes [Tomlinson et al., 1997; Blauth et al., 2001; Dumez et al., 2006]).

The degradation of the starch granule in Arabidopsis leaves is catalyzed primarily by β-amylases and isoamylase 3 (Wattebled et al., 2005; Delatte et al., 2006; Fulton et al., 2008). Normal rates of degradation require phosphorylation of the starch polymers by two glucan, water dikinases, GWD1 (Ritte et al., 2002) and GWD3 (or PWD, for phosphoglucan water, dikinase; Baunsgaard et al., 2005; Kötting et al., 2005), followed by dephosphorylation by a phosphoglucan phosphatase, STARCH EXCESS4 (SEX4; Kötting et al., 2009). Maltose produced by starch degradation is exported from the chloroplast by a maltose transporter and further metabolized to hexose phosphates in the cytosol (Zeeman et al., 2007; Supplemental Fig. S1). Mutations in numerous components of this pathway result in a starch-excess phenotype, in which the starch

[1] This work was supported by a Marie Curie studentship (EU Early Stage Training program no. 019727) to C.V. and by a Core Strategic Grant to the John Innes Centre from the Biotechnology and Biological Sciences Research Council.

* Corresponding author; e-mail trevor.wang@bbsrc.ac.uk.

The author responsible for distribution of materials integral to the findings presented in this article in accordance with the policy described in the Instructions for Authors (www.plantphysiol.org) is: Trevor L. Wang (trevor.wang@bbsrc.ac.uk).

[W] The online version of this article contains Web-only data.

[OA] Open Access articles can be viewed online without a subscription.

www.plantphysiol.org/cgi/doi/10.1104/pp.110.161844

content of leaves at the end of the night is higher than that of wild-type plants.

These studies have also revealed the importance of starch turnover for the productivity of the plant. Mutants of Arabidopsis that are essentially unable to synthesize transitory starch, or with reduced rates of starch degradation at night, have a reduced rate of growth and delayed flowering time relative to wild-type plants under most conditions (Caspar et al., 1985, 1991; Eimert et al., 1995; Corbesier et al., 1998; Smith and Stitt, 2007). However, it is not known whether information about the nature and importance of starch turnover in Arabidopsis is widely applicable. Plant species differ considerably in the extent to which starch is stored in leaves at night as well as in diurnal patterns of growth and metabolic demand. The function and regulation of starch metabolism in heterotrophic organs and its importance in major physiological and developmental processes such as perenniality, vegetative regrowth, symbiotic nitrogen fixation, and the accumulation of seed storage reserves cannot be studied easily in Arabidopsis and remain largely unknown. These processes represent traits of agronomic value in legumes (Fabaceae), a family that includes some of the most agriculturally important forage (e.g. alfalfa [*Medicago sativa*] and clover [*Trifolium* spp.]), grain (e.g. pea [*Pisum sativum*] and common bean [*Phaseolus vulgaris*]), and oilseed (e.g. soybean [*Glycine max*]) crops.

Some information is already available about starch metabolism in pea and other legume crops (Martin and Smith, 1995; Wang et al., 1998b, and refs. therein). However, characteristics including large genome sizes and recalcitrant transformation and regeneration have limited progress on these species. There is insufficient information to allow either an overview of the nature and importance of starch metabolism in legumes or a meaningful comparison with the detailed picture emerging for Arabidopsis. The development of both *Lotus japonicus* and *Medicago truncatula* as legume model systems, and the wide range of genetic and genomic resources generated for them, offer the opportunity for a systematic analysis.

To elucidate the pathway of starch synthesis and degradation in legumes and provide resources for future experimentation, we screened an ethyl methanesulfonate (EMS)-mutagenized population of *L. japonicus* (Perry et al., 2003) for mutants altered in transitory starch metabolism and carried out genetic mapping to identify the mutation responsible for their phenotype. We also used TILLING (for Targeting Induced Local Lesions IN Genomes; McCallum et al., 2000) to confirm that the mutations identified were indeed responsible for the mutant phenotype and to obtain additional mutations in genes known to affect leaf starch content in other species. We present the results of molecular and phenotypic analyses on the mutants that provide novel insights into the structure-function relationship of the AGPase and GWD1 enzymes. In addition, our analyses reveal new information on the nature and importance of starch metabolism for plant growth and development in *L. japonicus*. The importance of starch accumulation and degradation and a comparison with pathways in other plant species are also discussed.

RESULTS AND DISCUSSION

Metabolism of Leaf Starch in *L. japonicus*

To examine the extent of diurnal starch turnover in leaves of *L. japonicus*, plants of the two wild-type ecotypes commonly used in research on this species, Miyakojima MG-20 and Gifu B-129 (referred to as MG-20 and Gifu, respectively), were grown in a 12-h-light/12-h-dark cycle in a growth chamber. Their leaf starch contents were measured at the end of the day and the end of the night at 2-week intervals during their first 10 weeks of growth. For the first 6 weeks, the two ecotypes showed similar, strong diurnal changes in starch content. The starch content was in excess of 7.5 mg g^{-1} fresh weight at the end of the day and less than 0.6 mg g^{-1} fresh weight at the end of the night (Fig. 1; Supplemental Table S1). This pattern is very similar to that in Arabidopsis plants under the same growth conditions (Yu et al., 2001, 2005; Baunsgaard et al., 2005; Fulton et al., 2008). In contrast to the situation in Arabidopsis, starch levels in older *L. japonicus* plants increased at the end of both the day and the night. At 8 weeks, the diurnal amplitude of change in starch content was unchanged, but leaves had about 14 mg starch g^{-1} fresh weight at the end of the day and retained 5 mg starch g^{-1} fresh weight at the end of the night. Between 8 and 10 weeks, leaf starch content increased dramatically. In Gifu, a diurnal

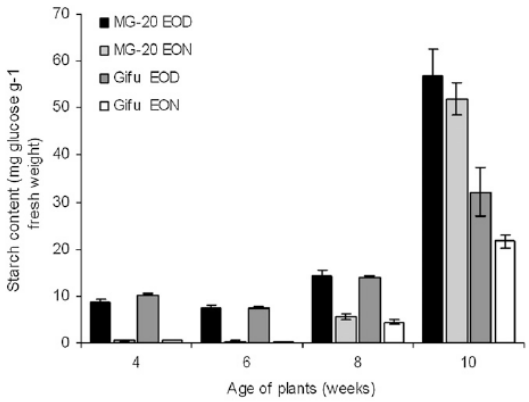

Figure 1. Diurnal changes in leaf starch content through the development of *L. japonicus* plants. Plants were grown in 12 h of light and 12 h of dark. Mature leaves were harvested at the end of the day (EOD) and the end of the night (EON) and assayed for starch content at the indicated times after germination. Values are means ± SE of measurements on six samples, each of which consisted of three fully expanded leaves taken from the top of two plants.

turnover of about 10 mg starch g^{-1} fresh weight was maintained, but starch content at the end of the night was 20 mg g^{-1} fresh weight. In MG-20, starch content was over 50 mg g^{-1} fresh weight throughout the diurnal cycle. Increases in leaf starch content with leaf and/or plant age have been observed in several other species, including tobacco (*Nicotiana tabacum*; Matheson and Wheatley, 1962; Ölçer et al., 2001) and soybean (Ainsworth et al., 2006). It should be mentioned, however, that both the timing and magnitude of the rise in starch content with plant age in *L. japonicus* were highly dependent on the growth conditions (data not shown).

In Silico Identification of Genes Involved in Starch Metabolism in *L. japonicus*

We first listed the Arabidopsis genes involved in the metabolism of leaf starch (Supplemental Table S2). This included genes encoding enzymes involved in the partitioning of photoassimilates into starch, in the synthesis and degradation of starch, and in the subsequent metabolism of maltose (Zeeman et al., 2007, 2010; Fulton et al., 2008; Kötting et al., 2009). Recent progress in EST and genome sequencing projects in *L. japonicus* allowed us to identify the orthologs of the Arabidopsis genes in this species (Supplemental Table S2). Whenever possible, these genes were mapped on the genetic linkage map of *L. japonicus* (Fig. 2) using the marker information provided by the Miyakogusa genome database available at http://www.kazusa.jp/lotus/index.html (Sato et al., 2008).

We were able to identify *L. japonicus* genes encoding all of the classes of enzymes involved in starch metabolism in Arabidopsis, but there were several differences in isoform representation. For instance, we could not find *L. japonicus* sequences orthologous to Arabidopsis genes encoding the glucan, water dikinase GWD2 and the β-amylases BAM2 and BAM4 (Supplemental Table S2). These genes may be present but in an unsequenced region of the genome (9% of the gene space has not been sequenced; Sato et al., 2008) or expressed at a low level and so not represented in the EST collection. Alternatively, there may be differences in the composition of some gene families between the two species. We also found duplications of several starch metabolism genes in *L. japonicus*, including AGPase large subunit isoform 2 (APL2), starch synthase 2 (SS2), granule-bound starch synthase (GBSS), α-amylase 3 (AMY3), β-amylase 3 (BAM3), and cytosolic glucan phosphorylase PHS2 (also known as Pho2 in some species). Duplication of genes encoding SS2 and GBSS exist in numerous species, including other legumes and cereals (Pan et al., 2009). Interestingly, the duplications appear to have independent origins in different groups of plants. The legume duplication resulted from a whole-genome duplication within

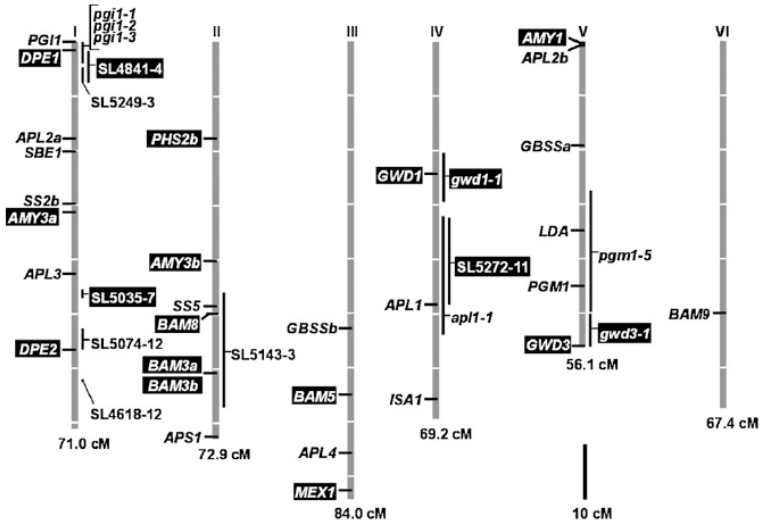

Figure 2. Chromosomal locations of starch metabolism genes of *L. japonicus*, and map positions of mutations discovered in the forward genetic screen. The genetic linkage map of *L. japonicus* is derived from a cross between the ecotypes Gifu and MG-20 (maternal and paternal parents, respectively). For each chromosome, the number is given at the top and the size (in cM) is given at the bottom (data from http://www.kazusa.or.jp/lotus/index.html). Genes involved in the synthesis and degradation of starch (lettered in white and black, respectively) are shown on the left of each chromosome. Mutations from the forward genetic screen are shown on the right of each chromosome. Identified mutations are labeled with allele numbers; mapped intervals of the mutations yet to be characterized are labeled with the SL number of the mutant lines. The starch metabolism genes are listed in Supplemental Table S2. Full details of the alleles are given in Supplemental Tables S4 and S6.

Rosid clade I, whereas the cereal duplication resulted from the whole-genome duplication at the base of the grass lineages, well after the divergence of the monocots and dicots (Pan et al., 2009).

Forward Genetic Screens to Identify Mutants Affected in Starch Metabolism

To identify mutants, we used a collection of lines impaired in starch metabolism from a screen on 1,428 M2 families (17,100 plants) from seeds of Gifu mutagenized with EMS (Perry et al., 2003). Our screen utilized the fact that decolorized leaves of wild-type plants stain strongly with iodine solution at the end of the day, when starch content is high, and much less strongly at the end of the night, when starch content is low (Fig. 3). We used this to isolate mutants that had either lower levels of leaf starch than wild-type plants at the end of the day ("synthesis mutants") or higher levels of leaf starch than wild-type plants at the end of a dark period ("degradation mutants"). Because starch content at the end of a normal night varied from batch to batch and with glasshouse conditions, screening for degradation mutants was usually performed on plants subjected to an extended night of up to 44 h. The clearest results were obtained on young plants (about 4 weeks old) in which starch content was generally low at the end of the night (Fig. 1).

The screens led to the selection of 10 synthesis and six degradation mutants (Fig. 3). Allelism tests suggested that the mutations defined at least five loci for the synthesis mutants and four loci for the degradation mutants. The selected mutant lines were outcrossed at least once to MG-20 to reduce numbers of background mutations introduced by EMS mutagenesis and to establish a mapping population. Segregation ratios of the F2 progeny (data not shown) indicated a recessive monogenic mode of inheritance for all the starch mutant phenotypes, consistent with the nature of such mutations in other species.

Genetic Linkage Mapping and TILLING as Complementary Approaches to Identify Mutations Affecting Starch Metabolism

To discover genes necessary for starch metabolism in *L. japonicus*, we took two approaches: mapping, to

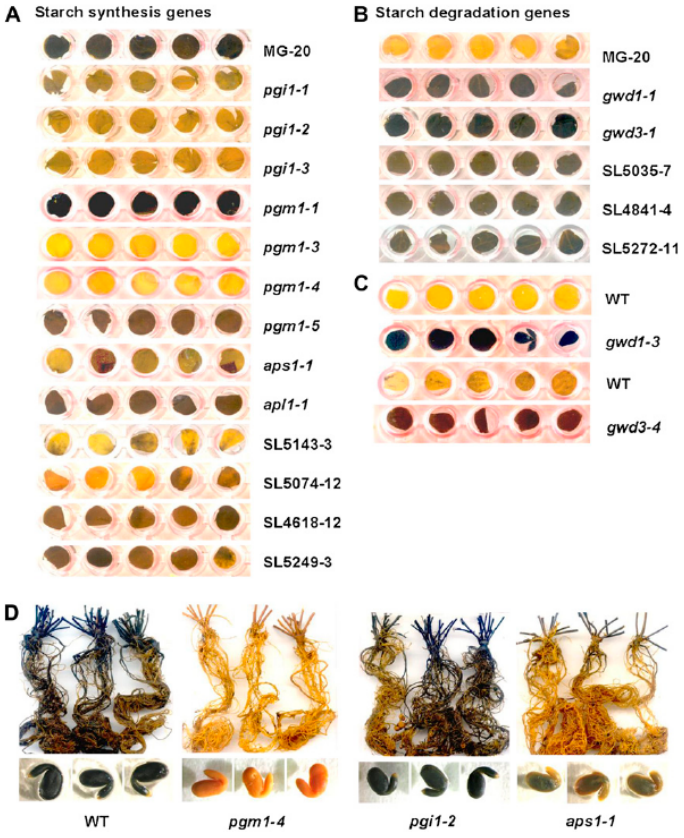

Figure 3. Iodine staining of starch synthesis and degradation mutants. A to C, Iodine staining of leaves of mutants obtained from the forward genetic screen and from TILLING. All mutant lines shown here except *gwd1-3* and *gwd3-4* were derived from outcrosses of the original mutant with MG-20. Each leaflet is from a different plant. Plants were grown in 16 h of light and 8 h of dark and were approximately 4 weeks old at the time of harvest. The name of the mutant allele is given where this is known (Supplemental Table S5). A, Starch synthesis mutants from the forward genetic screen and TILLING. Leaflets were harvested at the end of the day. B and C, Mutants from the forward genetic screen (B) and TILLING (C). Leaf phenotypes of the *gwd1-3* and *gwd3-4* TILLING mutants are shown in comparison with those of their segregating wild types (WT). Leaflets were harvested at the end of an extended night of up to 44 h. D, Starch contents of roots and embryos of wild-type and starch synthesis mutant plants. Plants were harvested when approximately 3 months old. Roots and embryos were decolorized prior to staining with iodine solution. Note that roots and embryos of wild-type plants have high starch contents, those of *pgm1-4* have no detectable starch, those of the *aps1-1* mutant have drastically reduced starch contents, and those of *pgi1-2* (SL4308-12) appear very similar to the wild type.

identify the mutations responsible for the phenotypes identified above, and TILLING, to identify mutations in selected genes encoding enzymes known to be necessary for starch metabolism in other plant species (Supplemental Table S2). TILLING was also used to identify additional mutant alleles of genes for which only one mutant allele was isolated from the forward genetic screen.

We initially carried out rough mapping on the forward screen mutant lines by bulk segregant analysis, using genomic DNA from mutants isolated from F2 populations from crosses with MG-20. Microsatellite simple sequence repeat (SSR) markers evenly distributed over the arms of each of the six chromosomes of *L. japonicus* (three to four SSR markers per chromosome) were selected from the markers developed by the Kazusa DNA Research Institute (http://www.kazusa.jp/lotus/index.html; Supplemental Table S3). The mapping interval thus identified (Supplemental Table S4) was confirmed by further mapping on the mutant individuals.

Using information from the genome sequence of *L. japonicus* (Sato et al., 2008), we searched within the confirmed interval for candidate genes (Fig. 2; Supplemental Table S2). Synteny with the genomes of the legume species soybean (http://www.phytozome.net/soybean) and *M. truncatula* (http://www.medicago.org/genome/) were also used in some cases where the *L. japonicus* genome sequence was not available. Where sequencing of candidate genes (for primers, see Supplemental Table S5) revealed mutations, biochemical and genetic approaches were used to check rigorously that the mutations were indeed responsible for the starch phenotype. As described below, we were able to identify the mutated genes in six out of the 10 synthesis mutants and three out of the six degradation mutants.

TILLING was carried out using two DNA populations of *L. japonicus* (GENPOP and STARPOP; Perry et al., 2009). Most of the mutants isolated were heterozygous (Perry et al., 2009), so homozygous mutant, heterozygous, and wild-type segregants in the M3 generation were identified by sequencing (for primers, see Supplemental Table S5).

Mutations in the Starch Synthesis Genes *LjPGI1*, *LjPGM1*, *LjAPL1*, *LjAPL2*, and *LjAPS1*

Based on knowledge gained from Arabidopsis (see introduction and Supplemental Fig. S1), we examined whether the almost starchless and low-starch plants (synthesis mutants) selected in the forward screen lacked pPGM, pPGI, or AGPase. As described below, mutations affecting these three enzymes accounted for the phenotypes of six of the 10 synthesis mutants.

Three of the synthesis mutants from the forward screen (SL4308-12, SL4715-2, and SL5069-2) had leaf starch contents that were only 10% of wild-type values (Table I), but their embryo and root starch contents were indistinguishable by iodine staining from those of wild-type plants (Fig. 3 for SL4308-12; data not shown). This pattern of starch distribution is also seen in the Arabidopsis *pgi1* mutant (Yu et al., 2000). The three mutants were shown by crossing to be allelic, and the mutations in all three mapped to the same interval at the top of chromosome I. The *LjPGI1* gene is located in this interval (Fig. 2; Supplemental Tables S2 and S4). Sequencing of the *PGI1* gene in the three mutants revealed two mutations that create stop codons (*pgi1-1*, SL4715-2; *pgi1-2*, SL4308-12) and one (*pgi1-3*, SL5069-2) at a splice-site junction (Fig. 4; Supplemental Table S6). Native gel electrophoresis followed by activity staining on protein extracts from leaves revealed two bands of PGI activity in wild-type extracts, attributable to the cytosolic and plastidial isoforms of the enzyme (Shaw and Prasad, 1970). The band attributable to the plastidial isoform was missing in extracts of the mutants (Supplemental Fig. S2), consistent with the specific loss of the plastidial isoform of PGI in the *pgi1* mutants.

One of the synthesis mutants, SL4725-4, appeared from iodine staining and starch quantification to lack starch in leaves, stems, roots, and embryos, suggesting that it might be a *pgm1* mutant (Fig. 3; Table I). Arabidopsis, tobacco, and pea mutants lacking pPGM are starchless in all plant parts examined (Caspar et al., 1985; Hanson and McHale, 1988; Harrison et al., 1998). In a second mutant (SL4867-11) with a strongly reduced starch content relative to wild-type plants in all organs examined, the mutation mapped to an interval of about 10 centimorgan (cM) on chromosome V, in which the *PGM1* gene is located (Fig. 2; Supplemental Tables S2 and S4). Sequencing revealed that the *PGM1* gene in SL4725-4 contained a mutation affecting a splice-site

Table I. *Starch content at the end of the day in leaves of mutants with starchless or low-starch phenotypes*

Values are means ± SE of measurements on six samples, each consisting of fully expanded leaves from the upper part of the shoot of a single plant. n.d., Not detected.

Genotype[a]	Starch Content	
	Wild Type	Mutant
	mg Glc equivalents g^{-1} fresh wt	
PGM1		
pgm1-3	25.3 ± 6.4	n.d.
pgm1-4	20.1 ± 4.8	n.d.
pgm1-5	29.7 ± 6.2	6.1 ± 1.3
PGI1		
pgi1-1	17.2 ± 5.9	1.83 ± 0.35
pgi1-2	50.6 ± 4.7	4.56 ± 1.90
APS1		
aps1-1	47.0 ± 4.1	3.73 ± 1.29
APL1		
apl1-1	59.6 ± 10.5	12.7 ± 2.0

[a]For each genotype, F3 homozygous mutant and wild-type plants for analysis were selected by genotyping individual plants in a single F2 population derived from a cross between the original mutant in Gifu and MG-20. Plants were grown for 7 weeks, as described for starch quantification in "Materials and Methods."

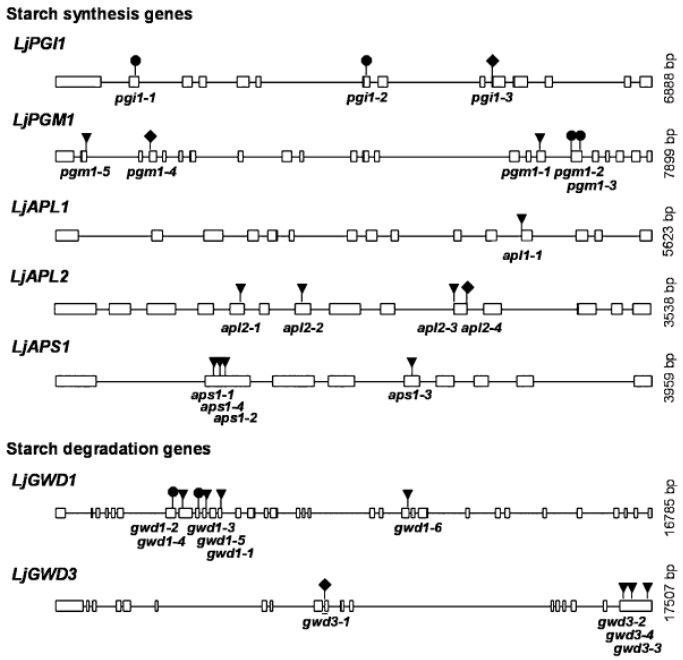

Figure 4. Structures of the starch metabolism genes and positions of the nonsilent mutations discovered in the forward genetic screen and by TILLING. Boxes and lines indicate exons and introns, respectively. Only the TILLING mutations leading to a starch phenotype and/or predicted by the PARSESNP program to have position-specific scoring matrix values greater than 0 are shown. The length of the gene sequence (in bp) is given on the right. The symbols above the gene specify the mutation type and position: octagons, stop codons; diamonds, splice site junction mutations; triangles, amino acid changes. Details of the nature and position of the mutations are given in Supplemental Table S6.

junction, and the gene in SL4867-11 contained a mutation predicted to result in the amino acid change G95D. These mutants are referred to as *pgm1-4* and *pgm1-5*, respectively (Fig. 4; Supplemental Table S6). Native gel electrophoresis followed by activity staining on protein extracts from leaves revealed two bands of PGM activity in wild-type extracts, attributable to the cytosolic (PGM2) and plastidial (PGM1) isoforms of the enzyme (Harrison et al., 1998). The band attributable to the plastidial isoform was missing from extracts of the mutants, confirming that chloroplastic PGM activity is strongly reduced or absent in both cases (Supplemental Fig. S2). We used TILLING to select lines homozygous for three additional mutant alleles of the *PGM1* gene. Two of the alleles (*pgm1-2* from SL755-1 and *pgm1-3* from SL1837-1; Fig. 4; Supplemental Table S6) contained mutations creating stop codons; both of the mutant lines appeared from iodine staining to lack starch in all plant parts and were identical in phenotype to *pgm1-4* (Fig. 3; described in more detail below). The mutation in the third allele (*pgm1-1* from SL4490-1) was predicted to result in the amino acid change D436N. Activity of the plastidial isoform of PGM was reduced in *pgm1-1* (Supplemental Fig. S2), but no reduction in starch content of the leaves was apparent from iodine staining (Fig. 3).

We used similar approaches to identify the mutation accounting for the phenotype of another synthesis mutant, SL5127-5, in which leaf starch content at the end of the day is typically reduced by about 80% (Table I). The mutation mapped to an interval on chromosome IV encompassing a gene encoding a large subunit of AGPase, APL1 (Fig. 2; Supplemental Tables S2 and S4). AGPase in higher plants is a heterotetramer composed of two small (APS) and two large (APL) subunits. Many species possess one or two *APS* genes and several *APL* genes that are differentially expressed between organs (Crevillén et al., 2003, 2005, and refs. therein). At least one *APS* gene and six *APL* genes are present in the *L. japonicus* genome (Supplemental Table S2). In Arabidopsis, loss of the small subunit (in the *adg1* mutant) almost eliminates AGPase activity and starch synthesis (Lin et al. 1988a; Wang et al., 1998a), and loss of the major leaf isoform of the large subunit (in the *adg2* mutant) reduces activity by 95% and starch synthesis by 60% (Lin et al., 1988b; Wang et al., 1997). Sequencing revealed a single mutation in the *APL1* gene of SL5127-5, predicted to result in the amino acid change S400L. To discover whether this mutation can account for the starch phenotype of the mutant, we assayed AGPase activity in extracts of wild-type and mutant leaves. Activity was 93% lower in mutant than in wild-type extracts (Table II). Activity in extracts made from mixtures of wild-type and mutant leaves was 98.5% of that predicted from separate extracts of the two genotypes; hence, the large difference in activity is likely to result from a loss of APL function in the mutant rather than from the presence of inhibitory substances in the mutant leaf.

To understand further the importance of AGPase subunits in *L. japonicus*, we used TILLING to identify

Table II. *AGPase activities in leaves of the apl and aps synthesis mutants*

Values are means ± SE of measurements on three plants.

Genotype[a]	AGPase Activity
	nmol min^{-1} g^{-1} fresh wt
MG-20	1,457 ± 41
Gifu	1,367 ± 140
apl1-1	105 ± 9
apl1-2	1,166 ± 166
apl2-1	1,844 ± 32
apl2-3	1,996 ± 63
apl2-4	1,364 ± 174
aps1-1	439 ± 10
aps1-2	1,376 ± 160
aps1-3	1,412 ± 168

[a]Plants were grown in a glasshouse as described in "Materials and Methods" and harvested 10 h into the 16-h light period when 7 to 12 weeks old.

mutations in a second large subunit gene, *APL2*, and in the single small subunit gene, *APS1*. For *APL2*, we isolated four alleles containing mutations predicted to have a deleterious effect on activity of the encoded protein. None of these had an effect on starch content (assessed by iodine staining) in any of the organs examined, including roots, leaves, and embryos (data not shown). In contrast, plants carrying one of the four mutant alleles identified for APS1 (*aps1-1* from SL529-1), which had a mutation predicted to bring about the amino acid change A111T (Supplemental Fig. S4; Supplemental Table S6), displayed a strong reduction in starch content in leaves, roots, and embryos (Fig. 3). AGPase activity in leaves of this mutant was about 70% lower than in wild-type leaves (Table II), and leaf starch content was reduced by up to 90% (Table I).

Mutations in the Starch Degradation Genes *LjGWD1* and *LjGWD3*

Following the same approach as for the starch synthesis mutants, we identified the mutations responsible for the starch-excess phenotype of three of the starch degradation mutants. The mutations in SL5215-2 and SL5358-3 mapped to the same interval on chromosome IV, and the mutation in line SL5104-12 mapped to the top of chromosome V (Fig. 2; Supplemental Table S4). These two intervals encompass genes encoding *GWD1* (Ritte et al., 2002) and *GWD3* (Baunsgaard et al., 2005; Kötting et al., 2005), respectively (Fig. 2; Supplemental Table S2). In Arabidopsis, the *gwd1* (or *sex1*) mutant has a severe starch-excess phenotype and reduced growth under short-day conditions (Caspar et al., 1991; Yu et al., 2001). The *gwd3* (*pwd*) mutant (Baunsgaard et al., 2005; Kötting et al., 2005) also has a starch-excess phenotype, although less severe than that of *gwd1*. Sequencing revealed that SL5215-2 and SL5358-3 both carry a mutation in *GWD1*, while SL5104-12 has a mutation in *GWD3*. Although SL5215-2 and SL5358-3 were independently selected, they carry the same mutation in *GWD1*, predicted to result in the amino acid change E566K (Fig. 4; Supplemental Table S6). Plants carrying this mutation are referred to as *gwd1-1* mutants. The mutation in *GWD3* affects a splice-site junction and results in the nucleotide change G7871A (Fig. 4; Supplemental Table S6).

To confirm that the mutations identified in these two genes were responsible for the starch-excess phenotype of the *gwd1-1* and *gwd3-1* mutants, we generated additional mutant alleles by TILLING. We targeted a region of the *LjGWD1* gene encompassing the sequence encoding the second of the two putative starch-binding domains of the protein (SBD, Carbohydrate-Binding Module [CBM45] family; Mikkelsen et al., 2006) and a second region encoding part of the phospho-His domain of the enzyme (Yu et al., 2001). Two mutant lines isolated by TILLING (from SL1833-1 and SL3001-1, *gwd1-2* and *gwd1-3*, respectively; Fig. 4; Supplemental Table S6) had point mutations in *GWD1* leading to stop codons. Leaves of both mutants showed very strong starch-excess phenotypes (Fig. 3), stronger than that of *gwd1-1*, and quantification confirmed very high levels of starch in the *gwd1-2* mutant (end-of-night values: wild type, 0.9 ± 0.3, *gwd1-2*, 43.1 ± 3.3 mg g^{-1} fresh weight [mean ± SE of at least five replicates]; Supplemental Fig. S3A). Immunoblotting with an antiserum to GWD1 from potato (*Solanum tuberosum*) revealed that an immunoreactive protein of the expected mass was present in extracts of wild-type plants but missing in extracts of the *gwd1-2* mutant (Supplemental Fig. S3B). Several other mutant alleles were identified by TILLING, but none were predicted by the PARSESNP (see "Materials and Methods") program to have a deleterious effect on enzyme function, and leaves of the homozygous mutants did not have a starch-excess phenotype (data not shown).

TILLING performed on *LjGWD3* targeted the region encoding the nucleotide-binding domain involved in the dikinase activity of the enzyme (Kötting et al., 2005). A suite of mutant alleles with missense change mutations was identified. Homozygous mutants for one of these alleles, *gwd3-4* (from SL639-1; Fig. 4; Supplemental Table S6) had a clear starch-excess phenotype in leaves (Fig. 3). The mutation in this line is predicted to affect a residue (amino acid change G980E) that is identical across all the predicted protein homologs of LjGWD3 we analyzed and lies within a conserved motif (PWD_ARATH, Q6ZY51; PWD_ORYSA, NP_001066613; putative homologs in *Vitis vinifera*, XP_002265211; *Ricinus communis*, XP_002518612; and *Sorghum bicolor*, XP_002453659 [multiple sequence alignment not shown]). The starch-excess phenotypes of both *gwd3-1* and *gwd3-4* strongly suggest that LjGWD3 plays an important role in the degradation of starch in leaves of *L. japonicus*. It seems likely that, as in Arabidopsis, LjGWD3 acts in synergy with LjGWD1 to phosphorylate the starch granule as a prerequisite for degradation (Baunsgaard et al., 2005; Kötting et al., 2005).

Isolation of Mutants Affected in Novel Proteins Involved in Starch Metabolism in *L. japonicus*

We mapped the chromosomal locations of the mutations responsible for the remaining four synthesis mutants (SL5249-3, SL5143-3, SL5074-12, and SL4618-12) and three degradation mutants (SL4841-4, SL5035-7, and SL5272-11) from the forward screen. To date, four of the mutations have been mapped to intervals of less than 5 cM (synthesis mutants SL5249-3 and SL4618-12 and degradation mutants SL4841-4 and SL5035-7; Fig. 2; Supplemental Table S4). No obvious candidate genes are present in these intervals, such as those encoding pathway enzymes or established regulators. Hence, the genes responsible for the phenotypes are likely to encode previously undiscovered components of starch metabolism pathways.

Altogether, this comprehensive collection of starch metabolism mutants of *L. japonicus* is a valuable resource for further study of starch metabolism in general and its importance in legumes in particular. To illustrate this, we report below new information about the structure-function relationships of AGPase and GWD1 derived from study of the mutations affecting these enzymes in *L. japonicus* and provide new insights into the importance of starch metabolism in *L. japonicus* through the analysis of the phenotypes of the *pgm1* and *gwd1* mutants.

Identification of Novel Amino Acid Residues Important for the Activity of the LjAPL1 and LjGWD1 Enzymes

The nature of the mutation in the *APL1* gene of *L. japonicus* (in line SL5127-5, from the forward screen) was unexpected in the light of our current understanding of the structure-function relationships of the enzyme. Although leaves of the *apl1* mutant have only 7% of the AGPase activity of wild-type leaves (Table II), the mutation changes an amino acid (S400L; Supplemental Fig. S4) not known previously to be important for enzyme activity. The crystal structure of the small subunit of AGPase from potato tubers (Jin et al., 2005) and mutagenesis studies (Ballicora et al., 1998; Greene et al., 1998; Kavakli et al., 2002) have enabled the identification of residues important for either substrate affinity or sensitivity to the allosteric effectors inorganic phosphate and 3-phosphoglycerate. The strong sequence similarities between the small and large subunits (48% identity at the amino acid level between LjAPL1 and StAPS) allowed us to use this three-dimensional structure to analyze the impact of the mutation in *apl1*. The mutated residue (Ser-400; equivalent to Ser-331 in the potato small subunit) is positioned at the interface between subunits (Supplemental Fig. S5). It is tempting to speculate that this residue is crucial for activity because it is involved in interaction between the subunits. Consistent with this idea, Cross et al. (2005) identified a 55-amino acid region of the potato small subunit including Ser-331 that influences both the catalytic and the allosteric properties of the enzyme by modulating interaction between the subunits. However, preliminary in silico analysis indicates that the change from Ser to Leu at this position is unlikely to affect subunit interaction (Supplemental Fig. S5); the backbone, rather than the side chain, of the residue at this position is involved in subunit interaction. The side chain of Ser-400, however, interacts with other amino acids in the β-helix domain in which it is located. These interactions are lost when a Leu is substituted for this Ser residue. We suggest that Ser-400 may be important for the three-dimensional structure of the large subunit itself and hence for heterotetramer stability as a whole.

The mutation in *gwd1-1* also provides new information about the structure-function relationships of an enzyme essential for normal starch metabolism. The mutation (E566K) lies in the second of the two starch-binding domains (SBD-1 and SBD-2) located in the N-terminal region of the GWD1 protein (Mikkelsen et al., 2006). These domains have been classified into the newly defined CBM45 family in the CAZy database (http://www.cazy.org). Members of this family are also found in an extraplastidial glucan, water dikinase of unknown function (GWD2; Glaring et al., 2007) and in plastidial α-amylases. Expression of an N-terminally truncated form of the Arabidopsis plastidial α-amylase AMY3 has established that the CBM module is not required for the catalytic activity of this enzyme (Yu et al., 2005). Expression of a truncated form of Arabidopsis GWD1, lacking SBD-1, indicates that this module may be important in determining both the specific activity and the glucan substrate preference of the enzyme (Mikkelsen et al., 2006). However, nothing is known thus far about the role of SBD-2. None of the reported Arabidopsis *gwd1* mutants carry mutations in the SBD-2 module (Yu et al., 2001). Our results indicate that the SBD-2 module is crucial for the in vivo function of the enzyme. The Glu at position 566 is conserved at the equivalent position in GWD1 from other species and lies in a generally conserved region (Supplemental Fig. S6) predicted to be a coiled-coil domain.

Importance of Starch Metabolism for Plant Growth, Development, and Nodule Function in *L. japonicus*

We used our synthesis and degradation mutants to examine whether loss of normal starch metabolism affected growth and development and especially the legume-specific capacity for nitrogen fixation in *Rhizobium*-containing root nodules. The essentially starchless phenotype of the *pgm1-4* mutant (Figs. 3 and 5) indicates that plastidial PGM1 is necessary for starch synthesis throughout the plant. Interestingly, this mutant grows normally even under relatively short days (12 h of light and 12 h of dark; Fig. 5). This is also true of the equivalent mutant in pea (*rug3*; Harrison, 1996). In contrast, although the almost starchless *pgm1* mutant of Arabidopsis grows at approximately the same rate as the wild type under

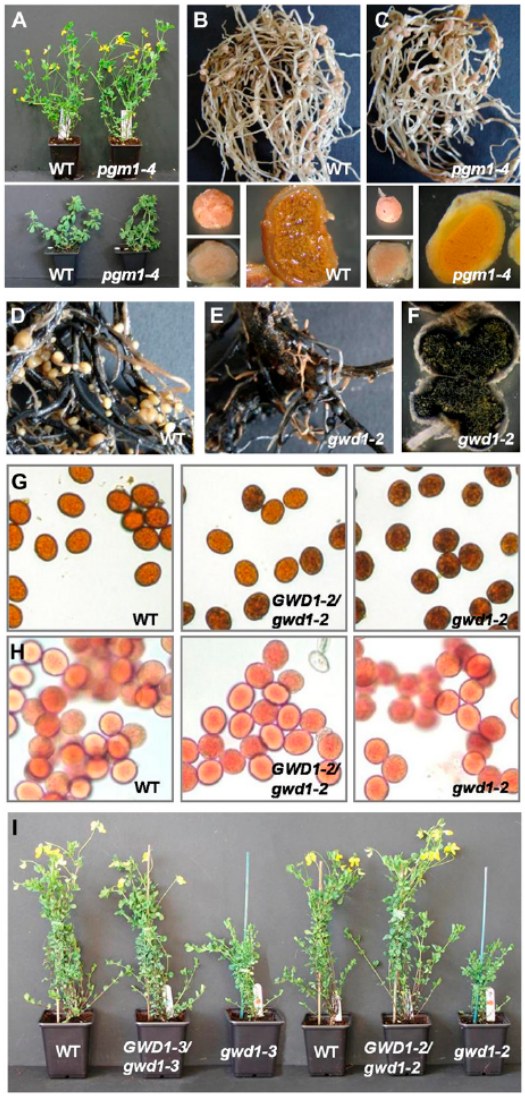

Figure 5. Phenotypes of the *pgm1-4* and *gwd1-2/3* mutants. A, Plants grown in 16 h of light and 8 h of dark (top) and 12 h of light and 12 h of dark (bottom). B and C, Root systems and nodules of 3-month-old plants grown in 16 h of light and 8 h of dark and inoculated with *M. loti* at 6 weeks. Nodules are shown either whole (top left), cut open (bottom left) or cut open and stained with iodine (right). The cortical zone and noninfected cells in wild-type (WT) nodules contain starch. Mutant nodules contain no starch. D to F, Iodine staining of root systems and of the interior of a nodule of a mutant plant (F; compare with the wild type shown in B). Plants were grown in 16 h of light and 8 h of dark and were 6 months old. G and H, Pollen grains from plants stained with iodine (G) and acetocarmine (H). The mutation increases the starch content of pollen but does not affect its viability. I, Three-month-old wild-type, heterozygous, and mutant segregants for *gwd1-3* (left three plants) and *gwd1-2* (right three plants).

continuous light, it grows much more slowly under 12-h-light/12-h-dark conditions (Caspar et al., 1985).

Both the *gwd1-2* and *gwd1-3* mutants accumulated excessive amounts of starch in their leaves, roots, stems, nodules, and pollen (Figs. 3 and 5; Supplemental Fig. S3). These mutants showed severe growth defects, including chlorosis, premature leaf senescence, and very poor or no seed set. Only a small proportion of mutant plants in a given batch produced flowers, and they did so about 2 months later than wild-type plants. These characteristics were present regardless of the daylength under which the plants were grown. This is in contrast to the situation in Arabidopsis, in which *gwd1* (*sex1*) knockout mutants display almost no growth phenotype under long days but retain very high starch contents and can reproduce even under short days when growth is significantly retarded (Caspar et al., 1991). Thus, loss of GWD seems to have much more serious consequences for *L. japonicus* than for Arabidopsis.

It is not clear why growth rates are reduced in some mutant plants impaired in leaf starch synthesis or degradation or why mutations in homologous starch-metabolism genes have different consequences for growth in *L. japonicus* and Arabidopsis. In Arabidopsis, genetic and environmental factors that reduce carbohydrate availability at night can also cause temporary cessation of growth (Smith and Stitt, 2007). It may be that there is variation between genes and species in the extent to which mutations affecting starch turnover result in reduced carbohydrate availability and hence cessation of growth during the night. Alternatively, for starch-excess mutants, the severity of the phenotype may depend on the extent to which starch accumulation physically impairs normal chloroplast functions.

We explored further the causes of the loss of fertility in *gwd1-2* and *gwd1-3* mutants. In the progeny of plants heterozygous for either mutant allele, segregation did not follow the Mendelian ratio of 1:2:1 mutant:heterozygote:wild type. From 219 progeny of a *gwd1-2* heterozygote, 13 were mutants, 116 were heterozygotes, and 90 were wild type. For 202 progeny of a *gwd1-3* heterozygote, 15 were mutants, 98 were heterozygotes, and 89 were wild type. The low numbers (6%–7%) of homozygous mutant plants suggested that loss of GWD1 is partially lethal at the gametophyte stage, or that mutant embryos generally failed to mature, or that mutant seeds did not germinate. In tomato (*Solanum lycopersicum*), loss of GWD1 leads to pollen with an abnormally high starch content that fails to germinate (Nashilevitz et al., 2009). However, two lines of evidence suggested that pollen from *L. japonicus gwd1* mutants is at least partially viable despite its high starch content. First, heterozygous plants could be obtained in the F1 progeny of recip-

rocal crosses made between heterozygote and wild-type plants. Second, staining the pollen with acetocarmine, a dye used to assess whether pollen grains have matured, showed no differences between the wild type, heterozygotes, and homozygous mutants (Fig. 5).

Most *gwd1* flowers did not produce pods, and when they did, pods and embryos often aborted early in development. However, fully developed mutant pods and seeds could be obtained by detaching flowers and placing the peduncles in Murashige and Skoog liquid medium supplemented with 3% Suc (data not shown). This result suggested that the effect of the mutation on the production of viable seed was maternal rather than due to a defect in embryo development. As a further test, we analyzed embryos and seeds from 40 pods each of wild-type and heterozygous (*GWD1-2/gwd1-2*) plants from the same segregating population. Both the number of seeds per pod and the average seed weight were very similar for the two genotypes (an average of 9.1 and 10.2 seeds per pod for heterozygous and wild-type plants, respectively, and an average seed weight of 1.0 mg for both genotypes). Similar results were obtained for the *gwd1-3* mutation (data not shown). These data support the idea that reduced production of viable seeds on homozygous mutant plants is a maternal effect. However, genotyping of each individual mature embryo from heterozygous plants was not wholly consistent with a maternal effect. Out of 63 mature seeds, only seven contained homozygous mutant embryos (one in nine rather than the expected one in four). Thus, mutant embryos were disadvantaged whether in mutant or heterozygous pods. The effect of the *gwd1* mutations on fertility thus appears to be complex. Gametophytic, maternal, and embryo effects may all be involved. In general, our mutants show that the phosphorylation of starch via the glucan, water dikinases GWD1 and GWD3 is essential for normal starch degradation in most parts of the *L. japonicus* plant and that this, in turn, is crucial for normal plant growth and development.

Legume nodules generally contain starch in cortical cells and noninfected cells within the infected zone (Gordon, 1992; Gordon and James, 1997; Szczyglowski et al., 1998). In *pgm1-4* mutants inoculated with *Mesorhizobium loti*, nodules had a normal pink color, and their size and number per root system were similar to those of wild-type segregants (Fig. 5). In spite of the apparent lack of starch in the nodules, assays for nitrogen fixation (acetylene reduction) revealed no statistically significant differences (Student's t test P value of greater than 0.05) between mutant, heterozygote, and wild-type plants 36 d after inoculation (0.57 ± 0.06, 0.75 ± 0.11, and 0.67 ± 0.20 μmol ethylene h^{-1} root system^{-1}, respectively; mean $\pm$ SE of five root systems). Thus, storage of carbon as starch in the nodule is not necessary for normal nodule function under our growth conditions. At two stages of nodule development, nodules on *gwd1-2* plants contained about 15 times more starch than nodules on wild-type plants (Supplemental Fig. S3C). Nonetheless, mutant nodules were capable of nitrogen fixation. In one batch of plants, nitrogen fixation (acetylene reduction) was comparable in *gwd1* mutants and their segregating wild-type and heterozygous lines. In another batch, fixation was reduced in mutant relative to wild-type and heterozygous plants. Both batches showed that the *gwd1* mutants were capable of nitrogen fixation (Supplemental Fig. S3D). Taken together with the results of measurements on the nodules of *pgm1-4* mutant plants, these data indicate that starch storage and normal starch metabolism are not essential for nodule function.

CONCLUSION

We have linked the identification of candidate genes from rough mapping with TILLING reverse genetics to assemble a comprehensive suite of starch mutants in the model legume *L. japonicus*. This is a valuable new resource with which to examine the partitioning of carbon in relation to several crop traits of agronomic importance, such as nitrogen fixation and perenniality. Our research has additional significance. It shows that the main components of the pathways of leaf starch metabolism are conserved across different families and life histories. In contrast, the control of flux through these pathways and their importance in sustaining normal plant growth are very different in Arabidopsis and *L. japonicus*. Whereas a severe deficiency in starch synthesis has much less effect in *L. japonicus* than in Arabidopsis, loss of the capacity for starch degradation has much more profound consequences for plant growth. Further investigation of these differences and the genes affecting starch metabolism that were previously unknown could lead to a better understanding of the regulatory mechanisms linking the metabolism of starch with plant growth. Our analysis also revealed significant differences in starch metabolism between plants of MG20 and Gifu, two wild-type ecotypes of *L. japonicus* with large differences in several other traits, including biomass production. This finding is particularly interesting in light of the recent demonstration that rates of starch turnover are positively, causally linked to productivity in Arabidopsis (Sulpice et al., 2009). We suggest that *L. japonicus* is an excellent system with which to test the wider applicability of this finding.

MATERIALS AND METHODS

Plant Material and Growth Conditions

Initial screening for starch metabolism mutants was carried out as described by Perry et al. (2003, 2009). Plants for starch quantification were grown in a growth chamber on F2 compost (Levington; Scotts Professional) with 12 h of light and 12 h of dark at a light intensity of 100 μmol m^{-2} s^{-1} and day/night temperatures of 22°C/18°C. Plants for iodine staining, acetylene reduction assay, enzyme assay, and native gel electrophoresis were grown in a glasshouse on compost with 16 h of light and 8 h of dark (with or without supplementary lighting; minimum light intensity at 200 μmol m^{-2} s^{-1}) or in

a controlled-environment room (light intensity at 200 μmol m^{-2} s^{-1}; 75% humidity).

Plants for acetylene reduction assay were transferred from compost to perlite:vermiculite (1:1, v/v) at 7 weeks and fed twice a week with nutrient solution (Broughton and Dilworth, 1971) containing 0.1 mM KNO_3. Roots were truncated at the time of transfer to stimulate lateral root formation and hence nodule production upon inoculation with *Mesorhizobium loti* strain Tono.

For in vitro culture of pods, peduncles carrying mature flowers were cut and the ends were immediately immersed in distilled water. Peduncles were then surface sterilized with 10% (v/v) bleach (1% available chlorine) and rinsed repeatedly in sterile water. After recutting, peduncles were inserted through a hole in the lid of a 50-mL tube of sterile Murashige and Skoog medium (microelements and macroelements including vitamins, pH 5.7) with 3% (w/v) Suc and then kept for 4 weeks in a growth chamber with 16 h of light and 8 h of dark.

In Silico Analysis of Gene and Protein Sequences

Genes encoding known enzymes of starch metabolism in *Lotus japonicus* were identified from the Miyakogusa genome database (Kazusa DNA Research Institute; http://www.kazusa.jp/lotus/index.html; Sato et al., 2008) using gene names as keywords and/or by performing BLASTp with the protein sequences of their Arabidopsis (*Arabidopsis thaliana*) orthologs. Hits that included clones and selected genome assembly sequences were selected for further analyses. These included use of the ClustalW2 program (http://www.ebi.ac.uk/Tools/clustalw2/index.html) for protein sequence alignment of homologs and other members of the same gene family from other species. Alignments allowed the identification of problems associated with incorrect annotations, incorrect predictions, or incomplete sequences for the *L. japonicus* genes and proteins.

Retrieved coding sequences that were incorrectly predicted or partial were used to search for the contig containing the corresponding genomic sequence. A predicted full-length coding sequence was then obtained using FGENESH (http://linux1.softberry.com/berry.phtml), Genscan (http://genes.mit.edu/GENSCAN.html; Burge and Karlin, 1997; Burge, 1998), and GenomeScan (http://genes.mit.edu/genomescan.html; Yeh et al., 2001).

When orthologs of known genes could not be identified, BLASTn or tBLASTn searches were performed against the *L. japonicus* EST database (Dana-Farber Cancer Institute Gene Index of *L. japonicus*; http://compbio.dfci.harvard.edu/tgi/plant.html). Where possible, a partial or full-length coding sequence was obtained by aligning several EST clones, and the resulting sequence was used to search the Miyakogusa genome database or to screen transformation-competent bacterial artificial chromosome vector and bacterial artificial chromosome libraries.

Gene structures were predicted using the CODDLE program (for Codons Optimized to Discover Deleterious Lesions; http://www.proweb.org/coddle/), and PARSESNP (for Project Aligned Related Sequences and Evaluate SNPs; http://www.proweb.org/parsesnp/) was used to determine potential effects on protein function.

Isolation of Nucleic Acids

Genomic DNA was extracted with phenol:chloroform according to Heckmann et al. (2006). The DNA pellet was washed with 70% (v/v) aqueous ethanol, air dried, and resuspended in 50 to 100 μL of nuclease-free water. Samples of 1 μL were subjected to electrophoresis on 1% agarose gels to check integrity. Five- to 10-fold dilutions were used for further experiments.

Genotyping and Sequencing

Genotyping of individual plants was carried out using gene-specific primers (Supplemental Table S5). PCR primers were designed using Primer3 software (http://frodo.wi.mit.edu/cgi-bin/primer3/primer3_www.cgi; Rozen and Skaletsky, 2000). PCR was performed using ExTaq polymerase (Takara) following the manufacturer's instructions, and the products were sequenced.

TILLING

Primers were designed using Primer3 in the region identified by CODDLE as having the maximum likelihood of producing deleterious alleles following EMS mutagenesis. TILLING on the genes *LjPGM1*, *LjAPS1*, *LjAPL2*, and *LjGWD1* was performed as described previously (Horst et al., 2007) using gene-specific primers. TILLING for *LjGWD3* was carried out by RevGenUK (http://revgenuk.jic.ac.uk/) on an ABI3730 capillary sequencer following the method of Le Signor et al. (2009). Gene-specific primers used for TILLING are shown in Supplemental Table S4. The effect of the mutations was predicted using the PARSESNP program. Mutations resulting in the loss of a splicing site or a premature stop codon and those with a position-specific scoring matrix difference score greater than zero, or likely to have an effect according to our own analysis of a multiple sequence alignment, were selected for further analysis.

Mapping

Mapping populations were created from crosses between mutants (in the Gifu background) and the wild-type ecotype *L. japonicus* MG-20. F1 plants were allowed to self, and mutant plants were selected in the F2 generation based on iodine staining of leaves. Mapping was carried out using microsatellite SSR markers designed at the Kazusa DNA Research Institute (from Sigma Genosys, Sigma-Aldrich). Rough mapping was carried out initially by bulk segregant analysis (markers shown in Supplemental Table S2) on at least two pools of eight genomic DNA samples of mutants from F2 segregating populations. The mapping interval thus identified was confirmed on the mutant individuals. For five of the mutant lines shown in Supplemental Table S6 (SL5074-12, SL5249-3, SL4618-12, SL4841-4, and SL5035-7), finer mapping was performed on a larger set of mutant individuals from F2 segregating populations from a cross with MG-20. Finer mapping used SSR markers designed either at the Kazusa DNA Research Institute or with the Simple Sequence Repeat Identification Tool (Temnykh et al., 2001). SSR markers within the target regions were PCR amplified and fluorescently labeled (Schuelke, 2000). The method used multiplex PCR amplification and automated capillary electrophoresis analysis on an ABI 3730 DNA Analyzer (M. Groth, Biocenter Ludwig-Maximilians-Universität Munich) and GeneMapper software (Applied Biosystems).

Iodine Staining and Starch Quantification

Tissue was heated in 80% (v/v) aqueous ethanol to remove pigments before staining with iodine (Lugol's solution), except for embryos, which were incubated in chloroform:ethanol:water (5:5:1, v/v/v) prior to treatment with 80% ethanol.

For starch quantification, 50 to 200 mg of tissue was rapidly frozen in liquid nitrogen after harvest and then homogenized on dry ice using a pulverizing mill (MM300; Retsch). After extraction with perchloric acid (1 mL of 0.7 M), insoluble material was washed, heated to gelatinize starch, and incubated with amyloglucosidase and α-amylase prior to measurement of Glc on the solubilized material, according to Smith and Zeeman (2006).

Enzyme Assays

For assays of AGPase, leaf material (200–300 mg) was harvested on ice, extracted in 3 mL of 50 mM HEPES (pH 7.4), 1 mM EDTA, 2 mM $MgCl_2$, and 1 mM dithiothreitol and clarified by centrifugation at 4°C. Each assay contained 10 μL of soluble extract in 190 μL of 50 mM HEPES (pH 7.4), 15 mM $MgCl_2$, 15 mM 3-phosphoglycerate, 1.5 mM ATP, 0.5 mg mL^{-1} bovine serum albumin, 0.5 mM [U-^{14}C]Glc 1-P at 1 MBq $mmol^{-1}$, and 12.5 units mL^{-1} inorganic pyrophosphatase (from baker's yeast). After incubation for 10 min at 37°C, samples were processed by treatment with DEAE cellulose discs according to Ghosh and Preiss (1966) and the ADPGlc product was measured by liquid scintillation counting.

Gel Electrophoresis and Immunoblotting

Native gel electrophoresis for enzyme activities was modified from the method of Shaw and Prasad (1970). Samples of 200 to 300 mg of leaves were homogenized in 1 mL of cold 100 mM MOPS, pH 7.2, 1 mM EDTA, 1 mM dithiothreitol, and 10% (v/v) glycerol. Following centrifugation (10,000*g*, 10 min at 4°C), samples (50–100 μg of protein) of supernatant were subjected to electrophoresis on native polyacrylamide gels (7.5%) containing 1% (w/v) potato (*Solanum tuberosum*) starch. Gels were then incubated for 1 h at 37°C in 100 mM Tricine (pH 8), 10 mM $MgCl_2$, 0.25 mM NADP, 1 mM thiazolyl blue tetrazolium bromide, a trace of Meldola's blue (Sigma-Aldrich), 1 unit mL^{-1} Glc 6-P dehydrogenase from *Leuconostoc mesenteroides*, and either 7 mM Glc 1-P (PGM activity) or 8 mM Fru 6-P (PGI activity).

For immunoblotting, samples of frozen leaves were powdered and mixed with 2× Laemmli sample buffer. The homogenate was clarified by centrifu-

gation. Samples of 10 μg of protein were loaded onto SDS-polyacrylamide gels (4%–12% gradient). After electrophoresis, the gel was blotted onto a nitrocellulose membrane and probed with rabbit serum containing antibodies to potato GWD1 at a dilution of 1:1,000 (Yu et al., 2001).

Acetylene Reduction Assay

The amount of ethylene produced by whole root systems incubated with acetylene was quantified as described by Horst et al. (2007).

Novel sequence data from this article have been deposited in the GenBank/EMBL/DDBJ databases under the following accession numbers: AP011538, LjT05B14 (TM2333; DPE2); AP011539, LjB22L24 (BM2254; 5′ region of LjGWD1).

Supplemental Data

The following materials are available in the online version of this article.

Supplemental Figure S1. Pathway of transitory starch metabolism in Arabidopsis leaves.

Supplemental Figure S2. Separation of PGM and PGI isoforms by native gel electrophoresis.

Supplemental Figure S3. Phenotypes of *gwd1* TILLING mutants.

Supplemental Figure S4. Comparison of the amino acid sequences of *L. japonicus* AGPase subunits with those of other species.

Supplemental Figure S5. Predicted effect on AGPase function of the S400L amino acid change identified in the *L. japonicus* mutant *apl1-1*.

Supplemental Figure S6. Protein domains of *L. japonicus* GWD1, and comparison of its amino acid sequence with those of other species.

Supplemental Table S1. Diurnal changes in leaf starch content through the development of *L. japonicus* plants.

Supplemental Table S2. Orthologs in *L. japonicus* of the core set of genes encoding enzymes of starch metabolism in Arabidopsis.

Supplemental Table S3. Microsatellite SSR markers used for rough mapping of loci with mutant phenotype from the forward genetic screen.

Supplemental Table S4. Mapped interval and flanking microsatellite markers of the loci with mutant phenotypes from the forward genetic screen.

Supplemental Table S5. Primers used for gene sequencing, TILLING, and genotyping.

Supplemental Table S6. Mutant alleles of genes encoding enzymes of starch metabolism in *L. japonicus*.

ACKNOWLEDGMENTS

We thank Martin Groth (Biocenter Ludwig-Maximilians-Universität) for access to the ABI3730 mapping method and Dr. Gerhard Ritte (University of Potsdam) for the gift of GWD1 antibodies. We thank RevGenUK (http://revgenuk.jic.ac.uk/) for TILLING the *LjGWD3* gene.

Received June 28, 2010; accepted July 30, 2010; published August 10, 2010.

LITERATURE CITED

Ainsworth EA, Rogers A, Leakey ADB, Heady L, Gibon Y, Stitt M, Schurr U (2006) Does elevated atmospheric [CO_2] alter diurnal C uptake and the balance of C and N metabolites in growing and fully expanded soybean leaves? J Exp Bot **58:** 579–591

Ballicora MA, Fu Y, Nesbitt NM, Preiss J (1998) ADP-glucose pyrophosphorylase from potato tubers: site-directed mutagenesis studies of the regulatory sites. Plant Physiol **118:** 265–274

Baunsgaard L, Lütken H, Mikkelsen R, Glaring MA, Pham TT, Blennow A (2005) A novel isoform of glucan, water dikinase phosphorylates pre-phosphorylated α-glucans and is involved in starch degradation in *Arabidopsis*. Plant J **41:** 595–605

Blauth SL, Yao Y, Klucinec JD, Shannon JC, Thompson DB, Guiltinan MJ (2001) Identification of *Mutator* insertional mutants of starch-branching enzyme 2a in corn. Plant Physiol **125:** 1396–1405

Broughton WJ, Dilworth MJ (1971) Control of leghaemoglobin synthesis in snake beans. Biochem J **125:** 1075–1080

Burge C, Karlin S (1997) Prediction of complete gene structures in human genomic DNA. J Mol Biol **268:** 78–94

Burge CB (1998) Modeling dependencies in pre-mRNA splicing signals. *In* S Salzberg, D Searls, S Kasif, eds, Computational Methods in Molecular Biology. Elsevier Science, Amsterdam, pp 127–163

Caspar T, Huber SC, Somerville CR (1985) Alterations in growth, photosynthesis, and respiration in a starchless mutant of *Arabidopsis thaliana* (L.) deficient in chloroplast phosphoglucomutase. Plant Physiol **79:** 11–17

Caspar T, Lin TP, Kakefuda G, Benbow L, Preiss J, Somerville C (1991) Mutants of *Arabidopsis* with altered regulation of starch degradation. Plant Physiol **95:** 1181–1188

Corbesier L, Lejeune P, Bernier G (1998) The role of carbohydrates in the induction of flowering in *Arabidopsis thaliana*: comparison between the wild type and a starchless mutant. Planta **206:** 131–137

Crevillén P, Ballicora MA, Mérida A, Preiss J, Romero JM (2003) The different large subunit isoforms of *Arabidopsis thaliana* ADP-glucose pyrophosphorylase confer distinct kinetic and regulatory properties to the heterotetrameric enzyme. J Biol Chem **278:** 28508–28515

Crevillén P, Ventriglia T, Pinto F, Orea A, Mérida A, Romero JM (2005) Differential pattern of expression and sugar regulation of *Arabidopsis thaliana* ADP-glucose pyrophosphorylase-encoding genes. J Biol Chem **280:** 8143–8149

Cross JM, Clancy M, Shaw JR, Boehlein SK, Greene TW, Schmidt RR, Okita TW, Hannah LC (2005) A polymorphic motif in the small subunit of ADP-glucose pyrophosphorylase modulates interactions between the small and large subunits. Plant J **41:** 501–511

Delatte T, Umhang M, Trevisan M, Eicke S, Thorneycroft D, Smith SM, Zeeman SC (2006) Evidence for distinct mechanisms of starch granule breakdown in plants. J Biol Chem **281:** 12050–12059

Delvallé D, Dumez S, Wattebled F, Roldán I, Planchot V, Berbezy P, Colonna P, Vyas D, Chatterjee M, Ball S, et al (2005) Soluble starch synthase I: a major determinant for the synthesis of amylopectin in *Arabidopsis thaliana* leaves. Plant J **43:** 398–412

Dumez S, Wattebled F, Dauvillee D, Delvallé D, Planchot V, Ball SG, D'Hulst C (2006) Mutants of *Arabidopsis* lacking starch branching enzyme II substitute plastidial starch synthesis by cytoplasmic maltose accumulation. Plant Cell **18:** 2694–2709

Eimert K, Wang SM, Lue WL, Chen J (1995) Monogenic recessive mutations causing both late floral initiation and excess starch accumulation in *Arabidopsis*. Plant Cell **7:** 1703–1712

Fulton DC, Stettler M, Mettler T, Vaughan CK, Li J, Francisco P, Gil M, Reinhold H, Eicke S, Messerli G, et al (2008) β-AMYLASE4, a noncatalytic protein required for starch breakdown, acts upstream of three active β-amylases in *Arabidopsis* chloroplasts. Plant Cell **20:** 1040–1058

Ghosh HP, Preiss J (1966) Adenosine diphosphate glucose pyrophosphorylase: a regulatory enzyme in the biosynthesis of starch in spinach leaf chloroplasts. J Biol Chem **241:** 4491–4504

Glaring MA, Zygadlo A, Thorneycroft D, Schulz A, Smith SM, Blennow A, Baunsgaard L (2007) An extra-plastidial α-glucan, water dikinase from *Arabidopsis* phosphorylates amylopectin in vitro and is not necessary for transient starch degradation. J Exp Bot **58:** 3949–3960

Gordon AJ (1992) Carbon metabolism in the legume nodule. *In* CJ Pollock, JF Farrar, AJ Gordon, eds, Carbon Partitioning within and between Organisms. Bios Scientific Publishers, Oxford, pp 133–162

Gordon AJ, James CL (1997) Enzymes of carbohydrate and amino acid metabolism in developing and mature nodules of white clover. J Exp Bot **48:** 895–903

Greene TW, Kavakli IH, Kahn ML, Okita TW (1998) Generation of up-regulated allosteric variants of potato ADP-glucose pyrophosphorylase by reversion genetics. Proc Natl Acad Sci USA **95:** 10322–10327

Hanson KR, McHale NA (1988) A starchless mutant of *Nicotiana sylvestris* containing a modified plastid phosphoglucomutase. Plant Physiol **88:** 838–844

Harrison CJ (1996) The *rug3* locus of pea. PhD thesis. University of East Anglia, Norwich, UK

Harrison CJ, Hedley CL, Wang TL (1998) Evidence that the *rug3* locus of pea (*Pisum sativum* L.) encodes plastidial phosphoglucomutase confirms

that the imported substrate for starch synthesis in pea amyloplasts is glucose-6-phosphate. Plant J **13:** 753–762

Heckmann AB, Lombardo F, Miwa H, Perry JA, Bunnewell S, Parniske M, Wang TL, Downie JA (2006) *Lotus japonicus* nodulation requires two GRAS domain regulators, one of which is functionally conserved in a non-legume. Plant Physiol **142:** 1739–1750

Horst I, Welham T, Kelly S, Kaneko T, Sato S, Tabata S, Parniske M, Wang TL (2007) TILLING mutants of *Lotus japonicus* reveal that nitrogen assimilation and fixation can occur in the absence of nodule-enhanced sucrose synthase. Plant Physiol **144:** 806–820

Jin X, Ballicora MA, Preiss J, Geiger JH (2005) Crystal structure of potato tuber ADPglucose pyrophosphorylase. EMBO J **24:** 694–704

Kavakli IH, Kato C, Choi SB, Kim KH, Salamone PR, Ito H, Okita TW (2002) Generation, characterization, and heterologous expression of wild-type and up-regulated forms of *Arabidopsis thaliana* leaf ADP-glucose pyrophosphorylase. Planta **215:** 430–439

Keeling PL, Myers AM (2010) Biochemistry and genetics of starch synthesis. Annu Rev Food Sci Technol **1:** 271–303

Kötting O, Kossmann J, Zeeman SC, Lloyd J (2010) Regulation of starch metabolism: the age of enlightenment? Curr Opin Plant Biol **13:** 321–329

Kötting O, Pusch K, Tiessen A, Geigenberger P, Steup M, Ritte G (2005) Identification of a novel enzyme required for starch metabolism in Arabidopsis leaves: the phosphoglucan, water dikinase. Plant Physiol **137:** 242–252

Kötting O, Santelia D, Edner C, Eicke S, Marthaler T, Gentry MS, Comparot-Moss S, Chen J, Smith AM, Steup M, et al (2009) STARCH-EXCESS4 is a laforin-like phosphoglucan phosphatase required for starch degradation in *Arabidopsis thaliana*. Plant Cell **21:** 334–346

Kruckeberg AL, Neuhaus HE, Feil R, Gottlieb LD, Stitt M (1989) Decreased-activity mutants of phosphoglucose isomerase in the cytosol and chloroplast of *Clarkia xantiana*. Biochem J **261:** 457–467

Le Signor C, Savois V, Aubert G, Verdier J, Nicolas M, Pagny G, Moussy F, Sanchez M, Baker D, Clarke J, et al (2009) Optimizing TILLING populations for reverse genetics in *Medicago truncatula*. Plant Biotechnol J **7:** 430–441

Lin TP, Caspar T, Somerville C, Preiss J (1988a) Isolation and characterization of a starchless mutant of *Arabidopsis thaliana* (L.) Heynh lacking ADPglucose pyrophosphorylase activity. Plant Physiol **86:** 1131–1135

Lin TP, Caspar T, Somerville C, Preiss J (1988b) A starch deficient mutant of *Arabidopsis thaliana* with low ADPglucose pyrophosphorylase activity lacks one of the two subunits of the enzyme. Plant Physiol **88:** 1175–1181

Martin C, Smith AM (1995) Starch biosynthesis. Plant Cell **7:** 971–985

Matheson NK, Wheatley JM (1962) Starch changes in developing and senescing tobacco leaves. Aust J Biol Sci **15:** 445–458

McCallum CM, Comai L, Greene EA, Henikoff S (2000) Targeting Induced Local Lesions IN Genomes (TILLING) for plant functional genomics. Plant Physiol **123:** 439–442

Mikkelsen R, Suszkiewicz K, Blennow A (2006) A novel type carbohydrate-binding module identified in α-glucan, water dikinases is specific for regulated plastidial starch metabolism. Biochemistry **45:** 4674–4682

Nashilevitz S, Melamed-Bessudo C, Aharoni A, Kossmann J, Wolf S, Levy AA (2009) The *legwd* mutant uncovers the role of starch phosphorylation in pollen development and germination in tomato. Plant J **57:** 1–13

Ölçer H, Lloyd JC, Raines C (2001) Photosynthetic capacity is differentially affected by reductions in sedoheptulose-1,7-bisphosphatase activity during leaf development in transgenic tobacco plants. Plant Physiol **125:** 982–989

Pan X, Tang Y, Li M, Wu G, Jiang H (2009) Isoforms of GBSSI and SSII in four legumes and their phylogenetic relationship to their orthologs from other angiosperms. J Mol Evol **69:** 625–634

Perry J, Welham T, Brachmann A, Binder A, Charpentier M, Groth M, Haage K, Markmann K, Wang TL, Parniske M (2009) TILLING in *Lotus japonicus* identified large allelic series for symbiosis genes and revealed a bias in non-functional alleles towards hits in glycine codons. Plant Physiol **151:** 1281–1291

Perry JA, Wang TL, Welham TJ, Gardner S, Pike JM, Yoshida S, Parniske M (2003) A TILLING reverse genetics tool and a Web accessible collection of mutants of the legume *Lotus japonicus*. Plant Physiol **131:** 866–871

Ritte G, Lloyd JR, Eckermann N, Rottmann A, Kossmann J, Steup M (2002) The starch-related R1 protein is an α-glucan, water dikinase. Proc Natl Acad Sci USA **99:** 7166–7171

Rozen S, Skaletsky H (2000) Primer3 on the WWW for general users and for biologist programmers. Methods Mol Biol **132:** 365–386

Sato S, Nakamura Y, Kaneko T, Asamizu E, Kato T, Nakao M, Sasamoto S, Watanabe A, Ono A, Kawashima K, et al (2008) Genome structure of the legume, *Lotus japonicus*. DNA Res **15:** 227–239

Schuelke M (2000) An economic method for the fluorescent labelling of PCR fragments. Nat Biotechnol **18:** 233–234

Shaw CR, Prasad R (1970) Starch-gel electrophoresis of enzymes: a compilation of recipes. Biochem Genet **4:** 297–320

Smith AM, Stitt M (2007) Coordination of carbon supply and plant growth. Plant Cell Environ **30:** 1126–1149

Smith AM, Zeeman SC (2006) Quantification of starch in plant tissues. Nat Protoc **1:** 1342–1345

Streb S, Egli B, Eicke S, Zeeman SC (2009) The debate on the pathway of starch synthesis: a closer look at low-starch mutants lacking plastidial phosphoglucomutase supports the chloroplast-localized pathway. Plant Physiol **151:** 1769–1772

Sulpice R, Pyl ET, Ishihara H, Trenkamp S, Steinfath M, Witucka-Wall H, Gibon Y, Usadel B, Poree F, Piques MC, et al (2009) Starch as a major integrator in the regulation of plant growth. Proc Natl Acad Sci USA **106:** 10348–10353

Szczyglowski K, Shaw RS, Wopereis J, Copeland S, Hamburger D, Kasiborski B, Dazzo FB, de Bruijn FJ (1998) Nodule organogenesis and symbiotic mutants of the model legume *Lotus japonicus*. Mol Plant Microbe Interact **11:** 684–697

Temnykh S, DeClerck G, Lukashova A, Lipovich L, Cartinhour S, McCouch S (2001) Computational and experimental analysis of microsatellites in rice (*Oryza sativa* L.): frequency, length variation, transposon associations, and genetic marker potential. Genome Res **11:** 1441–1452

Tomlinson KL, Lloyd JR, Smith AM (1997) Importance of isoforms of starch-branching enzyme in determining the structure of starch in pea leaves. Plant J **11:** 31–43

Wang SM, Chu B, Lue WL, Yu TS, Eimert K, Chen J (1997) *adg2-1* represents a missense mutation in the ADPG pyrophosphorylase large subunit gene of *Arabidopsis thaliana*. Plant J **11:** 1121–1126

Wang SM, Lue WL, Yu TS, Long JH, Wang CN, Eimert K, Chen J (1998a) Characterization of *ADG1*, an *Arabidopsis* locus encoding for ADPG pyrophosphorylase small subunit, demonstrates that the presence of the small subunit is required for large subunit stability. Plant J **13:** 63–70

Wang TL, Bogracheva TY, Hedley CL (1998b) Starch: as simple as A, B, C? J Exp Bot **49:** 481–502

Wattebled F, Dong Y, Dumez S, Delvalle D, Planchot R, Berbezy P, Vyas D, Colonna P, Chatterjee M, Ball S, et al (2005) Mutants of Arabidopsis lacking a chloroplastic isoamylase accumulate phytoglycogen and an abnormal form of amylopectin. Plant Physiol **138:** 184–195

Yeh RF, Lim LP, Burge CB (2001) Computational inference of homologous gene structures in the human genome. Genome Res **11:** 803–816

Yu TS, Kofler H, Hausler RE, Hille D, Flugge UI, Zeeman SC, Smith AM, Kossmann J, Lloyd J, Ritte G, et al (2001) The *Arabidopsis sex1* mutant is defective in the R1 protein, a general regulator of starch degradation in plants, and not in the chloroplast hexose transporter. Plant Cell **13:** 1907–1918

Yu TS, Lue WL, Wang SM, Chen J (2000) Mutation of Arabidopsis plastid phosphoglucose isomerase affects leaf starch synthesis and floral initiation. Plant Physiol **123:** 319–326

Yu TS, Zeeman SC, Thorneycroft D, Fulton DC, Dunstan H, Lue WL, Hegemann B, Tung SY, Umemoto T, Chapple A, et al (2005) α-Amylase is not required for breakdown of transitory starch in Arabidopsis leaves. J Biol Chem **280:** 9773–9779

Zeeman SC, Kossmann J, Smith AM (2010) Starch: its metabolism, evolution and biotechnological modification in plants. Annu Rev Plant Biol **61:** 209–234

Zeeman SC, Smith SM, Smith AM (2007) The diurnal metabolism of leaf starch. Biochem J **401:** 13–28

Zhang X, Myers AM, James MG (2005) Mutations affecting starch synthase III in Arabidopsis alter leaf starch structure and increase the rate of starch synthesis. Plant Physiol **138:** 663–674

Supplemental materials of Vriet et al, 2010.

Genotype	Time of day	Starch content (mg Glc equivalents g^{-1} fresh weight)			
		Four weeks	Six weeks	Eight weeks	Ten weeks
MG-20	EOD	8.7 ± 0.8	7.5 ± 0.4	14.2 ± 1.3	56.9 ± 5.5
	EON	0.52 ± 0.15	0.36 ± 0.095	5.6 ± 0.1	52.0 ± 5.1
Gifu	EOD	10.3 ± 0.2	7.6 ± 0.2	14.1 ± 0.6	32.1 ± 3.4
	EON	0.59 ± 0.06	0.32 ± 0.11	4.5 ± 0.4	21.7 ± 1.4

Supplemental Table S1. Diurnal changes in leaf starch content through development of *L. japonicus* plants.

These data are displayed graphically in Figure 1. Details are as in Figure 1. EOD, end of day ; EON, end of night.

Enzyme	*in A. thaliana* Gene name	Locus	*in L. japonicus* Gene name	Predicted gene(s)		Clone name	Chr	Map position	Marker(s)
Phosphoglucoisomerase, plastidial	PGI1	At4g24620	PGI1	chr1.LjT29N14.30.nd		LjT29N14	1	0,0	TM0454
Phosphoglucomutase, plastidial	PGM1	At5g51820	PGM1	chr5.CM0953.200.nc		LjT17N13	5	44,9	TM0953
ADPglucose pyrophosphorylase Small subunit	APS1/ADG1	At5g48300	APS1	chr2.CM0191.60.nc		LjT45D07	2	72.1-72.5	TM0210-TM0324
ADPglucose pyrophosphorylase Large subunit 1	APL1/ADG2	At5g19220	APL1	chr4.CM0387.180.nc		LjT31N09	4	48,2	TM1865
ADPglucose pyrophosphorylase Large subunit 2	APL2	At1g27680	APL2	chr1.LjT34C24.40.nc		LjT34C24	1	17,7	TM0952
				chr5.CM0077.680.nc		LjT08B03	5	0,8	TM0822-TM0291
ADPglucose pyrophosphorylase Large subunit 3	APL3	At4g39210	APL3	chr1.CM0113.470.nd		LjT55F02	1	42,6	TM0113-TM0309
ADPglucose pyrophosphorylase Large subunit 4	APL4	At2g21590	APL4	chr3.CM0216.100.nd		LjT44D07	3	75,6	TM0527-TM0268
ADPglucose pyrophosphorylase Large subunit 5	n/a	n/a	APL5	LjB06P23.100.nc		LjB06P23	0		
Starch synthase I	ATSS1/SSI1	At5g24300	SS1	LjT38J19.80.nd	LjT38J19.60.nd	LjT38J19	0		
Starch synthase II	ATSS2	At3g01180	SS2	chr1.CM0141.60.nd	chr1.CM0141.220.nd	LjT58F09	1	29.3-29.7	TM1869-TM0141
				CM1835.140.nc			0		
Starch synthase III	ATSS3	At1g11720							
Starch synthase IV	ATSS4/SSIV	At4g18240							
Starch synthase V/Glycogen synthase-like	putative SSV	At5g65685	SS5	chr2.CM0177.660.nc		LjT10N22	2	48,5	TM0381*
Granule-bound starch synthase	putative GBSS	At1g32900	GBSS	chr3.CM0208.40.nd		LjT11A16	3	49.4-52.7	TM0406-TM0208
				chr5.LjT41L03.30.nd		LjT41L03	5	19,2	TM0431
Starch branching enzyme, class I	n/a	n/a	SBE1	chr1.CM0178.250.nc					
Starch branching enzyme, class II	SBE2.2	At5g03650				LjT29P11	1	20,1	TM0193
	BE3/SBE2.1	At2g36390							
Starch branching enzyme, class III	BE1	At3g20440							
Starch debranching enzyme: Isoamylase I	ATISA1/ISA1	At2g39930	ISA1	chr4.CM0004.550.nc		LjT15D01	4	65,6	TM0004*
Starch debranching enzyme: Isoamylase II	ATISA2/DBE1/BE2	At1g03310	ISA2	LjSGA_028198.1					
Starch debranching enzyme: Isoamylase III	ATISA3/ISA3	At4g09020							
Starch debranching enzyme: Pullulanase/Limit dextrinase	ATLDA/ATPU1/PU1	At5g04360	LDA	chr5.CM0909.690.nc		LjT34P16	5	34.8-36.8	BM1817-TM0138*
Glucan, water dikinase 1	GWD1/SEX1/SOP1/R1	At1g10760	GWD1	chr4.LjT08E06.100.nc		LjT08E06	4	24,2	TM0296
Glucan, water dikinase 2	ATGWD2/GWD2	At4g24450							
Glucan, water dikinase 3/phosphoglucan water dikinase	ATGWD3/PWD/OK1	At5g26570	GWD3	chr5.LjT42F22.140.nc	chr5.LjT42F22.160.nc	LjT42F22	5	56,1	TM1948
Protein phosphatase	ATPTPKIS1/DSP4/SEX4	At3g52180							
Alpha-amylase 1	ATAMY1/AMY1	At4g25000	AMY1	chr5.CM0852.300.nc		LjT30K21	5	0,4	TM0089*-TM1392
Alpha-amylase 2	ATAMY2/AMY2	At1g76130	AMY2	LjSGA_020916.1					
Alpha-amylase 3	ATAMY3/AMY3	At1g69830	AMY3	chr2.CM0608.610.nc		LjT38H08	2	40,3	TM1534
				chr1.CM0410.400.nd		LjT26M18	1	31,3	TM1701
Beta-amylase 1	BAM1/BMY7	At3g23920	BAM1	LjSGA_011445.1	LjSGA_032725.2				
Beta-amylase 2	BAM2/BMY9	At4g00490							
Beta-amylase 3	BAM3/BMY8/CT-BMY	At4g17090	BAM3	chr2.CM0021.1220.nd		LjT16A17	2	60,9	TM0521
				chr2.CM0021.1150.nd	chr2.CM0021.1290.nd	LjT16A17	2	60,9	TM0521
Beta-amylase 4	BAM4/BMY6	At5g55700							
Beta-amylase 5	BAM5/BMY1/RAM1	At4g15210	BAM5	chr3.CM0152.120.nc		LjT45C16	3	64,8	TM0203
Beta-amylase 6	BAM6/BMY5	At2g32290	BAM6	LjSGA_030993.1					
Beta-amylase 7	BAM7/BMY4	At2g45880	BAM7	LjT34L14.60.nc		LjT34L14	0		
Beta-amylase 8	BAM8/BMY2	At5g45300	BAM8	chr2.CM0803.520.nc		LjT10G21	2	49.3-50.1	TM0974-TM0803
Beta-amylase 9	BAM9/BMY3	At5g18670	BAM9	chr6.LjT15B19.140.nd		LjT15B19	6	49,9	TM0756
Disproportionating enzyme/D enzyme	DPE1	At5g64860	DPE1	chr1.CM0032.500.nc		LjT07E21	1	1,6	TM032-TM1730
Transglucosidase	DPE2	At2g40840	DPE2	LjSGA_007380.1	LjSGA_011298.1	LjT05B14	1	56,6	TM2333
Alpha-glucan phosphorylase, plastidial	PHS1	At3g29320							
Alpha-glucan phosphorylase, cytosolic	ATPHS2/PHS2	At3g46970	PHS2	LjB08M07.80.nc		LjB08M07	0		
				chr2.CM0373.1170.nd		LjT47H03	2	17,7	TM1491
Maltose transporter	MEX1/RCP1	At5g17520	MEX1	chr3.CM0127.650.nc		LjT44D21	3	82,4	TM0127

Supplemental Table S2. Orthologs in *L. japonicus* of the core set of genes encoding enzymes of starch metabolism in Arabidopsis.

The core set of Arabidopsis genes was taken from information in Smith et al. (2004; 2005), Zeeman et al. (2007), Fulton et al. (2008) and Kötting et al. (2009). Candidate genes in *L. japonicus* were retrieved by searching the Miyakogusa genome database developed by the Kasuza DNA Research Institute (http://www.kazusa.jp/lotus/index.html; Sato et al., 2008), then manually analyzed at the level of predicted amino acid sequence. The Table shows only the genes with coverage greater than 30% and greater than 50% identity at the amino acid level with the Arabidopsis orthologous genes. The map positions (in cM) are from the *L. japonicus* genetic linkage map from a cross between the ecotypes Gifu and MG-20 (maternal and paternal parents, respectively). All markers are SSR markers, except those marked with an asterix (*), which are dCAPs markers. The map position and markers that are underlined are the closest to the gene of those presented. Genes located on Selected Genome Assembly (LjSGA) sequences are unmapped (corresponding chromosome given as 0) since these sequences are not anchored to the genome. Additional information on clones, including the corresponding contig, its accession number and marker sequences, is given in the Miyakogusa database (under 'Clone list'). No clones, LjSGA or EST sequence hits could be obtained in *L. japonicus* for three of the Arabidopsis genes: *GWD2*, *BAM2* and *BAM4*. Several sequence hits could be identified for the genes SS3, SS4, SBE1, SBE3, ISA3, SEX4, and PHS1, but they could not be assigned with good confidence as the orthologs in *L. japonicus* of the Arabidopsis genes. Details of bioinformatic analyses performed to generate this table are in Materials and Methods. Chr, chromosome.

Marker	Chromosome	Map position
TM0193	1	20.1
TM0438	1	42.6
TM0143	1	66.2
TM0065	2	14.0
TM0076	2	46.0
TM0002	2	67.3
TM0080	3	12.5
TM0005	3	34.0
TM0049	3	55.1
TM0616	3	70.4
TM0182	4	8.8
TM0030	4	32.2
TM0046	4	53.8
TM0034	5	4.8
TM0048	5	27.6
TM0036	5	49.7
TM0302	6	14.0
TM0013	6	36.9
TM0336	6	57.6

Supplemental Table S3. Microsatellite SSR markers used for rough mapping of mutant phenotypes from the forward genetic screen.

The map positions are in cM and correspond to the location of the markers on the genetic linkage map of *L. japonicus* (see Fig. 2).

Mutant line	Mutant class	Chromosome	Mapped interval	Flanking markers	Recombination frequency
SL4308-12	synthesis	1	0.0	TM0102-TM0192	7/19
SL4715-2	synthesis	1	0.0-1.2	TM0102-TM0039	6/13
SL5069-2	synthesis	1	0.0-4.0	TM0058-TM0094	9/17
SL4725-4	synthesis	-	-	-	-
SL4867-11	synthesis	5	27.6-49.7	TM0048-TM0366	n/a
SL5127-5	synthesis	4	32.2-53.8	TM0030-TM0046	n/a
SL5074-12	synthesis	1	52.6-56.6	TM0107-TM0098	4/112
SL5249-3	synthesis	1	4.8-7.6	TM0063-TM0982	5/75
SL4618-12	synthesis	1	62.2	TM2089-BM1994	6/286
SL5143-3	synthesis	2	46.0-67.3	TM0076-TM0002	4/24
SL5215-2	breakdown	4	20.5-29.4	TM283-TM0500	5/19
SL5358-3	breakdown	4	21.3-32.2	TM0131-TM0030	4/24
SL5104-12	breakdown	5	50.1-56.1	TM0703-TM1948	1/24
SL4841-4	breakdown	1	1.6-7.6	TM0032-TM0982	11/87
SL5035-7	breakdown	1	45.4-47.0	TM0989-TM0001	8/131
SL5272-11	breakdown	4	32.2-47.8	TM0030-TM0387	5/16

Supplemental Table S4. Mapped interval and flanking microsatellite markers of mutant phenotypes from the forward genetic screen

Mutant class was determined by iodine staining of leaflets at the end of the day (revealing synthesis mutants) and the end of the night (revealing degradation mutants). The mapped interval corresponds to the upper and lower limit (given in cM) of the interval in which the loci of the mutant phenotype maps. The map positions are from the *L. japonicus* linkage map (see Fig. 2). Recombination frequencies are the number of recombinants obtained with both flanking markers divided by the total number of mutants analyzed. The mutation in line SL4725-4 was not mapped because the mutated gene was successfully identified by a candidate gene approach based on the starch-free phenotype of the plant.

A

Gene	Primer name	Primer sequence 5'-3'	Position
PGI1	LjPGI1_1F	TGGTCAAAACCTGAAAACAAAACAC	-79
	LjPGI1_1R	TTCCAATTTCCATCCCAGTATTTCC	1118
	LjPGI1_2F	GGAATGAGTTTTGCTAAATGTTCTT	1311
	LjPGI1_2R	TCATCATTGCATAGTCATACAGAAA	2472
	LjPGI1_3F	GCTAAATTTTGACTCGCTCCCAATC	3484
	LjPGI1_3R	ATAGAGTCCATTAGGCTGGTTCAGA	3982
	LjPGI1_4F	ATTGTTGCTCAGGAGCCCTAGTTTC	4822
	LjPGI1_4R	AACTCATGCTTTCATGAGGATCCAG	5841
	LjPGI1_5F	CGAAGTCCATGATTATGCCACTAAA	6431
	LjPGI1_5R	CCAAAACAACTTATTGCAACCTGCT	6983
PGM1	LjPGM1_1F	GTGGCACCTGTGTTTCCTTT	-178
	LjPGM1_1R	TGCAATACAAAAGCCAGCAG	1407
	LjPGM1_2F	TGTTCAATTCATTGCCTCCA	1238
	LjPGM1_2R	CCTGGTGAGGAAGACCCTCT	2843
	LjPGM1_3F	CCCAGTTCATGGAAAATGAGA	2850
	LjPGM1_3R	TTGAATTCTTTCCTCTGTGGTG	4485
	LjPGM1_4F	AAACGGGCTCCTAGTGTTGA	5818
	LjPGM1_1634R	CATCTGCAAACTGGAGGACA	7315
	LjPGM1_1374F	TGACCACATTCGTGAGAAAGA	6463
	LjPGM1_4R	CGGGAACAGGTTGATTCACT	8257
APL1	LjAPL1_1F	CACACAGTGCTTCATGTGGA	-98
	LjAPL1_1R	CTGCCATAGAAACCCCAGAG	1401
	LjAPL1_2F	GGTGGTACCAGCTGTTTGGT	1188
	LjAPL1_2R	TTGCTTTCAGGTCTGCTCCT	2837
	LjAPL1_3F	GGAAAATTCGCACCTCAAAG	2635
	LjAPL1_3R	TGGACATCCAACCACATGAA	4356
	LjAPL1_4F	AAGCACCAAAGCCTTATTGG	4203
	LjAPL1_4R	GCGGCATTGGAATATCAAGA	5794
GWD1/SEX1	LjGWD1_6F	GGAGGGCAGATCTGGAATTT	-1349
	LjGWD1_6R	GAACAAACAGAATCCAATCAAAA	325
	LjGWD1_7F	GAGTGTCAGCAAAGGCAAGA	105
	LjGWD1_7R	CTCCCTCATCTTTTCCTGGT	1802
	LjGWD1_8F	AGGTCTCCTGAATTGACTGGA	1477
	LjGWD1_8R	TCAAATAAGCAAAAAGTGCAAAA	3466
	LjGWD1_9F	GAAAAAGCTGGGAAGCCTAA	3305
	LjGWD1_9R	TGGCTAGCTGGTTAGTGTGC	4993
	LjGWD1_10F	GAGAGGCATGGCAACAATCT	4801
	LjGWD1_10R	TCCAACCTTCAGTGTCCTCA	6233
	LjGWD1_11F	TCAGAAAGGTCCTGCAATCA	5699
	LjGWD1_11R	TGACAACAACCACCAACACC	6401
	LjGWD1_1F	TCTCTCCAGGCACTGATTGA	6033
	LjGWD1_1R	CGTAAGCTAAGGATCGCAAA	7523
	LjGWD1_2F	CAGTTTTCATGCCCTGGACT	8767
	LjGWD1_2R	TGGCATATCTGGTGTCAGGA	10401
	LjGWD1_3F	ACTTGACGTGCTTGCACCAT	11234
	LjGWD1_3R	TGAAAACTTCCCTGGATCAAA	12963
	LjGWD1_4F	TGTGTTCTCAAGCCCAGTTT	13551
	LjGWD1_4R	CTTCTCTTGTTCGCCAGGAT	15239
	LjGWD1_5F	TGCCCCCATTTTAATGTTGT	15569
	LjGWD1_5R	TCAAACACACAGATTCACCAAA	17133

B

Gene	Primer name	Primer sequence 5'-3'	Position
PGM1	LjPGM1_TILL_2F(T2F)	GGTGCTCTGGATCGTGTTGCTGAA	6257
	LjPGM1_TILL_2R(T2R)	TCCAGAAAAACGGTGGGGAAACAA	7558
APL2	LjAPL2_TILL_1F	AAAGCAGACCCAAAAAGTGTGGCTTCC	358
	LjAPL2_TILL_1R	TGTCAACATGCTGCAAATTTTGGCAAT	1643
	LjAPL2_TILL_2F	TGAAGGCATGCCACTTGATTTTCTTGA	1320
	LjAPL2_TILL_2R	ATGCTGTGATGCAGGATAAGTGTGTGC	2817
APS1	LjAPS1_TILL_2F	GCATAGGCGGAACCAGGAAAAACC	698
	LjAPS1_TILL_2R	TCCAATGGAAGTTGCACCAGGAAT	1981
	LjAPS1_TILL_1F	TGCCCAGCAGAGTCCTGAGAATCC	1253
	LjAPS1_TILL_1R	GACGGAGGCAAATATCGTGGTTGG	2582
GWD1/SEX1	LjGWD1_TILL_1F	CAAAGTAGATCGTTCTTTCACCTTGACCA	9502
	LjGWD1_TILL_1R	ATGCTCATTTTCCTGGGAAGCAAACAC	10685
	LjGWD1_TILL 2F	GGAGGAATATGAAGCAGCTCGACAAGA	3124
	LjGWD1_TILL 2R	AGCCACATGCTTTGCCACAAAATTACA	4702
GWD3/PWD	LjGWD3_TILL_1F	AGAGGTTCAAGGTCCGGAAT	16320
	LjGWD3_TILL_1R	GGCAGTAGGGGTCAAACAAC	17825

Supplemental Table S5. Primers used for gene sequencing, TILLING and genotyping.

The position given for each primer sequence corresponds to the nucleotide position of its 5' end from the start codon of the gene. For candidate genes from the forward genetic screen mutation, primers were designed to cover the whole coding sequence. A, primers for gene sequencing and genotyping in relation to mutations discovered in the forward genetic screen. B, primers for gene sequencing and genotyping in relation to mutations isolated by TILLING.

Gene	Mutant line	Allele name	Nucleotide change	Effect of the mutation	Source of the mutation
LjPGI1	SL4715-2	*pgi1-1*	C917T	Q200*	Forward screen
	SL4308-12	*pgi1-2*	G3602A	W360*	Forward screen
	SL5069-2	*pgi1-3*	G5047A	Splice-site junction	Forward screen
LjPGM1	SL4725-4	*pgm1-4*	G1233A	Splice-site junction	Forward screen
	SL4867-11	*pgm1-5*	G377A	G95D	Forward screen
	SL4490-1	*pgm1-1*	G6413A	D436N	TILLING
	SL0755-1	*pgm1-2*	G6848A	W467*	TILLING
	SL1837-1	*pgm1-3*	G6932A	W495*	TILLING
LjAPL1	SL5127-5	*apl1-1*	C4408T	S400L	Forward screen
LjAPL2	SL0933-1	*apl2-1*	G1104A	D236N	TILLING
	SL0443-1	*apl2-2*	G1471A	G275E	TILLING
	SL0501-1	*apl2-3*	C2369T	P383S	TILLING
	SL4318-1	*apl2-4*	G2453A	Splice-site junction	TILLING
LjAPS1	SL0529-1	*aps1-1*	G1059A	A111T	TILLING
	SL4504-1	*aps1-2*	G1129A	S134N	TILLING
	SL5072-1	*aps1-3*	G2379A	A359T	TILLING
	SL4723-1	*aps1-4*	C1077T	L117F	TILLING
LjGWD1	SL5215-2	*gwd1-1*	G4633A	E566K	Forward screen
	SL5358-3	*gwd1-1*	G4633A	E566K	Forward screen
	SL1833-1	*gwd1-2*	G3303A	W303*	TILLING
	SL3001-1	*gwd1-3*	G3994A	W456*	TILLING
	SL4958-1	*gwd1-4*	G3491A	R324K	TILLING
	SL0176-1	*gwd1-5*	C4236T	P497L	TILLING
	SL5535-1	*gwd1-6*	G9912A	A968T	TILLING
LjGWD3	SL5104-12	*gwd3-1*	G7871A	Splice-site junction	Forward screen
	SL0692-1	*gwd3-2*	G16648A	G890E	TILLING
	SL4648-1	*gwd3-3*	C17437T	P1153L	TILLING
	SL0639-1	*gwd3-4*	G16918A	G980E	TILLING

Supplemental Table S6. Mutant alleles of genes encoding enzymes of starch metabolism in *L. japonicus*.

For mutations identified by TILLING, the table shows only those giving rise to alterations at splice sites, to stop codons (*), or to missense changes leading to a starch phenotype, or with PSSM values given by PARSESNP >0.

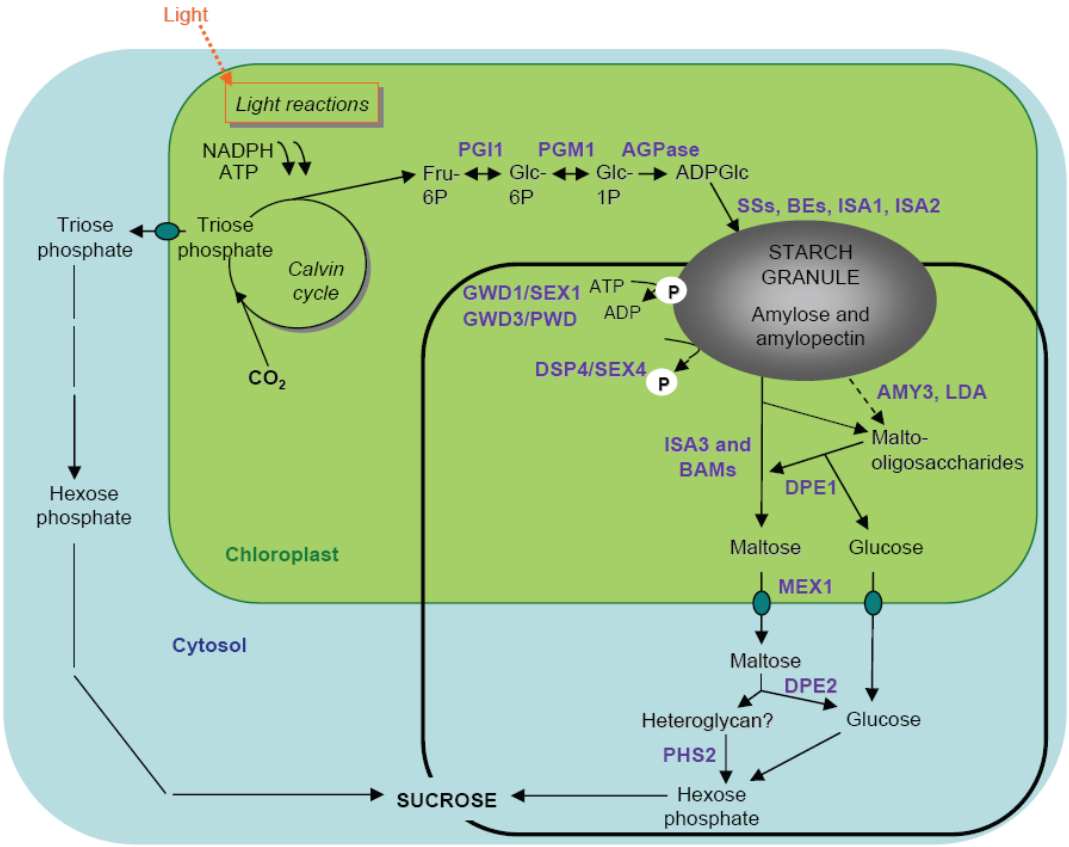

Supplemental Figure S1. Pathway of transitory starch metabolism in Arabidopsis leaves.

The diagram is modified from Smith et al. (2005) and Zeeman et al. (2007). The black bordered box encloses the reactions taking place during the night: the other reactions take place during the day. Names of members of the core set of starch metabolic enzymes (Supplemental Table S1) are in bold and in blue. PGI1, phosphoglucoisomerase, plastidal isoform; PGM1, phosphoglucomutase, plastidial isoform; AGPase, ADPglucose pyrophosphorylase; SSs, starch synthases (SS1, SS2, SS3, SS4, GBSS); BEs, starch branching enzymes (SBE1, SBE2, SBE3); ISA1, ISA2, ISA3, isoamylases (debranching enzymes); GWD1/SEX1, alternative abbreviations for glucan water dikinase 1; GWD3/PWD, alternative abbreviations for phosphoglucan, water dikinase; DPE1, disproportionating enzyme; AMY3, alpha-amylase 3; LDA, limit dextrinase (also called pullulanase: debranching enzyme); BAMs, beta-amylases (BAM3 and BAM4); MEX1, maltose transporter; DPE2, maltose transglucosidase; PHS2, glucan phosphorylase, cytosolic isoform.

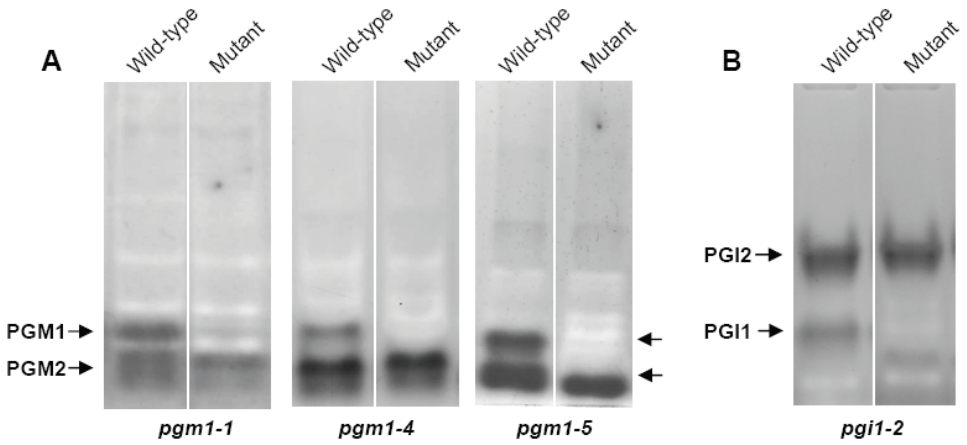

Supplemental Figure S2. Separation of PGM and PGI isoforms by native gel electrophoresis.

The positions of bands corresponding to the activity of the plastidial and cytosolic isoforms of the enzymes are indicated by arrowheads. The experiment was repeated on three different mutant and segregating wild-type plants for each genotype; representative results are displayed for one plant of each genotype. For each genotype, wild-type and mutant lanes are from the same gel. A, gels treated to reveal PGM activity. Each lane contained 100 µg of protein from a soluble extract of leaves. B, gel treated to reveal PGI activity. Each lane contained 50 µg of protein from a soluble extract of leaves.

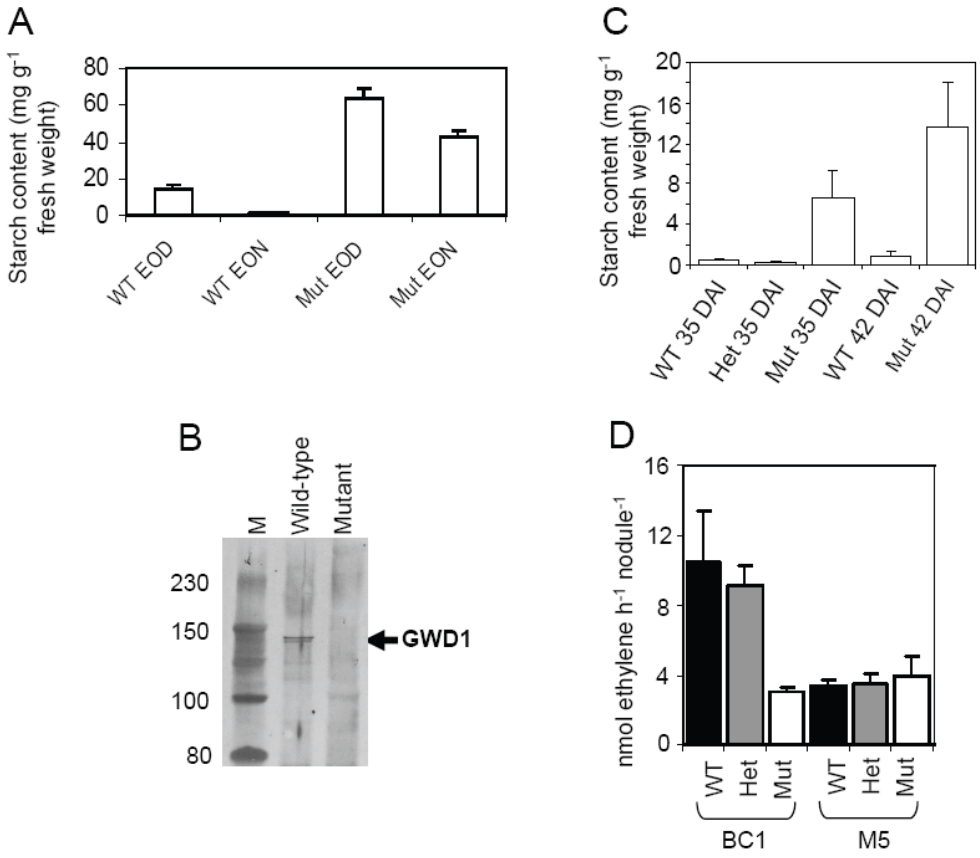

Supplemental Figure S3. Phenotypes of *gwd1* TILLING mutants.

A, Elevated starch content of leaves in *gwd1-2* leaves at end of day (EOD) and end of night (EON). Values are means ± SE of measurements on at least five, 6 week old plants. Plants were from lines derived by outcrossing to MG-20 and selfing F2 segregants. B, Absence of GWD1 protein in *gwd1-3* leaves. Samples of 10 µg protein from soluble extracts of leaves of the *gwd1-3* mutant and its wild-type segregant were subjected to electrophoresis on a 4-12% gradient polyacrylamide-SDS gel, electroblotted onto a nitrocellulose membrane, and probed with rabbit serum containing antibodies to potato GWD1 at a dilution of 1/1000. M is molecular mass markers, values in kD. C, Elevated starch contents of *gwd1-2* nodules. Nodules were harvested from individual *gwd1-2* plants and segregating heterozygous and wild-type plants from the first outcross to MG-20 at 35 and 42 days after inoculation (DAI) with *Mesorhizobium loti*, and assayed for starch content. Values are means ± SE of measurements on five plants, except for WT at 42 DAI for which four plants were used. D, ethylene released in an acetylene reduction assay for nitrogenase activity on root systems of *gwd1-2* mutants and their wild-type and heterozygous segregants. Plants were from lines derived either by outcrossing to MG20 (BC1), or directly from the original mutant in Gifu (M5).

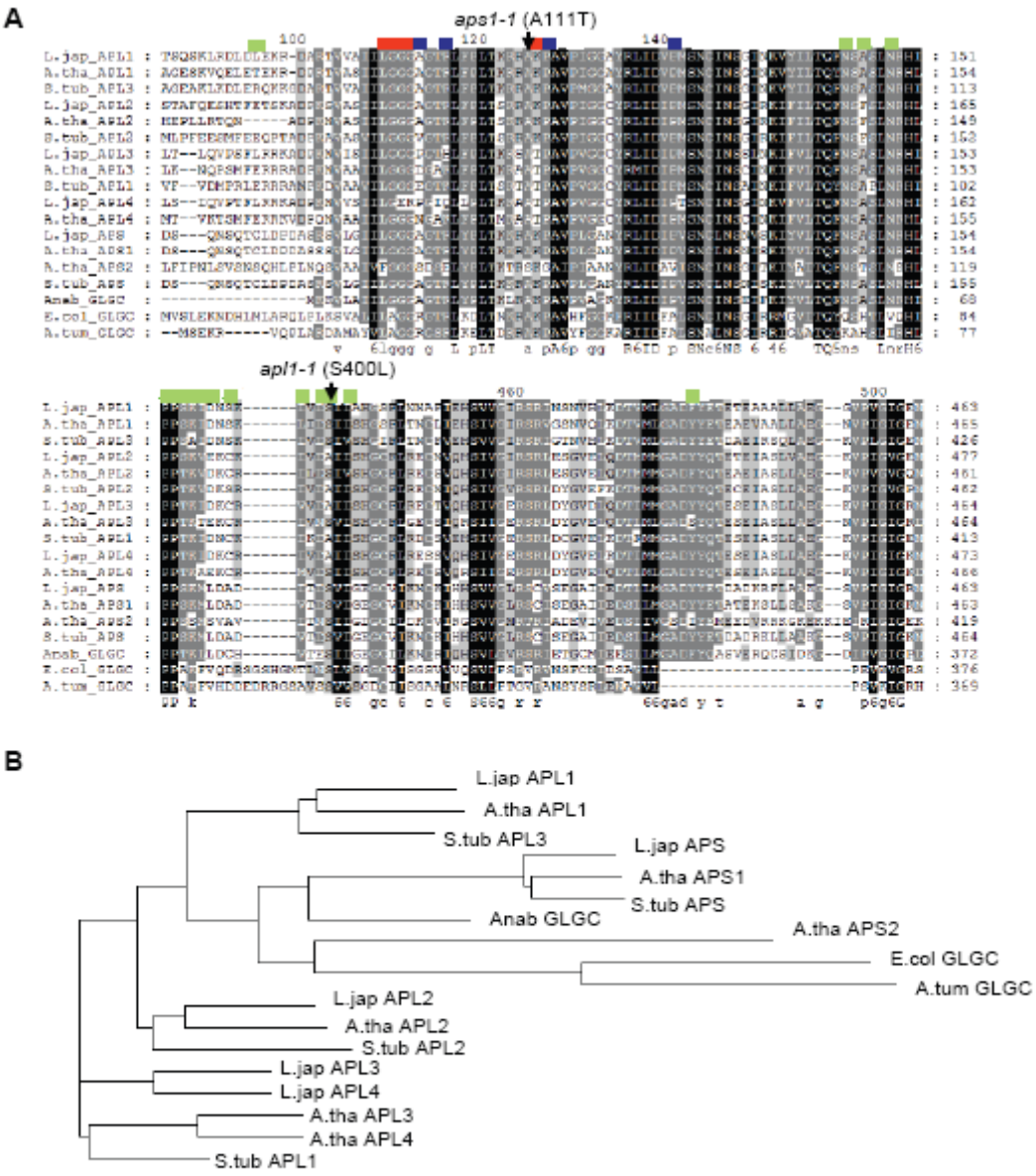

Supplemental Figure S4. Comparison of the amino acid sequences of *L. japonicus* AGPase subunits with those of other species.

Continued on next page

Supplemental Figure S4. Comparison of the amino acid sequences of *L. japonicus* AGPase subunits with those of other species.

Continued.

A, Comparison of two regions of the small and large subunits from *L. japonicus* (L.jap) genes carrying the mutations *aps1-1* and *apl1-1* with homologs from species including bacteria [*E. coli* (E.col) and *A. tumefaciens* (A.tum)], cyanobacteria [*Anabena* sp. (Anab)] and plants [*Arabidopsis thaliana* (A.tha) and *S. tuberosum* (S.tub)]. GLGC is the single gene product responsible for AGPase activity in bacteria and cyanobacteria. The alignment was made with the programs Clustal W2 (default settings) and GeneDoc. Strictly conserved residues are highlighted in black, less conserved residues are in grey. The positions of the *aps1-1* and *apl1-1* mutations are indicated by arrows. Residues marked in red interact with the substrates ADPGlc and/or ATP in the *S. tuberosum* APS protein (Jin et al., 2005); those marked in blue may be important in the regulatory properties of the enzyme (Kavakli et al., 2001; 2002). Residues marked in green are those involved in subunit interactions according to Jin et al. Note that in this alignment the residue in the potato APS protein equivalent to *L. japonicus* S400 is S401. Jin et al. numbered this residue as S331; their numbering is used in Supplemental Figure S6. The 55 amino-acid motif identified by Cross et al. (2005) as being critical for interaction between the small and the large subunit corresponds to amino acids 368-468 in the potato APS sequence on our alignment. Accession numbers for the sequences are: A.tha APL1, P55229; A.tha APL2, P55230; A.tha APL3, P55231; A.tha APL4, Q9SIK1, S.tub APL1, Q00081 ; S.tub APL2, P55242; S.tub APL3, P55243; A.tha APS1, P55228; A.tha APS2, Q7YKW3; S.tub APS, P23509; E.col GLGC, P046V1; A.tum GLGC, P39669: Anab GLGC, P30521. For origins of *L. japonicus* sequences see Supplemental Table S2. B, Guide tree made with the Clustal W2 program, showing the phylogenetic relationships between the AGPase proteins.

Additional literature

Kavakli IH, Park JS, Slattery CJ, Salamone PR, Frohlick J, Okita TW (2001) Analysis of allosteric effector binding sites of potato ADP-glucose pyrophosphorylase through reverse genetics. J Biol Chem 276: 40834–40840.

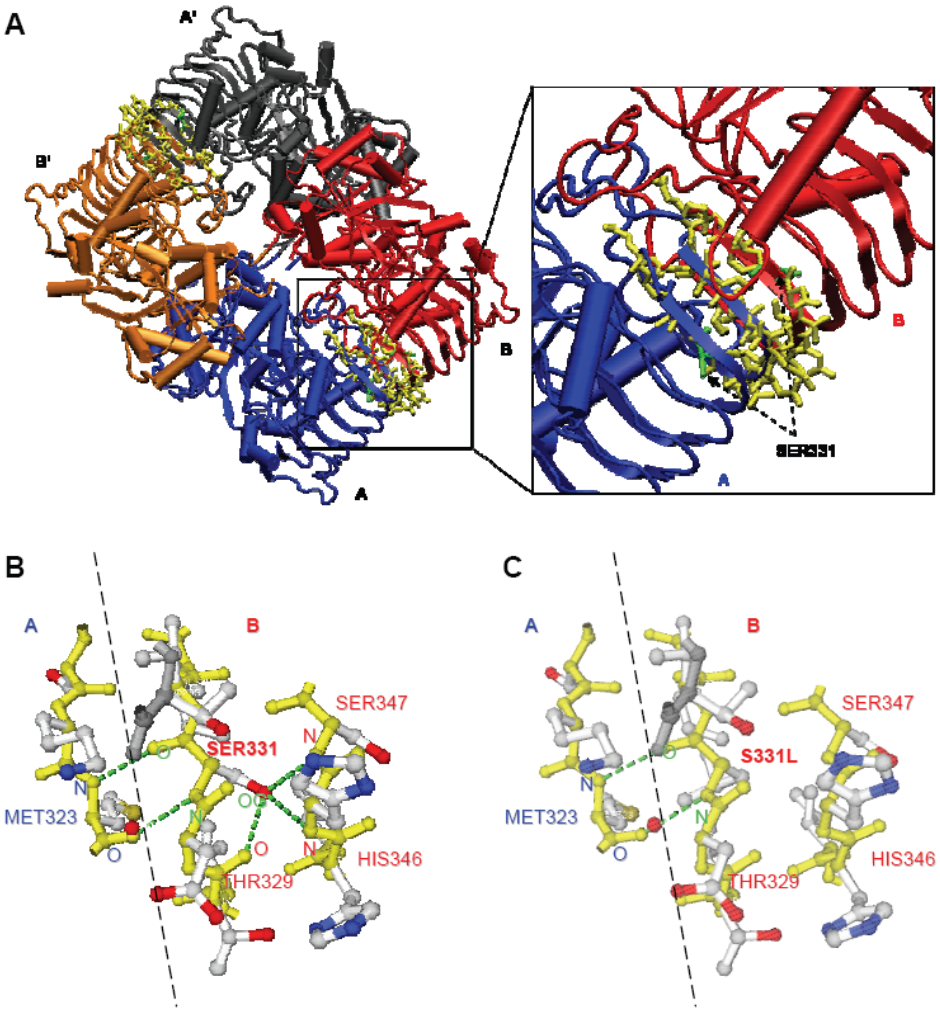

Supplemental Figure S5. Predicted effect on AGPase function of the S400L amino acid change identified in the *L. japonicus* mutant *apl1-1*.

A, Position of S331, the residue equivalent to S400 of the *L. japonicus* APL1, in the three dimensional structure of the small subunit of the potato tuber AGPase. The representation was generated by the VMD program from the crystallographic structure obtained by Jin et al. (2005), entered on the RCSB PDB databank with the PDB ID 1YP2. The residues at the interface between monomer A and B of the small subunit homotetramer are highlighted in yellow and enlarged on the right. The residue S331 is highlighted in green and indicted by arrows. B, Closer view of residues at the interface between subunits. C, *In silico* mutagenesis of S331 using the program Swiss PDB Viewer. The serine 331 residue was replaced by a leucine residue to simulate the effect of the mutation identified in *apl1-1*. The change brings about a disruption of the interaction of the side chain of this residue with other residues of the β-helix domain, suggesting a possible effect of the amino acid change S400L on the stability of this domain.

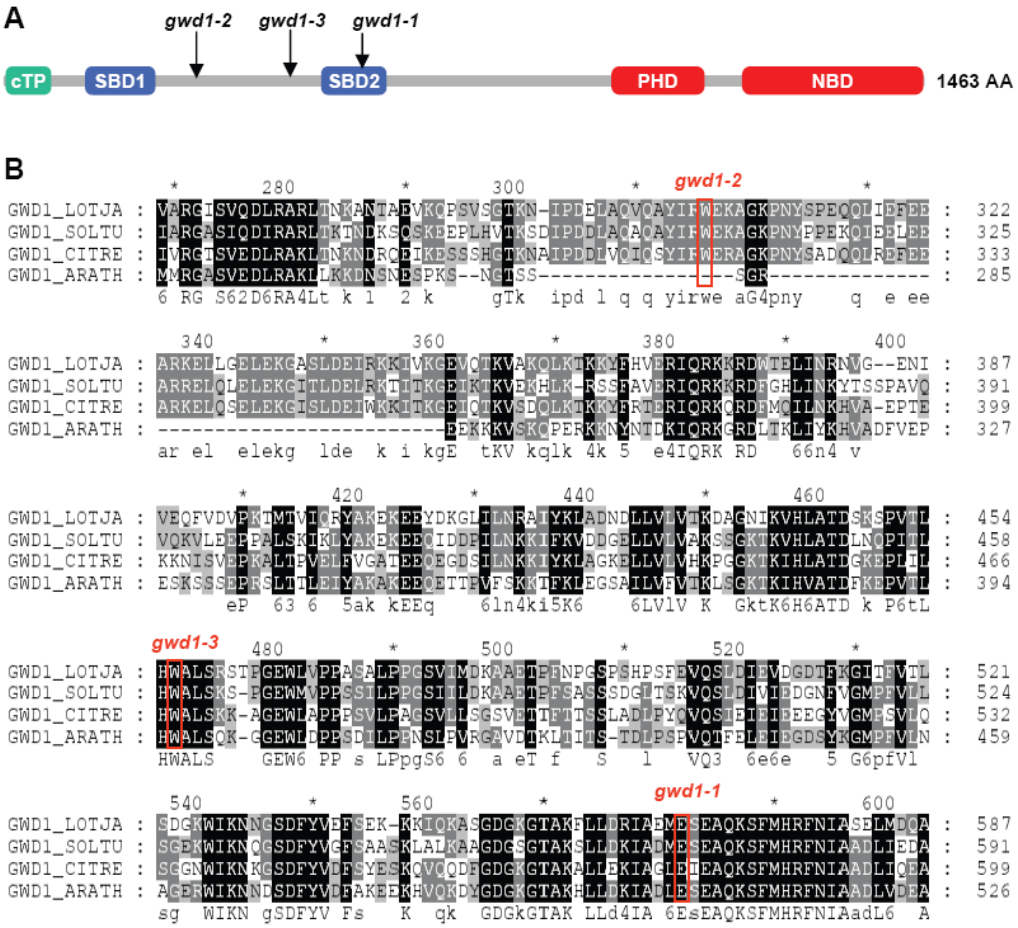

Supplemental Figure S6. Protein domains of the *L. japonicus* glucan water, dikinase 1, and comparison of its amino acid sequence with those of other species.

Continued on next page

Supplemental Figure S6. Protein domains of the *L. japonicus* glucan water, dikinase 1, and comparison of its amino acid sequence with those of other species.

Continued.

A, Location of the putative protein domains of LjGWD1 as defined by Yu et al. (2001) for its Arabidopsis homolog. cTP, chloroplast Transit Peptide (amino acids 1-75); SBD, Starch Binding Domain (amino acids 132-247 and 505-602); PHD, Phospho-Histidine Domain (amino acids 963-1112); NBD, Nucleotide Binding Domain (amino acids 1164-1462). B, Comparison of the region of GWD1 of *L. japonicus* carrying the *gwd1-1*, *gwd1-2* and *gwd1-3* mutations with the corresponding amino acid sequence in *Solanum tuberosum* (GWD1_SOLTU; Q9AWA5), *Citrus reticulata* (GWD1_CITRE; Q8LPT9), and *Arabidopsis thaliana* (GWD1_ARATH; Q9SAC6). The alignment was made with the programs Clustal W2 (default settings) and GeneDoc. Strictly conserved residues are highlighted in black, less conserved residues are in grey. Amino acids changed in plants carrying the *gwd1-1, gwd1-2 and gwd1-3* alleles and their equivalent residues in the GWD1 proteins of other species are boxed in red.
It is interesting to note that the *gwd1-2* mutation (W303*) lies within a region predicted to be coding for *GWD1* from *L. japonicus*, potato and *Citrus reticulata*, but non-coding for *GWD1* from Arabidopsis. The fact that in *L. japonicus* this mutation leads to a strong degradation phenotype, indistinguishable from the phenotype produced by another stop-codon mutant allele (*gwd1-3*; W456*) demonstrates that, at least for this species, the region is indeed translated.

Abbreviations

3PGA	3-phosphoglycerate
ABA	abscisic acid
ADP	adenosine 5'-diphosphate
ADPGlc	ADP-glucose
ADPGT	ADP-glucose/ADP transporter
AGPase	ADPglucose pyrophosphorylase
AM	arbuscular mycorrhiza
AMY	alpha-amylase
ARATH	*Arabidopsis thaliana*
ATP	adenosine 5'-triphosphate
BAC	bacterial artificial chromosome
BAM	beta-amylase
BCIP/NBT	5-bromo-4-chloro-3-indolyl phosphate/p-nitroblue tetrazolium chloride
BE	starch-branching enzyme
Bicine	bis (2-hydroxyethyl) glycine
bp	base pair
BSA	bovine serum albumine
BSA	bulk segregant analysis
C	carbon
CBM	carbohydrate-binding module
cDNA	complementary DNA
CER	controlled environment room
Chr	chromosome
cM	centiMorgan
CODDLE	codons optimized to discover deleterious lesions
CTAB	cetyltrimethylammonium bromide
d	days
dap	days after pollination
DBE	starch debranching enzyme
dCAPS	derived cleaved amplified polymorphic sequences
dH_2O	distilled water
DNA	desoxyribonucleic acid

DPE	disproportionating enzyme (aka D-enzyme and ransglucosidase)
dpi	days post inoculation
DSP4	dual-specificity protein phosphatase (aka PTPKIS1 and SEX4)
DTT	dithiothreitol
DW	dry weight
EC	enzyme commission number
EDTA	ethylenediaminetetraacetic acid
EFα	elongation factor alpha
EMS	ethyl methane sulfonate
ENU	N-ethyl-N-nitrosourea
EOD	end of the day
EON	end of the night
EST	expressed sequence tag
FDA	fluorescein fluorescein diacetate
FK	fructokinase
Fru	fructose
Fru6P	fructose-6-phosphate
FW	fresh weight
G6PDH	glucose-6-phosphate dehydrogenase
G6PT	glucose-6-phosphate/phosphate transporter
GBSS	granule bound starch synthase
GC-MS	gas chromatography-mass spectrometry
GH	glycoside hydrolases
Glc	glucose
Glc1P	glucose-1-phophate
Glc6P	glucose-6-phophate
GRIN	Germplasm Resource Information Network
GT	glycosyl-transferases
GWD	glucan water dikinase
HEPES	4-(2-hydroxyethyl)piperazine-1-ethanesulfonic acid
HK	hexokinase
HPAEC-PAD	High Performance Anion Exchange Chromatography with Pulsed Amperometric Detection
HPLC	high peformance liquid chromatography
Inv	invertase
ISA	isoamylase (aka pullulanase)
JIC	John Innes Centre

Da	Dalton
LD	long day
LDA	limit dextrinase
LM	light microscopy
LMU	Ludwig-Maximilians-Universität
LOTJA	*Lotus japonicus* (aka *L. Japonicus*)
LS	large subunit
LSF1	LIKE SEX4 (aka PTPKIS2)
MALDI-ToF	matrix-assisted laser desorption/ionization time-of-flight
MEX1	maltose transporter 1
MOS	malto-oligosaccharides
mRNA	messenger RNA
MS	Murashige & Skoog
Mya	million years ago
N	nitrogen
N_2	atmospheric nitrogen
NAD, NADH	nicotinamide adenine dinucleotide
NADP, NADPH	nicotinamide adenine dinucleotide phosphate
NEB	New England Biolabs
NH4	ammonium
NIL	Near Isogenic Line
NMD	nonsense-mediated decay
nt	nucleotide
ORYSA	*Orysa sativa*
PAGE	polyacrylamide gel electrophoresis
PAR	photosynthetically active radiation
PARSESNP	project aligned related sequences and evaluate SNPs
PCR	polymerase chain reaction
PEPC	phosphoenolpyruvate carboxylase
PGI	phosphoglucoisomerase
PGM	phosphoglucomutase
PHD	phospho-histidine domain
PHS	alpha-glucan phosphorylase
Pi	inorganic phosphate
PMSF	phenylmethanesulfonylfluoride
POPTR	*Populus trichocarpa*
PPi	Inorganic pyrophosphate

PSSM	position-specific scoring matrix
PVPP	polyvinylpolypyrrolidone
PWD	phosphoglucan, water dikinase
qRT-PCR	quantitative reverse transcription PCR
QTL	Quantitative Trait Locus
RGR	Relative Growth Rate
RIL	Recombinant Inbred Line
RNA	ribonucleic acid
RNAi	RNA interference
RT	room temperature
RT	room temperature
RT-PCR	reverse transcription PCR
SBD	starch binding domain
SBE	starch branching enzyme
SBE	starch branching enzyme
SD	short day
SD	standard deviation
SDS	sodium dodecyl sulfate
SE	standard error of the mean
SEX	starch excess
SGA	selected genome assembly
SIFT	sorting intolerant from tolerant
SNF	symbiotic nitrogen fixation
SNP	single nucleotide polymorphism
SNPs	single nucleotide polymorphisms
SnRK1	sucrose non-fermenting-1-related protein kinase 1
SORBI	*Sorghum bicolor*
SP	starch phosphorylase
SS	small subunit
SS	starch synthase
SSR	simple sequence repeat
SSRIT	Simple Sequence Repeat Identification Tool
Susy	sucrose synthase
T6P	trehalose-6-phosphate
TAC	transformation-competent artificial chromosome
TAE	Tris Acetate EDTA
TBE	Tris Borate EDTA

T-DNA	transfer DNA
TEM	transmission electron microscopy
TEMED	N,N,N',N'-tetramethylethylenediamine
TILLING	targeting induced local lesions in genomes
TP	triose-phosphate
TPT	triose-phosphate transporter
Tricine	N-(tri(hydroxymethyl)methyl)glycine
Tris	3-N-tris(hydroxymethyl)aminomethane
TSL	The Sainsbury Laboratory
U	Units of enzyme activity (one μmol/min)
UBQ10	Ubiquitin 10
UDP	Uridine diphosphate
UGPase	UDP-glucose pyrophosphorylase
USDA/ARS	United States Department of Agriculture/Agriculture Research Service
UV	ultraviolet
V/v	Volume by volume
VITVI	*Vitis vinifera*
W/v	Weight by volume
WGD	whole genome duplication
WT	wild-type

Bibliography

Aerts R, Chapin FS (2000) The mineral nutrition of wild plants revisited: A re-evaluation of processes and patterns. Advances in Ecological Research, Vol 30 **30:** 1-67

Ainsworth EA, Rogers A, Leakey ADB, Heady L, Gibon Y, Stitt M, Schurr U (2006). Does elevated atmospheric [CO_2] alter diurnal C uptake and the balance of C and N metabolites in growing and fully expanded soybean leaves? J Exp Bot **58:** 579-591

Ajjawi I, Lu Y, Savage LJ, Bell SM, Last RL (2010) Large-Scale Reverse Genetics in Arabidopsis: Case Studies from the Chloroplast 2010 Project. Plant Physiology **152:** 529-540

Akihiro T, Mizuno K, Fujimura T (2005) Gene expression of ADP-glucose pyrophosphorylase and starch contents in rice cultured cells are cooperatively regulated by sucrose and ABA. Plant and Cell Physiology **46:** 937-946

Alonso-Blanco C, Koornneef M (2000) Naturally occurring variation in Arabidopsis: an underexploited resource for plant genetics. Trends in Plant Science **5:** 22-29

Al-Shehbaz, I.A., O'Kane Jr., S.L. (2002) Taxonomy and phylogeny of Arabidopsis (Brassicaceae). In: Somerville, C.R., Meyerowitz, E.M. (Eds.), The Arabidopsis Book. American Society of Plant Biologists, Rockville, MD, doi: 10.1199/tab.0009, <www.aspb.org/publications/arabidopsis/>.

Anderson JM, Okita TW, Preiss J (1990) Enhancing carbon flow into starch: the role of ADP glucose pyrophosphorylase. The molecular and cellular biology of the potato.**:** 159-180

Ap Rees T (1980) Assessment of the contributions of metabolic pathways to plant respiration. Davies, D. D. (Ed.). the Biochemistry of Plants: a Comprehensive Treatise, Vol. 2. Metabolism and Respiration. Xvi+687p. Academic Press, Inc.: New York, N.Y., USA; London, England. Illus**:** P1-30

Ap Rees T (1985) The organization of glycolysis and the oxidative pentose phosphate pathway in plants. Douce, R. and D. a. Day (Ed.). Encyclopedia of Plant Physiology New Series, Vol. 18. Higher Plant Cell Respiration. Xvi+522p. Springer-Verlag: Berlin, West Germany; New York, N.Y., USA. Illus**:** 391-417

Arambarri AM (2000) A cladistic analysis of the new world species of Lotus L. (Fabaceae, Loteae). Cladistics-the International Journal of the Willi Hennig Society **16:** 283-297

Arambarri AM (2000) A cladistic analysis of the Old World species of *Lotus* L. (Fabaceae, Loteae). Canadian Journal of Botany-Revue Canadienne De Botanique **78:** 351-360

Asamizu E, Nakamura Y, Sato S, Tabata S (2004) Characteristics of the *Lotus japonicus* gene repertoire deduced from large-scale expressed sequence tag (EST) analysis. Plant Molecular Biology **54:** 405-414

Avice JC, Ourry A, Lemaire G, Boucaud J (1996) Nitrogen and carbon flows estimated by N-15 and C-13 pulse-chase labeling during regrowth of alfalfa. Plant Physiology **112:** 281-290

Baier MC, Barsch A, Kuster H, Hohnjec N (2007) Antisense repression of the *Medicago truncatula* nodule-enhanced sucrose synthase leads to a handicapped nitrogen fixation mirrored by specific alterations in the symbiotic transcriptome and metabolome. Plant Physiology **145:** 1600-1618

Ball K, Preiss J (1994) Allosteric sites of the large subunit of the spinach leaf adpglucose pyrophosphorylase. Journal of Biological Chemistry **269:** 24706-24711

Ball S, Guan HP, James M, Myers A, Keeling P, Mouille G, Buleon A, Colonna P, Preiss J (1996) From glycogen to amylopectin: A model for the biogenesis of the plant starch granule. Cell **86:** 349-352

Ballicora MA, Fu YB, Nesbitt NM, Preiss J (1998) ADP-Glucose pyrophosphorylase from potato tubers. Site-directed mutagenesis studies of the regulatory sites. Plant Physiology **118:** 265-274

Balmer Y, Koller A, del Val G, Manieri W, Schurmann P, Buchanan BB (2003) Proteomics gives insight into the regulatory function of chloroplast thioredoxins. Proceedings of the National Academy of Sciences of the United States of America **100:** 370-375

Battey NH, Tooke F (2002) Molecular control and variation in the floral transition. Current Opinion in Plant Biology **5:** 62-68

Baunsgaard L, Lutken H, Mikkelsen R, Glaring MA, Pham TT, Blennow A (2005) A novel isoform of glucan, water dikinase phosphorylates pre-phosphorylated alpha-glucans and is involved in starch degradation in Arabidopsis. Plant Journal **41:** 595-605

Bena G (2001) Molecular phylogeny supports the morphologically based taxonomic transfer of the "medicagoid" Trigonella species to the genus *Medicago* L. Plant Systematics and Evolution **229:** 217-236

Benedito VA, Torres-Jerez I, Murray JD, Andriankaja A, Allen S, Kakar K, Wandrey M, Verdier J, Zuber H, Ott T, Moreau S, Niebel A, Frickey T, Weiller

G, He J, Dai XB, Zhao PX, Tang YH, Udvardi MK (2008) A gene expression atlas of the model legume *Medicago truncatula*. Plant Journal **55:** 504-513

Bernier G, Havelange A, Houssa C, Petitjean A, Lejeune P (1993) Physiological signals that induce flowering. Plant Cell **5:** 1147-1155

Bhattacharyya MK, Smith AM, Ellis THN, Hedley C, Martin C (1990) The wrinkled-seed character of pea described by mendel is caused by a transposon-like insertion in a gene encoding starch-branching enzyme. Cell **60:** 115-122

Bird AR, Brown IL, Topping DL (2000) Starches, resistant starches, the gut microflora and human health. Curr Issues Intest Microbiol **1:** 25-37

Blasing OE, Gibon Y, Gunther M, Hohne M, Morcuende R, Osuna D, Thimm O, Usadel B, Scheible WR, Stitt M (2005) Sugars and circadian regulation make major contributions to the global regulation of diurnal gene expression in Arabidopsis. Plant Cell **17:** 3257-3281

Blauth SL, Kim KN, Klucinec J, Shannon JC, Thompson D, Guiltinan M (2002) Identification of Mutator insertional mutants of starch-branching enzyme 1 (sbe1) in *Zea mays* L. Plant Molecular Biology **48:** 287-297

Blennow A, Engelsen SB, Nielsen TH, Baunsgaard L, Mikkelsen R (2002) Starch phosphorylation: a new front line in starch research. Trends in Plant Science **7:** 445-450

Boehlein SK, Shaw JR, Stewart JD, Hannah LC (2008) Heat stability and allosteric properties of the maize endosperm ADP-glucose pyrophosphorylase are intimately intertwined. Plant Physiology **146:** 289-299

Boehlein SK, Shaw JR, Stewart JD, Hannah LC (2009) Characterization of an Autonomously Activated Plant ADP-Glucose Pyrophosphorylase. Plant Physiology **149:** 318-326

Bogracheva TY, Cairns P, Noel TR, Hulleman S, Wang TL, Morris VJ, Ring SG, Hedley CL (1999) The effect of mutant genes at the r, rb, rug3, rug4, rug5 and lam loci on the granular structure and physico-chemical properties of pea seed starch. Carbohydrate Polymers **39:** 303-314

Borisjuk L, Rolletschek H, Radchuk R, Weschke W, Wobus U, Weber H (2004) Seed development and differentiation: A role for metabolic regulation. Plant Biology **6:** 375-386

Borisjuk L, Rolletschek H, Walenta S, Panitz R, Wobus U, Weber H (2003) Energy status and its control on embryogenesis of legumes: ATP distribution within *Vicia faba* embryos is developmentally regulated and correlated with photosynthetic capacity. Plant Journal **36:** 318-329

Borovsky D, Smith EE, Whelan WJ (1975) Mechanism of branching enzyme action and its influence on structure of amylopectin. Biochemical Society Transactions **3:** 48-49

Boyce PJ, Volenec JJ (1992) Taproot carbohydrate concentrations and stress tolerance of contrasting alfalfa genotypes. Crop Science **32:** 757-761

Bradford MM (1976) Rapid and sensitive method for quantitation of microgram quantities of protein utilizing principle of protein-dye binding. Analytical Biochemistry **72:** 248-254

Brand K, Dugi KA, Brunzell JD, Nevin DN, SantamarinaFojo S (1996) A novel A->G mutation in intron I of the hepatic lipase gene leads to alternative splicing resulting in enzyme deficiency. Journal of Lipid Research **37:** 1213-1223

Brewin NJ (1991) Development of the legume root nodule. Annual Review of Cell Biology **7:** 191-226

Broughto.Wj, Dilworth MJ (1971) Control of leghaemoglobin synthesis in snake beans. Biochemical Journal **125:** 1075-&

Brown RA, Rosenberg NJ, Hays CJ, Easterling WE, Mearns LO (2000) Potential production and environmental effects of switchgrass and traditional crops under current and greenhouse-altered climate in the central United States: a simulation study. Agriculture Ecosystems & Environment **78:** 31-47

Buchanan BB, Balmer Y (2005) Redox regulation: A broadening horizon. Annual Review of Plant Biology **56:** 187-220

Burge C, Karlin S (1997) Prediction of complete gene structures in human genomic DNA. Journal of Molecular Biology **268:** 78-94

Burge CB (1998) Modeling dependencies in pre-mRNA splicing signals. Computational Methods in Molecular Biology **32:** 129-164

Burton RA, Bewley JD, Smith AM, Bhattacharyya MK, Tatge H, Ring S, Bull V, Hamilton WDO, Martin C (1995) Starch branching enzymes belonging to distinct enzyme families are differentially expressed during pea embryo development. Plant Journal **7:** 3-15

Bustos R, Fahy B, Hylton CM, Seale R, Nebane NM, Edwards A, Martin C, Smith AM (2004) Starch granule initiation is controlled by a heteromultimeric isoamylase in potato tubers. Proceedings of the National Academy of Sciences of the United States of America **101:** 2215-2220

Calenge F, Saliba-Colombani V, Mahieu S, Loudet O, Daniel-Vedele F, Krapp A (2006) Natural variation for carbohydrate content in Arabidopsis. Interaction with complex traits dissected by quantitative genetics. Plant Physiology **141:** 1630-1643

Cannon SB, Sterck L, Rombauts S, Sato S, Cheung F, Gouzy J, Wang XH, Mudge J, Vasdewani J, Scheix T, Spannagl M, Monaghan E, Nicholson C, Humphray SJ,

Schoof H, Mayer KFX, Rogers J, Quetier F, Oldroyd GE, Debelle F, Cook DR, Retzel EF, Roe BA, Town CD, Tabata S, Van de Peer Y, Young ND (2006) Legume genome evolution viewed through the *Medicago truncatula* and *Lotus japonicus* genomes. Proceedings of the National Academy of Sciences of the United States of America **103:** 14959-14964

Carlini DB, Stephan W (2003) *In vivo* introduction of unpreferred synonymous codons into the Drosophila Adh gene results in reduced levels of ADH protein. Genetics **163:** 239-243

Caspar T, Huber SC, Somerville C (1985) Alterations in growth, photosynthesis, and respiration in a starchless mutant of *Arabidopsis thaliana* (L) deficient in chloroplast phosphoglucomutase activity. Plant Physiology **79:** 11-17

Caspar T, Lin TP, Kakefuda G, Benbow L, Preiss J, Somerville C (1991) Mutants of arabidopsis with altered regulation of starch degradation. Plant Physiology **95:** 1181-1188

Cassman KG, Dobermann A, Walters DT, Yang H (2003) Meeting cereal demand while protecting natural resources and improving environmental quality. Annual Review of Environment and Resources **28:** 315-358

Chamary JV, Hurst LD (2005) Evidence for selection on synonymous mutations affecting stability of mRNA secondary structure in mammals. Genome Biology **6**

Chang YF, Chan WK, Imam JS, Wilkinson MF (2007) Alternatively spliced T-cell receptor transcripts are up-regulated in response to disruption of either splicing elements or reading frame. Journal of Biological Chemistry **282:** 29738-29747

Chapman GW, Mendicin.J, Pallas JE (1972) Hydrolysis of maltodextrins by a beta-amylase isolated from leaves of vicia-faba. Biochimica Et Biophysica Acta **276:** 491-&

Chatterton NJ, Silvius JE (1981) Photosynthate partitioning into starch in soybean leaves. Irradiance level and daily photosynthetic period duration effects. Plant Physiology **67:** 257-260

Chen BY, Janes HW, Gianfagna T (1998) PCR cloning and characterization of multiple ADP-glucose pyrophosphorylase cDNAs from tomato. Plant Science **136:** 59-67

Chen BY, Wang Y, Janes HW (1998) ADP-glucose pyrophosphorylase is localized to both the cytoplasm and plastids in developing pericarp of tomato fruit. Plant Physiology **116:** 101-106

Chen X, Salamini F, Gebhardt C (2001) A potato molecular-function map for carbohydrate metabolism and transport. Theoretical and Applied Genetics **102:** 284-295

Chia T, Thorneycroft D, Chapple A, Messerli G, Chen J, Zeeman SC, Smith SM, Smith AM (2004) A cytosolic glucosyltransferase is required for conversion of starch to sucrose in Arabidopsis leaves at night. Plant Journal **37:** 853-863

Chinnasamy G, Bal AK (2003) Seasonal changes in carbohydrates of perennial root nodules of beach pea. Journal of Plant Physiology **160:** 1185-1192

Chourey PS, Taliercio EW, Carlson SJ, Ruan YL (1998) Genetic evidence that the two isozymes of sucrose synthase present in developing maize endosperm are critical, one for cell wall integrity and the other for starch biosynthesis. Molecular and General Genetics **259:** 88-96

Clauss MJ, Koch MA (2006) Poorly known relatives of *Arabidopsis thaliana*. Trends in Plant Science **11:** 449-459

Colbert T, Till BJ, Tompa R, Reynolds S, Steine MN, Yeung AT, McCallum CM, Comai L, Henikoff S (2001) High-throughput screening for induced point mutations. Plant Physiology **126:** 480-484

Colebatch G, Desbrosses G, Ott T, Krusell L, Montanari O, Kloska S, Kopka J, Udvardi MK (2004) Global changes in transcription orchestrate metabolic differentiation during symbiotic nitrogen fixation in *Lotus japonicus*. Plant Journal **39:** 487-512

Colebatch G, Kloska S, Trevaskis B, Freund S, Altmann T, Udvardi MK (2002) Novel aspects of symbiotic nitrogen fixation uncovered by transcript profiling with cDNA arrays. Molecular Plant-Microbe Interactions **15:** 411-420

Comai L, Henikoff S (2006) TILLING: practical single-nucleotide mutation discovery. Plant Journal **45:** 684-694

Commuri PD, Keeling PL (2001) Chain-length specificities of maize starch synthase I enzyme: studies of glucan affinity and catalytic properties. Plant Journal **25:** 475-486

Comparot-Moss S, Denyer K (2009) The evolution of the starch biosynthetic pathway in cereals and other grasses. Journal of Experimental Botany **60:** 2481-2492

Comparot-Moss S, Kotting O, Stettler M, Edner C, Graf A, Weise SE, Streb S, Lue WL, MacLean D, Mahlow S, Ritte G, Steup M, Chen J, Zeeman SC, Smith AM (2010) A Putative Phosphatase, LSF1, Is Required for Normal Starch Turnover in Arabidopsis Leaves. Plant Physiology **152:** 685-697

Cooper JL, Till BJ, Laport RG, Darlow MC, Kleffner JM, Jamai A, El-Mellouki T, Liu S, Ritchie R, Nielsen N, Bilyeu KD, Meksem K, Comai L, Henikoff S (2008) TILLING to detect induced mutations in soybean. BMC Plant Biology **8:** Article No.: 9

Corbesier L, Lejeune P, Bernier G (1998) The role of carbohydrates in the induction of flowering in *Arabidopsis thaliana*: comparison between the wild type and a starchless mutant. Planta **206:** 131-137

Coruzzi G, Bush DR (2001) Nitrogen and carbon nutrient and metabolite signaling in plants. Plant Physiology **125:** 61-64

Coruzzi GM, Zhou L (2001) Carbon and nitrogen sensing and signaling in plants: emerging 'matrix effects'. Current Opinion in Plant Biology **4:** 247-253

Cox TS, Bender M, Picone C, Van Tassel DL, Holland JB, Brummer EC, Zoeller BE, Paterson AH, Jackson W (2002) Breeding perennial grain crops. Critical Reviews in Plant Sciences **21:** 59-91

Cox TS, Glover JD, Van Tassel DL, Cox CM, DeHaan LR (2006) Prospects for developing perennial-grain crops. Bioscience **56:** 649-659

Craig J, Barratt P, Tatge H, Dejardin A, Handley L, Gardner CD, Barber L, Wang T, Hedley C, Martin C, Smith AM (1999) Mutations at the rug4 locus alter the carbon and nitrogen metabolism of pea plants through an effect on sucrose synthase. Plant Journal **17:** 353-362

Crevillen P, Ballicora MA, Merida A, Preiss J, Romero JM (2003) The different large subunit isoforms of *Arabidopsis thaliana* ADP-glucose pyrophosphorylase confer distinct kinetic and regulatory properties to the heterotetrameric enzyme. Journal of Biological Chemistry **278:** 28508-28515

Crevillen P, Ventriglia T, Pinto F, Orea A, Merida A, Romero JM (2005) Differential pattern of expression and sugar regulation of Arabidopsis thaliana ADP-glucose pyrophosphorylase-encoding genes. Journal of Biological Chemistry **280:** 8143-8149

Critchley JH, Zeeman SC, Takaha T, Smith AM, Smith SM (2001) A critical role for disproportionating enzyme in starch breakdown is revealed by a knock-out mutation in Arabidopsis. Plant Journal **26:** 89-100

Cross JM, Clancy M, Shaw JR, Boehlein SK, Greene TW, Schmidt RR, Okita TW, Hannah LC (2005) A polymorphic motif in the small subunit of ADP-glucose pyrophosphorylase modulates interactions between the small and large subunits. Plant Journal **41:** 501-511

Cross JM, von Korff M, Altmann T, Bartzetko L, Sulpice R, Gibon Y, Palacios N, Stitt M (2006) Variation of enzyme activities and metabolite levels in 24 arabidopsis accessions growing in carbon-limited conditions. Plant Physiology **142:** 1574-1588

Dalmais M, Schmidt J, Le Signor C, Moussy F, Burstin J, Savois V, Aubert G, Brunaud V, de Oliveira Y, Guichard C, Thompson R, Bendahmane A (2008)

UTILLdb, a *Pisum sativum in silico* forward and reverse genetics tool. Genome Biology **9**

Dam S, Laursen BS, Ornfelt JH, Jochimsen B, Staerfeldt HH, Friis C, Nielsen K, Goffard N, Besenbacher S, Krusell L, Sato S, Tabata S, Thogersen IB, Enghild JJ, Stougaard J (2009) The Proteome of Seed Development in the Model Legume *Lotus japonicus*. Plant Physiology **149:** 1325-1340

De Souza JG, Da Silva JV (1987) Partitioning of carbohydrates in annual and perennial cotton *Gossypium hirsutum* L. Journal of Experimental Botany **38:** 1211-1218

Degtjareva GV, Kramina TE, Sokoloff DD, Samigullin TH, Valiejo-Roman CM, Antonov AS (2006) Phylogeny of the genus Lotus (Leguminosae, Loteae): evidence from nrITS sequences and morphology. Canadian Journal of Botany-Revue Canadienne De Botanique **84:** 813-830

Dejardin A, Rochat C, Wuilleme S, Boutin JP (1997) Contribution of sucrose synthase, ADP-glucose pyrophosphorylase and starch synthase to starch synthesis in developing pea seeds. Plant Cell and Environment **20:** 1421-1430

Delatte T, Trevisan M, Parker ML, Zeeman SC (2005) Arabidopsis mutants Atisa1 and Atisa2 have identical phenotypes and lack the same multimeric isoamylase, which influences the branch point distribution of amylopectin during starch synthesis. Plant Journal **41:** 815-830

Delatte T, Trevisan M, Parker ML, Zeeman SC (2006) Arabidopsis mutants Atisa1 and Atisa2 have identical phenotypes and lack the same multimeric isoamylase, which influences the branch point distribution of amylopectin during starch synthesis. (vol 41, pg 815, 2005). Plant Journal **45:** 870-870

Delatte T, Umhang M, Trevisan M, Eicke S, Thorneycroft D, Smith SM, Zeeman SC (2006) Evidence for distinct mechanisms of starch granule breakdown in plants. Journal of Biological Chemistry **281:** 12050-12059

Delvalle D, Dumez S, Wattebled F, Roldan I, Planchot V, Berbezy P, Colonna P, Vyas D, Chatterjee M, Ball S, Merida A, D'Hulst C (2005) Soluble starch synthase I: a major determinant for the synthesis of amylopectin in Arabidopsis thaliana leaves. Plant Journal **43:** 398-412

Denyer K, Barber LM, Edwards EA, Smith AM, Wang TL (1997) Two isoforms of the GBSSI class of granule-bound starch synthase are differentially expressed in the pea plant (*Pisum sativum* L.). Plant Cell and Environment **20:** 1566-1572

Denyer K, Clarke B, Hylton C, Tatge H, Smith AM (1996) The elongation of amylose and amylopectin chains in isolated starch granules. Plant Journal **10:** 1135-1143

Denyer K, Dunlap F, Thorbjornsen T, Keeling P, Smith AM (1996) The major form of ADP-glucose pyrophosphorylase in maize endosperm is extra-plastidial. Plant Physiology **112:** 779-785

Desbrosses GG, Kopka J, Udvardi MK (2005) *Lotus japonicus* metabolic profiling. Development of gas chromatography-mass spectrometry resources for the study of plant-microbe interactions. Plant Physiology **137:** 1302-1318

Deschamps P, Colleoni C, Nakamura Y, Suzuki E, Putaux JL, Buleon A, Haebel S, Ritte G, Steup M, Falcon LI, Moreira D, Loffelhardt W, Raj JN, Plancke C, d'Hulst C, Dauvillee D, Ball S (2008) Metabolic symbiosis and the birth of the plant kingdom. Molecular Biology and Evolution **25:** 536-548

Deschamps P, Moreau H, Worden AZ, Dauvillee D, Ball SG (2008) Early gene duplication within chloroplastida and its correspondence with relocation of starch metabolism to chloroplasts. Genetics **178:** 2373-2387

Dhont C, Castonguay Y, Nadeau P, Belanger G, Chalifour FP (2002) Alfalfa root carbohydrates and regrowth potential in response to fall harvests. Crop Science **42:** 754-765

Dhont C, Castonguay Y, Nadeau P, Belanger G, Drapeau R, Laberge S, Avice JC, Chalifour FP (2006) Nitrogen reserves, spring regrowth and winter survival of field-grown alfalfa (*Medicago sativa*) defoliated in the autumn. Annals of Botany **97:** 109-120

Dickinso.Db, Preiss J (1969) ADP glucose pyrophosphorylase from maize endosperm. Archives of Biochemistry and Biophysics **130:** 119-&

Dixon RA, Sumner LW (2003) Legume natural products: Understanding and manipulating complex pathways for human and animal health. Plant Physiology **131:** 878-885

Djemel N, Guedon D, Lechevalier A, Salon C, Miquel M, Prosperi JM, Rochat C, Boutin JP (2005) Development and composition of the seeds of nine genotypes of the Medicago truncatula species complex. Plant Physiology and Biochemistry **43:** 557-566

Domoney C, Duc G, Ellis THN, Ferrandiz C, Firnhaber C, Gallardo K, Hofer J, Kopka J, Kuster H, Madueno F, Munier-Jolain NG, Mayer K, Thompson R, Udvardi M, Salon C (2006) Genetic and genomic analysis of legume flowers and seeds. Current Opinion in Plant Biology **9:** 133-141

Dong ZC, Zhao Z, Liu CW, Luo JH, Yang J, Huang WH, Hu XH, Wang TL, Luo D (2005) Floral patterning in *Lotus japonicus*. Plant Physiology **137:** 1272-1282

Doyle EA, Lane AM, Sides JM, Mudgett MB, Monroe JD (2007) An alpha-amylase (At4g25000) in Arabidopsis leaves is secreted and induced by biotic and abiotic stress. Plant Cell and Environment **30:** 388-398

Doyle JJ, Luckow MA (2003) The rest of the iceberg. Legume diversity and evolution in a phylogenetic context. Plant Physiology **131:** 900-910

Dumez S, Wattebled F, Dauvillee D, Delvalle D, Planchot V, Ball SG, D'Hulst C (2006) Mutants of Arabidopsis lacking starch branching enzyme II substitute plastidial starch synthesis by cytoplasmic maltose accumulation. Plant Cell **18:** 2694-2709

Edner C, Li J, Albrecht T, Mahlow S, Hejazi M, Hussain H, Kaplan F, Guy C, Smith SM, Steup M, Ritte G (2007) Glucan, water dikinase activity stimulates breakdown of starch granules by plastidial beta-amylases. Plant Physiology **145:** 17-28

Edwards A, Borthakur A, Bornemann S, Venail L, Denyer K, Waite D, Fulton D, Smith A, Martin C (1999) Specificity of starch synthase isoforms from potato. European Journal of Biochemistry **266:** 724-736

Edwards A, Vincken JP, Suurs LCJM, Visser RGF, Zeeman S, and Smith A, Martin C (2002) Discrete forms of amylose are synthesized by isoforms of GBSSI in pea. The Plant Cell **14:** 1767-1785

Edwards J, ap Rees T (1986) Sucrose partitioning in developing embryos of round and wrinkled varieties of pisum-sativum. Phytochemistry **25:** 2027-2032

Egli DB, Leggett JE, Cheniae A (1980) Carbohydrate-levels in soybean leaves during reproductive growth. Crop Science **20:** 468-473

Eimert K, Wang SM, Lue WL, Chen JC (1995) Monogenic recessive mutations causing both late floral initiation and excess starch accumulation in Arabidopsis. Plant Cell **7:** 1703-1712

El-Lithy ME, Clerkx EJM, Ruys GJ, Koornneef M, Vreugdenhil D (2004) Quantitative trait locus analysis of growth-related traits in a new Arabidopsis recombinant. Plant Physiology **135:** 444-458

El-Lithy ME, Rodrigues GC, van Rensen JJS, Snel JFH, Dassen H, Koornneef M, Jansen MAK, Aarts MGM, Vreugdenhil D (2005) Altered photosynthetic performance of a natural Arabidopsis accession is associated with atrazine resistance. Journal of Experimental Botany **56:** 1625-1634

Emmanuel E, Yehuda E, Melamed-Bessudo C, Avivi-Ragolsky N, Levy AA (2006) The role of AtMSH2 in homologous recombination in *Arabidopsis thaliana*. Embo Reports **7:** 100-105

Fankhauser JJ, Volenec JJ (1989) Root vs shoot effects on herbage regrowth and carbohydrate-metabolism of alfalfa. Crop Science **29:** 735-740

Farrar JF, Williams ML (1991) The effects of increased atmospheric carbon-dioxide and temperature on carbon partitioning, source-sink relations and respiration. Plant Cell and Environment **14:** 819-830

Fettke J, Hejazi M, Smirnova J, Hochel E, Stage M, Steup M (2009) Eukaryotic starch degradation: integration of plastidial and cytosolic pathways. Journal of Experimental Botany **60:** 2907-2922

Fettke J, Malinova I, Eckermann N, Steup M (2009) Cytosolic heteroglycans in photoautotrophic and in heterotrophic plant cells. Phytochemistry **70:** 696-702

Finan TM, Wood JM, Jordan DC (1983) Symbiotic properties of C4-dicarboxylic acid transport mutants of *Rhizobium leguminosarum*. Journal of Bacteriology **154:** 1403-1413

Fincher GB (1989) Molecular and cellular biology associated with endosperm mobilization in germinating cereal grains. Annual Review of Plant Physiology and Plant Molecular Biology **40:** 305-346

Force A, Lynch M, Pickett FB, Amores A, Yan YL, Postlethwait J (1999) Preservation of duplicate genes by complementary, degenerative mutations. Genetics **151:** 1531-1545

Fordham-Skelton AP, Chilley P, Lumbreras V, Reignoux S, Fenton TR, Dahm CC, Pages M, Gatehouse JA (2002) A novel higher plant protein tyrosine phosphatase interacts with SNF1-related protein kinases via a KIS (kinase interaction sequence) domain. Plant Journal **29:** 705-715

Franchi GG, Bellani L, Nepi M, Pacini E (1996) Types of carbohydrate reserves in pollen: Localization, systematic distribution and ecophysiological significance. Flora **191:** 143-159

Fritzius T, Aeschbacher R, Wiemken A, Wingler A (2001) Induction of *ApL3* expression by trehalose complements the starch-deficient Arabidopsis mutant *adg2-1* lacking ApL1, the large subunit of ADP-glucose pyrophosphorylase. Plant Physiology **126:** 883-889

Frugoli J, Harris J (2001) Medicago truncatula on the move! Plant Cell **13:** 458-463

Fujita N, Taira T (1998) A 56 kDa protein is a novel granule-bound starch synthase existing in the pericarps, aleurone layers, and embryos of immature seed in diploid wheat (*Triticum monococcum* L.). Planta **207:** 125-132

Fulton DC, Stettler M, Mettler T, Vaughan CK, Li J, Francisco P, Gil D, Reinhold H, Eicke S, Messerli G, Dorken G, Halliday K, Smith AM, Smith SM, Zeeman SC (2008) beta-AMYLASE4, a noncatalytic protein required for starch breakdown, acts upstream of three active beta-amylases in Arabidopsis chloroplasts. Plant Cell **20:** 1040-1058

Gallardo K, Le Signor C, Vandekerckhove J, Thompson RD, Burstin J (2003) Proteomics of *Medicago truncatula* seed development establishes the time frame of diverse metabolic processes related to reserve accumulation. Plant Physiology **133:** 664-682

Gallardo K, Thompson R, Burstin J (2008) Reserve accumulation in legume seeds. Comptes Rendus Biologies **331:** 755-762

Galvez L, Gonzalez EM, Arrese-Igor C (2005) Evidence for carbon flux shortage and strong carbon/nitrogen interactions in pea nodules at early stages of water stress. Journal of Experimental Botany **56:** 2551-2561

Garnier E, Laurent G (1994) Leaf anatomy, specific mass and water-content in congeneric annual and perennial grass species. New Phytologist **128:** 725-736

Geigenberger P, Kolbe A, Tiessen A (2005) Redox regulation of carbon storage and partitioning in response to light and sugars. Journal of Experimental Botany **56:** 1469-1479

Gentry MS, Dowen RH, Worby CA, Mattoo S, Ecker JR, Dixon JE (2006) An Unexpected Link between Neuronal Degeneration in Lafora Disease Patients and Starch Metabolism in Unicellular Eukaryotes and Kingdom Plantae. Molecular Biology of the Cell **17**

Gentry MS, Dowen RH, Worby CA, Mattoo S, Ecker JR, Dixon JE (2007) The phosphatase laforin crosses evolutionary boundaries and links carbohydrate metabolism to neuronal disease. Journal of Cell Biology **178:** 477-488

Georgelis N, Braun EL, Hannah LC (2008) Duplications and functional divergence of ADP-glucose pyrophosphorylase genes in plants. Bmc Evolutionary Biology **8**

Georgelis N, Braun EL, Shaw JR, Hannah LC (2007) The two AGPase subunits evolve at different rates in angiosperms, yet they are equally sensitive to activity-altering amino acid changes when expressed in bacteria. Plant Cell **19:** 1458-1472

Georgelis N, Shaw JR, Hannah LC (2009) Phylogenetic Analysis of ADP-Glucose Pyrophosphorylase Subunits Reveals a Role of Subunit Interfaces in the Allosteric Properties of the Enzyme. Plant Physiology **151:** 67-77

Gepts P, Beavis WD, Brummer EC, Shoemaker RC, Stalker HT, Weeden NF, Young ND (2005) Legumes as a model plant family. Genomics for food and feed report of the cross-legume advances through genomics conference. Plant Physiology **137:** 1228-1235

Ghosh HP, Preiss J (1966) Adenosine diphosphate glucose pyrophosphorylase - a regulatory enzyme in biosynthesis of starch in spinach leaf chloroplasts. Journal of Biological Chemistry **241:** 4491-&

Gibon Y, Blasing OE, Palacios-Rojas N, Pankovic D, Hendriks JHM, Fisahn J, Hohne M, Gunther M, Stitt M (2004) Adjustment of diurnal starch turnover to short days: depletion of sugar during the night leads to a temporary inhibition of carbohydrate utilization, accumulation of sugars and post-translational activation of ADP-glucose pyrophosphorylase in the following light period. Plant Journal **39:** 847-862

Gibon Y, Usadel B, Blaesing OE, Kamlage B, Hoehne M, Trethewey R, Stitt M (2006) Integration of metabolite with transcript and enzyme activity profiling during diurnal cycles in Arabidopsis rosettes. Genome Biology **7**

Gibson SI (2005) Control of plant development and gene expression by sugar signaling. Current Opinion in Plant Biology **8:** 93-102

Giroux MJ, Hannah LC (1994) ADP-glucose pyrophosphorylase in shrunken-2 and brittle-2 mutants of maize. Molecular & General Genetics **243:** 400-408

Giroux MJ, Shaw J, Barry G, Cobb BG, Greene T, Okita T, Hannah LC (1996) A single gene mutation that increases maize seed weight. Proceedings of the National Academy of Sciences of the United States of America **93:** 5824-5829

Glaring MA, Zygadlo A, Thorneycroft D, Schulz A, Smith SM, Blennow A, Baunsgaard L (2007) An extra-plastidial alpha-glucan, water dikinase from Arabidopsis phosphorylates amylopectin in vitro and is not necessary for transient starch degradation. Journal of Experimental Botany **58:** 3949-3960

Glover JD (2005) The necessity and possibility of perennial grain production systems. Renewable Agriculture and Food Systems **20:** 1-2

Glover JD, Cox CM, Reganold JP (2007) Future farming: A return to roots? Scientific American **297:** 82-89

Golombek S, Rolletschek H, Wobus U, Weber H (2001) Control of storage protein accumulation during legume seed development. Journal of Plant Physiology **158:** 457-464

Gondo T, Sato S, Okumura K, Tabata S, Akashi R, Isobe S (2007) Quantitative trait locus analysis of multiple agronomic traits in the model legume *Lotus japonicus*. Genome **50:** 627-637

Gong JM, Waner DA, Horie T, Li SL, Horie R, Abid KB, Schroeder JI (2004) Microarray-based rapid cloning of an ion accumulation deletion mutant in *Arabidopsis thaliana*. Proceedings of the National Academy of Sciences of the United States of America **101:** 15404-15409

Gonzalez EM, Gordon AJ, James CL, Arreseigor C (1995) The role of sucrose synthase in the response of soybean nodules to drought. Journal of Experimental Botany **46:** 1515-1523

Gordon AJ (1992) Carbon metabolism in the legume nodule. Carbon Partitioning : within and between Organisms**:** 133-162

Gordon AJ, James CL (1997) Enzymes of carbohydrate and amino acid metabolism in developing and mature nodules of white clover. Journal of Experimental Botany **48:** 895-903

Gordon AJ, Minchin FR, James CL, Komina O (1999) Sucrose synthase in legume nodules is essential for nitrogen fixation. Plant Physiology **120:** 867-877

Gordon AJ, Minchin FR, Skot L, James CL (1997) Stress-induced declines in soybean N-2 fixation are related to nodule sucrose synthase activity. Plant Physiology **114:** 937-946

Gordon AJ, Mitchell DF, Ryle GJA, Powell CE (1987) Diurnal production and utilization of photosynthate in nodulated white clover. Journal of Experimental Botany **38:** 84-98

Gordon AJ, Ryle GJA, Mitchell DF, Lowry KH, Powell CE (1986) The effect of defoliation on carbohydrate, protein and leghemoglobin content of white clover nodules. Annals of Botany **58:** 141-154

Gordon AJ, Thomas BJ, James CL (1995) The location of sucrose synthase in root-nodules of white clover. New Phytologist **130:** 523-530

Graf A, Schlereth A, Stitt M, Smith AM (2010) Circadian control of carbohydrate availability for growth in Arabidopsis plants at night. Proceedings of the National Academy of Sciences of the United States of America **107:** 9458-9463

Graham PH, Vance CP (2003) Legumes: Importance and constraints to greater use. Plant Physiology **131:** 872-877

Greene EA, Codomo CA, Taylor NE, Henikoff JG, Till BJ, Reynolds SH, Enns LC, Burtner C, Johnson JE, Odden AR, Comai L, Henikoff S (2003) Spectrum of chemically induced mutations from a large-scale reverse-genetic screen in arabidopsis. Genetics **164:** 731-740

Greene TW, Hannah LC (1998) Adenosine diphosphate glucose pyrophosphorylase, a rate-limiting step in starch biosynthesis. Physiologia Plantarum **103:** 574-580

Greene TW, Kavakli IH, Kahn ML, Okita TW (1998) Generation of up-regulated allosteric variants of potato ADP-glucose pyrophosphorylase by reversion genetics. Proceedings of the National Academy of Sciences of the United States of America **95:** 10322-10327

Grime JP, Hunt R (1975) Relative growth-rate - its range and adaptive significance in a local flora. Journal of Ecology **63:** 393-422

Guan HP, Preiss J (1993) Differentiation of the properties of the branching isozymes from maize (*Zea-mays*). Plant Physiology **102:** 1269-1273

Hajirezaei MR, Bornke F, Peisker M, Takahata Y, Lerchl J, Kirakosyan A, Sonnewald U (2003) Decreased sucrose content triggers starch breakdown and respiration in stored potato tubers (*Solanum tuberosum*). Journal of Experimental Botany **54:** 477-488

Han Y, Sun FJ, Rosales-Mendoza S, Korban SS (2007) Three orthologs in rice, Arabidopsis, and Populus encoding starch branching enzymes (SBEs) are different from other SBE gene families in plants. Gene **401:** 123-130

Handberg K, Stougaard J (1992*) Lotus japonicus*, an autogamous, diploid legume species for classical and molecular-genetics. Plant Journal **2:** 487-496

Handford MG, Carr JP (2007) A defect in carbohydrate metabolism ameliorates symptom severity in virus-infected *Arabidopsis thaliana*. Journal of General Virology **88:** 337-341

Hansen PI, Spraul M, Dvortsak P, Larsen FH, Blennow A, Motawia MS, Engelsen SB (2009) Starch Phosphorylation-Maltosidic Restrains upon 3 '- and 6 '-Phosphorylation Investigated by Chemical Synthesis, Molecular Dynamics and NMR Spectroscopy. Biopolymers **91:** 179-193

Hanson KR, McHale NA (1988) A starchless mutant of nicotiana-sylvestris containing a modified plastid phosphoglucomutase. Plant Physiology **88:** 838-844

Harmer SL, Hogenesch LB, Straume M, Chang HS, Han B, Zhu T, Wang X, Kreps JA, Kay SA (2000) Orchestrated transcription of key pathways in Arabidopsis by the circadian clock. Science **290:** 2110-2113

Harrison CJ (1996) The rug3 locus of pea. PhD thesis, University of East Anglia, Norwich

Harrison CJ, Hedley CL, Wang TL (1998) Evidence that the rug3 locus of pea (*Pisum sativum* L.) encodes plastidial phosphoglucomutase confirms that the imported substrate for starch synthesis in pea amyloplasts is glucose-6-phosphate. Plant Journal **13:** 753-762

Harrison CJ, Mould RM, Leech MJ, Johnson SA, Turner L, Schreck SL, Baird KM, Jack PL, Rawsthorne S, Hedley CL, Wang TL (2000) The rug3 locus of pea encodes plastidial phosphoglucomutase. Plant Physiology **122:** 1187-1192

Harrison J, Jamet A, Muglia CI, Van de Sype G, Aguilar OM, Puppo A, Frendo P (2005) Glutathione plays a fundamental role in growth and symbiotic capacity of *Sinorhizobium meliloti.* Journal of Bacteriology **187:** 168-174

Hayashi M, Miyahara A, Sato S, Kato T, Yoshikawa M, Taketa M, Pedrosa A, Onda R, Imaizumi-Anraku H, Bachmair A, Sandal N, Stougaard J, Murooka Y, Tabata S, Kawasaki S, Kawaguchi M, Harada K (2001) Construction of a genetic

linkage map of the model legume *Lotus japonicus* using an intraspecific F2 population. DNA Research **8:** 301-310

Hendriks JHM, Kolbe A, Gibon Y, Stitt M, Geigenberger P (2003) ADP-glucose pyrophosphorylase is activated by posttranslational redox-modification in response to light and to sugars in leaves of Arabidopsis and other plant species. Plant Physiology **133:** 838-849

Henikoff S, Till BJ, Comai L (2004) TILLING. Traditional mutagenesis meets functional genomics. Plant Physiology **135:** 630-636

Herbers K, Takahata Y, Melzer M, Mock HP, Hajirezaei M, Sonnewald U (2000) Regulation of carbohydrate partitioning during the interaction of potato virus Y with tobacco. Molecular Plant Pathology **1:** 51-59

Hirose T, Ohdan T, Nakamura Y, Terao T (2006) Expression profiling of genes related to starch synthesis in rice leaf sheaths during the heading period. Physiologia Plantarum **128:** 425-435

Hofer J, Turner L, Moreau C, Ambrose M, Isaac P, Butcher S, Weller J, Dupin A, Dalmais M, Le Signor C, Bendahmane A, Ellis N (2009) Tendril-less Regulates Tendril Formation in Pea Leaves. Plant Cell **21:** 420-428

Hoffmann WA, Poorter H (2002) Avoiding bias in calculations of relative growth rate. Annals of Botany **90:** 37-42

Horst I, Welham T, Kelly S, Kaneko T, Sato S, Tabata S, Parniske M, Wang TL (2007) TILLING mutants of *Lotus japonicus* reveal that nitrogen assimilation and fixation can occur in the absence of nodule-enhanced sucrose synthase. Plant Physiology **144:** 806-820

Hossain MS, Umehara Y, Kouchi H (2006) A novel Fix(-) symbiotic mutant of *Lotus japonicus*, Ljsym105, shows impaired development and premature deterioration of nodule infected cells and symbiosomes. Molecular Plant-Microbe Interactions **19:** 780-788

Hu FY, Tao DY, Sacks E, Fu BY, Xu P, Li J, Yang Y, McNally K, Khush GS, Paterson AH, Li ZK (2003) Convergent evolution of perenniality in rice and sorghum. Proceedings of the National Academy of Sciences of the United States of America **100:** 4050-4054

Huang XH, Feng Q, Qian Q, Zhao Q, Wang L, Wang AH, Guan JP, Fan DL, Weng QJ, Huang T, Dong GJ, Sang T, Han B (2009) High-throughput genotyping by whole-genome resequencing. Genome Research **19:** 1068-1076

Huber SC, Hanson KR (1992) Carbon partitioning and growth of a starchless mutant of *Nicotiana sylvestris*. Plant Physiology **99:** 1449-1454

Hughes RK, Desforges N, Selwood C, Smith R, Speirs I, Sinnaeve G, Gorton PG, Wiseman J, Jumel K, Harding SE, Hill SE, Street V, Wang TL, Hedley CL (2001) Genes affecting starch biosynthesis exert pleiotropic effects on the protein content and composition of pea seeds. Journal of the Science of Food and Agriculture **81:** 877-882

Hussain H, Mant A, Seale R, Zeeman S, Hinchliffe E, Edwards A, Hylton C, Bornemann S, Smith AM, Martin C, Bustos R (2003) Three isoforms of isoamylase contribute different catalytic properties for the debranching of potato glucans. Plant Cell **15:** 133-149

Ihemere U, Arias-Garzon D, Lawrence S, Sayre R (2006) Genetic modification of cassava for enhanced starch production. Plant Biotechnology Journal **4:** 453-465

Imaizumi-Anraku H, Takeda N, Charpentier M, Perry J, Miwa H, Umehara Y, Kouchi H, Murakami Y, Mulder L, Vickers K, Pike J, Downie JA, Wang T, Sato S, Asamizu E, Tabata S, Yoshikawa M, Murooka Y, Wu GJ, Kawaguchi M, Kawasaki S, Parniske M, Hayashi M (2005) Plastid proteins crucial for symbiotic fungal and bacterial entry into plant roots. Nature **433:** 527-531

Jander G, Norris SR, Rounsley SD, Bush DF, Levin IM, Last RL (2002) Arabidopsis map-based cloning in the post-genome era. Plant Physiology **129:** 440-450

Jenner HL, Winning BM, Millar AH, Tomlinson KL, Leaver CJ, Hill SA (2001) NAD malic enzyme and the control of carbohydrate metabolism in potato tubers. Plant Physiology **126:** 1139-1149

Jiang QY, Gresshoff PM (1997) Classical and molecular genetics of the model legume *Lotus japonicus*. Molecular Plant-Microbe Interactions **10:** 59-68

Jin XS, Ballicora MA, Preiss J, Geiger JH (2005) Crystal structure of potato tuber ADP-glucose pyrophosphorylase. Embo Journal **24:** 694-704

Jobling S (2004) Improving starch for food and industrial applications. Current Opinion in Plant Biology **7:** 210-218

Jobling SA, Schwall GP, Westcott RJ, Sidebottom CM, Debet M, Gidley MJ, Jeffcoat R, Safford R (1999) A minor form of starch branching enzyme in potato (*Solanum tuberosum* L.) tubers has a major effect on starch structure: cloning and characterisation of multiple forms of SBE A. Plant Journal **18:** 163-171

Jobling SA, Westcott RJ, Tayal A, Jeffcoat R, Schwall GP (2002) Production of a freeze-thaw-stable potato starch by antisense inhibition of three starch synthase genes. Nature Biotechnology **20:** 295-299

Jones TWA, Gottlieb LD, Pichersky E (1986) Reduced enzyme-activity and starch level in an induced mutant of chloroplast phosphoglucose isomerase. Plant Physiology **81:** 367-371

Juliano BO, Varner JE (1969) Enzymic degradation of starch granules in cotyledons of germinating peas. Plant Physiology **44:** 886-&

Kavakli IH, Greene TW, Salamone PR, Choi SB, Okita TW (2001) Investigation of subunit function in ADP-glucose pyrophosphorylase. Biochemical and Biophysical Research Communications **281:** 783-787

Kavakli IH, Kato C, Choi SB, Kim KH, Salamone PR, Ito H, Okita TW (2002) Generation, characterization, and heterologous expression of wild-type and up-regulated forms of *Arabidopsis thaliana* leaf ADP-glucose pyrophosphorylase. Planta **215:** 430-439

Kawaguchi M, Motomura T, Imaizumi-Anraku H, Akao S, Kawasaki S (2001) Providing the basis for genomics in *Lotus japonicus*: the accessions Miyakojima and Gifu are appropriate crossing partners for genetic analyses. Molecular Genetics and Genomics **266:** 157-166

Kawaguchi M, Pedrosa-Harand A, Yano K, Hayashi M, Murooka Y, Saito K, Nagata T, Namai K, Nishida H, Shibata D, Sato S, Tabata S, Harada K, Sandal N, Stougaard J, Bachmair A, Grant WF (2005) *Lotus burttii* takes a position of the third corner in the Lotus molecular genetics triangle. DNA Research **12:** 69-77

Kawasaki S, Murakami Y (2000) Genome analysis of *Lotus japonicus*. Journal of Plant Research **113:** 497-506

Keiller D, Smith H (1989) Control of carbon partitioning by light quality mediated by phytochrome. Plant Science **63:** 25-29

Kerr PS, Rufty TW, Huber SC (1985) Changes in nonstructural carbohydrates in different parts of soybean (*glycine max* L Merr) plants during a light dark cycle and in extended darkness. Plant Physiology **78:** 576-581

Kim D, Hwang SK, Okita TW (2007) Subunit interactions specify the allosteric regulatory properties of the potato tuber ADP-glucose pyrophosphorylase. Biochemical and Biophysical Research Communications **362:** 301-306

Kim IJ, Noh SJ, Lee BH, Jo J, Kim YS, Chung WI (2001) Molecular characterization of cDNA clones for ADP-glucose pyrophosphorylase from Citrus. Biochimica Et Biophysica Acta-Gene Structure and Expression **1518:** 324-328

Kim TH, Ourry A, Boucaud J, Lemaire G (1993) Partitioning of nitrogen derived from N2 fixation and reserves in nodulated *Medicago sativa* L. during regrowth. Journal of Experimental Botany **44:** 555-562

Kirchberger S, Leroch M, Huynen MA, Wahl M, Neuhaus HE, Tjaden J (2007) Molecular and biochemical analysis of the plastidic ADP-glucose transporter (ZmBT1) from *Zea mays*. Journal of Biological Chemistry **282**

Kitajima A, Asatsuma S, Okada H, Hamada Y, Kaneko K, Nanjo Y, Kawagoe Y, Toyooka K, Matsuoka K, Takeuchi M, Nakano A, Mitsui T (2009) The Rice alpha-Amylase Glycoprotein Is Targeted from the Golgi Apparatus through the Secretory Pathway to the Plastids. Plant Cell **21:** 2844-2858

Kleczkowski LA (2000) Is leaf ADP-glucose pyrophosphorylase an allosteric enzyme? Biochimica Et Biophysica Acta-Protein Structure and Molecular Enzymology **1476:** 103-108

Kleczkowski LA, Villand P, Lonneborg A, Olsen OA, Luthi E (1991) Plant ADP-glucose pyrophosphorylase - recent advances and biotechnological perspectives (a review). Zeitschrift Fur Naturforschung C-a Journal of Biosciences **46:** 605-612

Knox KJE, Clarke PJ (2005) Nutrient availability induces contrasting allocation and starch formation in resprouting and obligate seeding shrubs. Functional Ecology **19:** 690-698

Koch K (2004) Sucrose metabolism: regulatory mechanisms and pivotal roles in sugar sensing and plant development. Current Opinion in Plant Biology **7:** 235-246

Koch KE, Nolte KD, Duke ER, McCarty DR, Avigne WT (1992) Sugar levels modulate differential expression of maize sucrose synthase genes. Plant Cell **4:** 59-69

Kolbe A, Tiessen A, Schluepmann H, Paul M, Ulrich S, Geigenberger P (2005) Trehalose 6-phosphate regulates starch synthesis via posttranslational redox activation of ADP-glucose pyrophosphorylase. Proceedings of the National Academy of Sciences of the United States of America **102:** 11118-11123

Koornneef M, Alonso-Blanco C, Vreugdenhil D (2004) Naturally occurring genetic variation in *Arabidopsis thaliana*. Annual Review of Plant Biology **55:** 141-172

Kotting O, Pusch K, Tiessen A, Geigenberger P, Steup M, Ritte G (2005) Identification of a novel enzyme required for starch metabolism in Arabidopsis leaves. The phosphoglucan, water dikinase. Plant Physiology **137:** 242-252

Kotting O, Santelia D, Edner C, Eicke S, Marthaler T, Gentry MS, Comparot-Moss S, Chen J, Smith AM, Steup M, Ritte G, Zeeman SC (2009) STARCH-EXCESS4 Is a Laforin-Like Phosphoglucan Phosphatase Required for Starch Degradation in Arabidopsis thaliana. Plant Cell **21:** 334-346

Kouchi H, Yoneyama T (1984) Dynamics of carbon photosynthetically assimilated in nodulated soya bean-plants under steady-state conditions 1. Development and application of 13CO2 assimilation system at a constant 13C abundance. Annals of Botany **53:** 875-882

Kruger NJ, ap Rees T (1983) maltose metabolism by pea chloroplasts. Planta **158:** 179-184

Kuchuk N, Komarnitski I, Shakhovsky A, Gleba Y (1990) Genetic-transformation of medicago species by agrobacterium-tumefaciens and electroporation of protoplasts. Plant Cell Reports **8:** 660-663

Lacognata U, Willmitzer L, Mullerrober B (1995) Molecular cloning and characterization of novel isoforms of potato ADP-glucose pyrophosphorylase. Molecular & General Genetics **246:** 538-548

Laemmli UK, Beguin F, Gujerkel.G (1970) A factor preventing major head protein of bacteriophage T4 from random aggregation. Journal of Molecular Biology **47:** 69-&

Lammer D, Cai XW, Arterburn M, Chatelain J, Murray T, Jones S (2004) A single chromosome addition from *Thinopyrum elongatum* confers a polycarpic, perennial habit to annual wheat. Journal of Experimental Botany **55:** 1715-1720

Le BH, Wagmaister JA, Kawashima T, Bui AQ, Harada JJ, Goldberg RB (2007) Using genomics to study legume seed development. Plant Physiology **144:** 562-574

Le Signor C, Savois V, Aubert G, Verdier J, Nicolas M, Pagny G, Moussy F, Sanchez M, Baker D, Clarke J, Thompson R (2009) Optimizing TILLING populations for reverse genetics in *Medicago truncatula*. Plant Biotechnology Journal **7:** 430-441

Lee SK, Hwang SK, Han M, Eom JS, Kang HG, Han Y, Choi SB, Cho MH, Bhoo SH, An G, Hahn TR, Okita TW, Jeon JS (2007) Identification of the ADP-glucose pyrophosphorylase isoforms essential for starch synthesis in the leaf and seed endosperm of rice (*Oryza sativa* L.). Plant Molecular Biology **65:** 531-546

Leister D, Varotto C, Pesaresi P, Niwergall A, Salamini F (1999) Large-scale evaluation of plant growth in *Arabidopsis thaliana* by non-invasive image analysis. Plant Physiology and Biochemistry **37:** 671-678

Li X, Song YJ, Century K, Straight S, Ronald P, Dong XN, Lassner M, Zhang YL (2001) A fast neutron deletion mutagenesis-based reverse genetics system for plants. Plant Journal **27:** 235-242

Lin TP, Caspar T, Somerville C, Preiss J (1988) Isolation and characterization of a starchless mutant of *Arabidopsis thaliana* (L) Heynh lacking ADP-glucose pyrophosphorylase activity. Plant Physiology **86:** 1131-1135

Lin TP, Caspar T, Somerville CR, Preiss J (1988) A starch deficient mutant of *Arabidopsis thaliana* with low ADP-glucose pyrophosphorylase activity lacks one of the 2 subunits of the enzyme. Plant Physiology **88:** 1175-1181

Lin TP, Spilatro SR, Preiss J (1988) Subcellular-localization and characterization of amylases in Arabidopsis leaf. Plant Physiology **86:** 251-259

Lin Y, Ulanov AV, Lozovaya V, Widholm J, Zhang GR, Guo JH, Goodman HM (2006) Genetic and transgenic perturbations of carbon reserve production in

Arabidopsis seeds reveal metabolic interactions of biochemical pathways. Planta **225:** 153-164

Lizotte PA, Henson CA, Duke SH (1990) Purification and characterization of pea epicotyl beta-amylase. Plant Physiology **92:** 615-621

Lloyd JR, Landschutze V, Kossmann J (1999) Simultaneous antisense inhibition of two starch-synthase isoforms in potato tubers leads to accumulation of grossly modified amylopectin. Biochemical Journal **338:** 515-521

Lodwig EM, Hosie AHF, Bordes A, Findlay K, Allaway D, Karunakaran R, Downie JA, Poole PS (2003) Amino-acid cycling drives nitrogen fixation in the legume - Rhizobium symbiosis. Nature **422:** 722-726

Logendra S, Putman JD, Janes HW (1990) The influence of light period on carbon partitioning, translocation and growth in tomato. Scientia Horticulturae **42:** 75-83

Lorberth R, Ritte G, Willmitzer L, Kossmann J (1998) Inhibition of a starch-granule-bound protein leads to modified starch and repression of cold sweetening. Nature Biotechnology **16:** 473-477

Lu Y, Gehan JP, Sharkey TD (2005) Daylength and circadian effects on starch degradation and maltose metabolism. Plant Physiology **138:** 2280-2291

Lu Y, Gehan JP, Sharkey TD (2005) Daylength and circadian effects on starch degradation and maltose metabolism. Plant Physiology **138:** 2280-2291

Lu Y, Sharkey TD (2004) The role of amylomaltase in maltose metabolism in the cytosol of photosynthetic cells. Planta **218:** 466-473

Lu Y, Sharkey TD (2006) The importance of maltose in transitory starch breakdown. Plant Cell and Environment **29:** 353-366

Lu Y, Steichen JM, Yao J, Sharkey TD (2006) The role of cytosolic alpha-glucan phosphorylase in maltose metabolism and the comparison of amylomaltase in Arabidopsis and Escherichia coli. Plant Physiology **142:** 878-889

Ludewig F, Sonnewald U, Kauder F, Heineke D, Geiger M, Stitt M, Muller-Rober BT, Gillissen B, Kuhn C, Frommer WB (1998) The role of transient starch in acclimation to elevated atmospheric CO2. Febs Letters **429:** 147-151

Macdonal.Pw, Strobel GA (1970) Adenosine diphosphate-glucose pyrophosphorylase control of starch accumulation in rust-infected wheat leaves. Plant Physiology **46:** 126-&

Magori S, Kawaguchi M (2009) Long-distance control of nodulation: Molecules and models. Molecules and Cells **27:** 129-134

Mansoor S, Amin I, Hussain M, Zafar Y, Briddon RW (2006) Engineering novel traits in plants through RNA interference. Trends in Plant Science **11:** 559-565

Marillonnet S, Wessler SR (1997) Retrotransposon insertion into the maize waxy gene results in tissue-specific RNA processing. Plant Cell **9:** 967-978

Marino R, Ponnaiah M, Krajewski P, Frova C, Gianfranceschi L, Pe ME, Sari-Gorla M (2009) Addressing drought tolerance in maize by transcriptional profiling and mapping. Molecular Genetics and Genomics **281:** 163-179

Martin C, Smith AM (1995) Starch biosynthesis. Plant Cell **7:** 971-985

Martindale W, Leegood RC (1997) Acclimation of photosynthesis to low temperature in *Spinacia oleracea* L. 1. Effects of acclimation on CO_2 assimilation and carbon partitioning. Journal of Experimental Botany **48:** 1865-1872

Matheson NK, Wheatley JM (1962) Starch changes in developing and senescing tobacco leaves. Australian Journal of Biological Sciences **15:** 445

Matheson NK, Wheatley JM (1963) Diurnal-nocturnal changes in starch of tobacco leaves. Australian Journal of Biological Sciences **16:** 70

Matt P, Schurr U, Klein D, Krapp A, Stitt M (1998) Growth of tobacco in short-day conditions leads to high starch, low sugars, altered diurnal changes in the Nia transcript and low nitrate reductase activity, and inhibition of amino acid synthesis. Planta **207:** 27-41

McCallum CM, Comai L, Greene EA, Henikoff S (2000) Targeting induced local lesions in genomes (TILLING) for plant functional genomics. Plant Physiology **123:** 439-442

McKibbin RS, Muttucumaru N, Paul MJ, Powers SJ, Burrell MM, Coates S, Purcell PC, Tiessen A, Geigenberger P, Halford NG (2006) Production of high-starch, low-glucose potatoes through over-expression of the metabolic regulator SnRK1. Plant Biotechnology Journal **4:** 409-418

Melzer S, Lens F, Gennen J, Vanneste S, Rohde A, Beeckman T (2008) Flowering-time genes modulate meristem determinacy and growth form in *Arabidopsis thaliana.* Nature Genetics **40:** 1489-1492

Messerli G, Nia VP, Trevisan M, Kolbe A, Schauer N, Geigenberger P, Chen JC, Davison AC, Fernie AR, Zeeman SC (2007) Rapid classification of phenotypic mutants of Arabidopsis via metabolite fingerprinting. Plant Physiology **143:** 1484-1492

Meyer RC, Steinfath M, Lisec J, Becher M, Witucka-Wall H, Torjek O, Fiehn O, Eckardt A, Willmitzer L, Selbig J, Altmann T (2007) The metabolic signature related to high plant growth rate in *Arabidopsis thaliana*. Proceedings of the National Academy of Sciences of the United States of America **104:** 4759-4764

Michaels SD, Amasino RM (2000) Memories of winter: vernalization and the competence to flower. Plant Cell and Environment **23:** 1145-1153

Michelmore RW, Paran I, Kesseli RV (1991) Identification of markers linked to disease-resistance genes by bulked segregant analysis - a rapid method to detect markers in specific genomic regions by using segregating populations. Proceedings of the National Academy of Sciences of the United States of America **88:** 9828-9832

Mikkelsen R, Mutenda KE, Mant A, Schurmann P, Blennow A (2005) alpha-Glucan, water dikinase (GWD): A plastidic enzyme with redox-regulated and coordinated catalytic activity and binding affinity. Proceedings of the National Academy of Sciences of the United States of America **102:** 1785-1790

Mikkelsen R, Suszkiewicz K, Blennow A (2006) A novel type carbohydrate-binding module identified in alpha-glucan, water dikinases is specific for regulated plastidial starch metabolism. Biochemistry **45:** 4674-4682

Minchin FR, Pate JS (1974) Diurnal functioning of legume root nodule. Journal of Experimental Botany **25:** 295-308

Mine M, Brivet M, Touati G, Grabowski P, Abitbol M, Marsac C (2003) Splicing error in E1 alpha pyruvate dehydrogenase mRNA caused by novel intronic mutation responsible for lactic acidosis and mental retardation. Journal of Biological Chemistry **278:** 11768-11772

Mitra RM, Gleason CA, Edwards A, Hadfield J, Downie JA, Oldroyd GED, Long SR (2004) A Ca2+/calmodulin-dependent protein kinase required for symbiotic nodule development: Gene identification by transcript-based cloning. Proceedings of the National Academy of Sciences of the United States of America **101:** 4701-4705

Mooney BP (2009) The second green revolution? Production of plant-based biodegradable plastics. Biochemical Journal **418:** 219-232

Moore B, Zhou L, Rolland F, Hall Q, Cheng WH, Liu YX, Hwang I, Jones T, Sheen J (2003) Role of the Arabidopsis glucose sensor HXK1 in nutrient, light, and hormonal signaling. Science **300:** 332-336

Morgan JAW, Bending GD, White PJ (2005) Biological costs and benefits to plant-microbe interactions in the rhizosphere. Journal of Experimental Botany **56:** 1729-1739

Munier-Jolain N, Salon C (2003) Can sucrose content in the phloem sap reaching field pea seeds (*Pisum sativum* L.) be an accurate indicator of seed growth potential? Journal of Experimental Botany **54:** 2457-2465

Munne-Bosch S (2007) Aging in perennials. Critical Reviews in Plant Sciences **26:** 123-138

Munne-Bosch S (2008) Do perennials really senesce? Trends in Plant Science **13:** 216-220

Munoz-Bertomeu J, Cascales-Minana B, Irles-Segura A, Mateu I, Nunes-Nesi A, Fernie AR, Segura J, Ros R (2010) The Plastidial Glyceraldehyde-3-Phosphate Dehydrogenase Is Critical for Viable Pollen Development in Arabidopsis. Plant Physiology **152:** 1830-1841

Myers AM, Morell MK, James MG, Ball SG (2000) Recent progress toward understanding biosynthesis of the amylopectin crystal. Plant Physiology **122:** 989-997

Nakamura T, Vrinten P, Hayakawa K, Ikeda J (1998) Characterization of a granule-bound starch synthase isoform found in the pericarp of wheat. Plant Physiology **118:** 451-459

Nakamura Y, Takahashi J, Sakurai A, Inaba Y, Suzuki E, Nihei S, Fujiwara S, Tsuzuki M, Miyashita H, Ikemoto H, Kawachi M, Sekiguchi H, Kurano N (2005) Some cyanobacteria synthesize semi-amylopectin type alpha-polyglucans instead of glycogen. Plant and Cell Physiology **46:** 539-545

Nashilevitz S, Melamed-Bessudo C, Aharoni A, Kossmann J, Wolf S, Levy AA (2009) The legwd mutant uncovers the role of starch phosphorylation in pollen development and germination in tomato. Plant Journal **57:** 1-13

Neuhaus HE, Stitt M (1990) Control analysis of photosynthate partitioning - impact of reduced activity of ADP-glucose pyrophosphorylase or plastid phosphoglucomutase on the fluxes to starch and sucrose in *Arabidopsis thaliana* (L) Heynh. Planta **182:** 445-454

Neuhaus HE, Wagner R (2000) Solute pores, ion channels, and metabolite transporters in the outer and inner envelope membranes of higher plant plastids. Biochimica Et Biophysica Acta-Biomembranes **1465:** 307-323

Niittyla T, Comparot-Moss S, Lue WL, Messerli G, Trevisan M, Seymour MDJ, Gatehouse JA, Villadsen D, Smith SM, Chen JC, Zeeman SC, Alison MS (2006) Similar protein phosphatases control starch metabolism in plants and glycogen metabolism in mammals. Journal of Biological Chemistry **281:** 11815-11818

Niittyla T, Messerli G, Trevisan M, Chen J, Smith AM, Zeeman SC (2004) A previously unknown maltose transporter essential for starch degradation in leaves. Science **303:** 87-89

Nishi A, Nakamura Y, Tanaka N, Satoh H (2001) Biochemical and genetic analysis of the effects of amylose-extender mutation in rice endosperm. Plant Physiology **127:** 459-472

Ohdan T, Francisco PB, Sawada T, Hirose T, Terao T, Satoh H, Nakamura Y (2005) Expression profiling of genes involved in starch synthesis in sink and source organs of rice. Journal of Experimental Botany **56:** 3229-3244

Okita TW, Nakata PA, Anderson JM, Sowokinos J, Morell M, Preiss J (1990) The subunit structure of potato tuber ADPglucose pyrophosphorylase. Plant Physiology **93:** 785-790

Olcer H, Lloyd JC, Raines CA (2001) Photosynthetic capacity is differentially affected by reductions in sedoheptulose-1,7-bisphosphatase activity during leaf development in transgenic tobacco plants. Plant Physiology **125:** 982-989

Oldroyd GED, Downie JA (2004) Calcium, kinases and nodulation signalling in legumes. Nature Reviews Molecular Cell Biology **5:** 566-576

Oldroyd GED, Downie JM (2008) Coordinating nodule morphogenesis with rhizobial infection in legumes. Annual Review of Plant Biology **59:** 519-546

Ourry A, Kim TH, Boucaud J (1994) Nitrogen reserve mobilization during regrowth of *Medicago sativa* L. (relationships between availability and regrowth yield). Plant Physiology **105:** 831-837

Ozga JA, van Huizen R, Reinecke DM (2002) Hormone and seed-specific regulation of pea fruit growth. Plant Physiology **128:** 1379-1389

Pacini E (1996) Types and meaning of pollen carbohydrate reserves. Sexual Plant Reproduction **9:** 362-366

Pacini E, Franchi GG (1988) Amylogenesis and amylolysis during pollen grain development. In Cresti, M., P. Gori and E. Pacini (Ed.). Sexual Reproduction in Higher Plants; Tenth International Symposium, Siena, Italy, May 30-June 4, 1988. Xiii+502p. Springer-Verlag New York, Inc.: Secaucus, New Jersey, USA; Berlin, West Germany. Illus**:** 181-186

Pacini E, Viegi L (1995) Total polysaccharide content of developing pollen in 2 angiosperm species. Grana **34:** 237-241

Pagani F, Raponi M, Baralle FE (2005) Synonymous mutations in CFTR exon 12 affect splicing and are not neutral in evolution. Proceedings of the National Academy of Sciences of the United States of America **102:** 6368-6372

Pan XX, Tang YY, Li MR, Wu GJ, Jiang HW (2009) Isoforms of GBSSI and SSII in Four Legumes and Their Phylogenetic Relationship to Their Orthologs from Other Angiosperms. Journal of Molecular Evolution **69:** 625-634

Panitz R, Borisjuk L, Manteuffel R, Wobus U (1995) Transient expression of storage-protein genes during early embryogenesis of vicia faba - synthesis and metabolization of vicilin and legumin in the embryo, suspensor and endosperm. Planta **196:** 765-774

Park SW, Chung WI (1998) Molecular cloning and organ-specific expression of three isoforms of tomato ADP-glucose pyrophosphorylase gene. Gene **206:** 215-221

Patrick JW, Offler CE (2001) Compartmentation of transport and transfer events in developing seeds. Journal of Experimental Botany **52:** 551-564

Patron NJ, Keeling PJ (2005) Common evolutionary origin of starch biosynthetic enzymes in green and red algae. Journal of Phycology **41:** 1131-1141

Paul MJ, Stitt M (1993) Effects of nitrogen and phosphorus deficiencies an levels of carbohydrates, respiratory enzymes and metabolites in seedlings of tobacco and their response to exogenous sucrose. Plant Cell and Environment **16:** 1047-1057

Periappuram C, Steinhauer L, Barton DL, Taylor DC, Chatson B, Zou JT (2000) The plastidic phosphoglucomutase from Arabidopsis. A reversible enzyme reaction with an important role in metabolic control. Plant Physiology **122:** 1193-1199

Perry J, Brachmann A, Welham T, Binder A, Charpentier M, Groth M, Haage K, Markmann K, Wang TL, Parniske M (2009) TILLING in *Lotus japonicus* Identified Large Allelic Series for Symbiosis Genes and Revealed a Bias in Functionally Defective Ethyl Methanesulfonate Alleles toward Glycine Replacements. Plant Physiology **151:** 1281-1291

Perry J, Welham T, Cheminant S, Parniske M, Wang T (2005) Tilling. Springer

Perry JA, Wang TL, Welham TJ, Gardner S, Pike JM, Yoshida S, Parniske M (2003) A TILLING reverse genetics tool and a web-accessible collection of mutants of the legume *Lotus japonicus*. Plant Physiology **131:** 866-871

Petreikov M, Shen S, Yeselson Y, Levin I, Bar M, Schaffer AA (2006) Temporally extended gene expression of the ADP-Glc pyrophosphorylase large subunit (AgpL1) leads to increased enzyme activity in developing tomato fruit. Planta **224:** 1465-1479

Pohjanvirta R, Wong JMY, Li W, Harper PA, Tuomisto J, Okey AB (1998) Point mutation in intron sequence causes altered carboxyl-terminal structure in the aryl hydrocarbon receptor of the most 2,3,7,8-tetrachlorodibenzo-p-dioxin-resistant rat strain. Molecular Pharmacology **54:** 86-93

Poorter H, Garnier E (1999) Ecological significance of inherent variation in relative growth rate and its components. In: Pugnaire FI & Valladares F (eds). Handbook of Plant Functional Ecology. Marcel Dekker, New York, pp. 81-120.

Poorter H, van Rijn CPE, Vanhala TK, Verhoeven KJF, de Jong YEM, Stam P, Lambers H (2005) A genetic analysis of relative growth rate and underlying components in Hordeum spontaneum. Oecologia **142:** 360-377

Porch TG, Blair MW, Lariguet P, Galeano C, Pankhurst CE, Broughton WJ (2009) Generation of a Mutant Population for TILLING Common Bean Genotype BAT 93. Journal of the American Society for Horticultural Science **134:** 348-355

Preiss J, Sivak MN (1998) Biochemistry, molecular biology and regulation of starch synthesis. Genetic Engineering **20:** 177-223

Rainbird RM, Atkins CA, Pate JS (1983) Diurnal-variation in the functioning of cowpea nodules. Plant Physiology **72:** 308-312

Remington DL, Ungerer MC, Purugganan MD (2001) Map-based cloning of quantitative trait loci: progress and prospects. Genetics Research **78:** 213-218

Ritte G, Heydenreich M, Mahlow S, Haebel S, Kotting O, Steup M (2006) Phosphorylation of C6- and C3-positions of glucosyl residues in starch is catalysed by distinct dikinases. Febs Letters **580:** 4872-4876

Ritte G, Lloyd JR, Eckermann N, Rottmann A, Kossmann J, Steup M (2002) The starch-related R1 protein is an alpha-glucan, water dikinase. Proceedings of the National Academy of Sciences of the United States of America **99:** 7166-7171

Ritte G, Lorberth R, Steup M (2000) Reversible binding of the starch-related R1 protein to the surface of transitory starch granules. Plant Journal **21:** 387-391

Ritte G, Scharf A, Eckermann N, Haebel S, Steup M (2004) Phosphorylation of transitory starch is increased during degradation. Plant Physiology **135:** 2068-2077

Ritte G, Steup M, Kossmann J, Lloyd JR (2003) Determination of the starch-phosphorylating enzyme activity in plant extracts. Planta **216:** 798-801

Rohde A, Bhalerao RP (2007) Plant dormancy in the perennial context. Trends in Plant Science **12:** 217-223

Roldan I, Wattebled F, Lucas MM, Delvalle D, Planchot V, Jimenez S, Perez R, Ball S, D'Hulst C, Merida A (2007) The phenotype of soluble starch synthase IV defective mutants of *Arabidopsis thaliana* suggests a novel function of elongation enzymes in the control of starch granule formation. Plant Journal **49:** 492-504

Rolland F, Baena-Gonzalez E, Sheen J (2006) Sugar sensing and signaling in plants: Conserved and novel mechanisms. Annual Review of Plant Biology **57:** 675-709

Rolland F, Moore B, Sheen J (2002) Sugar sensing and signaling in plants. Plant Cell **14:** S185-S205

Rolletschek H, Borisjuk L, Radchuk R, Miranda M, Heim U, Wobus U, Weber H (2004) Seed-specific expression of a bacterial phosphoenolpyruvate carboxylase in *Vicia narbonensis* increases protein content and improves carbon economy. Plant Biotechnology Journal **2:** 211-219

Rosche E, Blackmore D, Tegeder M, Richardson T, Schroeder H, Higgins TJV, Frommer WB, Offler CE, Patrick JW (2002) Seed-specific overexpression of a potato sucrose transporter increases sucrose uptake and growth rates of developing pea cotyledons. Plant Journal **30:** 165-175

Rosti S, Rudi H, Rudi K, Opsahl-Sorteberg HG, Fahy B, Denyer K (2006) The gene encoding the cytosolic small subunit of ADP-glucose pyrophosphorylase in barley endosperm also encodes the major plastidial small subunit in the leaves. Journal of Experimental Botany **57:** 3619-3626

Rozen S, Skaletsky H (2000) Primer3 on the WWW for general users and for biologist programmers. Methods Mol Biol **132:** 365-386

Ryle GJA, Powell CE, Gordon AJ (1988) Responses of N2 fixation-linked respiration to host-plant energy status in white clover acclimated to a controlled environment. Journal of Experimental Botany **39:** 879-887

Salanoubat M, Belliard G (1989) The steady-state level of potato sucrose synthase messenger-rna is dependent on wounding, anaerobiosis and sucrose concentration. Gene **84:** 181-185

Sandal N, Krusell L, Radutoiu S, Olbryt M, Pedrosa A, Stracke S, Sato S, Kato T, Tabata S, Parniske M, Bachmair A, Ketelsen T, Stougaard J (2002) A genetic linkage map of the model legume *Lotus japonicus* and strategies for fast mapping of new loci. Genetics **161:** 1673-1683

Sandal N, Petersen TR, Murray J, Umehara Y, Karas B, Yano K, Kumagai H, Yoshikawa M, Saito K, Hayashi M, Murakami Y, Wang XW, Hakoyama T, Imaizumi-Anraku H, Sato S, Kato T, Chen WL, Hossain MS, Shibata S, Wang TL, Yokota K, Larsen K, Kanamori N, Madsen E, Radutoiu S, Madsen LH, Radu TG, Krusell L, Ooki Y, Banba M, Betti M, Rispail N, Skot L, Tuck E, Perry J, Yoshida S, Vickers K, Pike J, Mulder L, Charpentier M, Muller J, Ohtomo R, Kojima T, Ando S, Marquez AJ, Gresshoff PM, Harada K, Webb J, Hata S, Suganuma N, Kouchi H, Kawasaki S, Tabata S, Parniske M, Szczyglowski K, Kawaguchi M, Stougaard J (2006) Genetics of symbiosis in *Lotus japonicus*: Recombinant inbred lines, comparative genetic maps, and map position of 35 symbiotic loci. Molecular Plant-Microbe Interactions **19:** 80-91

Sanwal GG, Greenber.E, Hardie J, Cameron EC, Preiss J (1968) Regulation of starch biosynthesis in plant leaves: activation and inhibition of ADPglucose pyrophosphorylase. Plant Physiology **43:** 417-427

Sato S, Nakamura Y, Kaneko T, Asamizu E, Kato T, Nakao M, Sasamoto S, Watanabe A, Ono A, Kawashima K, Fujishiro T, Katoh M, Kohara M, Kishida Y, Minami C, Nakayama S, Nakazaki N, Shimizu Y, Shinpo S, Takahashi C, Wada T, Yamada M, Ohmido N, Hayashi M, Fukui K, Baba T, Nakamichi T, Mori H, Tabata S (2008) Genome Structure of the Legume, *Lotus japonicus*. DNA Research **15:** 227-239

Sato S, Tabata S (2006) *Lotus japonicus* as a platform for legume research. Current Opinion in Plant Biology **9:** 128-132

Satoh H, Nishi A, Yamashita K, Takemoto Y, Tanaka Y, Hosaka Y, Sakurai A, Fujita N, Nakamura Y (2003) Starch-branching enzyme I-deficient mutation specifically affects the structure and properties of starch in rice endosperm. Plant Physiology **133:** 1111-1121

Satoh H, Shibahara K, Tokunaga T, Nishi A, Tasaki M, Hwang SK, Okita TW, Kaneko N, Fujita N, Yoshida M, Hosaka Y, Sato A, Utsumi Y, Ohdan T, Nakamura Y (2008) Mutation of the plastidial alpha-glucan phosphorylase gene in rice affects the synthesis and structure of starch in the endosperm. Plant Cell **20:** 1833-1849

Schafer G, Heber U, Heldt HW (1977) Glucose-transport into spinach-chloroplasts. Plant Physiology **60:** 286-289

Schaffer R, Landgraf J, Accerbi M, Simon V, Larson M, Wisman E (2001) Microarray analysis of diurnal and circadian-regulated genes in Arabidopsis. Plant Cell **13:** 113-123

Schauser L, Handberg K, Sandal N, Stiller J, Thykjaer T, Pajuelo E, Nielsen A, Stougaard J (1998) Symbiotic mutants deficient in nodule establishment identified after T-DNA transformation of *Lotus japonicus*. Molecular and General Genetics **259:** 414-423

Schauser L, Roussis A, Stiller J, Stougaard J (1999) A plant regulator controlling development of symbiotic root nodules. Nature **402:** 191-195

Scheidig A, Frohlich A, Schulze S, Lloyd JR, Kossmann J (2002) Downregulation of a chloroplast-targeted beta-amylase leads to a starch-excess phenotype in leaves. Plant Journal **30:** 581-591

Schneegurt MA, Sherman DM, Sherman LA (1997) Composition of the carbohydrate granules of the cyanobacterium, Cyanothece sp strain ATCC 51142. Archives of Microbiology **167:** 89-98

Schnyder H, de Visser R (1999) Fluxes of reserve-derived and currently assimilated carbon and nitrogen in perennial ryegrass recovering from defoliation. The regrowing tiller and its component functionally distinct zones. Plant Physiology **119:** 1423-1435

Schuelke M (2000) An economic method for the fluorescent labeling of PCR fragments. Nature Biotechnology **18:** 233-234

Schulze J (2004) How are nitrogen fixation rates regulated in legumes? Journal of Plant Nutrition and Soil Science-Zeitschrift Fur Pflanzenernahrung Und Bodenkunde **167:** 125-137

Schulze W, Stitt M, Schulze ED, Neuhaus HE, Fichtner K (1991) A quantification of the significance of assimilatory starch for growth of *Arabidopsis thaliana* L Heynh. Plant Physiology **95:** 890-895

Senoura T, Isono N, Yoshikawa M, Asao A, Hamada S, Watanabe K, Ito H, Matsui H (2004) Characterization of starch synthase I and II expressed in early developing seeds of kidney bean (*Phaseolus vulgaris* L.). Bioscience Biotechnology and Biochemistry **68:** 1949-1960

Servaites JC, Geiger DR (2002) Kinetic characteristics of chloroplast glucose transport. Journal of Experimental Botany **53:** 1581-1591

Shalit A, Rozman A, Goldshmidt A, Alvarez JP, Bowman JL, Eshed Y, Lifschitz E (2009) The flowering hormone florigen functions as a general systemic regulator of growth and termination. Proceedings of the National Academy of Sciences of the United States of America **106:** 8392-8397

Shannon JC, Pien FM, Cao HP, Liu KC (1998) Brittle-1, an adenylate translocator, facilitates transfer of extraplastidial synthesized ADP-glucose into amyloplasts of maize endosperms. Plant Physiology **117:** 1235-1252

Shaw CR, Prasas R (1970) Starch gel electrophoresis of enzymes - A compilation of recipes. Biochemical Genetics **4:** 297-320

Singh RJ, Chung GH, Nelson RL (2007) Landmark research in legumes. Genome **50:** 525-537

Singh S, Choi SB, Modi MK, Okita TW (2002) Isolation and characterization of cDNA clones encoding ADP-glucose pyrophosphorylase (AGPase) large and small subunits from chickpea (*Cicer arietinum* L.). Phytochemistry **59:** 261-268

Sissons MJ, Lance RCM, Wallace W (1994) Bound and free forms of barley limit dextrinase. Cereal Chemistry **71:** 520-521

Sissons MJ, Macgregor AW (1994) Hydrolysis of barley starch granules by alpha-glucosidases from malt. Journal of Cereal Science **19:** 161-169

Slade AJ, Knauf VC (2005) TILLING moves beyond functional genomics into crop improvement. Transgenic Research **14:** 109-115

Smeekens S (2000) Sugar-induced signal transduction in plants. Annual Review of Plant Physiology and Plant Molecular Biology **51:** 49-81

Smidansky ED, Clancy M, Meyer FD, Lanning SP, Blake NK, Talbert LE, Giroux MJ (2002) Enhanced ADP-glucose pyrophosphorylase activity in wheat endosperm increases seed yield. Proceedings of the National Academy of Sciences of the United States of America **99:** 1724-1729

Smidansky ED, Martin JM, Hannah LC, Fischer AM, Giroux MJ (2003) Seed yield and plant biomass increases in rice are conferred by deregulation of endosperm ADP-glucose pyrophosphorylase. Planta **216:** 656-664

Smidansky ED, Meyer FD, Blakeslee B, Weglarz TE, Greene TW, Giroux MJ (2007) Expression of a modified ADP-glucose pyrophosphorylase large subunit in wheat seeds stimulates photosynthesis and carbon metabolism. Planta **225:** 965-976

Smith AM (2001) The biosynthesis of starch granules. Biomacromolecules **2:** 335-341

Smith AM (2008) Prospects for increasing starch and sucrose yields for bioethanol production. Plant Journal **54:** 546-558

Smith AM, Stitt M (2007) Coordination of carbon supply and plant growth. Plant Cell and Environment **30:** 1126-1149

Smith AM, Zeeman SC (2006) Quantification of starch in plant tissues. Nature Protocols **1:** 1342-1345

Smith AM, Zeeman SC, Smith SM (2005) Starch degradation. Annual Review of Plant Biology **56:** 73-98

Smith AM, Zeeman SC, Thorneycroft D, Smith SM (2003) Starch mobilization in leaves. Journal of Experimental Botany **54:** 577-583

Smith MW, Doolittle RF (1992) Anomalous phylogeny involving the enzyme glucose-6-phosphate isomerase. Journal of Molecular Evolution **34:** 544-545

Smith SM, Fulton DC, Chia T, Thorneycroft D, Chapple A, Dunstan H, Hylton C, Zeeman SC, Smith AM (2004) Diurnal changes in the transcriptome encoding enzymes of starch metabolism provide evidence for both transcriptional and posttranscriptional regulation of starch metabolism in arabidopsis leaves. Plant Physiology **136:** 2687-2699

Smithwhite BJ, Preiss J (1992) Comparison of proteins of ADP-glucose pyrophosphorylase from diverse sources. Journal of Molecular Evolution **34:** 449-464

Sokolov LN, Dejardin A, Kleczkowski LA (1998) Sugars and light/dark exposure trigger differential regulation of ADP-glucose pyrophosphorylase genes in *Arabidopsis thaliana* (thale cress). Biochemical Journal **336:** 681-687

Sokolov LN, Dominguez-Solis JR, Allary AL, Buchanan BB, Luan S (2006) A redox-regulated chloroplast protein phosphatase binds to starch diurnally and functions in its accumulation. Proceedings of the National Academy of Sciences of the United States of America **103:** 9732-9737

Sonnewald U, Basner A, Greve B, Steup M (1995) A 2nd L-type isozyme of potato glucan phosphorylase - cloning, antisense inhibition and expression analysis. Plant Molecular Biology **27:** 567-576

Sonnewald U, Willmitzer L (1992) molecular approaches to sink-source interactions. Plant Physiology **99:** 1267-1270

Stark DM, Timmerman KP, Barry GF, Preiss J, Kishore GM (1992) Regulation of the amount of starch in plant-tissues by adp glucose pyrophosphorylase. Science **258:** 287-292

Stinard PS, Robertson DS, Schnable PS (1993) Genetic isolation, cloning, and analysis of a mutator-induced, dominant antimorph of the maize amylose extender1 locus. Plant Cell **5:** 1555-1566

Stitt M (1996) Metabolic regulation of photosynthesis. Advances in Photosynthesis; Photosynthesis and the environment**:** 151-190

Stitt M, ap Rees T (1980) carbohydrate breakdown by chloroplasts of *Pisum sativum*. Biochimica Et Biophysica Acta **627:** 131-143

Stitt M, Bulpin PV, Rees TA (1978) Pathway of starch breakdown in photosynthetic tissues of pisum-sativum. Biochimica Et Biophysica Acta **544:** 200-214

Stitt M, Heldt HW (1981) Physiological rates of starch breakdown in isolated intact spinach chloroplasts. Plant Physiology **68:** 755-761

Stitt M, Krapp A (1999) The interaction between elevated carbon dioxide and nitrogen nutrition: the physiological and molecular background. Plant Cell and Environment **22:** 583-621

Sturm A, Tang GQ (1999) The sucrose-cleaving enzymes of plants are crucial for development, growth and carbon partitioning. Trends in Plant Science **4:** 401-407

Sturre MJG, Shirzadian-Khorramabad R, Schippers JHM, Chin-A-Woeng TFC, Hille J, Dijkwel PP (2009) Method for the identification of single mutations in large genomic regions using massive parallel sequencing. Molecular Breeding **23:** 51-59

Sugimoto T, Tanaka K, Monma M, Kawamura Y, Saio K (1989) Phosphoenolpyruvate carboxylase level in soybean seed highly correlates to its contents of protein and lipid. Agricultural and Biological Chemistry **53:** 885-887

Sulpice R, Pyl ET, Ishihara H, Trenkamp S, Steinfath M, Witucka-Wall H, Gibon Y, Usadel B, Poree F, Piques MC, Von Korff M, Steinhauser MC, Keurentjes JJB, Guenther M, Hoehne M, Selbig J, Fernie AR, Altmann T, Stitt M (2009) Starch as a major integrator in the regulation of plant growth. Proceedings of the National Academy of Sciences of the United States of America **106:** 10348-10353

Sun Z, Henson CA (1990) Degradation of native starch granules by barley alpha-glucosidases. Plant Physiology **94:** 320-327

Sweetlove LJ, Trethewey RN, Muller-Rober B, Hill SA (1998) High flux control coefficient for potato tuber ADPglucose pyrophosphorylase. Journal of Experimental Botany **49:** 61-62

Szczyglowski K, Shaw RS, Wopereis J, Copeland S, Hamburger D, Kasiborski B, Dazzo FB, de Bruijn FJ (1998) Nodule organogenesis and symbiotic mutants of the model legume *Lotus japonicus*. Molecular Plant-Microbe Interactions **11:** 684-697

Szydlowski N, Ragel P, Raynaud S, Lucas MM, Roldan I, Montero M, Munoz FJ, Ovecka M, Bahaji A, Planchot V, Pozueta-Romero J, D'Hulst C, Merida A (2009) Starch Granule Initiation in Arabidopsis Requires the Presence of Either Class IV or Class III Starch Synthases. Plant Cell **21:** 2443-2457

Ta TC, Macdowall FDH, Faris MA (1990) Utilization of carbon and nitrogen reserves of alfalfa roots in supporting N2-fixation and shoot regrowth. Plant and Soil **127:** 231-236

Tadege M, Wang TL, Wen JQ, Ratet P, Mysore KS (2009) Mutagenesis and Beyond! Tools for Understanding Legume Biology. Plant Physiology **151:** 978-984

Takeda Y, Guan HP, Preiss J (1993) Branching of amylose by the branching isoenzymes of maize endosperm. Carbohydrate Research **240:** 253-263

Taliercio EW, Romano G, Scheffler J, Ayre BG (2009) Expression of genes associated with carbohydrate metabolism in cotton stems and roots. BMC Plant Biology **9:** Article No.: 11

Tarrago JF, Nicolas G (1976) Starch degradation in cotyledons of germinating lentils. Plant Physiology **58:** 618-621

Tauberger E, Fernie AR, Emmermann M, Renz A, Kossmann J, Willmitzer L, Trethewey RN (2000) Antisense inhibition of plastidial phosphoglucomutase provides compelling evidence that potato tuber amyloplasts import carbon from the cytosol in the form of glucose-6-phosphate. Plant Journal **23:** 43-53

Temnykh S, DeClerck G, Lukashova A, Lipovich L, Cartinhour S, McCouch S (2001) Computational and experimental analysis of microsatellites in rice (*Oryza sativa* L.): Frequency, length variation, transposon associations, and genetic marker potential. Genome Research **11:** 1441-1452

Tetlow IJ, Morell MK, Emes MJ (2004) Recent developments in understanding the regulation of starch metabolism in higher plants. Journal of Experimental Botany **55:** 2131-2145

Tetlow IJ, Wait R, Lu ZX, Akkasaeng R, Bowsher CG, Esposito S, Kosar-Hashemi B, Morell MK, Emes MJ (2004) Protein phosphorylation in amyloplasts regulates starch branching enzyme activity and protein-protein interactions. Plant Cell **16:** 694-708

Thimm O, Blasing O, Gibon Y, Nagel A, Meyer S, Kruger P, Selbig J, Muller LA, Rhee SY, Stitt M (2004) MAPMAN: a user-driven tool to display genomics data

sets onto diagrams of metabolic pathways and other biological processes. Plant Journal **37:** 914-939

Thomas H, Howarth CJ (2000) Five ways to stay green. Journal of Experimental Botany **51**: 329-337.

Thomas H, Thomas HM, Ougham H (2000) Annuality, perenniality and cell death. Journal of Experimental Botany **51:** 1781-1788

Thorbjornsen T, Villand P, Denyer K, Olsen OA, Smith AM (1996) Distinct isoforms of ADPglucose pyrophosphorylase occur inside and outside the amyloplasts in barley endosperm. Plant Journal **10:** 243-250

Thummler F, Verma DPS (1987) Nodulin-100 of soybean is the subunit of sucrose synthase regulated by the availability of free heme in nodules. Journal of Biological Chemistry **262:** 14730-14736

Tiessen A, Prescha K, Branscheid A, Palacios N, McKibbin R, Halford NG, Geigenberger P (2003) Evidence that SNF1-related kinase and hexokinase are involved in separate sugar-signalling pathways modulating post-translational redox activation of ADP-glucose pyrophosphorylase in potato tubers. Plant Journal **35:** 490-500

Till B, Colbert TG, Tompa R, Steine M, McCallum CM, Henikoff S, Reynolds SH, Comai L (2001) A high-throughput method for identifying induced point mutations in plants. Plant Biology (Rockville) **2001:** 181

Till BJ, Cooper J, Tai TH, Colowit P, Greene EA, Henikoff S, Comai L (2007) Discovery of chemically induced mutations in rice by TILLING. BMC Plant Biology **7:** Article No.: 19

Till BJ, Reynolds SH, Weil C, Springer N, Burtner C, Young K, Bowers E, Codomo CA, Enns LC, Odden AR, Greene EA, Comai L, Henikoff S (2004) Discovery of induced point mutations in maize genes by TILLING. BMC Plant Biology **4**

Till BJ, Reynolds SH, Weil C, Springer N, Burtner C, Young K, Bowers E, Codomo CA, Enns LC, Odden AR, Greene EA, Comai L, Henikoff S (2004) Discovery of induced point mutations in maize genes by TILLING. BMC Plant Biology **4**

Tjaden J, Mohlmann T, Kampfenkel K, Henrichs G, Neuhaus HE (1998) Altered plastidic ATP/ADP-transporter activity influences potato (*Solanum tuberosum* L.) tuber morphology, yield and composition of tuber starch. Plant Journal **16:** 531-540

Tomlinson KL, Lloyd JR, Smith AM (1997) Importance of isoforms of starch-branching enzyme in determining the structure of starch in pea leaves. Plant Journal **11:** 31-43

Trethewey RN, Smith AM, Leegood RC, Kennedy R (2000) Starch metabolism in leaves. Photosynthesis: Physiology and metabolism**:** 205-231

Tsai HL, Lue WL, Lu KJ, Hsieh MH, Wang SM, Chen J (2009) Starch Synthesis in Arabidopsis Is Achieved by Spatial Cotranscription of Core Starch Metabolism Genes. Plant Physiology **151:** 1582-1595

Tuncel A, Kavakli IH, Keskin O (2008) Insights into subunit interactions in the heterotetrameric structure of potato ADP-glucose pyrophosphorylase. Biophysical Journal **95:** 3628-3639

Udvardi MK, Tabata S, Parniske M, Stougaard J (2005) *Lotus japonicus*: Legume research in the fast lane. Trends in Plant Science **10:** 222-228

Usadel B, Blasing OE, Gibon Y, Retzlaff K, Hoehne M, Gunther M, Stitt M (2008) Global transcript levels respond to small changes of the carbon status during progressive exhaustion of carbohydrates in Arabidopsis rosettes. Plant Physiology **146:** 1834-1861

Van Laere AS, Nguyen M, Braunschweig M, Nezer C, Collette C, Moreau L, Archibald AL, Haley CS, Buys N, Tally M, Andersson G, Georges M, Andersson L (2003) A regulatory mutation in IGF2 causes a major QTL effect on muscle growth in the pig. Nature **425:** 832-836

Vance CP, Gantt JS (1992) Control of nitrogen and carbon metabolism in root-nodules. Physiologia Plantarum **85:** 266-274

Varshney RK, Close TJ, Singh NK, Hoisington DA, Cook DR (2009) Orphan legume crops enter the genomics era! Current Opinion in Plant Biology **12:** 202-210

Vigeolas H, Mohlmann T, Martini N, Neuhaus HE, Geigenberger P (2004) Embryo-specific reduction of ADP-Glc pyrophosphorylase leads to an inhibition of starch synthesis and a delay in oil accumulation in developing seeds of oilseed rape. Plant Physiology **136:** 2676-2686

Volenec JJ, Boyce PJ, Hendershot KL (1991) Carbohydrate-metabolism in taproots of *Medicago sativa* L during winter adaptation and spring regrowth. Plant Physiology **96:** 786-793

Vriet C, Welham T, Brachmann A, Pike M, Pike J, Perry J, Parniske M, Sato S, Tabata S, Smith AM, Wang TL (2010) A Suite of Lotus japonicus Starch Mutants Reveals both Conserved and Novel Features of Starch Metabolism. Plant Physiology **154:** 643-655

Vrinten PL, Nakamura T (2000) Wheat granule-bound starch synthase I and II are encoded by separate genes that are expressed in different tissues. Plant Physiology **122:** 255-263

Walsh KB, Layzell DB (1986) Carbon and nitrogen assimilation and partitioning in soybeans exposed to low root temperatures. Plant Physiology **80:** 249-255

Walsh KB, Vessey JK, Layzell DB (1987) Carbohydrate supply and N2 fixation in soybean - the effect of varied daylength and stem girdling. Plant Physiology **85:** 137-144

Wang D, Shi J, Carlson SR, Cregan PB, Ward RW, Diers BW (2003) A low-cost, high-throughput polyacrylamide gel electrophoresis system for genotyping with microsatellite DNA markers. Crop Science **43:** 1828-1832

Wang D-K, Sun Z-X, Tao Y-Z (2006) Application of TILLING in plant improvement. Acta Genetica Sinica **33:** 957-964

Wang RH, Farrona S, Vincent C, Joecker A, Schoof H, Turck F, Alonso-Blanco C, Coupland G, Albani MC (2009) PEP1 regulates perennial flowering in *Arabis alpina*. Nature **459:** 423-U138

Wang SJ, Yeh KW, Tsai CY (2001) Regulation of starch granule-bound starch synthase I gene expression by circadian clock and sucrose in the source tissue of sweet potato. Plant Science **161:** 635-644

Wang SM, Chu B, Lue WL, Yu TS, Eimert K, Chen JC (1997) adg2-1 represents a missense mutation in the ADPG pyrophosphorylase large subunit gene of *Arabidopsis thaliana*. Plant Journal **11:** 1121-1126

Wang TL, Bogracheva TY, Hedley CL (1998) Starch: As simple as A, B, C? Journal of Experimental Botany **49:** 481-502

Wang TL, Domoney C, Hedley CL, Casey R, Grusak MA (2003) Can we improve the nutritional quality of legume seeds? Plant Physiology **131:** 886-891

Wang TL, Hadavizideh A, Harwood A, Welham TJ, Harwood WA, Faulks R, Hedley CL (1990) An analysis of seed development in *Pisum-sativum* .XIII. The chemical induction of storage product mutants. Plant Breeding **105:** 311-320

Wang, T.L., and Hedley, C. (1991) Seed development in peas: Knowing your three "r"s (or four, or five). Seed Sci. Res. 1:3-14.

Wardlaw IF (1990) Tansley review no 27 - the control of carbon partitioning in plants. New Phytologist **116:** 341-381

Wattebled F, Dong Y, Dumez S, Delvalle D, Planchot R, Berbezy P, Vyas D, Colonna P, Chatterjee M, Ball S, D'Hulst C (2005) Mutants of Arabidopsis lacking a chloroplastic isoamylase accumulate phytoglycogen and an abnormal form of amylopectin. Plant Physiology **138:** 184-195

Wattebled F, Dong Y, Dumez S, Delvalle D, Planchot R, Berbezy P, Vyas D, Colonna P, Chatterjee M, Ball S, D'Hulst C (2005) Mutants of Arabidopsis lacking a chloroplastic isoamylase accumulate phytoglycogen and an abnormal form of amylopectin. Plant Physiology **138:** 184-195

Wattebled F, Planchot V, Dong Y, Szydlowski N, Pontoire B, Devin A, Ball S, D'Hulst C (2008) Further Evidence for the Mandatory Nature of Polysaccharide Debranching for the Aggregation of Semicrystalline Starch and for Overlapping Functions of Debranching Enzymes in Arabidopsis Leaves. Plant Physiology **148:** 1309-1323

Weber A, Servaites JC, Geiger DR, Kofler H, Hille D, Groner F, Hebbeker U, Flugge UI (2000) Identification, purification, and molecular cloning of a putative plastidic glucose translocator. Plant Cell **12:** 787-801

Weber H, Borisjuk L, Heim U, Buchner P, Wobus U (1995) Seed coat-associated invertases of fava-bean control both unloading and storage functions - cloning of cdnas and cell-type-specific expression. Plant Cell **7:** 1835-1846

Weber H, Borisjuk L, Wobus U (2005) Molecular physiology of legume seed development. Annual Review of Plant Biology **56:** 253-279

Weeden NF, Gottlieb LD (1982) Dissociation, reassociation, and purification of plastid and cytosolic phosphoglucose isomerase isozymes. Plant Physiology **69:** 717-723

Weigelt K, Kuster H, Rutten T, Fait A, Fernie AR, Miersch O, Wasternack C, Emery RJN, Desel C, Hosein F, Muller M, Saalbach I, Weber H (2009) ADP-Glucose Pyrophosphorylase-Deficient Pea Embryos Reveal Specific Transcriptional and Metabolic Changes of Carbon-Nitrogen Metabolism and Stress Responses. Plant Physiology **149:** 395-411

Weise SE, Weber APM, Sharkey TD (2004) Maltose is the major form of carbon exported from the chloroplast at night. Planta **218:** 474-482

Welham T, Pike J, Horst I, Flemetakis E, Katinakis P, Kaneko T, Sato S, Tabata S, Perry J, Parniske M, Wang TL (2009) A cytosolic invertase is required for normal growth and cell development in the model legume, *Lotus japonicus*. Journal of Experimental Botany **60:** 3353-3365

Wienkoop S, Saalbach G (2003) Proteome analysis. Novel proteins identified at the peribacteroid membrane from *Lotus japonicus* root nodules. Plant Physiology **131:** 1080-1090

Williams LE, Dejong TM, Phillips DA (1982) Effect of changes in shoot carbon-exchange rate on soybean root nodule activity. Plant Physiology **69:** 432-436

Wingler A, Fritzius T, Wiemken A, Boller T, Aeschbacher RA (2000) Trehalose induces the ADP-glucose pyrophosphorylase gene, ApL3, and starch synthesis in Arabidopsis. Plant Physiology **124:** 105-114

Wingler A, Purdy S, MacLean JA, Pourtau N (2006) The role of sugars in integrating environmental signals during the regulation of leaf senescence. Journal of Experimental Botany **57:** 391-399

Worby CA, Gentry MS, Dixon JE (2006) Laforin, a dual specificity phosphatase that dephosphorylates complex carbohydrates. Journal of Biological Chemistry **281:** 30412-30418

Wuriyanghan H, Zhang B, Cao WH, Ma BA, Lei G, Liu YF, Wei W, Wu HJ, Chen LJ, Chen HW, Cao YR, He SJ, Zhang WK, Wang XJ, Chen SY, Zhang JS (2009) The Ethylene Receptor ETR2 Delays Floral Transition and Affects Starch Accumulation in Rice. Plant Cell **21:** 1473-1494

Yan HB, Pan XX, Jiang HW, Wu GJ (2009) Comparison of the starch synthesis genes between maize and rice: copies, chromosome location and expression divergence. Theoretical and Applied Genetics **119:** 815-825

Yano M, Sasaki T (1997) Genetic and molecular dissection of quantitative traits in rice. Plant Molecular Biology **35:** 145-153

Yeh RF, Lim LP, Burge CB (2001) Computational inference of homologous gene structures in the human genome. Genome Research **11:** 803-816

Young ND, Cannon SB, Sato S, Kim D, Cook DR, Town CD, Roe BA, Tabata S (2005) Sequencing the genespaces of *Medicago truncatula* and *Lotus japonicus*. Plant Physiology **137:** 1174-1181

Yu SK, Blennow A, Bojko M, Madsen F, Olsen CE, Engelsen SB (2002) Physico-chemical characterization of floridean starch of red algae. Starch-Starke **54:** 66-74

Yu TS, Kofler H, Hausler RE, Hille D, Flugge UI, Zeeman SC, Smith AM, Kossmann J, Lloyd J, Ritte G, Steup M, Lue WL, Chen JC, Weber A (2001) The Arabidopsis sex1 mutant is defective in the R1 protein, a general regulator of starch degradation in plants, and not in the chloroplast hexose transporter. Plant Cell **13:** 1907-1918

Yu TS, Lue WL, Wang SM, Chen JC (2000) Mutation of arabidopsis plastid phosphoglucose isomerase affects leaf starch synthesis and floral initiation. Plant Physiology **123:** 319-325

Yu TS, Zeeman SC, Thorneycroft D, Fulton DC, Dunstan H, Lue WL, Hegemann B, Tung SY, Umemoto T, Chapple A, Tsai DL, Wang SM, Smith AM, Chen J, Smith SM (2005) alpha-Amylase is not required for breakdown of transitory starch in Arabidopsis leaves. Journal of Biological Chemistry **280:** 9773-9779

Zeeman SC, Ap Rees T (1999) Changes in carbohydrate metabolism and assimilate export in starch-excess mutants of Arabidopsis. Plant Cell and Environment **22:** 1445-1453

Zeeman SC, Delatte T, Messerli G, Umhang M, Stettler M, Mettler T, Streb S, Reinhold H, Kotting O (2007) Starch breakdown: recent discoveries suggest distinct pathways and novel mechanisms. Functional Plant Biology **34:** 465-473

Zeeman SC, Northrop F, Smith AM, ap Rees T (1998) A starch-accumulating mutant of *Arabidopsis thaliana* deficient in a chloroplastic starch-hydrolysing enzyme. Plant Journal **15:** 357-365

Zeeman SC, Smith SM, Smith AM (2004) The breakdown of starch in leaves. New Phytologist **163:** 247-261

Zeeman SC, Smith SM, Smith AM (2007) The diurnal metabolism of leaf starch. Biochemical Journal **401:** 13-28

Zeeman SC, Thorneycroft D, Schupp N, Chapple A, Weck M, Dunstan H, Haldimann P, Bechtold N, Smith AM, Smith SM (2004) Plastidial alpha-glucan phosphorylase is not required for starch degradation in Arabidopsis leaves but has a role in the tolerance of abiotic stress. Plant Physiology **135:** 849-858

Zeeman SC, Tiessen A, Pilling E, Kato KL, Donald AM, Smith AM (2002) Starch synthesis in Arabidopsis. Granule synthesis, composition, and structure. Plant Physiology **129:** 516-529

Zeeman SC, Umemoto T, Lue WL, Au-Yeung P, Martin C, Smith AM, Chen J (1998) A mutant of Arabidopsis lacking a chloroplastic isoamylase accumulates both starch and phytoglycogen. Plant Cell **10:** 1699-1711

Zeng Y, Wu Y, Avigne WT, Koch KE (1998) Differential regulation of sugar-sensitive sucrose synthases by hypoxia and anoxia indicate complementary transcriptional and postranscriptional responses. Plant Physiology (Rockville) **116:** 1573-1583

Zhang X, Szydlowski N, Delvalle D, D'Hulst C, James MG, Myers AM (2008) Overlapping functions of the starch synthases SSII and SSIII in amylopectin biosynthesis in Arabidopsis. BMC Plant Biology **8:** Article No.: 96

Zhang XL, Myers AM, James MG (2005) Mutations affecting starch synthase III in arabidopsis alter leaf starch structure and increase the rate of starch synthesis. Plant Physiology **138:** 663-674

Zhang YH, Shewry PR, Jones H, Barcelo P, Lazzeri PA, Halford NG (2001) Expression of antisense SnRK1 protein kinase sequence causes abnormal pollen development and male sterility in transgenic barley. Plant Journal **28:** 431-441

Zhang YHP, Evans BR, Mielenz JR, Hopkins RC, Adams MWW (2007) High-yield hydrogen production from starch and water by a synthetic enzymatic pathway. PLoS One **2:** e456

Zheng GH, Han HL, Bhatty RS (1998) Physicochemical properties of zero amylose hull-less barley starch. Cereal Chemistry **75:** 520-524

Zhou YC, Chan K, Wang TL, Hedley CL, Offler CE, Patrick JW (2009) Intracellular sucrose communicates metabolic demand to sucrose transporters in developing pea cotyledons. Journal of Experimental Botany **60:** 71-85

Zrenner R, Salanoubat M, Willmitzer L, Sonnewald U (1995) Evidence of the crucial role of sucrose synthase for sink strength using transgenic potato plants (*Solanum tuberosum* L). Plant Journal **7:** 97-107